

**INVESTIGATING THE MECHANISMS UNDERLYING  
EFFECTS OF TESTOSTERONE ON BLOOD PRESSURE  
IN NORMOTENSIVE AND HYPERTENSIVE RATS**

**LOH SU YI**

**FACULTY OF MEDICINE  
UNIVERSITY OF MALAYA  
KUALA LUMPUR**

**2017**

**INVESTIGATING THE MECHANISMS  
UNDERLYING EFFECTS OF TESTOSTERONE ON  
BLOOD PRESSURE IN NORMOTENSIVE AND  
HYPERTENSIVE RATS**

**LOH SU YI**

**THESIS SUBMITTED IN FULFILMENT OF THE  
REQUIREMENTS FOR THE DEGREE OF DOCTOR OF  
PHILOSOPHY**

**FACULTY OF MEDICINE  
UNIVERSITY OF MALAYA  
KUALA LUMPUR**

**2017**

**UNIVERSITY OF MALAYA**  
**ORIGINAL LITERARY WORK DECLARATION**

Name of Candidate: **LOH SU YI**

Matric No: **MHA140012**

Name of Degree: **DOCTOR OF PHILOSOPHY**

Title of Project Paper/Research Report/Dissertation/Thesis (“this Work”):

**INVESTIGATING THE MECHANISMS UNDERLYING  
EFFECTS OF TESTOSTERONE ON BLOOD PRESSURE IN  
NORMOTENSIVE AND HYPERTENSIVE RATS**

Field of Study: **PHYSIOLOGY**

I do solemnly and sincerely declare that:

- (1) I am the sole author/writer of this Work;
- (2) This Work is original;
- (3) Any use of any work in which copyright exists was done by way of fair dealing and for permitted purposes and any excerpt or extract from, or reference to or reproduction of any copyright work has been disclosed expressly and sufficiently and the title of the Work and its authorship have been acknowledged in this Work;
- (4) I do not have any actual knowledge nor do I ought reasonably to know that the making of this work constitutes an infringement of any copyright work;
- (5) I hereby assign all and every rights in the copyright to this Work to the University of Malaya (“UM”), who henceforth shall be owner of the copyright in this Work and that any reproduction or use in any form or by any means whatsoever is prohibited without the written consent of UM having been first had and obtained;
- (6) I am fully aware that if in the course of making this Work I have infringed any copyright whether intentionally or otherwise, I may be subject to legal action or any other action as may be determined by UM.

Candidate’s Signature

Date:

Subscribed and solemnly declared before,

Witness’s Signature

Date:

Name:

Designation:

## ABSTRACT

The influences of sex hormones on the blood pressure regulation have been known since decades. These were evidence by men, with higher testosterone level having higher blood pressure and incidence of hypertension as compared to the age-matched women. Besides, women after menopause who have higher testosterone to estrogen ratio possessing greater blood pressure as compared to women before menopause. Based on these observations, I hypothesized that testosterone might play an important role in causing the blood pressure to increase via affecting the sodium and water handling in the kidney and expression of genes that are involved in the blood pressure regulation in the brain. Therefore in this study, expression of proteins that are involved in sodium and water handling in kidney and gene profiling in the cardiovascular center of the brain were investigated under testosterone influence. This study was performed on normotensive and hypertensive rats which were gonadectomized and subsequently were given testosterone treatment. Two groups were employed which were gonadectomized male normotensive rats receiving sub-chronic (seven days) testosterone treatment and gonadectomized male and female normotensive and hypertensive rats receiving chronic (six weeks) testosterone treatment. Sub-chronic testosterone treatment increased the blood pressure and expression levels of epithelial sodium channel (ENaC) in the kidneys while expression levels of aquaporin (AQP) (AQP-1, 2, 3, 4, 6 and 7) were differentially regulated. Plasma aldosterone, sodium and glucose levels were increased but osmolality and urea levels were decreased. In these rats, co-administration of flutamide (androgen receptor antagonist) and finasteride (5 $\alpha$ -reductase inhibitor) prevented the testosterone effects. Chronic testosterone treatment resulted in an increase in the blood pressure but ENaC and AQP expressions in the kidney decreased and increased, respectively. Plasma aldosterone, sodium, osmolality and urea levels were decreased. Chronic testosterone treatment also resulted in up-regulations of 1575, 23

and 34 genes in the paraventricular nucleus (PVN), nucleus of solitary tract (NTS) and rostral ventrolateral medulla (RVLM), respectively. However, 252, 23 and 23 genes in these respective regions of the brain were down-regulated. Based on the fold changes of the genes relevant to blood pressure regulation, and following mRNA and protein validations, it was found that two genes in the PVN could be involved in mediating testosterone effects namely *Ephx2* and *Fcrl2*. In overall, testosterone was found to increase the blood pressure, however in kidney, the mechanisms involved differ between periods of exposure. Sub-chronic exposure to testosterone could lead to sodium retention via the related increases in plasma aldosterone and kidney ENaC levels while chronic exposure to testosterone could lead to a decrease in sodium retention via the related decreases in plasma aldosterone and kidney ENaC levels. In both cases, testosterone exposure might also lead to water retention via increasing the kidney AQP expression. In view that chronic testosterone treatment affects the regulation of genes in the cardiovascular center of the brain, mainly the novel *Ephx2* and *Fcrl2* genes, therefore, it could be suggested that the blood pressure increased following chronic exposure to testosterone might be mediated through the mechanisms involving the brain rather than kidneys.

## ABSTRAK

Peranan hormon seks dalam pengawal-aturan tekanan darah telah diketahui sejak dekad lalu. Antara buktinya adalah lelaki dengan paras testosteron yang tinggi menunjukkan tekanan darah dan bilangan kes tekanan darah tinggi lebih tinggi berbanding dengan wanita pada usia sama. Selain itu, wanita selepas putus haid mempunyai nisbah testosteron kepada estrogen yang lebih tinggi yang mungkin menyebabkan tekanan darah yang lebih tinggi berbanding dengan wanita sebelum putus haid. Berdasarkan pemerhatian-pemerhatian ini, saya menghipotesiskan bahawa testosteron memainkan peranan yang penting dalam peningkatan tekanan darah di mana ia mempengaruhi ekspresi protein-protein yang terlibat dalam proses pengendalian natrium dan air di buah pinggang dan gen-gen dalam pusat kawalan tekanan darah di otak. Oleh yang demikian, dalam kajian ini, tindakan testostosterone ke atas ekspresi protein-protein yang terlibat di dalam proses pengendalian natrium dan air di ginjal dan profil ekspresi gen dalam pusat kawalan kardiovaskular di otak dikaji. Kajian ini menggunakan tikus normotensif dan hipertensif di mana gonadektomi dilakukan dan testosteron diberikan. Terdapat dua kumpulan eksperimen iaitu tikus-tikus jantan normotensif yang digonadektomi menerima testosteron secara sub-kronik (tujuh hari) dan tikus-tikus jantan dan betina normotensif and hipertensif yang digonadektomi menerima testosteron secara kronik (enam minggu). Pemberian testosteron secara sub-kronik menyebabkan kenaikan tekanan darah dan ekspresi *epithelial sodium channel* (ENaC) dalam ginjal manakala kesannya ke atas ekspresi *aquaporin* (AQP) (AQP-1, 2, 3, 4, 6 dan 7) adalah berbeza-beza. Dalam plasma, kepekatan aldosteron, natrium dan glukosa meningkat manakala paras osmolaliti manakala paras urea menurun. Pemberian bersama *flutamide* (antagonis reseptor androgen) dan *finasteride* (perencat 5 $\alpha$ -reduktase) kepada tikus-tikus ini menghalang tindakan testosteron. Sementara itu, pemberian testosteron secara kronik menyebabkan kenaikan tekanan darah manakala

penurunan and peningkatan masing-masing dalam ekspresi ENaC and AQP di ginjal. Kepekatan aldosteron, natrium, osmolaliti dan urea dalam plasma juga menurun. Pemberian testosteron secara kronik ini juga mengakibatkan peningkatan dalam ekspresi gen iaitu sebanyak 1575, 23 dan 34 masing-masing di *paraventricular nucleus* (PVN), *nucleus of solitary tract* (NTS) dan *rostral ventrolateral medulla* (RVLM). Pada masa yang sama, ekspresi gen iaitu sebanyak 252, 23 dan 23 masing-masing dalam bahagian-bahagian otak ini menurun. Berdasarkan tahap perubahan dalam ekspresi gen-gen yang terlibat dalam pengawal-aturan tekanan darah, dan diikuti oleh pengesahan paras mRNA dan protein, didapati bahawa dua gen dalam PVN iaitu *Ephx2* and *Fcrl2* mungkin memainkan peranan yang penting dalam tindakan testosteron ini. Secara keseluruhannya, testosteron menyebabkan peningkatan tekanan darah, walau bagaimanapun, mekanisme-mekanisme dalam ginjal yang terlibat adalah berbeza-beza bergantung kepada jangka masa pemberian. Pemberian testosteron secara sub-kronik mungkin membawa kepada retensi natrium dengan meningkatkan kepekatan aldosteron dalam plasma dan ekspresi ENaC dalam ginjal manakala pemberian testosteron secara kronik mungkin menyebabkan pengurangan dalam retensi natrium dengan menurunkan kepekatan aldosteron dalam plasma dan ekspresi ENaC dalam ginjal. Dalam kedua-dua kes ini, pemberian testosteron mungkin juga menjurus kepada retensi air dengan meningkatkan ekspresi AQP dalam ginjal. Memandangkan pemberian testosteron secara kronik juga menyebabkan perubahan ekspresi gen-gen dalam pusat kawalan kardiovaskular di otak, termasuklah gen novel *Ephx2* and *Fcrl2*, oleh itu, dicadangkan bahawa peningkatan tekanan darah akibat penerimaan testosteron secara kronik mungkin dikawal-atur melalui mekanisme-mekanisme dalam otak dan bukannya ginjal.

## ACKNOWLEDGEMENTS

I would like to take this opportunity to convey my heartfelt thanks and sincere appreciation to all those who have made this journey possible. First and foremost, I would like to express my deepest gratitude to my supervisor, Associate Professor Dr. Naguib Salleh for his patient guidance, inspiring advice and valuable support throughout the course of this study. Without his constant and untiring encouragements, this thesis would not have been possible.

My sincere appreciation is extended to Professor Dr. Ruby Husain, Head, Department of Physiology for her kind assistance and support throughout the study period. I would also like to thank all lecturers and staff of Department of Physiology and Medical Biotechnology Laboratory for their help and cooperation in making my research work smooth. I am also appreciative of all my lab buddies for their support and encouragement during the long hours in the lab.

With this opportunity, I must also thank the Bright Sparks Unit of University of Malaya for sponsoring my graduate studies. Besides, I also gratefully acknowledge the grant funding received toward my research project from University of Malaya.

Last but not least, I would also like to extend my deepest gratitude to my family members for their unflagging love and support since the day I was born. Without them, I would not have reached this stage of education. Thank you for giving me the freedom to pursue my dreams. Lastly, I would like to express my sincere thanks again to all those who have directly or indirectly contributed to my research work. Thank you.

## TABLE OF CONTENTS

Abstract .....	iii
Abstrak .....	v
Acknowledgements .....	vii
Table of Contents .....	viii
List of Figures .....	xvii
List of Tables.....	xxii
List of Symbols and Abbreviations.....	xxiv
List of Appendices .....	xxvii
<b>CHAPTER 1: GENERAL INTRODUCTION .....</b>	<b>1</b>
1.1 Research background.....	1
1.2 Significance of study .....	5
1.3 Research questions and hypotheses .....	6
1.4 Objectives .....	8
<b>CHAPTER 2: LITERATURE REVIEW.....</b>	<b>9</b>
2.1 Testosterone.....	9
2.1.1 Metabolisms of testosterone.....	10
2.1.2 Testosterone, health and diseases .....	12
2.2 Regulation of blood pressure .....	13
2.2.1 Sexual dimorphism in blood pressure .....	14
2.2.2 Testosterone-induced high blood pressure .....	17
2.3 The roles of kidney in blood pressure regulation .....	23
2.3.1 Renal sodium handling.....	24
2.3.1.1 The effects of testosterone on sodium handling.....	26

2.3.1.2	Epithelial Sodium Channel (ENaC) .....	27
2.3.2	Regulation of water balance .....	28
2.3.2.1	The effects of testosterone on water balance .....	29
2.3.2.2	Aquaporins (AQPs) .....	30
2.4	Central Nervous System (CNS) and blood pressure.....	34
2.4.1	Paraventricular Nucleus (PVN) of hypothalamus .....	37
2.4.2	Nucleus of the solitary tract (NTS) of brainstem .....	38
2.4.3	Rostral Ventrolateral medulla (RVLM) of brainstem .....	40
2.4.4	Testosterone influences blood pressure regulation via CNS .....	41
2.5	Animal Models .....	44
2.5.1	Sprague Dawley (SD).....	45
2.5.2	Wistar Kyoto (WKY) .....	46
2.5.3	Spontaneously Hypertensive Rats (SHR).....	46
2.6	Transcriptomics .....	47
2.6.1	RNA-Seq (RNA-Sequencing) .....	47
2.6.2	RNA-Seq gene expression profiling.....	49
<b>CHAPTER 3: MATERIALS AND METHODS .....</b>		<b>51</b>
3.1	Materials .....	51
3.1.1	Animals and animal facilities .....	51
3.1.2	Chemicals and consumables.....	51
3.1.2.1	Anesthesia and post-surgeries .....	51
3.1.2.2	Hormonal treatments .....	52
3.1.2.3	Carotid artery cannulation.....	52
3.1.2.4	Blood collection and analysis.....	52
3.1.2.5	RNA extraction and quality control .....	52
3.1.2.6	cDNA synthesis and qPCR .....	53

3.1.2.7	RNASeq .....	53
3.1.2.8	Protein extraction and quantification .....	54
3.1.2.9	SDS-PAGE and Western blotting .....	54
3.1.2.10	Immunohistochemistry studies.....	54
3.2	Experimental design and animal preparation .....	55
3.2.1	Effects of orchidectomy and sub-chronic testosterone treatment in normotensive male rats.....	56
3.2.2	Effects of gonadectomies in normotensive and hypertensive male and female rats .....	57
3.2.3	Changes in blood pressure across estrous cycle in normotensive and hypertensive female rats.....	58
3.2.4	Effect of chronic testosterone treatment in normotensive and hypertensive female rats .....	59
3.3	Surgical procedures .....	60
3.3.1	Sham-operation .....	60
3.3.2	Orchidectomy .....	61
3.3.3	Ovariectomy .....	61
3.4	Identification of estrous cycle.....	62
3.5	Hormonal treatment.....	63
3.5.1	Sub-chronic testosterone treatment via subcutaneous injection.....	64
3.5.2	Chronic testosterone treatment via Silastic tubing implantation.....	64
3.6	Cannulation of carotid artery .....	65
3.7	Blood analysis.....	66
3.8	Kidney .....	67
3.8.1	Real-time quantitative polymerase chain reaction (qPCR) .....	67
3.8.1.1	RNA extraction .....	68

3.8.1.2	RNA quantification and quality control .....	68
3.8.1.3	cDNA synthesis .....	69
3.8.1.4	qPCR procedure .....	70
3.8.2	Western blotting .....	71
3.8.2.1	Protein extraction .....	71
3.8.2.2	Protein quantification .....	72
3.8.2.3	Preparation of SDS-PAGE gel .....	72
3.8.2.4	Sample preparation and running the gel electrophoresis.....	74
3.8.2.5	Protein transfer .....	74
3.8.2.6	Membrane blocking.....	75
3.8.2.7	Incubation with primary and secondary antibodies.....	75
3.8.2.8	Protein bands visualization.....	77
3.8.3	Immunohistochemistry .....	77
3.8.3.1	Whole animal perfusion fixation.....	77
3.8.3.2	Tissue processing and sectioning .....	79
3.8.3.3	Deparaffinization, rehydration and antigen retrieval .....	80
3.8.3.4	Immunoperoxidase staining .....	81
3.8.3.5	Immunofluorescence staining .....	82
3.9	Paraventricular nucleus (PVN), nucleus of the solitary tract (NTS) and rostral ventrolateral medulla (RVLM) .....	85
3.9.1	Transcriptome analysis with RNA-Seq.....	86
3.9.1.1	Sample preparation.....	86
3.9.1.2	RNA extraction .....	89
3.9.1.3	RNA quantification and quality control .....	90
3.9.1.4	Library preparation and quality control .....	91
3.9.1.5	Library qualification via qPCR .....	93

3.9.1.6	MiSeq library quality control .....	95
3.9.1.7	HiSeq sequencing .....	97
3.9.1.8	Data analysis .....	101
3.9.2	Real-time quantitative polymerase chain reaction (qPCR) .....	103
3.9.2.1	Sample preparation and RNA extraction .....	103
3.9.2.2	RNA quantification and quality control .....	103
3.9.2.3	cDNA synthesis .....	103
3.9.2.4	qPCR procedures .....	104
3.9.3	Immunohistochemistry .....	105
3.9.3.1	Whole animal perfusion fixation .....	105
3.9.3.2	Tissue preparation and sectioning .....	106
3.9.3.3	Double immunofluorescence staining .....	106
3.10	Statistical analysis .....	107

**CHAPTER 4: EFFECTS OF TESTOSTERONE ON MEAN ARTERIAL PRESSURE (MAP) ..... 108**

4.1	Introduction .....	108
4.2	Results .....	110
4.2.1	Effects of orchidectomy and sub-chronic testosterone treatment on MAP and plasma testosterone levels in male normotensive rats .....	110
4.2.2	Effects of gonadectomy on MAP and plasma testosterone levels in male and female normotensive and hypertensive rats .....	112
4.2.3	Changes in MAP and plasma testosterone levels across estrous cycle in female normotensive and hypertensive rats .....	114
4.2.4	Effects of chronic testosterone treatment on MAP and plasma testosterone levels in female normotensive and hypertensive rats .....	116
4.3	Discussion .....	118

**CHAPTER 5: EFFECTS OF SUB-CHRONIC TESTOSTERONE TREATMENT  
ON EPITHELIAL SODIUM CHANNEL (ENAC) EXPRESSION IN KIDNEYS ....**

..... 123

5.1 Introduction..... 123

5.2 Results ..... 125

5.2.1 Hormonal and biochemical blood parameters ..... 125

5.2.2  $\alpha$ -ENaC mRNA and protein expression levels..... 127

5.2.3  $\beta$ -ENaC mRNA and protein expression levels..... 129

5.2.4  $\gamma$ -ENaC mRNA and protein expression levels ..... 131

5.2.5 Distribution of  $\alpha$ -ENaC protein in nephrons ..... 133

5.2.6 Distribution of  $\beta$ -ENaC protein in nephrons ..... 133

5.2.7 Distribution of  $\gamma$ -ENaC protein in nephrons ..... 133

5.3 Discussion..... 142

**CHAPTER 6: EFFECTS OF SUB-CHRONIC TESTOSTERONE TREATMENT  
ON AQUAPORINS (AQP) EXPRESSION IN KIDNEYS ..... 147**

6.1 Introduction..... 147

6.2 Results ..... 149

6.2.1 *Aqp* mRNA expression levels..... 149

6.2.2 Classical aquaporin (AQP-1, 2, 4 and 6) protein levels ..... 152

6.2.3 Aquaglyceroporin (AQP-3 and 7) protein levels..... 153

6.2.4 Distribution of AQP-1 and AQP-3 proteins in nephrons ..... 156

6.2.5 Distribution of AQP-2 and AQP-4 proteins in nephrons ..... 157

6.2.6 Distribution of AQP-6 and AQP-7 proteins in nephrons ..... 157

6.3 Discussion..... 161

**CHAPTER 7: EFFECTS OF CHRONIC TESTOSTERONE TREATMENT ON EPITHELIAL SODIUM CHANNEL (ENaC) IN KIDNEYS..... 164**

7.1	Introduction.....	164
7.2	Results .....	166
7.2.1	Hormonal and biochemical blood parameters.....	166
7.2.2	$\alpha$ , $\beta$ and $\gamma$ -ENaC mRNA and protein levels in kidneys of WKY rats. ....	170
7.2.3	Distribution of $\alpha$ , $\beta$ and $\gamma$ -ENaC proteins in kidneys of WKY rats .....	173
7.2.4	$\alpha$ , $\beta$ and $\gamma$ -ENaC mRNA and protein levels in kidneys of SHR rats.....	176
7.2.5	Distribution of $\alpha$ , $\beta$ and $\gamma$ -ENaC proteins in kidneys of SHR rats .....	179
7.3	Discussion.....	182

**CHAPTER 8: EFFECTS OF CHRONIC TESTOSTERONE TREATMENT ON AQUAPORIN (AQP) EXPRESSION IN KIDNEYS..... 186**

8.1	Introduction.....	186
8.2	Results .....	188
8.2.1	AQP mRNA expression in kidneys of normotensive WKY rats .....	188
8.2.2	AQP protein expression in kidneys of normotensive WKY rats.....	190
8.2.3	Distribution of AQP proteins in kidney of normotensive WKY rats ....	193
8.2.4	AQP mRNA expression in kidneys of hypertensive SHR rats .....	198
8.2.5	AQP protein expression in kidneys of hypertensive SHR rats.....	200
8.2.6	Distribution of AQP proteins in kidney of hypertensive SHR rats .....	203
8.3	Discussion.....	208

**CHAPTER 9: EFFECTS OF CHRONIC TESTOSTERONE TREATMENT ON TRANSCRIPTOMES IN PVN, NTS AND RVLM..... 212**

9.1	Introduction.....	212
9.2	Results .....	214

9.2.1	RNA quality assessment prior to library preparation for RNASeq.....	214
9.2.2	cDNA library quality assessment and quantification .....	217
9.2.3	MiSeq library quality control of pooled library .....	217
9.2.4	HiSeq sequencing of pooled library .....	217
9.2.5	Transcriptome data analysis .....	222
9.2.5.1	Paraventricular nucleus (PVN).....	222
9.2.5.2	Nucleus of the solitary tract (NTS) .....	226
9.2.5.3	Rostral ventrolateral medulla (RVLM) .....	229
9.3	Discussion.....	233

**CHAPTER 10: EFFECTS OF CHRONIC TESTOSTERONE TREATMENT ON  
SELECTED GENES EXPRESSION IN PVN, NTS AND RVLM.....237**

10.1	Introduction.....	237
10.2	Results .....	239
10.2.1	Verification of RNA-Seq analysis by qPCR .....	239
10.2.1.1	Paraventricular nucleus (PVN).....	239
10.2.1.2	Nucleus of Solitary tract (NTS) .....	252
10.2.1.3	Rostral ventrolateral medulla (RVLM) .....	265
10.2.2	Distribution of Ephx2 and Fcrl2 proteins in PVN.....	276
10.3	Discussion.....	279

**CHAPTER 11: CONCLUSION AND FUTURE STUDIES .....283**

11.1	Conclusion.....	283
11.2	Limitation of the present study .....	286
11.3	Future studies.....	286

References .....	287
List of Publications and Papers Presented .....	329
Appendices.....	331

University of Malaya

## LIST OF FIGURES

Figure 2.1 Structure of cholesterol and testosterone. ....	11
Figure 2.2 Gonadal pathways for testosterone formation in Leydig cell. ....	11
Figure 2.3 Biosynthetic pathways of testosterone from cholesterol precursor. ....	12
Figure 2.4 Summary of renal regulation of blood pressure. ....	24
Figure 2.5 The amount of sodium reabsorbed along the kidney nephron. ....	25
Figure 2.6 Structure of ENaC and cellular transport of sodium reabsorption. ....	28
Figure 2.7 Structure of aquaporins. ....	33
Figure 2.8 Involvement of AQPs in epithelial water transport. ....	33
Figure 2.9 Schematic illustration showing the keys hypothalamic circuits that mediate the osmosensitive neural pathways in the CNS. ....	37
Figure 2.10 Schematic diagram of major physiological systems in CNS and PNS that are involved in the regulation of blood pressure. ....	44
Figure 2.11 Overview of library preparation for RNA-Seq. ....	49
Figure 3.1 Identification of estrous cycle stages in female rats. ....	63
Figure 3.2 Testosterone treatments via subcutaneous Silastic tubing implantation. ....	65
Figure 3.3 Surgical procedures for cannulation of carotid artery. ....	66
Figure 3.4 RNA analysis by agarose gel electrophoresis. ....	69
Figure 3.5 Preparation for protein transfer. ....	75
Figure 3.6 Whole animal perfusion fixation procedures. ....	78
Figure 3.7 Histology slide of kidney cortex. ....	85
Figure 3.8 Coronal rat brain atlas diagrams from Paxinos and Watson (2009) and toluidine blue staining of neurons. ....	88
Figure 3.9 Simplified flow chart of RNA-Seq library preparation using ScriptSeq Complete Gold Kit (low input). ....	93
Figure 3.10 Workflow for transcriptome analysis study by RNA-Seq. ....	102

Figure 4.1 Effects of orchidectomy and sub-chronic testosterone treatment on MAP and plasma testosterone levels in male normotensive rats.....	111
Figure 4.2 Effects of gonadectomy on MAP and plasma testosterone levels in male and female normotensive and hypertensive rats. ....	113
Figure 4.3 Changes in MAP and plasma testosterone levels across estrous cycle in female normotensive and hypertensive rats. ....	115
Figure 4.4 Effects of chronic testosterone treatment on MAP and plasma testosterone levels in female normotensive and hypertensive rats.....	117
Figure 5.1 Effects of sub-chronic testosterone treatment on mRNA and protein expression levels of $\alpha$ -ENaC in kidneys. ....	128
Figure 5.2 Effects of sub-chronic testosterone treatment on mRNA and protein expression levels of $\beta$ -ENaC in kidneys. ....	130
Figure 5.3 Effects of sub-chronic testosterone treatment on mRNA and protein expression levels of $\gamma$ -EnaC in kidneys. ....	132
Figure 5.4 Immunoperoxidase images showing the distribution of $\alpha$ -ENaC proteins in nephrons following sub-chronic testosterone treatment. ....	135
Figure 5.5 Immunoperoxidase images showing the distribution of $\beta$ -ENaC proteins in nephrons following sub-chronic testosterone treatment. ....	136
Figure 5.6 Immunoperoxidase images showing the distribution of $\gamma$ -ENaC proteins in nephrons following sub-chronic testosterone treatment. ....	137
Figure 5.7 Immunofluorescence images showing the distribution of $\alpha$ , $\beta$ and $\gamma$ -ENaC proteins in nephrons following sub-chronic testosterone treatments.....	138
Figure 5.8 Immunofluorescence images showing the effects of co-administration of flutamide or finasteride with sub-chronic testosterone treatments on the distribution of $\alpha$ -ENaC in nephrons.....	139
Figure 5.9 Immunofluorescence images showing the effects of co-administration of flutamide or finasteride with sub-chronic testosterone treatments on the distribution of $\beta$ -ENaC in nephrons.....	140
Figure 5.10 Immunofluorescence images showing the effects of co-administration of flutamide or finasteride with sub-chronic testosterone treatments on protein expression levels of $\gamma$ -ENaC in nephrons. ....	141
Figure 6.1 Effects of sub-chronic testosterone treatment on mRNA expression levels of AQP subunits in kidneys.....	151

Figure 6.2 Effects of sub-chronic testosterone treatment on expression levels of classical aquaporin subunit proteins in kidneys. ....	154
Figure 6.3 Effects of sub-chronic testosterone treatment on expression levels of aquaglyceroporin proteins in kidneys. ....	155
Figure 6.4 Effects of sub-chronic testosterone treatment on the distribution of AQP-1 (green) and AQP-3 (red) proteins in nephrons. ....	158
Figure 6.5 Effects of chronic testosterone treatment on the distribution of AQP-2 (red) and AQP-4 (green) proteins in nephrons. ....	159
Figure 6.6 Effects of sub-chronic testosterone treatment on the distribution of AQP-6 (green) and AQP-7 (red) proteins in nephrons. ....	160
Figure 7.1 Effects of chronic testosterone treatment on mRNA and protein expression levels of $\alpha$ , $\beta$ and $\gamma$ -ENaC subunits in kidneys of normotensive WKY rats. ....	172
Figure 7.2 Effects of chronic testosterone treatment on the distribution of $\alpha$ , $\beta$ and $\gamma$ -ENaC proteins in kidneys of normotensive WKY rats as observed by immunoperoxidase staining. ....	174
Figure 7.3 Effects of chronic testosterone treatments on the distribution of $\alpha$ , $\beta$ and $\gamma$ -ENaC in kidneys of normotensive WKY rats as observed by immunofluorescence staining. ....	175
Figure 7.4 Effects of chronic testosterone treatment on mRNA and protein expression levels of $\alpha$ , $\beta$ and $\gamma$ -ENaC in kidneys of hypertensive SHR rats. ....	178
Figure 7.5 Effects of chronic testosterone treatment on the distribution of $\alpha$ , $\beta$ and $\gamma$ -ENaC in kidneys of hypertensive SHR rats as observed by immunoperoxidase staining. ....	180
Figure 7.6 Effects of chronic testosterone treatment on the distribution of $\alpha$ , $\beta$ and $\gamma$ -ENaC in kidneys of hypertensive SHR rats as observed by immunofluorescence staining. ....	181
Figure 8.1 Effects of chronic testosterone treatment on mRNA expression levels of AQP subunits in kidneys of normotensive WKY rats. ....	189
Figure 8.2 Effects of chronic testosterone treatment on protein expression levels of classical aquaporins in kidneys of normotensive WKY rats. ....	191
Figure 8.3 Effects of chronic testosterone treatment on protein expression levels of aquaglyceroporins in kidneys of normotensive WKY rats. ....	192

Figure 8.4 Effects of chronic testosterone treatment on distributions of AQP-1 (green) and AQP-3 (red) proteins in cortical nephron of normotensive WKY rats. ....	195
Figure 8.5 Effects of chronic testosterone treatment on distributions of AQP-2 (red) and AQP-4 (green) proteins in cortical nephron of normotensive WKY rats. ....	196
Figure 8.6 Effects of chronic testosterone treatment on distributions of AQP-6 (green) and AQP-7 (red) proteins in cortical nephron of normotensive WKY rats. ....	197
Figure 8.7 Effects of chronic testosterone treatment on mRNA expression levels of AQP subunits in the kidneys of hypertensive SHR rats.....	199
Figure 8.8 Effects of chronic testosterone treatment on protein expression levels of classical aquaporins in kidneys of hypertensive SHR rats.....	201
Figure 8.9 Effects of chronic testosterone treatment on protein expression levels of aquaglyceroporins in kidneys of hypertensive SHR rats. ....	202
Figure 8.10 Effects of chronic testosterone treatment on distributions of AQP-1 (green) and AQP-3 (red) proteins in cortical nephron of hypertensive SHR rats. ....	205
Figure 8.11 Effects of chronic testosterone treatment on distributions of AQP-2 (red) and AQP-4 (green) proteins in cortical nephron of hypertensive SHR rats.....	206
Figure 8.12 Effects of chronic testosterone treatment on distributions of AQP-6 (green) and AQP-7 (red) proteins in cortical nephron of hypertensive SHR rats. ....	207
Figure 9.1 RNA quality assessment report with Agilent Bioanalyzer.....	216
Figure 9.2 Library quality assessment report with Agilent Bioanalyzer. ....	218
Figure 9.3 Venn diagram showing intersection of number of genes changes in PVN in SMO compared to SMS and in SFT compared to SFO. ....	223
Figure 9.4 Venn diagram showing intersection of number of genes changes in NTS in SMO compared to SMS and in SFT compared to SFO. ....	226
Figure 9.5 Venn diagram showing intersection of number of genes changes in RVLM in SMO compared to SMS and in SFT compared to SFO. ....	230
Figure 10.1 Selection of reference gene with constant expression in PVN.....	241
Figure 10.2 qPCR determinations of up-regulated genes by chronic testosterone treatment based on the transcriptome analysis of PVN. ....	242
Figure 10.3 qPCR determinations of genes down-regulated by chronic testosterone treatment based on transcriptome analysis of PVN. ....	248

Figure 10.4 Effects of chronic testosterone treatment on mRNA expression levels of arginine vasopressin (AVP) in PVN. ....	251
Figure 10.5 Selection of reference gene with constant expression in NTS. ....	254
Figure 10.6 qPCR determinations of genes up-regulated by testosterone treatment based on the transcriptome analysis of NTS. ....	255
Figure 10.7 qPCR determinations of genes down-regulated by testosterone treatment based on NTS transcriptome analysis. ....	260
Figure 10.8 Selection of reference gene with constant expression in RVLM. ....	267
Figure 10.9 qPCR determinations of genes up-regulated by testosterone treatment based on the transcriptome analysis of RVLM. ....	268
Figure 10.10 qPCR determinations of genes down-regulated by testosterone treatment based on the transcriptome analysis of RVLM. ....	273
Figure 10.11 Effects of chronic testosterone treatment on the distribution of Ephx2 (red) and Fcrl2 (green) in PVN of normotensive WKY rats. ....	277
Figure 10.12 Effects of chronic testosterone treatment on the distribution of Ephx2 (red) and Fcrl2 (green) in PVN of hypertensive SHR rats. ....	278

## LIST OF TABLES

Table 2.1 Sexual dimorphism in blood pressure.....	16
Table 2.2 Summary of mechanisms that involved in testosterone-induced changes in blood pressure. ....	19
Table 3.1 Forward and reverse primer sequences for ENaC, AQP and GAPDH.....	71
Table 3.2 Preparation of SDS-PAGE gel.....	73
Table 3.3 List of primary and secondary antibodies used in Western blotting.....	76
Table 3.4 Sequence of tissue processing.....	79
Table 3.5 List of primary and secondary antibodies used in immunoperoxidase and immunofluorescence staining. ....	84
Table 3.6 The position of SBS Reagents in TruSeq v3 sequencing mode.....	100
Table 3.7 The position of PE Reagents for Read 1 and Read 2 in TruSeq v3 sequencing mode.....	100
Table 3.8 List of primary and secondary antibodies used for double immunofluorescence staining in PVN. ....	107
Table 5.1 Effects of sub-chronic testosterone treatment on hormonal and biochemical parameters in blood plasma.....	126
Table 7.1 Effects of chronic testosterone treatment on hormonal and biochemical parameters in blood plasma of normotensive WKY rats. ....	168
Table 7.2 Effects of chronic testosterone treatment on hormonal and biochemical parameters in blood plasma of hypertensive SHR rats. ....	169
Table 9.1 Quality control assessment of RNA extracted from PVN, RVLM and NTS. ....	215
Table 9.2 Quality control assessment of cDNA library. ....	219
Table 9.3 MiSeq quality control assessment of pooled library.....	220
Table 9.4 Summary report of HiSeq run.....	221
Table 9.5 Expression changes of selected genes in PVN based on edgeR analysis of SMO compared to SMS and SFT compared to SFO. ....	224

Table 9.6 Expression changes of selected genes in NTS based on edgeR analysis of SMO compared to SMS and SFT compared to SFO. ....	227
Table 9.7 Expression changes of selected genes in RVLM based on edgeR analysis of SMO compared to SMS and SFT compared to SFO. ....	231
Table 10.1 Summary of fold changes, both from edgeR analysis of RNA-Seq data and qPCR analysis, of genes up-regulated by chronic testosterone treatment based on the transcriptome analysis of PVN.....	246
Table 10.2 Summary of fold changes, both from edgeR analysis of RNA-Seq data and qPCR analysis, of genes down-regulated by chronic testosterone treatment based on the transcriptome analysis of PVN.....	250
Table 10.3 Summary of fold changes, both from edgeR analysis of RNA-Seq data and qPCR analysis, of genes up-regulated by chronic testosterone treatment based on the transcriptome analysis of NTS. ....	258
Table 10.4 Summary of fold changes, both from edgeR analysis of RNA-Seq data and qPCR analysis, of genes down-regulated by chronic testosterone treatment based on the transcriptome analysis of NTS. ....	263
Table 10.5 Summary of fold changes, both from edgeR analysis of RNA-Seq data and qPCR analysis, of genes up-regulated by chronic testosterone treatment based on the transcriptome analysis of RVLM. ....	271
Table 10.6 Summary of fold changes, both from edgeR analysis of RNA-Seq data and qPCR analysis, of genes down-regulated by chronic testosterone treatment based on the transcriptome analysis of RVLM. ....	275

## LIST OF SYMBOLS AND ABBREVIATIONS

×g	:	Times gravity
μg	:	Microgram
μl	:	Microliter
μm	:	Micrometer
μM	:	Micromolar
ACE	:	Angiotensin converting enzyme
ANS	:	Autonomic nervous system
AR	:	Androgen receptor
AVP	:	Arginine vasopressin
AQP	:	Aquaporin
bp	:	Base pair
BSA	:	Bovine serum albumin
CD	:	Collecting duct
cDNA	:	Complementary DNA
CNS	:	Central nervous system
DBP	:	Diastolic blood pressure
ddH <sub>2</sub> O	:	Double-distilled water
DHT	:	5α-dihydrotestosterone
DNA	:	Deoxyribonucleic acid
DT	:	Distal convoluted tubule
<i>e.g.</i>	:	<i>exempli gratia</i> (for example)
ENaC	:	Epithelial sodium channel
FN	:	Finasteride
FU	:	Flutamide

g	:	gram
G	:	Glomerulus
HRP	:	Horseradish peroxidase
<i>i.e.</i>	:	<i>id est</i> (that is/namely)
kg	:	Kilogram
MAP	:	Mean arterial pressure
mg	:	Milligram
mM	:	Millimolar
MnPO	:	Median preoptic nucleus
mol	:	Mole
mRNA	:	Messenger RNA
ng	:	Nanogram
nm	:	Nanometer
nM	:	Nanomolar
NTS	:	Nucleus of solitary tract
OVLT	:	Organum vasculosum of the lamina terminalis
OXT	:	Oxytocin
PBS	:	Phosphate-buffered saline
PBST	:	Phosphate-buffered saline with Tween-20
PCOS	:	Polycystic ovary syndrome
PFA	:	Paraformaldehyde
pM	:	Picomolar
PNS	:	Peripheral nervous system
PSNS	:	Parasympathetic nervous system
PT	:	Proximal convoluted tubule
PVN	:	Paraventricular nucleus

qPCR	:	Real-time quantitative polymerase chain reaction
RAS	:	Renin-angiotensin-aldosterone system
RNA	:	Ribonucleic acid
RNA-Seq	:	RNA-Sequencing
rRNA	:	Ribosomal RNA
rpm	:	Revolutions per minute
RVLM	:	Rostral ventrolateral medulla
SBP	:	Systolic blood pressure
SD	:	Sprague Dawley
SDS-PAGE	:	Sodium dodecyl sulfate-polyacrylamide gel electrophoresis
SEM	:	Standard error of mean
SFO	:	Subfornical organ
SHR	:	Spontaneously hypertensive rat
SNA	:	Sympathetic nerve activity
SNS	:	Sympathetic nervous system
v/v	:	Volume/volume
WKY	:	Wistar Kyoto
w/v	:	Weight/volume

## LIST OF APPENDICES

Appendix A: Publications.....	331
Appendix B: Buffer preparation.....	337
Appendix C: Forward and reverse primer sequences for target genes in PVN, NTS and RVLM.....	339
Appendix D: Hi-Seq sequencing report.....	341

University of Malaya

## CHAPTER 1: GENERAL INTRODUCTION

### 1.1 Research background

Hypertension is the major risk factor for many diseases including stroke, heart disease and kidney diseases which may lead to substantial morbidity. Gender bias and gender differences in blood pressure regulation have long been observed, however the underlying mechanisms are not fully understood and are likely to be multifaceted (Maas & Appelman, 2010; Maranon & Reckelhoff, 2013; Regitz-Zagrosek & Seeland, 2012). Many studies had revealed the lower prevalence of hypertension in premenopausal women as compared to age-matched men. However, the incidence of hypertension in women increases sharply after menopause, suggesting the involvement of sex hormones in protecting the females against hypertension (Hinojosa-Laborde et al., 2000; Regitz-Zagrosek & Seeland, 2012). To date, various studies have focused on the roles of female sex hormone *i.e.* estrogen in blood pressure regulation. Nevertheless, despite the limited evidences on the detrimental effects of androgen such as induces vasoconstriction (Ammar et al., 2004; Song et al., 2010), and increases in blood pressure (Liu & Ely, 2011; Reckelhoff et al., 1998), the mechanisms underlying blood pressure regulation by androgen remains unknown.

Previous studies reported that in rats, blood pressure in males was higher than aged-matched females. The high blood pressure in male rats can be overcome by castration while in female rats, ovariectomy has been shown to cause an increase in blood pressure (Ito et al., 2006; Liu et al., 2016; Martin et al., 2005; Martin et al., 2012; Reckelhoff et al., 1998). Nonetheless, there are also controversial studies which showed that ovariectomy did not alter the blood pressure (Dias et al., 2010; Giménez et al., 2006; Jazbutyte et al., 2006; Martin et al., 2012). Administration of testosterone to male and

female rats has been shown to cause the blood pressure to increase (Davis et al., 2012; Dubey et al., 2002; Mishra et al., 2016; Reckelhoff et al., 2000), suggesting the important roles of testosterone in blood pressure control and its contribution to the gender-related differences in prevalence of hypertension. To date, limited studies with regard to the mechanisms in which testosterone could cause the increase in blood pressure were reported. One of the evidence showed that testosterone exerts its effects via renin-angiotensin-aldosterone system (RAS) whereby a linear correlation between testosterone level and plasma renin activity and angiotensinogen mRNA level have been reported (Chen et al., 1992; Ellison et al., 1989).

Sex hormones have been reported to exert influences on the cardiovascular system (Pol et al., 2006; Yang et al., 2000). *In vivo* studies showed that estrogen and testosterone modulate cerebrovascular tone via prostanoid mechanisms (Gonzales et al., 2005; Momoi et al., 2003). Additionally, studies have revealed the impact of sex hormones on renal function. The regulation of body water and sodium in the kidney were reported to be affected by the changes in sex hormone levels (Stachenfeld, 2008). One of the well-known renal membrane-bound proteins *i.e.* epithelial sodium channel (ENaC) which plays an essential role in the control of sodium balance have been shown to be regulated by sex hormones (Gambling et al., 2004). Studies reported that expression of  $\alpha$ - ENaC subunit could be enhanced by testosterone (Kienitz et al., 2006a; Quinkler et al., 2005). However, the *in vivo* effects of testosterone on ENaC expression in the kidney remained unclear.

Apart from the sodium balance, the kidney roles in maintaining body water balance could also affect the blood pressure as blood volume is tightly regulated by these mechanisms. Aquaporins (AQPs), a ubiquitous membrane protein, have been long-

known for its role in facilitating the water transport across the cell membranes. To date, numerous studies documented the association between the increased AQPs levels in kidney and the pathogenesis of hypertension (Graffe et al., 2012; Lee et al., 2006; Schuoler et al., 2015). Previously, increases in blood pressure and sodium retention have been shown to be associated with greater sensitivity to osmotic stimulation in men (Stachenfeld et al., 2001). These testosterone roles in osmoregulation were further supported by the studies in gilt-head sea bream (Sangiao-Alvarellos et al., 2006). Studies have also reported that the higher expression level of AQP-1 in the kidneys of male rats was down-regulated by gonadectomies and restored by testosterone replacements (Herak-Kramberger et al., 2015). Nevertheless, the effects of testosterone on AQP subunits expression in kidney remain to be further elucidated.

In addition, the effects of testosterone on blood pressure could also involve the central mechanisms. Earlier human and animal data have indicated the significant differences between males and females with regards to the basic function of the autonomic nervous system (ANS) (Abhishekh et al., 2013; Ng et al., 1993). Data showed that males tend to have a higher sympathetic drive while females tend to have higher parasympathetic and cardiac autonomic activities. These gender differences were proposed to be due to the developmental differences or the effects of male and female sex hormones on autonomic regulations (Barnett et al., 1999; Dart et al., 2002; Sevre et al., 2001). Previous studies also reported higher circulating antidiuretic vasopressin (AVP) levels and cardiovascular and antidiuretic actions of AVP in males than females (Ishunina & Swaab, 1999; Stachenfeld et al., 2001; Wang et al., 1993). The possible effects of sex hormones in contributing to these differences were proposed and supported by large distributions of androgen and estrogen receptors in the hypothalamic nuclei of the brain known to produce AVP (Sar & Stumpf, 1980; Simerly et al., 1990;

Somponpun & Sladek, 2002; Xue et al., 2013). Estrogen and androgens have been proposed to regulate arterial blood pressure and control the release of AVP (Auger et al., 2011; Grassi et al., 2013; Heritage et al., 1981; Stachenfeld, 2008; Wenner & Stachenfeld, 2012). However, despite these limited information, the molecular mechanisms underlying the central regulation of blood pressure by testosterone have yet to be documented.

In the present study, effects of testosterone on blood pressure and the potential mechanisms underlying its effects were investigated in both the normotensive and hypertensive rats. The first part of the thesis investigated the correlation between plasma testosterone level and the mean arterial pressure (MAP) using sub-chronic (seven days) and chronic (six weeks) treatment models. The findings indicated the MAP increased by testosterone. In this study, it was hypothesized that these effects of testosterone could involve the regulation of sodium and water balance in the kidney whereby changes in the expression levels of proteins that are involved in sodium and water handling in kidneys, *i.e.* ENaC and AQP, following sub-chronic and chronic testosterone treatment could explain changes in the blood pressure. In addition, these effects of testosterone were also being proposed to involve the central regulatory mechanisms, in which changes in gene expression profiles in the paraventricular nucleus (PVN), nucleus of solitary tract (NTS) and rostral ventrolateral medulla (RVLM) of the brain following chronic testosterone treatment were identified by using high-throughput RNA sequencing (RNA-Seq) technique.

## **1.2 Significance of study**

The present study is important as to elucidate the sexual dimorphism in the regulation of blood pressure in view that men, having high testosterone level, were found to have a higher prevalence of hypertension as compared to aged-matched premenopausal women. The outcomes of this study can provide a better understanding of the reasons underlying higher blood pressure in men than aged-matched women before menopause and higher blood pressure in women after menopause, which could be due to the more effect of testosterone. This study not only revealed the impact of sex hormones in blood pressure regulation but highlighted the importance of gender differences to consider during the development of antihypertensive treatments.

### 1.3 Research questions and hypotheses

- i. Males showed significantly higher blood pressure than aged-matched females. Orchidectomy in males reduced while testosterone treatment increased the blood pressure in females – What are the changes in blood pressure following sub-chronic (seven days) and chronic (six weeks) testosterone treatments in normotensive and hypertensive conditions?

**Hypothesis:** The blood pressure was higher in males than females, decreased by orchidectomies and increased by both sub-chronic and chronic testosterone treatments, regardless of the normotensive or hypertensive conditions.

- ii. Impaired sodium excretion and excessive sodium reabsorption exhibit a close relationship with the pathogenesis of hypertension and testosterone was shown to influence the concentration of sodium plasma. Previous study reported up-regulation of  $\alpha$ -*Enac* mRNA level in human proximal tubule cell line by testosterone – What were the *in vivo* effects of testosterone on  $\alpha$ ,  $\beta$  and  $\gamma$ -ENaC expression levels in the kidneys?

**Hypothesis:** Testosterone causes changes in plasma sodium level and expression levels of  $\alpha$ ,  $\beta$  and  $\gamma$ -ENaC in the kidneys.

- iii. Long-term blood pressure regulation involves changes in the blood volume and body water balance plays an important role in the maintenance of blood pressure. Higher expressions of AQP-1 in the kidney of males than females were reduced by gonadectomy but were increased by testosterone replacement – What were the changes in expression levels of other AQP subunits in the kidneys following testosterone treatments?

**Hypothesis:** In addition to AQP-1, testosterone could induce changes in expression levels of other AQP subunits in the kidneys.

- iv. Central nervous system (CNS) is the most important physiological mechanisms that are involved in the regulation of blood pressure. Testosterone has been suggested to regulate blood pressure via central mechanisms – What are the potential genes in the cardiovascular center that could be involved in the regulation of blood pressure by testosterone?

**Hypothesis:** Comparisons of transcriptomes of the specific cardiovascular center *i.e.* paraventricular nucleus (PVN), nucleus of the solitary tract (NTS) and rostral ventrolateral medulla (RVLM) allow the identification of potential genes that might play a role in testosterone-induced changes in the blood pressure.

## 1.4 Objectives

This study was performed in order to answer the research questions and to justify the hypotheses made. The main objective of the present study is to investigate the effects of testosterone on blood pressure and the mechanisms underlying these effects. Upon the completion of the study, it was anticipated that the following objectives will be achieved.

The specific objectives of the study were:

To investigate effects of testosterone in male and female normotensive and hypertensive rat models with regards to the following parameters:

- i. blood pressure.
- ii. hormonal and biochemical blood parameters *i.e.* plasma levels of aldosterone, electrolytes, osmolality, glucose, urea and creatinine.
- iii. expression levels of proteins that are involved in sodium handling in kidneys *i.e.* epithelial sodium channel (ENaC).
- iv. expression levels of proteins that are involved water handling in kidneys *i.e.* aquaporins (AQPs).
- v. gene expression profiles of the specific areas of the cardiovascular center in the brain *i.e.* paraventricular nucleus (PVN), nucleus of the solitary tract (NTS) and rostral ventrolateral medulla (RVLM)

## CHAPTER 2: LITERATURE REVIEW

### 2.1 Testosterone

Testosterone is an anabolic sex hormone classed under androgens, primarily biosynthesized and secreted from testicular Leydig cells (Ruiz-Cortés, 2012). In general, testosterone is dubbed the male sex steroid hormone as males produce more and require more testosterone than females. It is well-known that testosterone and its biologically active form, 5 $\alpha$ -dihydrotestosterone (DHT) are required in men for spermatocytogenesis and development of male sexual characteristics (Hu et al., 2010). In addition to these roles, to date, several pieces of evidences have shown the involvement of testosterone in different systems which includes cardiovascular physiology (Tambo et al., 2016), bone integrity (Johnson & Rendano, 1984) and neuronal growth (Estrada et al., 2006).

Testosterone, composed of 19 carbon atoms with no side chain, is synthesized from cholesterol. A series of enzymes are involved in these pathways in which the side chain at C-17 of cholesterol precursor is converted into a hydroxyl group, the double bond at C-6 is transferred to C-4 and the hydroxyl group at C-3 is oxidized into a carbonyl group (Freeman et al., 2001). Biosynthesis of testosterone in Leydig cells is mainly controlled by gonadotropin luteinizing hormone (LH), released from the anterior pituitary gland. The binding of LH to its G-protein coupled receptors initiates a cascade of events which includes activation of adenylate cyclase (AC), increased in conversion of adenosine triphosphate (ATP) to cyclic adenosine monophosphate (cAMP) and activation of cAMP-dependent protein kinase (PKA) (Cooke et al., 1992; Luo et al., 1998; Manna et al., 2007; Papadopoulos, 2010). Following the stimulation of PKA by cAMP, the mobilization of cholesteryl esters stored in lipid droplets by cholesteryl ester hydrolase, transport of cholesterol to the inner mitochondrial membrane and expression

levels of genes that are involved in the regulation of testosterone production were enhanced (Hu et al., 2010). Pregnenolone that produced from cholesterol in mitochondrial by CYP11A (cholesterol side-chain cleavage) is transferred to smooth endoplasmic reticulum for further modification (Parker & Schimmer, 1995; Payne & Hales, 2004). These modification processes involved numerous enzymatic reactions where testosterone is produced and transferred into the blood stream (Hu et al., 2010; Michels & Hoppe, 2008).

### **2.1.1 Metabolisms of testosterone**

Like other steroid hormones, testosterone derived from cholesterol and the structure of this hormone is similar across all mammals, reptiles, birds and fish (Ye et al., 2011). The production of testosterone from the testes is regulated by hypothalamus and pituitary gland through chemicals and hormones circulating in the bloodstream. This communication is known as the hypothalamic-hypophyseal portal system (Amory & Bremner, 2001). In the body, testosterone can be metabolized into two biological active hormones. First, the  $5\alpha$ -reductase, an enzyme highly expressed in the male prostate, genital skin and testes, is responsible for converting testosterone into a more potent androgen, DHT (Duskova & Pospisilova, 2011; Sherbet & Auchus, 2007). Second, the aromatization of testosterone into a potent estrogen, estradiol is facilitated by aromatase enzyme present in the gonads, brain, placenta and adipose tissues (Drago et al., 1982; Sherbet & Auchus, 2007). In addition, testosterone can also be reduced by  $17\beta$ -hydroxysteroid dehydrogenase into an inactive metabolite, androstenedione (Ofner, 1955; Sherbet & Auchus, 2007).

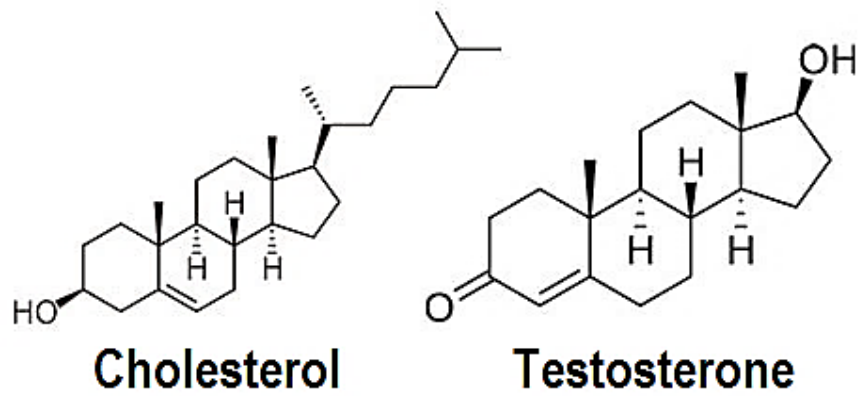


Figure 2.1 Structure of cholesterol and testosterone.

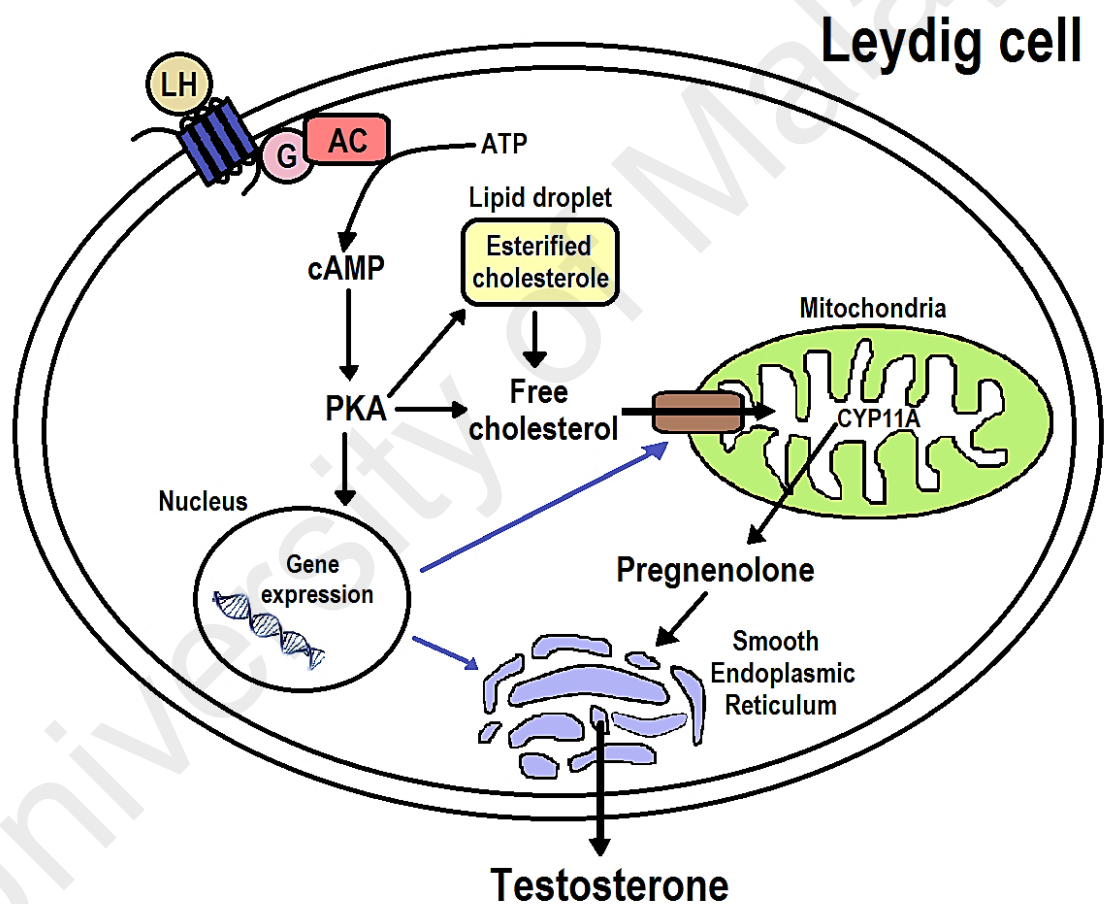
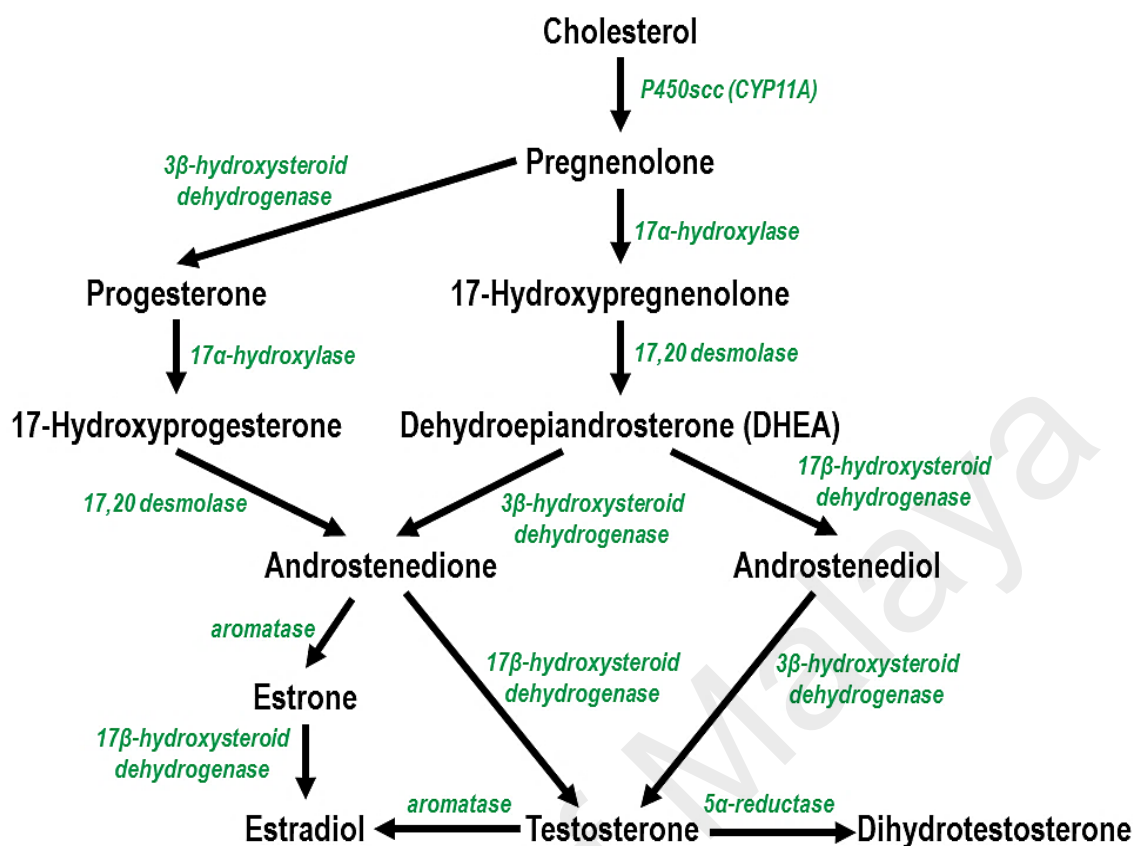


Figure 2.2 Gonadal pathways for testosterone formation in Leydig cell.

The image was produced by drawing with modification from Papadopoulos (Papadopoulos, 2010).



**Figure 2.3 Biosynthetic pathways of testosterone from cholesterol precursor.** Enzymes that are responsible for the corresponding catalysis are shown in green. Cholesterol is first metabolized into pregnenolone in mitochondria. Subsequent catalytic activities occur in the smooth endoplasmic reticulum to form testosterone.

### 2.1.2 Testosterone, health and diseases

Apart from the reproductive and sexual functions, testosterone has also been reported to exert significant effects on the insulin sensitivity (Lee et al., 2005; Pitteloud et al., 2005), glucose homeostasis and lipid metabolism (Rao et al., 2013; Saad, 2009). These clustering effects could eventually lead to the pathogenesis of type 2 diabetes mellitus (T2DM), metabolic syndrome (MetS) and cardiovascular disease (CVD) (Nettleship et al., 2009; Saad, 2009; Shores et al., 2014). In general, testosterone level peaks during adolescence and early adulthood in men and gradually decreases with age. It has been well-known that low level of testosterone may result in decreased muscle mass, increased body fat, vasomotor instability and decreased bone mineral density (McLeod-Sordjan, 2015). Nonetheless, numerous studies in animals, cells and clinical trials have documented the metabolic and vascular action of testosterone in which the decrease in

serum testosterone level have been suggested to be associated with the risk of CVD incident in aged men (Kelly & Jones, 2013a, 2013b). In addition, clinical studies on androgen deprivation therapy (ADT) in prostate carcinoma patients have also reported increased risk of T2DM and CVD following blockage of production or effects of testosterone (Tivesten et al., 2015). However, testosterone replacement therapy has resulted in a discrepant finding in regard to the role of testosterone in cardiovascular events where increased risk of cardiovascular problems was reported (Finkle et al., 2014; Seftel, 2015). To date, there is growing evidence that testosterone has influences on the development of T2DM, MetS and CVD, however the effects and mechanisms underlying the effects remained unclear and convoluted. Nevertheless, several studies have suggested the role of testosterone in acting at the molecular level to control the expression of important regulatory proteins involved in insulin action, glycolysis, lipid metabolisms and cardiovascular system which in turn contribute to the pathogenesis of these diseases (Eyster et al., 2007; Kelly & Jones, 2013a; Phillip et al., 1992; Vodo et al., 2013).

## **2.2 Regulation of blood pressure**

The pressure or force exerted by circulating blood against the inner walls of the blood vessel is generally known as blood pressure. The maintenance of blood pressure at a normal level is critical in maintaining optimal oxygen delivery to tissues and homeostasis balance. In general, there are two basic mechanisms in the regulation of blood pressure. Short-term mechanisms involved the regulation of blood vessel diameter, heart rate and heart contractility while long-term mechanisms involved the regulation of blood volume (Charkoudian & Rabbitts, 2009; Jones et al., 2004). Autonomic nervous system (ANS) which includes sympathetic nervous system (SNS) and parasympathetic nervous system (PSNS), and renin-angiotensin-aldosterone system

(RAS) are known to play important roles in blood pressure regulation in which they respond immediately towards the changes in blood pressure via baroreflex mechanisms (Guyton et al., 1972). These mechanisms are of great importance for time-to-time stabilization of blood pressure however in some conditions, the blood pressure is not completely restored. The initiation of long-term mechanisms which also involved SNS and RAS stimulates the release of renin in the juxtaglomerular apparatus of the kidney via direct renal sympathetic nerve activity (SNA) (Lohmeier, 2001). This activation leads to changes in kidney tubular reabsorption of sodium and water, thereby providing a long-term control of body fluid volumes and arterial pressure (Cowley & Roman, 1989).

### **2.2.1 Sexual dimorphism in blood pressure**

To date, sex differences in the regulation of blood pressure are still not well understood and are likely to be multifaceted. Many studies have proved the prevalence of hypertension in premenopausal women to be lower than men of the same age, however the incidence of hypertension in women increases steeply after menopause, which revealed the importance of sex differences in pathophysiology of hypertension and the possibility of female sex hormones to exhibit some protections against the development of hypertension (Hinojosa-Laborde et al., 2000; Maas & Appelman, 2010; Regitz-Zagrosek & Seeland, 2012). Similar to humans, gender differences in blood pressure also exist in animals. Three mechanisms proposed to contribute to the development of hypertension, affected by sex hormones are the SNS, RAS and endothelial system (Davidson & Duchon, 2007; Hinojosa-Laborde et al., 2000). Besides sex hormones, sex chromosome is also known to play an important role in sex differences, yet there are limitations in studies of the sex chromosome effects on gender differences, as it is difficult to manipulate sex chromosome effect independently of the effects of the

gonadal hormones (Ji et al., 2010). Previous studies have demonstrated the reduction of blood pressure in male spontaneously hypertensive rats (SHR) by castration almost to the level observed in aged-matched females (Chen & Meng, 1991; Martin et al., 2005; Reckelhoff et al., 1998). On the other hand, ovariectomy was shown to augment the risk of hypertension in the female SHR rat (Ito et al., 2006). Nevertheless, these findings were inconsistent as several studies had also reported no changes in the blood pressure (Reckelhoff & Granger, 1999; Tatchum-Talom et al., 2011). Meanwhile, administration of exogenous testosterone into ovariectomized female rats was shown to result in exacerbation of hypertension almost to the level found in intact males (Liu & Ely, 2011; Reckelhoff & Granger, 1999; Reckelhoff et al., 1998; Reckelhoff et al., 2000). Table 2.1 shows the reported sexual dimorphism in blood pressure.

**Table 2.1 Sexual dimorphism in blood pressure.**

No.	Model	Population/ Strain	Findings	Reference
1	Human	Students from University of Minnesota	<ul style="list-style-type: none"> <li>Higher SBP and DBP in young men than young women.</li> </ul>	(Boynton & Todd, 1947)
2	Human	United States population	<ul style="list-style-type: none"> <li>Higher prevalence of elevated blood pressure in men than women.</li> </ul>	(Stamler et al., 1976)
3	Rat	Deoxycorticosterone-salt hypertension rat	<ul style="list-style-type: none"> <li>Higher SBP in males than females.</li> </ul>	(Ouchi et al., 1987)
4	Rat	New Zealand genetically hypertensive rat	<ul style="list-style-type: none"> <li>Males showed higher blood pressure than females.</li> </ul>	(Ashton & Balment, 1991)
5	Rat	Dahl salt-sensitive rats	<ul style="list-style-type: none"> <li>Higher SBP in males than females.</li> </ul>	(Crofton et al., 1993)
6	Human	Pittsburgh high school cohort	<ul style="list-style-type: none"> <li>Higher increment in mean DBP in men than women.</li> </ul>	(Yong et al., 1993)
7	Human	Danish population	<ul style="list-style-type: none"> <li>Men showed higher 24-hour mean blood pressure than women.</li> </ul>	(Wiinberg et al., 1995)
8	Rat	Spontaneously hypertensive rat	<ul style="list-style-type: none"> <li>Higher MAP in males than females.</li> <li>Orchiectomy reduced the MAP in males.</li> <li>Testosterone treatment increased the MAP in ovariectomized females.</li> </ul>	(Reckelhoff et al., 2000)
9	Human	Pre- and postpubertal cohort	<ul style="list-style-type: none"> <li>Greater increment in SBP in men than women during pubertal growth.</li> </ul>	(Shankar et al., 2005)
10	Human	Young-adult Nigerians (age between 18-35)	<ul style="list-style-type: none"> <li>Higher SBP response during and after exercise in men than women.</li> </ul>	(Dimkpa et al., 2008)
11	Human	United States population (age between 18-39)	<ul style="list-style-type: none"> <li>Men had higher prevalence of hypertension than women regardless of race and ethnicity.</li> </ul>	(Cutler et al., 2008)
12	Human	Pomerania women	<ul style="list-style-type: none"> <li>Positive association between total testosterone, blood pressure and prevalent of hypertension in women.</li> </ul>	(Ziemens et al., 2013)
13	Mice	FVB/N and C56BL/6 mice	<ul style="list-style-type: none"> <li>Greater MAP in males than females.</li> </ul>	(Barsha et al., 2016)

Abbreviations: DBP: diastolic blood pressure; MAP: mean arterial pressure; SBP: systolic blood pressure.

### 2.2.2 Testosterone-induced high blood pressure

Studies on animals have strongly suggested the pro-hypertensive roles of testosterone. Lower level of testosterone have been suggested to protect against cardiovascular disease and studies using animal models have further supported the role of testosterone as a pro-hypertensive hormone (Dubey et al., 2002). Studies on humans and animals have generated a significant amount of evidence showing higher blood pressure in males than females. This phenomenon is also observed in different strains of rats which include SHR, Dahl salt-sensitive, deoxycorticosterone acetate (DOCA)-salt hypertensive and New Zealand hypertensive rats (Dubey et al., 2002; Reckelhoff, 2001). A number of mechanisms by which testosterone induces high blood pressure and accelerate the progression of hypertension have been documented. The balance of vasomotor tone: vasodilators (NO and prostacyclin) and vasoconstrictors, is very important to maintain the body blood pressure homeostasis. Both estrogen and testosterone can modulate the cerebrovascular tone via prostanoid mechanisms where estrogen appears to shift the prostanoid balance toward vasodilation while testosterone enhances vasoconstriction (Gonzales et al., 2005). For instance, testosterone was shown to increase the number of human endothelial cells that secrete endothelin-1, a potent vasoconstrictor, which was also accompanied by the up-regulation of endothelin-1 secretory activity (Pearson et al., 2008). Intramuscular testosterone treatment was also reported to increase the coronary arterial reactivity to thromboxane A<sub>2</sub> and enhance its constriction (Schorr et al., 1994). Earlier, Kumai *et al.* (1995) had also demonstrated the raised tyrosine hydroxylase activity in adrenal medulla and in the aorta and mesenteric arteries by administering testosterone into castrated male SHR, which then lead to the increased catecholamine synthesis and high blood pressure (Kumai et al., 1995). This finding was further verified by Liu & Ely (2011) where they observed increased kidney vasoconstrictor norepinephrine level in testosterone-treated female SHR, which

believed to be responsible for the enhanced sodium reabsorption of the kidney (Liu & Ely, 2011). In addition, testosterone was also found to exert adverse effects towards kidney function where it decreases the glomerular filtration rate, induces glomerulosclerosis and proteinuria (Liu & Ely, 2011; Muraoka, 2001). Together, these effects could result in elevated blood pressure and eventually lead to hypertension. Table 2.2 summarizes the mechanisms that involved in testosterone-induced changes in blood pressure.

University of Malaya

**Table 2.2 Summary of mechanisms that involved in testosterone-induced changes in blood pressure.**

No.	Model	Mechanisms	Findings	Reference
1	Rat (WKY)	RAAS	<ul style="list-style-type: none"> <li>▪ Orchidectomy lowered renal angiotensinogen mRNA levels in the males.</li> <li>▪ Testosterone treatment increased renal angiotensinogen mRNA in orchidectomized males and normal females.</li> </ul>	(Ellison et al., 1989)
2	Rat (SHR)	RAS	<ul style="list-style-type: none"> <li>▪ Orchidectomy reduced plasma renin and renal and hepatic angiotensinogen mRNA.</li> <li>▪ Testosterone replacement restored plasma renin and renal and hepatic angiotensinogen mRNA.</li> </ul>	(Chen et al., 1992)
3	Rat (WKY and SHR)	SNS	<ul style="list-style-type: none"> <li>▪ Orchidectomy reduced while testosterone replacement restored epinephrine and norepinephrine levels in adrenal medulla of males.</li> <li>▪ Orchidectomy-induced decreased activity and mRNA expression level of tyrosine hydroxylase restored by testosterone replacement in males.</li> </ul>	(Kumai et al., 1995)
4	Rat (SHR)	Pressure-natriuresis	<ul style="list-style-type: none"> <li>▪ Lower level of sodium excreted by males than females and castrated males.</li> <li>▪ Testosterone treatment blunted pressure-natriuresis in ovariectomized females.</li> </ul>	(Reckelhoff et al., 1998)
5	Human (Transsexual)	Vascular function	<ul style="list-style-type: none"> <li>▪ Increased plasma endothelin level in transsexuals taking masculinizing level of testosterone.</li> </ul>	(Van Kesteren et al., 1998)
6	Human (Transsexual)	Cardiac function	<ul style="list-style-type: none"> <li>▪ Androgen administration to females (transsexuals) increased plasma total homocysteine level.</li> </ul>	(Giltay et al., 1998)
7	Rat	Vascular function	<ul style="list-style-type: none"> <li>▪ Testosterone inhibited vasodilation effect of adenosine in isolated heart in a concentration-dependent manner.</li> </ul>	(Ceballos et al., 1999)

**Table 2.2 continued.**

No.	Model	Mechanisms	Findings	Reference
8	Rat (SD)	Cardiac function	<ul style="list-style-type: none"> <li>Testosterone treatment increased expression levels of AR, <math>\beta</math>1-adrenergic receptor and calcium regulatory proteins (<i>i.e.</i> L-type calcium channel and Na/Ca exchanger) in ventricular myocytes.</li> </ul>	(Golden et al., 2004)
9	Rat (SD)	RAS Renal function	<ul style="list-style-type: none"> <li>Reduced serum angiotensin II level in DHT-treated males.</li> <li>DHT treatment in males increased the expression levels of renal angiotensinogen and Na/H exchanger and the volume reabsorptive rate in proximal tubule of the kidney.</li> </ul>	(Quan et al., 2004)
10	Cell culture and rat (HKC-8 and Wistar)	Renal Function	<ul style="list-style-type: none"> <li>Testosterone treatment increased <math>\alpha</math>-ENaC mRNA expression via AR in HKC-8 cells.</li> <li>Testosterone treatment up-regulated <math>\alpha</math>-ENaC mRNA expression levels in the kidneys of orchidectomized males.</li> </ul>	(Quinkler et al., 2005)
11	Rat (SHR/y and WKY)	Renal Function	<ul style="list-style-type: none"> <li>Urinary sodium and potassium concentration and plasma aldosterone level increased by orchidectomy and restored by testosterone replacement in males.</li> <li>Relative kidney weight reduced by orchidectomy and increased by testosterone replacement in males.</li> </ul>	(Toot et al., 2008)
12	Rat (SHR)	Renal Function SNS	<ul style="list-style-type: none"> <li>Testosterone treatment reduced sodium excretion and elevated glomerulosclerosis in normal and ovariectomized females.</li> <li>Plasma level of norepinephrine increased upon testosterone treatment in normal and ovariectomized females.</li> </ul>	(Liu & Ely, 2011)
13	Cell culture (human vascular endothelial cells and smooth muscle cells)	Vascular function	<ul style="list-style-type: none"> <li>Testosterone induced DNA synthesis and growth in human vascular endothelial cells.</li> <li>Testosterone and DHT enhanced proliferation of smooth muscle cells.</li> </ul>	(Nheu et al., 2011)

**Table 2.2 continued.**

No.	Model	Mechanisms	Finding	Reference
14	Rat (Wistar)	RAS	<ul style="list-style-type: none"> <li>▪ Castration reduced while testosterone treatment restored plasma renin activity and level of angiotensin II.</li> <li>▪ In castrated rats, higher sodium excretion and creatinine clearance were abolished by the administration of testosterone.</li> </ul>	(Hu et al., 2011)
15	Rat (Wistar)	Cardiac function Vascular function	<ul style="list-style-type: none"> <li>▪ Testosterone enhanced aortic strips NO production in females.</li> <li>▪ Testosterone treatment in females induced endothelial NO production, DNA synthesis and inhibited platelet aggregation in endothelial cell cultures obtained from the aortic ring.</li> </ul>	(Campelo et al., 2012)
16	Rat (WKY and SHR)	Vascular function	<ul style="list-style-type: none"> <li>▪ Testosterone induced ROS generation by increasing expression of NADPH oxidase in WKY vascular smooth muscle cells.</li> <li>▪ Testosterone increased ROS production via activation of c-Src-dependent pathway in SHR vascular smooth muscle cells.</li> </ul>	(Chignalia et al., 2012)
17	Rat (Wistar)	RAS Cardiac function	<ul style="list-style-type: none"> <li>▪ Orchidectomy increased while testosterone replacement reduced AT<sub>2</sub>R expression in the hearts of males.</li> <li>▪ Increased cardiac fibrosis and cardiac cell apoptosis in orchidectomized male rats with heart failure reversed by testosterone replacement.</li> </ul>	(Kang et al., 2012)
18	Rat (SD)	Vascular function	<ul style="list-style-type: none"> <li>▪ Prenatal exposure of testosterone reduced endothelial-dependent acetylcholine relaxation and expression of Kcnn3 channel, thus indicated the blunting of endothelial cell-associated relaxation by testosterone.</li> </ul>	(Chinnathambi et al., 2013)

**Table 2.2 continued.**

No.	Model	Mechanisms	Findings	Reference
19	Rat (SD)	Renal function	<ul style="list-style-type: none"> <li>Testosterone was suggested to accelerate the progression of kidney injury as administration of testosterone increased the urinary excretion of protein and NGAL, an index of tubulointerstitial injury, in rats with reduced renal mass.</li> </ul>	(Illiescu et al., 2014)
20	Cell culture (Vascular smooth muscle cells isolated from Wistar rats)	Vascular function	<ul style="list-style-type: none"> <li>Testosterone induced ROS generation in a concentration- and time-dependent manner.</li> <li>Testosterone was suggested to exert pro-apoptotic effects such as induced cleavage of procaspase-3 and procaspase-8 and increased expressions of FasL and TNF-<math>\alpha</math>.</li> </ul>	(Lopes et al., 2014)
21	Human (PCOS patients)	SNS Vascular function	<ul style="list-style-type: none"> <li>Elevated multiunit muscle SNS activity and impaired endothelial function were found in women with PCOS, a hyperandrogenic disorder.</li> </ul>	(Lambert et al., 2015)
22	Rat (HAF)	SNS	<ul style="list-style-type: none"> <li>Adrenergic blockade or renal denervation reduced the higher MAP in HAF rats but not controls.</li> <li>Hypothalamic MC4R expression was higher in HAF rats, and CNS MC4R antagonist reduced MAP in HAF rats.</li> </ul>	(Maranon et al., 2015)
23	Rat (SD)	Cardiac function	<ul style="list-style-type: none"> <li>Lower expression of AT<sub>2</sub>R in the aortas of males than females.</li> <li>Castration elevated while testosterone replacement restored the expression level of AT<sub>2</sub>R in the aortas of males.</li> </ul>	(Mishra et al., 2016)

Abbreviations: AR: androgen receptor; AT<sub>2</sub>R: angiotensin II type-2 receptor; CNS: central nervous system; DHT: 5 $\alpha$ -dihydrotestosterone; DNA: deoxyribonucleic acid; ENaC: epithelial sodium channel; HAF: hyperandrogenemia female rat; HKC-8: human renal proximal tubular cell line; MC4R: melanocortin-4 receptor; mRNA: messenger ribonucleic acid; NADPH: nicotinamide adenine dinucleotide phosphate; NGAL: neutrophil gelatinase-associated lipocalin; NO: nitric oxide; PCOS: polycystic ovary syndrome; RAS: renin-angiotensin-aldosterone system; ROS: reactive oxygen species; SD: Sprague Dawley rat; SNS: sympathetic nervous system; SHR: Spontaneously hypertensive rat; WKY: Wistar Kyoto rat.

### **2.3 The roles of kidney in blood pressure regulation**

It has been known for decades that kidney plays an important role in the regulation of blood pressure. Kidney influences blood pressure primarily by inducing constriction of blood vessels and regulating the volume of circulating blood (Crowley et al., 2006; Navar, 1997). As discussed earlier, kidney is known to be involved in the long-term blood pressure regulation where water and sodium reabsorption in kidney tubules are regulated via SNS and RAS. Renal perfusion pressure is monitored by juxtaglomerular cells, specialized smooth muscle cells located mainly in the afferent arteriole while concentration of sodium is monitored by macula densa, specialized cells in the distal tubule of the kidney (Barrett et al., 2010). A drop in blood pressure and sodium level stimulates the release of renin by juxtaglomerular cells, which then cleaves angiotensinogen, produced from liver, into angiotensin I. Angiotensin converting enzyme (ACE), found mainly in lungs, converted angiotensin I into angiotensin II, a potent vasoconstrictor, thereby increases the blood pressure and cardiac output (Barrett et al., 2010; Suzuki & Saruta, 2004). As proximal convoluted tubules (PT), distal convoluted tubules (DT) and thick ascending limb of Henle's loop are highly innervated, renin secretions are also induced by the direct action of norepinephrine on adrenergic receptors on juxtaglomerular cells following stimulation of these renal sympathetic nerves (Barrett et al., 2010; Weinberger et al., 1975). Due to the vital roles of the kidney in blood pressure regulation, it is known that abnormal activation of kidney function by RAS and SNS could increase the risk of cardiovascular disease and eventually contribute to the development of hypertension (Coffman & Crowley, 2008; Manrique et al., 2009; Phillips, 2005). Figure 2.4 summarizes renal regulation of blood pressure.

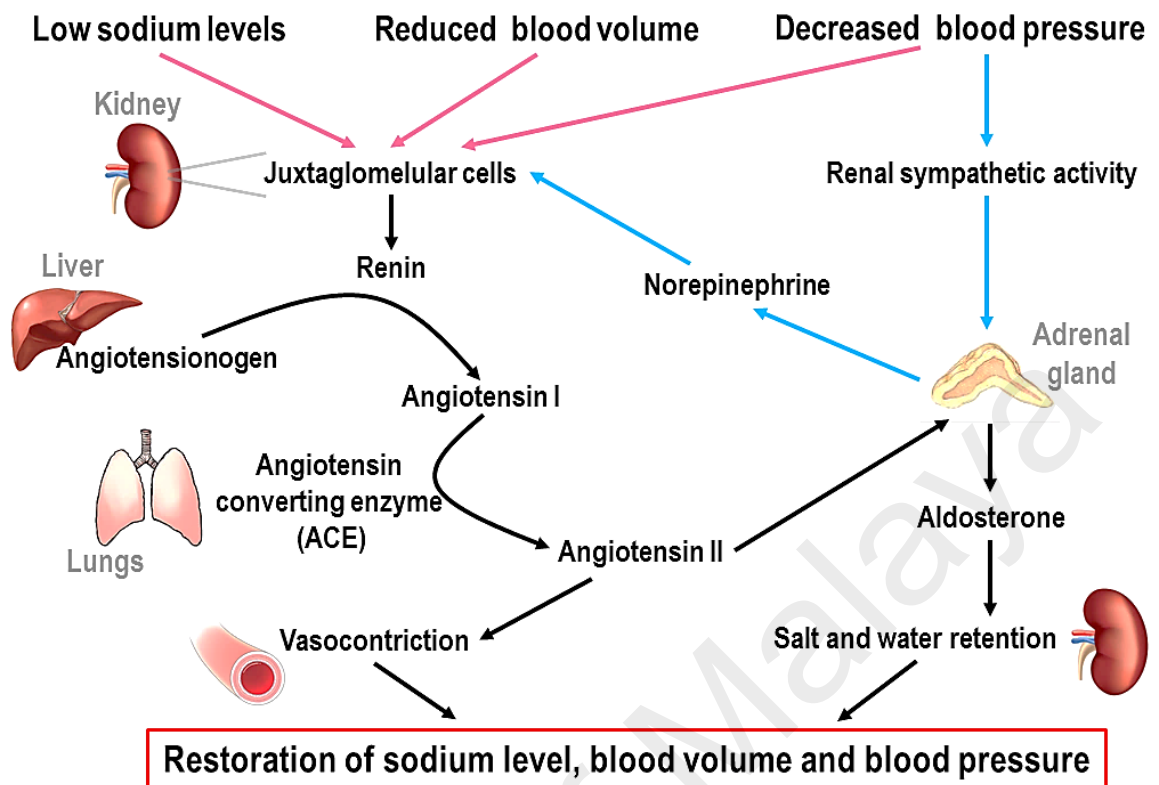


**Figure 2.4 Summary of renal regulation of blood pressure.**

Pink arrows: Low sodium levels, reduced blood volume and decreased blood pressure were detected and juxtaglomerular cells were signaled. Blue arrows: Activation of renal SNA by the decreased in blood pressure, stimulate juxtaglomerular cells. Black arrows: Stimulation of RAS pathway to restore sodium levels, blood volume and blood pressure.

### 2.3.1 Renal sodium handling

As the concentration of solute (sodium) is highly integrated with the regulation of blood volume, renal sodium handling is known to be associated with blood pressure regulation. Previously, abnormalities in these mechanisms have been demonstrated in the development of hypertension (Matsubara, 2004; Song et al., 2006). Following the RAS activation, the adrenal gland is also stimulated by angiotensin II to secrete aldosterone, a peptide that stimulates sodium and water reabsorption in renal tubules. Enhanced sodium and water reabsorption increased the blood volume, generating more pressure in the blood vessels, thereby increasing the blood pressure (Harrison-Bernard, 2009). Meanwhile, norepinephrine, released upon activation of renal sympathetic nerves by increased blood volume, caused an increase in tubular reabsorption of sodium via

adrenergic stimulation (Gill, 1979). Pressure-natriuresis control also known to play a critical role in renal-regulated blood pressure as activation of renal-pressure-natriuresis mechanisms by increased blood pressure induced the increase in sodium excretion, thus leading to long-term changes in blood pressure (Suzuki & Saruta, 2004). Under normal condition, these mechanisms work to maintain the blood pressure and body fluid volume at normal levels. Malfunctioned pressure-natriuresis mechanisms have been identified in most cases of chronic hypertension in which sodium excretion remained regardless the increased blood pressure (Hall et al., 1990; Ivy & Bailey, 2014; Moreno et al., 2001). Figure 2.5 shows sodium reabsorption along the kidney nephron.

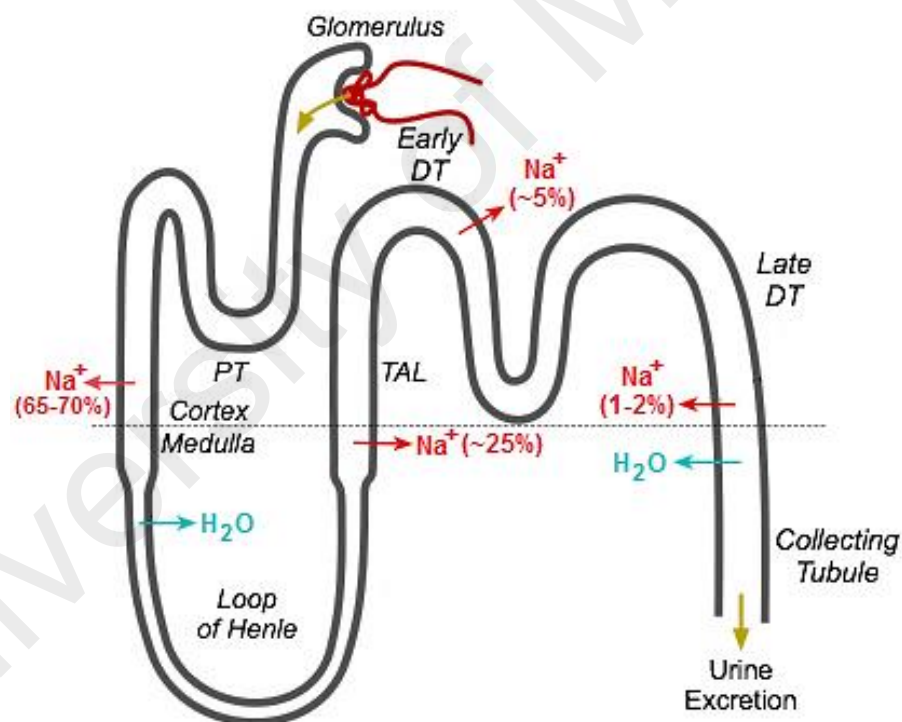


**Figure 2.5 The amount of sodium reabsorbed along the kidney nephron.**

Glomerular capillary hydrostatic pressure filters water and sodium into Bowman's space. A large amount of sodium (60-70%) in urine is reabsorbed in PT while approximately 25% and 5% are removed in TAL and DT. The amount of sodium reabsorption in collecting ducts is quantitatively low (1-2%) however this mechanism, which depends on the tubular concentration of sodium and stimulation of hormones *i.e.* aldosterone, may significantly alter the final concentration of sodium excreted in urine. The image was modified from Klabunde (Klabunde, 2011). Abbreviations: DT: distal convoluted tubule; PT: proximal convoluted tubule; TAL: thick ascending limb of Henle's loop.

### 2.3.1.1 The effects of testosterone on sodium handling

It has been long reported that from puberty onward, men exhibit higher blood pressure compare to women, which revealed the gender differences in prevalence of hypertension (Burt et al., 1995; Liu et al., 2003). Until today, numerous studies have proposed that this phenomenon is primarily due to the effects of sex hormones. A number of *in vivo* studies using different animal models have documented the detrimental influences of testosterone upon blood pressure (Jenkins et al., 1994; Khalid et al., 2002; Reckelhoff et al., 1998). Testosterone could accelerate the development of hypertension via a variety of pathways. Impaired sodium excretion and excessive sodium reabsorption have been known to exhibit a close relationship with the pathogenesis of hypertension and testosterone have been found to influence the mechanisms involved in sodium handling in kidney (Liu & Ely, 2011). Earlier, a study has reported pressure-natriuresis response to be shifted rightward in male rats at which male rats appear to excrete less sodium than females at similar arterial pressure (Reckelhoff & Granger, 1999). Using hypertensive SHR rat model, scientists have observed the increase in blood pressure with blunted pressure-natriuresis relationship in males and testosterone-supplemented ovariectomized females (Reckelhoff et al., 1998). Previously, Hu *et al.* (2011) have demonstrated the involvement of RAS in testosterone-induced sodium retention as they observed lower plasma renin activity and angiotensin concentration in castrated male rats than intact and testosterone-treated castrated male rats (Hu et al., 2011). Additionally, studies on animal models of hypertension have also suggested the enhanced renal norepinephrine content and release by testosterone (Jones et al., 1998; Liu & Ely, 2011). Testosterone replacement restored the castration-induced decreased metabolism and release of norepinephrine, thus indicating the antinatriuresis effects of testosterone (Lara et al., 1985).

### 2.3.1.2 Epithelial Sodium Channel (ENaC)

Epithelial sodium channel (ENaC), a renal membrane-bound protein, has been known to play an essential role in the control of sodium balance in the distal connecting tubules (Warnock & Rossier, 2005). This channel consisted of 3 homologous subunits ( $\alpha$ ,  $\beta$ ,  $\gamma$ ). The  $\alpha$ -subunit is required for active sodium conductance whereas the presence of  $\beta$ - and  $\gamma$ -subunits will enhance the activity of the channel (Schild, 2010). The RAS pathway is known to be involved in the controls of ENaC and the mineralocorticoid hormone, aldosterone is the most-established major regulator of ENaC where it stimulates the sodium transport in renal collecting duct (CD) by enhancing the expression and activity of ENaC (Garty, 2000; Loffing & Schild, 2005). Apart from that, some studies have documented the potential of insulin and vasopressin to also regulate the ENaC and alter the sodium reflux in the kidney (Kamynina & Staub, 2002; Rotin & Schild, 2008; Schild, 2010). Loss of functional mutation in ENaC has been reported to cause hypotension (pseudohypoaldosteronism type 1) whereas prolonged activation of renal ENaC, as observed in Liddle's syndrome, leads to severe hypertension (Bubien, 2010). In general, ENaC provides the rate limiting step for sodium and fluid reabsorption into the bloodstream, at which the increases in the abundance and activity of ENaC were reported to induce sodium retention and result in elevated blood pressure. In 2000-an, the expression of ENaC have been found to be differentially regulated by female sex hormones *i.e.* estrogen and progesterone (Gambling et al., 2004), thus suggesting that the differential in sodium handling which result in the gender differences in blood pressure may possibly due to the sexual dimorphism in the regulation of ENaC. Furthermore, Quinkler *et al.* (2005) have also demonstrated the up-regulation of mRNA expression of  $\alpha$ -ENaC in human proximal tubule cell line HKC-8 by testosterone (Quinkler et al., 2005). Figure 2.6 shows the structure of ENaC and cellular transport of sodium reabsorption.

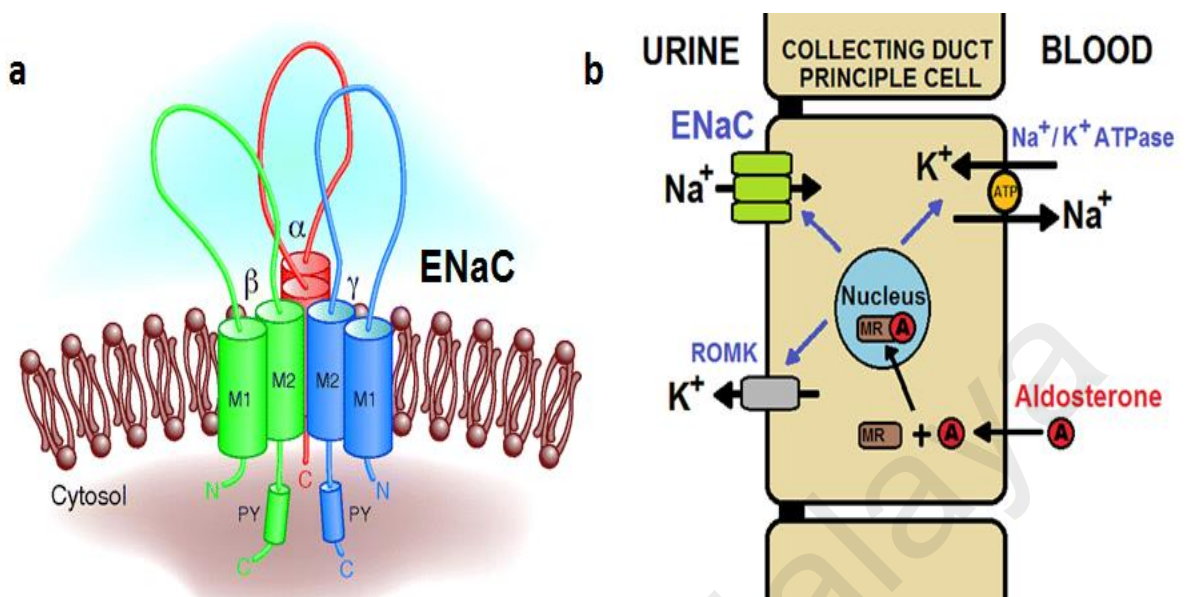


**Figure 2.6 Structure of ENaC and cellular transport of sodium reabsorption.**

(a) Structure of ENaC. Heterotrimeric ENaC consists of three different subunits ( $\alpha$ ,  $\beta$  and  $\gamma$ ). Each of the subunits consists of two membrane-spanning domains (M1 and M2), an extracellular loop, an intracellular amino- (N-) and carboxyl- (C-) termini. The roles of ENaC in blood pressure regulation have been shown in Liddle syndrome where the increased activity due to the deletions of PY (Proline-Proline-X-Tyrosine) motif at C-termini of  $\beta$  or  $\gamma$  subunits caused the development of hypertension (Schild et al., 1996). Image sourced from Bhalla and Hallows (Bhalla & Hallows, 2008). (b) Sodium flux through ENaC represents the rate-limiting step of sodium reabsorption in the kidney. Aldosterone is the most important hormone that modulates the activity of ENaC in the kidney. Binding of aldosterone to the mineralocorticoid receptor (MR) stimulates sodium reabsorption from tubular urine by activating ENaC and  $\text{Na}^+/\text{K}^+$ -ATPase in the kidney. Activation renal outer medullary potassium channel (ROMK) by aldosterone also induces active secretion of potassium into the urine. This concentration of potassium provides a feedback control on aldosterone synthesis where potassium depletion reduces aldosterone secretion. The image was produced by modification from Stockand *et al.* (Stockand et al., 2000).

### 2.3.2 Regulation of water balance

Besides sodium intake and excretion, water balance is also known to be monitored under long-term blood pressure regulation (Osborn, 1991). The fluid balance is tightly regulated in the body in order to maintain adequate volume to generate the normal blood pressure necessary to deliver sufficient blood and oxygen to all tissues. The maintenance of water balance is achieved by regulating the balance between water gained and water losses. As discussed earlier, kidney is involved in the regulation of blood pressure by regulating blood volume. Kidney is known as the fluid exchange

platform as it allowed the alteration in blood composition and volume via active solute exchange, water reabsorption and urine excretion activities (Cowley & Roman, 1989). Direct controls of kidney on the excretion of urine enable conservation of water and concentration of urine during water loss and vice versa. In addition to aldosterone in RAS mechanisms, these controls are also regulated by arginine vasopressin (AVP), also known as antidiuretic hormone (ADH), that is produced and released from hypothalamus (Zeisberger et al., 1988). During water loss or dehydration, the osmotic pressure in the blood increased as a result of concentrated blood solutes (Solomon, 2016). These changes are detected by osmoreceptors, specialized receptors that are sensitive to increasing plasma osmolality in the brain (Danziger & Zeidel, 2015; Piantadosi, 2003). Pituitary gland is then signaled to release ADH which traveled through bloodstream to the kidney. Upon the stimulation from ADH, more water is reabsorbed in the CD of the kidney and urine is concentrated (Piantadosi, 2003). In addition, increased blood's osmotic pressure also stimulates the thirst center in the hypothalamus that results in the sensation of thirst and desire to drink (Solomon, 2016). In contrast, increased blood volume detected by stretch receptors in the atria of the heart reduced the production of ADH in hypothalamus and water reabsorption in kidney, thereby diluted urine is excreted (Kamat, 2013; Koizumi & Yamashita, 1978).

#### **2.3.2.1 The effects of testosterone on water balance**

Renal-body fluid balance has been known to influence the blood pressure in which a shift in pressure-natriuresis mechanisms could lead to the changes in blood pressure (Hall, 2003). To date, numerous studies have documented the roles of testosterone in the pathogenesis of higher blood pressure in males however the effects of testosterone on fluid transport in the kidney remained unclear. Previously, the induction of fluid secretion by testosterone have been demonstrated in *in vitro* studies using Madin-Darby

canine kidney cells (Sandhu et al., 1997). It is suggested that testosterone influences water transport mechanisms via endocrine systems *i.e.* RAS and ADH. Testosterone activates RAS mechanisms by enhancing renin secretion level and ACE activity, which eventually resulted in increased renal tubular sodium and water reabsorption (Komukai et al., 2010; Reckelhoff et al., 2005). The correlation between testosterone, ADH and water reabsorption have not been fully elucidated and contradicting effects of testosterone on the expression levels of AVP have been reported (Catudioc-Vallero et al., 2000). Recently, testosterone replacement therapy was reported to cause water retention and/or edema in which the increase in fluid retention could eventually lead to swelling and an increase in blood pressure (Osterberg et al., 2014). These findings have therefore supported the roles of testosterone in body fluid and blood pressure regulation.

### **2.3.2.2 Aquaporins (AQPs)**

Aquaporins (AQPs) are a family of pore-forming integral membrane proteins with low molecular weight (monomer size ~30 kDa) that appear at the cell membrane to facilitate passive fluid transport (Benga, 2009; Gomes et al., 2009). In general, AQPs are well-known for its role in transporting water molecules across plasma membranes in many cell types, however they are impermeable to charged species such as  $H^+$  and  $OH^-$  ions (Chakrabarti et al., 2004). AQPs are usually expressed in membranes as homotetramers in which each monomer consist of six transmembrane  $\alpha$ -helical domains connected by five loops, with hydrophilic amino ( $-NH_2$ ) and carboxyl ( $-COOH$ ) termini oriented towards the cytosol (Verkman et al., 2014; Verkman & Mitra, 2000). Among the five connecting loops, loops *b* and *e* which are hydrophobic in nature, contain highly conserved asparagine-proline-alanine (NPA) motifs that overlap in the center of the pore where water flows through (Benga, 2009; Gomes et al., 2009; Lehmann et al., 2008). Different AQP subunits possess differences in peptide sequences and thus

differences in the size of the pores and type of molecules that are able to be transported (Rastogi et al., 2008).

AQP-1 is the first membrane water channel functionally identified as a member of AQPs in erythrocyte and kidney membranes (Benga, 2012; Denker et al., 1988). To date, at least thirteen different AQPs have been found in mammalian tissues (AQP0-AQP12) (Ishibashi et al., 2009; Lehmann et al., 2008). While most AQPs are exclusively water transport channels, some of them also facilitate the transports of other small uncharged solutes such as glycerol (Hara-Chikuma & Verkman, 2006), urea (Li & Wang, 2014; Litman et al., 2009), carbon dioxide and nitric oxide (Herrera & Garvin, 2011; Wang & Tajkhorshid, 2010) across the membrane. AQPs have been divided into three subgroups based on their absorptivity: (i) classical aquaporins (AQP-0, 1, 2, 4, 5, 6, 8) which are permeable to water only, (ii) aquaglyceroporins (AQP-3, 7, 9, 10) which are permeable to water, glycerol, urea and other solutes and (iii) super-aquaporins or also known as subcellular aquaporins (AQP-11 and AQP-12) which have low homology (~20%) with other AQPs and have poorly conserved NPA boxes (Ishibashi, 2006; Ishibashi et al., 2009).

In mammals, AQPs play important roles in many organs in the body that require a high rate of water flux, such as kidney (Agarwal & Gupta, 2008), brain (Badaut et al., 2002), lungs (Verkman et al., 2000) and salivary glands (Ishikawa & Ishida, 2000; Kruse et al., 2006) and therefore they are known to be involved in numerous physiological processes. Amongst all thirteen AQPs, at least 6 AQPs (AQP-1, 2, 3, 4, 6 and 7) have been identified to be expressed in the kidneys (Agarwal & Gupta, 2008). AQP-2 is the most characterized AQPs where it plays a critical role in the mechanisms of water retention and urine concentration in kidney collecting ducts. Loss-of-function

mutation in AQP-2 have been reported in the rare genetic disease nephrogenic diabetes insipidus (NDI) in which the kidney fails to concentrate the urine (Deen et al., 1994) while numerous studies have indicated the correlation between the increased expression of AQP-2 in the kidney with the pathogenesis of hypertension (Buemi et al., 2004; Lee et al., 2000). Despite the limited information with regards to the roles of other renal AQPs in the development of high blood pressure, higher expressions of AQP-1, 2 and 3 in the kidney of hypertensive SHR rats than normotensive Wistar Kyoto (WKY) rats were reported, thereby suggesting the involvement of these AQPs in the development of hypertension in SHR (Lee et al., 2006).

AQPs have been known to express in female and male reproductive systems in which their expressions were altered by sex hormones (Huang et al., 2006; Snyder et al., 2009). Earlier, orchidectomies were reported to abolish the expression of AQP-3 in the epididymal epithelium of male Sprague Dawley (SD) rats (Hermo et al., 2004). In addition, testosterone has been shown to increase the expression levels of AQP-1, 5 and 7 in the uterus of ovariectomized female SD rats (Salleh et al., 2015). Besides reproductive organs, the expression levels of AQP-4 have also been shown to be up-regulated by testosterone in culture astrocytes (Gu et al., 2003). Recently, Herak-Kramberger *et al.* (2015) have demonstrated the higher mRNA and protein expression of AQP-1 in the kidney in males than females to be decreased by gonadectomies and increased by testosterone replacement (Herak-Kramberger et al., 2015). Figure 2.7 shows the structure of aquaporins while figure 2.8 shows the involvement of AQPs in epithelial water transport.

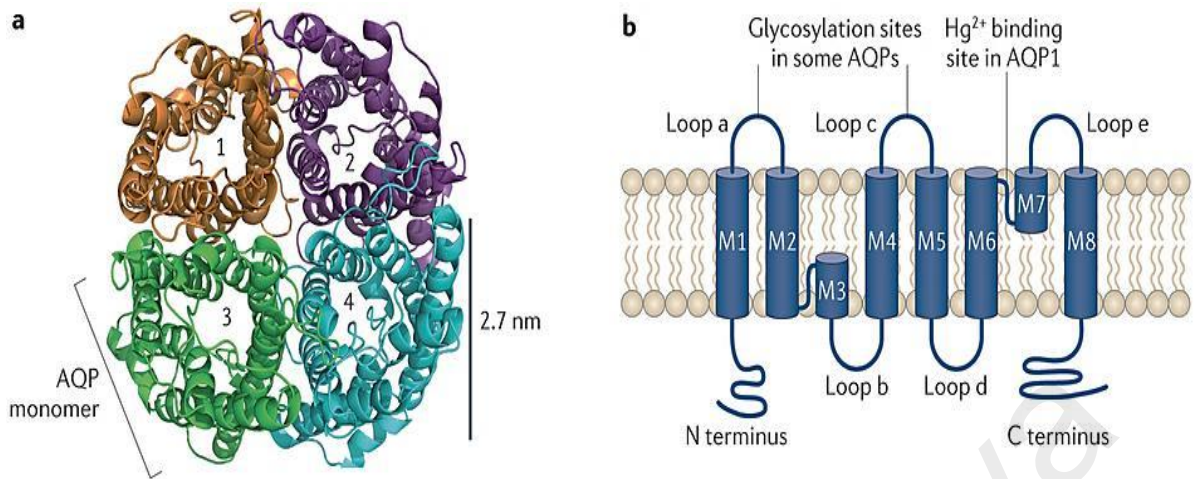


**Figure 2.7 Structure of aquaporins.**

(a) A top view of the extracellular face of an AQP-1 homotetramer, with monomers labeled 1 to 4. AQP monomers assemble to form tetramers in the membrane. (b) Each AQP monomer consists of six membrane-spanning  $\alpha$ -helical domains (M1, M2, M4, M5, M6 and M8) with five linkers (Loop a-e) and cytoplasmically-oriented amino (-NH<sub>2</sub>) and carboxyl (-COOH) termini. Two short helical segments, M3 and M5 form functional water pores with highly conserved NPA motifs in loop b and e. Image sourced from Verkman *et al.* (Verkman et al., 2014).

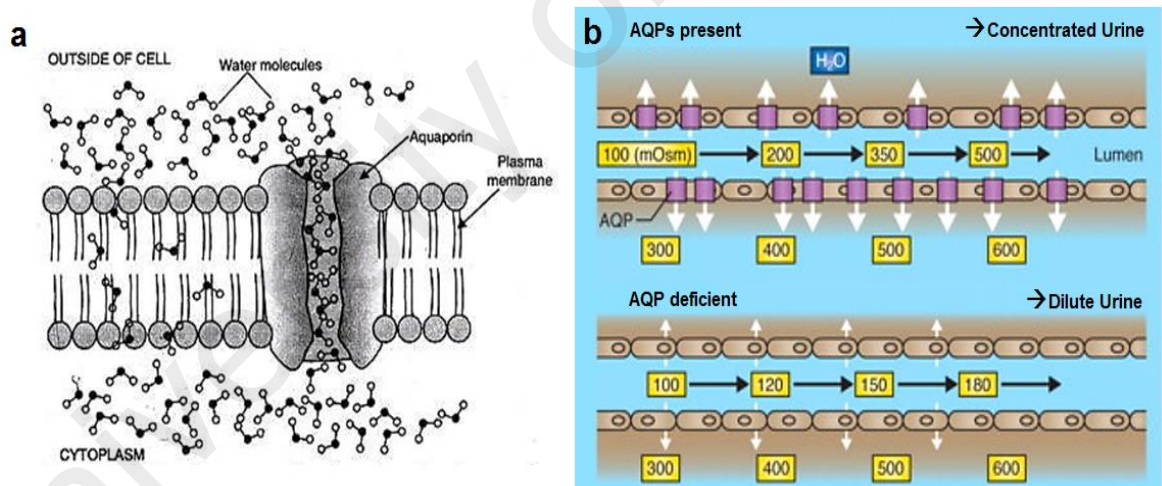


**Figure 2.8 Involvement of AQP in epithelial water transport.**

(a) Water is transported across plasma membrane via simple diffusion through the lipid bilayer. The presence of water selective channels, AQPs allow more rapid movement of water across cell membranes in many cell types. Image sourced from Biology Discussion (<http://www.biologydiscussion.com/plants/absorption-of-water/absorption-of-water-in-plants-with-diagram/22718>). (b) AQPs play an important role in rapid water transport in the kidney. Impaired urinary concentrating ability is observed in AQP deficient models as reduced transepithelial water permeability in the kidney tubules prevented osmotic equilibration of luminal fluid. Numbers represent hypothetical fluid osmolalities (mOsm). The image sourced from Verkman (Verkman, 2011).

## 2.4 Central Nervous System (CNS) and blood pressure

Central nervous system (CNS) is the most important physiological system for blood pressure controls in all mammals. These areas consist of a large number of brain nuclei which are located in the hypothalamus, brainstem and spinal cord and communicate with each other via a meshwork of interconnecting neurons. It has been known for some time that central hypothalamic and brainstem structures exert integrative control over neuroendocrine, autonomic and behavioral mechanisms in regulating blood pressure homeostasis. The principle osmoreceptors in the CNS that detect the changes in blood volume or pressure are located in the forebrain lamina terminalis (Stocker et al., 2008; Toney & Stocker, 2010). These areas consist of the subfornical organ (SFO), the organum vasculosum of the lamina terminalis (OVLT) and the median preoptic nucleus (MnPO) (Toney & Stocker, 2010). As the SFO and the OVLT are circumventricular organs, structures in the brain that are lack of normal blood-brain barrier, therefore these neurons can respond to circulating factors present in the blood that other neurons in the brain cannot (Stocker et al., 2013). In addition, these neurons are also intrinsically osmosensitive in which they are stimulated by physiological fluctuations in blood or cerebral spinal fluid (CSF) osmolality (Anderson et al., 2000; Ciura & Bourque, 2006). Meanwhile, the MnPO which located between the SFO and the OVLT, possess an intrinsic capability to detect changes in extracellular sodium levels via  $Na_x$  channel, a concentration-sensitive sodium channel (Choe & Bourque, 2014). It has been known that the MnPO receives and integrates a diverse array of inputs from the SFO and the OVLT which eventually project to the magnocellular neurons in the supraoptic nucleus (SON) and the paraventricular nucleus (PVN) (Burbach et al., 2001; Choe & Bourque, 2014; Ermisch et al., 1992; Renaud, 1994). Nevertheless, there are also direct neural pathways from the SFO to the PVN and SON via the OVLT where hormonal, SNS and

behavioral mechanisms are activated in order to restore the body fluid balance and blood pressure (Rossi & Chen, 2001).

The hypothalamic SON and PVN magnocellular neurons mediate the neuroendocrine reflexes through its axons which terminate at the blood capillaries of the posterior pituitary (PP) (Bargmann, 1966), at which the biologically active AVP and oxytocin (OXT) are stored until mobilized for secretion into the circulation (Fitzsimmons et al., 1994). A rise in plasma osmolality during dehydration is detected by intrinsic magnocellular neuron osmoreceptor mechanisms (Bourque et al., 2002; Zhang & Bourque, 2003) and specialized osmoreceptive neurons in the circumventricular organs (SFO and OVLT) that project to the magnocellular neurons (Anderson et al., 2000; Bourque et al., 1994; McKinley et al., 2004) and provide direct excitatory inputs to shape the firing activity of magnocellular neurons for hormone secretion (Hu & Bourque, 1992; Nissen et al., 1994). In addition, the internuclear connection between the SON and PVN also plays a role in synchronizing the firing patterns of the neurons for hormones release in PP (Rossi & Chen, 2001). Upon release, AVP travels through the blood stream and binds to its specific receptor located in the kidney where it increases the permeability of renal CD, reducing the renal water excretion and thus promoting water conservation (Stockand, 2010). Although some studies have also revealed the natriuretic activity of OXT (Haanwinckel et al., 1995; Soares et al., 1999), yet this hormone is best known for its role in milk ejection and uterine contraction during parturition (Blanks & Thornton, 2003; Leng et al., 2005).

Apart from that, the PVN also contains parvocellular neurons that can directly or indirectly influence SNA through descending projections to the brainstem, notably

the rostral ventrolateral medulla (RVLM), and the intermediolateral cell column (IML) of the spinal cord, which in turn regulate the arterial pressure and blood volume (Pyner, 2009; Shafon et al., 1998). Increased activity of RVLM is transmitted to IML of the spinal cord in which sympathetic nervous activity and blood pressure are increased (Kumagai et al., 2012). Apart from that, the PVN and RVLM neurons are also involved in the response of cardiovascular activity to changing environmental demands, mediated via the baroreflex (Patel & Schmid, 1988; Saigusa et al., 2003). Meanwhile, gamma-aminobutyric acid (GABA) interneurons and neuronal nitric oxide synthase (nNOS)-containing neurons of PVN are known to connect with the afferents of the nucleus of the solitary tract (NTS) where cardiac and vasomotor sympathetic activities are mediated (Affleck et al., 2012). Additionally, activation of arterial baroreceptors by increased blood volume or pressure stimulates the barosensitive NTS neurons which project directly to RVLM or indirectly via the inhibitory interneurons in the caudal ventrolateral medulla (CVLM) neurons which in turn inhibits the excitatory interneurons that project to RVLM and activate sympathetic nervous activity (Agarwal et al., 1990; Dampney & Horiuchi, 2003; O'Donoghue et al., 2002; Sun & Guyenet, 1985). Figure 2.9 shows the schematic illustration showing the keys hypothalamic circuits that mediate the osmosensitive neural pathways in the CNS.

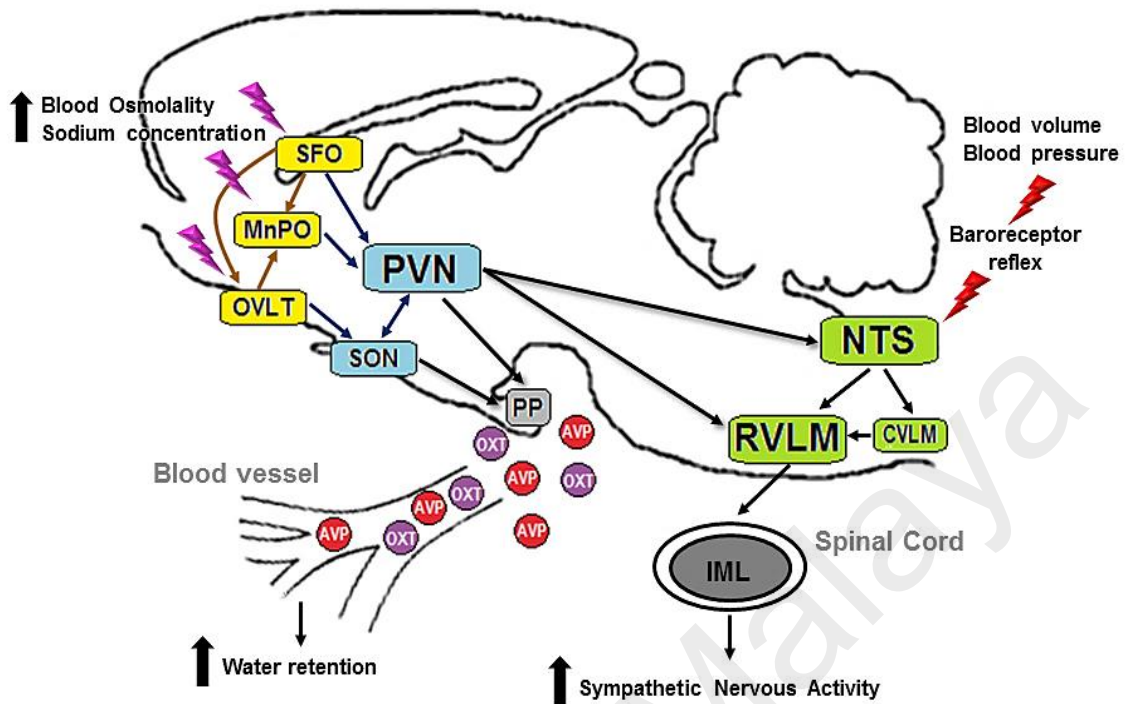


**Figure 2.9 Schematic illustration showing the keys hypothalamic circuits that mediate the osmosensitive neural pathways in the CNS.**

Increased blood osmolality or sodium concentration stimulates SFO, OVLT and MnPO which induced the activity in SON and PVN. The magnocellular neurons in SON and PVN project their axons to PP in which AVP and OXT are secreted into the blood. AVP travels through blood stream and binds to its receptor at kidney, thereby inducing water retention activities. The interconnection between SON and PVN allows the synchronization of firing synaptic inputs to PP following excitation. Regulation of sympathetic nervous activity occurred via the projections from PVN to NTS and RVLM. Stimulation of arterial baroreceptors excites NTS which in turn directly or indirectly via CVLM inhibited the excitatory neurons that project to RVLM and eventually decreased the activity of sympathetic cardiomotor and vasoconstrictor neurons.

#### 2.4.1 Paraventricular Nucleus (PVN) of hypothalamus

Hypothalamic paraventricular nucleus (PVN) is an important mediator in homeostatic control (Hazell et al., 2012) at which it plays a key role in neuroendocrine autonomic functions of the brain (Xia & Krukoff, 2003). Due to the capability of PVN to regulate sympathetic nervous activity, it is also known to be the most important cardiovascular regulatory center where it involves actively in the sympathetic control of blood pressure (Badoer, 2001; Blair et al., 1996). PVN neurons have been reported to be sensitive to both glutamate and GABA as studies have shown the presence of glutamate interneurons within the neurons and GABA interneurons at the halo zone surrounding

PVN (Csaki et al., 2000; Roland & Sawchenko, 1993). These neurotransmitters are in responsible to mediate the input of excitatory and inhibitory signals from other hypothalamic nuclei to PVN (Cui et al., 2001; Li & Pan, 2007; Tasker et al., 1998). As indicated earlier, PVN is a heterogeneous nucleus which composed of large magnocellular neurons and small parvocellular neurons (van den Pol, 1982). The axons of magnocellular neurons project to the PP where they involve in the hypothalamo-hypophysial neurosecretory system while the axons of parvocellular neurons project to various sites within the CNS that are known to be important in autonomic sympathetic nerve regulation (Ferguson et al., 2008). The well-revealed projections of parvocellular neurons are the projections to the pre-sympathetic RVLM and sympathetic IML of the thoracolumbar spinal cord (Pyner & Coote, 2000). Both projections were shown to innervate sympathetic preganglionic motoneurons at the end point (Dampney, 1994; Hosoya et al., 1991) and thus PVN was suggested to influence the sympathetic nervous activity directly via its spinal projections and indirectly via RVLM. Previously, the PVN neurons with the projection to the RVLM of the brainstem were shown to play an important role in the regulation of sympathetic nervous activity involved in the maintenance of normal blood pressure (Badoer, 2001). These neurons are activated by various homeostatic challenges including dehydration (Holbein et al., 2014) and appears to take part in the regulation the sympathetic outflow originated from PVN (Tagawa & Dampney, 1999).

#### **2.4.2 Nucleus of the solitary tract (NTS) of brainstem**

The nucleus of the solitary tract (NTS) is a cluster of sensory nucleus in the dorsomedial medulla that receives cardiovascular, visceral, respiratory, and gustatory information from various visceral afferents (Andresen et al., 2004; Jean, 1991). This information is ultimately directed to the postganglionic parasympathetic and

sympathetic pathways through the NTS neurons projected to the nucleus ambiguus (NA) and RVLM (Andresen et al., 2004). The intermediate third and the commissural subnucleus of NTS are termed as the cardiovascular NTS due to the reasons that they contain many cardiovascular-mediated neurotransmitters and are richly innervated by fibers emerged from different regions of brains that are actively involved in cardiovascular control (Colombari et al., 2001). By playing the role as the main site of termination of baroreceptor afferent nerves (Miura & Reis, 1972), this area of NTS could also mediate the baroreceptor reflexes on sympathetic discharge. Previously, baroreceptor afferent fibers raised from aortic arch and carotid sinus have been revealed to project to the secondary neurons located in the intermediate and caudal NTS via the aortic depressor nerves and carotid sinus nerves (Accorsi-Mendonça & Machado, 2013), in which NTS could influences the synaptic mechanisms of cardiovascular reflexes in normal as well as in pathophysiological conditions such as hypertension. Meanwhile, the involvement of commissural neurons of NTS in blood pressure regulation has been elucidated in the study of hypertension induced by aortic baroreceptor denervation where the lesions of this subnucleus were reported to prevent hypertension (Sato et al., 1999). These findings were further supported by the electrophysiological studies where they demonstrated the enhanced excitation of RVLM vasomotor by NTS through the projection of neurons in commissural NTS to RVLM (Koshiya & Guyenet, 1996). In overall, several lines of evidence indicated that there are two major regions in NTS that could possibly regulate the blood pressure, commissural NTS seems to play a role in maintaining the status of hypertension while intermediate NTS exhibits opposite effect as the inhibition of this region leads to chronic hypertension (Colombari et al., 2001).

### **2.4.3 Rostral Ventrolateral medulla (RVLM) of brainstem**

Numerous evidences from studies on a variety of species suggested that the rostral ventrolateral medulla (RVLM), a dense longitudinal column of cells laid within the ventrolateral aspect of medullary reticular formation, ventral to the retrofacial nucleus, plays a vital role in maintaining tonic sympathetic nervous activity and basal blood pressure (Bourassa et al., 2009; Dampney et al., 1987). The RVLM contains neurons that project to the spinal cord IML and densely innervates the sympathetic preganglionic motoneurons (Dampney et al., 1987). It is known that the resting sympathetic tone and arterial blood pressure are highly dependent on the level of cardio-acceleratory and vasoconstrictor tone originating from RVLM as sympathetic premotor neurons of RVLM is considered to be the final common pathway for several cardiovascular responses (Coote et al., 1997). Some of the cardiovascular effects stimulating the PVN are also mediated through these RVLM spinal neurons (Badoer, 2001). To date, RVLM has been extensively studied with regards to the regulation of sympathetic tone and baroreflex. The central baroreceptor pathway controlling sympathetic vasomotor responses involved a complex chain of neurons initiated from NTS to a region of CVLM that then projected to the RVLM and in turn directed the descending influence upon sympathetic preganglionic neurons in the spinal cord (Dampney, 1994; Saigusa et al., 2003). Following an increase in baroreceptor afferent activity, the projection from CVLM to RVLM is inhibited, leading to the suppression in sympathetic vasomotor outflow (Sved et al., 2001). In general, the RVLM contains barosensitive sympathetic premotor neurons that are responsible for maintaining the sympathetic vasomotor outflow through spinal cord.

#### **2.4.4 Testosterone influences blood pressure regulation via CNS**

The CNS communicates with various organs in the circulatory system via peripheral nervous systems (PNS). The PNS is divided into somatic nervous systems (SoNS) and autonomic nervous systems (ANS), that further broken down into the sympathetic nervous system (SNS) and parasympathetic nervous system (PSNS). The ANS and its SNS routes are shown to contribute to the pathogenesis of hypertension and thus CNS, which regulates the activity of ANS and SNS, is known to play a pivotal role in the development and maintenance of high blood pressure (Mancia & Grassi, 2014; Marvar et al., 2011; Wyss, 1993). Of the many physiological systems which are involved in the blood pressure regulation, the CNS is probably the most important. In general, most neurons that are involved in blood pressure regulation are concentrated in the brainstem nonetheless these control neurons are extended from the hypothalamus to the thoracic spinal cord. Numerous studies have documented their role in both short-term and long-term blood pressure regulation where abnormal elevation in sympathetic controls of cardiomotor, renal and vascular tone are identified as the major factors in development of essential hypertension (Burns et al., 2007; Joyner et al., 2010; Oparil et al., 2003). Many fluctuations in blood flow occur as a result of alteration in input signals from CNS to the circulatory system via these pathways.

Angiotensin II is known to modulate blood pressure via its actions on the CNS and thus the activation of CNS is suggested in angiotensin-induced hypertension. Circulating angiotensin II is detected by circumventricular organ, SFO in CNS via its angiotensin II AT1 receptors (Braga, 2011), in addition, the neural pathways from SFO to SON and PVN also use angiotensin II as neurotransmitters (Akaishi et al., 1980). Previously, injection of angiotensin I and II into the CNS resulted in increased blood pressure in rats (Fink et al., 1980). The influences of angiotensin II on CNS are further

elucidated by the studies on angiotensin II-induced hypertension in which significant neuronal activations of SFO, SON, PVN, NTS and CVLM were observed upon subcutaneous infusion of angiotensin II (Davern & Head, 2007). Nevertheless, the intracerebroventricular infusion of flutamide, an androgen receptor (AR) antagonist, in the CNS significantly attenuates the development of angiotensin II-induced hypertension in male mice, thereby suggesting the roles of male hormone *i.e.* testosterone and central ARs in potentiating sensitivity to angiotensin II via centrally mediated mechanisms (Xue et al., 2007). Moreover, testosterone has also been suggested to enhance the responsiveness actions towards angiotensin II via activation of central RAS, which in turn modulates the renal SNA and eventually contributes to the development of hypertension (Ojeda et al., 2010).

Apart from that, testosterone has also been known to mediate blood pressure controls by altering the gene expression levels of important components in the CNS. Tyrosine hydroxylase is a rate-limiting enzyme of catecholamine biosynthesis while alpha 2B-adrenoceptor plays a critical role in regulating neuronal signals from sympathetic nerves and from adrenergic neurons in the CNS. Several pieces of evidence have reported the increased expression levels of hypothalamic tyrosine hydroxylase and alpha 2B-adrenoceptor in the pathogenesis of hypertension (Carbajosa et al., 2015; Kanagy, 2005). Recently, studies on cafeteria-diet-induced hypertension have revealed the increased blood pressure to be accompanied by the up-regulation of gene expression of hypothalamic tyrosine hydroxylase and alpha 2B-adrenoceptor subtype in male and testosterone-treated female rats (Plut et al., 2002). These findings have indicated that testosterone may contribute to the development of cafeteria-induced hypertension by altering the gene expression in the central mechanisms.

Meanwhile, numerous studies have documented the interaction of AVP with SNS and RAS in maintaining the blood pressure. AVP is suggested to be involved in the regulation of sympathetic outflow in blood pressure control as earlier, the intracerebroventricular infusion of exogenous AVP was shown to stimulate the sympathetic vasomotor activity and produce long-lasting increases in blood pressure and heart rate in rats (Berecek & Swords, 1990). To date, several lines of evidence revealed the alteration in AVP expression by testosterone. Previously, the *in vitro* studies on human SH-SY5Y neuroblastoma cell lines have reported an increase in the expression level of AVP upon testosterone treatment (Grassi et al., 2013). This effect of testosterone is further supported by the studies on epigenetic control of AVP expression in which the mRNA expression level of AVP within the bed nucleus of the stria terminalis in the brain was shown to be reduced by orchidectomy and restored by testosterone replacement in male rats (Auger et al., 2011). In addition, the involvement of testosterone in mediating the hyperosmotic responses have also been reported as the hyperosmotic-induced enhanced AVP mRNA levels in SON were shown to be prevented by orchidectomy and restored by testosterone replacement (O'Keefe et al., 1995). The expression level of AVP in medial parvocellular PVN of hypothalamus has also recently been reported to be up-regulated by testosterone and thus these findings have further supported the roles of testosterone in regulating the central mechanisms and blood pressure control (Williamson & Viau, 2008). Figure 2.10 shows the schematic diagram of major physiological systems in CNS and PNS that are involved in the regulation of blood pressure.

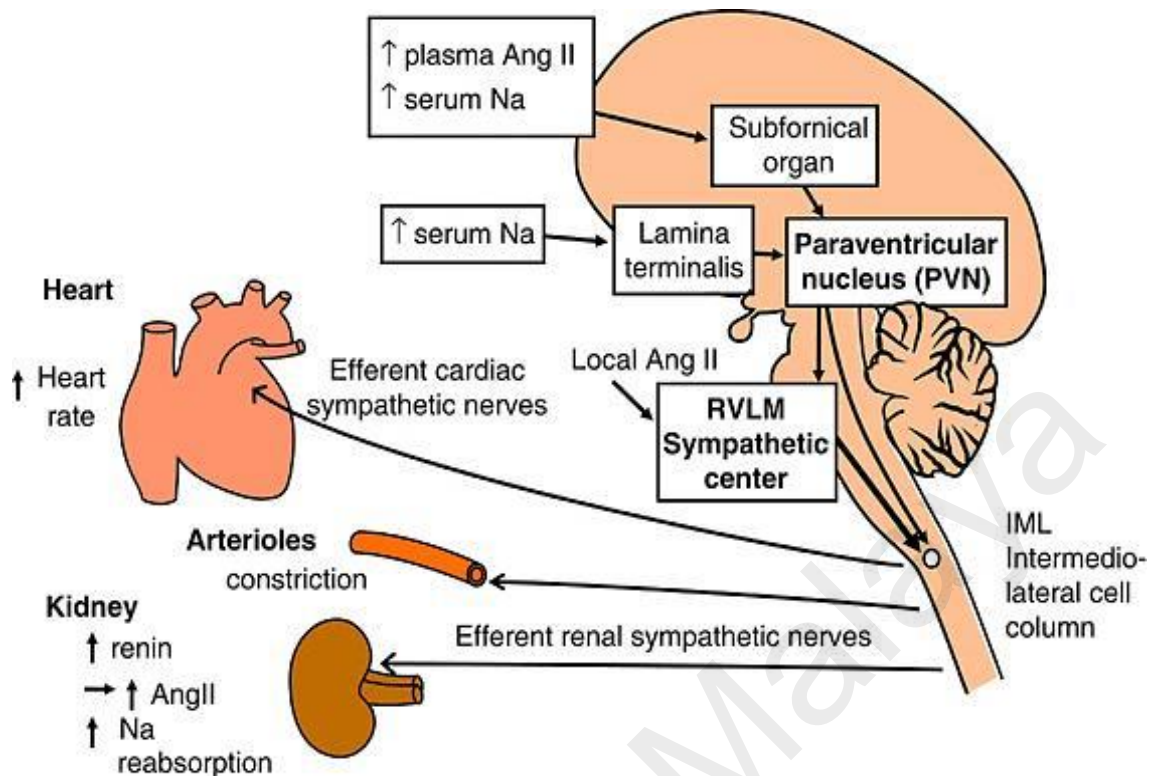


**Figure 2.10 Schematic diagram of major physiological systems in CNS and PNS that are involved in the regulation of blood pressure.**

Circumventricular organ, SFO and lamina terminalis responded to elevations in plasma angiotensin II and/or serum sodium levels by increasing the efferent sympathetic activity via activation of PVN. Enhanced neuronal signals transmitted from PVN to RVLM and IML of the spinal cord, stimulating the PNS to heart, arterioles and kidney that may collectively cause the increase in blood pressure. Image sourced from Kumagai *et al.* (Kumagai *et al.*, 2012).

## 2.5 Animal Models

To date, the success rate of clinical trials remained low due to the flawed preclinical research and thus the use of animal models is pivotal in bridging the translation gap to the clinic. The ultimate aim of animal experimental research is to explain the perplexing problems encountered in clinical practice and to examine new approaches prior to clinical trials (Isselhard & Kusche, 1998). In many cases, using humans as research subjects is not feasible and thus animal models generally serve as the first subject to allow us to extrapolate knowledge on a particular disease and develop a new cure for it. The selection of animal model is important to mimic the normal physiology of human and conditions of interest in which to answer the scientific and clinical questions (Denayer *et al.*, 2014). The choice of suitable models for pre-clinical trials not only

relies on the understanding of the species-specific anatomy and physiology but also its analogous relationship to humans. Small animals such as rat and mice are the most extensively used models in many experimental studies due to their small sizes, abbreviated life cycles, reproductive affluence, inexpensive and most importantly, the well-establishment of the backgrounds (Chow et al., 2007). The growing numbers of research in using rat models have led to the emergence of genetic-manipulated models in which the modern-day research is able to select the models with the genetic background specifically to represent the human diseases' condition of interest.

### **2.5.1 Sprague Dawley (SD)**

Sprague Dawley (SD) is an outbred multipurpose breed of albino rats. This strain was developed in 1925 by Robert W. Dawley using a female Wistar rat and a hybrid hooded male of unknown origin. The original SD rat colony was obtained and established by Harlan (now Harlan Sprague Dawley) in 1980 through the acquisition of a commercial firm, Sprague Dawley Inc. in Madison, Wisconsin (Chow et al., 2007; Kraus, 1979). It is extensively used due in part to the efficiency of their calmness, good reproduction performance and ease of handling. The SD rats have been suggested to be a sustainable and reproducible model for studies on oral submucous fibrosis and spinal cord injury as appreciable results are obtained within reasonable periods using a limited number of rats (Garcia-Lopez et al., 1996; Maria et al., 2015). Currently, the SD strain has gradually become the most popular laboratory animal model for research in renal and cardiovascular diseases (Grossman, 2010; Latendresse et al., 2001; Leong et al., 2015; Wang et al., 2015).

### **2.5.2 Wistar Kyoto (WKY)**

Wistar rat is an outbred albino rats that named after Professor Casper Wistar. In 1906, the Wistar strain was developed at the Wistar Institute in Philadelphia for the used in biological and medical research. This strain is notably the first laboratory rat strain developed to serve as an experimental model at a time when *Mus musculus* (house mouse) was primarily used (Alexandru, 2011; Chow et al., 2007). The Wistar Kyoto (WKY) strain was established in 1971 by employing normotensive descendants of Wistar colony in Kyoto (Kurtz & Morris, 1987). The WKY rats are currently one of the most used rat models for experimental laboratory research. The SHR and WKY rats strain were both developed from the same parental Wistar rats and thus normotensive WKY rats are almost exclusively used as the corresponding control for SHR in many studies on human essential hypertension (Doggrell & Brown, 1998).

### **2.5.3 Spontaneously Hypertensive Rats (SHR)**

Spontaneously hypertensive rat (SHR) is a well-known genetic animal model for studies in essential hypertension and cardiovascular disease. In 1963, Okamoto and Aoki developed the SHR strain by selectively inbreeding Wistar rats with highest blood pressure (Okamoto & Aoki, 1963) and today, this strain has become the most studied animal model of human essential hypertension (Leong et al., 2015; Pinto et al., 1998). Previously, SHR strain was described to develop almost 100% of the incidence of hypertension and present hypertensive cardiovascular diseases in high frequency at the advanced stage of hypertension (Okamoto & Aoki, 1963). The spontaneously and consistency of SHR strain to develop moderate to severe hypertension have affirmed its suitability as an excellent material in hypertension research and a counterpart for clinical essential hypertension (Trippodo & Frohlich, 1981). In addition, the specific and uniform predisposition of SHR to hypertension and cardiovascular diseases has

allowed the scientists to achieve reliable and reproducible outcomes that can be correlated with the existing clinical findings (Folkow, 1982).

## **2.6 Transcriptomics**

Transcriptome is a collection of gene readouts, also known as ribonucleic acid (RNA) transcripts, encoded by the genome of a particular cell, tissue or organism. Transcriptomics is the study of a complete set of RNA transcripts (transcriptome) that are expressed at a specific time or under certain circumstances. Amongst all types of RNA, one of the most abundant forms of RNA, messenger RNA (mRNA) plays an important role in directing the synthesis of proteins in the cytoplasm. Comparisons of transcriptomes enable the identification of genes that are differentially regulated in distinct cell populations at a specific time under different treatment. In 1991, Adams *et al.* performed the first mammalian transcriptomes profiling on human brain complementary DNA (cDNA) through the generation of expressed sequence tag (EST) libraries (Adams *et al.*, 1991). This technology represented one of the earliest application which then followed by the development of Sanger sequencing of cDNA and microarrays (Sanger *et al.*, 1977; Schena *et al.*, 1995). Nonetheless, the latest revolution of novel high-throughput sequencing technologies represented by short-read, also known as second or next generation RNA-Seq (RNA-Sequencing), has then dominated the field since 2008 and become the technologies of choice for transcriptomics studies today (McGettigan, 2013).

### **2.6.1 RNA-Seq (RNA-Sequencing)**

RNA-Seq (RNA-Sequencing), also known as whole-transcriptome shotgun sequencing, refers to the use of high-throughput next generation sequencing (NGS) technologies in identification and quantification of RNA contents inside a given sample

(Chu & Corey, 2012; Morin et al., 2008). Roche 454 was the first commercially successful next generation system. In 2006, Bainbridge *et al.* have published the first RNA-Seq paper on transcriptome profiling of a human prostate cancer cell line, LNCaP (Bainbridge et al., 2006). The use of RNA-Seq has then exploded due to its ability to quantify a large dynamic range of expression levels via absolute quantification. In general, a typical RNA-Seq workflow consists of the following steps: sample preparation, RNA extraction, library preparation, sequencing and data analysis. During library preparation, rRNA is first removed and a pool of RNA (total or fractionated *i.e.* rRNA-depleted or poly(A)<sup>+</sup> RNA) is fragmented and reverse transcribed into a library of cDNA fragments with adaptors attached to one or both end (3' and 5' ends). The library, with or without amplification, is then sequenced on a high-throughput platform in which the short sequences are read from one end (single-end sequencing) or both ends (pair-end sequencing). The sequencing data obtained vary according to the RNA sequencing technologies used, nonetheless the sequence “reads” are typically 30-400bp (Wang et al., 2009). Currently, several sequencing platforms are commercially available and more are under active development. To date, the pyrosequencing-based Roche 454 system, the sequencing-by-ligation-based Applied Biosystem SOLiD system and the sequencing-by-synthesis-based Illumina Genome Analyzer (GA)/MiSeq/HiSeq machines are the most commonly used sequencing platforms (Wolf, 2013). Figure 2.11 shows the overview of library preparation for RNA-Seq.

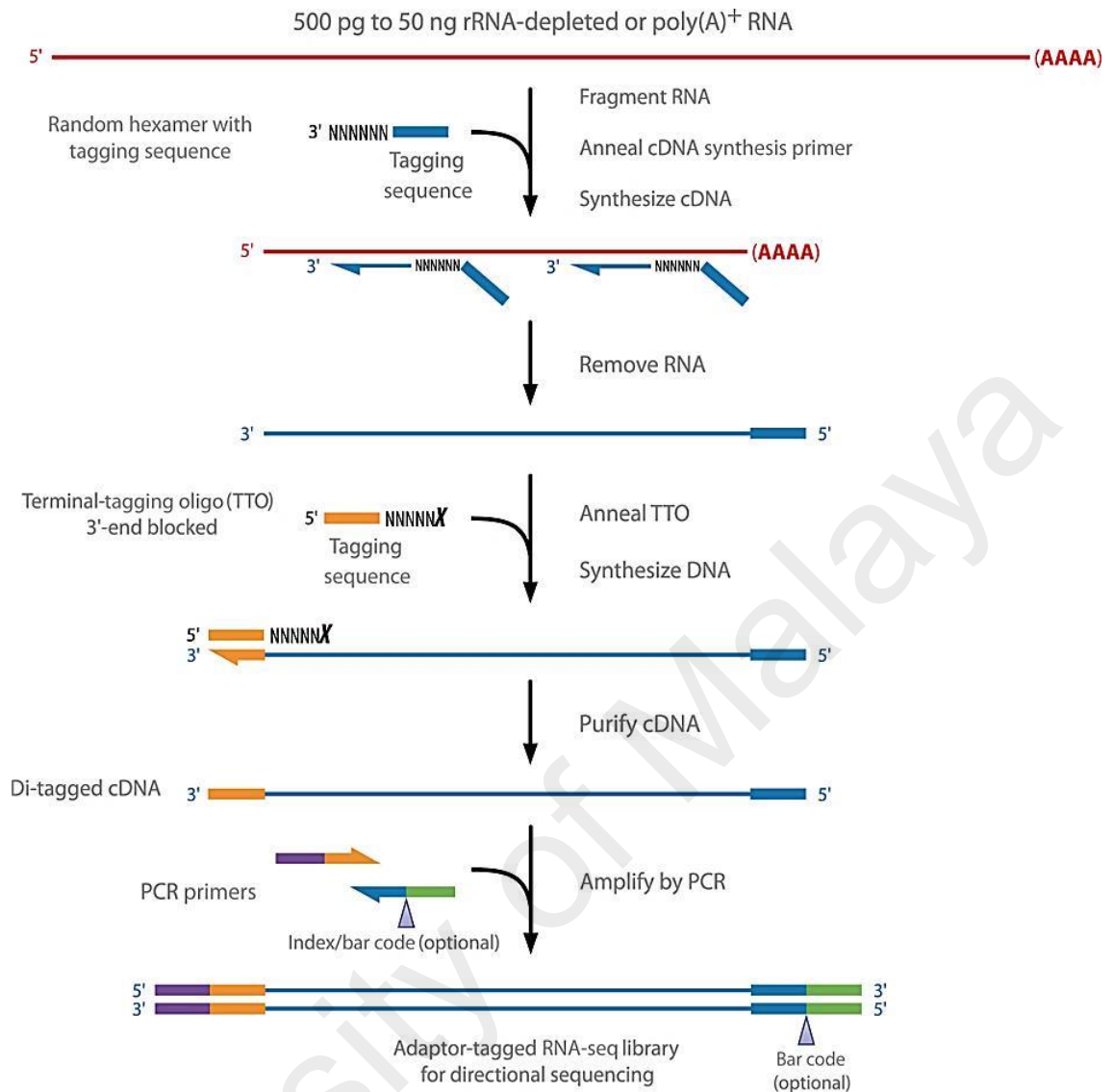


**Figure 2.11 Overview of library preparation for RNA-Seq.**

500pg to 50ng of rRNA-depleted or poly(A)<sup>+</sup> RNA (mRNA) is first fragmented into smaller pieces and converted to cDNA using 5'-tagged random primers. The cDNA is further tagged at its 3' end and subjected to purification. The di-tagged cDNA is then amplified using polymerase chain reaction (PCR) method in which the addition of adaptor sequences (optional index/bar code for user identification purpose) is added. Lastly, the purification of the amplified library is performed and the library is ready for sequencing. This protocol is based on Illumina ScriptSeq v2 RNA-Seq Library Preparation Kit. Image sourced from Pease and Sooknanan (Pease & Sooknanan, 2012).

## 2.6.2 RNA-Seq gene expression profiling

Traditional gene expression studies that focus on a single gene or a limited number of genes could restrict the overall understanding of gene alteration and their complex interactions. Analysis and comparison of the whole collection of RNA transcripts (transcriptomes) in a cell population allow the identification of differentially expressed

genes in response to certain treatments. By counting the number of transcripts, the amount of gene activity, also known as gene expression can be determined. Gene expression profiling is the characterization of the pattern of genes expressed at the level of transcription at once to create a global picture of cellular function. In 1992, the first gene expression profiling via high-throughput methods was demonstrated with the development of differential display method (Liang & Pardee, 1992). Today, gene expression profiling with the use of RNA-Seq technology is a powerful tool that has greatly improved our ability to quantify and profile all active genes in a specific cell, tissue or organism (Mortazavi et al., 2008; Trapnell et al., 2012). The recent breakthroughs in high-throughput RNA-Seq technologies not only ease the detection of dynamic changes in gene expression but also allow the assessment of the whole transcriptome under different conditions. This high-throughput technology often provides enormous insights in which the detail information on mapping and annotation of transcripts, novel sequences, transcriptional start site, splice variants and alternative promoter usage can be obtained (Han et al., 2015). At present, RNA-Seq has become the preferred technique to measure the absolute abundance of transcripts as the high sensitivity of RNA-Seq allowed an unlimited dynamic range of detection with high-resolution quantification of differentially expressed genes (Mantione et al., 2014).

## CHAPTER 3: MATERIALS AND METHODS

### 3.1 Materials

#### 3.1.1 Animals and animal facilities

Sprague Dawley (SD), Wistar Kyoto (WKY) and Spontaneously Hypertensive (SHR) rats at eight (8) weeks of age were obtained from Animal Experimental Unit (AEU), Faculty of Medicine, University of Malaya (UM). All procedures were carried out in highly sterilized conditions with the approval from Institutional Animal Care and Use Committee (IACUC), University of Malaya (ethic number: 2014-05-07/physio/R/NS). All animals are kept in a well-maintained environment with standardized temperature ( $22\pm 1^{\circ}\text{C}$ ), humidity ( $50\pm 5\%$ ) and 12:12 hours light-dark cycle. Animals had free access to standard rodent chow (Harlan, Germany) and tap water *ad libitum* throughout the whole study.

#### 3.1.2 Chemicals and consumables

##### 3.1.2.1 Anesthesia and post-surgeries

Betadine® 10% PVPI antiseptic solution and EMLA (Eutectic Mixture of Local Anesthetics) 5% cream were purchased from Betadine (Singapore) and AstraZeneca (London, UK) respectively. Ethanol was obtained from VWR International, (Pennsylvania, USA). Anesthetic agents, ketamine and xylazine were from Ilium, Troy Laboratories Private Ltd. (Australia), kombitrim antibiotic was from Kela Laboratoria N.V. (Hoogstraten, Belgium) and meloxicam was from Intas Pharmaceuticals Ltd. (India). All Ethicon™ suture needles were supplied by Ethicon, Inc. (New Jersey, USA).

### **3.1.2.2 Hormonal treatments**

Bovine serum albumin (BSA), finasteride (FN), flutamide (FU), peanut oil, sodium chloride (NaCl), sodium phosphate dibasic ( $\text{Na}_2\text{HPO}_4$ ) and testosterone propionate were purchased from Sigma-Aldrich (USA). Ethanol and sodium phosphate dibasic ( $\text{NaH}_2\text{PO}_4$ ) were purchased from VWR International (Pennsylvania, USA) and Calbiochem (Darmstadt, Germany) respectively. Silastic® silicone laboratory tubing (catalog no.: 508-008) and Dow Corning®732 multi-purpose silicone sealant were supplied by Dow Corning Corporation (Michigan, USA).

### **3.1.2.3 Carotid artery cannulation**

Heparin, pentobarbital sodium salt, sodium chloride (NaCl) and thimerosal (Merthiolate) were purchased from Sigma-Aldrich (USA).

### **3.1.2.4 Blood collection and analysis**

Heparin was obtained from Sigma-Aldrich (USA). Mouse, rat, human aldosterone ELISA kit (catalog no.: ab136933) was supplied by Abcam (Cambridge, UK). Testosterone ELISA kits (catalog no.: ADI-900-065) were purchased from Enzo Life Sciences, Inc. (Farmingdale, New York, USA).

### **3.1.2.5 RNA extraction and quality control**

Agarose and ethylenediamine tetraacetic acid (EDTA) were from Calbiochem (USA) while boric acid was from QRëC, Quality Reagent Chemical (New Zealand). Chloroform and ethanol were purchased from Merck Specialties Private Ltd. (Mumbai) and VWR International (Pennsylvania, USA) respectively. QIAzol® lysis buffer (catalog no.: 79306) and RNeasy® mini kit (catalog no.: 74106) were obtained from Qiagen (Germany). NucleoSpin® RNA kit (catalog no.: 740955) was supplied by

Macherey-Nagel (Düren, Germany). Tris base and RNA marker (catalog no.: G3191) were from Promega Corporation (USA) and RNA loading dye (2X) (catalog no.: R0641) were from Thermo Fisher Scientific (Rockford, USA).

### **3.1.2.6 cDNA synthesis and qPCR**

iScript™ Reverse Transcription Supermix for RT-qPCR (catalog no.: 170-8841) was supplied by Bio-Rad Laboratories (California, USA) while QuantiTect® reverse transcription kit (catalog no.: 205313) and QuantiNova® SYBR® green PCR Kit (catalog no.: 208056) were purchased from Qiagen (Germany).

### **3.1.2.7 RNASeq**

Hydrochloric acid (HCl) and sodium hydroxide (NaOH) were from QRëC, Quality Reagent Chemical (New Zealand). Sodium acetate, toluidine blue and Tween-20 were from Sigma-Aldrich (USA). Ethanol was from VWR International (Pennsylvania, USA) and Tris base was from Promega Corporation (USA). Tissue-Tek Optimal Cutting Temperature (OCT) compound (catalog no.: 4583) was supplied by Sakura Finetek Europe (Netherlands). Agilent RNA 6000 Nano Kit (catalog no.: 5067-1511) and Agilent High Sensitivity DNA Kit (catalog no.: 5067-4626) were products from Agilent Technologies, Inc. (California, USA). Qubit RNA High Sensitivity Assay Kit (catalog no.: Q32852) and Qubit dsDNA High Sensitivity Assay Kit (catalog no.: Q32851) were purchased from Life Technologies (California, USA). KAPA Library Quantification Kit (catalog no.: KR0405) was from Kapa Biosystems (South Africa). MiSeq Reagent Kit v2 (catalog no.: MS-102-2001), ScriptSeq™ Complete Gold Kit (Human/Mouse/Rat) – Low input (catalog no.: SCL6G), TruSeq Paired-End (PE) Cluster Kit v3-cBOT-HS (catalog no.: PE-401-3001) and TruSeq SBS Kit v3-HS (200 cycles) (catalog no.: FC-401-3001) were purchased by Illumina, Inc. (California, USA).

### **3.1.2.8 Protein extraction and quantification**

EZblock™ protease inhibitor cocktail (catalog no.: K271-500) and RIPA buffer solution (catalog no.: 2114-100) were obtained from BioVision Inc. (California, USA). Micro BCA™ Protein Assay Kit (catalog no.: 23235) was purchased from Thermo Fisher Scientific (Rockford, USA).

### **3.1.2.9 SDS-PAGE and Western blotting**

Ammonium persulfate, β-mercaptoethanol, bromophenol blue, glycerol, glycine, isopropanol (2-Propanol), potassium phosphate monobasic (KH<sub>2</sub>PO<sub>4</sub>), sodium chloride (NaCl) and Tween-20 were purchased from Sigma-Aldrich (USA). Ethanol and methanol were from VWR International (Pennsylvania, USA), hydrochloric acid (HCl) was from QR&C, Quality Reagent Chemical (New Zealand) and Tris base was from Promega Corporation (USA). Sodium dodecyl sulfate (SDS), sodium phosphate dibasic (Na<sub>2</sub>HPO<sub>4</sub>) and tetramethylethylenediamine (TEMED) were products from Calbiochem (USA). 30% acrylamide/bis solution 19:1 (catalog no.: 161-0154), 10X tris/glycine/SDS electrophoresis buffer (catalog no.: 161-0732) and Immun-Blot® polyvinylidene difluoride (PVDF) membrane (catalog no.: 162-0177) were supplied by Bio-Rad Laboratories, Inc. (USA). Amersham ECL prime blocking agent (catalog no.: RPN418) and Amersham™ ECL™ rainbow™ markers – full range (catalog no.: RPN800E) were purchased from GE Healthcare Life Sciences (Buckinghamshire, UK). SuperSignal West Dura Extended Duration Substrate (catalog no.: 34075) was from Thermo Fisher Scientific (Rockford, USA)

### **3.1.2.10 Immunohistochemistry studies**

Aluminium potassium sulfate (alum), bovine serum albumin (BSA), gelatin, hydrogen peroxidase (H<sub>2</sub>O<sub>2</sub>), paraformaldehyde (PFA), potassium chloride (KCl),

potassium phosphate monobasic ( $\text{KH}_2\text{PO}_4$ ), sodium chloride ( $\text{NaCl}$ ), sodium iodate ( $\text{NaIO}_3$ ), sucrose, Tween-20 and xylene were purchased from Sigma-Aldrich (USA). Acetic acid (glacial), ethanol and methanol were obtained from VWR International (Pennsylvania, USA). Sodium phosphate dibasic ( $\text{Na}_2\text{HPO}_4$ ) was from Calbiochem (Darmstadt, Germany) and Triton X-100 was from Promega Corporation (USA). Haematoxylin, paraffin wax, sodium citrate were products from Merck Specialties Pvt. Ltd. (Germany). Tissue-Tek Optimal Cutting Temperature (OCT) compound (catalog no.: 4583) was from Sakura Finetek Europe (Netherlands). Pierce diaminobenzidine tetrahydrochloride (DAB) substrate kit and poly-L-lysine glass slide were supplied by Thermo Fisher Scientific (Rockford, USA). Dibutylphthalate polystyrene xylene (DPX) mounting medium was from Ajax Finechem Pty Ltd. (New South Wales, Australia) and UltraCruz® mounting medium (catalog no.: sc-24941) was from Santa Cruz Biotechnology, Inc (Texas, USA).

### **3.2 Experimental design and animal preparation**

This study was divided into two main parts: (A) functional study to investigate the influences of sex hormones *i.e.* testosterone on blood pressure and (B) molecular mechanisms study to elucidate the potential mechanisms underlying these testosterone effects of blood pressure. A preliminary study on the effects of orchidectomy and sub-chronic testosterone treatment was first performed in normotensive rats (refer **Section 3.2.1**). Following that, in order to further improve the understanding of these effects in pathophysiology of hypertension, the effects of (i) gonadectomies *i.e.* ovariectomy and orchidectomy (refer **Section 3.2.2**), (ii) estrous cycle (refer **Section 3.2.3**) and (iii) chronic testosterone treatment (refer **Section 3.2.4**) were investigated in both normotensive and hypertensive rats.

### 3.2.1 Effects of orchidectomy and sub-chronic testosterone treatment in normotensive male rats

Male Sprague Dawley (SD) rats at eight (8) weeks of age were divided into eight (8) experimental groups with n = 6 per group.

Group 1 : Sham-operated intact male receiving vehicle oil only [S]

Group 2 : Orchidectomized male receiving vehicle oil only [O]

Group 3 : Orchidectomized male receiving 125µg/kg/day testosterone [T125]

Group 4 : Orchidectomized male receiving 250µg/kg/day testosterone [T250]

Group 5 : Orchidectomized male receiving 125µg/kg/day testosterone plus flutamide (8mg/kg/day) [T125+FU]

Group 6 : Orchidectomized male receiving 250µg/kg/day testosterone plus flutamide (8mg/kg/day) [T250+FU]

Group 7 : Orchidectomized male receiving 125µg/kg/day testosterone plus finasteride (5mg/kg/day) [T125+FN]

Group 8 : Orchidectomized male receiving 250µg/kg/day testosterone plus finasteride (5mg/kg/day) [T250+FN]

All sham-operations and orchidectomies (refer **Section 3.3**) were performed at eight (8) weeks of age. After two weeks (2) of recovery period, hormonal treatments were initiated at ten (10) weeks of age. All treatments were given via subcutaneous injection (refer **Section 3.5.1**) for seven (7) consecutive days. At the end of the hormonal treatment, animals (n = 6 per group) at eleven (11) weeks of age were subjected to cannulation of carotid artery (refer **Section 3.6**). After the completion of blood pressure measurement, blood sample was collected from carotid artery into chilled blood collection tubes containing lithium heparin (TUD Sdn Bhd., Malaysia) and centrifuged immediately (refer **Section 3.7**). Meanwhile, another cohort of animals (n = 6 per group) receiving the same treatments were sacrificed (between 0800 to 1200) via

decapitation using a specialized rodent guillotine (Harvard Apparatus, Holliston, USA). Trunk blood was collected into chilled blood collection tubes containing lithium heparin (TUD Sdn Bhd., Malaysia) and subjected to further processing (refer **Section 3.7**). Tissues (whole kidneys) were collected, snap-frozen in powdered dry ice and stored at -80°C until further used.

### **3.2.2 Effects of gonadectomies in normotensive and hypertensive male and female rats**

Male and female Wistar Kyoto (WKY) and Spontaneously Hypertensive (SHR) rats were used in this experiment in which eight (8) experimental groups were designed with n = 6 per group.

Group 1 : WKY sham-operated intact male

Group 2 : WKY orchidectomized male

Group 3 : WKY sham-operated intact female

Group 4 : WKY ovariectomized female

Group 5 : SHR sham-operated intact male

Group 6 : SHR orchidectomized male

Group 7 : SHR sham-operated intact female

Group 8 : SHR ovariectomized female

All sham-operations, orchidectomies and ovariectomies (refer **Section 3.3**) were performed at eight (8) weeks of age. At sixteen (16) weeks of age, animals (n = 6 per group) were subjected to cannulation of carotid artery (refer **Section 3.6**). At the end of the procedure, blood sample was collected from carotid artery into chilled blood collection tubes containing lithium heparin (TUD Sdn Bhd., Malaysia) and processed immediately (refer **Section 3.7**).

### 3.2.3 Changes in blood pressure across estrous cycle in normotensive and hypertensive female rats

Intact female Wistar Kyoto (WKY) and Spontaneously Hypertensive (SHR) rats were divided into eight (8) experimental groups according to their stage of estrous cycle. At least 5 animals per cycle were determined.

Group 1 : WKY female at proestrus stage (Ps)

Group 2 : WKY female at estrus stage (Es)

Group 3 : WKY female at metestrus stage (Ms)

Group 4 : WKY female at diestrus stage (Ds)

Group 5 : SHR female at proestrus stage (Ps)

Group 6 : SHR female at estrus stage (Es)

Group 7 : SHR female at metestrus stage (Ms)

Group 8 : SHR female at diestrus stage (Ds)

At sixteen (16) weeks of age, all animals ( $n = 5-8$  per group) were subjected to cannulation of carotid artery (refer **Section 3.6**). Vaginal smears (refer **Section 3.4**) were performed in order to determine the stage of estrous cycle prior to cannulation of carotid artery. Upon the completion of blood pressure recording, blood sample was collected from carotid artery into chilled blood collection tubes containing lithium heparin (TUD Sdn Bhd., Malaysia) and processed immediately (refer **Section 3.7**). The measurement of estrogen and progesterone levels were carried out by Division of Laboratory Medicine, University Malaya Medical Centre (UMMC) in order to further validate the stage of estrous cycle of the female rats (Sjahfirdi et al., 2011).

### 3.2.4 Effect of chronic testosterone treatment in normotensive and hypertensive female rats

Male and female Wistar Kyoto (WKY) and Spontaneously Hypertensive (SHR) rats were divided into eight (8) experimental groups with  $n = 6$  per group.

Group 1 : WKY sham-operated intact male [WMS]

Group 2 : WKY orchidectomized male [WMO]

Group 3 : WKY ovariectomized female [WFO]

Group 4 : WKY ovariectomized female receiving testosterone treatment [WFT]

Group 5 : SHR sham-operated intact male [SMS]

Group 6 : SHR orchidectomized male [SMO]

Group 7 : SHR ovariectomized female (without treatment) [SFO]

Group 8 : SHR ovariectomized female receiving testosterone treatment [SFT]

All sham-operations, orchidectomies and ovariectomies (refer **Section 3.3**) were performed at eight (8) weeks of age. After two (2) weeks of recovery period, which coincide with the age of the rats at ten (10) weeks old, testosterone treatments were initiated via Silastic tubing implantation (refer **Section 3.5.2**) for six (6) weeks of period. Meanwhile, all non-testosterone-treated groups were also implanted with empty Silastic tubing. At sixteen (16) weeks of age, all animals ( $n = 6$  per group) were subjected to cannulation of carotid artery (refer **Section 3.6**). After the completion of the procedure, blood sample was collected from carotid artery into chilled blood collection tubes containing lithium heparin (TUD Sdn Bhd., Malaysia) and transferred for further processing (refer **Section 3.7**). In the meantime, another cohort of animals ( $n = 15$  per group for **Section 3.9.1**;  $n = 6$  per group for **Section 3.9.2**) under the same experimental conditions was sacrificed (between 0800 to 1200) via decapitation using a specialized rodent guillotine (Harvard Apparatus, Holliston, USA). Trunk blood was collected into chilled blood collection tubes containing lithium heparin (TUD Sdn Bhd.,

Malaysia) and processed accordingly (refer **Section 3.7**). Tissues (whole kidneys and brains) were harvested and immediately snap-frozen in powdered dry ice prior to storage at -80°C.

### **3.3 Surgical procedures**

Sham-operation, orchidectomy and ovariectomy were performed at eight (8) weeks of age before they are considered adults in aseptic conditions. All procedures were carried out under ketamine: xylazine (80mg/kg: 8mg/kg, intraperitoneal injection) anesthesia. A heat pad was used to maintain body temperature and vital signs were regularly monitored. All surgical instruments were sterilized using hot beads sterilizer (Fine Science Tools, California, USA) prior to surgery. All areas for surgeries were shaved and disinfected by using 70% (v/v) ethanol and Betadine antiseptic solution. Upon the recovery of consciousness after anesthesia, animals were returned to the animal holding area and monitored regularly. All animals were given intramuscular injection of Kombitrim (1mg/kg) antibiotic for three (3) days consecutively to prevent any post-surgical wound infection. Meloxicam (1mg/kg, subcutaneous injection) was also given to all animals for three (3) consecutive days for the purpose of relieving pain. After all surgical procedures, all animals were left for two (2) weeks in order to ensure a full recovery and elimination of effects of endogenous sex hormones prior to the following hormonal treatments.

#### **3.3.1 Sham-operation**

Sham operation for orchidectomy in male was done by making an anterior midline incision in the scrotum, exposing the testes and reinserting intact into the scrotum. Meanwhile, the sham-operation for ovariectomy in female was performed by making a small incision in the caudal end of the ribs on lateral side through the skin and muscle

layers in which the ovary found between the fats in the peritoneal cavity were exposed and then reinserted intact into the peritoneal cavity. All incisions were closed and sutured using Ethicon sutures.

### **3.3.2 Orchidectomy**

Orchidectomy was carried out by first making an anterior midline incision in the scrotum, sac that contains testicles. Each testicle was exposed through the surgical incision and testicular fat pads were gently separated. The cauda epididymis, caput epididymis, vas deferens and testicular blood vessel was gently exposed in which a single ligature was performed around the blood vessel using Ethicon sutures to prevent bleeding upon removal of testis. Blood vessel, cauda epididymis and caput epididymis were then severed and testicle was removed. The remaining content was inserted back into the scrotal sac (Idris, 2012). Following the completion of the same procedure on the other testicle, the incision was closed and sutured using Ethicon sutures.

### **3.3.3 Ovariectomy**

Animal was placed in left lateral position and caudal end of the ribs on the lateral side of the animal was identified. A small incision was made in the skin and subcutaneous connective tissues from the underlying muscle were separated. A second incision was then made through the muscle layers in order to gain entry into the peritoneal cavity. Using blunt-end forceps, ovary was gently retracted from the surrounding fat pads in the peritoneal cavity. Oviduct and artery extending towards the ovary were singly ligated using Ethicon sutures to prevent bleeding upon removal of ovary. Oviduct and blood vessel were then severed and ovary was removed. The remaining parts of the oviduct were gently pushed back into the peritoneal cavity (Parhizkar et al., 2008) and incisions in muscle and skin were closed and sutured using

Ethicon sutures. Same procedures were repeated for the other ovary.

### **3.4 Identification of estrous cycle**

In order to determine the stage of estrous cycle, vaginal smears were performed using normal saline [0.9% (w/v) sodium chloride (NaCl) solution]. The tip of the plastic pipette filled with ten 10µl of normal saline was inserted into the vagina of female rat in which the saline was flushed into the vagina and the fluid was retrieved. The vaginal flushing was placed onto a glass slide and viewed immediately (unstained) under a light microscope. The stages of estrous cycle were determined based on the cellular type and relative proportion of each type present in the vaginal flushing. Three (3) types of cells that are present in the vaginal were distinguished according to their morphologies: (i) leukocytes, round and small, (ii) nucleated epithelial cells, generally round to polygonal and nucleated and (iii) cornified epithelial cells, irregular shaped and lack of nuclei (Figure 3.1). The major feature of proestrus stage (Ps) is the presence of predominately the nucleated epithelial cells while estrus stage (Es) is characterized by the presence of primarily the cornified epithelial cells. Metestrus stage (Ms) is however the stage where a combination of all cellular types is present. Lastly, diestrus stage (Ds) which is the longest stage of estrus cycle, is identified by the predominance of leukocytes, however moderate numbers of nucleated epithelial cells and low numbers of cornified epithelial cells may also be observed (Cora et al., 2015; Marcondes et al., 2002). Figure 3.1 shows identification of estrous cycle stages in female rats.

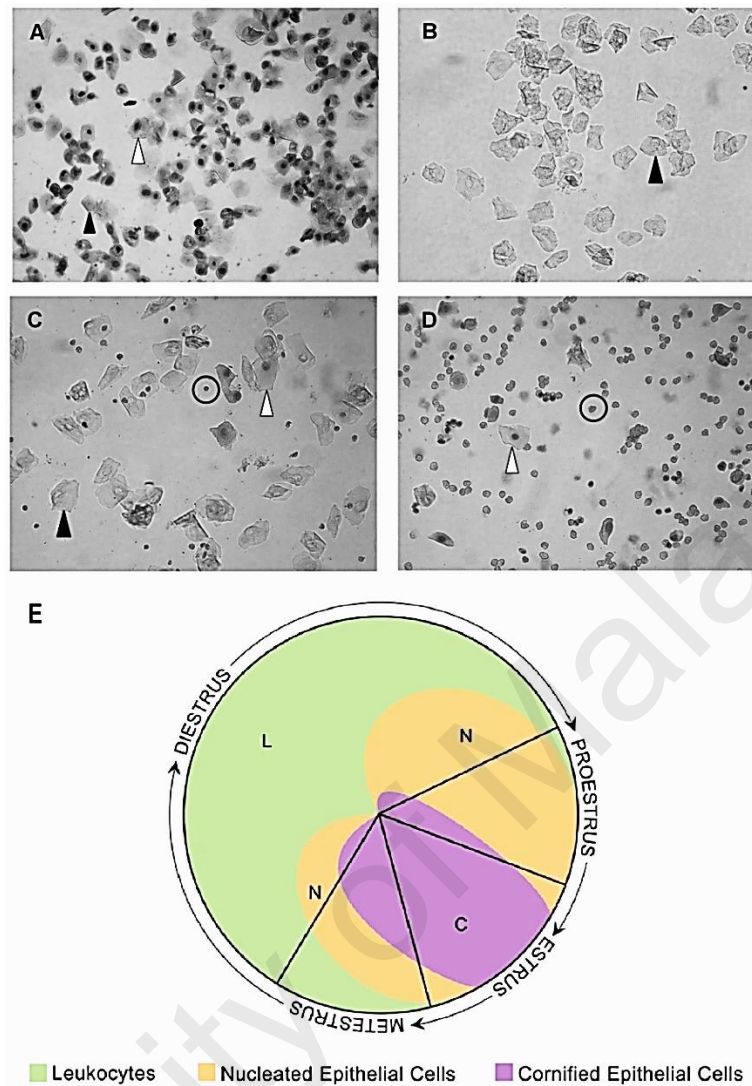


**Figure 3.1 Identification of estrous cycle stages in female rats.**

Leukocytes (circle), nucleated epithelial cells (white arrow) and cornified epithelial cells (black arrow) were presented in vaginal. In general, estrous cycle in rodent is divided into four (4) stages: **(A)** proestrus (Ps), **(B)** estrus (Es), **(C)** metestrus (Ms) and **(D)** diestrus (Ds). **(E)** Visual representation of the cellular types and relative proportion of each cellular types present during the four (4) stages of the estrous cycle in female rat. One complete estrous cycle takes about four (4) to five (5) days. Images sourced from Byers *et al.* and Cora *et al.* (Byers *et al.*, 2012; Cora *et al.*, 2015)

### 3.5 Hormonal treatment

All hormonal treatments were initiated two (2) weeks after sham-operation, orchidectomy and ovariectomy in order to ensure the removal of majority of the endogenous sex hormones in the blood circulation and so to avoid potential confounding effects of these hormones.

### **3.5.1 Sub-chronic testosterone treatment via subcutaneous injection**

In sub-chronic testosterone treatment, exogenous testosterone was given to the animals via subcutaneous injection at the back of the neck for seven (7) consecutive days. Peanut oil was used as the vehicle oil in this experiment. Testosterone propionate, flutamide (FU), an androgen receptor (AR) blocker and finasteride (FN), a 5 $\alpha$ -reductase inhibitor were dissolved in peanut oil to be delivered to the rats. FU and FN were given one (1) hour prior to the respective testosterone injection in order to ensure a total blockage of AR and 5 $\alpha$ -reductase prior to the administration of exogenous testosterone.

### **3.5.2 Chronic testosterone treatment via Silastic tubing implantation**

In chronic testosterone treatment, exogenous testosterone was given to the animals via subcutaneous Silastic tubing implantation at the back of the shoulder for six (6) weeks of period (Figure 3.2). Ten milligrams (10mg) of testosterone propionate was weighted and packed into a Silastic laboratory tubing (inner diameter (ID): 0.062mm; outer diameter (OD): 0.125mm; length: 19mm). Both ends of the tubing were then sealed with multi-purpose silicone adhesive (Ely et al., 1991). Tubing were incubated in albumin buffered primer solution at 4°C for overnight and soaked in 70% (v/v) ethanol for at least two (2) hours before implanting them. Empty Silastic tubing with both ends sealed were given to non-testosterone treated groups in order to eliminate possible changes due to the implantation of Silastic tubing and post-surgeries effects. Subcutaneous Silastic tubing implantation procedures were performed under ketamine: xylazine (80mg/kg: 8mg/kg, intraperitoneal injection) anesthesia. The area at the back of the shoulder of the animal was shaved and disinfected by using 70% (v/v) ethanol and Betadine antiseptic solution prior to insertion. A small incision was made and the tubing was placed subcutaneously under the skin at the back of the shoulder. The incision was then closed and sutured using Ethicon sutures. All tubing were replaced

three (3) weeks after the first tubing implanted following the same procedures discussed. Reimplantation on multiple occasions should not cause infection as long as sterile and aseptic techniques are adhered. After surgery, all animals were given intramuscular injection of Kombitrim (1mg/kg) antibiotic for three (3) days consecutively to prevent any post-surgical wound infection. EMLA 5% cream were applied onto the wound to reduce the pain after every surgery. Figure 3.2 shows testosterone treatments via subcutaneous Silastic tubing implantation.

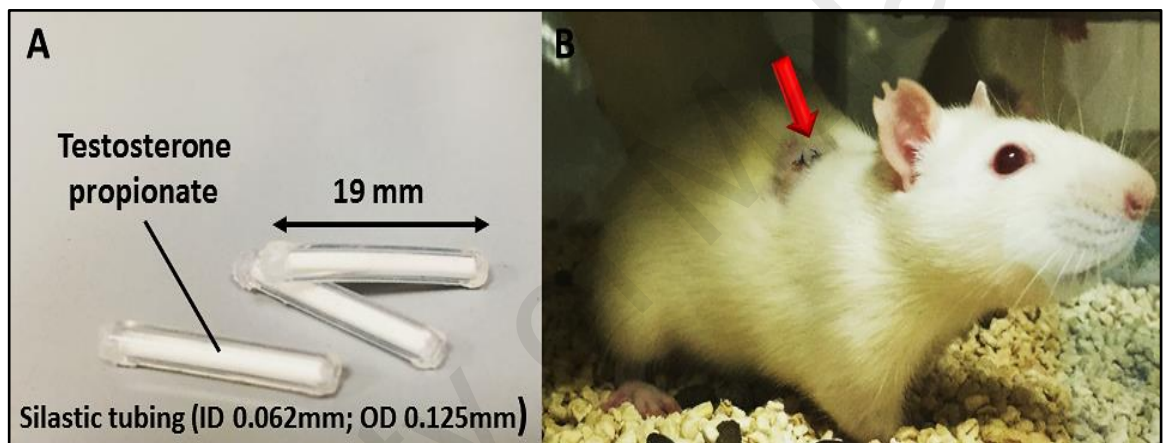


**Figure 3.2 Testosterone treatments via subcutaneous Silastic tubing implantation.** (A) 19mm-length Silastic tubing pre-packed with 10mg of testosterone propionate powder to be implanted into the rats. (B) Silastic tubing was subcutaneously implanted at the back of the shoulder (red arrow) of the rats.

### 3.6 Cannulation of carotid artery

Animals were first anesthetized via intraperitoneal injection of pentobarbital sodium (65mg/kg). Cannulation of carotid artery procedures were carried out as described by Parasuraman *et al.* (Parasuraman & Raveendran, 2012). In brief, a small incision was made in the trachea for tracheostomy. Using the visual aid of vagus nerve, carotid artery was identified and a cannula pre-filled with heparinized normal saline (0.5IU/ml) was inserted into the carotid artery (Figure 3.3). The cannula was connected to a syringe filled with heparinized saline and a pressure transducer (MLT0380/D; ADInstruments, Dunedin, New Zealand). The blood pressure of the animal was monitored using the

PowerLab Data acquisition system (PowerLab 4/35; ADInstruments, Dunedin, New Zealand). Blood pressure was recorded for at least 10 minutes following 10-15 minutes of stabilization. The blood pressure data were analyzed using LabChart version 6.0 (ADInstruments, Dunedin, New Zealand) in which average systolic blood pressure (SBP) and diastolic blood pressure (DBP) were obtained. Mean arterial blood pressure (MAP) was calculated as  $DBP + [(SBP-DBP)/3]$ . Figure 3.3 shows surgical procedures for cannulation of carotid artery.

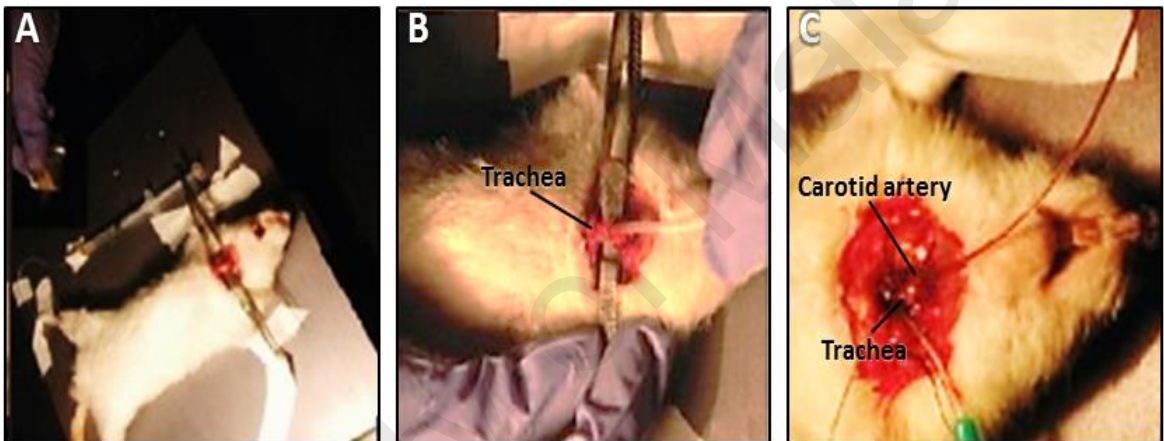


**Figure 3.3 Surgical procedures for cannulation of carotid artery.**

(A) Experimental rat was placed in ventral recumbency and a small incision was made at the neck of the rat for tracheotomy and cannulation of carotid artery. (B) Tracheostomy: A small incision was made at the cartilage tissue of trachea and a short tube was inserted. (C) Cannulation of carotid artery: Carotid artery was cannulated with a cannula that was pre-filled with heparinized saline (0.5IU/ml) and connected to a pressure transducer and PowerLab Data acquisition system. Images were modified and sourced from Parasuraman *et al.* (Parasuraman & Raveendran, 2012).

### 3.7 Blood analysis

All blood samples (from carotid artery and trunk blood) were kept on ice and processed immediately within two (2) hours. Plasma was separated by centrifuging whole blood sample at 3,000rpm for 20 minutes at 4°C. The supernatant, designated plasma was carefully removed from the cell pellet, transferred into a new polypropylene tube and stored in -80°C until further used. The levels of testosterone and aldosterone in the blood plasma were determined using competitive enzyme-linked immunosorbent

assay (ELISA) kit. All assays, in triplicate, were performed following the manufacturers' guidelines with the lowest assay sensitivity limit of approximately 5.67pg/ml and 4.7pg/ml for testosterone and aldosterone respectively. Absorbance values were read at 405nm using a microplate reader (Infinite M1000 Pro, Tecan, Switzerland) and the plasma levels of testosterone and aldosterone were expressed as pg/ml. Quantitative determination of sodium ( $\text{Na}^+$ ), chloride ( $\text{Cl}^-$ ), potassium ( $\text{K}^+$ ), calcium ( $\text{Ca}^{2+}$ ), glucose, urea and creatinine in the plasma sample were performed using automated ADVIA 2400 Chemistry System (Siemens Healthcare Diagnostics, Eschborn, Germany) while plasma osmolality was measured by an osmometer (Osmomat 030-D, Gonotec, Berlin, Germany) based on the method of freezing point depression.

### **3.8 Kidney**

Following the hormonal treatment in **Section 3.2.1** and **3.2.4**, kidneys were collected in order to investigate the changes in gene expression levels of epithelial sodium channel (ENaC) and aquaporin (AQP) upon sub-chronic and chronic testosterone treatments.

#### **3.8.1 Real-time quantitative polymerase chain reaction (qPCR)**

To date, real-time quantitative polymerase chain reaction (qPCR) is the most emerging method of choice for rapid and reliable quantification of mRNA expression level using fluorescent dyes (Ginzinger, 2002). qPCR was carried out to determine and measure the changes in the RNA expression levels in the kidneys under testosterone influences. In this experiment, two-step qPCR was performed in which the reverse transcription of RNA extracted from the tissue into cDNA was carried out independently prior to the level detection in qPCR step.

### **3.8.1.1 RNA extraction**

Approximately 50mg of kidney tissue was weighed and disrupted using a rotor-stator homogenizer (Heidolph DIAX 600, Ballerup, Denmark) in Qiazol lysis buffer. The separation of RNA, DNA and protein phases was initiated by adding chloroform and centrifuging at 12,000×g for 15 minutes at 4°C. The obtained total RNA was then purified and cleaned up using the Macherey-nagel NucleoSpin RNA extraction kit. After centrifugation, the upper RNA layer was added to 70% (v/v) ethanol and transferred to Nucleospin RNA column. The following steps were performed following the manufacturer's instruction in which the contaminating DNAs were removed by adding rDNase solution and pure RNAs were eluted using RNase-free water. All extracted RNAs were stored in -80°C until further used.

### **3.8.1.2 RNA quantification and quality control**

The quality and total yield of the extracted RNA were assessed using a Nanodrop spectrophotometer (NanoDrop™ 2000/2000c, Thermo Fisher Scientific, USA). One microliter (1µl) of the RNA sample was placed on the lower measurement pedestal where the absorbance measurement for nucleic acid was read from 220nm to 340nm. The concentration of RNA in ng/µl, the ratio of absorbance at 260nm to 280nm (A260/280) and 260nm to 230nm (A260/230) were obtained using the default wavelength of 340nm for the bichromatic normalization. Meanwhile, agarose gel electrophoresis was then carried out to further examine the integrity of the RNA samples (Figure 3.4). RNA loading dye was added to all RNA samples in 1:1 ratio. After 10 minutes of incubation at 70°C, the pre-prepared samples were chilled and loaded onto 1% (w/v) agarose gels. All electrophoresis were run for 45 minutes at 90 volts in tris-borate-EDTA (TBE) buffer using a horizontal electrophoresis system (Wide Mini-Sub Cell GT Cell System, Bio-Rad Laboratories, China). The gel was observed

and captured using a BioSpectrum imaging system with high sensitivity CCD camera (Ultra-Violet Products Ltd., Cambridge, UK). Figure 3.4 shows RNA analysis by agarose gel electrophoresis.

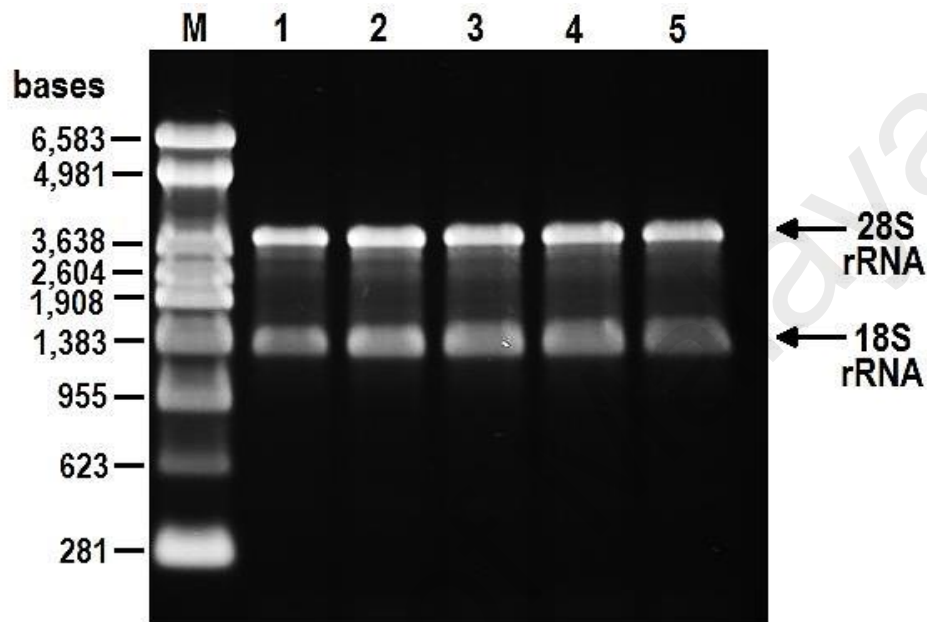


**Figure 3.4 RNA analysis by agarose gel electrophoresis.**

Representative agarose gel image showing the 28S and 18S rRNA bands of the total RNA extracted. A good quality RNA generally shows a 28S: 18S rRNA ratio of approximately 2:1 and without smearing (indicator for degradation). Abbreviations: M: RNA marker; 1-5: total RNA extracted; rRNA: ribosomal RNA).

### 3.8.1.3 cDNA synthesis

cDNA synthesis was carried out using Biorad iScript Reverse Transcription Supermix for RT-qPCR kit following the manufacturer's manual. In brief, 4 $\mu$ l of iScript RT supermix was added to 16 $\mu$ l of sample containing 600ng of input total RNA. All reactions were run on a StepOne Plus Real-Time PCR System (Applied Biosystems, California, USA) at 25°C for 5 minutes, followed by 42°C for 30 minutes and lastly 85°C for 5 minutes. cDNAs were then transferred into new microcentrifuge tubes and kept in -20°C until further used.

#### 3.8.1.4 qPCR procedure

Real-time qPCRs were performed to measure the steady state mRNA level in kidneys. Primers for *Scnn1a*, *Scnn1b*, *Scnn1g*, *Aqp1*, *Aqp2*, *Aqp3*, *Aqp4*, *Aqp6*, *Aqp7* and *Gapdh* (Table 3.1) were designed using the NCBI PrimerBLAST tool (<http://www.ncbi.nlm.nih.gov/tools/primer-blast/>) based on the following specifications: primer size of 18 to 22bp, product size of 70 to 250bp, melting temperature of 59 to 60°C and GC contents between 40 to 60%. All primers were synthesized by Integrated DNA Technologies and primers efficiency was validated using serial dilutions of cDNA prior to all experiments. Earlier synthesized cDNAs were used as the template and all experiments were carried out in duplicate using QuantiNova SYBR Green PCR Kit on StepOne Plus Real-Time PCR Systems (Applied Biosystems, California, USA). A total of 12µl of reaction mixture containing 6µl of 2x SYBR Green PCR master mix, 2µl of QN ROX reference dye, 0.7µM of forward primer, 0.7µM of reverse primer and 2µl of cDNA were prepared in each well. The real-time cycle program was set according to the manufacturer's protocol in which the PCR was initiated by heat activation at 95°C for 2 minutes, followed by 40 cycles of denaturation step at 95°C for 5 seconds and annealing/extension step at 60°C for 10 seconds. The housekeeping gene *Gapdh* was selected as the internal reference gene and relative mRNA quantifications were performed using StepOne Software version 2.3 and based on  $2^{-\Delta\Delta Ct}$  method (Livak & Schmittgen, 2001). Table 3.1: shows primers' sequences for ENaC, AQP and GAPDH.

**Table 3.1 Forward and reverse primer sequences for ENaC, AQP and GAPDH.**

Target	Gene name	Forward primer sequence (5' → 3')	Reverse primer sequence (5' → 3')
ENaC	<i>Scnn1a</i>	CCTAAGCCCAAGGGAGTTGA	ACACTACAAGGCTTCCGACA
	<i>Scnn1b</i>	TGGACATTGGTCAGGAGGAC	AGCAGCACCCCAATAGAAGT
	<i>Scnn1g</i>	TGAGGCTTCCGAGAAATGGT	AATACTGTTGGCTGGGCTCT
AQP	<i>Aqp1</i>	ACCCACTGGAGAGAAACCAG	AGAGTAGCGATGCTCAGACC
	<i>Aqp2</i>	AACTACCTGCTGTTCCCCTC	ACTTCACGTTCCCTCCCAGTC
	<i>Aqp3</i>	GAACCCTGCTGTGACCTTTG	AGTGTGTAGATGGGCAGCTT
	<i>Aqp4</i>	ACACGAAAGATCAGCATCGC	TGACCAGGTAGAGGATCCCA
	<i>Aqp6</i>	GGATCTTCTGGGTAGGACCG	ACGGTCTTGGGTGTCAGGAAA
	<i>Aqp7</i>	TATCTTCGCCATCACGGACA	CCCAAGAACGCAAACAAGGA

### 3.8.2 Western blotting

Western blotting is also known as immunoblotting as antibodies are used to specifically detect its target proteins. This method was first introduced in 1979 by Towbin *et al.* (1979) in their attempts to identify rRNA binding proteins (Towbin *et al.*, 1979). Nevertheless, it is now widely used in research to separate and identify specific proteins in the midst of a complex protein mixture extracted from cells or tissues (Mahmood & Yang, 2012). In addition, this method also allows the quantification of protein concentration in which qualitative or semi-quantitative data about a specific protein could be obtained by comparing the protein expression levels amongst the experimental groups. In this experiment, Western blotting is performed in order to identify the changes in the expression levels of ENaC and AQP proteins in the kidneys under testosterone influences.

#### 3.8.2.1 Protein extraction

Approximately 80mg kidney tissues were weighed and cut into smaller pieces. The tissues were then submerged in one 1ml RIPA buffer solution containing protease inhibitors and homogenized for 30 seconds using a rotor-stator homogenizer (Heidolph DIAX 600, Ballerup, Denmark). Following 5 minutes incubation in ice, the total

proteins were obtained by centrifugation at 14,000×g for 15 minutes at 4°C. The supernatants were transferred to new clean microcentrifuge tubes and stored at -20°C until further used.

### **3.8.2.2 Protein quantification**

Thermo Fisher Scientific micro bicinchoninic acid (BCA) protein assay kit was used to determine the concentration of extracted proteins. BCA, sodium salt, is a water-soluble compound that forms an intense purple complex that exhibits strong absorbance at 562nm with cuprous ion ( $\text{Cu}^{+1}$ ) in an alkaline environment. This assay utilizes BCA as the detection reagent in which it reacted with  $\text{Cu}^{+1}$  produced in the reaction of protein with alkaline  $\text{Cu}^{+2}$  (Smith et al., 1985). Therefore, this method provides an extremely sensitive calorimetric detection for quantification of total protein. All procedures were carried out according to the manufacturer's instructions. In brief, a serial dilution of bovine serum albumin (BSA) standard was first prepared in following concentrations: 0, 0.5, 1, 2.5, 5, 10, 20, 40 and 200µg/ml. All standards or samples, in triplicate, were added to the working BCA reagents at the ratio of 1:1. After two (2) hours of incubation at 37°C, the absorbance was read at a wavelength of 562nm using a microplate reader (Infinite® M1000 PRO, Tecan, Switzerland). The concentrations of the proteins were determined using the standard curve plotted based on the absorbance of the serial dilution of standards.

### **3.8.2.3 Preparation of SDS-PAGE gel**

In 1970, the sodium dodecyl sulfate-polyacrylamide gel electrophoresis (SDS-PAGE) was first employed in a scientific study on bacteriophage T4 by U.K. Laemmli (Laemmli, 1970). In general, this method allows the separation of proteins based on its molecular mass by using a discontinuous polyacrylamide gel as a support medium and

sodium dodecyl sulfate (SDS) to denature the proteins. The SDS-PAGE gel can be divided into two (2) different parts: stacking gel and separating gel. The stacking gel generally consists of four percent (4%) acrylamide with lower pH *i.e.* pH6.8 and lies on top of separating gel. Meanwhile, the concentrations of acrylamide that were used in the separating gel with higher pH *i.e.* pH8.8 are highly dependent on the size of the target proteins in the samples. In the current experiment, 10% and 12% acrylamide separating gels were used for the protein separation. The compositions of the gels were shown in Table 3.2. The separating gel was first prepared and poured into the casting frames. A thin layer of isopropanol or ethanol was added on top of the gel to remove the bubbles and prevent the gel from drying. After the complete polymerization of the separating gel, the gel surface was then briefly washed with ddH<sub>2</sub>O and any excessive fluid was discarded. The pre-prepared stacking gel was pipetted onto the solidified separating gels until overflow and the well-forming comb was then inserted. Following the complete gelation of the stacking gel, the comb was gently removed and the ready SDS-PAGE gel was set in the cell buffer dam. Table 3.2 shows the preparation of SDS-PAGE gel.

**Table 3.2 Preparation of SDS-PAGE gel.**

<b>Stock solution</b>	<b>4%</b>	<b>10%</b>	<b>12%</b>
	<b>Stacking gel</b>	<b>Separating gel</b>	<b>Separating gel</b>
ddH <sub>2</sub> O (μl)	2975	3800	3200
0.5M Tris, pH6.8 (μl)	1250	-	-
1.5M Tris, pH8.8 (μl)	-	2600	2600
30% Acrylamide/Bis solution 19:1 (μl)	670	3400	4000
10% (w/v) SDS (μl)	50	100	100
10% (w/v) AP (μl)	50	100	100
TEMED (μl)	5	10	10

The table shows the compositions for 4% stacking gel and 10% and 12% separating gels. The amount indicated is for the preparation of two (2) gels. AP and TEMED were added at the last step right before added into the casting frames to prevent early gelation or polymerization. Abbreviations: AP: ammonium persulfate; SDS: sodium dodecyl sulfate; TEMED: tetramethylethylenediamine.

#### **3.8.2.4 Sample preparation and running the gel electrophoresis**

SDS-PAGE was conducted using a vertical electrophoresis system (Mini-PROTEAN Tetra Cell System, Bio-Rad Laboratories, China). Thirty micrograms (30µg) of protein samples were mixed with the sample loading buffer (4X) at a ratio of 3: 1 and boiled for 10 minutes to denature the proteins. The SDS-PAGE system was set up by filling the chamber with tris/glycine/SDS running buffer and connected to a power supply system (PowerPac™ Basic Power Supply, Bio-Rad Laboratories, Singapore). Amersham ECL full range rainbow molecular weight protein markers were loaded into well with at least one well of each gel. After few minutes of cooling down, the pre-prepared protein samples were loaded into the remaining wells and the electrophoresis was run at a constant voltage of 100 volts for approximately 2 hours. Once the front dye reached the bottom of the gel, the electrophoresis was stopped and the gel was carefully removed from the glass plates.

#### **3.8.2.5 Protein transfer**

Upon the completion of the electrophoresis separation, the proteins were then transferred from the gel to a membrane using a blotting system (QNX-700: Quadra Mini-Vertical PAGE/Blotting System with internal cooling, CBS Scientific Company Inc., USA). There are two types of membranes for Western blotting: nitrocellulose and polyvinylidene difluoride (PVDF). In this experiment, the PVDF membranes were used due to its higher binding capacity and greater sensitivity in detection. PVDF membranes were first activated by soaking in methanol for 2 minutes. The activated PVDF membranes and gels were then washed in the transfer buffer for 5 minutes. Foam pads and filter papers were also pre-soaked in the transfer buffer for a few minutes. Using the blotting cassettes, the PVDF membrane and gel were sandwiched between foam pads and filter papers as shown in Figure 3.5(A). The blotting cassettes were inserted into the

core and placed into the blotting chamber (Figure 3.5(B)). The blotting system was then set up by filling the chamber with chilled transfer buffer and connected to a power supply system (PowerPac™ Basic Power Supply, Bio-Rad Laboratories, Singapore). The protein transfer by electrophoresis was conducted at a constant voltage of 100 volts for 1 hour and 45 minutes. Figure 3.5 shows preparation for protein transfer.

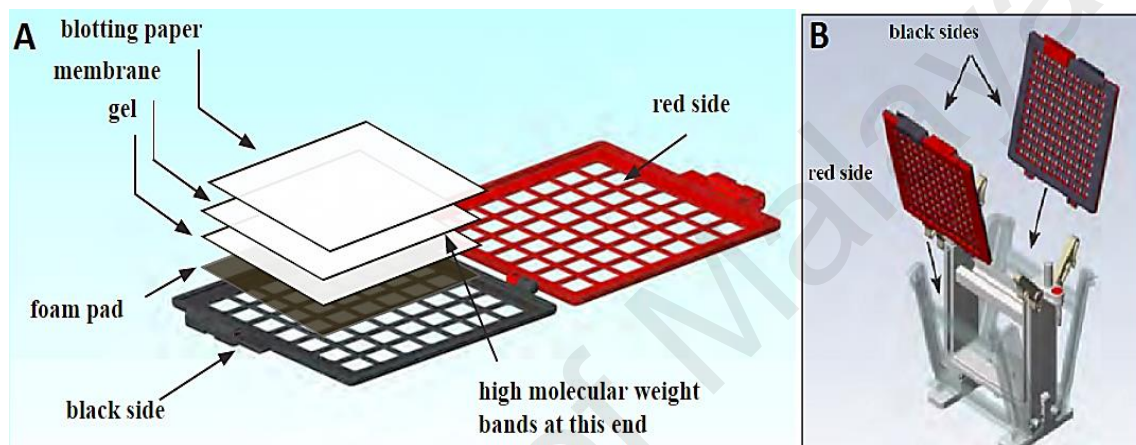


**Figure 3.5 Preparation for protein transfer.**

(A) The arrangement of blotting stack following the order (from black side): foam pad, gel, PVDF membrane and blotting paper (filter paper). (B) Blotting cassettes were inserted into the core with black side facing inward and red side facing outward. Images sourced from [www.cbsscientific.com](http://www.cbsscientific.com).

### 3.8.2.6 Membrane blocking

After the completion of the protein transfer, the membranes were removed from the blotting sandwiches and washed with ddH<sub>2</sub>O for 5 minutes. The membranes were then blocked with 2% (w/v) Amersham ECL prime blocking agent in phosphate buffer saline (PBS) for 1 hour at room temperature. After blocking, the membranes were rinsed and washed twice with PBS containing Tween-20 (PBST) for 5 minutes at room temperature.

### 3.8.2.7 Incubation with primary and secondary antibodies

The primary and secondary antibodies that were used in the immunoblotting are

shown in Table 3.3. In this experiment, the primary and secondary antibodies were diluted to in PBST at the ratio of 1: 1000 and 1: 2500 respectively. The blocked membranes were incubated with the diluted primary antibody for overnight at 4°C with agitation. Following 3 times of 5 minutes washes with PBST at room temperature, the membranes were then incubated with appropriate horseradish peroxidase (HRP)-conjugated secondary antibodies for 1 hour at room temperature with agitation. After incubation, the membranes were rinsed and washed for 3 times, 5 minutes each in PBST at room temperature. Table 3.3 shows the list of primary and secondary antibodies used in Western blotting.

**Table 3.3 List of primary and secondary antibodies used in Western blotting.**

<b>Target protein</b>	<b>Primary antibody</b>	<b>Secondary antibody</b>
<b>ENaC-<math>\alpha</math></b>	Goat polyclonal (sc-22239)	Donkey anti-goat IgG-HRP (sc-2020)
<b>ENaC-<math>\beta</math></b>	Mouse monoclonal (sc-25354)	Goat anti-mouse IgG-HRP (sc-2005)
<b>ENaC-<math>\gamma</math></b>	Rabbit polyclonal (sc-21014)	Goat anti-rabbit IgG-HRP (sc-2004)
<b>Aqp1</b>	Goat polyclonal (sc-9878)	Donkey anti-goat IgG-HRP (sc-2020)
<b>Aqp2</b>	Rabbit polyclonal (sc-28629)	Goat anti-rabbit IgG-HRP (sc-2004)
<b>Aqp3</b>	Rabbit polyclonal (sc-20811)	Goat anti-rabbit IgG-HRP (sc-2004)
<b>Aqp4</b>	Goat polyclonal (sc-9888)	Donkey anti-goat IgG-HRP (sc-2020)
<b>Aqp6</b>	Goat polyclonal (sc-14969)	Donkey anti-goat IgG-HRP (sc-2020)
<b>Aqp7</b>	Rabbit polyclonal (sc-28625)	Goat anti-rabbit IgG-HRP (sc-2004)
<b>GAPDH</b>	Rabbit polyclonal (sc-25778)	Goat anti-rabbit IgG-HRP (sc-2004)

All primary and secondary antibodies were purchased from Santa Cruz Biotechnology (USA).

### **3.8.2.8 Protein bands visualization**

The target protein bands were visualized by using SuperSignal West Dura Extended Duration Substrate detection kit according to the manufacture's manual. This kit provides a luminol-based enhanced chemiluminescent substrate for HRP with stable light output and high sensitivity detection via a CCD-based imaging system. Working solution was first prepared by mixing the stable peroxidase solution and the luminol/enhancer solution at a ratio of 1: 1. The membranes were then incubated with the working solution for 5 minutes at room temperature. The protein bands were visualized and captured using a gel imaging system with high sensitivity CCD camera (Ultra-Violet Products Ltd., Cambridge, UK). The intensity of each band was analyzed by using Image J software (Version 1.47, National Institutes of Health (NIH), USA). Housekeeping gene, GAPDH was selected as the control reference gene and the ratios of target proteins against GAPDH were calculated. All experiments were performed in triplicate and average ratios were determined.

### **3.8.3 Immunohistochemistry**

Immunohistochemistry is a common technique used to detect the distribution of a protein of interest in a specific tissue. In general, the interaction of target antigens with specific antibodies conjugated with an enzyme or a visible label allowed the visualization and identification of the specific target protein in tissues. In the present study, immunohistochemistry was carried out in order to elucidate the distribution and localization of ENaC and AQP in kidneys and their changes upon testosterone influences.

#### **3.8.3.1 Whole animal perfusion fixation**

Animals were first anesthetized via intraperitoneal injection of pentobarbital sodium

(65mg/kg). Whole animal perfusion fixation procedures were carried out as described by Gage *et al.* (Gage et al., 2012). In brief, a lateral incision through the integument and abdominal wall just beneath the rib cage was first made, followed by an incision along the diaphragm. The entire pleural cavity was exposed by cutting through the rib cage up to the collarbone at both sides. A blunted perfusion needle connected to a peristaltic pump (LongerPump, Langer Instruments, USA) was gently passed through the tip of the left ventricle of the heart and inserted into the ascending aorta. A hemostat was used to secured the needle and prevent leakage (Figure 3.6). Once the perfusion was initiated, a small incision was made at the right atrium of the heart to create an outlet. The animal was first perfused with PBS (100ml/100g body weight) at a flow rate of 15ml/minute to remove and wash the blood out from the body. Fixation was initiated by replacing PBS with 4% (w/v) paraformaldehyde (PFA) solution (100ml/100g body weight). The perfusion was stopped once the appropriate amount of fixative was reached. Kidneys were collected and fixed in 4% (w/v) PFA solution containing 30% (w/v) sucrose for overnight to three (3) days at 4°C. Figure 3.6 shows whole animal perfusion fixation procedures.

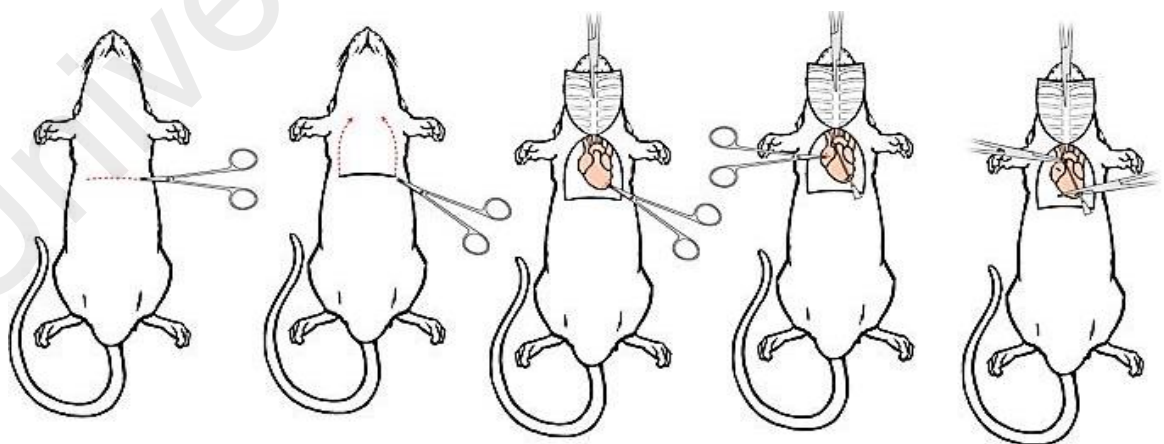


**Figure 3.6 Whole animal perfusion fixation procedures.**

A lateral incision was first made below the rib cage and the pleural cavity was exposed by cutting the rib cage until the collarbone. Perfusion needle was inserted through the left ventricle of the heart into the ascending aorta. Image sourced from Gage *et al.* (Gage et al., 2012).

### 3.8.3.2 Tissue processing and sectioning

After the immersion-fixation, all kidneys were processed using an automated tissue processing machine (Semi-enclosed Benchtop Tissue Processor, Leica, Germany). The tissue processing procedure for paraffin sections is divided into 3 parts: dehydration, clearing and wax infiltration. As melted paraffin wax is hydrophobic, all kidneys were first dehydrated in order to be infiltrated with the wax. The dehydration process was performed by immersing the tissues in a series of ethanol solution in increasing concentrations until pure. Nevertheless, wax and ethanol are largely immiscible and thus xylene was then used as an intermediate solvent to displace ethanol which then displaced by molten paraffin wax. The sequences of tissue processing procedures are shown in Table 3.4.

**Table 3.4 Sequence of tissue processing.**

<b>Step</b>	<b>Solution</b>	<b>Incubation time (hour)</b>
<b>1</b>	50% Ethanol	1
<b>2</b>	70% Ethanol	1
<b>3</b>	80% Ethanol	1
<b>4</b>	95% Ethanol	1
<b>5</b>	95% Ethanol	1
<b>6</b>	100% Ethanol (Pure)	1
<b>7</b>	100% Ethanol (Pure)	1
<b>8</b>	Xylene	1
<b>9</b>	Xylene	1
<b>10</b>	Xylene	1
<b>11</b>	Wax	1
<b>12</b>	Wax	1

All tissues were processed accordingly (approximately 12 hours) using an automated tissue processing machine prior to tissue embedding process.

After twelve (12) hours of tissue processing, the tissues were ready to be embedded in paraffin wax to maintain the natural shape and architecture of the tissue for longer term. The embedding procedure was carried out using a paraffin embedding station (Tissue Embedding Histo-Center II-N, Thermolyne Corporation, USA). In brief, a mold

was filled with molten paraffin wax and processed tissue was carefully placed into it. A cassette was placed on top of the mold, more molten wax was added and the whole thing was left on cold plate. Once the wax was completely solidified, the mold was removed. All paraffin blocks were kept at 4°C until further used.

All paraffin-embedded blocks were trimmed as necessary and subjected to sectioning using a microtome (ARM3600, Histo-Line Laboratories, Italy). The block was inserted into the microtome chuck and orientated to expose the tissue surface facing the blade. All embedded kidneys were sectioned coronally at a thickness of five micrometers (5µm). The paraffin ribbon of sections was placed on the surface of a water bath (Tissue Float Bath model 1052, GFL Gesellschaft für Labortechnik GmbH, Germany) at 37°C to allow them to flatten out. The floating sections were then mounted onto poly-L-lysine coated glass slides and allowed to dry on a hot plate (Slide/Tissue Drying Bench model 12801, MEDAX GmbH & Co, KG, Germany) at 37°C for 30 minutes. In order to ensure a complete dehydration and proper adhesion of the tissues to the slides, all glass slides were further dried in an oven at 37°C for overnight prior to the following immunoperoxidase and immunofluorescence staining processes.

### **3.8.3.3 Deparaffinization, rehydration and antigen retrieval**

Prior to immunostaining procedures, the deparaffinization and rehydration of tissue sections were performed in order to remove the embedding materials and allow the penetration of water-soluble dyes. All tissue sections were deparaffinized in 3 changes of xylene, 5 minutes each and rehydrated in a series of ethanol in decreasing concentrations (2 changes of 100% (v/v) ethanol and 2 changes in 95% (v/v) ethanol), 10 minutes each. Slides were then washed in 2 changes of PBS, 5 minutes each to remove the excessive alcohol residues. Methylene bridges were formed during tissue

fixation procedures and the cross-linking of proteins could cause the masking of antigenic sites and a reduction in the available epitopes for antibody binding. For that reason, antigen retrieval was performed to unmask the antigenic epitopes and allow the binding of antibodies and detection of target proteins. Tissue sections were immersed in sodium citrate buffer, the most commonly used buffer for antigen retrieval, and incubated at 95°C for 10 minutes. The slides were allowed to cool to room temperature for approximately 20 minutes, followed by 2 washes in PBS, 5 minutes each, before proceeding to the following immunoperoxidase or immunofluorescence staining.

#### **3.8.3.4 Immunoperoxidase staining**

In order to quench endogenous peroxidase activity, peroxidase blocking was performed with 3% (v/v) hydrogen peroxidase (H<sub>2</sub>O<sub>2</sub>) in methanol at room temperature for 30 minutes. Following two (2) washes in water for 5 minutes each, all tissue sections were blocked with 5% (w/v) BSA at room temperature for 1 hour to suppress the non-specific binding of immunoglobulin G (IgG). The slides were then washed in PBS three (3) times for 5 minutes each and incubated with primary antibody at a ratio of 1: 100 in 5% (w/v) BSA at 4°C for overnight. On the next day, tissue sections were first gently rinsed and washed in PBS three (3) times for 5 minutes each. All slides were then incubated with appropriate HRP-conjugated secondary antibodies at a ratio of 1: 200 in 5% (w/v) BSA at room temperature for 1 hour and 30 minutes. After three (3) washes in PBS for 5 minutes each, the sections were incubated in diaminobenzidine tetrahydrochloride (DAB) substrate solution at room temperature for 5 to 10 minutes. Once optimal staining was achieved, sections were rinsed with water to quench excess DAB reaction. The slides were then counterstained with Mayer's hematoxylin for about 30 seconds to visualize the nuclei and immediately washed gently with water. All slides were dehydrated through an ascending concentration of ethanol (70%, 80%, 90% and

100% (v/v) for 30 seconds each) and three (3) times of xylene bath for 30 seconds each before mounted with dibutylphthalate polystyrene xylene (DPX) mounting medium and coverslipped. All slides were left overnight in a fume hood to ensure complete dryness. All experiments were carried out on four (4) different biological replicates. The primary and secondary antibodies that were used in immunoperoxidase staining are shown in Table 3.5. All slides were observed and captured using Nikon DS Ri1 12 megapixel camera (Nikon, Tokyo, Japan) attached to Nikon Eclipse 80i microscope (SEO Enterprises Inc., Lakeland, FL, USA) at a fixed exposure time. Dark-brown stains appeared at the sites where HRP-conjugated antibodies were bind. All immunoperoxidase images were taken at 40x magnifications. Glomerulus (G), distal convoluted tubule (DT), proximal convoluted tubule (PT) and collecting duct (CD) in the kidney cortex were identified and labeled in all representative immunoperoxidase images based on the atlas of histology (Figure 3.7) (Eroschenko, 2005).

#### **3.8.3.5 Immunofluorescence staining**

For immunofluorescence staining, all sections were first incubated with appropriate 10% (v/v) normal serum in PBS at room temperature for 1 hour in order to block the non-specific binding of IgG. After one (1) wash in PBS for 5 minutes, primary antibody at a ratio of 1: 100, prepared in appropriate 1.5% (v/v) blocking serum, was added on to the sections and incubated at 4°C for overnight. On the following day, slides were washed three (3) times in PBS for 5 minutes each and incubated with appropriate IgG-fluorochrome-conjugated secondary antibodies at a ratio of 1: 200 at room temperature for 45 minutes. Following another three (3) washes in PBS for 5 minutes each, coverslips were mounted onto the slides with Ultra Cruz Mounting Medium to prevent photo-bleaching and permanently sealed with nail polisher. All slides were well kept and protected from light. The primary and secondary antibodies that were used in

immunofluorescence staining are shown in Table 3.5. The fluorescence signals from the tissues were visualized and captured using a confocal laser scanning fluorescent microscope equipped with argon/krypton laser (Leica TCS SP5 II; Leica Microsystems, Wetzlar, Germany). All experiments were performed in four (4) biological replicates and high magnification immunofluorescence images were taken with 63x oil immersion objective lens. All images were subjected to post-process by using LAS AF Lite software (Leica Microsystems, Wetzlar, Germany) and Adobe Photoshop (Adobe Systems Incorporated, California, USA). G, DT, PT and CD in the kidney cortex were identified and labeled in all representative immunofluorescence images based on the atlas of histology (Figure 3.7) (Eroschenko, 2005). Table 3.5: List of primary and secondary antibodies used in immunoperoxidase and immunofluorescence staining while Figure 3.7 shows the histology slide of kidney cortex.

**Table 3.5 List of primary and secondary antibodies used in immunoperoxidase and immunofluorescence staining.**

<b>Target protein</b>	<b>Primary antibody</b>	<b>HRP-conjugated secondary antibody for immunoperoxidase staining</b>	<b>Fluorochrome-conjugated secondary antibody for immunofluorescence staining</b>
<b>ENaC-<math>\alpha</math></b>	Rabbit polyclonal (PA1-920A)	Goat anti-rabbit IgG-HRP (sc-2004)	Donkey anti-rabbit IgG, DyLight 550 (SA5-10039)
<b>ENaC-<math>\beta</math></b>	Rabbit monoclonal (PA5-28909)	Goat anti-rabbit IgG-HRP (sc-2004)	Donkey anti-rabbit IgG, DyLight 550 (SA5-10039)
<b>ENaC-<math>\gamma</math></b>	Rabbit polyclonal (PA11-922)	Goat anti-rabbit IgG-HRP (sc-2004)	Donkey anti-rabbit IgG, DyLight 488 (SA5-10038)
<b>Aqp1</b>	Goat polyclonal (sc-9878)	Donkey anti-goat IgG-HRP (sc-2020)	Donkey anti-goat IgG, DyLight 488 (SA5-10086)
<b>Aqp2</b>	Rabbit polyclonal (sc-28629)	Goat anti-rabbit IgG-HRP (sc-2004)	Donkey anti-rabbit IgG, DyLight 550 (SA5-10039)
<b>Aqp3</b>	Rabbit polyclonal (sc-20811)	Goat anti-rabbit IgG-HRP (sc-2004)	Donkey anti-rabbit IgG, DyLight 550 (SA5-10039)
<b>Aqp4</b>	Goat polyclonal (sc-9888)	Donkey anti-goat IgG-HRP (sc-2020)	Donkey anti-goat IgG, DyLight 488 (SA5-10086)
<b>Aqp6</b>	Goat polyclonal (sc-14969)	Donkey anti-goat IgG-HRP (sc-2020)	Donkey anti-goat IgG, DyLight 488 (SA5-10086)

Primary and secondary antibodies were purchased from Santa Cruz Biotechnology (USA) and Thermo Fisher Scientific (USA).

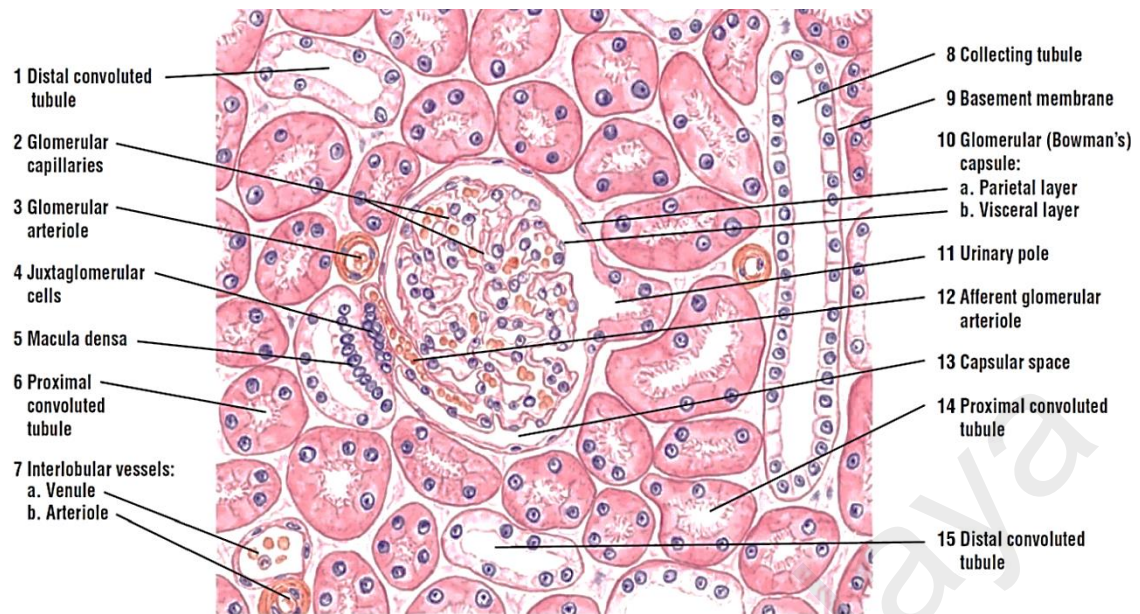


**Figure 3.7 Histology slide of kidney cortex.**

Both distal convoluted tubule (DT) and proximal convoluted tubule (PT) consist of cuboidal epithelium and are highly convoluted, nonetheless, PTs are longer, irregular in shape and have an extensive brush border (uneven luminal surface) while DTs are usually well-rounded with smooth luminal surface. On the other hand, collecting ducts (CDs) are easily distinguished from DT and PT by their well-lined cuboidal or squamous epithelium cells with distinct boundaries between adjacent cells as their cells do not interdigitate. Image sourced from *diFiore's Atlas of Histology with Functional Correlations* (Eroschenko, 2005).

### **3.9 Paraventricular nucleus (PVN), nucleus of the solitary tract (NTS) and rostral ventrolateral medulla (RVLM)**

Brain samples were collected upon the completion of hormonal treatment in **Section 3.2.4**. Paraventricular nucleus (PVN), nucleus of the solitary tract (NTS) and rostral ventrolateral medulla (RVLM) were collected (refer **Section 3.10.1.1**) and subjected to transcriptome and gene expression analysis. The transcriptome analysis using RNA-Seq was first performed on the hypertensive model (refer **Section 3.2.4**; experimental treatment groups: SMS, SMO, SFO and SFT) to reveal and identify potential candidate genes that are fundamental in the development of testosterone-induced high blood pressure by comparing the relative measure of transcriptional activity across the treatment groups. Gene expression analysis via qPCR was then performed on both normotensive and hypertensive models (refer **Section 3.2.4**; experimental treatment

groups: WMS, WMO, WFO, WFT, SMS, SMO, SFO and SFT) in order to further evaluate the expression changes of the potential candidate genes under both conditions.

### **3.9.1 Transcriptome analysis with RNA-Seq**

Transcriptome analysis by RNA-Seq, which based on next-generation sequencing technology, is now a gold standard technique to compare the differential gene expression profile of a specific cell or tissue. This technique allows the identification and detection of novel transcripts, splice variants as well as the changes in gene expression (Han et al., 2015). In the present studies, transcriptome analysis through RNA-Seq was performed on three cardiovascular-related areas in the brain *i.e.* PVN, NTS and RVLM. Hypertensive rat (refer **Section 3.2.4**; experimental treatment groups: SMS, SMO, SFO and SFT) was selected as the model for the current experiment as this study aimed to identify those genes that are fundamental in blood pressure regulation. Following the completion of sequencing steps, the genes that are differentially expressed in these areas upon testosterone treatment were identified using DESeq and edgeR, well-known statistical methods for differential expression analysis of digital gene expression data.

#### **3.9.1.1 Sample preparation**

Brains tissues (n = 3 per group where 5 samples were pooled to obtain n = 1, refer **Section 3.9.1.2**) were collected. Frozen brain was first mounted onto Tissue-Tek Optimal Cutting Temperature (OCT) compound on a chuck and placed in the cryostat (Shandon Cryotome FE and FSE Cryostats, Thermo Fisher Scientific, USA). Sixty micrometers (60µm) rostral-to-caudal sections were sliced and stained with 1% (w/v) toluidine blue in 70% (v/v) ethanol in order to facilitate the identification of the target areas in the brain. The sections were observed under a light microscope (Olympus

CX31 Binocular Microscope, New York Microscope Company, New York, USA) and mapped based on the atlas of rat brain in stereotaxic coordinates (Paxinos & Watson, 2007). Upon the identification of PVN, NTS and RVLM (Figure 3.8), a 1-mm diameter sample corer (catalog no.: 18035-01; Fine Science Tools, California, USA) was then used to collect the target areas from the unstained tissues. Figure 3.8 shows the coronal rat brain atlas diagrams from Paxinos and Watson (2009) and toluidine blue staining of neurons.

University of Malaya

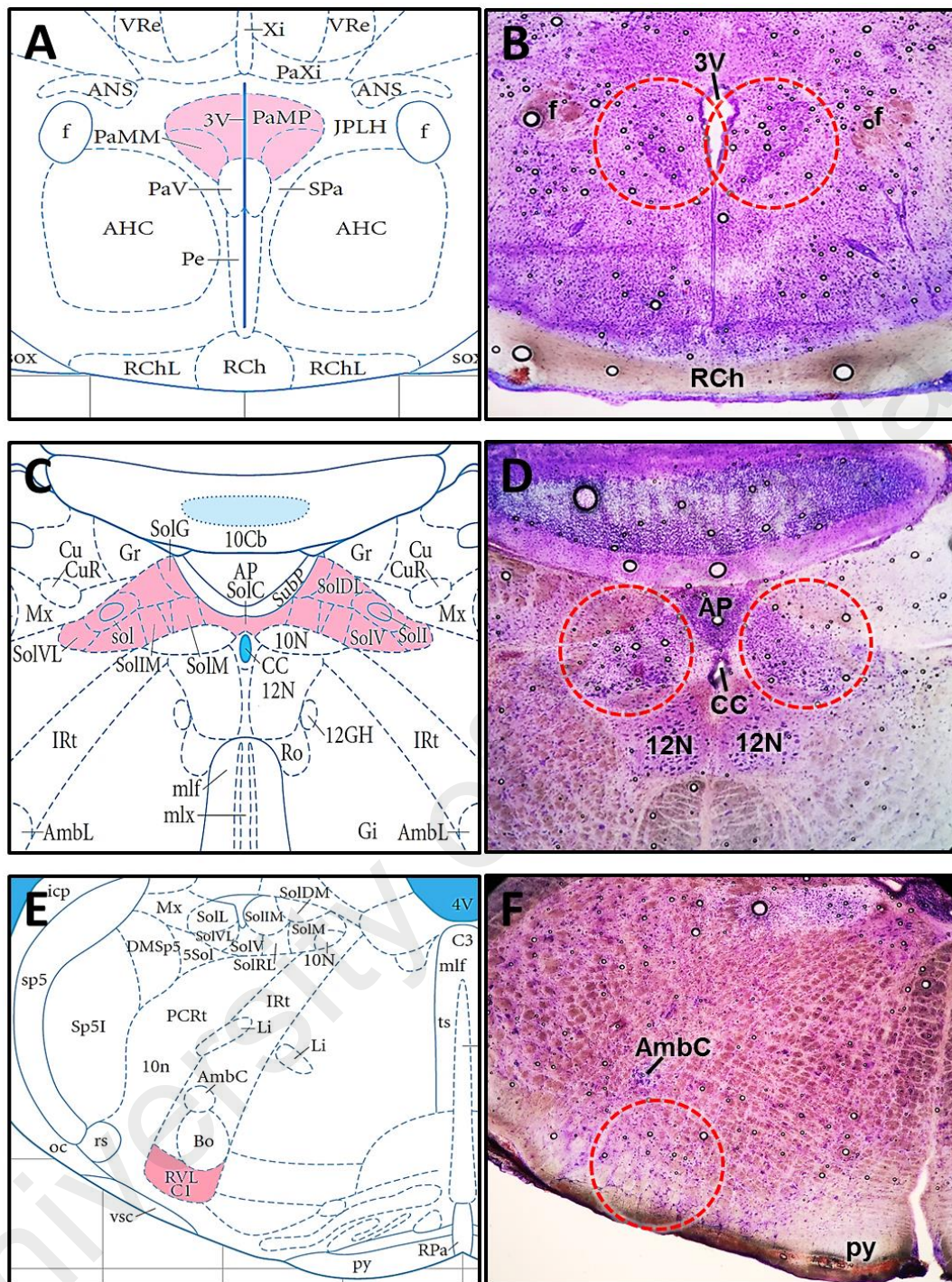


**Figure 3.8 Coronal rat brain atlas diagrams from Paxinos and Watson (2009) and toluidine blue staining of neurons.**

Schematic representations of coronal sections obtained from *The Rat Brain: In Stereotaxic Coordinates*, 6th edition (Paxinos & Watson, 2007) indicating the locations of (A) PVN, (C) NTS and (E) RVL (pink). Representative images of toluidine blue-stained coronal section (60µm) of frozen rat brain showing the sites of (B) PVN, (D) NTS and (F) RVL. PVN and NTS were easily identified by their intense blue-stained neurons while RVL was identified by using AmbC as a reference marker. All targeted areas (red circle) were collected using a 1-mm diameter sample corer. Abbreviations: 3V: 3rd ventricle; 4V: 4th ventricle; 5Sol: trigeminal-solitary transition zone; 10Cb: 10th cerebellar lobule (nodule); 10N: dorsal motor nucleus of vagus; 10n: vagus nerve; 12GH: hypoglossal nucleus, geniohyoid part; 12N: hypoglossal nucleus; AHC: anterior hypothalamic area, central part; AmbC: ambiguous nucleus, compact part; AmbL:

ambiguus nucleus, loose part; ANS: accessory neurosecretory nuclei; AP: area postrema; Bo: Botzinger complex; C3: C3 adrenaline cells; CC: central canal; Cu: cuneate nucleus; CuR: cuneate nucleus, rotundus part; DMSp5: dorsomedial spinal trigeminal nucleus; f: fornix; Gi: gigantocellular reticular nucleus; Gr: gracile nucleus; icp: inferior cerebellar peduncle (restiform body); IRt: intermediate reticular nucleus; JPLH: juxtaparaventricular part of lateral hypothalamus; Li: linear nucleus of the medulla; mlf: medial longitudinal fasciculus; mlx: medial lemniscus decussation; Mx: matrix region of the medulla; oc: olivocerebellar tract; PaMM: paraventricular hypothalamic nucleus, medial magnocellular part; PaMP: paraventricular hypothalamic nucleus, medial parvicellular part; PaV: paraventricular hypothalamic nucleus, ventral part; PaXi: paraxiphoid nucleus of thalamus; PCRt: parvicellular reticular nucleus; Pe: periventricular hypothalamic nucleus; py: pyramidal tract; RCh: retrochiasmatic area ; RChL: retrochiasmatic area, lateral part; Ro: nucleus of Roller; RPa: raphe pallidus nucleus; rs: rubrospinal tract; RVL: rostroventrolateral reticular nucleus; sol: solitary tract; SolC: nucleus of the solitary tract, commissural part; SolDL: solitary nucleus, dorsolateral part; SolDM: nucleus of solitary tract, dorsomedial part; SolG: nucleus of the solitary tract, gelatinous part; SolI: nucleus of the solitary tract, interstitial part; SolIM: nucleus of the solitary tract, intermediate part; SolL: nucleus of the solitary tract, lateral part; SolM: nucleus of the solitary tract, medial part; SolRL: nucleus of the solitary tract, rostromedial part; SolV: solitary nucleus, ventral part; SolVL: nucleus of the solitary tract, ventrolateral part; sox: supraoptic decussation; sp5: spinal trigeminal tract; Sp5I: spinal trigeminal nucleus, interpolar part; SPa: subparaventric zone of the hypothalamus; SubP: subpostrema area; ts: tectospinal tract; VRe: ventral reunions thalamic nucleus; vsc: ventral spinocerebellar tract; Xi: xiphoid thalamic nucleus.

### 3.9.1.2 RNA extraction

Three hundred microliter (300 $\mu$ l) of QIAzol lysis reagent was added into each sample and 5 samples were pooled as n = 1. Separations of RNA, genomic DNA and proteins phase were initiated by adding chloroform and centrifugation at 12,000 $\times$ g at 4 $^{\circ}$ C for 15 minutes. The upper RNA layer was transfer to a new tube and one volume of 70% (v/v) ethanol was added to promote the selective binding of RNA to the RNeasy membrane. The following RNA purification steps were carried out using Qiagen RNeasy Mini Kit according to manufacturer's protocol. In brief, the sample was first transferred to RNeasy spin column placed in a 2ml collection tube and centrifuged at 8,000 $\times$ g at 24 $^{\circ}$ C for 15 seconds to wash away all contaminants while RNA binds to the membrane. Desaltation was then performed by adding 700 $\mu$ l of RW1 buffer (stringent wash buffer), followed by two (2) washes with 500 $\mu$ l of RPE buffer (mid wash buffer). Lastly, RNA was eluted by adding 30 $\mu$ l of RNase-free water and centrifugation at

8,000×g at 24°C for 1 minute. RNAs were then transferred and stored in -80°C until further used.

### **3.9.1.3 RNA quantification and quality control**

RNA is a sensitive polymeric molecule and extremely susceptible to degradation. Thus, in order to ensure the success of subsequent downstream RNA-Seq, several methods of RNA quality assessment were carried out. The yield and purity of the extracted RNA were first examined by measuring the UV absorption of the sample using a spectrophotometer (NanoDrop™ 2000/2000c; Thermo Fisher Scientific, USA). In brief, 1µl of RNA sample was pipetted onto the lower optical pedestal and the ratios of absorbance at 260nm to 280nm (A260/A280) and 260nm to 230nm (A260/A230) were obtained. The integrity of RNA was further confirmed using Agilent RNA 6000 Nano Kit on Agilent 2100 bioanalyzer instrument (Agilent Technologies, Santa Clara, California, USA) following the manufacturer's protocol. In general, RNA samples and marker were loaded onto the RNA Nano chip in which the nucleic acid fragments were electrophoretically separated based on their size and an electropherogram was generated. Finally, the concentrations of the RNA samples were quantified using Qubit RNA High Sensitivity Assay Kit following the manufacturer's instructions. This assay allows a better accuracy in measuring the concentration of the RNA as it is highly selective towards RNA over double-stranded DNA. Briefly, pre-prepared Qubit RNA assay working solution was added to the standards or RNA samples in a total volume of 200µl. The reaction mixture was then vortexed for 3 seconds and allowed to stand at room temperature for 2 minutes. Lastly, the absorbance reading of the sample was measured on Qubit 2.0 Fluorometer (Life Technologies, Carlsbad, California, USA) and the concentration of the RNA was calculated based on the following equation.

$$\text{Concentration of RNA (ng/ml)} = \text{QF value (ng/ml)} \times \frac{200}{x}$$

where *QF value* = the value given by the Qubit 2.0 Fluorometer (ng/ml)

*x* = the microliters of RNA samples added to the assay

#### 3.9.1.4 Library preparation and quality control

Following the quality and integrity analysis of all RNA samples, RNA-Seq libraries were prepared using ScriptSeq Complete Gold Kit (Human/Mouse/Rat), which composed of Ribo-Zero Gold rRNA removal reagents and ScriptSeq v2 RNA-Seq Library Preparation Kit (Figure 3.9). All library preparation procedures were carried out according to the manufacturer's user guide. Ribo-Zero reaction buffer and rRNA removal solution which contained rRNA probes were first added to 1µg of total RNA samples to remove both cytoplasmic and mitochondrial rRNAs. The rRNA-depleted RNA samples were then purified using ethanol precipitation technique in which RNAs were precipitated by adding sodium acetate and 100% (v/v) ethanol, followed by two (2) washes with 70% (v/v) ethanol and air dried. These purified rRNA-depleted RNA pellets were then dissolved in clean RNase-free water and further processed using ScriptSeq v2 RNA-Seq Library Preparation Kit, following the manufacturer's instruction, in order to produce cDNA sequencing libraries. In general, the RNA samples were first fragmented in RNA fragmentation solution into short fragments, which served as the templates for cDNA synthesis. These templates were annealed with random cDNA synthesis primer and the first-strand cDNAs were synthesized in the presence of cDNA premix (oligo dT), dithiothreitol (DTT) and reverse transcriptase. These single-stranded cDNAs were then labeled with 3'-terminal-tagging oligos and di-tagged single-stranded cDNAs were generated. Finally, all RNA-Seq libraries were labeled with an index and double-stranded cDNAs were produced and amplified by PCR using ScriptSeq index reverse PCR primer, forward PCR primer, FailSafe PCR

premix (oligo dT) and FailSafe PCR enzyme. It is essential to ensure the high quality of the initial starting material for library preparation as well as the samples as they progress through the preparation workflow and thus the library quality controls were performed. The yield and quality of the RNA-Seq libraries were assessed using Agilent High Sensitivity DNA Kit following the manufacturer's protocol. In brief, the samples and marker were loaded onto the High Sensitivity DNA chip and run on Agilent 2100 bioanalyzer instrument (Agilent Technologies, Santa Clara, California, USA). The nucleic acid fragments in the samples were electrophoretically separated based on their size and an electropherogram was generated. The concentrations of the RNA-Seq libraries were also quantified using Qubit dsDNA High Sensitivity Assay Kit following the manufacturer's guidance. Freshly prepared Qubit dsDNA assay working solution was first added to the standards or sample libraries in a total volume of 200µl. Following 3 seconds of vortexing and 2 minutes of incubation at room temperature, the fluorescence signal of the sample was read by Qubit 2.0 Fluorometer (Life Technologies, Carlsbad, California, USA) and the concentration of the cDNA was calculated based on the equation shown.

$$\text{Concentration of cDNA (ng/ml)} = QF \text{ value (ng/ml)} \times \frac{200}{x}$$

where *QF value* = the value given by the Qubit 2.0 Fluorometer (ng/ml)

*x* = the microliters of cDNA libraries samples added to the assay

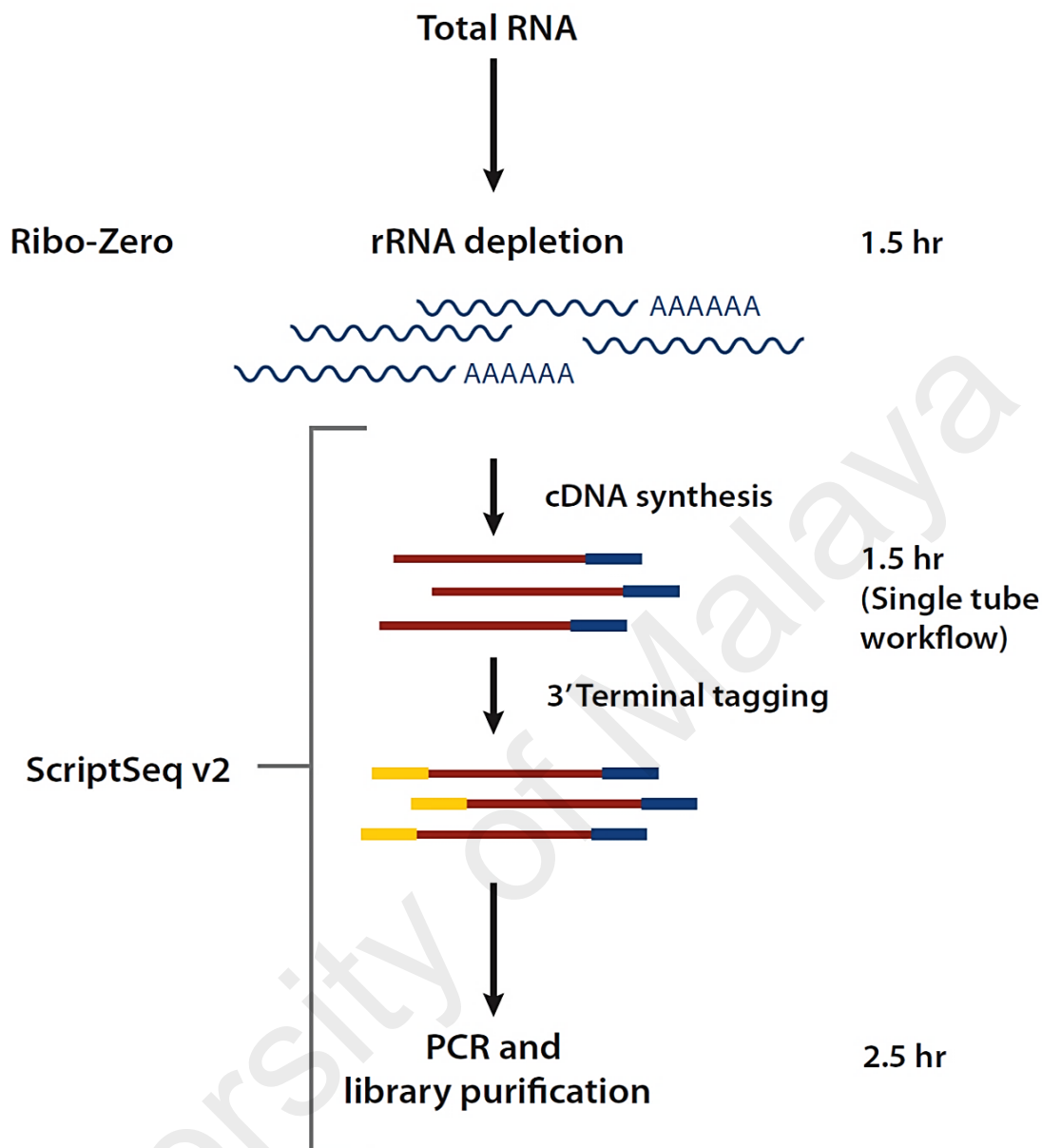


**Figure 3.9 Simplified flow chart of RNA-Seq library preparation using ScriptSeq Complete Gold Kit (low input).**

After the quality and integrity analysis of the RNA samples, ribosomal RNAs (rRNAs) were first removed by Ribo-Zero Gold rRNA removal reagents using sequence-specific oligos and bead-based extraction method. RNA-Seq libraries were then generated from rRNA-depleted RNA samples using the ScriptSeq v2 RNA-Seq Library Preparation Kit in which these RNAs were first fragmented, reverse transcribed using 5'-tagged primers, followed by 3'-tagging, index-labeling and PCR amplification.

### 3.9.1.5 Library qualification via qPCR

In order to ensure the optimum output of the downstream sequencing analysis, the quantification of the number of amplifiable molecules in prepped library was performed using KAPA Library Quantification Kit according to the manufacturer's manual.

Following the RNA-Seq library validation analysis through bioanalyzer and Qubit assay, the unit for concentration of cDNA in all RNA-Seq libraries were first converted from *ng/ml* (obtained from Qubit assay) to *nM* based on the following equation.

$$\text{Concentration of cDNA (nM)} = \frac{\text{Concentration of cDNA (ng/ml)}}{600\text{g/mol} \times L \text{ value(bp)}} \times 10^6$$

Where *L value* = the average library fragment length given by Bioanalyzer (bp)

660g/mol = average mass of 1bp dsDNA

The concentration of cDNA in RNA-Seq library was then normalized into 10nM by adding 5 $\mu$ l of cDNA library stock with appropriate volume of elution buffer (10mM Tris-HCl, pH 8.0) containing 0.1% (v/v) Tween-20. A 10,000-fold dilution of 10nM-normalized libraries was performed prior to the setup of the qPCR reaction as to ensure the coverage of the libraries concentration within the dynamic range of the DNA standards (0.0002pM, 0.002pM, 0.02pM, 0.2pM, 2pM and 20pM) provided in the KAPA kit. All assays were performed in triplicate in which a total of 20 $\mu$ l of reaction mixture containing 10 $\mu$ l of 2x KAPA SYBR fast qPCR master mix, 2 $\mu$ l of 10x primer premix, 4 $\mu$ l of PCR-grade and 4 $\mu$ l of DNA standard or diluted library cDNA water was loaded into each well of the Eco qPCR plate. Real-time thermal cycle reaction was then performed on Eco real-time PCR system (Illumina, San Diego, California, USA) according the manufacturer's protocol *i.e.* an initial denaturation at 95°C for 5 minutes, followed by 35 cycles of denaturation at 95°C for 30 seconds and annealing/extension at 60°C for 45 seconds. The concentration of cDNA in each library was analyzed and quantified based on the amplification activity using Eco real-time PCR system software version 5.0 (Illumina, San Diego, California, USA). Using the mean quantity of cDNA estimated by qPCR, the concentration of undiluted 10nM-normalized cDNA libraries were calculated based on the following equation.

$$\text{Concentration of } 10\text{nM-normalized cDNA (nM)} = \frac{\text{Eco value (pM)}}{1000} \times \frac{452 \text{ bp}}{L \text{ value (bp)}} \times DF$$

where *Eco value* = mean quantity of cDNA given by Eco real-time PCR system (pM)

1000 = pM to nM

452bp = the average fragment length of KAPA Illumina DNA standard

*L value* = the average library fragment length given by Bioanalyzer (bp)

*DF* = dilution factor (10,000-fold)

Finally, the concentration of cDNA in RNA-Seq library was normalized into 4nM by adding 5µl of 10nM-normalized cDNA library stock with appropriate volume of elution buffer (10mM Tris-HCl, pH 8.0) containing 0.1% (v/v) Tween-20.

### 3.9.1.6 MiSeq library quality control

Three microliter (3µl) from 36 prepped 4nM RNA-Seq libraries (3 targeted brain areas of 4 treatment groups with n = 3, giving a total number of 36 samples) were pooled and sequenced on the Illumina MiSeq platform (Illumina, San Diego, California, USA) using MiSeq Reagent Kit v2. The purposes of MiSeq sequencing are to validate the efficiency of the library clustering and identify the possible under- or over-clustering of the particular library as a result of sample pooling. The volume of each library pooled was adjusted based on the outcomes of MiSeq library sequencing in order to ensure an optimum performance and high output of the downstream HiSeq sequencing. In order to obtain one milliliter (1ml) of 20pM denatured library, 5µl of 4nM pooled was added to 5µl of 0.2N sodium hydroxide (NaOH), vortexed, centrifuged at 280×g for 1 minute, incubated at room temperature for 5 minutes and finally diluted with 990µl of HT1 (hybridization buffer). Six hundred microliter (600µl) of 20pM denatured library was pipetted into the load sample reservoir on the reagent cartridge. The paired-end single lane flow cell (standard 14 tiles) was rinsed with nuclease-free water, dried and cleaned

with alcohol wipe before placing in the flow cell compartment on the MiSeq sequencer. The reagents and the reagent cartridge were then loaded into the reagent chiller compartment in which the reagents were held at proper temperature. Using the MiSeq control software (MSC), the MiSeq sequencing run was initiated and the quality scores (Q-score) of each cycle that indicate the probability of wrong base call was closely monitored using the Real Time Analysis (RTA) software during the run. After the run completed, the number of clusters passing filter (PF) and the percentage of clusters passing filter (%PF), an indication of signal purity from each cluster, were obtained and analyzed using MiSeq Reporter software. The number of reads per microliter ( $\mu\text{l}$ ) for each library and the volume of library to achieve an ideal number of reads were estimated based on the equations below.

$$\text{Reads } /\mu\text{l} = PF \times \frac{\%PF}{100\% \times V}$$

$$\text{Ideal reads} = \frac{T \text{ reads}}{LP \text{ value}}$$

$$\text{Volume of 4nM library} = \frac{\text{Ideal reads}}{\text{Reads}/\mu\text{l}}$$

where  $PF$  = the number of clusters that passed the quality filter

$\%PF$  = the percentage of clusters passing filter

$V$  = the volume of library in pooled library ( $3\mu\text{l}$ )

$T \text{ reads}$  = the total reads of pooled library given by a single MiSeq run

$LP \text{ value}$  = the number of libraries pooled (36 libraries)

The sample library used in the following HiSeq run were then prepared by re-polling the 36 prepped 4nM RNA-Seq libraries based on the volume determined from the MiSeq sequencing analysis.

### 3.9.1.7 HiSeq sequencing

The sequencing of the re-pooled 4nM library sample after MiSeq optimization step was accomplished using the HiSeq2500 sequencing platform (Illumina, San Diego, California, USA). The library sequencing run was performed on HiSeq high output mode with a single flow cell for 100bp, paired-end (2×100bp) reads, in which a minimum output of 30 million single cluster reads was predicted.

TruSeq Paired-End (PE) Cluster Kit v3- cBOT-HS was first used to cluster the sequencing flow cell using an automated cBOT Cluster Station (Illumina, San Diego, California, USA). Prior to the cluster generation, library denaturation and dilution was carried out to obtain a 20pM denatured library by adding 5µl of re-pooled 4nM library sample to 5µl of nuclease-free water and 10µl freshly prepared 0.1N sodium hydroxide (NaOH), the sample was then vortexed, centrifuged at 280×g for 1 minute and incubated at room temperature for 5 minutes before diluting with 980µl of HT1 (hybridization buffer). One hundred twenty microliters (120µl) of prepared 20pM denatured library was loaded into each tube of an 8-tube strip. The 96-well cBot reagent plate prefilled with cluster generation reagents was thawed in room temperature water bath and placed onto the reagent stage while the flow cell was rinsed with clean deionized water, dried and positioned on the thermal stage with the port holes facing upward. The single-use manifold was then placed over the flow cell and aligned with the guide pins on the thermal stage before securing with the flow cell clamp. Lastly, the 8-tube strip containing prepared 20pM denatured library was loaded in an orientation that the tubes were numbered from right to left on the template row and the cluster generation run was initiated upon the successful completion of the pre-run check.

The subsequent sequencing workflow was carried out on the high output single-

indexed mode in a 4-camera epifluorescence HiSeq 2500 sequencer using TruSeq SBS Kit v3-HS (200 cycles). For both Read 1 and Read 2 sequencing, ICB (incorporation mix) was prepared by adding 2 tubes of LFN36 (long read nucleotide mix) and 1.1ml of EDP (enhanced DNA polymerase) to 47ml of ICB stock buffer. The caps of all SBS reagents (ICB, PW1, SRE, CMR, SB1, SB2 and SB3) were replaced with funnel caps before placing in an associated numbered position onto the SBS reagent rack for flow cell A (Table 3.6). Meanwhile, HP3 solution for Read 1 single-indexed run was prepared by diluting 175 $\mu$ l of HP3 stock solution to 3325 $\mu$ l of PW1 (wash buffer). The Read 1 indexing reagents, HP3 (diluted), HP8 and HT2 were then placed onto the PE reagent rack at the position 17, 18 and 19 respectively while 15ml conical tubes filled with 10ml of laboratory-grade water were placed onto the unused positions (Table 3.7). The reagent priming was performed by placing the priming flow cell on the flow cell holder and measuring the volume of waste collected from each flow cell waste tubes (1.75ml per tube). The Read 1 sequencing run was then initiated by replacing the priming flow cell with the clustered flow cell from cBot and the running progress was monitored through the Real-Time Analysis (RTA) software. Upon the completion of Read 1 sequencing and index reads, the ICB buffer on position 1 of SBS reagent rack was replaced with a freshly prepared ICB (Table 3.6). HP3 solution for Read 2 paired-end run was prepared by diluting 150 $\mu$ l of HP3 stock solution was diluted with 2850 $\mu$ l of PW1 (wash buffer). The Read 2 paired-end resynthesis reagents, RMR, LMX2, BMX, AMX2, APM2, AT2, HP7, HP3 (diluted) and HT2 were then placed onto the PE reagent rack at the position 10, 11, 12, 13, 14, 15, 16, 18 and 19 respectively and the sequencing run was resumed (Table 3.7).

During the sequencing run, images analysis data was generated by Instrument Control Software (ICS) on the instrument computer based on the run parameters

inserted in the run setup. The intensities of the images were then analyzed using Real-Time Analysis (RTA) software to produce a set of primary output files which includes a base call file (\*.bcl) and a filter file (\*.filter) for each tile (a small imaging area on the flow cell viewed by the camera) per cycle, a cluster location file (\*.locs) for each cluster on the flow cell and a statistics file (\*.stats) for each run cycle. Finally, using the bcl2fastq conversion software v1.8.4 (Illumina, San Diego, California, USA), the per cycle \*.bcl files, which contain the base call and associated quality score, were combined, demultiplexed based on the indexed adaptors and translated into per read FASTQ files, an industry standard format supported by a wide variety of next generation sequencing manufacturers. The generated FASTQ format files, which contain the information, raw sequences and quality scores for all reads that passed the quality filter, were used as the sequence input for alignment and gene expression quantification in the downstream secondary analysis steps.

**Table 3.6 The position of SBS Reagents in TruSeq v3 sequencing mode.**

Position	Reagent Name	Description
1	ICB	Incorporation Mix
2	PW1	25ml of PW1 or laboratory-grade water
3	SRE	Scan Mix Reagent
4	SBS Buffer 1 (SB1)	High Salt Buffer
5	SBS Buffer 2 (SB2)	Incorporation Wash Buffer
6	SBS Buffer 2 (SB2)	Incorporation Wash Buffer
7	CMR	Cleavage Mix Reagent
8	SBS Buffer 2 (SB3)	Cleavage Buffer

Cleavage mix reagent (CMR) and scan mix reagent (SRE) were thawed at 2°C to 8°C prior to use. Incorporation mix (ICB) at position 1 was prepared by mixing the ICB stock buffer with the long read nucleotide mix (LFN36) and the enhanced DNA polymerase (EDP). The cap of each reagent bottle was replaced with a funnel cap and placed onto the SBS reagent rack for flow cell A. CMR was loaded last in order to prevent cross contamination. Upon the completion of Read 1 and index reads, the ICB was replaced with freshly prepared ICB for Read 2 resynthesis.

**Table 3.7 The position of PE Reagents for Read 1 and Read 2 in TruSeq v3 sequencing mode.**

Position	Reagent Name	Description	Read 1	Read 2
10	RMR	Resynthesis Mix	-	✓
11	LMX2	Linearization Mix 2	-	✓
12	BMX	Blocking Mix	-	✓
13	AMX2	Amplification Mix 2	-	✓
14	APM2	AMX2 Premix	-	✓
15	AT2	100% Formamide	-	✓
16	HP7	Read 2 Sequencing Primer Mix	-	✓
17	HP8	Index 1 Sequencing Primer Mix	✓	-
18	HP3	Denaturation Solution	✓	✓
19	HT2	Wash Buffer	✓	✓

In Read 1 sequencing run, HP8, HP3 (diluted for Read 1) and HT2 were placed at the position 17, 18 and 19 respectively while 15ml conical tubes filled with laboratory-grade water were placed at the unused positions. In Read 2 resynthesis run, RMR, LMX2, BMX, AMX2, APM2, AT2, HP7, HP3 (diluted for Read 2) and HT2 were placed at the position 10, 11, 12, 13, 14, 15, 16, 18 and 19 respectively.

### 3.9.1.8 Data analysis

Three targeted brain areas (PVN, NTS and RVLM) of four (4) experimental treatment groups (refer **Section 3.2.4**; experimental treatment groups: SMS, SMO, SFO and SFT) were analyzed in biological triplicates, giving a total of 36 datasets. All data analysis protocols were performed in a terminal window of Unix-like operating system, Linux, with a bash shell. The Unix and R commands used for the differential expression analysis of RNASeq data were as described by Anders *et al.* (Anders et al., 2013). Paired-end RNA-Seq reads (2×100bp) were assembled, mapped and annotated to the rat (*Rattus norvegicus*) reference genome sequence assembly (rn5, FASTQ format downloaded from *Ensembl.org*) using TopHat (Trapnell et al., 2010), a well-known spliced read aligner, to generate sequence alignments. The default parameter settings were used, allowing only a maximum of two mismatches in the alignment. The aligned sequence files in BAM format (*accepted\_hits.bam*) were subsequently processed using HTSeq-count (Anders et al., 2015) for transcriptome raw hits counts. The raw reads count data output files were then assembled into a matrix and analyzed using the DESeq (Anders & Huber, 2010) and edgeR (Robinson et al., 2010) statistical tools. Both DESeq and edgeR methods quantified the readouts and compare the relative measure of differentially expressed genes by assuming a negative binomial distribution for the gene read count data. The results of differential gene expression analysis by DESeq and edgeR were presented in table form and saved as comma-separated values (\*.csv) files. The average read counts, fold changes and significant values (*P* value) were shown in the table and the following sorting analysis was performed using Microsoft Excel software (Microsoft Corporation, USA). Figure 3.10 shows the workflow for transcriptome analysis study by RNA-Seq.

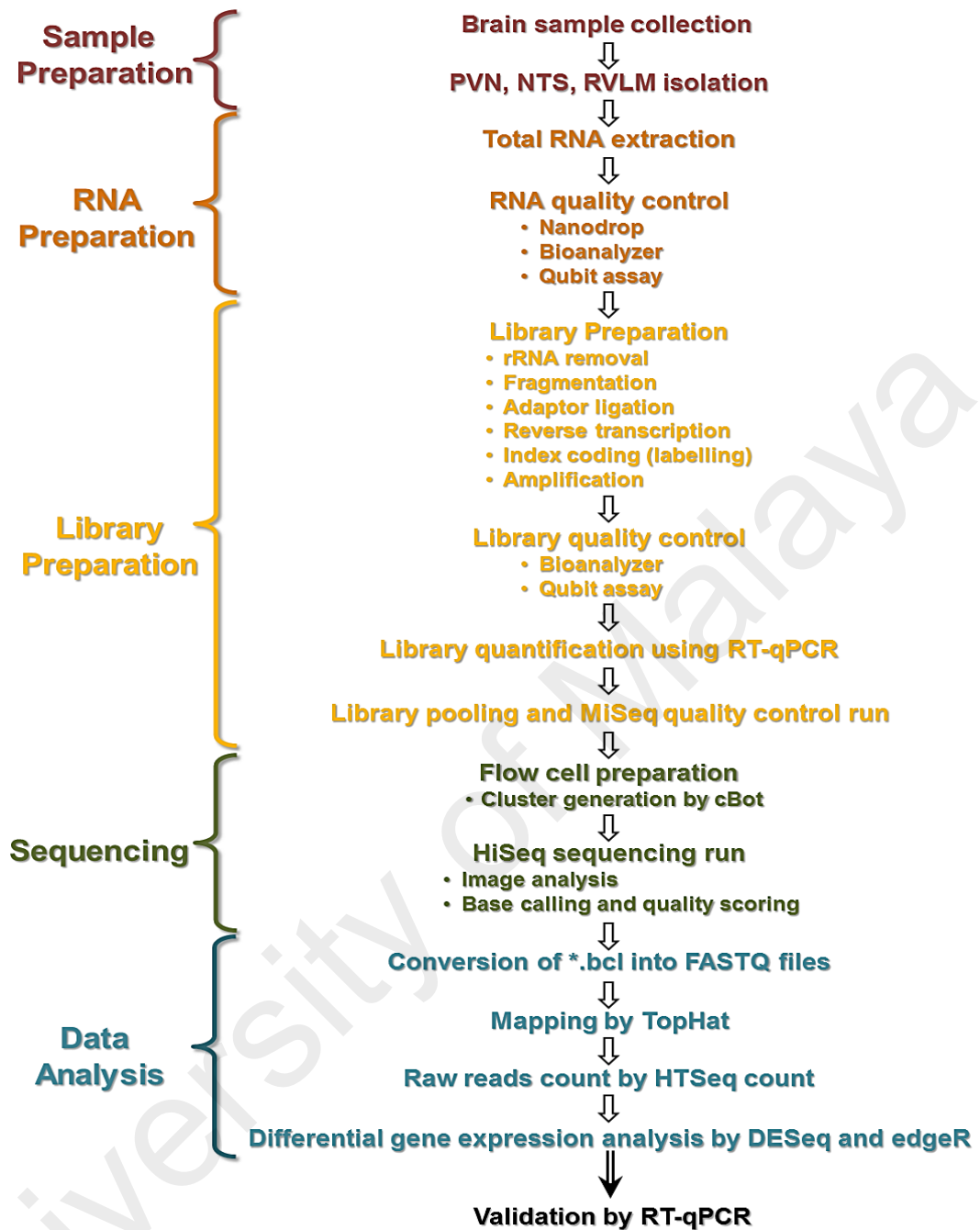


**Figure 3.100 Workflow for transcriptome analysis study by RNA-Seq.**

PVN, NTS and RVLM were isolated from the whole brain, RNAs were extracted and subjected to quality control assessments prior to library preparation. After the qPCR quantification, the prepped libraries were then normalized into 4nM, pooled and assessed via MiSeq quality control run. Following that, cluster generation was performed on cBot using the re-pooled library sample (based on the MiSeq analysis) prior to the sequencing on HiSeq high-throughput sequencing platform. Upon the completion of the sequencing run, the HiSeq data was obtained and converted into FASTQ format which then used as the sequence input for the subsequent analysis. RNA-Seq data was first assembled, mapped and annotated to the rat reference genome sequence using TopHat and the raw reads count data was then analyzed using the statistical tools, DESeq and edgeR. A number of candidate genes were identified and RT-qPCR was performed in order to further identify the changes in the expression levels of these genes.

### **3.9.2 Real-time quantitative polymerase chain reaction (qPCR)**

Lists of candidate genes expressed in PVN, RVLM and NTS were selected based on the differentially expressed genes analysis. qPCR was performed to validate and evaluate the expression changes of these genes. Both normotensive and hypertensive models (refer **Section 3.2.4**; experimental treatment groups: WMS, WMO, WFO, WFT, SMS, SMO, SFO and SFT) were used in the present experiment in order to study the differential expression of these potential genes in different hypertensive conditions.

#### **3.9.2.1 Sample preparation and RNA extraction**

Brains tissues (n = 6 per group) were collected following the completion of the hormonal treatment. PVN, NTS and RVLM were identified and isolated from the whole brain as described in **Section 3.9.1.1**. RNAs were extraction from these tissues according to the protocols mentioned in **Section 3.9.1.2**.

#### **3.9.2.2 RNA quantification and quality control**

Due to the limited and small tissue sample size, the yield and purity of the RNAs extracted from individual PVN, NTS and RVLM were assessed based on the absorbance readings at 260nm and 280nm. One microliter (1 $\mu$ l) of the RNA sample was loaded onto the lower optical measurement pedestal of a spectrophotometer (NanoDrop<sup>TM</sup> 2000/2000c, Thermo Fisher Scientific, USA) and the concentration of RNA in ng/ $\mu$ l, the ratio of absorbance at 260nm to 280nm (A<sub>260/280</sub>) and 260nm to 230nm (A<sub>260/230</sub>) were obtained.

#### **3.9.2.3 cDNA synthesis**

cDNA was synthesized from 150-300ng of total input RNA using Quantitect reverse transcription kit. The reverse transcription protocols were carried out according to the

manufacturer's guidelines with slight modification. In brief, 12µl of samples containing 150-300ng of RNAs were first added with 2µl of genomic DNA wipeout and immediately placed onto the ice after 2 minutes of incubation at 42°C. The reverse transcription master mix containing 1µl of reverse transcription primer mix, 1µl of QuantiScript reverse transcriptase and 4µl of QuantiScript reverse transcription buffer, was then added to the samples, followed by 30 minutes of incubation at 42°C and 3 minutes of incubation at 95°C. The newly synthesized cDNAs were stored at -20°C or immediately proceeded to qPCR.

#### 3.9.2.4 qPCR procedures

The expression levels of selected genes in PVN, NTS and RVLM were quantified using qPCR. All primers were designed using the NCBI PrimerBLAST tool (<http://www.ncbi.nlm.nih.gov/tools/primer-blast/>) according to the specifications discussed in **Section 3.8.1.4**. The sequences of the primers that were used in the current experiment were shown in **Appendix C**. All primers were synthesized by Integrated DNA Technologies and primers efficiency was validated using serial dilutions of cDNA prior to all experiments. The qPCR reaction assay was performed using QuantiNova SYBR Green PCR Kit on StepOne Plus Real-Time PCR Systems (Applied Biosystems, California, USA). In each assay (well), a total of 12µl of reaction mixture containing 6µl of 2x SYBR Green PCR master mix, 2µl of QN ROX reference dye, 0.7µM of forward primer, 0.7µM of reverse primer and 2µl of earlier synthesized cDNA was prepared. All assays were carried out in duplicate. The assay cycle was programmed according to the manufacturer's protocol in which the PCR reaction was first activated by heat at 95°C for 2 minutes, followed by 40 cycles of denaturation step at 95°C for 5 seconds and annealing/extension steps at 60°C for 10 seconds. The expression levels of housekeeping genes, *Rpl19*, *Gapdh* and *Actb* in PVN, NTS and RVLM were evaluated

and *Rpl19* was selected as the reference genes for all three areas. The relative mRNA quantifications were calculated based on the comparative  $2^{-\Delta\Delta Ct}$  method (Livak & Schmittgen, 2001).

### **3.9.3 Immunohistochemistry**

Hypothalamic PVN has been well-known for its role as the cardiovascular control central in the brain and thus immunohistochemistry was performed in order to evaluate the changes in protein expression and distribution of *Exphx2* and *Fcrl2*, genes identified from the differential gene expression analysis and validated via qPCR, in the PVN upon testosterone treatment. Both normotensive and hypertensive models were used in the present experiment in order to examine the differential expression of these proteins in different hypertensive conditions.

#### **3.9.3.1 Whole animal perfusion fixation**

Whole animal perfusion fixation procedures were carried out as described in **Section 3.8.3.1**. Upon the completion of the fixation flow, the brains were then collected. All brains were post-fixed and dehydrated in 30% (w/v) sucrose in 4% (w/v) PFA solution for overnight to three (3) days at 4°C. The brain was removed from the sucrose solution after it was seen to shank to the bottom (an indicator of complete dehydration). The brain was then briefly rinsed with distilled water, dried and placed onto a balance boat, which was then gently dipped on the surface of liquid nitrogen, allowing the slow frozen of the brain without cracking. The brain samples were transferred and stored at -80°C once they were completely frozen.

### 3.9.3.2 Tissue preparation and sectioning

Frozen perfused brain was first mounted onto Tissue-Tek Optimal Cutting Temperature (OCT) compound on a chuck and placed in the cryostat (Shandon Cryotome FE and FSE Cryostats, Thermo Fisher Scientific, USA). Forty micrometers (40µm) rostral-to-caudal sections were sliced and tissue sections of the regions of interest were collected in 24-wells plates containing cold PBS. In order to affirm the correct regions of interest collected, the sections of tissues were then observed under a light microscope (Olympus CX31 Binocular Microscope, New York Microscope Company, New York, USA) and PVN was identified based on the atlas of rat brain in stereotaxic coordinates (Paxinos & Watson, 2007). Tissue sections that containing PVN were kept in PBS at 4°C until further process (not longer than 2 weeks).

### 3.9.3.3 Double immunofluorescence staining

Brain sections containing PVN were washed three (3) times in PBS for 5 minutes each and blocked in 5% (w/v) BSA in PBS containing 0.3% (v/v) TritonX-100 for 30 minutes at room temperature with constant agitation. The sections were then transferred and incubated with primary antibodies (*Ephx2* and *Fcrl2*) at a ratio of 1: 100 in 5% (w/v) BSA in PBS containing 0.3% (v/v) TritonX-100 at 4°C for overnight, with gentle agitation. Next day, following three (3) washes with PBS, 5 minutes each, all sections were incubated with appropriate fluorochrome-conjugated secondary antibodies at a ratio of 1: 500 in 5% (w/v) BSA in PBS containing 0.3% (v/v) Triton X-100 at room temperature for 2 hours. After the incubation, the sections were then washed three (3) times in PBS for 5 minutes each under aluminum foil covered, mounted onto the glass slides with 0.5% (w/v) gelatin using a fine brush and air-dried in dark area. In order to preserve the fluorescence staining signals of the tissue sections, the glass slides were coverslipped with UltraCruz Mounting Medium and permanently sealed with nail

polisher. All experiments were performed in four (4) biological replicates. The primary and secondary antibodies that were used in this experiment are listed in Table 3.8. The fluorescent signals were observed and captured using a confocal laser scanning fluorescent microscope equipped with argon/krypton laser (Leica TCS SP5 II; Leica Microsystems, Wetzlar, Germany). High magnification immunofluorescence images were taken with 20x oil immersion objective lens and representative images were presented. All images were subjected to post-process by using LAS AF Lite software (Leica Microsystems, Wetzlar, Germany) and Adobe Photoshop (Adobe Systems Incorporated, California, USA).

**Table 3.8 List of primary and secondary antibodies used for double immunofluorescence staining in PVN.**

<b>Target Protein</b>	<b>Primary antibody</b>	<b>Fluorochrome-conjugated secondary antibody</b>
<b>Ephx2</b>	Rabbit polyclonal (orb5166)	Donkey anti-rabbit IgG, Dy Light 550 (SA5-10039)
<b>Fcrl2</b>	Goat polyclonal (sc-161583)	Donkey anti-goat IgG, Dy Light 488 (SA5-10086)

Primary antibody, rabbit anti-Ephx2 and goat anti-Fcrl2, were purchased from Biorbyt Ltd. (UK) and Santa Cruz Biotechnology, Inc. (Texas, USA) respectively while all secondary antibodies were purchased from Thermo Fisher Scientific (USA).

### **3.10 Statistical analysis**

All data were analyzed with SPSS Statistics (IBM Analytics, New York, USA) and Graphpad Prism (GraphPad Software, California, USA) and are expressed as mean  $\pm$  standard error of mean (SEM). Independent unpaired Student's *t*-test was used to detect the statistically significant differences between two groups. Comparisons between more than two groups were made using one-way analysis of variances (ANOVA) with Tukey's *post-hoc* test. Probability level less than 0.05 ( $P < 0.05$ ) was considered as significant.

## CHAPTER 4: EFFECTS OF TESTOSTERONE ON MEAN ARTERIAL PRESSURE (MAP)

### 4.1 Introduction

The relationship between sex hormones and blood pressure has long been observed (Hughes et al., 1989; Wenner & Stachenfeld, 2012). Gender difference in blood pressure has been well documented in which men have higher blood pressure as compared to aged-matched women before menopause (Dubey et al., 2002; Maranon & Reckelhoff, 2013; Sandberg & Ji, 2012). Studies have shown that testosterone plays a role in the gender difference in blood pressure regulation, however the outcomes of the studies were contradicting. Previously, studies have reported an inverse relationship between blood pressure and plasma testosterone levels in men (Fogari et al., 2005; Khaw & Barrett-Connor, 1988; Vlachopoulos et al., 2016). Nevertheless, there are also evidence of the association between the higher plasma testosterone levels with the higher blood pressure and arterial stiffness in men (Fogari et al., 2005; Svartberg et al., 2004) while in women, an increase in risk of hypertension was observed in patient with high plasma testosterone level *i.e.* polycystic ovary syndrome (PCOS) (Chen et al., 2007; Echiburú et al., 2016).

Effects of testosterone on blood pressure regulation have been documented in animals. In hypertensive rats, the level of testosterone was shown to correlate with the mean arterial pressure (MAP) (Dubey et al., 2002; Filgueira et al., 2012; Jenkins et al., 1994; Liu & Ely, 2011; Reckelhoff et al., 2000). However, in some studies, testosterone was found to have no effect on the blood pressure (Ganten et al., 1989; Mishra et al., 2016). Thus, in the current study, the effects of testosterone deficiency following orchidectomy and sub-chronic (seven days) testosterone replacement on blood pressure

in normotensive male rats were first examined. The involvement of androgen receptor (AR) and 5 $\alpha$ -dihydrotestosterone (DHT) were also accessed by co-administrating with the AR blocker, flutamide and 5 $\alpha$ -reductase inhibitor, finasteride. In addition, the effects of longer-term gonadectomies on blood pressure and plasma testosterone levels were also investigated in both normotensive and hypertensive rats in order to elucidate the influences of this hormone in the pathophysiology of hypertension.

In females, the effects of sex steroid hormones on blood pressure are far more complex and less well understood as compared to effects of these hormones on blood pressure in males. To date, numerous studies have shown the influences of estrogen on blood pressure in females (De Melo et al., 2016; Goldman et al., 2009; Takezawa et al., 1994). Nonetheless, there are limited findings with regards to the effect of testosterone on blood pressure regulation in females. The level of testosterone was found to fluctuate throughout female reproductive cycle, which suggested that this hormone could possibly responsible for the mild blood pressure fluctuation observed throughout the cycle (Falvo et al., 1974; Linton et al., 2016; Rothman et al., 2011; Rush & Blake, 1982). This study examined the changes in blood pressure as well as plasma testosterone level throughout the female reproductive cycle under both normotensive and hypertensive conditions. Additionally, in view of the limited information available and an effort to avoid possible conflicting effects of other male factors, *e.g.* Y chromosome (Ely et al., 1994) and female hormones (Maranon & Reckelhoff, 2013), the effects of chronic (six weeks) testosterone treatment on blood pressure were then investigated in ovariectomized female rats.

## 4.2 Results

### 4.2.1 Effects of orchidectomy and sub-chronic testosterone treatment on MAP and plasma testosterone levels in male normotensive rats

In Figure 4.1(A), MAP in male normotensive SD rats significantly decreased following orchidectomy ( $P<0.05$ ). Administration of 125 $\mu\text{g}/\text{kg}/\text{day}$  testosterone resulted in MAP to increase ( $P<0.05$ ). Significant increase in MAP was also observed following 250 $\mu\text{g}/\text{kg}/\text{day}$  testosterone treatment ( $P<0.05$ ). Co-administration of flutamide with 125 $\mu\text{g}/\text{kg}/\text{day}$  and 250 $\mu\text{g}/\text{kg}/\text{day}$  testosterone resulted in significant decrease in MAP ( $P<0.05$ ). Significant decreases in MAP were also seen when finasteride was concomitantly given with 125 $\mu\text{g}/\text{kg}/\text{day}$  and 250 $\mu\text{g}/\text{kg}/\text{day}$  testosterone.

In Figure 4.1(B), plasma testosterone level in male rats markedly decreased following orchidectomy ( $P<0.05$ ). In orchidectomized male rats, plasma testosterone level significantly increased following treatment with 125 $\mu\text{g}/\text{kg}/\text{day}$  and 250 $\mu\text{g}/\text{kg}/\text{day}$  testosterone, ( $P<0.05$ ). No changes in plasma testosterone level were observed following co-treatment with flutamide or finasteride with 125 $\mu\text{g}/\text{kg}/\text{day}$  or 250 $\mu\text{g}/\text{kg}/\text{day}$  testosterone.

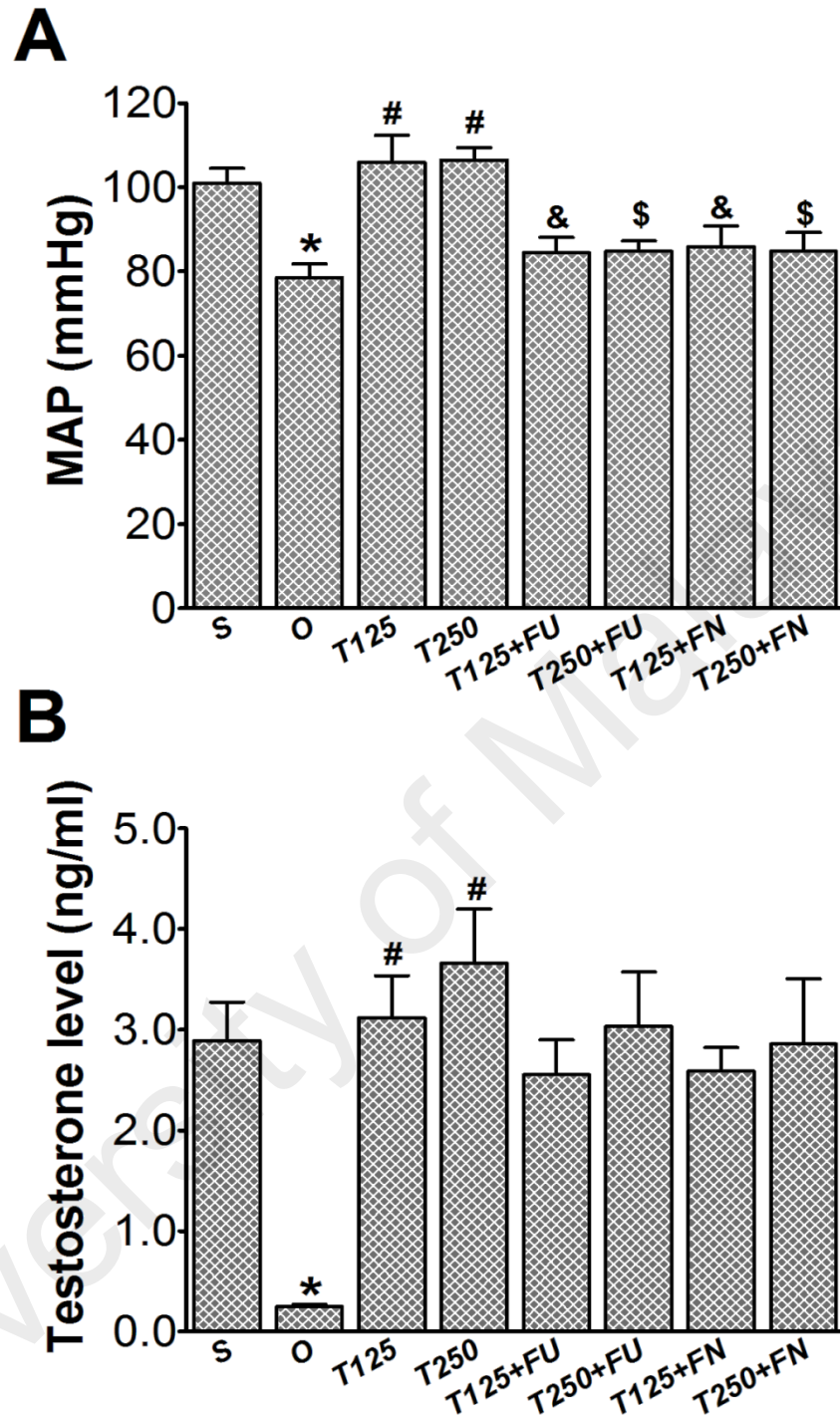


**Figure 4.1** Effects of orchidectomy and sub-chronic testosterone treatment on MAP and plasma testosterone levels in male normotensive rats.

(A) Mean arterial pressure (MAP) in orchidectomized male normotensive SD rats receiving 7 days of sub-chronic testosterone treatment were measured via cannulation of carotid artery. Sham-operation and orchidectomy were carried out at 8 weeks of age while sub-chronic testosterone treatments were initiated at 10 weeks of age. (B) Plasma testosterone levels were quantified using the ELISA method. Data are presented as mean  $\pm$  SEM ( $n = 6-8$ /group, one way ANOVA); \* $P < 0.05$  compared to S; # $P < 0.05$  compared to O; & $P < 0.05$  compared to T125; \$ $P < 0.05$  compared to T250. Abbreviations: MAP: mean arterial pressure; S: sham operated; O: orchidectomized; T125: 125 $\mu$ g/kg/day testosterone-treated; T250: 250 $\mu$ g/kg/day testosterone-treated rats; FU: flutamide; FN: finasteride.

#### **4.2.2 Effects of gonadectomy on MAP and plasma testosterone levels in male and female normotensive and hypertensive rats**

In Figure 4.2(A), MAP of WKY rats ranged from 50 to 100mmHg while SHR rats ranged from 100 to 200mmHg. MAP of sham-operated intact male rats was higher than sham-operated intact female rats in both rat strains ( $P<0.001$ ). In male rats, orchidectomy significantly decreased the MAP ( $P<0.01$  for WKY rats and  $P<0.001$  for SHR rats). In female rats, ovariectomy significantly decreased the MAP ( $P<0.05$  for WKY rats and  $P<0.01$  for SHR rats).

In Figure 4.2(B), highest plasma testosterone level was observed in sham-operated intact male SHR rats. Orchidectomy significantly decreased plasma testosterone levels in both male WKY ( $P<0.001$ ) and SHR ( $P<0.05$ ) rats. Similarly, ovariectomy reduced plasma testosterone levels in female rats of both strains ( $P <0.01$ ).

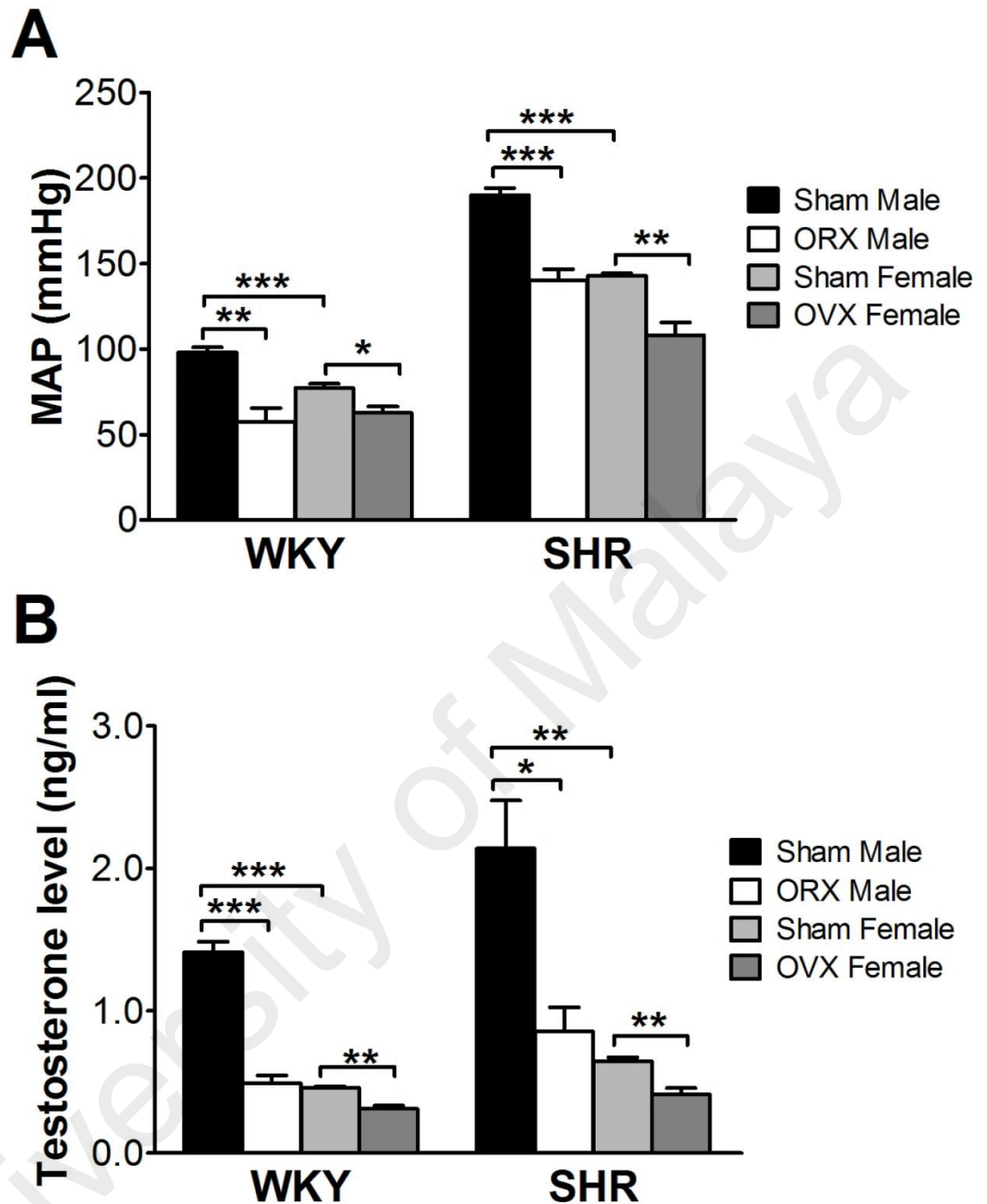


**Figure 4.2** Effects of gonadectomy on MAP and plasma testosterone levels in male and female normotensive and hypertensive rats.

(A) Mean arterial blood pressure (MAP) of 16 weeks old WKY and SHR male and female rats were measured by cannulation of carotid artery. Sham-operation and gonadectomy were performed at 8 weeks of age. (B) Plasma testosterone levels were assessed using blood collected from carotid arteries at the end of the experiment. Data are presented in mean  $\pm$  SEM ( $n = 6$ /group; unpaired student's  $t$ -test); \* $P < 0.05$ , \*\* $P < 0.01$ , \*\*\* $P < 0.001$ . Abbreviations: MAP: mean arterial pressure; WKY: Wistar Kyoto rat; SHR: Spontaneously hypertensive rat; Sham: sham-operated intact; ORX: orchidectomized; OVX: ovariectomized.

#### **4.2.3 Changes in MAP and plasma testosterone levels across estrous cycle in female normotensive and hypertensive rats**

Figure 4.3(A) showed the MAP of 16 weeks old intact female normotensive WKY and hypertensive SHR rats, grouped according to their estrous phases: proestrus (Ps), estrus (Es), metestrus (Ms) and diestrus (Ds). No significant differences in MAP were reported across the estrous cycle stages in both female WKY and SHR rats.

In Figure 4.3(B), plasma testosterone levels of female WKY rats ranged from 0.38 to 0.57ng/ml while female SHR rats ranged from 0.54 to 0.65ng/ml. Similarly, plasma testosterone levels in both strains were not significantly different across stages of the estrous cycle.

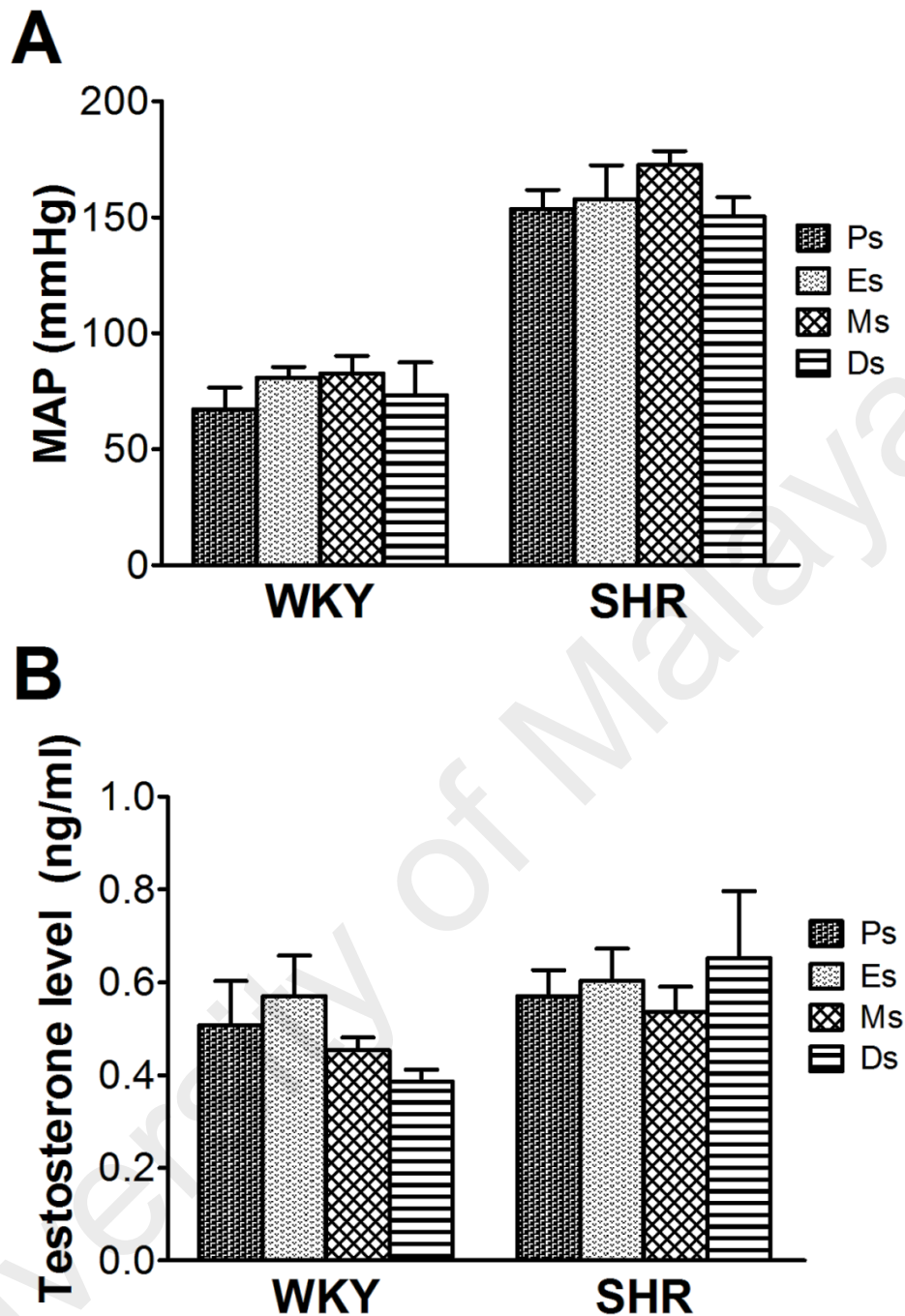


**Figure 4.3 Changes in MAP and plasma testosterone levels across estrous cycle in female normotensive and hypertensive rats.**

(A) Mean arterial blood pressure (MAP) of 16 weeks old intact female normotensive WKY and hypertensive SHR rats were measured by cannulation of carotid artery. The stages of estrous cycle were defined based on the vaginal smears and blood analysis of estrogen and progesterone. (B) Plasma testosterone levels were assessed using blood collected from carotid arteries at the end of the experiment. Data are presented in mean  $\pm$  SEM ( $n = 5-8/\text{group}$ ; unpaired student's  $t$ -test). Abbreviations: MAP: mean arterial pressure; WKY: Wistar Kyoto rat; SHR: Spontaneously hypertensive rat; Ps: proestrus; Es: estrus; Ms: metestrus; Ds: diestrus.

#### **4.2.4 Effects of chronic testosterone treatment on MAP and plasma testosterone levels in female normotensive and hypertensive rats**

In Figure 4.4(A), six weeks treatment in ovariectomized female rats with testosterone resulted in significant increase in MAP ( $P < 0.05$  for WKY and  $P < 0.01$  for SHR). Concordantly, in Figure 4.4(B), plasma testosterone levels were markedly increased in ovariectomized female rats of both strains receiving testosterone treatment ( $P < 0.001$ ).

University of Malaya

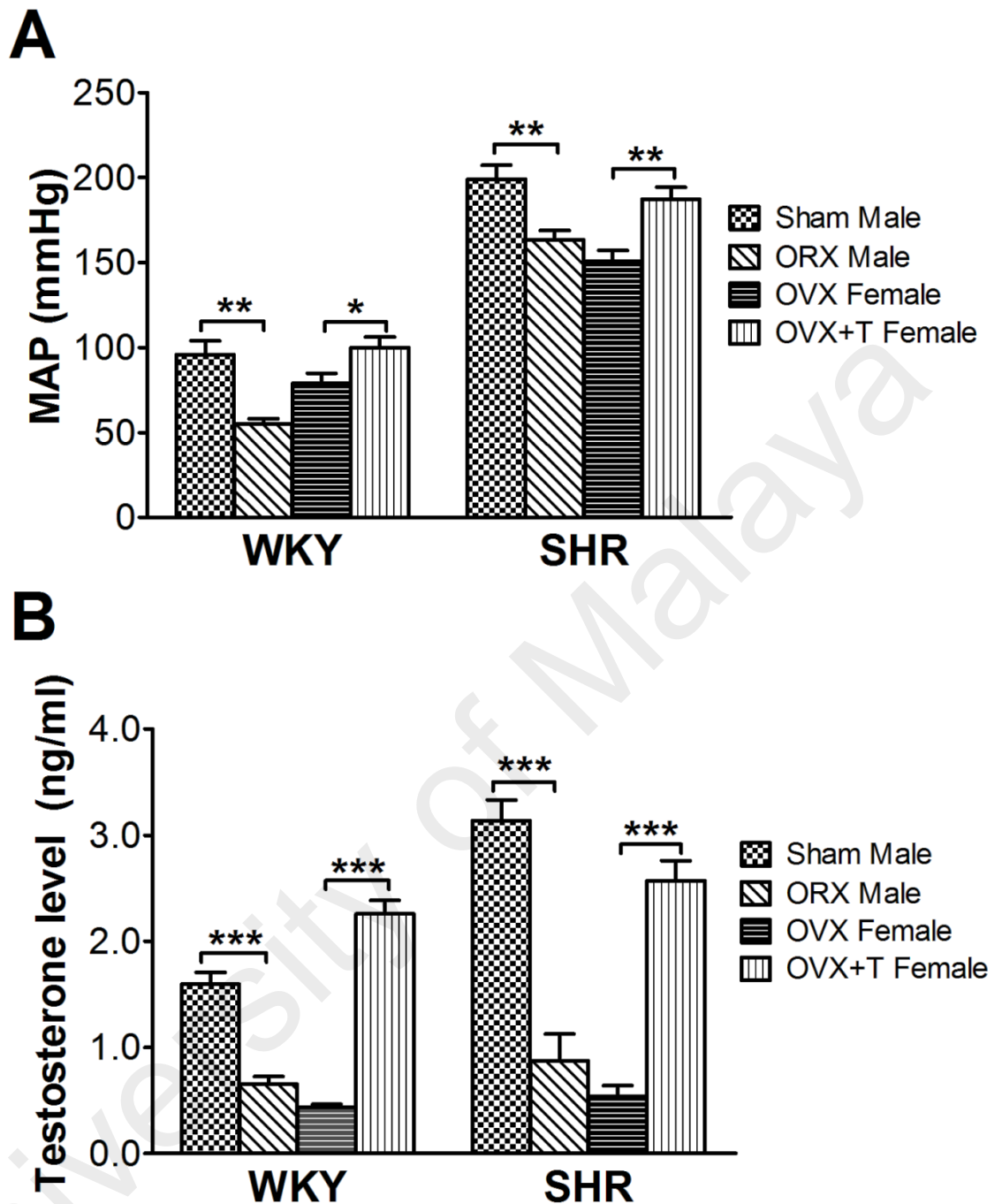


**Figure 4.4** Effects of chronic testosterone treatment on MAP and plasma testosterone levels in female normotensive and hypertensive rats.

(A) Mean arterial blood pressure (MAP) of 16 weeks old WKY and SHR male and female rats were measured by cannulation of the carotid artery. Sham-operation and gonadectomies were carried out at 8 weeks of age. At 10 weeks of age, OVX+T female rats were treated with testosterone implants for 6 weeks. (B) Plasma testosterone levels were assessed using blood collected from carotid arteries at the end of the experiment. Data are presented in mean  $\pm$  SEM ( $n = 6/\text{group}$ ; unpaired student's  $t$ -test); \* $P < 0.05$ , \*\* $P < 0.01$ , \*\*\* $P < 0.001$ . Abbreviations: MAP: mean arterial pressure; WKY: Wistar Kyoto rat; SHR: Spontaneously hypertensive rat; Sham: sham-operated intact; ORX: orchidectomized; OVX: ovariectomized; T: testosterone.

### 4.3 Discussion

Sex hormones are known to play an important role in the blood pressure regulation in both males and females (Burt et al., 1995; Hay, 2016; Huang et al., 2016; Maranon & Reckelhoff, 2013). In the present study, a positive correlation between plasma testosterone level and MAP was identified. In normotensive rats, the MAP was decreased by orchidectomy and was restored by sub-chronic testosterone treatment. The decrease in MAP was in parallel with the decrease in plasma testosterone level as a result of the removal of endogenous testosterone by orchidectomy while the increase in MAP was in parallel with the increase in plasma testosterone level following sub-chronic testosterone treatment in orchidectomized rats. Together, these findings suggested that testosterone plays a role in causing the blood pressure to increase. The involvement of testosterone in inducing an increase in MAP was further supported by the observed effects following the co-administration of flutamide *i.e.* blocking of AR inhibited the effects of testosterone in which a reduction in the MAP was found. In addition, the MAP was also decreased by the co-administration of finasteride, indicating that the effect of testosterone could be mediated via DHT. The present findings were in agreement with the previous findings that flutamide decreases the blood pressure in SHR and Wistar male rats (Hofmann et al., 2012; Reckelhoff et al., 1999; Vasudevan et al., 2012).

In general, the MAP was found to be higher in intact (naïve) male and rats when compared to intact (naïve) female rats under both normotensive and hypertensive states, which is in agreement with the previous reports by others (Chen & Meng, 1991; Dalpiaz et al., 2015; Maris et al., 2005; Masubuchi et al., 1982; Pijacka et al., 2016). In this study, gonadectomies performed prior to pubertal age *i.e.* 8 weeks were found to decrease the MAP (at 16 weeks of age) in both male and female normotensive and

hypertensive rats. These findings were also consistent with the report by Masubuchi *et al.* (1982) where a reduce in blood pressure (at 17 weeks of age) in adult male and female SHR rats following gonadectomies was shown (Masubuchi *et al.*, 1982). In addition to the MAP, the present study also found that in male rats, orchietomy resulted in a decrease in the level of endogenous testosterone while in female rats, ovariectomy also caused the level of endogenous testosterone to decrease.

To date, there were conflicting reports with regards to the effect of ovariectomy on MAP (Davis *et al.*, 2012; Liu *et al.*, 2016; Xue *et al.*, 2013). In normotensive SD rats, ovariectomy was found to result in no changes in the MAP when compared to the intact female rats (Xue *et al.*, 2009). Similarly, in another study, gonadectomy in female SD rats was reported to also not cause significant changes in blood pressure as compared to the intact rats, however an increase in the sensitive towards deoxycorticosterone-salt-induced increased in blood pressure was shown (Crofton & Share, 1997). Ovariectomy, performed at 6 weeks of age, in Dahl salt-sensitive female rats which were given low sodium diet was found not causing any significant changes in the blood pressure at 12 weeks of age, however at 16 weeks of age, a significantly higher blood pressure was shown in these rats than those intact rats, and these differences persisted up to the age of 84 weeks (Hinojosa-Laborde *et al.*, 2004).

In contrast to that, the present findings and several other findings indicated that ovariectomy reduced the blood pressure in female rats. Stachowiak *et al.* (1991) reported that 28 days after ovariectomy, the blood pressure in female rats markedly decreased which was associated with a marked atrophy of the adrenal cortices (Stachowiak *et al.*, 1991). A recent study also indicated a trend of a reduction in the blood pressure of SD female rats at 24 weeks of age following ovariectomy, which

performed at 7 weeks of age (Chinnathambi et al., 2012). A study conducted in 12 weeks old Wistar rats indicated that there was a transient decrease in MAP, measured by using a tail cuff, 2 weeks after ovariectomy yet subsequently returned to the pre-ovariectomized values (Laudański & Cudnoch-Jędrzejewska, 2001). In this study, we measured MAP in anesthetized female rats via cannulation of carotid artery which showed similar results. It is hypothesized that the decrease in MAP following ovariectomy in female rats may be, at least partly, mediated by suppression of adrenal secretory activity, due to the lack of circulating estrogens, which are known to stimulate the release of hypophyseal adrenocorticotrophic hormone (ACTH). In addition, estrogen has also been shown to increase the renin-angiotensin system (RAS) activity (O'Hagan et al., 2012; Safari et al., 2015) and therefore the decrease in the level of estrogen following removal of endogenous source of estrogen via ovariectomy could result in an alleviation in estrogen-induced increased RAS activity and thus leading towards a reduction in blood pressure.

This study has shown that there was no significant difference in MAP across the estrous cycle in both normotensive and hypertensive female rats. Previous studies have also demonstrated that blood pressure did not change throughout the estrous cycle in rodents (Capone et al., 2009; Ebine et al., 2016). Liu and Ely also reported that the blood pressure did not change throughout the estrous cycle in female SHR rats (Liu & Ely, 2011), which is in agreement with the current findings. The fact that there were no changes in blood pressure observed throughout the estrous cycle indicated that fluctuations in endogenous sex steroid hormone levels throughout the cycle had no influences on the blood pressure. Despite the high estrogen level at Es stage and the high progesterone level at Ds stage, these hormones seem not having an influence on the blood pressure. In addition, in contrast with the earlier reports (Falvo et al., 1974;

Rush & Blake, 1982), the plasma testosterone levels did not change significantly throughout the estrous cycle. Therefore, it can be concluded that in intact female rats, the changes in blood pressure may also depend on other factors rather than the fluctuating levels of sex-steroid hormones.

Changes in plasma testosterone levels were found to positively correlate with MAP, as seen in male and female intact and gonadectomized rats and in gonadectomized male and female rats receiving exogenous testosterone treatment. The increase in MAP in ovariectomized normotensive and hypertensive female rats following exogenous testosterone treatment strengthened the argument that testosterone increases the blood pressure as this model eliminates the effects of male sex chromosome which have been implicated in causing higher blood pressure in males as compared to females (Ellis et al., 2000; Ely et al., 2010; Molina et al., 2016). These findings were supported by the findings by Reckelhoff *et al.* (Reckelhoff et al., 1998) who demonstrated an increase in MAP in testosterone-treated female hypertensive SHR rats. In this study, the increase in MAP was also seen in testosterone-treated normotensive female rats, indicating that testosterone-induced increase in blood pressure is regardless of the normotensive or hypertensive states. In addition, the findings in male rats in which orchidectomy caused a decrease in blood pressure have also further supported the view that testosterone is involved in causing the blood pressure to increase.

Together, these results demonstrated a positive correlation between plasma testosterone level and MAP and further supported the roles of testosterone in causing the blood pressure to increase. In addition, these findings could partly explain the higher blood pressure in men than age-matched women before menopause and the elevated blood pressure in women after menopause (Regitz-Zagrosek, 2012), which could be

associated with the high plasma testosterone level in men or the relative testosterone excess due to the dramatic fall of estrogen in women after menopause (Secreto et al., 2016; Yasui et al., 2012).

University of Malaya

## CHAPTER 5: EFFECTS OF SUB-CHRONIC TESTOSTERONE TREATMENT ON EPITHELIAL SODIUM CHANNEL (ENaC) EXPRESSION IN KIDNEYS

### 5.1 Introduction

Testosterone has been shown to cause the blood pressure to increase (refer **Chapter 4**). However, mechanisms that underlie the effect of this hormone are currently not well understood. Epithelial sodium channel (ENaC), which consists of three homologous subunits ( $\alpha$ ,  $\beta$  and  $\gamma$ ) plays an important role in sodium reabsorption in kidneys (Soundararajan et al., 2012; Warnock & Rossier, 2005). The  $\alpha$ -subunit is absolutely required for sodium conductance while  $\beta$  and  $\gamma$ -subunits are needed to enhance the channel expression and activity at the cell surface (Schild, 2010; Warnock & Rossier, 2005). Expression of ENaC in kidneys was under aldosterone influence (Garty, 2000; Nesterov et al., 2012; Quinn et al., 2014). Besides aldosterone, other hormones that could influence kidney ENaC expression include insulin and vasopressin (Kamynina & Staub, 2002; Mironova et al., 2012; Rossier, 2014; Schild, 2010). Loss-of-function mutations in ENaC could lead to renal sodium wasting and hypotension, while conversely, its prolonged activation could lead to renal sodium retention and severe hypertension (Bubien, 2010; Pao, 2012). Expression of ENaC in kidneys could also be affected by sex hormones *i.e.* estrogen and progesterone (Gambling et al., 2004; Heo et al., 2013; Yusef et al., 2014). There were evidence which suggest the involvement of testosterone in regulating kidney ENaC expression (Fan et al., 2015). Quan and colleagues reported that dihydrotestosterone (DHT) injection to adult male Sprague-Dawley (SD) rats could increase sodium reabsorption in kidney proximal tubules, suggesting that this could be mediated via ENaC (Quan et al., 2004). Meanwhile, administration of testosterone in spontaneous hypertensive (SHR) rats was found to

decrease the pressure-induced natriuresis, again pointing towards the involvement of ENaC (Reckelhoff et al., 1998).

To date, the information with regard to effects of testosterone on ENaC expression in kidneys were far from complete. Quinkler *et al.* (2005) reported that incubation of human kidney proximal tubule cell line with testosterone but not DHT caused an increase in  $\alpha$ -ENaC mRNA level which could be antagonized by flutamide (Quinkler et al., 2005). However, no changes in expression for  $\beta$  and  $\gamma$ -ENaC were detected in these cells. An earlier study showed that sub-chronic (14 days) treatment of orchidectomized male Wistar rats with testosterone resulted in elevated  $\alpha$ -Enac mRNA level and a trend to increase in expression of  $\beta$  and  $\gamma$ -ENaC in kidney homogenates (Kienitz et al., 2006b). Nevertheless, testosterone was found to cause a trend to reduce while DHT significantly decreased expression of  $\alpha$ ,  $\beta$  and  $\gamma$ -ENaC subunits in the kidney of ovariectomized female Wistar rat (Kienitz et al., 2009). Based on these findings, it is postulated that testosterone could affect expression of all ENaC subunits *i.e.*  $\alpha$ ,  $\beta$  and  $\gamma$  in the kidneys, in which their co-existence will lead to a fully functioning ENaC channel and enhanced sodium reabsorption, which may contribute to the rise in blood pressure under testosterone influence (Hanukoglu & Hanukoglu, 2016). Therefore, in this part of the thesis, the effects of sub-chronic (seven days) testosterone exposure on expression levels of  $\alpha$ ,  $\beta$  and  $\gamma$ -ENaC in kidneys were examined. The changes in the related hormonal and biochemical parameters which include the plasma levels of aldosterone, electrolytes ( $\text{Na}^+$ ,  $\text{K}^+$ ,  $\text{Cl}^-$  and  $\text{Ca}^{2+}$ ), osmolality, glucose, urea and creatinine were also accessed. In addition, the possible involvements of androgen receptor (AR) and DHT in mediating these effects of testosterone were also investigated.

## 5.2 Results

### 5.2.1 Hormonal and biochemical blood parameters

In Table 5.1, administration of 125µg/kg/day testosterone resulted in plasma level of testosterone to be 13.5 folds greater than its level in non-treated orchidectomized rats. Treatment with 250µg/kg/day testosterone resulted in plasma testosterone level to be 16.5 folds greater than in non-treated orchidectomized rats. Meanwhile, plasma aldosterone level was increased by approximately 2 folds as compared to non-treated orchidectomized rats following treatments of both 125 and 250µg/kg/day testosterone.

Plasma osmolality and potassium ( $K^+$ ) levels were significantly increased by orchidectomy ( $P<0.05$ ) and decreased upon the administration of 125 ( $P<0.05$ ) and 250µg/kg/day ( $P<0.05$ ) testosterone. On the other hand, a decrease ( $P<0.05$ ) in plasma sodium ( $Na^+$ ) level following orchidectomy were significantly increased by both 125 ( $P<0.05$ ) and 250µg/kg/day ( $P<0.05$ ) testosterone treatments. No significant differences in plasma levels of chloride ( $Cl^-$ ) and calcium ( $Ca^{2+}$ ) were observed amongst all treatment groups.

Reduced plasma glucose level in orchidectomized rats ( $P<0.05$ ) were significantly increased by 125 ( $P<0.05$ ) and 250µg/kg/day ( $P<0.05$ ) testosterone treatments. Plasma levels of urea and creatinine were significantly increased following orchidectomy. Nevertheless, the administration of 125 and 250µg/kg/day ( $P<0.05$ ) testosterone in orchidectomized rats significant restored the plasma levels of urea and creatinine.

**Table 5.1 Effects of sub-chronic testosterone treatment on hormonal and biochemical parameters in blood plasma.**

Group	S	O	T125	T250
<b>Testosterone</b> (ng/ml)	2.89 ± 0.38	0.25 ± 0.02*	3.37 ± 0.40 <sup>#</sup>	4.12 ± 0.59 <sup>#</sup>
<b>Aldosterone</b> (pg/ml)	207.89 ± 23.66	107.85 ± 20.34*	206.11 ± 30.65 <sup>#</sup>	230.03 ± 31.35 <sup>#</sup>
<b>Sodium, Na<sup>+</sup></b> (mmol/L)	141.0 ± 0.84	135.4 ± 1.21*	140.0 ± 1.05 <sup>#</sup>	140.4 ± 1.03 <sup>#</sup>
<b>Osmolality</b> (mOsmol/kg)	299.6 ± 1.03	307.0 ± 2.12*	295.4 ± 1.29 <sup>#</sup>	293.8 ± 1.32 <sup>#</sup>
<b>Chloride, Cl<sup>-</sup></b> (mmol/L)	99.0 ± 0.55	100.4 ± 0.40	99.8 ± 0.97	99.0 ± 0.71
<b>Potassium, K<sup>+</sup></b> (mmol/L)	5.25 ± 0.20	6.55 ± 0.21*	5.40 ± 0.29 <sup>#</sup>	5.03 ± 0.27 <sup>#</sup>
<b>Calcium, Ca<sup>2+</sup></b> (mmol/L)	2.58 ± 0.02	2.58 ± 0.04	2.56 ± 0.05	2.58 ± 0.06
<b>Glucose</b> (mmol/L)	10.65 ± 0.68	8.15 ± 0.44*	9.88 ± 0.39 <sup>#</sup>	11.03 ± 0.84 <sup>#</sup>
<b>Urea</b> (mmol/L)	5.86 ± 0.49	7.46 ± 0.44*	6.08 ± 0.30 <sup>#</sup>	4.88 ± 0.32 <sup>#</sup>
<b>Creatinine</b> (μmol/L)	18.20 ± 0.66	23.20 ± 1.02*	19.00 ± 0.84 <sup>#</sup>	19.20 ± 1.24 <sup>#</sup>

Data are expressed as mean ± SEM (n = 6-8/group, one-way ANOVA); \**P*<0.05 compared to S; <sup>#</sup>*P*<0.05 compared to O. Abbreviations: S: sham-operated intact; O: orchidectomized; T125: 125μg/kg/day testosterone-treated; T250: 250μg/kg/day testosterone-treated rats.

### 5.2.2 $\alpha$ -ENaC mRNA and protein expression levels

In Figure 5.1(A), the levels of  $\alpha$ -Enac mRNA were highest following testosterone-only treatment. Co-treatment with flutamide or finasteride caused  $\alpha$ -Enac mRNA levels to decrease ( $P<0.05$ ). The effect of flutamide was greater in rats which received 125 $\mu$ g/kg/day testosterone when compared to 250 $\mu$ g/kg/day testosterone. However, the effect of finasteride in rats treated with 125 $\mu$ g/kg/day testosterone was not significantly different when compared to its effect in rats treated with 250 $\mu$ g/kg/day testosterone.

In Figure 5.1(B) and 5.1(C), the expression level of  $\alpha$ -ENaC protein was highest in rats which received 250 $\mu$ g/kg/day testosterone. In these rats, co-administration of flutamide or finasteride caused  $\alpha$ -ENaC protein expression level to decrease ( $P<0.05$ ). Flutamide effect was greater in rats treated with 125 $\mu$ g/kg/day testosterone than in rat treated with 250 $\mu$ g/kg/day testosterone. However, following co-administration of finasteride, no significant difference in  $\alpha$ -ENaC protein expression level was observed between rats which received 125 $\mu$ g/kg/day testosterone and rats which received 250 $\mu$ g/kg/day testosterone.

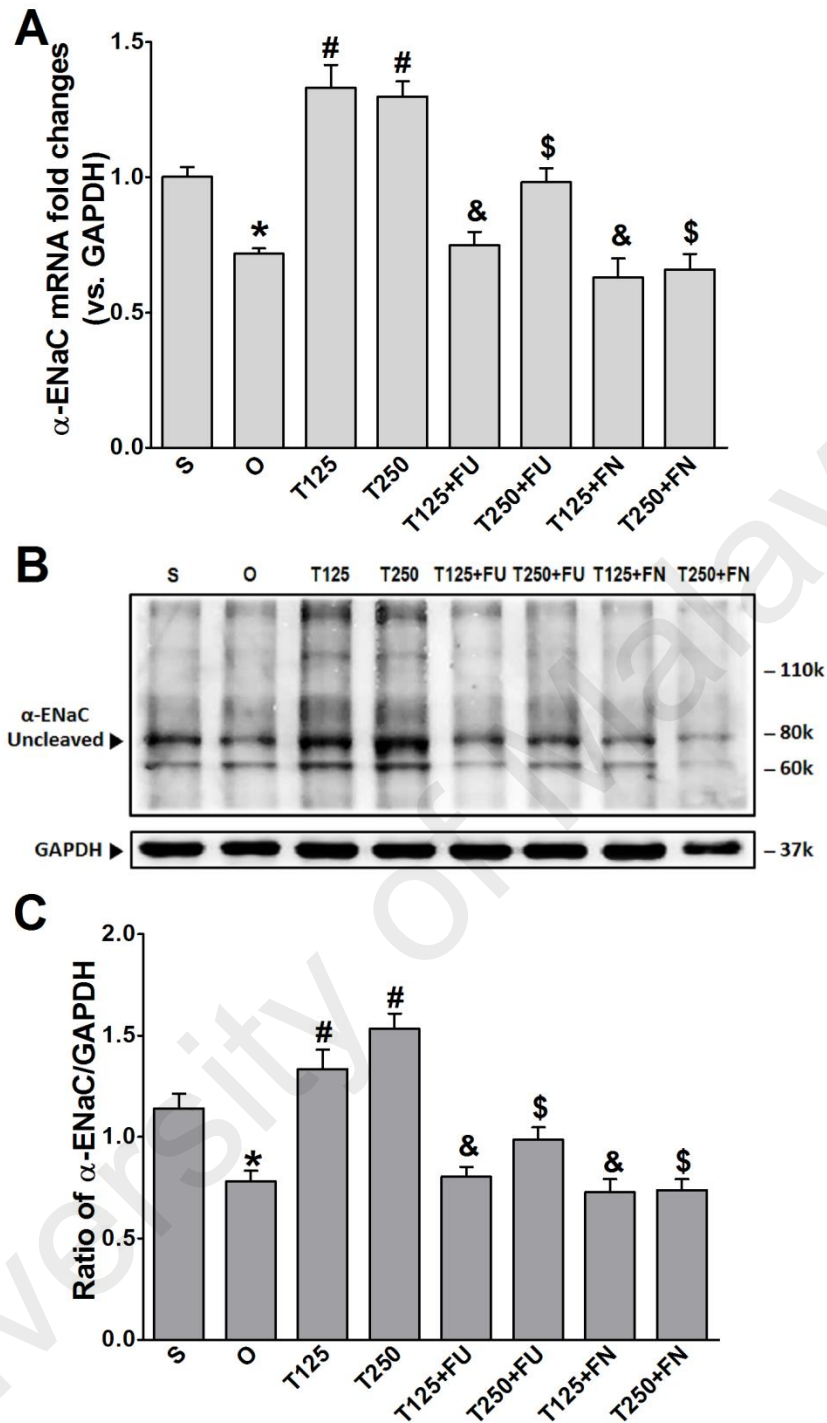


**Figure 5.1** Effects of sub-chronic testosterone treatment on mRNA and protein expression levels of  $\alpha$ -ENaC in kidneys.

(A)  $\alpha$ -Enac mRNA level, (B) representative whole membrane image of  $\alpha$ -ENaC protein band and (C) average ratio of band intensity of  $\alpha$ -ENaC to housekeeping protein, GAPDH of three replicate blots. Molecular weight of  $\alpha$ -ENaC protein = 78kDa (uncleaved). Values represent in mean  $\pm$  SEM (n = 4/group, one-way ANOVA); \* $P$ <0.05 compared to S; # $P$ <0.05 compared to O; & $P$ <0.05 compared to T125; \$ $P$ <0.05 compared to T250. Abbreviations: S: sham operated; O: orchidectomized; T125: 125 $\mu$ g/kg/day testosterone-treated; T250: 250 $\mu$ g/kg/day testosterone-treated rats; FU: flutamide; FN: finasteride.

### 5.2.3 $\beta$ -ENaC mRNA and protein expression levels

In Figure 5.2(A), the level of  $\beta$ -*Enac* mRNA was highest in rats which received testosterone-only treatment. In these rats, co-administration of flutamide or finasteride resulted in  $\beta$ -*Enac* mRNA level to decrease ( $P<0.05$ ). The effect of flutamide was greater in rats which received 125 $\mu$ g/kg/day testosterone when compared to rats which received 250 $\mu$ g/kg/day testosterone. However, co-administration of finasteride did not cause  $\beta$ -*Enac* mRNA level in rats which received 125 $\mu$ g/kg/day testosterone to be difference from rats which received 250 $\mu$ g/kg/day testosterone.

In Figure 5.2(B) and 5.2(C), the level of expression of  $\beta$ -ENaC protein was highest in rats which received 250 $\mu$ g/kg/day testosterone. In these rats, co-administration of flutamide or finasteride resulted in  $\beta$ -ENaC protein expression level to decrease ( $P<0.05$ ). The effects of flutamide were greater in rats which received 125 $\mu$ g/kg/day testosterone when compared to rats which received 250 $\mu$ g/kg/day testosterone. However, co-administration of finasteride did not cause  $\beta$ -ENaC protein expression level in rats which received 125 $\mu$ g/kg/day testosterone to be different from rats which received 250 $\mu$ g/kg/day testosterone.

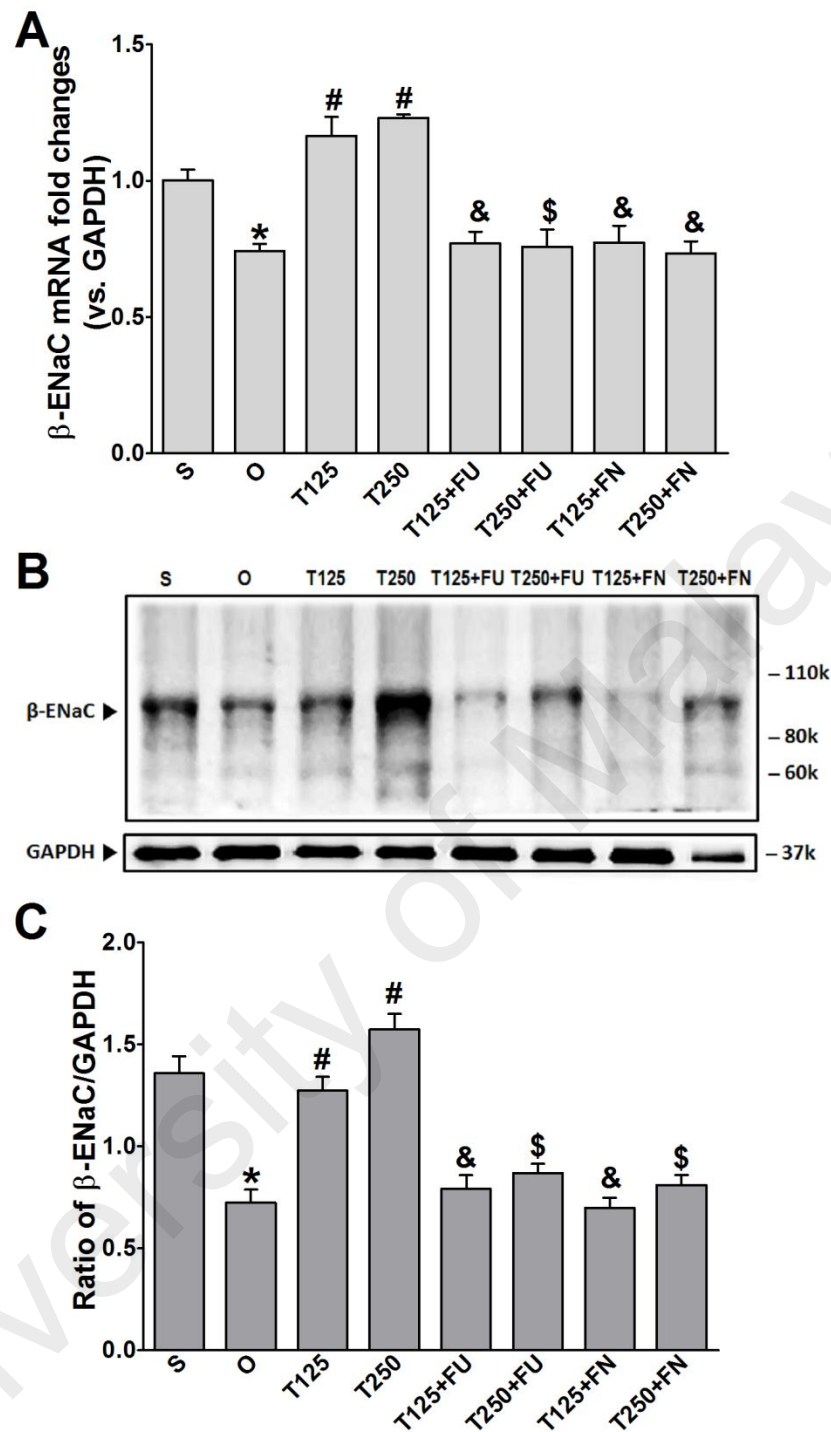


**Figure 5.2 Effects of sub-chronic testosterone treatment on mRNA and protein expression levels of  $\beta$ -ENaC in kidneys.**

(A)  $\beta$ -Enac mRNA level, (B) representative whole membrane image of  $\beta$ -ENaC protein band and (C) average ratio of band intensity of  $\beta$ -ENaC to housekeeping protein, GAPDH of three replicate blots. Molecular weight of  $\beta$ -ENaC protein = 99kDa. Values represent in mean  $\pm$  SEM (n = 4/group, one-way ANOVA). \* $P$ <0.05 compared to S; # $P$ <0.05 compared to O; & $P$ <0.05 compared to T125; \$ $P$ <0.05 compared to T250. Abbreviations: S: sham operated; O: orchidectomized; T125: 12 $\mu$ g/kg/day testosterone-treated; T250: 250 $\mu$ g/kg/day testosterone-treated rats; FU: flutamide; FN: finasteride.

#### 5.2.4 $\gamma$ -ENaC mRNA and protein expression levels

In Figure 5.3(A), the level of  $\gamma$ -*Enac* mRNA was highest in rats which received 250 $\mu$ g/kg/day testosterone. In these rats, co-administration of flutamide or finasteride resulted in  $\gamma$ -*Enac* mRNA level to decrease ( $P < 0.05$ ). The effect of flutamide was not significantly different between rats which received 125  $\mu$ g/kg/day testosterone and rats which received 250 $\mu$ g/kg/day testosterone. Similarly, the effect of finasteride in rats which received 125 $\mu$ g/kg/day testosterone was not significantly different from its effect in rats which received 250 $\mu$ g/kg/day testosterone.

In Figure 5.3(B) and 5.3(C), the level of  $\gamma$ -ENaC proteins was highest in rats which received 250 $\mu$ g/kg/day testosterone. In these rats, co-administration of flutamide or finasteride resulted in  $\gamma$ -ENaC protein expression level to decrease ( $P < 0.05$ ). Co-administration of flutamide with testosterone did not cause  $\gamma$ -ENaC protein expression level in rats which received 125 $\mu$ g/kg/day testosterone to be different from rats which received 250 $\mu$ g/kg/day testosterone. In contrast, co-administration of finasteride with testosterone caused a greater decrease in the level of this protein in rats which received 250 $\mu$ g/kg/day testosterone when compared to rats which received 125 $\mu$ g/kg/day testosterone.

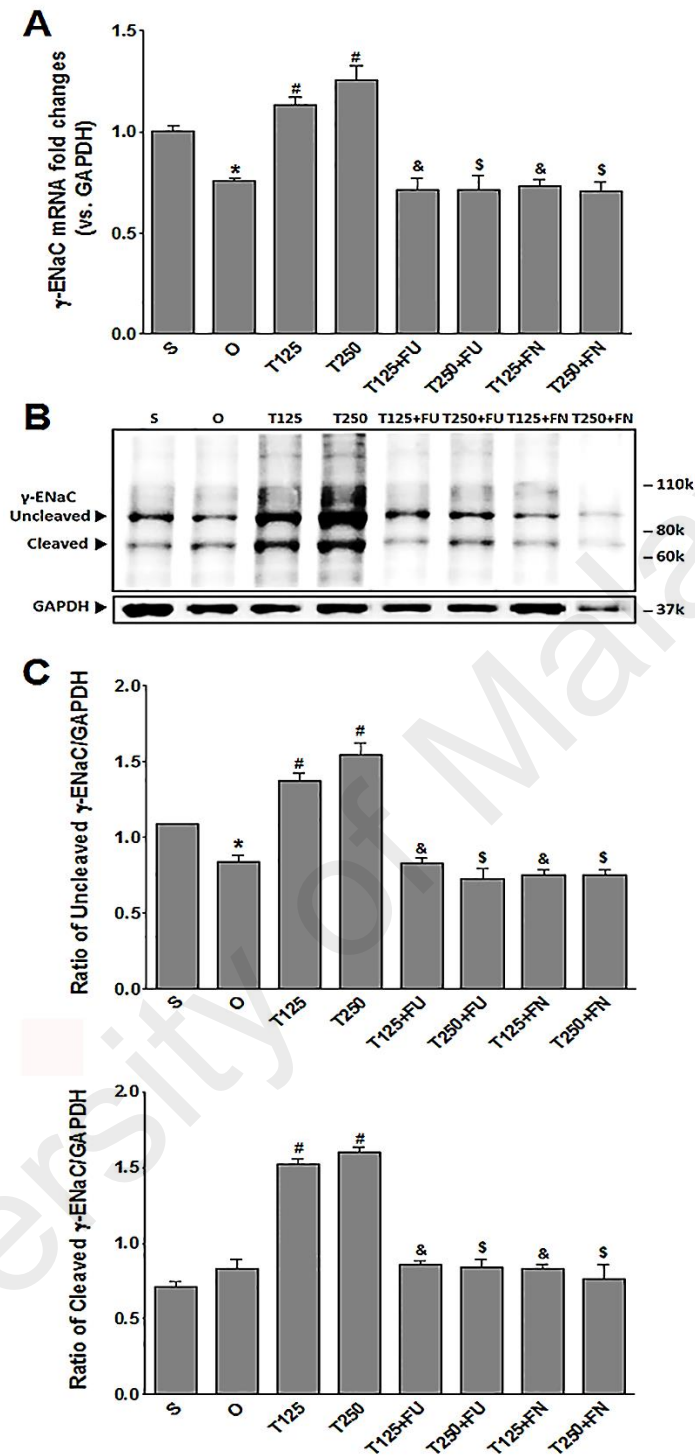


**Figure 5.3** Effects of sub-chronic testosterone treatment on mRNA and protein expression levels of  $\gamma$ -EnaC in kidneys.

(A)  $\gamma$ -Enac mRNA level, (B) representative whole membrane image of  $\gamma$ -EnaC protein band and (C) average ratio of band intensity of  $\alpha$ -EnaC (cleaved and uncleaved forms) to housekeeping protein, GAPDH of three replicate blots. Molecular weight of  $\gamma$ -EnaC = 75kDa (cleaved/unglycosylated) and 85kDa (uncleaved). Values represent in mean  $\pm$  SEM (n = 4/group, one-way ANOVA). \* $P$ <0.05 compared to S; # $P$ <0.05 compared to O; & $P$ <0.05 compared to T125; \$ $P$ <0.05 compared to T250. Abbreviations: S: sham operated; O: orchidectomized; T125: 125 $\mu$ g/kg/day testosterone-treated; T250: 250 $\mu$ g/kg/day testosterone-treated rats; FU: flutamide; FN: finasteride.

### **5.2.5 Distribution of $\alpha$ -ENaC protein in nephrons**

Based on the immunoperoxidase images (Figure 5.4), relatively high distribution of  $\alpha$ -ENaC protein could be seen in the distal tubules and collecting duct of 125 and 250 $\mu$ g/kg/day testosterone-treated rats, with a higher level in the latter compared to the former. Administration of flutamide or finasteride resulted in relative decreases in the amount of  $\alpha$ -ENaC proteins in 125 and 250 $\mu$ g/kg/day testosterone-treated rats. Similarly, in Figure 5.7, the immunofluorescence images showed comparatively higher distribution of  $\alpha$ -ENaC proteins in nephrons of rats which received 125 and 250 $\mu$ g/kg/day testosterone. In these rats, co-administration of flutamide or finasteride resulted in  $\alpha$ -ENaC protein distribution level to be relatively lower (Figure 5.8).

### **5.2.6 Distribution of $\beta$ -ENaC protein in nephrons**

Immunoperoxidase images showed relatively highest distribution of  $\beta$ -ENaC proteins in the distal tubules and collecting duct of rats receiving 250 $\mu$ g/kg/day testosterone treatment (Figure 5.5). Co-administration of flutamide or finasteride with 125 and 250 $\mu$ g/kg/day testosterone resulted in a relative decrease in the amount of  $\beta$ -ENaC protein distribution. Meanwhile, based on the immunofluorescence images (Figure 5.7), both 125 and 250 $\mu$ g/kg/day testosterone treatments relatively increased the  $\beta$ -ENaC protein distribution in nephrons in which the co-administration of flutamide or finasteride with testosterone resulted in relatively lower  $\beta$ -ENaC protein distribution level when compared to rats which received testosterone-only treatment (Figure 5.9).

### **5.2.7 Distribution of $\gamma$ -ENaC protein in nephrons**

Immunoperoxidase images showed relatively higher distribution of  $\gamma$ -ENaC proteins in the distal tubule and collecting ducts of 125 and 250 $\mu$ g/kg/day testosterone-treated rats (Figure 5.6). Administration of flutamide or finasteride in 125 and 250 $\mu$ g/kg/day

testosterone-treated rats resulted in a relative decrease in the amount of  $\gamma$ -ENaC protein distributed in the nephrons. Likewise, immunofluorescence images showing highly distributed  $\gamma$ -ENaC protein in the nephrons of 125 and 250 $\mu$ g/kg/day testosterone-treated rats (Figure 5.7). Nonetheless, the distributions of this protein were comparatively lower in the nephrons of those also received flutamide or finasteride (Figure 5.10).

University of Malaya

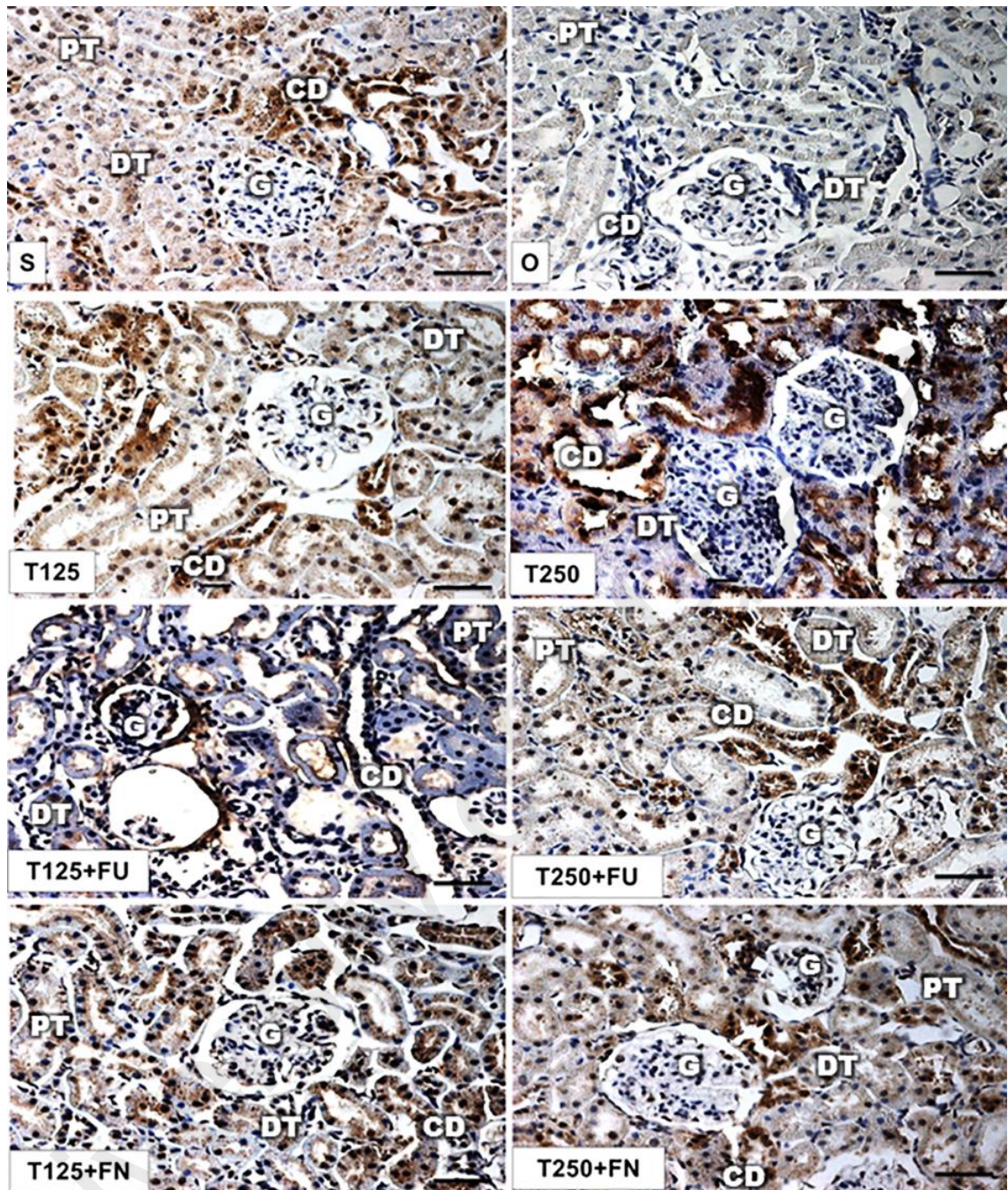


**Figure 5.4 Immunoperoxidase images showing the distribution of  $\alpha$ -ENaC proteins in nephrons following sub-chronic testosterone treatment.**

Representative immunoperoxidase images ( $n = 4/\text{group}$ ) of coronal sections of the kidney incubated  $\alpha$ -ENaC antibodies. Dark-brown staining indicates the sites of  $\alpha$ -ENaC protein localized. Abbreviations: S: sham operated; O: orchidectomized; T125: 125 $\mu\text{g}/\text{kg}/\text{day}$  testosterone-treated; T250: 250 $\mu\text{g}/\text{kg}/\text{day}$  testosterone-treated rats; G: glomeruli; PT: proximal convoluted tubule; DT: distal convoluted tubule; CD: collecting duct. Scale bar= 50 $\mu\text{M}$ .

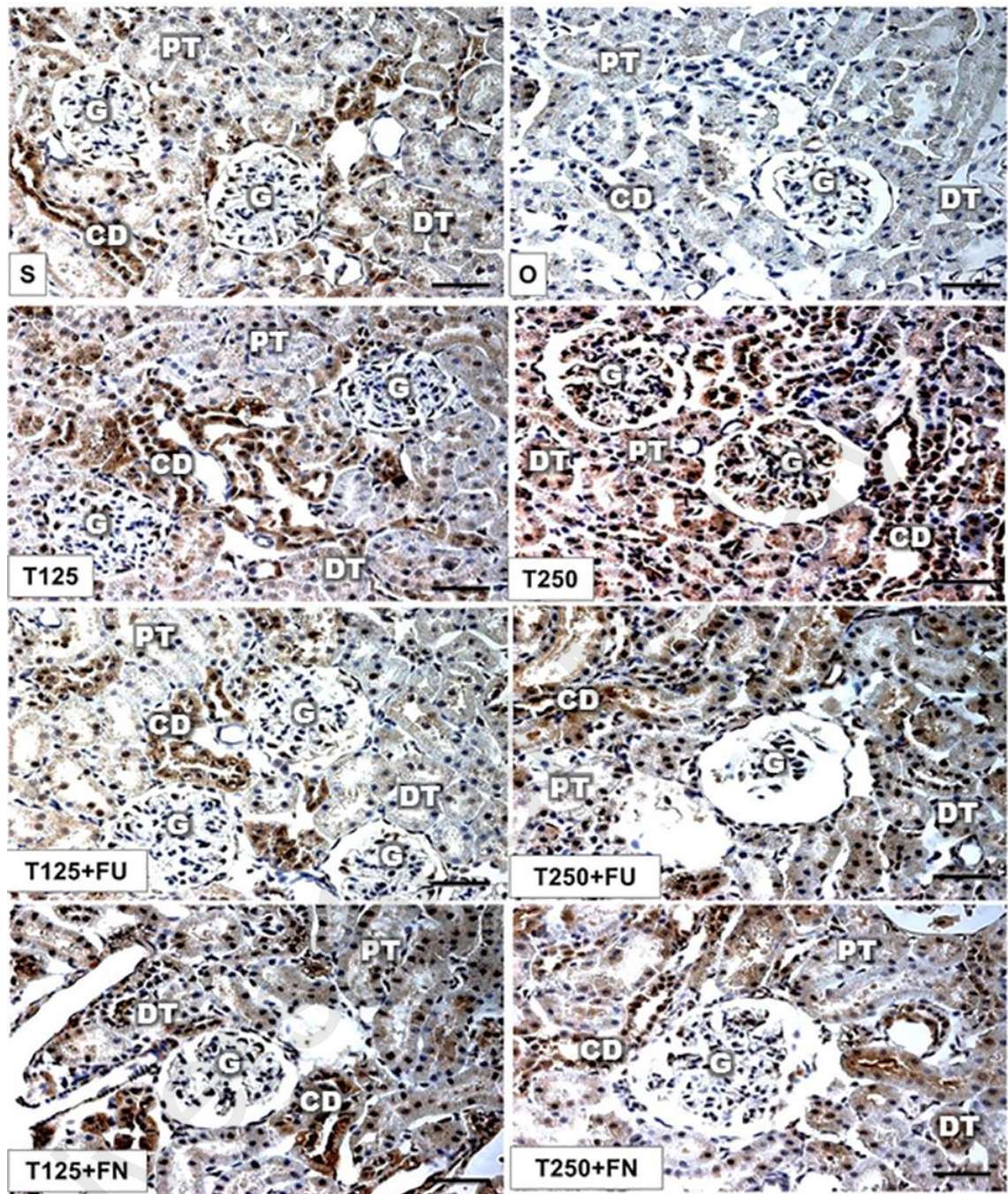


**Figure 5.5 Immunoperoxidase images showing the distribution of  $\beta$ -ENaC proteins in nephrons following sub-chronic testosterone treatment.**

Representative immunoperoxidase images ( $n = 4/\text{group}$ ) of coronal sections of the kidney incubated  $\beta$ -ENaC antibodies. Dark-brown staining indicates the sites of  $\beta$ -ENaC protein localized. Abbreviations: S: sham operated; O: orchidectomized; T125: 125 $\mu\text{g}/\text{kg}/\text{day}$  testosterone-treated; T250: 250 $\mu\text{g}/\text{kg}/\text{day}$  testosterone-treated rats; G: glomeruli; PT: proximal convoluted tubule; DT: distal convoluted tubule; CD: collecting duct. Scale bar= 50 $\mu\text{M}$ .

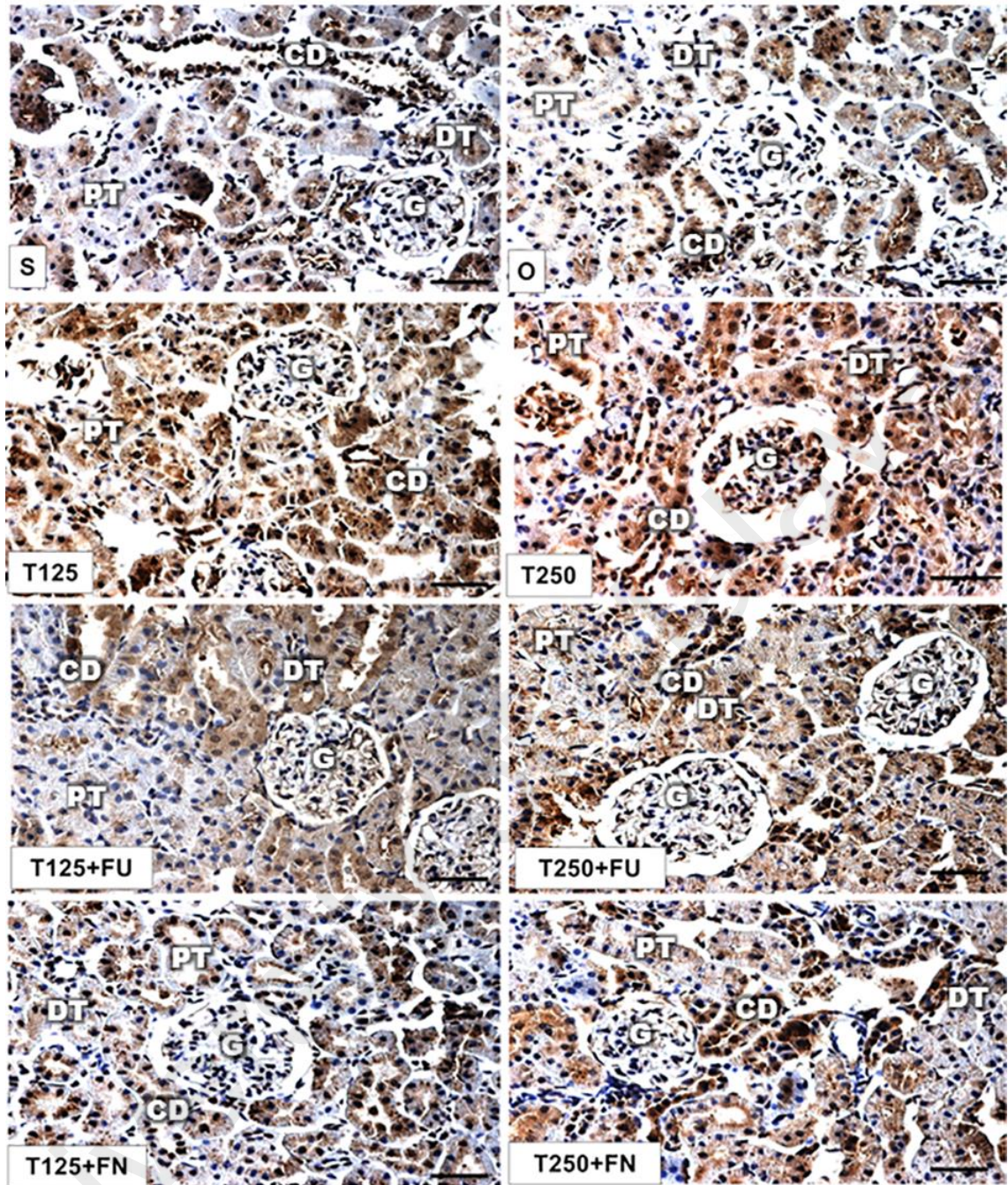


**Figure 5.6 Immunoperoxidase images showing the distribution of  $\gamma$ -ENaC proteins in nephrons following sub-chronic testosterone treatment.**

Representative immunoperoxidase images ( $n = 4/\text{group}$ ) of coronal sections of the kidney incubated  $\gamma$ -ENaC antibodies. Dark-brown staining indicates the sites of  $\gamma$ -ENaC protein localized. Abbreviations: S: sham operated; O: orchidectomized; T125: 125 $\mu\text{g}/\text{kg}/\text{day}$  testosterone-treated; T250: 250 $\mu\text{g}/\text{kg}/\text{day}$  testosterone-treated rats; G: glomeruli; PT: proximal convoluted tubule; DT: distal convoluted tubule; CD: collecting duct. Scale bar= 50 $\mu\text{M}$ .

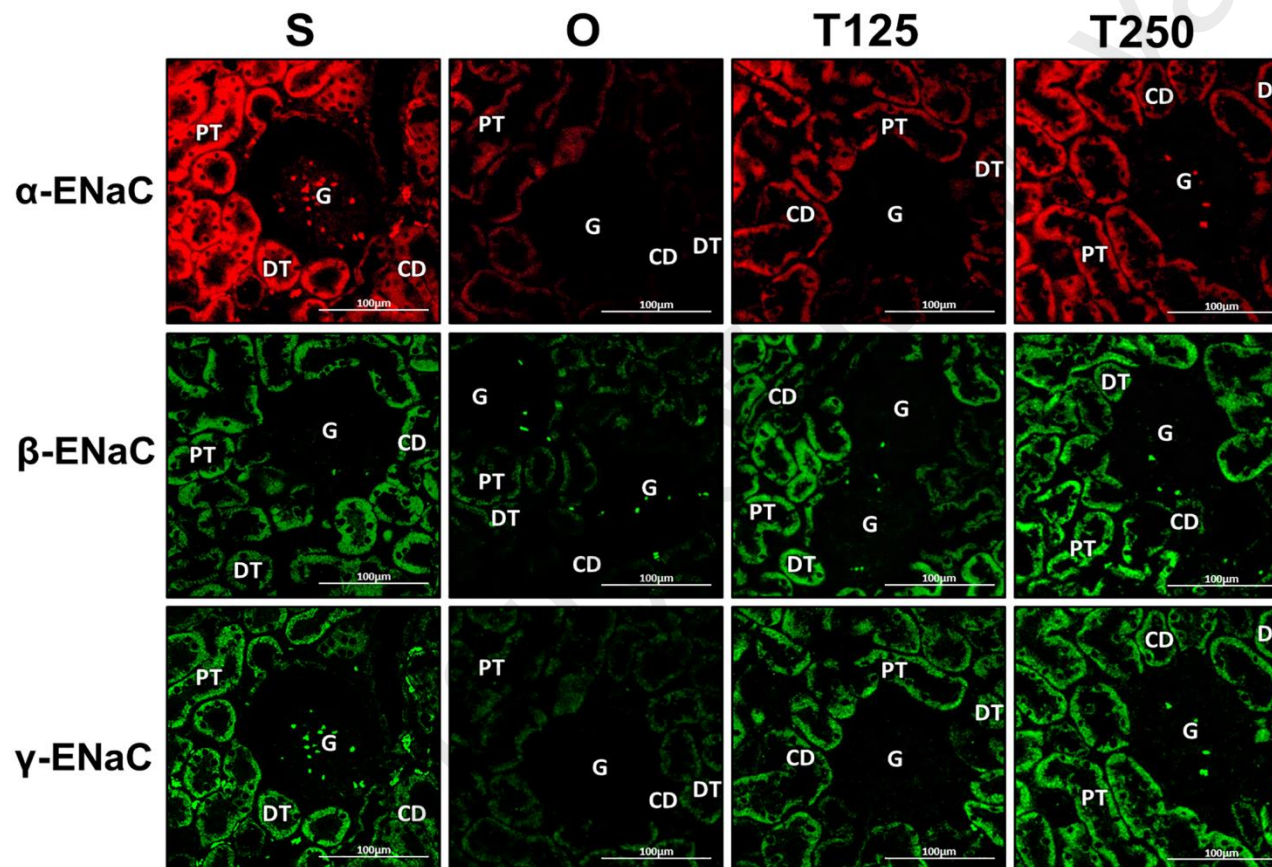


**Figure 5.7 Immunofluorescence images showing the distribution of  $\alpha$ ,  $\beta$  and  $\gamma$ -ENaC proteins in nephrons following sub-chronic testosterone treatments.**

Representative immunofluorescence images ( $n = 4/\text{group}$ ) of coronal sections of kidney incubated with  $\alpha$ ,  $\beta$  and  $\gamma$ -ENaC antibodies. Red or green fluorescence signals indicate the sites where ENaC subunit proteins were expressed. Abbreviations: S: sham operated; O: orchidectomized; T125: 125  $\mu\text{g}/\text{kg}/\text{day}$  testosterone-treated; T250: 250  $\mu\text{g}/\text{kg}/\text{day}$  testosterone-treated rats; G: glomeruli; PT: proximal convoluted tubule; DT: distal convoluted tubule; CD: collecting duct. Scale bar= 100  $\mu\text{M}$ .

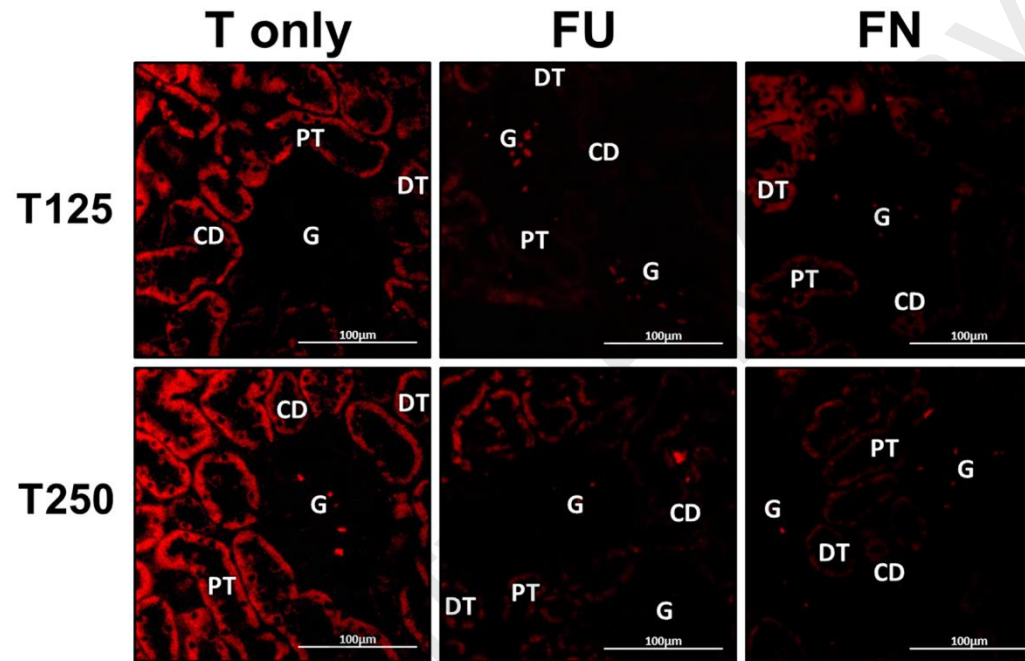


**Figure 5.8 Immunofluorescence images showing the effects of co-administration of flutamide or finasteride with sub-chronic testosterone treatments on the distribution of  $\alpha$ -ENaC in nephrons.**

Representative immunofluorescence images ( $n = 4/\text{group}$ ) of coronal sections of kidney incubated with  $\alpha$ -ENaC antibodies. Red fluorescence signals indicate sites where  $\alpha$ -ENaC subunit proteins were expressed. Abbreviations: S: sham operated; O: orchidectomized ; T125: 125µg/kg/day testosterone-treated; T250: 250µg/kg/day testosterone-treated rats; G: glomeruli; PT: proximal convoluted tubule; DT: distal convoluted tubule; CD: collecting duct. Scale bar= 100µM.

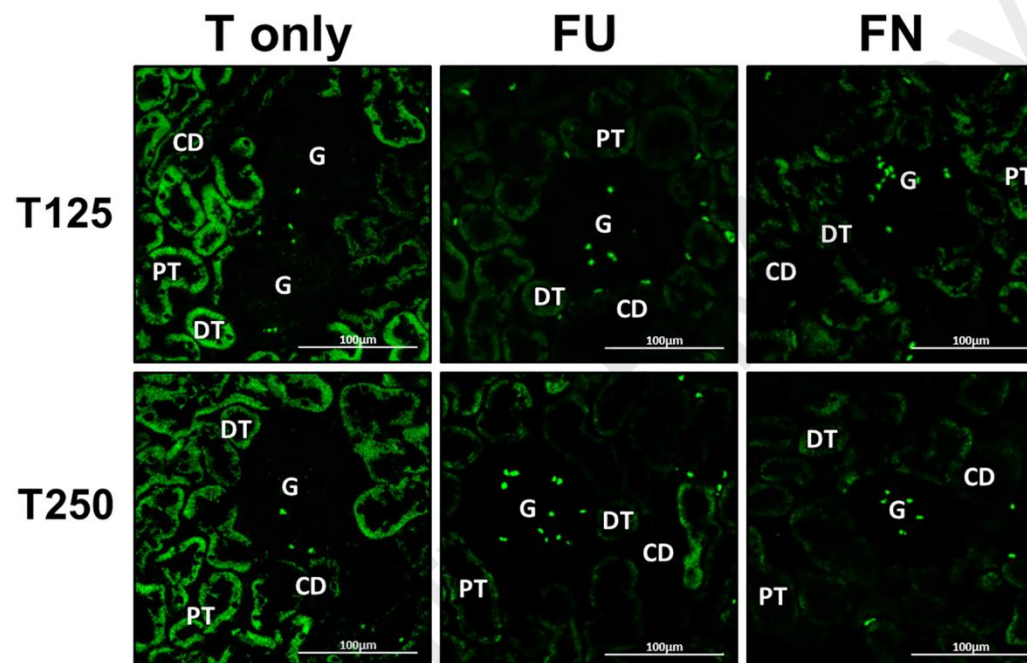


**Figure 5.9 Immunofluorescence images showing the effects of co-administration of flutamide or finasteride with sub-chronic testosterone treatments on the distribution of  $\beta$ -ENaC in nephrons.**

Representative immunofluorescence images ( $n = 4/\text{group}$ ) of coronal sections of kidney incubated with  $\beta$ -ENaC antibodies. Green fluorescence signals indicate sites where  $\beta$ -ENaC subunit proteins were expressed. Abbreviations: G: glomeruli; PT: proximal convoluted tubule; DT: distal convoluted tubule; CD: collecting duct; S: sham operated; O: orchidectomized; T125: 125 $\mu\text{g}/\text{kg}/\text{day}$  testosterone-treated; T250: 250 $\mu\text{g}/\text{kg}/\text{day}$  testosterone-treated rats. Scale bar= 100 $\mu\text{m}$ .

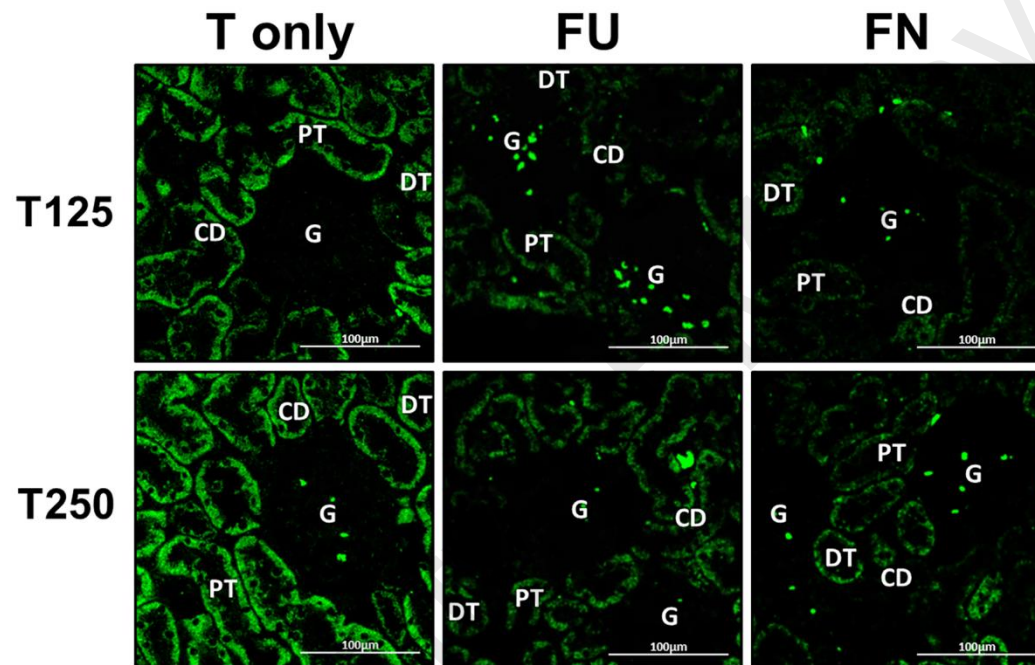


**Figure 5.10 Immunofluorescence images showing the effects of co-administration of flutamide or finasteride with sub-chronic testosterone treatments on protein expression levels of  $\gamma$ -ENaC in nephrons.**

Representative immunofluorescence images ( $n = 4/\text{group}$ ) of coronal sections of kidney incubated with  $\gamma$ -ENaC antibodies. Green fluorescence signals indicate sites where  $\gamma$ -ENaC subunit proteins were expressed. Abbreviations: S: sham operated; O: orchidectomized; T125: 125 $\mu\text{g}/\text{kg}/\text{day}$  testosterone-treated; T250: 250 $\mu\text{g}/\text{kg}/\text{day}$  testosterone-treated rats; G: glomeruli; PT: proximal convoluted tubule; DT: distal convoluted tubule; CD: collecting duct. Scale bar= 100 $\mu\text{M}$ .

### 5.3 Discussion

In this study, the dose-dependent increase in plasma testosterone level was observed when testosterone was subcutaneously injected to orchidectomized male rats at increasing doses which suggested that this hormone most likely was not metabolized as it bypassed the first-pass effect. Our data has revealed *in vivo* up-regulation in mRNAs and proteins expression levels of ENaC subunits' ( $\alpha$ ,  $\beta$  and  $\gamma$ ) in kidneys, which was accompanied by an increase in plasma aldosterone,  $\text{Na}^+$  and glucose levels, following seven days of sub-chronic testosterone treatments in orchidectomized adult male rats. Nonetheless, plasma osmolality,  $\text{K}^+$ , urea and creatinine were decreased while no changes in plasma levels of  $\text{Cl}^-$  and  $\text{Ca}^{2+}$  was observed between treatment groups. Osmolality, an osmotic pressure indicator of plasma, a measurement of the concentrations of all solutes present in the blood and varies depending on the concentration of the osmotically important solutes,  $\text{Na}^+$ ,  $\text{K}^+$ ,  $\text{Cl}^-$ , glucose and urea (Brownlow & Hutchins, 1982). Despite the increase in  $\text{Na}^+$  and glucose levels, a significant decrease in plasma  $\text{K}^+$  and urea levels could account for the observed decreased in plasma osmolality following sub-chronic testosterone treatments.

It was found that equal amount of  $\alpha$ -ENaC proteins was expressed in the orchidectomized male rats' kidneys following administration of 125 and 250 $\mu\text{g}/\text{kg}/\text{day}$  testosterone, however higher expressions of  $\beta$  and  $\gamma$ -ENaC proteins were found in the kidneys of rats which received 250 $\mu\text{g}/\text{kg}/\text{day}$  testosterone compared to 125 $\mu\text{g}/\text{kg}/\text{day}$  testosterone. The latter findings were consistent with the findings by Keinitz *et al.* (2006), who reported that administration of 500mg/kg testosterone for 14 days in male rats resulted in high level of  $\alpha$ -ENaC proteins in kidneys (Kienitz et al., 2006c). Another study has revealed that the level of  $\alpha$ -*Enac* mRNAs in human kidney cell line was enhanced by testosterone, however this hormone was found to have no significant

effects on  $\beta$  and  $\gamma$ -*Enac* mRNA levels (Quinkler et al., 2005). In contrast, in the present study, the levels of  $\beta$  and  $\gamma$ -ENaC mRNAs and proteins were highly up-regulated in the orchidectomized male rats' kidneys by testosterone treatments. Therefore, it is postulated that co-expression of all ENaC subunits ( $\alpha$ ,  $\beta$  and  $\gamma$ ) would result in a fully operating channel as their co-existence was required for the maximal ENaC channel function (Hamm et al., 2010).

In addition, the results also showed that the levels of expression of  $\alpha$ ,  $\beta$  and  $\gamma$ -ENaC mRNAs and proteins in the kidneys were significantly decreased following co-administration of flutamide with testosterone. The effect of flutamide on  $\alpha$  and  $\beta$ -ENaC but not  $\gamma$ -ENaC was found greater in rats which received 125 $\mu$ g/kg/day when compared to 250 $\mu$ g/kg/day testosterone. The reason behind this effect was unknown, however it is postulated that following high dose testosterone treatment *i.e.* at 250 $\mu$ g/kg/day, some of this hormone might be aromatized to estradiol in the adipose tissue, penis and brain (Schulster et al., 2016) while some bind to the tissue AR. The aromatized form of testosterone *i.e.* estradiol was known to cause an increase in  $\alpha$ -ENaC level in the kidneys (Gambling et al., 2004). This could perhaps explain the reason why lesser inhibition was seen following high dose testosterone treatment. In the meantime, at high dose, there was a possibility that testosterone could exert a non-genomic effect *i.e.* independent of AR (Foradori et al., 2008), which was not inhibited by flutamide (Mohd Mokhtar et al., 2014).

In this study, finasteride was found to inhibit testosterone effect in causing increases in ENaC subunits expressions in the kidneys, which suggested that DHT was involved. In the absence of DHT, levels of ENaC subunits in kidneys would be markedly decreased. Besides DHT, other hormone which was also known to cause expression

levels of  $\alpha$ ,  $\beta$  and  $\gamma$ -ENaC subunits in the kidneys to increase is aldosterone, which was reported to induce redistribution of all ENaC subunits to the apical membrane of kidneys' distal tubule and collecting ducts (Masilamani et al., 1999; Stachowiak et al., 1991). Administration of 125 and 250 $\mu$ g/kg/day testosterone increased plasma aldosterone level, suggesting that testosterone could increase the expression levels of ENaC subunits in the kidneys by inducing aldosterone secretion. In addition, redistribution of all ENaC subunits to the apical membrane of distal tubule and collecting duct under testosterone influence might produce a similar effect to that reported under aldosterone, in which this would result in fully functioning channels (Masilamani et al., 1999). The resultant effect would lead to increase in sodium reabsorption and thus higher plasma sodium level observed.

The effects of testosterone on ENaC subunits expressions and plasma sodium levels as observed in our study could help to explain the mechanisms underlying this hormone effects on kidneys' sodium handling as have been previously reported (Reckelhoff et al., 1998). Based on what has been known, this study provide additional information in which in kidneys of male rat model, testosterone was also found to enhance  $\beta$  and  $\gamma$ -ENaC subunits expressions in addition to the already known increase in  $\alpha$ -ENaC expression (Quinkler et al., 2005). These testosterone effects would likely result in a fully functioning channel which resulted in an increase in plasma sodium level. However, more works need to be done in order to confirm the optimal ENaC channel function at the apical membrane of the distal tubule and collecting duct epithelia for example by using a patch clamp in which kidney epithelial cells obtained from animals treated with testosterone will be exposed to a specific ENaC inhibitor such as amiloride (Edinger et al., 2012). If in the case where ENaC channels are functioning, inhibition by amiloride will result in reduced sodium conductance. Additionally, the involvement

of DHT can also be further confirmed by administering this compound directly to the rats and the involvement of genomic pathway *i.e.* AR-dependent, in mediating testosterone effects on ENaC expressions can be confirmed by using AR knock-out animal model.

Together, these results might be clinically relevant. The roles of testosterone in causing the development of hypertension have long been debated. So far there have been no studies implicating the direct involvement of this hormone in the development of this disease in males. Furthermore, molecular mechanisms underlying hypertension development that were linked to testosterone remain largely unknown. Several pieces of evidence showed that testosterone has a direct link to blood pressure. Reckelhoff *et al.* (1998) reported that in intact spontaneous male hypertensive (SHR) rats, elevated blood pressure was linked to high plasma testosterone level and this was further confirmed by the observations that ovariectomized female SHR rats that were given testosterone had an increase in blood pressure (Reckelhoff *et al.*, 1998). Furthermore, studies have shown that natriuresis was markedly reduced in intact male and testosterone-treated ovariectomized female SHR rats which indicated that higher amount of sodium was reabsorbed in the kidney under the influence of this hormone (Reckelhoff *et al.*, 1998). Similar findings were reported in humans whereby plasma testosterone level correlated with the blood pressure (Khaw & Barrett-Connor, 1988).

In overall, the current findings have provided evidence which might support the role of testosterone in causing a relatively higher blood pressure in males than females (refer **Chapter 4**). Increased in kidney sodium reabsorption, leading to higher plasma sodium level which may occur secondary to testosterone-induced up-regulation of ENaC might predispose the males to hypertension and could perhaps be the reason why males have a

higher incidence of this disease compared to age-matched females before menopause. The results also indicated that the differential effects of sex hormones on ENaC expression in the kidneys, followed by the changes in plasma sodium level, might contribute towards the reported gender differences in blood pressure (Reckelhoff, 2001; Reckelhoff et al., 1999).

University of Malaya

## CHAPTER 6: EFFECTS OF SUB-CHRONIC TESTOSTERONE TREATMENT ON AQUAPORINS (AQP) EXPRESSION IN KIDNEYS

### 6.1 Introduction

Aquaporin (AQP) is a membrane protein that facilitates the transport of water across the secretory epithelia (Benga, 2004). To date, thirteen AQP isoforms have been identified in the mammals (Park & Kwon, 2015). These isoforms can be classified into classical aquaporins (AQP-1, 2, 4, 5, 6 and 8) and aquaglyceroporins (AQP-3, 7, 9 and 10) (Kruse et al., 2006). AQP-1, 2, 3, 4, 6 and 7 have been reported to be expressed in kidneys (Agarwal & Gupta, 2008; Kruse et al., 2006; Nielsen et al., 2002; Park & Kwon, 2015). Expression of AQP subunits in the kidneys was found to be influenced by hormones. For example, AQP-2, an isoform which is highly expressed in the collecting ductal (CD) epithelium, is trafficked to the apical membrane by arginine vasopressin peptide (AVP) (Vukićević et al., 2016). Besides AVP, trafficking of AQP-2 and expression of its gene in the principal cells of the kidney CD was also found to be regulated by angiotensin II (Li et al., 2011) and aldosterone (de Seigneux et al., 2007). Recently, sex hormones *i.e.* estrogen has been reported to down-regulate AQP-2 expression in the kidneys at both mRNA and protein levels (Cheema et al., 2015). Nonetheless, the effects of testosterone on kidney AQP expression remained unclear.

There was evidence that testosterone could affect water handling in the kidney. In males with high testosterone levels, greater plasma volume was reported as compared to the aged-matched females (de Simone et al., 1991). In addition, males have higher blood pressure as compared to the age-matched females, which could partly be due to the relatively higher blood volume (Barrett et al., 2010). In view of these, it is postulated that higher blood pressure in males could be due to testosterone-induced

increases in the expression of AQP subunits in the kidneys. These effects of testosterone would eventually enhance the water reabsorption, subsequently could lead to increases in the plasma volume and blood pressure. Therefore, in this study, changes in the expression levels and distributions of AQP subunits that are presented in the kidney *i.e.* AQP-1, 2, 3, 4, 6 and 7, following sub-chronic exposure (seven days) to testosterone were studied. In addition, the roles of androgen receptor (AR) and dihydrotestosterone (DHT) in mediating these effects of testosterone were also investigated.

University of Malaya

## 6.2 Results

### 6.2.1 *Aqp* mRNA expression levels

In Figure 6.1(A), orchidectomy was found to cause *Aqp-1* mRNA levels in rats' kidneys to decrease ( $P < 0.05$ ). Administration of 125 µg/kg/day testosterone to orchidectomized rats caused *Aqp-1* mRNA level in the kidney to increase significantly ( $P < 0.05$ ). However, administration of 250 µg/kg/day testosterone to orchidectomized rats caused no significant changes to kidney *Aqp-1* mRNA levels. Co-administration of flutamide or finasteride to 125 µg/kg/day testosterone-treated orchidectomized rats resulted in *Aqp-1* mRNA level in the kidney to decrease ( $P < 0.05$ ). However, *Aqp-1* mRNA level did not change significantly following co-administration of flutamide or finasteride to 250 µg/kg/day testosterone-treated rats.

In Figure 6.1(B), orchidectomy was found to cause *Aqp-2* mRNA level in rats' kidneys to decrease ( $P < 0.05$ ). Following of orchidectomized rats with 125 µg/kg/day testosterone, no significant changes in *Aqp-2* mRNA level were observed. However, following the administration of 250 µg/kg/day testosterone, the level of *Aqp-2* mRNA in orchidectomized rats significantly increased ( $P < 0.05$ ). Co-administration of flutamide or finasteride resulted in *Aqp-2* mRNA level in both 125 µg/kg/day and 250 µg/kg/day testosterone-treated rats to decrease ( $P < 0.05$ ).

In Figure 6.1(C), orchidectomy was found to cause the level of *Aqp-3* mRNA in kidneys to increase ( $P < 0.05$ ). Treatment with 125 µg/kg/day testosterone to orchidectomized rats resulted in *Aqp-3* mRNA level in kidneys to decrease ( $P < 0.05$ ). A slight decrease in *Aqp-3* mRNA level in kidneys was observed in orchidectomized rats following administration of 250 µg/kg/day testosterone. Co-administration of flutamide

or finasteride resulted in *Aqp-3* mRNA level in 125µg/kg/day testosterone-treated but not 250µg/kg/day testosterone-treated rats' kidneys to significantly increase.

In Figure 6.1(D), *Aqp-4* mRNA level in kidneys was found to decrease following orchidectomy ( $P<0.05$ ). Treatment of 125µg/kg/day testosterone to orchidectomized male rats resulted in *Aqp-4* mRNA level in kidneys to increase ( $P<0.05$ ). Greater increases were observed following administration of orchidectomized male rats with 250µg/kg/day testosterone. Meanwhile, co-treatments of flutamide or finasteride to 125µg/kg/day and 250µg/kg/day testosterone-treated rats resulted in *Aqp-4* mRNA level in kidneys to decrease to the level observed in the non-treated orchidectomized rats ( $P<0.05$ ).

In Figure 6.1(E), orchidectomy was found to cause *Aqp-6* mRNA level in kidneys to decrease ( $P<0.05$ ). However, *Aqp-6* mRNA level in the kidney of orchidectomized rats increased significantly following testosterone treatment ( $P<0.05$ ), in which administration of 250µg/kg/day testosterone resulted in greater increase in *Aqp-6* mRNA level in the kidney when compared with 125µg/kg/day testosterone treatment. Co-administration of flutamide or finasteride to testosterone-treated rats resulted in *Aqp-6* mRNA level in kidneys to decrease significantly ( $P<0.05$ ).

In Figure 6.1(F), the level of *Aqp-7* mRNA in kidneys decreased following orchidectomy ( $P<0.05$ ). Administration of testosterone to orchidectomized male rats resulted in significant increase in *Aqp-7* mRNA level in kidneys ( $P<0.05$ ), with a greater increase observed in rats receiving 125µg/kg/day when compared to 250µg/kg/day testosterone-treated rats. In these rats, co-administration of flutamide or

finasteride to testosterone-treated male rats resulted in *Aqp-7* mRNA level in kidneys to decrease ( $P < 0.05$ ).

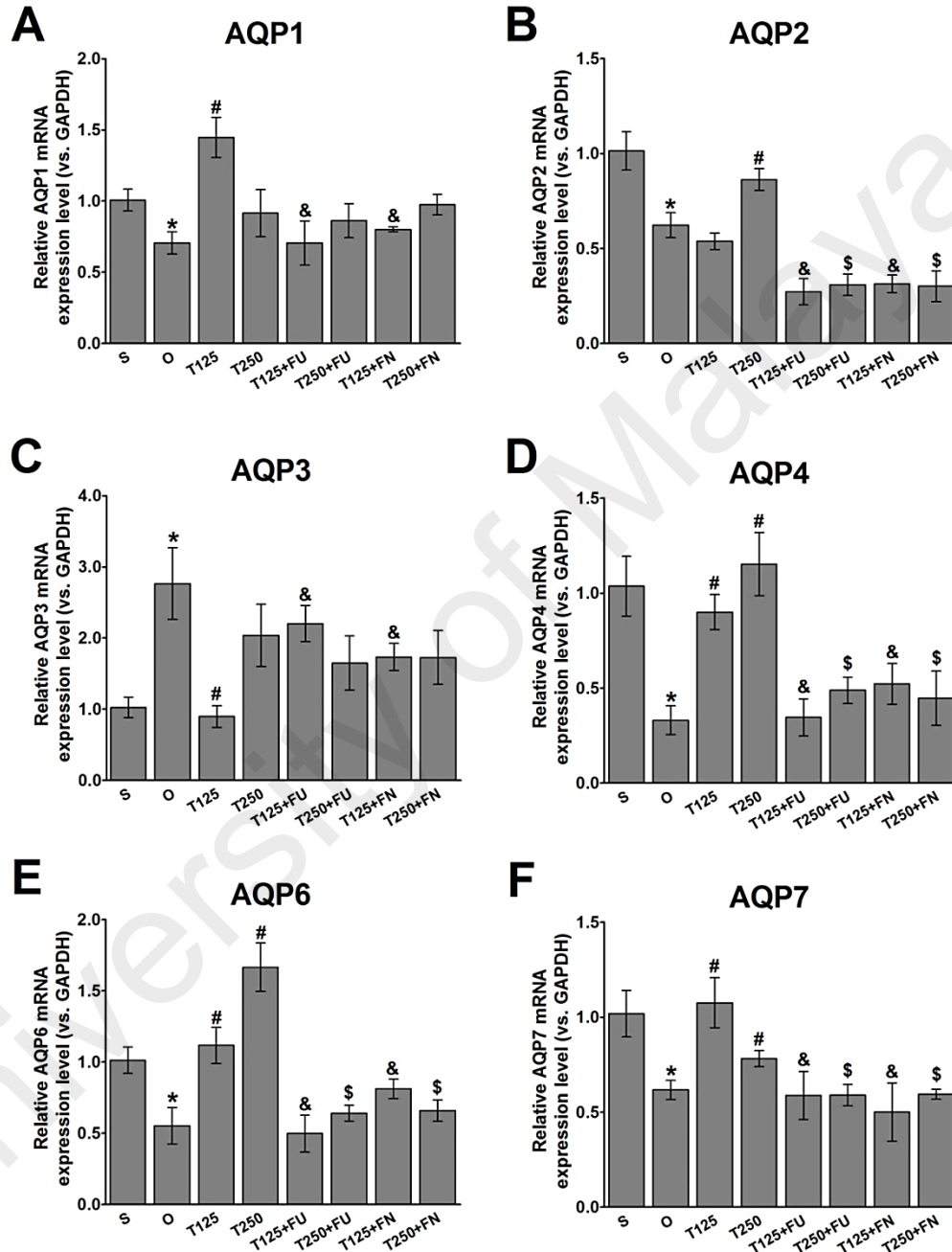


**Figure 6.1** Effects of sub-chronic testosterone treatment on mRNA expression levels of AQP subunits in kidneys.

Relative mRNA levels of (A) *Aqp-1*, (B) *Aqp-2*, (C) *Aqp-3*, (D) *Aqp-4*, (E) *Aqp-6* and (F) *Aqp-7* in the kidneys. Data are presented as mean  $\pm$  SEM ( $n = 5-6$ /group, one way ANOVA); \* $P < 0.05$  compared to S; # $P < 0.05$  compared to O; & $P < 0.05$  compared to T125; \$ $P < 0.05$  compared to T250. Abbreviations: S: sham operated; O: orchidectomized ; T125: 125 $\mu$ g/kg/day testosterone-treated; T250: 250 $\mu$ g/kg/day testosterone-treated rats; FU: flutamide; FN: finasteride.

### 6.2.2 Classical aquaporin (AQP-1, 2, 4 and 6) protein levels

In Figure 6.2(A) and 6.2(B), orchidectomy was found to cause AQP-1 protein level in kidneys to decrease ( $P<0.05$ ). The levels of AQP-1 protein in orchidectomized rats' kidneys markedly increased following 125 $\mu\text{g}/\text{kg}/\text{day}$  testosterone treatment ( $P<0.05$ ). However, no significant changes in AQP-1 protein level in kidneys were observed following administration of 250 $\mu\text{g}/\text{kg}/\text{day}$  testosterone to the orchidectomized male rats. Co-administration of flutamide to testosterone-treated rats resulted in AQP-1 protein level in kidneys to decrease ( $P<0.05$ ). However, co-administration of finasteride has no effect on AQP-1 protein expression level in the kidneys of rats receiving testosterone treatment.

Meanwhile, the level of AQP-2 protein in kidneys significantly decreased following orchidectomy ( $P<0.05$ ). Administration of 250 $\mu\text{g}/\text{kg}/\text{day}$  testosterone ( $P<0.05$ ) but not 125 $\mu\text{g}/\text{kg}/\text{day}$  testosterone resulted in AQP-2 protein level in orchidectomized rats' kidney to increase. In testosterone-treated orchidectomized rats, co-administration of flutamide or finasteride resulted in AQP-2 protein level in the kidney to decrease ( $P<0.05$ ).

The level of AQP-4 protein in kidneys significantly decreased following orchidectomy ( $P<0.05$ ). In orchidectomized rats, the level of this protein increased following testosterone treatments of 125 and 250 $\mu\text{g}/\text{kg}/\text{day}$  ( $P<0.05$ ). Co-administration of flutamide or finasteride in testosterone-treated orchidectomized male rats resulted in AQP-4 protein level in kidneys to decrease ( $P<0.05$ ).

The level of AQP-6 protein in kidneys significantly decreased following orchidectomy ( $P<0.05$ ). Administration of testosterone to orchidectomized male rats

resulted in AQP-6 protein level in kidneys to significantly increase ( $P<0.05$ ), with greater effects observed following administration of 250 $\mu$ g/kg/day testosterone. In orchidectomized rats which received testosterone, co-administration of flutamide or finasteride resulted in AQP-6 protein level in kidneys to decrease ( $P<0.05$ ).

### 6.2.3 Aquaglyceroporin (AQP-3 and 7) protein levels

In Figure 6.3(A) and 6.3(B), the level of AQP-3 protein in kidneys markedly increased following orchidectomy ( $P<0.05$ ). In orchidectomized male rats receiving 125 $\mu$ g/kg/day testosterone treatment, AQP-3 protein level markedly decreased ( $P<0.05$ ). However, no significant change was observed in rats treated with 250 $\mu$ g/kg/day testosterone. Co-administration of flutamide or finasteride to 125 $\mu$ g/kg/day testosterone-treated orchidectomized male rats resulted in AQP-3 protein expression level in kidneys to increase significantly ( $P<0.05$ ).

Meanwhile, the level of AQP-7 protein in kidneys significantly decreased following orchidectomy ( $P<0.05$ ). In orchidectomized male rats, treatment with 125 $\mu$ g/kg/day testosterone ( $P<0.05$ ) but not 250 $\mu$ g/kg/day testosterone resulted in marked increase in AQP-7 protein expression level in kidney. In 125 $\mu$ g/kg/day testosterone-treated orchidectomized male rats, co-administration of flutamide or finasteride resulted in AQP-7 protein expression level in kidneys to significantly decrease ( $P<0.05$ ).

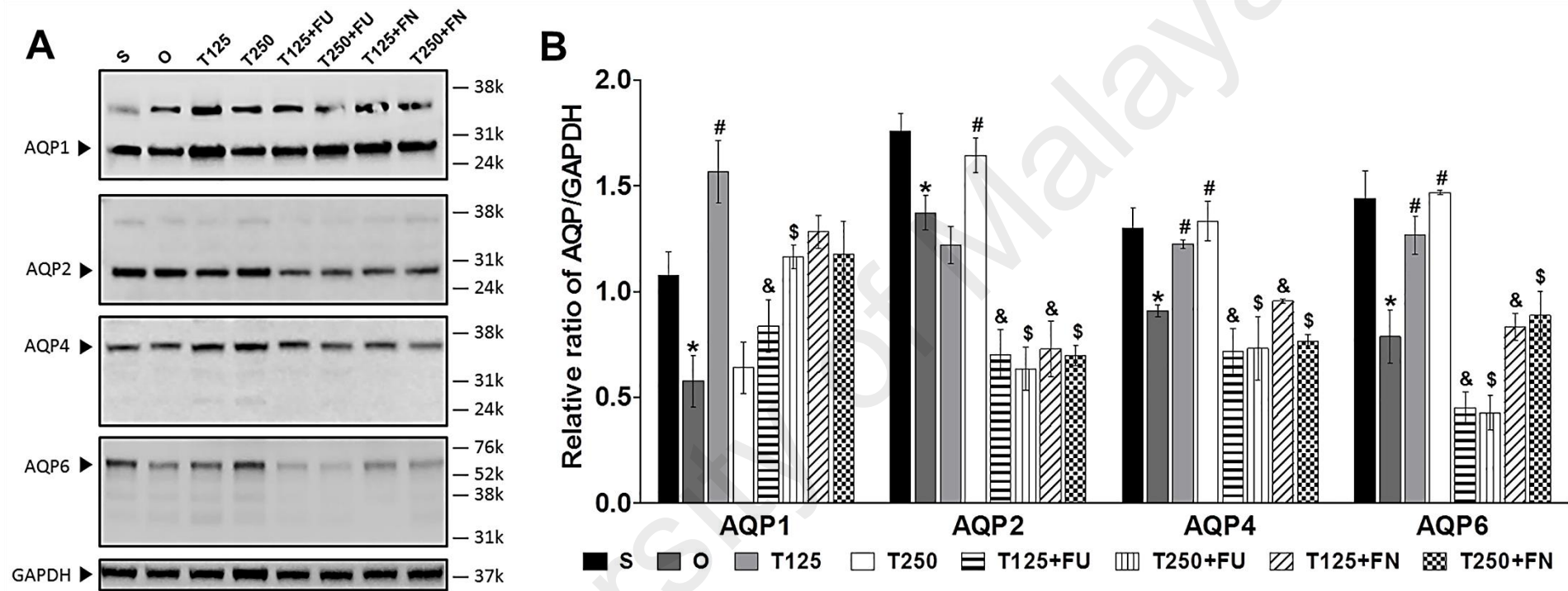


**Figure 6.2 Effects of sub-chronic testosterone treatment on expression levels of classical aquaporin subunit proteins in kidneys.**

(A) Representative immunoblot images of classical aquaporin *i.e.* AQP-1, AQP-2, AQP-4 and AQP-6. Molecular weight of targeted proteins = 28kDa (AQP-1), 29kDa (AQP-2), 34kDa (AQP-4) and 55kDa (AQP-6). (B) Average relative ratio of band intensities of AQP-1, AQP-2, AQP-3 and AQP-4 proteins to housekeeping protein, GAPDH (of three replicate blots). Data are presented as mean  $\pm$  SEM (n = 4/group, one way ANOVA); \* $P$ <0.05 compared to S; # $P$ <0.05 compared to O; & $P$ <0.05 compared to T125; \$ $P$ <0.05 compared to T250. Abbreviations: S: sham operated; O: orchidectomized; T125: 125 $\mu$ g/kg/day testosterone-treated; T250: 250 $\mu$ g/kg/day testosterone-treated rats; FU: flutamide; FN: finasteride.

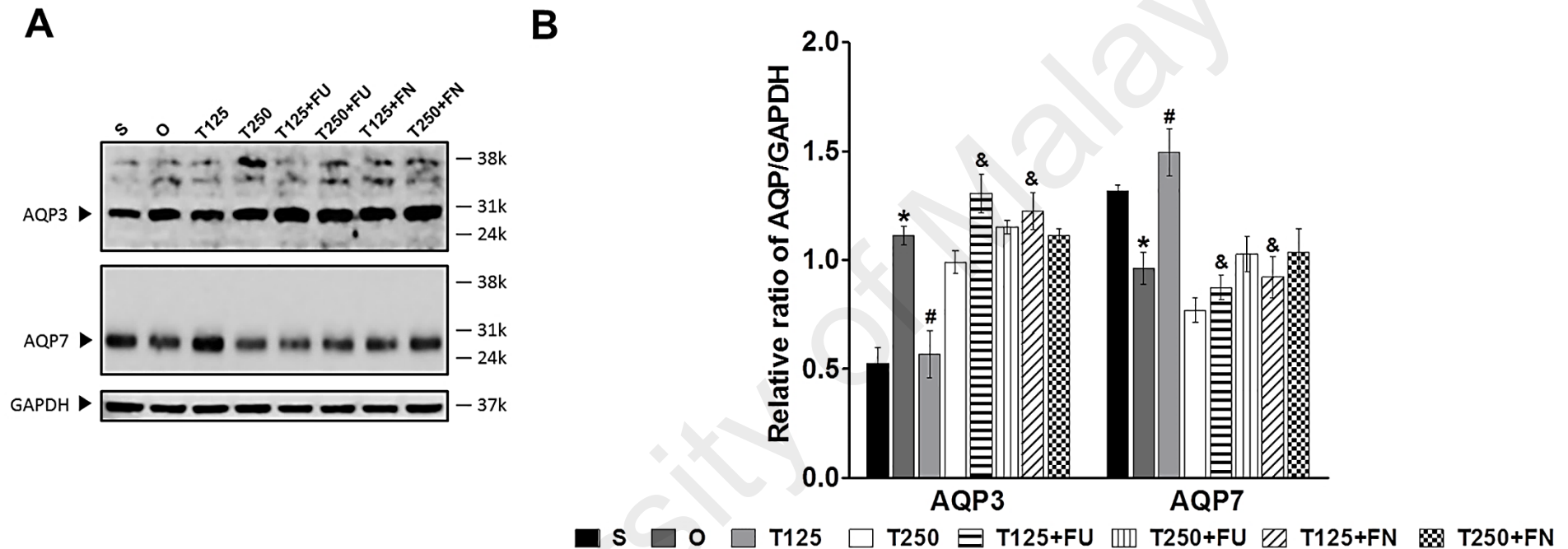


**Figure 6.3 Effects of sub-chronic testosterone treatment on expression levels of aquaglyceroporin proteins in kidneys.**

(A) Representative immunoblot images of aquaglyceroporin *i.e.* AQP-3 and AQP-7 in kidneys. Molecular weight of targeted proteins = 31kDa (AQP-3) and 22-33kDa (AQP-7). (B) Average relative ratio of band intensities of AQP-3 and AQP-7 proteins to housekeeping protein, GAPDH (of three replicate blots). Data are presented as mean  $\pm$  SEM (n = 4/group, one way ANOVA); \* $P$ <0.05 compared to S; # $P$ <0.05 compared to O; & $P$ <0.05 compared to T125; \$ $P$ <0.05 compared to T250. Abbreviations: S: sham operated; O: orchidectomized; T125: 125 $\mu$ g/kg/day testosterone-treated; T250: 250 $\mu$ g/kg/day testosterone-treated rats; FU: flutamide; FN: finasteride.

#### 6.2.4 Distribution of AQP-1 and AQP-3 proteins in nephrons

In Figure 6.4, AQP-1 protein (green fluorescent signal) could be seen in the proximal convoluted tubule (PT). A relatively high distribution of AQP-1 protein was seen in the sham-operated intact rats while in orchidectomized male rats, a relatively lower AQP-1 protein distribution was observed. Treatments with 125µg/kg/day and 250µg/kg/day testosterone resulted in relatively higher AQP-1 protein in PT as compared to orchidectomized rats. Co-administration of flutamide or finasteride with testosterone in these rats resulted in relatively lower levels of AQP-1 protein distribution in PT. AQP3 protein (red fluorescent signal) could be seen in the PT and CD, with relatively higher distribution in orchidectomized rats. Treatment of orchidectomized male rats with 125µg/kg/day testosterone resulted in comparably reduced AQP3 protein distribution in these nephron segments. However, no significant change was observed in orchidectomized rats received 250µg/kg/day testosterone. In 125µg/kg/day testosterone-treated orchidectomized rats, co-administration of flutamide or finasteride caused relatively increased in the distribution of the AQP-3 protein in PT and CD.

### **6.2.5 Distribution of AQP-2 and AQP-4 proteins in nephrons**

In Figure 6.5, both AQP-2 protein (red fluorescent signal) and AQP-4 protein (green fluorescent signal) could be seen to be distributed in CD. AQP2 was found to be expressed specifically at the apical membrane while AQP-4 was found to be expressed specifically at the basolateral membrane of CD. A comparably high distribution of these proteins could be seen in the kidneys of sham-operated intact rats. In orchidectomized male rats, testosterone treatments caused AQP-2 and AQP-4 protein distribution in CD to relatively increase. Relatively lower AQP-2 and AQP-4 distribution were observed in CD of testosterone-treated rats which also received co-treatment with flutamide or finasteride.

### **6.2.6 Distribution of AQP-6 and AQP-7 proteins in nephrons**

In Figure 6.6, AQP-6 protein (green fluorescent signal) could be seen to be distributed in CD while AQP-7 protein (red fluorescent signal) could be seen to be distributed in PT. Expression levels of these proteins were relatively higher in the sham-operated intact rats and relatively lower in male rats that underwent orchidectomy. In orchidectomized male rats, administration of testosterone caused the distribution of AQP-6 and AQP-7 proteins to be relatively increased. In these rats, co-administration of flutamide or finasteride resulted in AQP-6 and AQP-7 protein distributions in the kidneys to relatively decrease.

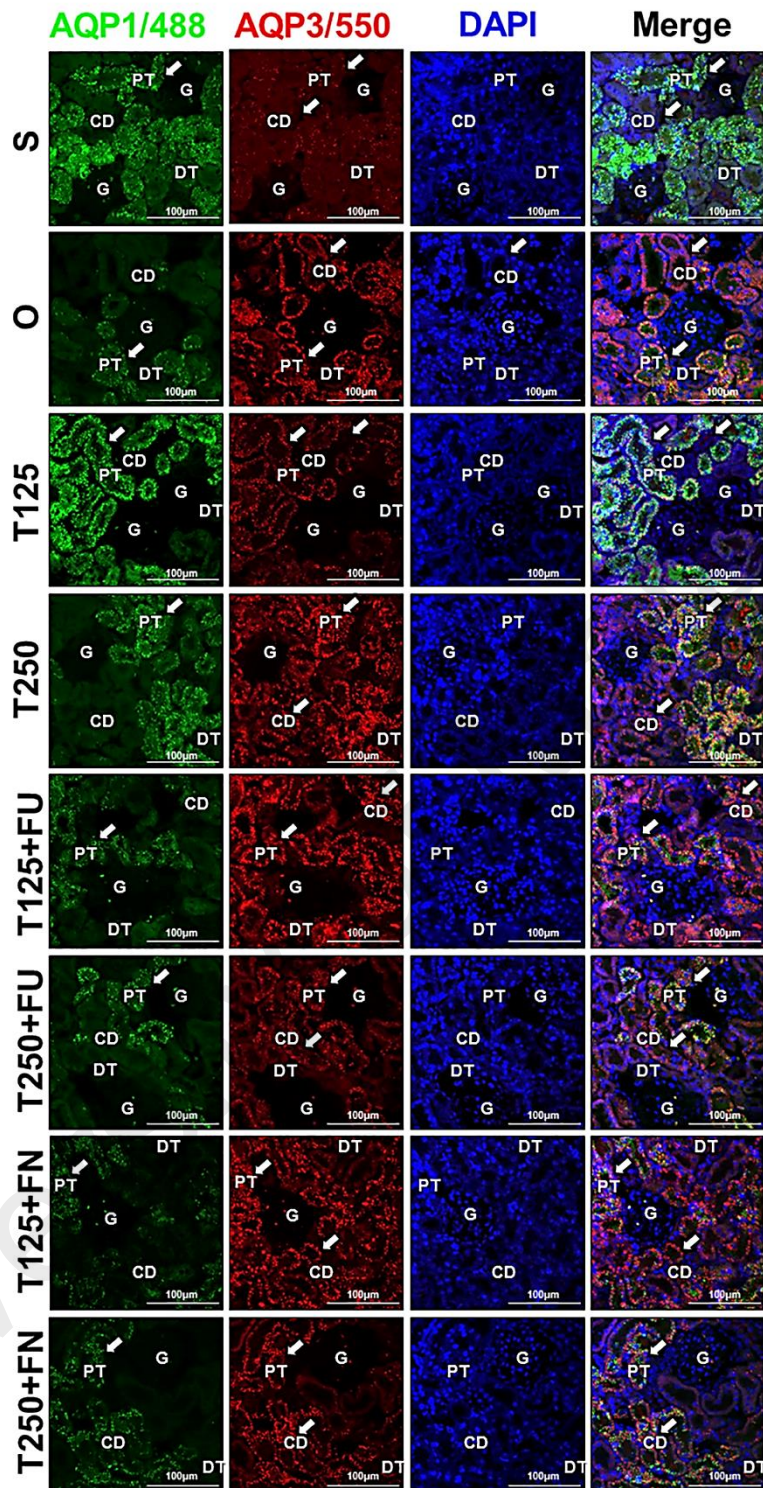


**Figure 6.4 Effects of sub-chronic testosterone treatment on the distribution of AQP-1 (green) and AQP-3 (red) proteins in nephrons.**

Representative confocal microscopic immunofluorescence images ( $n = 4/\text{group}$ ) of the nephrons showing the distribution of AQP-1 and AQP-3. AQP-1 was represented by green fluorescent signals while AQP-3 was represented by red fluorescent signals. Abbreviations: S: sham operated; O: orchidectomized; T125: 125 $\mu\text{g}/\text{kg}/\text{day}$  testosterone-treated; T250: 250 $\mu\text{g}/\text{kg}/\text{day}$  testosterone-treated rats; FU: flutamide; FN: finasteride; G: glomerulus; DT: distal convoluted tubule; PT: proximal convoluted tubule and CD: collecting duct. Scale bar = 100 $\mu\text{M}$ .

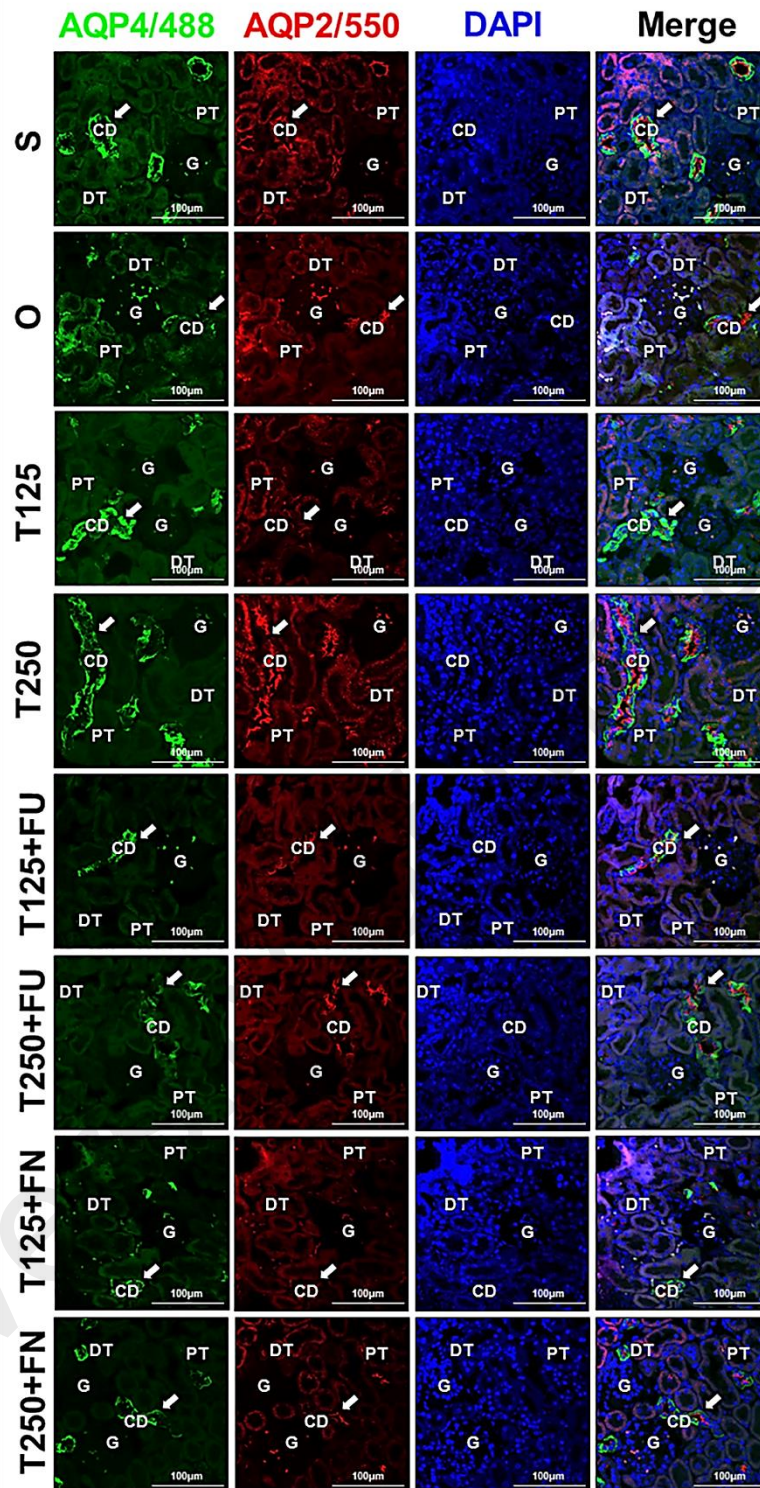


**Figure 6.5 Effects of chronic testosterone treatment on the distribution of AQP-2 (red) and AQP-4 (green) proteins in nephrons.**

Representative confocal microscopic immunofluorescence images (n = 4/group) showing the distribution of AQP-2 and AQP-4 in nephrons. AQP-2 was represented by red fluorescent signals while AQP-4 was represented by green fluorescent signals. Abbreviations: S: sham operated; O: orchidectomized; T125: 125µg/kg/day testosterone-treated; T250: 250µg/kg/day testosterone-treated rats; FU: flutamide; FN: finasteride; G: glomerulus; DT: distal convoluted tubule; PT: proximal convoluted tubule and CD: collecting duct. Scale bar = 100µM.

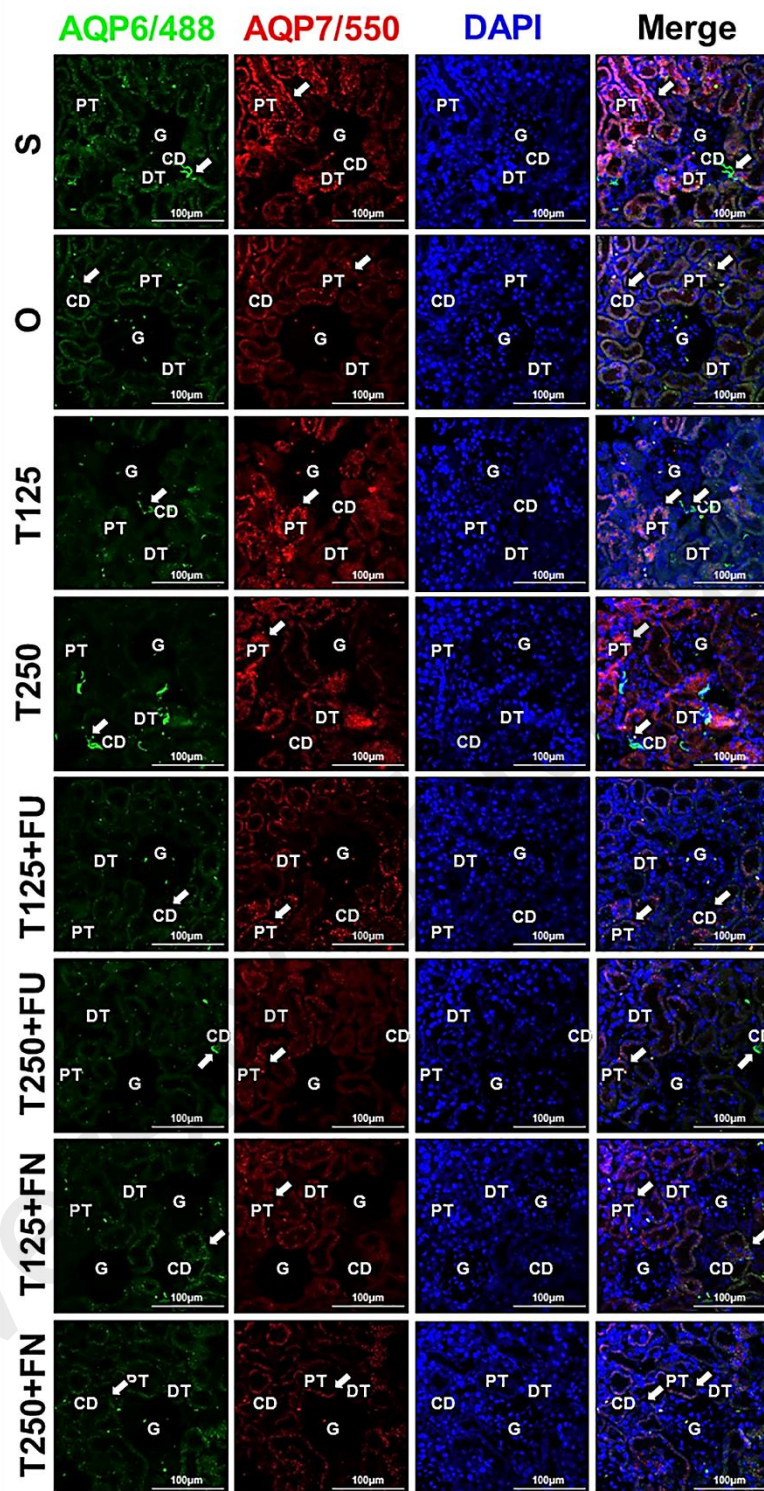


**Figure 6.6** Effects of sub-chronic testosterone treatment on the distribution of AQP-6 (green) and AQP-7 (red) proteins in nephrons.

Representative confocal microscopic immunofluorescence images (n = 4/group) showing the distribution of AQP-6 and AQP-7 in nephrons. AQP-6 was represented by green fluorescent signals while AQP-7 was represented by red fluorescent signals. Abbreviations: S: sham operated; O: orchidectomized; T125: 125 $\mu$ g/kg/day testosterone-treated; T250: 250 $\mu$ g/kg/day testosterone-treated rats; FU: flutamide; FN: finasteride; G: glomerulus; DT: distal convoluted tubule; PT: proximal convoluted tubule and CD: collecting duct. Scale bar = 100 $\mu$ M.

### 6.3 Discussion

This study revealed the effects of sub-chronic exposure to testosterone on expression levels and distribution of AQP subunits in kidneys. Sub-chronic testosterone treatment was found to cause AQP-1, 2, 4, 6 and 7 protein and mRNA levels in the kidneys to increase. However, testosterone treatment caused AQP-3 protein and mRNA levels in the kidneys to decrease. Treatment with 125µg/kg/day testosterone was found to produce greater increase in AQP-1 and 7 protein and mRNA levels as compared to treatment with 250µg/kg/day testosterone. The *vice-versa* effects of both testosterone doses were observed on AQP-2, 4 and 6 protein and mRNA levels. The observed differences in the effect of low dose *i.e.* 125µg/kg/day compared to high dose *i.e.* 250µg/kg/day testosterone indicated that testosterone displays dose-dependent effect. The similar observations have been reported elsewhere. In the aorta, low dose testosterone was reported to produce greater effects in inducing contraction when compared to high dose (Montano et al., 2008). The reason being was that testosterone at high dose could be aromatized to estrogen that might cause the opposite effects (Herak-Kramberger et al., 2015). The contradictory testosterone effects based on doses could also be due to the involvement of non-genomic pathways (Foradori et al., 2008; Wilson et al., 2011), which might occur following treatment with high-dose testosterone.

Immunofluorescence results showed that AQP-1 and 7 were expressed mainly in the PT while AQP-2, 4 and 6 were expressed in the CD. AQP-3 was distributed in most parts of the nephrons, except the DT and renal corpuscle. Our findings were consistent with other previous reports which indicate that AQP-1 was abundantly distributed in the PT and plays an essential role in urine concentrating mechanism (Vallon et al., 2000). AQP-2 was exclusively distributed in the principal cells of the CD and is regulated by AVP (Vukićević et al., 2016). AQP-3 and 4 were distributed at the basolateral

membrane of the CD and serves as the exit pathway for water reabsorbed via apical AQP-2 (Marlar et al., 2014). AQP-6 was presented in the vesicles within the intercalated cells of CD (Jin-Gon et al., 2014) while AQP-7 was abundantly distributed in the brush border of PT and involved in water reabsorption (Sohara et al., 2009).

In addition, the present results have also shown that the effects of testosterone were mainly mediated via AR and this finding was further supported by other findings which reported that AQP gene contains androgen-response elements (AREs) in the promoter region which is regulated androgens (Joseph et al., 2011; Moehren et al., 2008). In addition, testosterone was also found to exert its effects via DHT that regulates the expression of AQP in the kidney. Treatment of orchidectomized SD rats with DHT have been reported to cause a reduction in water excretion (Xu et al., 2009) while in the current study, inhibition of conversion of testosterone to DHT have caused the reduction in expression of all AQP subunits except AQP-3 in the kidney. Together, these findings have suggested the role of DHT in AQP-mediated water reabsorption in kidney whereby testosterone could also exert its effects by converting to DHT.

The observed differences in AQP-1, 2, 4, 6 and 7 distributions in different parts of the nephron under testosterone influences indicate that testosterone could play important role in regulation of body water homeostasis. Under the influence of testosterone, the elevated expression of AQP-1 and 7 in the PT could help to enhance water (and glycerol) reabsorption and lead to plasma volume expansion. The passive movement of water via AQP-1 and 7 occurs secondary to sodium reabsorption. Testosterone was also found to up-regulate the expression of AQP-2, 4 and 6 in the CD, however expression of AQP-3 was down-regulated by testosterone. The increased in the distribution of AQP-2 and 4 at the apical and basolateral membranes of CD indicated

that under the influence of testosterone, this nephron segment is highly permeable to water. Therefore, testosterone might produce effects that resemble AVP and aldosterone where both were reported to induce AQP-2 protein trafficking to the apical membrane of the CD (Takata et al., 2008). In fact, testosterone has been reported to help in restoring the AVP binding sites in kidneys (Herzberg et al., 1989). Together, these effects could collectively enhance the amount of water reabsorbed in the kidneys (Kwon et al., 2013; Marples et al., 1995).

In overall, the present study have demonstrated the differential effects of testosterone on the expressions of AQP subunits in the kidneys, which might in part contributed to the greater blood volume and higher blood pressure in the males than age-matched females. Elevated expressions of AQP-1, 2, 4, 6 and 7 in the kidney following sub-chronic testosterone treatments may lead to enhanced water reabsorption and thus increased blood volume and pressure. These findings have improved the understanding of the roles of testosterone in blood pressure regulation, which might then explain the higher blood pressure in males than females.

## CHAPTER 7: EFFECTS OF CHRONIC TESTOSTERONE TREATMENT ON EPITHELIAL SODIUM CHANNEL (ENAC) IN KIDNEYS

### 7.1 Introduction

It is well known that kidney plays an important role in regulating the blood pressure by modifying plasma sodium level (Meneton et al., 2005). In kidney distal convoluted tubules (DT) and collecting ducts (CD) and, the reabsorption of filtered sodium is under aldosterone influence (Meneton et al., 2005; Verrey et al., 2008). Evidence indicated that other hormones, including sex-steroid hormones, could also be involved in regulating sodium reabsorption in the kidney (Liu & Ely, 2011; Rouch et al., 2012). Indeed, sex hormone receptors such as androgen receptor (AR) (Kienitz et al., 2009; Quinkler et al., 2005), estrogen receptor (ER) (Graceli et al., 2013; Lane, 2008) and progesterone receptor (PR) (Graceli et al., 2013; Yanes et al., 2008) have been found to be expressed in the kidneys. Amongst the sex hormones, testosterone has been shown to directly influence sodium handling in the kidney. For instance, this hormone has been reported to promote sodium reabsorption along the nephron through up-regulation of the renin-angiotensin system (RAS) (Hu et al., 2011; Maranon & Reckelhoff, 2013; Yanes et al., 2009).

In kidney, reabsorption of filtered sodium in late DT and CD occurs through the apical epithelial sodium channel (ENaC), the rate-limiting step for sodium reabsorption in distal nephron that is known to play a major role in the regulation of sodium and water homeostasis and blood pressure (Butterworth, 2010; Marunaka et al., 2016). The sub-cellular localization and expression of ENaC in the kidney are regulated by hormones (Bubien, 2010). Aldosterone, the main mineralocorticoid hormone, is known to increase the insertion of ENaC subunits into the apical membrane of DT and CD

epithelial cells (Eaton et al., 1995; Frindt et al., 2008; Masilamani et al., 1999). Nevertheless, there is also evidence that sex hormones influence ENaC expression in the kidney (Gambling et al., 2004; Kienitz et al., 2009; Yusef et al., 2014). Higher mRNA abundance of  $\alpha$ ,  $\beta$  and  $\gamma$ -ENaC in the kidneys of females compared to males was abolished by ovariectomy, suggesting that ENaC expressions could be regulated by female sex hormones in the kidney (Gambling et al., 2004). Meanwhile, treatment with estrogen was found to increase the abundance of  $\alpha$ - and  $\gamma$ -ENaC (Gambling et al., 2004; Yusef et al., 2014). Despite the limited information with regard to the effects of testosterone on ENaC expression in the kidneys, earlier *in-vitro* and *in vivo* studies have shown the up-regulation of  $\alpha$ -ENaC mRNA expression level following treatment with testosterone (Kienitz et al., 2009; Quinkler et al., 2005).

In **Chapter 4**, chronic testosterone treatment was found to cause the increase in the mean arterial pressure (MAP) of ovariectomized female normotensive and hypertensive rats. Therefore, it is hypothesized that these increases in the blood pressure under testosterone influence could be mediated via the changes in expression level of  $\alpha$ ,  $\beta$  and  $\gamma$ -ENaC in the kidneys. These changes could then result in enhanced sodium reabsorption that ultimately causes the increase in blood pressure. In the present study, the effects of chronic (six weeks) testosterone treatment on ENaC expression in the kidney of both normotensive and hypertensive rats were investigated. In addition, the changes in the related hormonal and biochemical blood parameters which include plasma aldosterone, electrolytes ( $\text{Na}^+$ ,  $\text{K}^+$ ,  $\text{Cl}^-$  and  $\text{Ca}^{2+}$ ), osmolality, glucose, urea and creatinine levels were also examined.

## 7.2 Results

### 7.2.1 Hormonal and biochemical blood parameters

In Table 7.1 for WKY rats and Table 7.2 for SHR rats, plasma testosterone level was used as an indicator for success manipulations of the experimental models. Male SHR rats showed higher circulating plasma testosterone levels than male WKY rats. As expected, orchidectomy significantly reduced blood testosterone levels in both male WKY and SHR rats down to the same negligible levels ( $P < 0.01$ ). Ovariectomized female rats have lower testosterone levels than male rats of either strain, but testosterone levels were no difference between ovariectomized female SHR and WKY rats. Testosterone supplementation in ovariectomized female SHR and WKY rats increased the circulating levels of this hormone to the level seen in males ( $P < 0.01$  for WKY rats and  $P < 0.001$  for SHR rats).

Meanwhile, in orchidectomized male WKY rats, plasma aldosterone levels were significantly higher than sham-operated male WKY rats ( $P < 0.001$ ). Chronic testosterone treatment to ovariectomized female WKY rats had resulted in plasma aldosterone level to decrease ( $P < 0.01$ ). In male SHR rats, plasma aldosterone level significantly elevated following orchidectomy ( $P < 0.05$ ). In testosterone-treated ovariectomized female SHR rats, relatively lower plasma aldosterone levels were observed when compared to non-treated ovariectomized female SHR rats ( $P < 0.01$ ).

In Table 7.1, significant increases in plasma levels of  $\text{Na}^+$  ( $P < 0.05$ ), osmolality ( $P < 0.001$ ),  $\text{K}^+$  ( $P < 0.01$ ), urea ( $P < 0.05$ ) and creatinine ( $P < 0.01$ ) were observed in male WKY rats following orchidectomy. In ovariectomized female WKY rats, chronic testosterone treatment resulted in significant decreases in plasma  $\text{Na}^+$  ( $P < 0.001$ ),

osmolality ( $P<0.05$ ), urea ( $P<0.05$ ) and creatinine ( $P<0.01$ ) levels. No significant changes in plasma  $\text{Cl}^-$ ,  $\text{Ca}^{2+}$  and glucose levels were observed between different treatment groups.

In Table 7.2, plasma  $\text{Na}^+$  ( $P<0.01$ ), osmolality ( $P<0.05$ ),  $\text{K}^+$  ( $P<0.05$ ), urea ( $P<0.01$ ) and creatinine ( $P<0.01$ ) levels in male SHR rats were significantly increased following orchidectomy. In ovariectomized female SHR rats, plasma  $\text{Na}^+$  ( $P<0.05$ ), osmolality ( $P<0.05$ ),  $\text{K}^+$  ( $P<0.01$ ), urea ( $P<0.01$ ) and creatinine ( $P<0.001$ ) levels were significantly decreased in following chronic testosterone treatment. No significant changes in plasma  $\text{Cl}^-$ ,  $\text{Ca}^{2+}$  and glucose levels were noted between different treatment groups.

**Table 7.1 Effects of chronic testosterone treatment on hormonal and biochemical parameters in blood plasma of normotensive WKY rats.**

Group	WMS	WMO	WFO	WFT
<b>Testosterone</b> (ng/ml)	1.97 ± 0.24	0.62 ± 0.08 **	0.80 ± 0.05	2.19 ± 0.22 ##
<b>Aldosterone</b> (pg/ml)	75.53 ± 19.55	327.40 ± 37.18 ***	311.58 ± 48.85	170.84 ± 33.78 #
<b>Sodium, Na<sup>+</sup></b> (mmol/L)	140.50 ± 0.89	143.50 ± 0.22 *	144.50 ± 0.50	137.67 ± 0.76 ###
<b>Osmolality</b> (mOsmol/kg)	303.17 ± 0.79	311.67 ± 1.17 ***	305.83 ± 0.83	299.33 ± 2.20 #
<b>Chloride, Cl<sup>-</sup></b> (mmol/L)	102.88 ± 0.90	100.25 ± 1.05	103.25 ± 0.61	102.38 ± 1.21
<b>Potassium, K<sup>+</sup></b> (mmol/L)	4.82 ± 0.07	5.62 ± 0.13 **	4.93 ± 0.14	5.05 ± 0.14
<b>Calcium, Ca<sup>2+</sup></b> (mmol/L)	2.53 ± 0.02	2.67 ± 0.11	2.53 ± 0.05	2.43 ± 0.02
<b>Glucose</b> (mmol/L)	9.96 ± 1.42	12.15 ± 1.64	8.93 ± 0.29	9.28 ± 0.57
<b>Urea</b> (mmol/L)	7.34 ± 0.26	8.83 ± 0.55 *	8.23 ± 0.18	7.44 ± 0.27 #
<b>Creatinine</b> (μmol/L)	22.50 ± 2.32	36.75 ± 2.84 **	25.88 ± 1.19	20.00 ± 1.27 ###

Data are expressed as mean ± SEM (n = 6-8/group, unpaired student's *t*-test); \**P*<0.05, \*\**P*<0.01, \*\*\**P*<0.001 compared to WMS; #*P*<0.05, ##*P*<0.01, ###*P*<0.001 compared to WFO. Abbreviations: WMS: WKY sham-operated intact male; WMO: WKY orchidectomized male; WFO: WKY ovariectomized female; WFT: WKY testosterone-treated ovariectomized female rats.

**Table 7.2 Effects of chronic testosterone treatment on hormonal and biochemical parameters in blood plasma of hypertensive SHR rats.**

Group	SMS	SMO	SFO	SFT
<b>Testosterone</b> (ng/ml)	4.36 ± 0.61	0.53 ± 0.06 <sup>&amp;&amp;</sup>	0.60 ± 0.05	3.03 ± 0.26 <sup>\$\$\$</sup>
<b>Aldosterone</b> (pg/ml)	107.23 ± 19.77	422.54 ± 84.27 <sup>&amp;</sup>	420.41 ± 64.51	93.48 ± 29.87 <sup>\$\$</sup>
<b>Sodium, Na<sup>+</sup></b> (mmol/L)	141.67 ± 0.80	150.33 ± 2.11 <sup>&amp;&amp;</sup>	145.83 ± 1.35	140.67 ± 0.61 <sup>\$</sup>
<b>Osmolality</b> (mOsmol/kg)	309.00 ± 1.13	318.67 ± 3.63 <sup>&amp;</sup>	305.67 ± 0.80	301.17 ± 1.14 <sup>\$</sup>
<b>Chloride, Cl<sup>-</sup></b> (mmol/L)	102.25 ± 1.41	104.38 ± 1.28	104.00 ± 1.80	100.83 ± 2.14
<b>Potassium, K<sup>+</sup></b> (mmol/L)	5.33 ± 0.15	5.83 ± 0.14 <sup>&amp;</sup>	5.43 ± 0.18	4.68 ± 0.08 <sup>\$\$</sup>
<b>Calcium, Ca<sup>2+</sup></b> (mmol/L)	2.57 ± 0.03	2.63 ± 0.04	2.53 ± 0.02	2.60 ± 0.06
<b>Glucose</b> (mmol/L)	9.33 ± 0.56	9.18 ± 0.78	9.09 ± 0.43	8.17 ± 0.32
<b>Urea</b> (mmol/L)	7.58 ± 0.28	8.98 ± 0.32 <sup>&amp;&amp;</sup>	9.89 ± 0.29	8.55 ± 0.16 <sup>\$\$</sup>
<b>Creatinine</b> (μmol/L)	19.13 ± 0.90	25.63 ± 1.71 <sup>&amp;&amp;</sup>	22.14 ± 0.88	15.00 ± 0.58 <sup>\$\$\$</sup>

Data are expressed in mean ± SEM (n = 6-8/group, unpaired student's *t*-test); <sup>&</sup>*P*<0.05, <sup>&&</sup>*P*<0.01, <sup>&&&</sup>*P*<0.001 compared to SMS; <sup>\$</sup>*P*<0.05, <sup>\$\$</sup>*P*<0.01, <sup>\$\$\$</sup>*P*<0.001 compared to SFO. Abbreviations: SMS: SHR sham-operated intact male; SMO: SHR orchidectomized male; SFO: SHR ovariectomized female; SFT: SHR testosterone-treated ovariectomized female rats.

### 7.2.2 $\alpha$ , $\beta$ and $\gamma$ -ENaC mRNA and protein levels in kidneys of WKY rats.

$\alpha$ -*Enac* mRNA levels in kidneys of orchidectomized male WKY rats were higher than sham-operated male WKY rats in Figure 7.1(A). In contrast, chronic testosterone treatment in ovariectomized female WKY rats resulted in significant decrease in  $\alpha$ -*Enac* mRNA level ( $P<0.05$ ). No differences in mRNA levels were observed between orchidectomized male WKY and ovariectomized female WKY rats. In Figure 7.1(B) and Figure 7.1(C), expression levels of uncleaved  $\alpha$ -ENaC protein were highest in orchidectomized male WKY rats. Orchidectomized male WKY rats presented a trend to lower the level of uncleaved  $\alpha$ -ENaC protein when compared to sham-operated male WKY rats. In ovariectomized female WKY rats, chronic testosterone treatment resulted in expression levels of uncleaved  $\alpha$ -ENaC protein to significantly decrease ( $P<0.05$ ). Similar findings were observed for the cleaved  $\alpha$ -ENaC protein level. A significantly higher level of this protein was observed in orchidectomized male WKY rats when compared to sham-operated male WKY rats ( $P<0.05$ ). In ovariectomized female WKY rats, chronic testosterone treatment resulted in the level of cleaved  $\alpha$ -ENaC protein to decrease ( $P<0.05$ ).

In orchidectomized male WKY rats, the level of  $\beta$ -*Enac* mRNA was significantly higher when compared to intact sham-operated male WKY rats ( $P<0.05$ ) as shown in Figure 7.1(D). In ovariectomized female WKY rats, chronic testosterone treatment resulted in the level of  $\beta$ -*Enac* mRNA to decrease ( $P<0.05$ ). The level of  $\beta$ -*Enac* mRNA in intact sham-operated male WKY rats was not significantly different from ovariectomized female WKY rats which received chronic testosterone treatment. In Figure 7.1(E) and 7.1(F), expression levels of  $\beta$ -ENaC protein in orchidectomized male WKY rats were higher than sham-operated male WKY rats ( $P<0.05$ ). In ovariectomized female WKY rats, chronic testosterone treatment resulted in  $\beta$ -ENaC protein expression

level to decrease ( $P<0.05$ ). There were no differences in the levels of  $\beta$ -ENaC protein between orchidectomized male WKY rats and ovariectomized female WKY rats.

Ovariectomized female WKY rats showed highest level of  $\gamma$ -*Enac* mRNA in Figure 7.1(G). In male WKY rats, orchidectomy caused  $\gamma$ -*Enac* mRNA level to increase ( $P<0.01$ ). Meanwhile, in ovariectomized female WKY rats, chronic testosterone treatment resulted in  $\gamma$ -*Enac* mRNA level to decrease ( $P<0.05$ ). In Figure 7.1(H) and 7.1(I), the levels of uncleaved  $\gamma$ -ENaC protein were highest in ovariectomized female WKY rats. Expression levels of this protein were lower in sham-operated intact male WKY rats when compared to orchidectomized male WKY rats ( $P<0.05$ ). In ovariectomized female WKY rats, chronic testosterone treatment resulted in uncleaved  $\gamma$ -ENaC protein expression level to decrease ( $P<0.05$ ). The slightly highest cleaved  $\gamma$ -ENaC protein expression level was observed in ovariectomized female WKY rats. Expression levels of cleaved  $\gamma$ -ENaC protein were significantly higher in orchidectomized male WKY rats when compared to sham-operated male WKY rats ( $P<0.05$ ). However, regardless of statistical significance, in ovariectomized female WKY rats, chronic testosterone treatment resulted in a trend to decrease in the expression level of cleaved  $\gamma$ -ENaC protein.

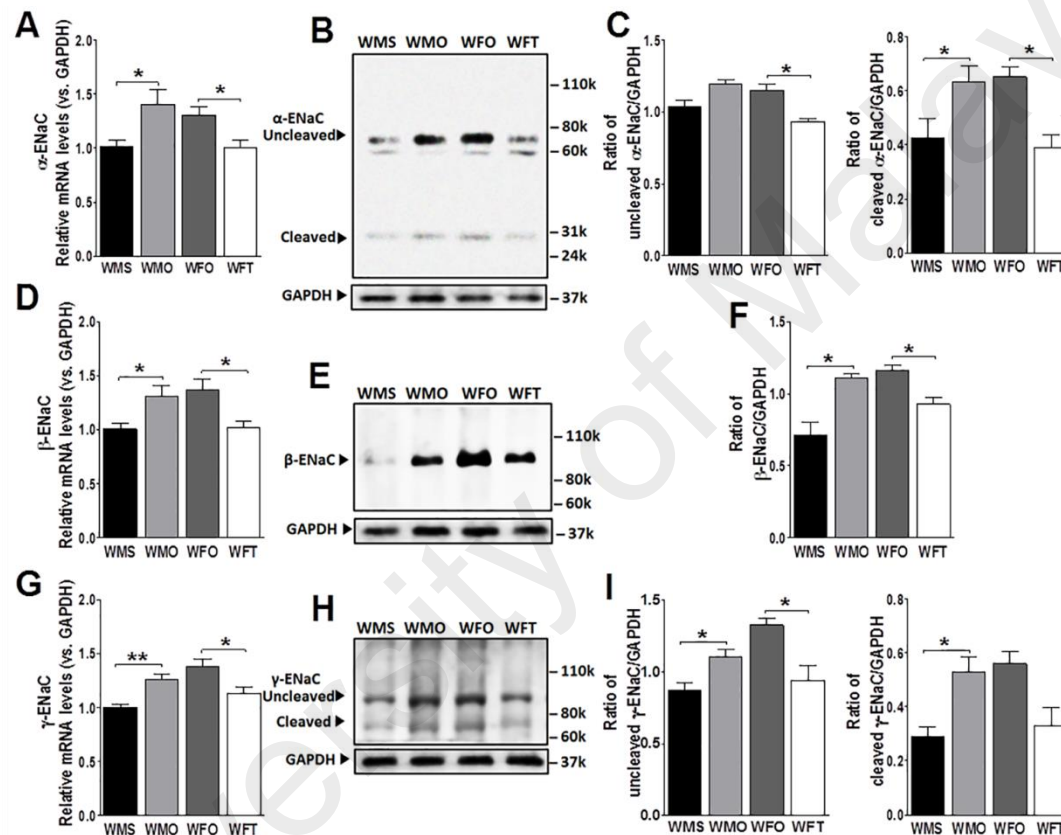


**Figure 7.1** Effects of chronic testosterone treatment on mRNA and protein expression levels of  $\alpha$ ,  $\beta$  and  $\gamma$ -ENaC subunits in kidneys of normotensive WKY rats.

(A) mRNA and (C) protein levels of  $\alpha$ -ENaC, (D) mRNA and (F) protein levels of  $\beta$ -ENaC and (G) mRNA and (I) protein levels of  $\gamma$ -ENaC in the kidney of normotensive WKY rats. Representative Western blotting images of (B)  $\alpha$ -ENaC (cleaved: 28kDa and uncleaved: 78kDa), (E)  $\beta$ -ENaC (99kDa) and (H)  $\gamma$ -ENaC (cleaved: 75kDa and uncleaved: 85kDa). Data are presented as mean  $\pm$  SEM ( $n = 6/\text{group}$ , unpaired student's  $t$ -test); \* $P < 0.05$ ; \*\* $P < 0.01$ . Abbreviations: WMS: WKY sham-operated intact male; WMO: WKY orchidectomized male; WFO: WKY ovariectomized female; WFT: WKY testosterone-treated ovariectomized female rats.

### 7.2.3 Distribution of $\alpha$ , $\beta$ and $\gamma$ -ENaC proteins in kidneys of WKY rats

Immunoperoxidase images showed that  $\alpha$ ,  $\beta$  and  $\gamma$ -ENaC proteins were distributed in distal convoluted tubule (DT) and collecting duct (CD), but not in renal corpuscles (Figure 7.2). Relatively higher expressions of all subunits were observed in orchidectomized male WKY when compared to sham-operated male WKY rats. In ovariectomized female WKY rats, chronic treatment with testosterone resulted in expression levels of  $\alpha$ ,  $\beta$  and  $\gamma$ -ENaC proteins in CD and DT to be relatively lower.

Immunofluorescence imaging revealed that  $\alpha$ ,  $\beta$  and  $\gamma$ -ENaC proteins were expressed in DT and CD of cortical nephrons (Figure 7.3). No expression was observed in PT and renal corpuscles. Meanwhile, in orchidectomized male WKY rats and ovariectomized female WKY rats, expression levels of  $\alpha$ ,  $\beta$  and  $\gamma$ -ENaC proteins in CD and DT were relatively higher when compared to sham-operated male WKY rats and testosterone-treated ovariectomized female WKY rats respectively.

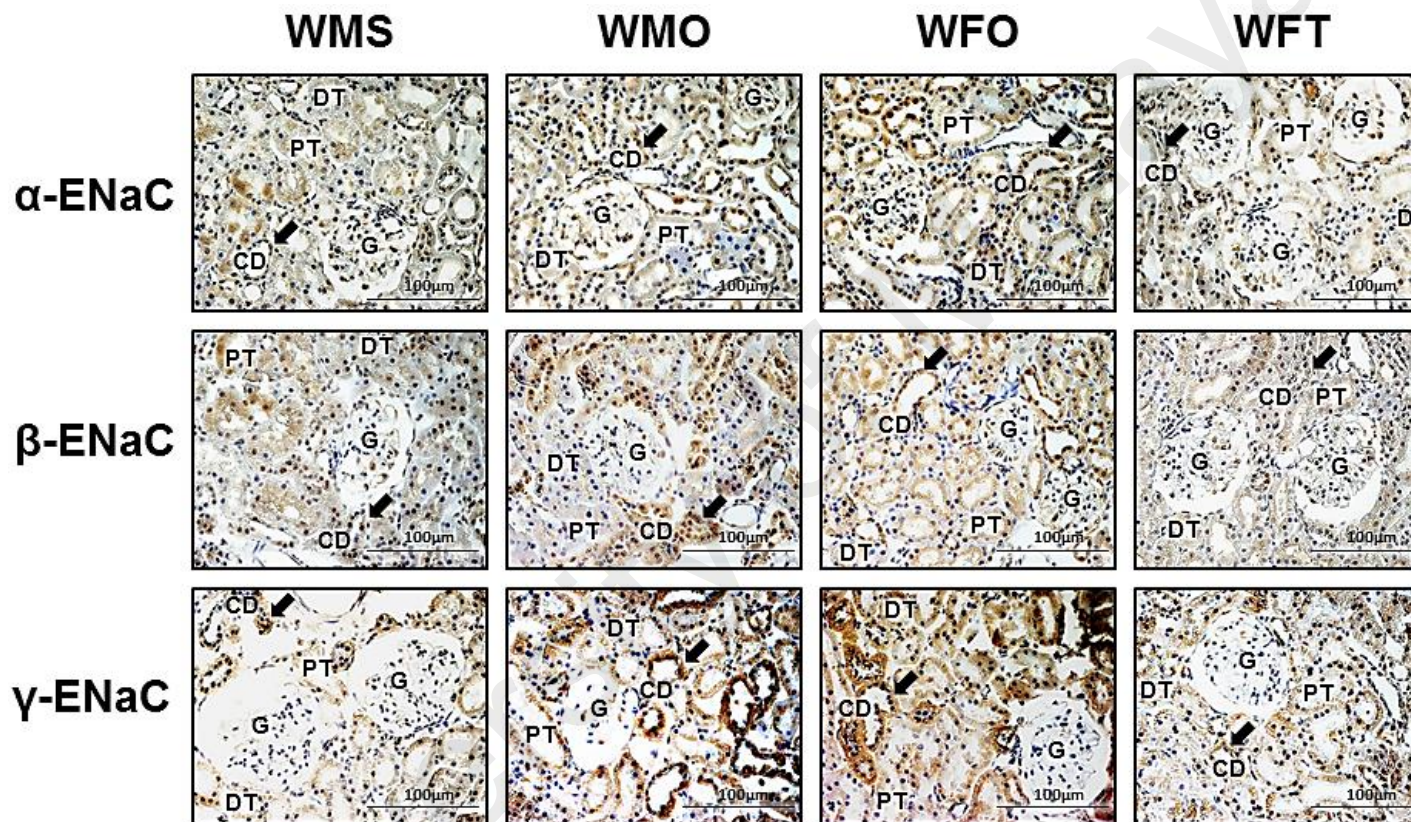


**Figure 7.2 Effects of chronic testosterone treatment on the distribution of  $\alpha$ ,  $\beta$  and  $\gamma$ -ENaC proteins in kidneys of normotensive WKY rats as observed by immunoperoxidase staining.**

Representative immunoperoxidase images (n = 4/group) of coronal sections of kidneys of normotensive WKY rats incubated with  $\alpha$ ,  $\beta$  and  $\gamma$ -ENaC antibodies. Dark-brown staining indicates the localization sites of ENaC subunits. Abbreviations: WMS: WKY sham-operated intact male; WMO: WKY orchidectomized male; WFO: WKY ovariectomized female; WFT: WKY testosterone-treated ovariectomized female rats; G: glomerulus; DT: distal convoluted tubule; PT: proximal convoluted tubule and CD: collecting duct. Scale bar= 100 $\mu$ M

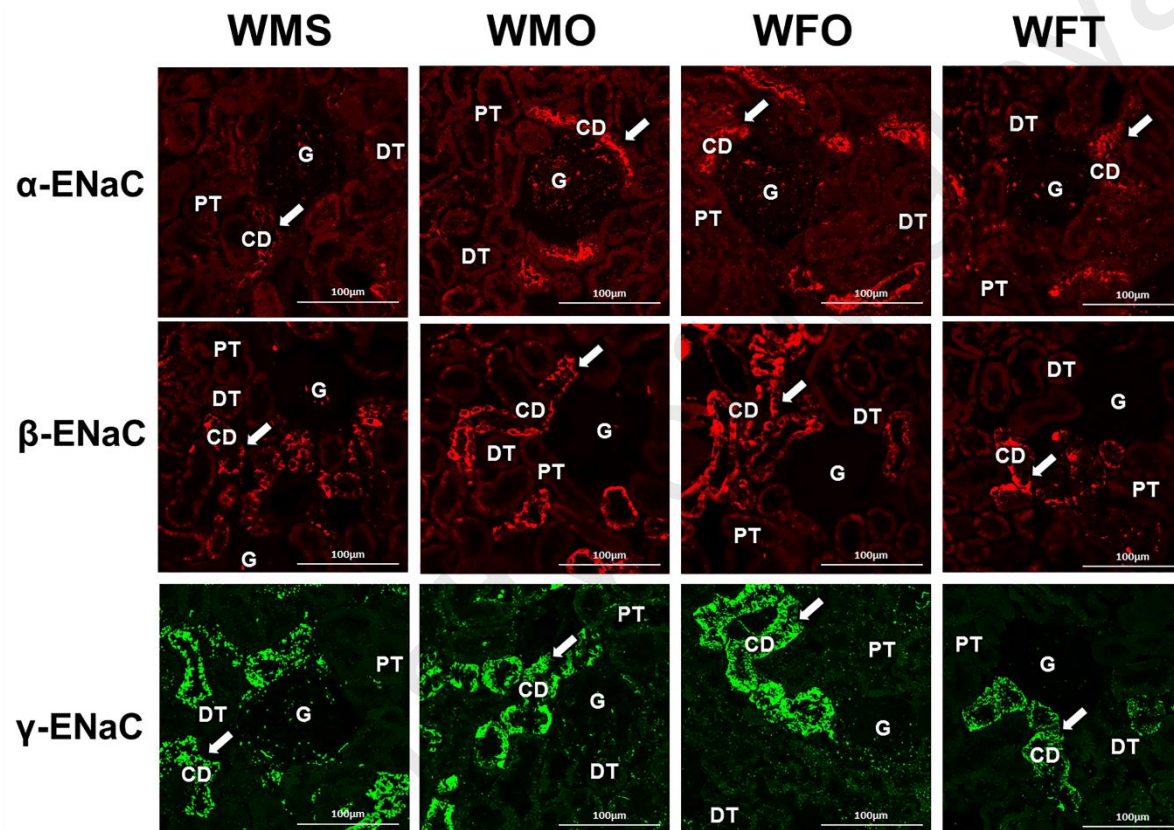


**Figure 7.3 Effects of chronic testosterone treatments on the distribution of  $\alpha$ ,  $\beta$  and  $\gamma$ -ENaC in kidneys of normotensive WKY rats as observed by immunofluorescence staining.**

Representative immunofluorescence images ( $n = 4/\text{group}$ ) of coronal sections of kidneys of normotensive WKY rats incubated with  $\alpha$ ,  $\beta$  and  $\gamma$ -ENaC antibodies. Red or green fluorescence signals indicate the sites where ENaC subunits were expressed. Abbreviations: WMS: WKY sham-operated intact male; WMO: WKY orchidectomized male; WFO: WKY ovariectomized female; WFT: WKY testosterone-treated ovariectomized female rats; G: glomerulus; DT: distal convoluted tubule; PT: proximal convoluted tubule and CD: collecting duct. Scale bar= 100 $\mu\text{M}$

#### 7.2.4 $\alpha$ , $\beta$ and $\gamma$ -ENaC mRNA and protein levels in kidneys of SHR rats

The level of  $\alpha$ -*Enac* mRNA was highest in ovariectomized female SHR rats in Figure 7.4(A). In male SHR rats, orchidectomy resulted in an approximately 1.5 folds increase in  $\alpha$ -*Enac* mRNA level compared to sham-operated male SHR rats ( $P<0.01$ ). In ovariectomized female SHR rats, chronic testosterone treatment resulted in  $\alpha$ -*Enac* mRNA level to decrease ( $P<0.001$ ). In Figure 7.4(B) and 7.4(C), the level of uncleaved  $\alpha$ -ENaC protein was highest in ovariectomized female SHR rats. Meanwhile, in male SHR rats, orchidectomy resulted in uncleaved  $\alpha$ -ENaC protein level to increase ( $P<0.05$ ). Chronic testosterone treatment to ovariectomized female SHR rats resulted in the expression level of uncleaved  $\alpha$ -ENaC protein to decrease ( $P<0.01$ ). The highest level of cleaved  $\alpha$ -ENaC protein was seen in orchidectomized male SHR rats and ovariectomized female SHR rats. A significant increase in the level of cleaved  $\alpha$ -ENaC protein was observed in male SHR rats following orchidectomy ( $P<0.05$ ). Meanwhile, chronic testosterone treatment in ovariectomized female SHR rats caused a significant decrease in the cleaved  $\alpha$ -ENaC protein expression level ( $P<0.05$ ).

In Figure 7.4(D), ovariectomized female SHR rats showed the highest  $\beta$ -*Enac* mRNA level. In male SHR rats, orchidectomy caused  $\beta$ -*Enac* mRNA level to increase ( $P<0.05$ ) while in ovariectomized female SHR rats, chronic testosterone treatment resulted in the  $\beta$ -*Enac* mRNA level to decrease ( $P<0.001$ ). In Figure 7.4(E) and 7.4(F), the level of  $\beta$ -ENaC protein was highest in ovariectomized female SHR rats. Orchidectomy caused  $\beta$ -ENaC protein expression level to increase in male SHR rats ( $P<0.05$ ). High  $\beta$ -ENaC protein expression level in ovariectomized female SHR rats was decreased following chronic testosterone treatment ( $P<0.01$ ).

Highest level of  $\gamma$ -*Enac* mRNA was shown in ovariectomized female SHR rats in Figure 7.4 (G).  $\gamma$ -*Enac* mRNA level in orchidectomized male SHR rats was significantly higher than sham-operated male SHR rats ( $P<0.01$ ). In ovariectomized female SHR rats, chronic testosterone treatment resulted in  $\gamma$ -*Enac* mRNA level to decrease ( $P<0.01$ ). There was no significant difference in  $\gamma$ -*ENaC* mRNA level between sham-operated male SHR rats and testosterone-treated ovariectomized female SHR rats. In Figure 7.4(H) and 7.4(I), highest level of uncleaved  $\gamma$ -ENaC protein was found in ovariectomized female SHR rats. Orchidectomized male SHR rats showed higher level of uncleaved  $\gamma$ -ENaC protein than the sham-operated male SHR rats ( $P<0.001$ ). In ovariectomized female SHR rats receiving chronic testosterone treatment, the level of uncleaved ENaC- $\gamma$  protein was significantly decreased ( $P<0.01$ ). Similarly, the highest expression level of cleaved  $\gamma$ -ENaC protein was observed in ovariectomized female SHR rats. Orchidectomy significantly increased the level of cleaved  $\gamma$ -ENaC protein as compared to sham-operated male SHR rats ( $P<0.01$ ) whilst chronic testosterone treatment in ovariectomized female SHR rats decreased the level of this protein as compared to non-treated ovariectomized female SHR rats ( $P<0.01$ ).

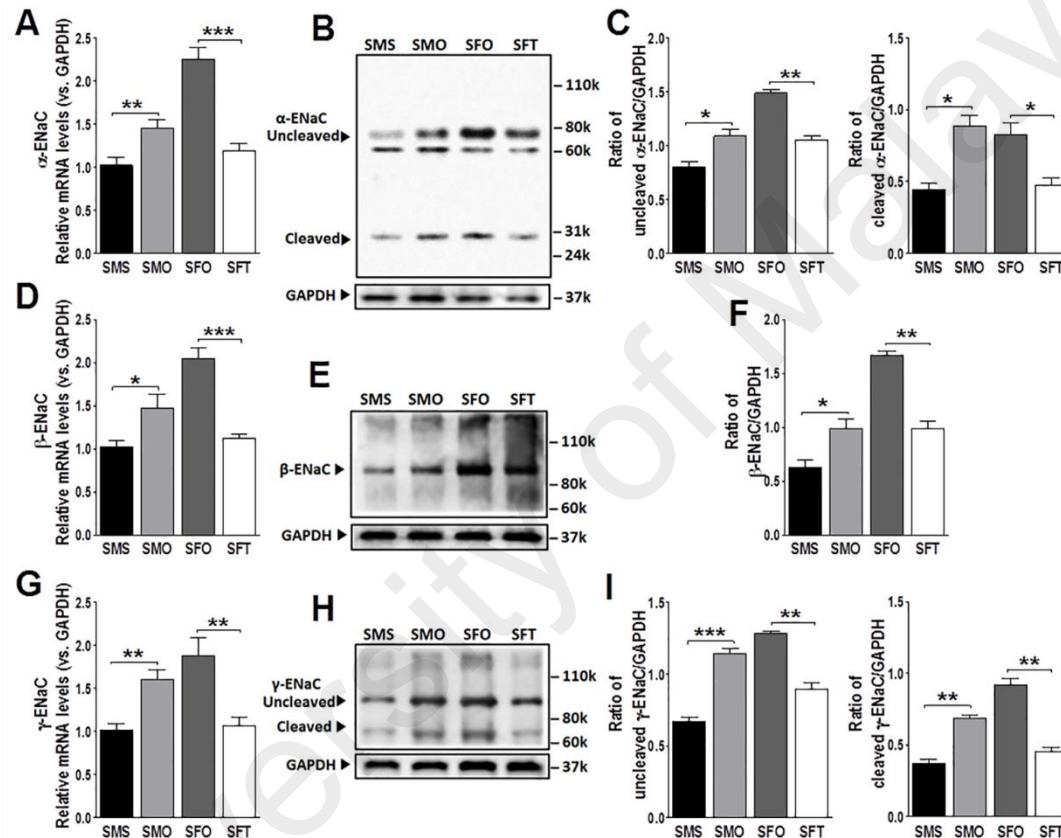


**Figure 7.4** Effects of chronic testosterone treatment on mRNA and protein expression levels of  $\alpha$ ,  $\beta$  and  $\gamma$ -ENaC in kidneys of hypertensive SHR rats.

(A) mRNA and (C) protein levels of  $\alpha$ -ENaC, (D) mRNA and (F) protein levels of  $\beta$ -ENaC and (G) mRNA and (I) protein levels of  $\gamma$ -ENaC in the kidney of hypertensive SHR rats. Representative Western blotting images of (B)  $\alpha$ -ENaC (cleaved: 28kDa and uncleaved: 78kDa), (E)  $\beta$ -ENaC (99kDa). and (H)  $\gamma$ -ENaC (cleaved: 75kDa and uncleaved: 85kDa). Data are presented as mean  $\pm$  SEM (n = 6/group, unpaired student's *t*-test); \**P*<0.05; \*\**P*<0.01; \*\*\**P*<0.001. Abbreviations: SMS: SHR sham-operated intact male; SMO: SHR orchidectomized male; SFO: SHR ovariectomized female; SFT: SHR testosterone-treated ovariectomized female rats.

### 7.2.5 Distribution of $\alpha$ , $\beta$ and $\gamma$ -ENaC proteins in kidneys of SHR rats

Immunoperoxidase images showed that  $\alpha$ ,  $\beta$  and  $\gamma$ -ENaC subunits were distributed mainly in DT and CD but not in renal corpuscles (Figure 7.5). Relatively higher  $\alpha$ ,  $\beta$  and  $\gamma$ -ENaC protein expression was observed in DT and CD of orchidectomized male SHR rats when compared to sham-operated male SHR rats. In ovariectomized female SHR rats, chronic testosterone treatment resulted in expression levels of  $\alpha$ ,  $\beta$  and  $\gamma$ -ENaC protein in DT and CD to be relatively lower when compared to non-treated ovariectomized female SHR rats.

Immunofluorescence imaging revealed that  $\alpha$ ,  $\beta$  and  $\gamma$ -ENaC proteins were expressed in DT and CD but not in renal corpuscles (Figure 7.6). In male SHR rats, orchidectomy caused  $\alpha$ ,  $\beta$  and  $\gamma$ -ENaC protein expression levels in DT and CD to be relatively higher when compared to sham-operated male SHR rats. In ovariectomized female SHR rats, chronic testosterone treatment resulted in relatively lower expression levels of  $\alpha$ ,  $\beta$  and  $\gamma$ -ENaC proteins in CD and DT when compared to non-treated ovariectomized female SHR rats.

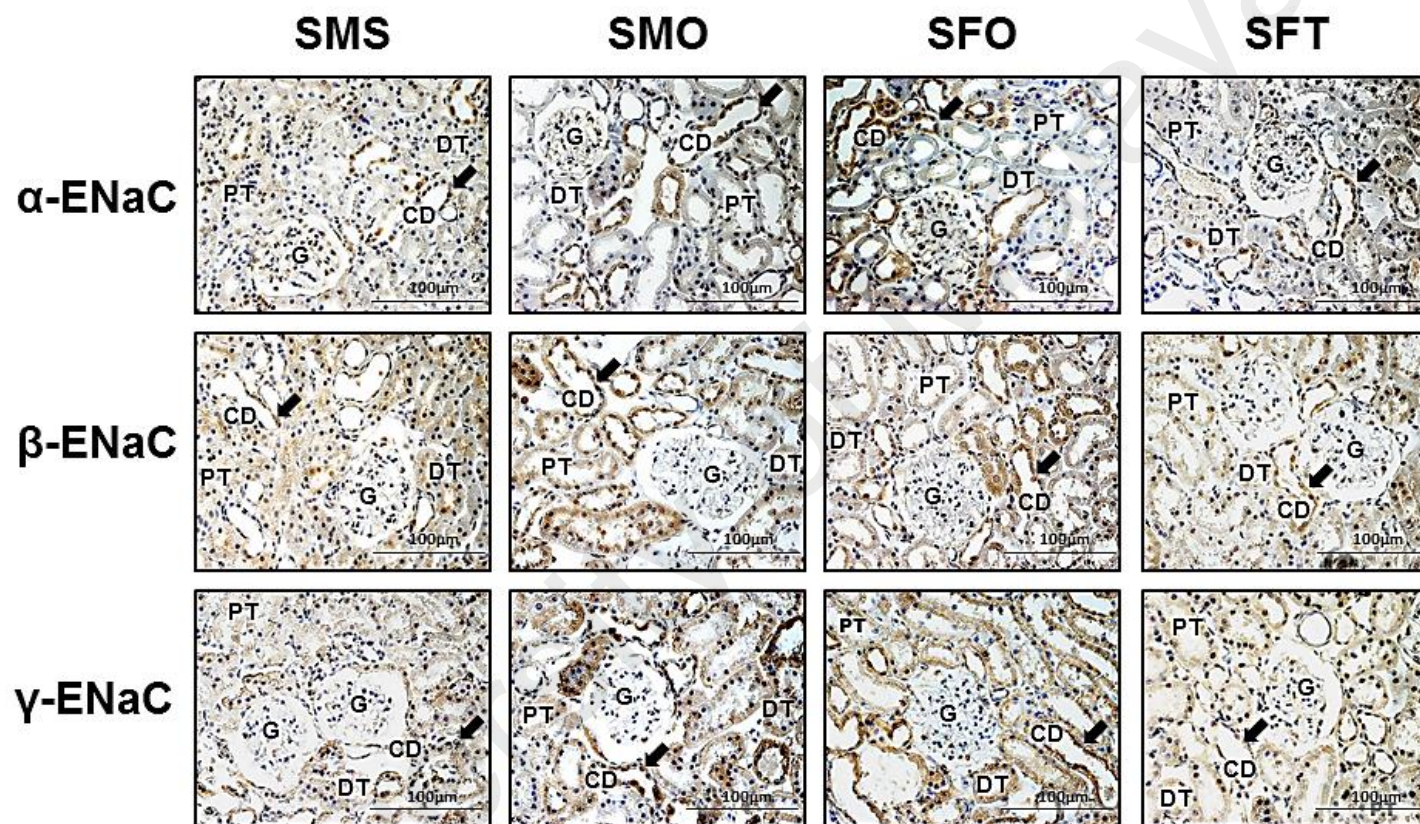


**Figure 7.5** Effects of chronic testosterone treatment on the distribution of  $\alpha$ ,  $\beta$  and  $\gamma$ -ENaC in kidneys of hypertensive SHR rats as observed by immunoperoxidase staining.

Representative immunoperoxidase images (n = 4/group) of coronal sections of kidneys of hypertensive SHR rats incubated with  $\alpha$ ,  $\beta$  and  $\gamma$ -ENaC antibodies. Dark-brown staining indicates the localization sites of ENaC subunits. Abbreviations: SMS: SHR sham-operated intact male; SMO: SHR orchidectomized male; SFO: SHR ovariectomized female; SFT: SHR testosterone-treated ovariectomized female rats; G: glomerulus; DT: distal convoluted tubule; PT: proximal convoluted tubule and CD: collecting duct. Scale bar= 100 $\mu$ M

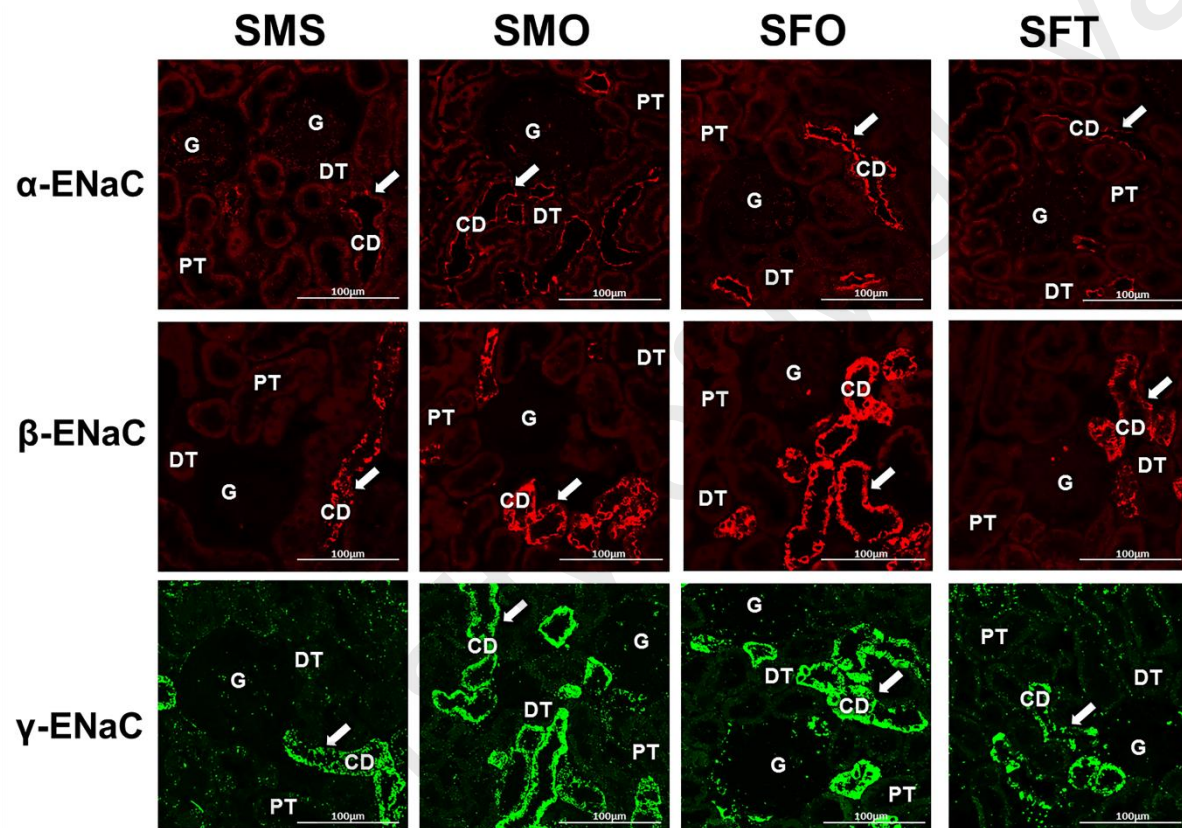


**Figure 7.6 Effects of chronic testosterone treatment on the distribution of  $\alpha$ ,  $\beta$  and  $\gamma$ -ENaC in kidneys of hypertensive SHR rats as observed by immunofluorescence staining.**

Representative immunofluorescence images ( $n = 4/\text{group}$ ) of coronal sections of kidneys of hypertensive SHR rats incubated with  $\alpha$ ,  $\beta$  and  $\gamma$ -ENaC antibodies. Red or green fluorescence signals indicate the sites where ENaC subunits were expressed. Abbreviations: SMS: SHR sham-operated intact male; SMO: SHR orchidectomized male; SFO: SHR ovariectomized female; SFT: SHR testosterone-treated ovariectomized female rats; G: glomerulus; DT: distal convoluted tubule; PT: proximal convoluted tubule and CD: collecting duct. Scale bar= 100 $\mu\text{M}$

### 7.3 Discussion

This study has revealed that when testosterone was given for a chronic duration to the ovariectomized female rats, there was a decreased in the expression levels of  $\alpha$ ,  $\beta$  and  $\gamma$ -ENaC in the kidneys. In addition, there was also a decrease in plasma aldosterone, sodium, osmolality, urea and creatinine levels. Similar effects could be seen in the male rats in which removal of the endogenous source of testosterone by orchidectomy increased the expression level of  $\alpha$ ,  $\beta$  and  $\gamma$ -ENaC in the kidney. These reductions were accompanied by the decreases in plasma aldosterone, sodium, osmolality, urea and creatinine levels. However, the plasma levels of chloride and calcium did not change, yet there was a significant increase in potassium levels following orchidectomy.

In addition, these results also indicated the differences in several parameters between normotensive WKY and hypertensive SHR rats. Besides MAP (refer **Chapter 4**), the intact hypertensive male rats have higher plasma testosterone and aldosterone levels. However, the electrolytes, osmolality, urea and creatinine levels were not markedly different as compared to the normotensive male rats. The observed higher level of plasma testosterone in male SHR rats, which is in agreement with the previous findings (Reckelhoff et al., 1998), was suggested to link with the hypertensive Y chromosome in SHR (SHR Yc) (Toot et al., 2011). Nevertheless, due to this feature, male SHR rats have been widely used to demonstrate androgen-dependent hypertension (Liu & Ely, 2011; Reckelhoff et al., 2000; Toot et al., 2012). Meanwhile, the higher plasma aldosterone level in male SHR rats could be resulted from the stimulation of renin-angiotensin-aldosterone (RAS) pathway in the former (Hu et al., 2011; Maranon & Reckelhoff, 2013; Reckelhoff et al., 2000; Yanes et al., 2009).

In this study, a Silastic tubing implant was used to deliver testosterone over six week period (Jenkins et al., 1994; Reckelhoff, 2001; Reckelhoff et al., 1998). By the end of the treatment period, the level of testosterone in female rats was found to be 3.5-fold higher than non-testosterone treated control. Previous *in-vitro* study showed that the released of sex-steroid hormones from a subcutaneous implant was proportional to the hormonal concentration within the implants (Cohen & Milligan, 1993), therefore this would produce a steady-state sex-steroid level in the blood (Ström et al., 2008). Nevertheless, the delivery of steroid hormones from the implant was also found to result in supra-physiological levels of these hormones in the blood (Quispe et al., 2015).

In the present study, expression of ENaC in female rats' kidneys was markedly decreased following chronic testosterone treatment. These results were in agreement with the previous finding in which two weeks treatment with testosterone to ovariectomized female rats resulted in ENaC subunits expression levels in the kidneys to decrease (Kienitz et al., 2009). Moreover, in addition to the earlier reported finding, it is found that these decreases in  $\alpha$ ,  $\beta$  and  $\gamma$ -ENaC expression levels in the kidneys of testosterone-treated female rats were accompanied by reductions in plasma levels of aldosterone, sodium and osmolality. Meanwhile, the protein distribution studies have indicated that the distribution of  $\alpha$ ,  $\beta$  and  $\gamma$ -ENaC in DT and CD were decreased following testosterone treatment to ovariectomized female rats. The decrease in the ENaC expression could be mediated via the decrease in plasma aldosterone levels as aldosterone has been reported to enhance sodium reabsorption by inducing the activity and expression of ENaC at the apical membrane of DT and CD in the kidney (Eaton et al., 1995; Masilamani et al., 1999).

The observed changes in kidney ENaC expression levels and plasma aldosterone and sodium levels in testosterone-treated ovariectomized female rats were supported by the finding in male rats following orchidectomy. In both WKY and SHR male rats, removal of the major source of endogenous testosterone by orchidectomy resulted in higher  $\alpha$ ,  $\beta$  and  $\gamma$ -ENaC expressions in DT and CD relative to intact rats. In concordant, plasma levels of aldosterone and sodium were found to be markedly increased in orchidectomized rats when compared to those intact rats. These findings were however in contrast with another previous finding which suggested that testosterone exacerbates hypertension by modulation of RAS (Reckelhoff et al., 1998) and causes an increase in plasma aldosterone level (Kau et al., 1999). The difference between our findings and others could be due to differences in testosterone doses, route of administration and duration of exposure to this drug. The reasons underlying the effects of chronic testosterone treatment on kidney ENaC expressions as observed in this study were unknown, thus warrant investigations. One possibility that removal of endogenous testosterone could reduce the renal perfusion pressure through decreased in MAP (refer **Chapter 4**), which in turn stimulating the release of renin, resulting in increased angiotensin II and subsequently aldosterone release. Besides, a number of different mechanisms might also be involved in mediating the effects of testosterone on MAP. For instance, recently, androgens *i.e.* DHT was reported to increase the levels of cytochrome P450 and 20-hydroxyecosatetraenoic acid in the kidney microvasculature that are involved in blood pressure regulation (Dalmasso et al., 2016). Meanwhile, the increased MAP in hyperandrogenemia female rats (HAF) was reported to be related to the activation of sympathetic nervous system (SNS), renal nerves, and melanocortin-4 receptor (MC4R) (Maranon et al., 2015). In addition, the changes in renal oxidative stress levels under the influence of testosterone might also be responsible for these effects (Lopez-Ruiz et al., 2010).

Despite the increased in MAP observed earlier (refer **Chapter 4**), the current finding indicated the reduction of ENaC expression by testosterone and therefore, it is suggested that these testosterone-mediated increase in blood pressure did not involve the up-regulation of ENaC expression levels in the kidneys. The outcomes of this study have excluded ENaC as one of the possible pathways by which testosterone mediate the blood pressure to increase. Further, these finding also supported the view that the increased in blood pressure under chronic testosterone exposure might involve other pathways such as the central regulation involving the brain.

University of Malaysia

## CHAPTER 8: EFFECTS OF CHRONIC TESTOSTERONE TREATMENT ON AQUAPORIN (AQP) EXPRESSION IN KIDNEYS

### 8.1 Introduction

To date, several mechanisms have been proposed to explain the gender differences in blood pressure regulation including differential effects of estrogens and androgens on expression and activity levels of components related to the renin-angiotensin system (RAS) (Komukai et al., 2010; Maric-Bilkan & Manigrasso, 2012; Vlachopoulos et al., 2016). Besides, changes in vascular reactivity, increases in endothelin and oxidative stress levels and possible activation of sympathetic nervous system (SNS) (Coutinho et al., 2013; Kelly & Jones, 2013b; Liu et al., 2016; Maranon et al., 2015; Reckelhoff, 2004; Tatchum-Talom et al., 2011) could also account for these differences. In addition, an increase in blood volume might also contribute towards the increase in blood pressure, and these could involve the kidneys (Broulik et al., 1973; Herak-Kramberger et al., 2015; Laragh, 1986; Probst et al., 2006).

Kidneys play an important role in the hormonal regulation of blood pressure (Wadei & Textor, 2012). Besides aldosterone (Quinn et al., 2014), the expression of kidney epithelial sodium channel (ENaC) was found to be regulated by testosterone in our previous findings (refer **Chapter 5** and **Chapter 7**). The increase in the number of active ENaC at the apical membrane of collecting ducts (CD) causes the increase in sodium entry, which could lead to secondary water reabsorption (Bubien, 2010; Hall, 2016). In the distal part of the nephron, which included the CD, the tight junctions are less permeable to water and therefore when sodium is reabsorbed, water moves from these tubular lumen into the blood via water channels named aquaporins (AQP) (Hall, 2016; Khurana, 2014; Pearce et al., 2014). Aldosterone and antidiuretic hormone

(ADH) were reported to control the water permeability of these segments in the nephron by regulating the expression of these channels (Lee & Kwon, 2007; Takata et al., 2004). Exaggerated expression of these channels in the kidneys was found to cause water retention as occur in hypothyroidism and in glucocorticoid-induced hypertension (Chen et al., 2015; Yeum et al., 2002). The increase in water retention could eventually lead to the increase in circulating fluid volume and thus blood pressure (Nadar & Lip, 2009; Wang et al., 2014).

Thirteen AQP isoforms have been identified in the mammals and are classified into classical aquaporins and aquaglyceroporins, based on their pore selectivity (King et al., 2004). Amongst these 13 AQPs, AQP-1, 2, 3, 4, 6 and 7 subunits were reported in the kidneys of rats and humans (Agarwal & Gupta, 2008; Nielsen et al., 1999). Therefore, it is hypothesized that testosterone could influence the expression level of these AQP subunits in the kidneys, thus causing the increase in water reabsorption and blood volume which subsequently causes the increase in blood pressure (refer **Chapter 4**). In this study, the changes in expression levels of AQP subunits in the kidneys under chronic testosterone treatment were examined in both normotensive and hypertensive conditions.

## 8.2 Results

### 8.2.1 AQP mRNA expression in kidneys of normotensive WKY rats

In Figure 8.1(A), *Aqp-1* mRNA level in the kidneys of male WKY rats was markedly decreased by orchidectomy ( $P<0.05$ ). In female WKY rats, chronic exposure to testosterone caused *Aqp-1* mRNA level to increase significantly ( $P<0.05$ ). In Figure 8.1(B), *Aqp-2* mRNA level in the kidneys of male WKY rats was markedly decreased following orchidectomy ( $P<0.05$ ). In ovariectomized female WKY rats, chronic testosterone treatment caused *Aqp-2* mRNA levels to increase ( $P<0.05$ ). In Figure 8.1(C), *Aqp-3* mRNA level in the kidney of male WKY rats significantly increased by orchidectomy ( $P<0.01$ ). In ovariectomized female WKY rats, testosterone treatment caused *Aqp-3* mRNA level to decreased ( $P<0.05$ ). In Figure 8.1(D), *Aqp-4* mRNA level significantly decreased in the kidney of male WKY rats following orchidectomy. ( $P<0.05$ ). In ovariectomized female WKY rats, testosterone treatment resulted in *Aqp-4* mRNA level to increase ( $P<0.01$ ). In Figure 8.1(E), no significant changes in *Aqp-6* mRNA level were observed between sham-operated intact and orchidectomized male WKY rats. Similarly, in ovariectomized female WKY rats, testosterone treatment did not cause significant changes in kidney *Aqp-6* mRNA level. In Figure 8.1(F), orchidectomy caused a marked reduction in *Aqp-7* mRNA level in the kidneys of male WKY rats ( $P<0.05$ ) whilst chronic testosterone treatment resulted in a significant increase in *Aqp-7* mRNA level in the kidneys of ovariectomized female WKY rats ( $P<0.05$ ).

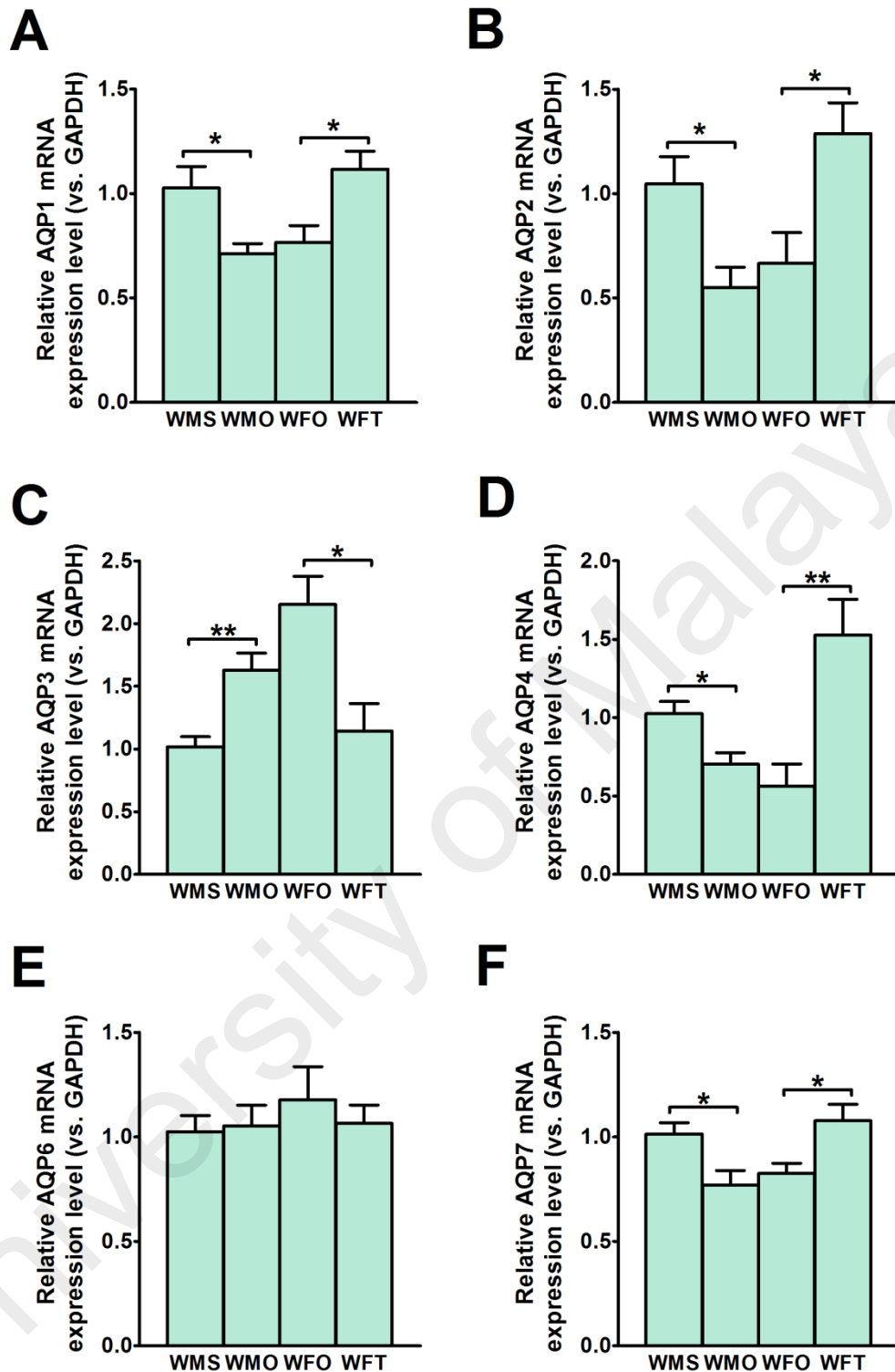


**Figure 8.1** Effects of chronic testosterone treatment on mRNA expression levels of AQP subunits in kidneys of normotensive WKY rats.

Effects of chronic testosterone treatment on (A) *Aqp-1*, (B) *Aqp-2*, (C) *Aqp-3*, (D) *Aqp-4*, (E) *Aqp-6* and (F) *Aqp-7* mRNA levels in the kidney of normotensive WKY rats. Data are expressed as mean  $\pm$  SEM (n = 6/group, unpaired student's *t*-test); \**P* < 0.05; \*\**P* < 0.01. Abbreviations: WMS: WKY sham-operated intact male; WMO: WKY orchidectomized male; WFO: WKY ovariectomized female; WFT: WKY testosterone-treated ovariectomized female rat.

### 8.2.2 AQP protein expression in kidneys of normotensive WKY rats

In Figure 8.2, the level of AQP-1 protein in the kidneys of male WKY rats was significantly decreased following orchidectomy ( $P<0.05$ ). In ovariectomized female WKY rats, testosterone treatment resulted in the level of AQP-1 protein to increase ( $P<0.05$ ). Meanwhile, orchidectomy significantly decreased AQP-2 protein expression level in the kidney of male WKY rats ( $P<0.05$ ). A significant increase in the expression levels of this protein was observed in the kidneys of ovariectomized female WKY rats following chronic testosterone treatment ( $P<0.05$ ).

In male WKY rats, AQP-4 protein expression level was significantly decreased following orchidectomy ( $P<0.01$ ). In ovariectomized female WKY rats, chronic testosterone treatment resulted in AQP-4 protein expression level in the kidney to increase ( $P<0.05$ ). A slight but no significant change in kidney AQP-6 protein expression level was observed in male following orchidectomy. Chronic testosterone exposure in ovariectomized female WKY rats did not cause any significant changes in the expression levels of AQP6 in the kidneys.

As for aquaglyceroporins (Figure 8.3), AQP-3 protein expression level in the kidneys of male WKY rats was significantly increased following orchidectomy ( $P<0.01$ ). Meanwhile, chronic testosterone treatment in ovariectomized female WKY rats caused a significant decrease in AQP-3 protein expression level ( $P<0.01$ ). In male WKY rats, orchidectomy was found to cause a significant decrease in the level of AQP-7 protein in the kidneys ( $P<0.001$ ). Meanwhile, regardless of statistical significance, chronic exposure of ovariectomized female WKY rats to testosterone resulted in a trend to increase in the level of AQP-7 protein in the kidneys.

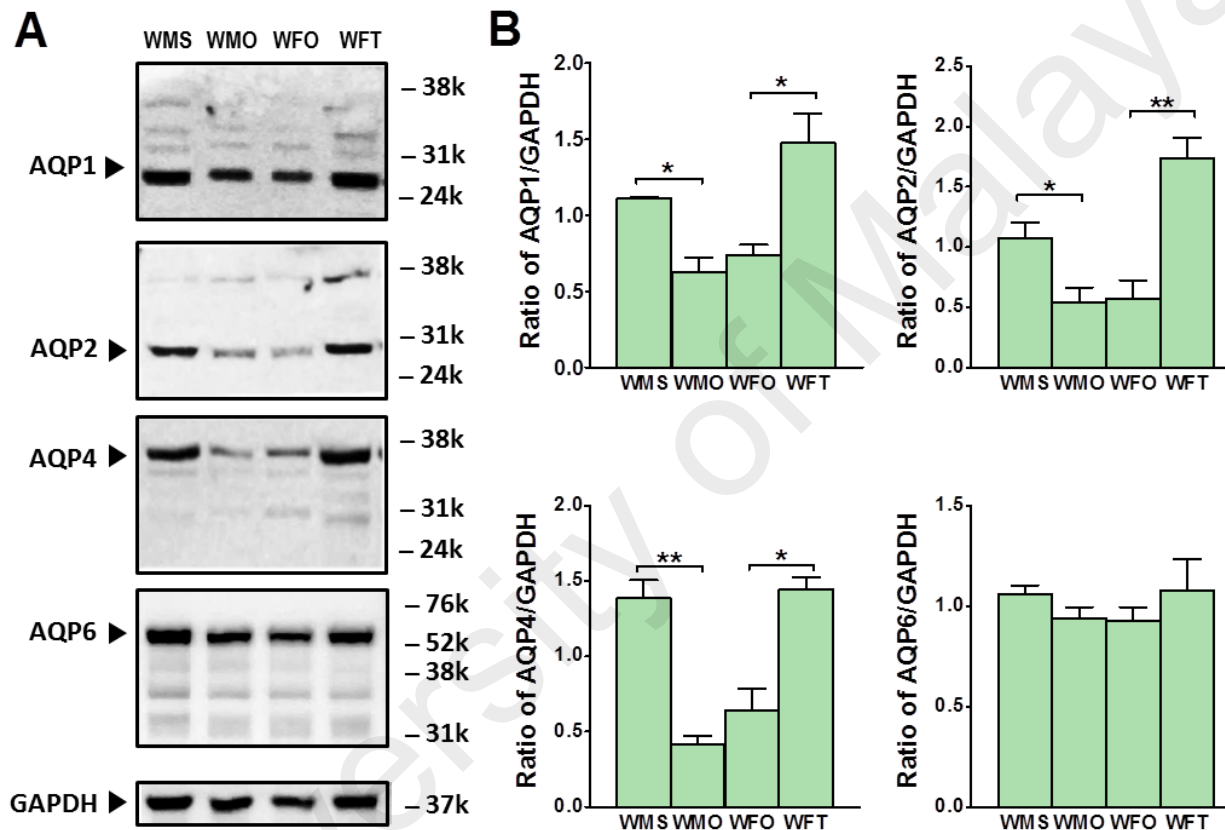


**Figure 8.2 Effects of chronic testosterone treatment on protein expression levels of classical aquaporins in kidneys of normotensive WKY rats.**

(A) Representative immunoblot images of the classical aquaporin *i.e.* AQP-1, AQP-2, AQP-4 and AQP-6. Molecular weight of targeted proteins = 28kDa (AQP-1), 29kDa (AQP-2), 34kDa (AQP-4) and 55kDa (AQP-6). (B) Average relative ratio of band intensities of AQP-1, AQP-2, AQP-4 and AQP-6 proteins to housekeeping protein, GAPDH (of three replicate blots). Data are expressed as mean  $\pm$  SEM ( $n = 6$ /group, unpaired student's *t*-test); \* $P < 0.05$ ; \*\* $P < 0.01$ . Abbreviations: WMS: WKY sham-operated intact male; WMO: WKY orchidectomized male; WFO: WKY ovariectomized female; WFT: WKY testosterone-treated ovariectomized female rat.

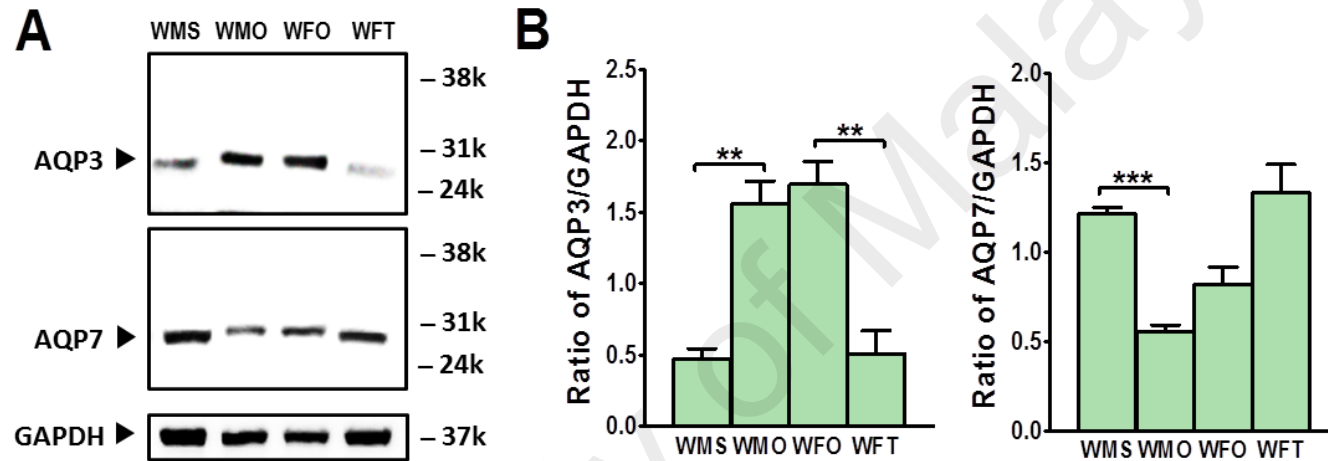


**Figure 8.3** Effects of chronic testosterone treatment on protein expression levels of aquaglyceroporins in kidneys of normotensive WKY rats.

(A) Representative immunoblot images of aquaglyceroporins *i.e.* AQP-3 and AQP-7. Molecular weight of targeted proteins = 31kDa (AQP-3) and 22-33kDa (AQP-7). (B) Average relative ratio of band intensities of AQP-3 and AQP-7 proteins to housekeeping protein, GAPDH (of three replicate blots). Data are expressed as mean  $\pm$  SEM ( $n = 6/\text{group}$ , unpaired student's *t*-test); \*\* $P < 0.01$ ; \*\*\* $P < 0.001$ . Abbreviations: WMS: WKY sham-operated intact male; WMO: WKY orchidectomized male; WFO: WKY ovariectomized female; WFT: WKY testosterone-treated ovariectomized female rat.

### 8.2.3 Distribution of AQP proteins in kidney of normotensive WKY rats

In Figure 8.4, AQP-1 protein (green fluorescent signals) was predominantly located in the proximal convoluted tubule (PT). AQP-3 (red fluorescent signals) was located in PT and collecting duct (CD). AQP-1 was not found in the glomeruli (G), distal convoluted tubules (DT) and CD while AQP-3 was not found in G and DT of normotensive male and female WKY rats. Higher AQP-1 protein was expressed in the kidneys of sham-operated intact male WKY rats relative to orchidectomized male rats. Chronic testosterone treatment in ovariectomized female WKY caused relatively lower distribution of AQP-1 in the kidney as compared to those non-treated. In contrast, comparably higher AQP-3 was expressed in orchidectomized male rats and non-treated ovariectomized female normotensive WKY rats as compared to the sham-operated intact male and testosterone-treated ovariectomized female WKY rats, respectively.

In Figure 8.5, AQP-2 (red fluorescent signals) and AQP-4 (green fluorescent signals) were exclusively distributed in the CD of normotensive WKY rats. AQP-2 was expressed at the apical membrane while AQP-4 was expressed at the basolateral membrane. Both AQP-2 and AQP-4 were not expressed in G, DT and PT. Relatively higher expression of AQP-2 and AQP-4 were observed in CD of sham-operated intact males and ovariectomized female WKY rats receiving chronic testosterone treatment when compared to orchidectomized male and non-treated ovariectomized female WKY rats, respectively.

In Figure 8.6, AQP-6 (green fluorescent signals) and AQP-7 (red fluorescent signals) were localized predominantly in PT and CD of normotensive WKY rats, respectively. AQP-6 was not expressed in the G, DT and CD while AQP-7 was not expressed in G, DT and PT. No marked changes in the fluorescent signals of AQP-6 in the kidneys

following orchidectomy in male or chronic testosterone treatment in ovariectomized female rats were observed. In ovariectomized female WKY rats receiving chronic testosterone treatment, relatively higher distribution of AQP-7 was observed when compared to those non-treated. A comparably lower AQP-7 distribution was observed in the kidney of orchidectomized male WKY rats when compared to sham-operated intact male WKY rats.

University of Malaya

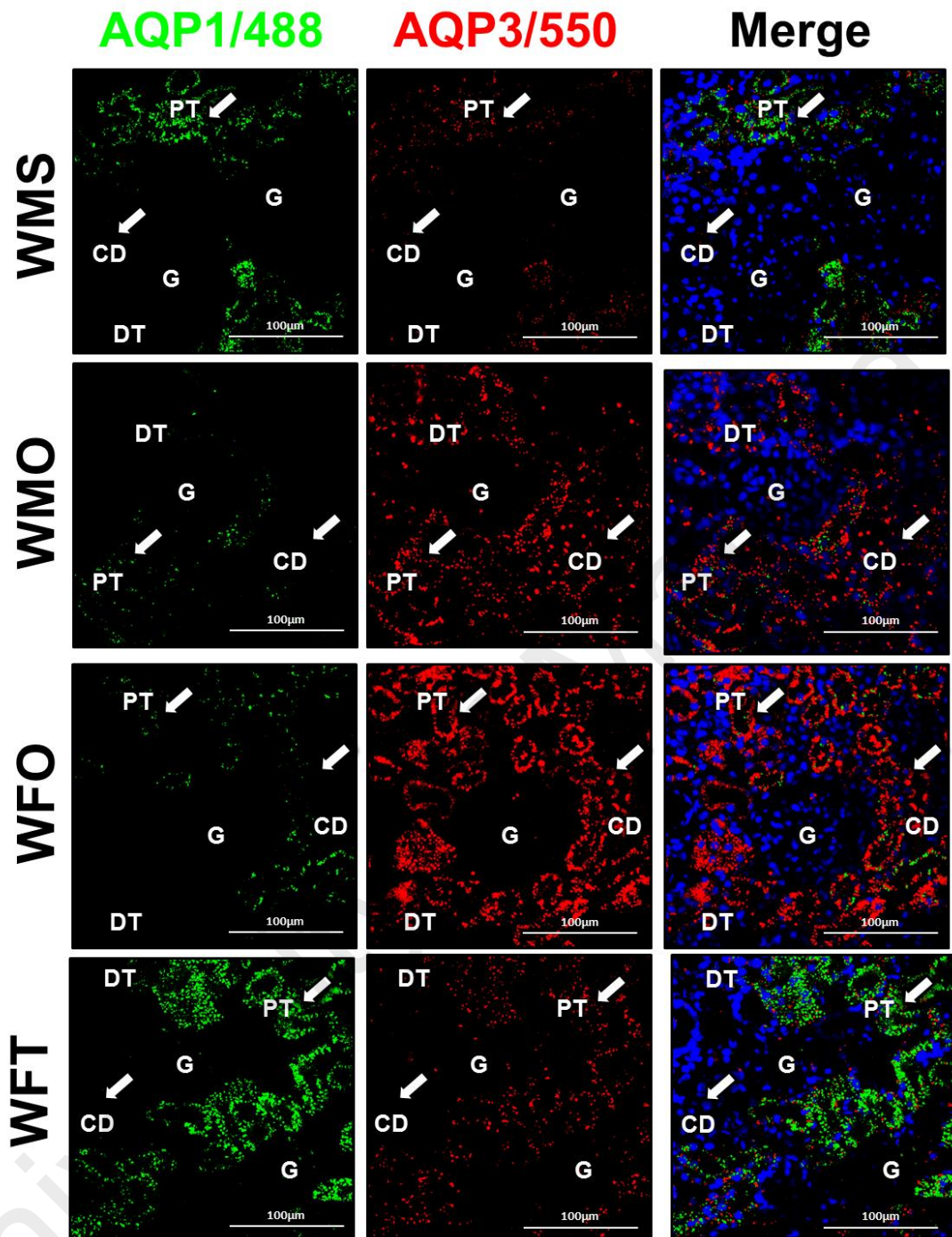


**Figure 8.4** Effects of chronic testosterone treatment on distributions of AQP-1 (green) and AQP-3 (red) proteins in cortical nephron of normotensive WKY rats. Distributions of AQP-1 and AQP-3 in the kidneys of normotensive WKY were assessed by double immunofluorescence staining. Representative confocal immunofluorescence images (n = 4/group) of the coronal sections of kidney cortex were presented. AQP-1, represented by green fluorescent signals, was expressed in PT while AQP-3, represented by red fluorescent signals, was expressed in PT and CD [white arrow heads]. Abbreviations: WMS: WKY sham-operated intact male; WMO: WKY orchidectomized male; WFO: WKY ovariectomized female; WFT: WKY testosterone-treated ovariectomized female rat; G: glomerulus; DT: distal convoluted tubule; PT: proximal convoluted tubule; CD: collecting duct. Scale bar = 100µM.

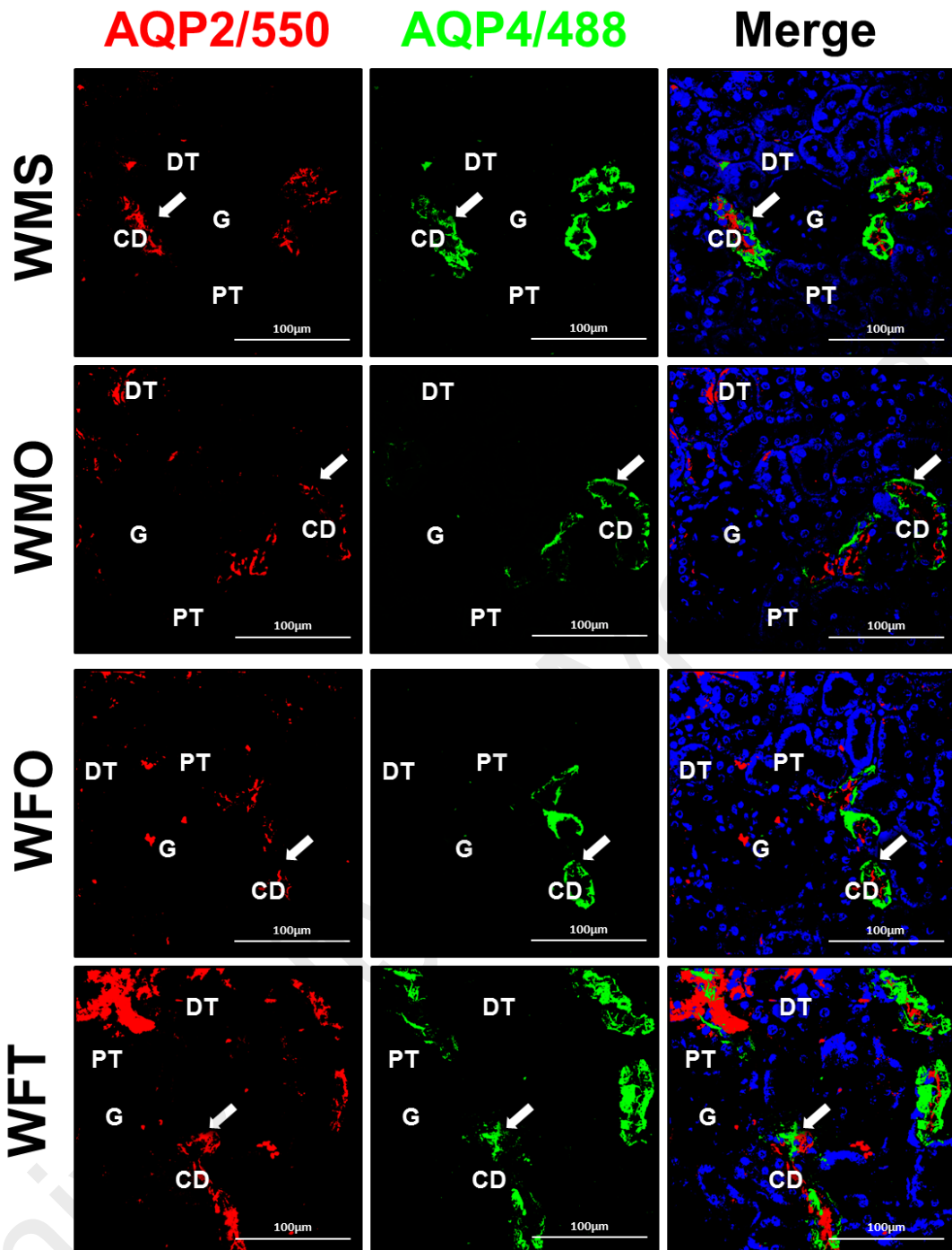


**Figure 8.5 Effects of chronic testosterone treatment on distributions of AQP-2 (red) and AQP-4 (green) proteins in cortical nephron of normotensive WKY rats.** Distributions of AQP-2 and AQP-4 in the kidneys of normotensive WKY were assessed by double immunofluorescence staining. Representative confocal immunofluorescence images ( $n = 4/\text{group}$ ) of the coronal sections of kidney cortex were presented. Both AQP-2, represented by red fluorescent signals and AQP-4, represented by green fluorescent signals were expressed in CD [white arrow heads]. Abbreviations: WMS: WKY sham-operated intact male; WMO: WKY orchidectomized male; WFO: WKY ovariectomized female; WFT: WKY testosterone-treated ovariectomized female rat; G: glomerulus; DT: distal convoluted tubule; PT: proximal convoluted tubule; CD: collecting duct. Scale bar =  $100\mu\text{M}$ .

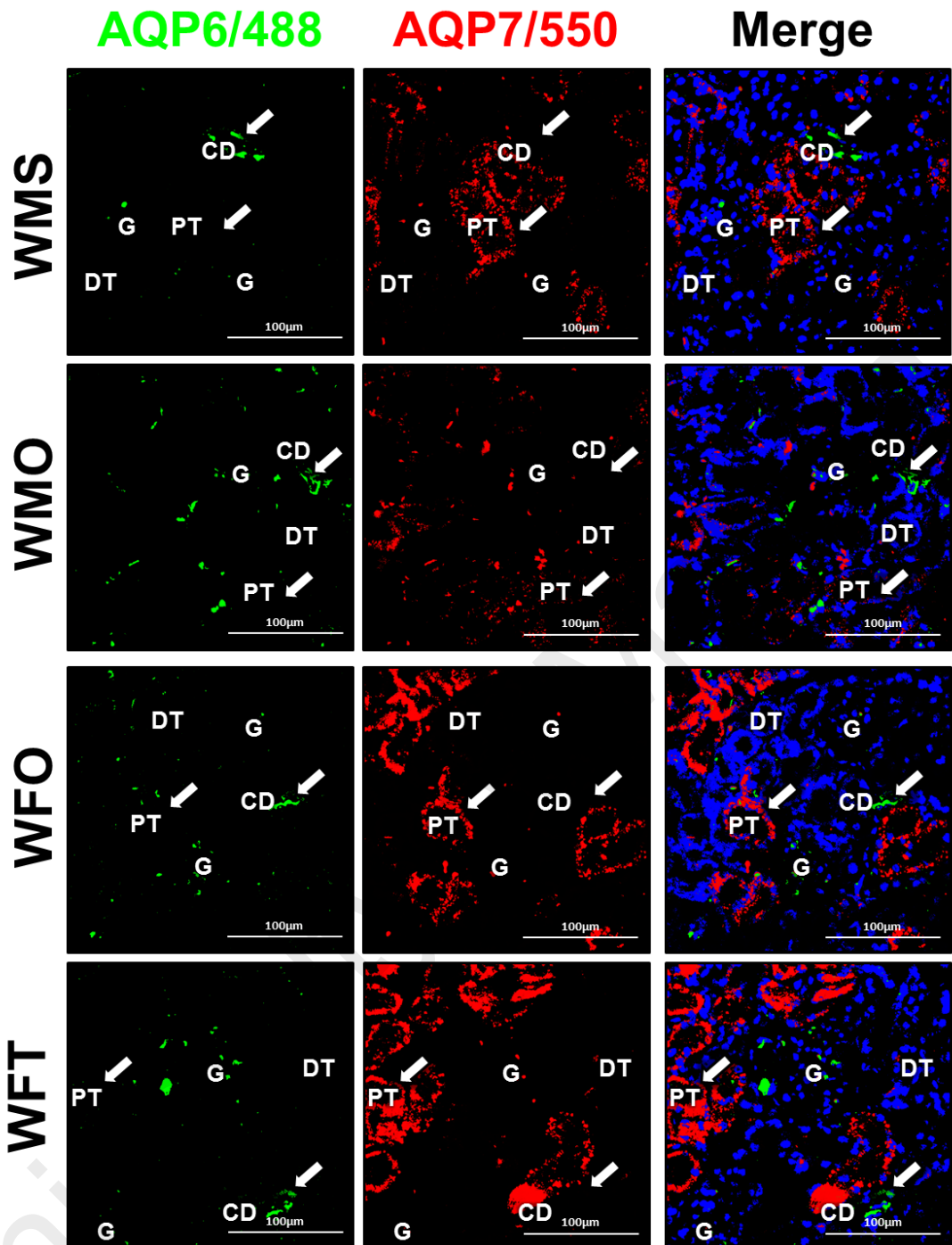


**Figure 8.6** Effects of chronic testosterone treatment on distributions of AQP-6 (green) and AQP-7 (red) proteins in cortical nephron of normotensive WKY rats. Distributions of AQP-6 and AQP-7 in the kidneys of normotensive WKY were assessed by double immunofluorescence staining. Representative confocal immunofluorescence images (n = 4/group) of the coronal sections of kidney cortex were presented. AQP6, represented by green fluorescent signals, was expressed in CD while and AQP-4, represented by red fluorescent signals, were expressed in PT [white arrow heads]. Abbreviations: WMS: WKY sham-operated intact male; WMO: WKY orchidectomized male; WFO: WKY ovariectomized female; WFT: WKY testosterone-treated ovariectomized female rat; G: glomerulus; DT: distal convoluted tubule; PT: proximal convoluted tubule; CD: collecting duct. Scale bar = 100µM.

#### 8.2.4 AQP mRNA expression in kidneys of hypertensive SHR rats

In Figure 8.7(A), *Aqp-1* mRNA level in the kidney of male SHR rats was significantly decreased following orchidectomy ( $P < 0.01$ ). In ovariectomized female SHR rats, chronic testosterone exposure caused *Aqp-1* mRNA level to increase ( $P < 0.05$ ). In Figure 8.7(B), orchidectomy markedly decreased *Aqp-2* mRNA level in the kidneys of male SHR rats ( $P < 0.05$ ). In testosterone-treated ovariectomized female SHR rats, a significantly higher *Aqp-2* mRNA level was observed when compared to those non-treated ( $P < 0.05$ ). In Figure 8.7(C), orchidectomized male SHR rats showed significantly lower *Aqp-3* mRNA level in the kidney when compared to sham-operated intact males ( $P < 0.05$ ). Chronic testosterone treatment caused *Aqp-3* mRNA level to increase in the kidneys of ovariectomized female SHR rats ( $P < 0.05$ ). In Figure 8.7(D), *Aqp-4* mRNA level in male SHR rats was significantly decreased by orchidectomy ( $P < 0.05$ ). In ovariectomized female SHR rats, chronic exposure to testosterone significantly increased *Aqp-4* mRNA level in the kidneys ( $P < 0.05$ ). In Figure 8.7(E), *Aqp-6* mRNA level was markedly lower in orchidectomized male when compared to sham-operated intact male SHR rats ( $P < 0.05$ ). A significantly higher level of *Aqp-6* mRNA was observed in the kidney of ovariectomized female SHR rats following chronic testosterone treatment ( $P < 0.001$ ). In Figure 8.7(F), a significant reduction in the level of *Aqp-7* mRNA in kidneys of male SHR rats following orchidectomy was observed ( $P < 0.01$ ). Meanwhile, ovariectomized female SHR rats following testosterone treatment showed significantly higher *Aqp-7* mRNA levels in the kidneys when compared to those non-treated ( $P < 0.01$ ).

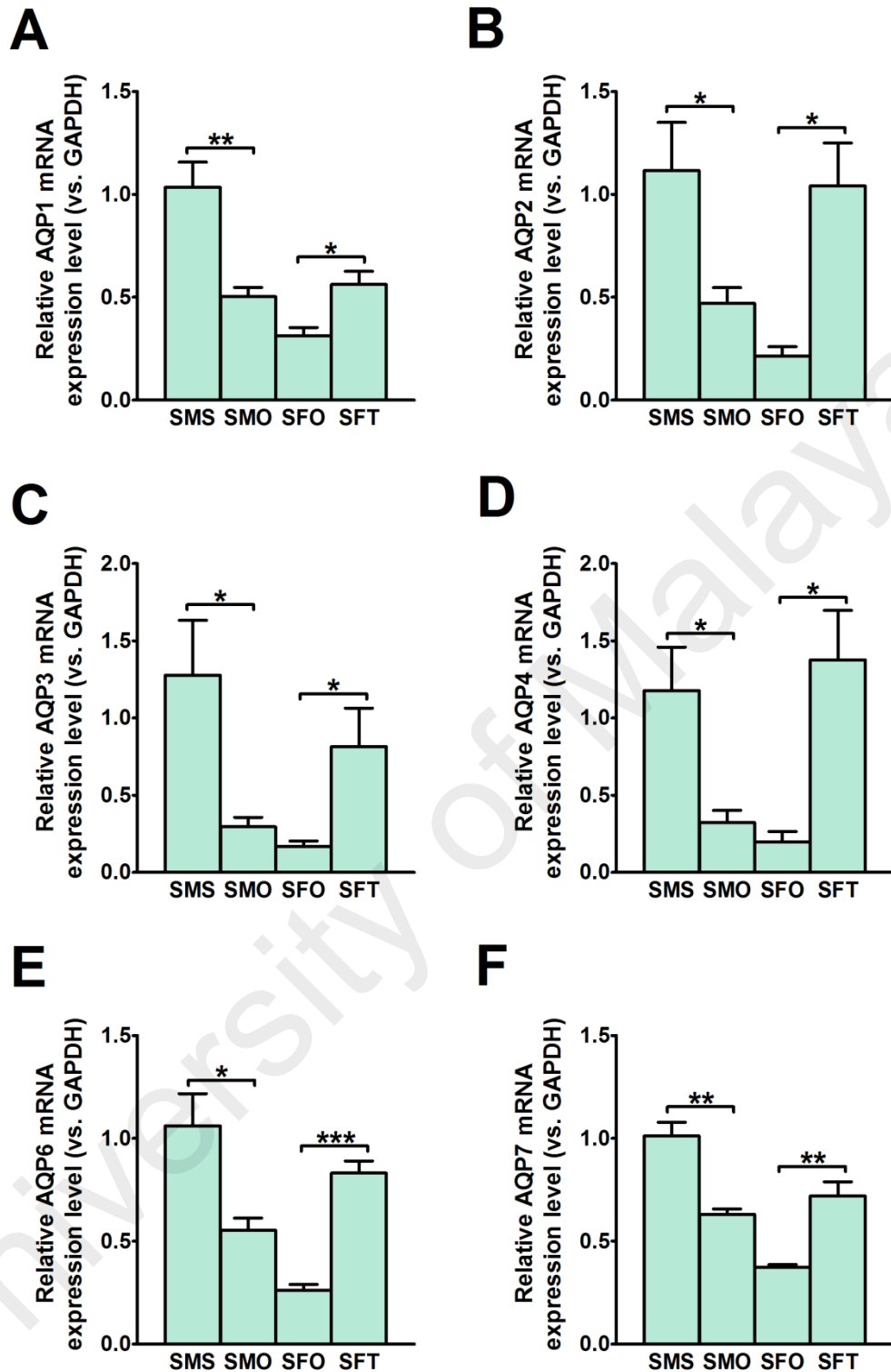


**Figure 8.7** Effects of chronic testosterone treatment on mRNA expression levels of AQP subunits in the kidneys of hypertensive SHR rats.

Effects of chronic testosterone treatment on (A) *Aqp-1*, (B) *Aqp-2*, (C) *Aqp-3*, (D) *Aqp-4*, (E) *Aqp-6* and (F) *Aqp-7* mRNA levels in the kidney of hypertensive SHR rats. Data are expressed as mean  $\pm$  SEM (n = 6/group, unpaired student's *t*-test); \* $P$ <0.05; \*\* $P$ <0.01; \*\*\* $P$ <0.001. Abbreviations: SMS: SHR sham-operated intact male; SMO: SHR orchidectomized male; SFO: SHR ovariectomized female; SFT: SHR testosterone-treated ovariectomized female rat.

### 8.2.5 AQP protein expression in kidneys of hypertensive SHR rats

In Figure 8.8, AQP-1 protein expression level in the kidney of male SHR rats was significantly decreased by orchidectomy ( $P < 0.05$ ). In ovariectomized female hypertensive SHR rats, chronic exposure to testosterone caused a significant increase in kidney AQP-1 protein expression level ( $P < 0.05$ ). A significant decrease in AQP-2 protein expression level was observed in male hypertensive SHR rats following orchidectomy ( $P < 0.05$ ). In ovariectomized female hypertensive SHR rats, chronic testosterone treatment caused AQP-2 protein expression level to significantly increase ( $P < 0.05$ ). For AQP-4, orchidectomy significantly decreased the level of this protein in the kidney of male SHR rats ( $P < 0.05$ ). Chronic testosterone treatment to ovariectomized female SHR rats increased the level of this protein ( $P < 0.05$ ). Similarly, AQP-6 protein level was markedly decreased following orchidectomy in male SHR rats ( $P < 0.01$ ) while significantly increased following chronic exposure to testosterone in ovariectomized female SHR rats ( $P < 0.01$ ).

As for aquaglyceroporins (Figure 8.9), the level of AQP-3 protein in the kidney of male SHR rats significantly decreased following orchidectomy ( $P < 0.001$ ). In ovariectomized female SHR rats, AQP-3 protein level significantly increased following chronic testosterone exposure ( $P < 0.01$ ). Likewise, AQP-7 protein expression level in male SHR rats significantly decreased by orchidectomy ( $P < 0.05$ ) while a significant increase in this protein level was observed following chronic testosterone treatment in ovariectomized female SHR rats ( $P < 0.05$ ).

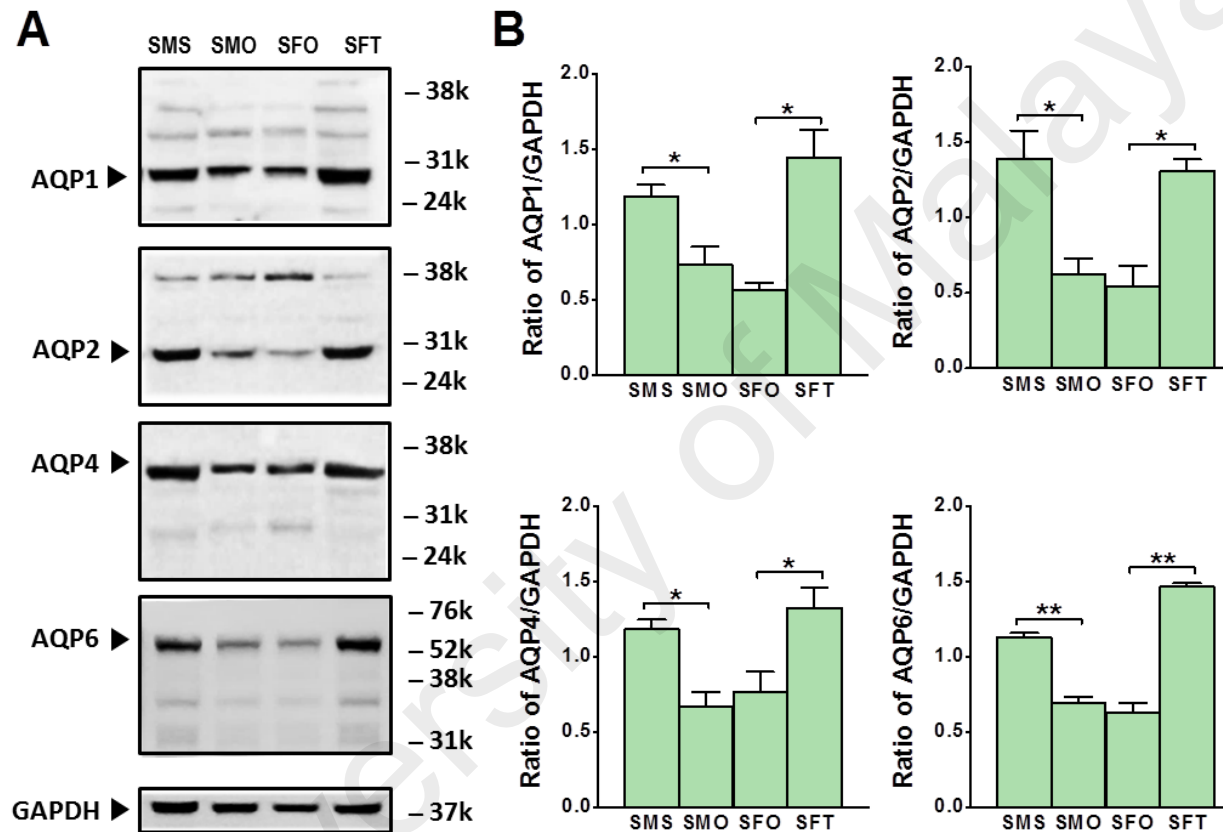


**Figure 8.8 Effects of chronic testosterone treatment on protein expression levels of classical aquaporins in kidneys of hypertensive SHR rats.**

(A) Representative immunoblot images of the classical aquaporin *i.e.* AQP-1, AQP-2, AQP-4 and AQP-6. Molecular weight of targeted proteins = 28kDa (AQP-1), 29kDa (AQP-2), 34kDa (AQP-4) and 55kDa (AQP-6). (B) Average relative ratio of band intensities of AQP-1, AQP-2, AQP-4 and AQP-6 proteins to housekeeping protein, GAPDH (of three replicate blots). Data are expressed as mean  $\pm$  SEM ( $n = 6$ /group, unpaired student's *t*-test); \* $P < 0.05$ ; \*\*\* $P < 0.01$ . Abbreviations: SMS: SHR sham-operated intact male; SMO: SHR orchidectomized male; SFO: SHR ovariectomized female; SFT: SHR testosterone-treated ovariectomized female rat.

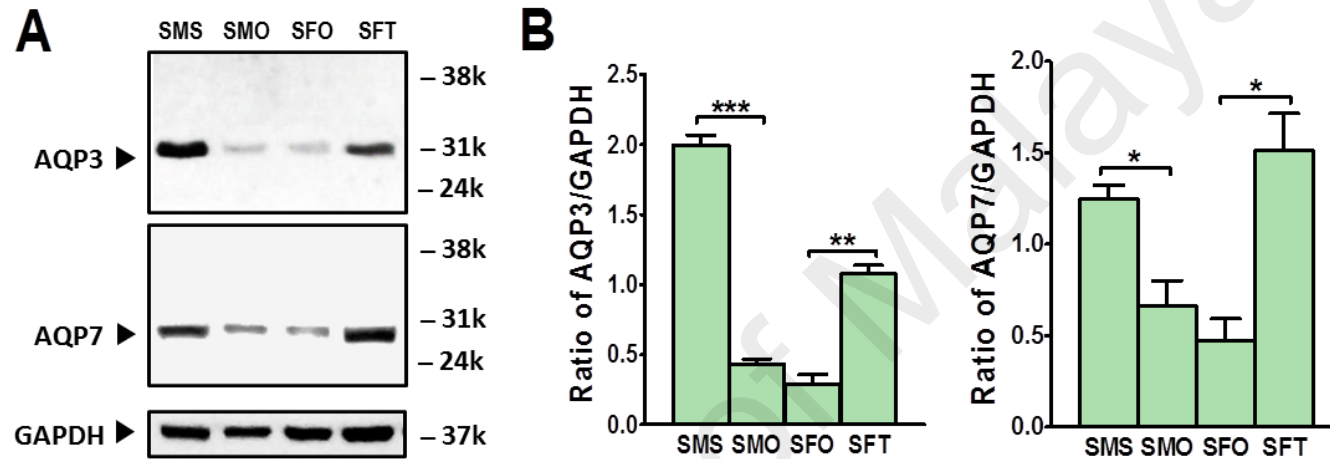


**Figure 8.9** Effects of chronic testosterone treatment on protein expression levels of aquaglyceroporins in kidneys of hypertensive SHR rats. **(A)** Representative immunoblot images of aquaglyceroporins *i.e.* AQP-3 and AQP-7. Molecular weight of targeted proteins = 31kDa (AQP-3) and 22-33kDa (AQP-7). **(B)** Average relative ratio of band intensities of AQP-3 and AQP-7 proteins to housekeeping protein, GAPDH (of three replicate blots). Data are expressed as mean  $\pm$  SEM (n = 6/group, unpaired student's *t*-test); \* $P$ <0.05; \*\* $P$ <0.01; \*\*\* $P$ <0.001. Abbreviations: SMS: SHR sham-operated intact male; SMO: SHR orchidectomized male; SFO: SHR ovariectomized female; SFT: SHR testosterone-treated ovariectomized female rat.

### 8.2.6 Distribution of AQP proteins in kidney of hypertensive SHR rats

In hypertensive SHR rats, AQP-1 (green fluorescent signals) protein was seen to distribute in the PT while AQP-3 (red) protein was seen to distribute in PT and CD (Figure 8.10). AQP-1 was not found in G, DT and CD while AQP-3 was not found in G and DT. Distribution of AQP-1 protein was relatively lower in orchidectomized as compared to sham-operated intact male SHR rats and in non-treated ovariectomized as compared to testosterone-treated ovariectomized female SHR rats. A relatively higher AQP-3 distribution was observed in sham-operated intact male rats when compared to orchidectomized male SHR rats. Lower AQP-3 was found to be distributed in the kidney of non-treated ovariectomized female SHR rats when relatively compared to those testosterone-treated.

In Figure 8.11, AQP-2 (red fluorescent signals) and AQP-4 (green fluorescent signals) proteins were found to be expressed at apical and basolateral membranes of CD, respectively. These proteins were not expressed in G, DT and PT. Distribution of AQP-2 in kidneys of SHR rats was relatively higher in sham-operated intact males when compared to those orchidectomized and in ovariectomized females receiving chronic testosterone treatment when compared to those non-treated. Likewise, comparably higher AQP-4 distributions were found in the CD of sham-operated intact male and testosterone-treated ovariectomized female when compared to orchidectomized male and non-treated ovariectomized female SHR rats, respectively.

AQP-6 (green fluorescent signals) was found to be distributed in CD while AQP-7 (red fluorescent signals) was found to be distributed in PT of hypertensive SHR rats. AQP-6 was not expressed in G, DT and PT while AQP-7 was not expressed in G, DT and CD. Relatively higher AQP-6 levels were observed in sham-operated intact male

and testosterone-treated ovariectomized female SHR rats when compared to orchidectomized male and non-treated ovariectomized female SHR rats, respectively. AQP-7 protein was expressed at a comparably higher level in the kidney of sham-operated intact male SHR rat when compared to orchidectomized male SHR rats. The distribution of this protein was also relatively higher in the kidney of ovariectomized female SHR rats receiving chronic testosterone treatment than those non-treated.

University of Malaya

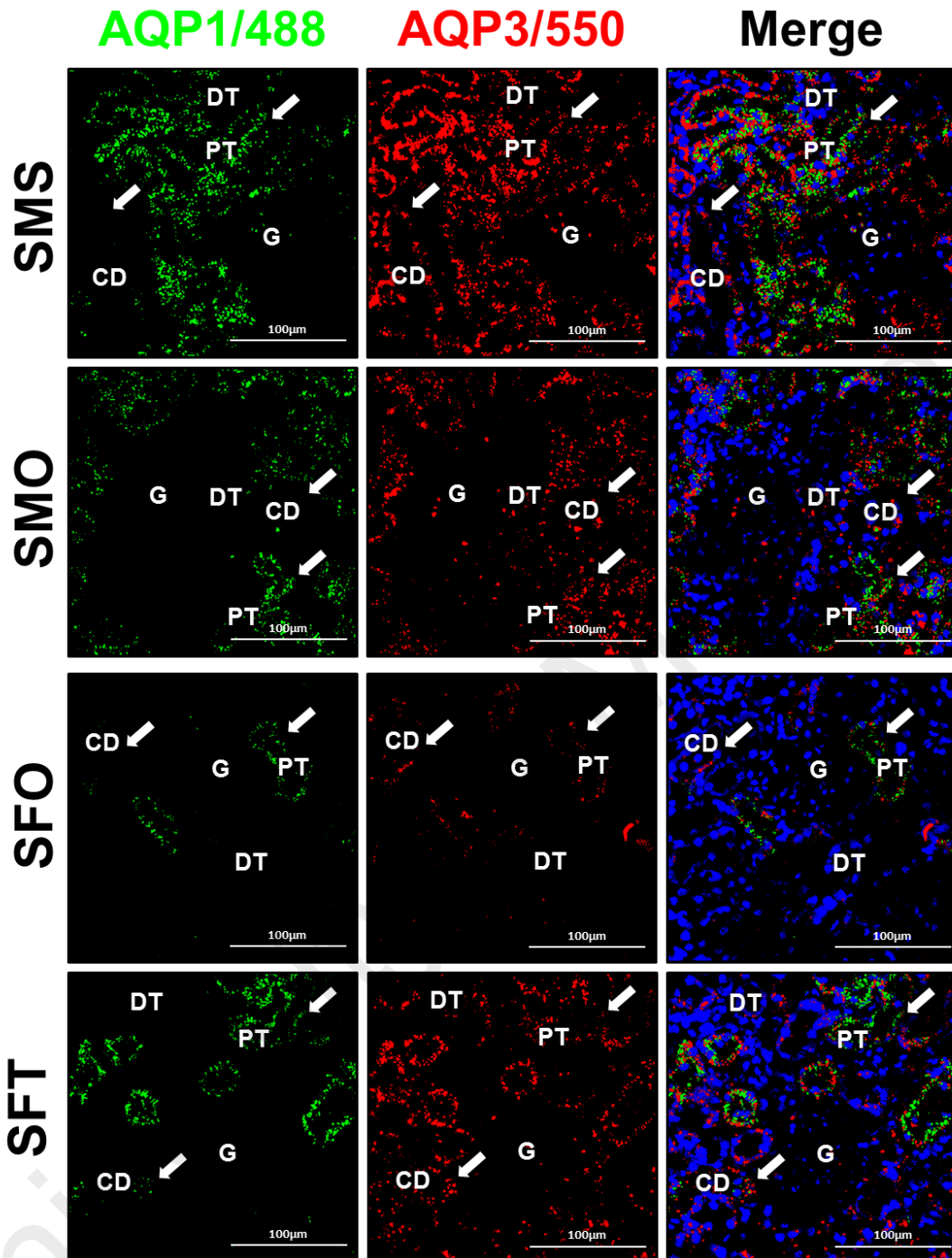


**Figure 8.10** Effects of chronic testosterone treatment on distributions of AQP-1 (green) and AQP-3 (red) proteins in cortical nephron of hypertensive SHR rats.

Distributions of AQP-1 and AQP-3 in the kidneys of hypertensive SHR were assessed by double immunofluorescence staining. Representative confocal immunofluorescence images ( $n = 4/\text{group}$ ) of the coronal sections of kidney cortex were presented. AQP-1, represented by green fluorescent signals, was expressed in PT while AQP-3, represented by red fluorescent signals, was expressed in PT and CD [white arrow heads]. Abbreviations: SMS: SHR sham-operated intact male; SMO: SHR orchidectomized male; SFO: SHR non-treated ovariectomized female; SFT: SHR testosterone-treated ovariectomized female rat; G: glomerulus; DT: distal tubule; PT: proximal tubule; CD: collecting duct. Scale bar =  $100\mu\text{M}$ .

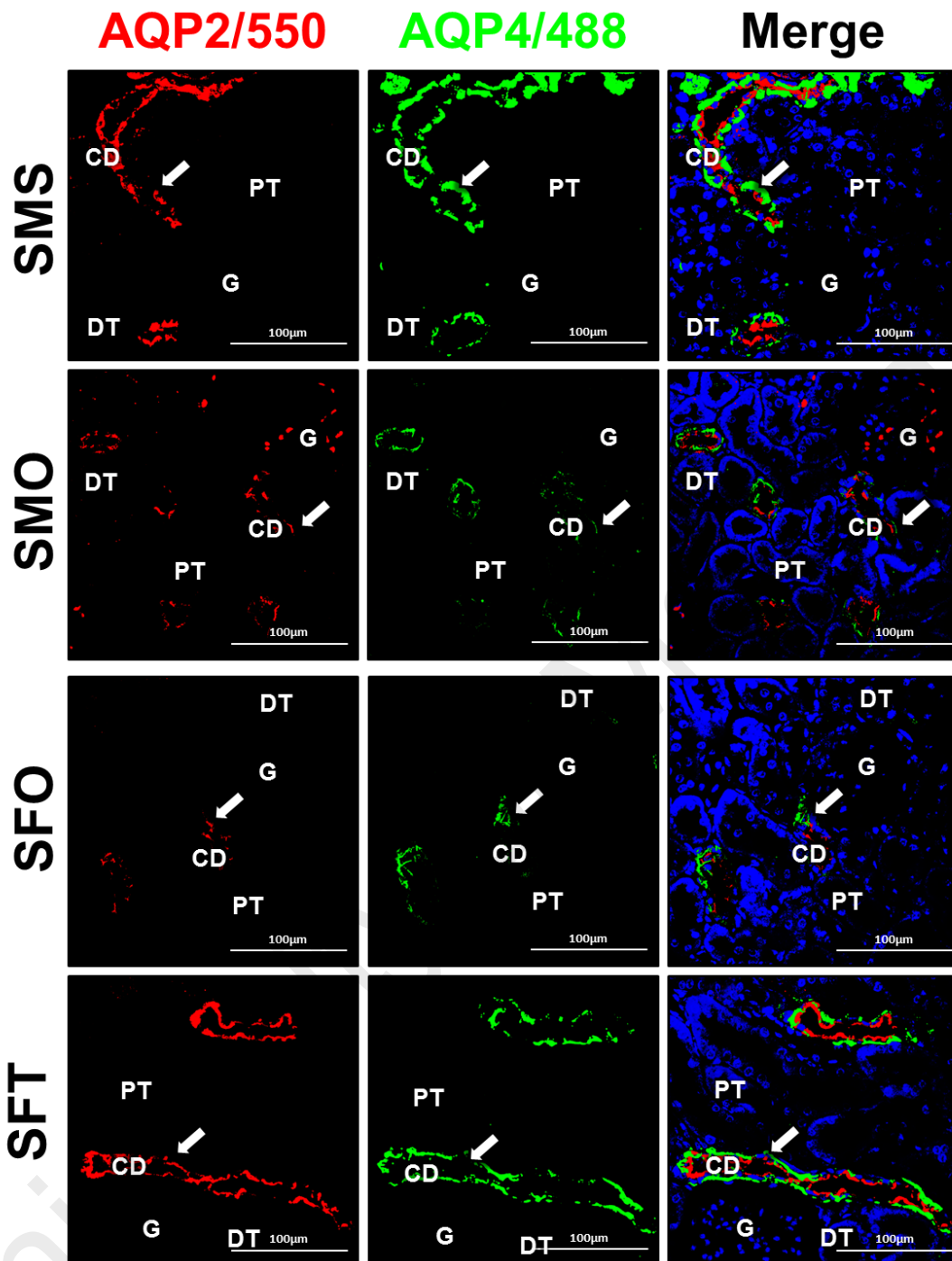


**Figure 8.11 Effects of chronic testosterone treatment on distributions of AQP-2 (red) and AQP-4 (green) proteins in cortical nephron of hypertensive SHR rats.**

Distributions of AQP-2 and AQP-4 in the kidneys of normotensive WKY were assessed by double immunofluorescence staining. Representative confocal immunofluorescence images (n = 4/group) of the coronal sections of kidney cortex were presented. Both AQP-2, represented by red fluorescent signals and AQP-4, represented by green fluorescent signals were expressed in CD [white arrow heads]. Abbreviations: SMS: SHR sham-operated intact male; SMO: SHR orchidectomized male; SFO: SHR ovariectomized female; SFT: SHR testosterone-treated ovariectomized female rat; G: glomerulus; DT: distal tubule; PT: proximal tubule; CD: collecting duct. Scale bar = 100µm.

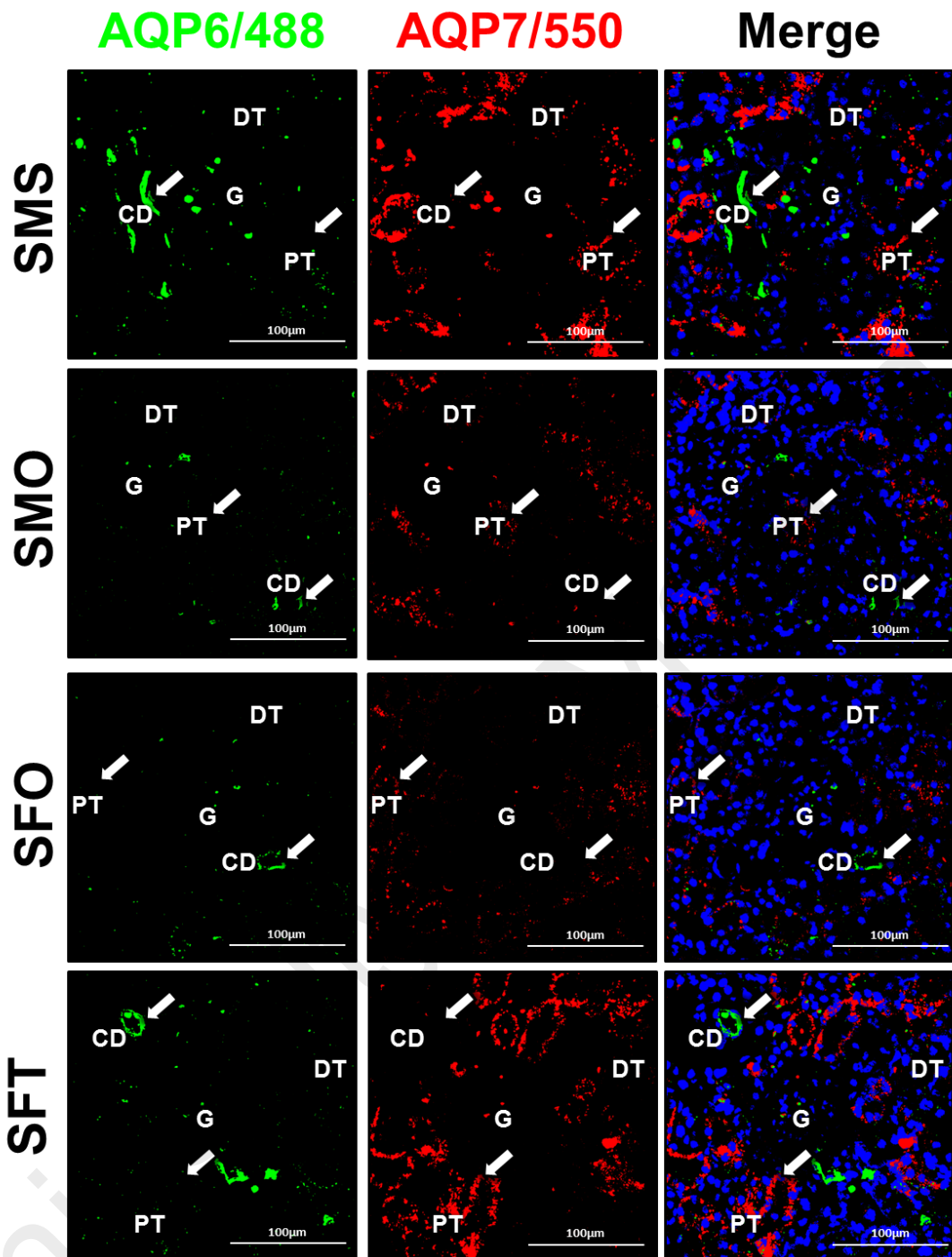


**Figure 8.12 Effects of chronic testosterone treatment on distributions of AQP-6 (green) and AQP-7 (red) proteins in cortical nephron of hypertensive SHR rats.**

Distributions of AQP-6 and AQP-7 in the kidneys of hypertensive SHR were assessed by double immunofluorescence staining. Representative confocal immunofluorescence images ( $n = 4/\text{group}$ ) of the coronal sections of kidney cortex were presented. AQP6, represented by green fluorescent signals, was expressed in CD while and AQP-4, represented by red fluorescent signals, were expressed in PT [white arrow heads]. Abbreviations: SMS: SHR sham-operated intact male; SMO: SHR orchidectomized male; SFO: SHR ovariectomized female; SFT: SHR testosterone-treated ovariectomized female rat; G: glomerulus; DT: distal tubule; PT: proximal tubule; CD: collecting duct. Scale bar = 100 $\mu\text{m}$ .

### 8.3 Discussion

In the present study, it is shown that chronic treatment with testosterone in ovariectomized normotensive females increased the expression of AQP-1, 2, 4 and 7 while, in ovariectomized hypertensive female rats, the expression of AQP-1, 2, 3, 4, 6 and 7 were increased. In these rats, ovariectomy resulted in endogenous estrogen level to fall and thus avoiding the possible conflicting effects of female hormones. The observed effects of chronic testosterone supplementation in females were supported by the findings in the male rats, in which removal of testes, a major source of endogenous testosterone had resulted in decreases in the expression levels of AQP-1, 2, 4 and 7 in normotensive rats and AQP-1, 2, 3, 4, 6 and 7 in hypertensive rats. Nonetheless, in normotensive rats, the levels of AQP-3 were increased by orchidectomy in males while decreased by chronic testosterone treatment in females. Meanwhile, the levels of AQP-6 were generally not affected by either orchidectomy or chronic testosterone treatment in these rats. In overall, testosterone was found to exert greater influence on the expression level of AQP subunits under hypertensive than normotensive conditions. These finding could likely contribute towards the progression of higher blood pressure in hypertensive rats as compared to normotensive rats (refer **Chapter 4**).

The observed effects of testosterone could have implications on kidney water movement. Increased in the expression of most AQP subunits could result in increased water reabsorption in the kidneys, in which this could lead to plasma volume expansion that would subsequently increase the blood pressure. Besides testosterone, other sex-steroid hormones for examples estrogen and progesterone have also been found to affect the regulation of body fluid homeostasis via their effects on the kidneys. These were supported by the presence of the sex hormone receptors in this organ (Curtis, 2009; Dubey & Jackson, 2001; Stachenfeld, 2008; Wenner & Stachenfeld, 2012). Estrogen

was also found to directly affect AQP expression in the kidneys (Cheema et al., 2015; Wei et al., 2014-05). In addition, the effect of sex hormones on AQP expression was not only limited to the kidney but was also found in other organs. For examples, testosterone has been reported to up-regulate the expression of AQP-4 in astrocytes (Gu et al., 2003) and AQP-1 (Herak-Kramberger et al., 2015; Salleh et al., 2015) and AQP-7 (Salleh et al., 2015) in uterus.

In this study, it is found that AQP-2 expression level in the CD markedly changed under testosterone influence. The remarkably higher AQP-2 expression could be seen in CD apical membrane in ovariectomized female normotensive and hypertensive rats receiving chronic testosterone treatment. Similarly, in male rats, orchidectomy markedly reduced AQP-2 expression at CD apical membrane with the effects more pronounce in hypertensive condition. The role of AQP-2 in the hormone-regulated water transport in kidneys has been well-documented. AQP-2 is exclusively expressed in the principal cells of CD and is under arginine vasopressin (AVP) regulation (Nielsen et al., 2002; Verkman, 2012). AVP acutely regulates water permeability of the kidney CD by trafficking AQP-2 from the intracellular vesicles to the apical plasma membrane and regulating the abundance of AQP-2 protein (Nielsen et al., 1999; Wilson et al., 2013). Besides AQP-2, our findings also indicated that in normotensive and hypertensive conditions, expression of AQP-4 at the basolateral membrane in ovariectomized female rats were enhanced by testosterone. Similarly, in the male rats, orchidectomy reduced the expression level of this protein, indicating the possible up-regulation of AQP-4 by testosterone. Our findings were consistent with the previous observations that expression of AQP-4 was observed at the basolateral membrane of CD where this channel serves as the exit pathway for water molecules that enter the CD via AQP-2 (Nielsen et al., 2002; Verkman, 2012). AQP-4 is responsible for the majority of

basolateral membrane water movement in the inner medullary CD as evidence from defective urinary concentrating ability in mice with *Aqp-4* gene knock-out (Chou et al., 1998; Ma et al., 1997a).

The present study have also showed that AQP1 was distributed in the PT in which expression was reduced following orchidectomy in males while in ovariectomized female rats, was markedly increased following chronic testosterone treatment. Schnermann *et al.* (2013) reported that in mice, deficiency of AQP-1, which is expressed in both apical and basolateral plasma membranes of PT could affect transcellular water movement (Schnermann et al., 2013). Therefore, the up-regulation of AQP-1 expression in PT by testosterone would likely to result in increased trans-epithelial water transport, which would ultimately cause increased plasma volume and blood pressure. On the other hand, AQP-3, which its levels were increased in hypertensive yet decreased in normotensive conditions by testosterone, was found to be expressed at the basolateral membrane of the CD. These findings were consistent with the report that AQP-3 was present at the basolateral membrane of CD principal cells which represent the exit pathways for water that was reabsorbed via apical AQP-2, and was regulated in part by vasopressin (Ecelbarger et al., 1995; Nielsen et al., 2002).

In addition, this study also showed that AQP-6 was expressed in CD while AQP-7 was expressed in PT. Under normotensive condition, the AQP-6 level was not affected by testosterone, however the level of this protein increased in hypertensive condition. In CD, AQP-6 resides in the intracellular membrane vesicles at apical, mid, and basolateral cytoplasm of type An intercalated cells, but was not observed in the plasma membrane, therefore this subunit most likely not involve in the transepithelial water transport (Yasui et al., 1999). Our findings were consistent with the report that AQP-7 is

abundantly expressed at the apical membrane of PT and has been identified as a novel pathway for glycerol reabsorption that occurs in this nephron segment (Sohara et al., 2006). *Aqp-1/Aqp-7* double knockout mice showed reduced urinary concentrating ability when compared to *Aqp-1* solo knockout mice, indicating the substantial contribution of AQP-7 to water reabsorption in the PT (Sohara et al., 2006). Testosterone caused the AQP-7 level to markedly increase, suggesting that this hormone could enhance water as well as glycerol absorption that would eventually affect both the plasma volume and glycerol levels.

In the present study, the observed up-regulation of AQP-2 and AQP-4 expression levels in the CD by testosterone in both normotensive and hypertensive conditions could lead to enhance water reabsorption from the lumen into the blood plasma. Although testosterone was found to down-regulate AQP-3 in CD under normotensive condition, however this effect might not cause significant changes in water exit through basolateral plasma membrane as AQP-4 expression was up-regulated. In the meantime, the up-regulation of AQP-1 and AQP-7 in PT could result in increased water reabsorption, leading to plasma volume expansion and thus high blood pressure. In overall, the changes in the expression levels of AQP subunits in the kidneys following orchidectomy (loss of endogenous testosterone) and chronic testosterone treatment could affect the plasma volume and subsequently resulted in the alteration in blood pressure (refer **Chapter 4**).

## CHAPTER 9: EFFECTS OF CHRONIC TESTOSTERONE TREATMENT ON TRANSCRIPTOMES IN PVN, NTS AND RVLM

### 9.1 Introduction

In addition to the kidney, gender-associated differences in sympathetic nervous system (SNS) are also known to contribute towards the differences in the blood pressure regulation (Hinojosa-Laborde et al., 1999; Maranon et al., 2015; Sabolic et al., 2007). It was reported that men typically have higher sympathetic nervous activity that could cause enhanced coronary vasoconstriction and thus higher blood pressure as compared to the age-matched premenopausal women (Hart & Joyner, 2010; Ng et al., 1993; Thangjam & Wangkheimayum, 2015). The paraventricular nucleus (PVN) of the hypothalamus and the nucleus of the solitary tract (NTS) and rostral ventrolateral medulla (RVLM) of the brainstem are of those important brain regions that play important roles in the central control of cardiovascular system, which involved the regulation of SNA (Hay, 2016; Martins-Pinge, 2011; Suzuki et al., 1989). Despite the evidence the showed the expressions of androgen and estrogen receptors in these brain regions (Bingham et al., 2006; Hamson et al., 2004; Haywood et al., 1999; Milner et al., 2007; Wu et al., 2009; Xue et al., 2013), the mechanisms underlying the central neural control of how sex hormones influence the blood pressure remain to be explored.

The influences of sex hormones on the cerebral vasculature have been reported to implicate a variety of disorders including cardiovascular diseases (Pol et al., 2006; Yang et al., 2000). Both estrogen and testosterone can modulate the cerebrovascular tone via prostanoid mechanisms where estrogen appears to shift the prostanoid balance toward vasodilation whereas testosterone enhances vasoconstriction (Gonzales et al., 2005), suggesting that the cerebrovascular functions could be dependent on the

estrogenic/androgenic balance in the males and females. Recently, chronic exposure to low level of  $17\beta$ -estradiol was shown to induce hypertension by causing the increase in superoxide level in RVLM (Subramanian et al., 2011). In this study, transcriptome analysis via RNASeq was performed on the pivotal brain regions *i.e.* PVN, NTS and RVLM following orchidectomy in male and chronic testosterone treatment in ovariectomized female hypertensive rats. These transcriptome data could thus provide a comprehensive view of the gene expression changes in these areas of the brain by testosterone under hypertensive conditions.

University of Malaysia

## 9.2 Results

### 9.2.1 RNA quality assessment prior to library preparation for RNASeq

In Table 9.1, in exception of some RNAs extracted from RVLM with ratio values of absorbance at 260nm versus 230nm ( $A_{260}/A_{230}$ ) below 1.7, the ratio of absorbance at 260nm versus 280nm ( $A_{260}/A_{280}$ ) and  $A_{260}/A_{230}$  for most RNA samples were within the ideal range *i.e.*  $A_{260}/A_{280}$  were within 1.8-2.2 and  $A_{260}/A_{230}$  were above 1.7. The 28S/18S ribosomal RNA (rRNA) ratios of all RNAs were around 2.0, ranged from the lowest 1.5 of sample NS1 to highest 2.4 of sample PV3. Except for sample PT1 (RIN number = 7.8), the RNA Integrity numbers (RIN) of all RNA samples were above the ideal value of 8. The concentrations of the RNA samples were quantified by using Qubit assay in which the highest concentration of RNA ranged from 165 to 255ng/ $\mu$ l were extracted from NTS, followed by 75 to 145ng/ $\mu$ l from PVN and the lowest concentration ranged from 40 to 70ng/ $\mu$ l from RVLM. In Figure 9.1, representative bioanalyzer electropherogram and gel-like images of all RNA samples showed two distinct peaks which corresponded to the 18S and 28S rRNA, with the 28S/18S ratios of 2.0, indicating high quality of RNAs input for the subsequent protocols.

**Table 9.1 Quality control assessment of RNA extracted from PVN, RVLM and NTS.**

Sample ID	A260/A280	A260/A230	rRNA ratio [28s/18s]	RIN	Qubit (ng/ $\mu$ l)
PS1	2.14	2.05	1.80	8.80	80.7
PS2	2.13	2.14	1.70	8.70	91.5
PS3	2.11	1.82	1.70	8.80	144.0
PO1	2.13	1.79	1.80	9.00	131.0
PO2	2.13	1.78	2.10	8.80	141.0
PO3	2.15	1.50	1.60	8.60	79.3
PV1	2.13	1.98	1.80	8.90	119.0
PV2	2.12	2.12	2.10	8.10	127.0
PV3	2.11	2.10	2.40	8.10	134.0
PT1	2.11	1.82	1.90	7.80	137.0
PT2	2.12	2.11	1.60	8.40	126.0
PT3	2.13	2.13	1.90	8.80	98.3
NS1	2.10	2.12	1.50	8.70	228.0
NS2	2.10	2.20	1.90	8.90	166.0
NS3	2.09	2.17	1.60	8.80	250.0
NO1	2.11	2.26	1.90	8.70	228.0
NO2	2.10	2.16	1.80	8.60	223.0
NO3	2.09	2.20	1.80	8.70	253.0
NV1	2.10	2.11	1.70	8.60	216.0
NV2	2.10	2.17	1.70	8.70	231.0
NV3	2.11	2.15	1.70	8.70	235.0
NT1	2.11	2.19	1.70	8.60	230.0
NT2	2.10	2.19	1.90	8.60	222.0
NT3	2.11	2.22	1.70	8.60	239.0
RS1	2.11	2.03	1.70	8.30	44.5
RS2	2.09	1.37	1.80	8.60	49.4
RS3	1.96	1.64	1.70	8.40	63.9
RO1	1.99	1.56	1.80	8.50	60.1
RO2	2.13	1.89	2.00	8.30	59.8
RO3	2.08	1.00	1.90	8.40	55.9
RV1	2.06	1.48	1.80	8.50	65.3
RV2	2.11	1.53	2.00	8.30	60.1
RV3	2.09	1.72	1.70	8.70	57.6
RT1	2.07	1.35	2.10	8.50	70.0
RT2	2.06	1.85	1.80	8.30	46.7
RT3	2.12	1.56	1.90	8.70	55.5

A number of quality control tests were performed on the RNA extracted from PVN, NTS and RVLM prior to library preparation. Ratios of A260/A280 and A260/A230 were obtained from Nanodrop while rRNA ratio and RIN number were generated from Agilent 2100 bioanalyzer. Concentrations of RNA were quantified using high sensitivity Qubit RNA assay. Abbreviations: RIN: RNA integrity number; P; PVN, R; RVLM, N; NTS, S; sham-operated intact male, O; orchidectomized male, V; ovariectomized female; T; testosterone-treated ovariectomized female.

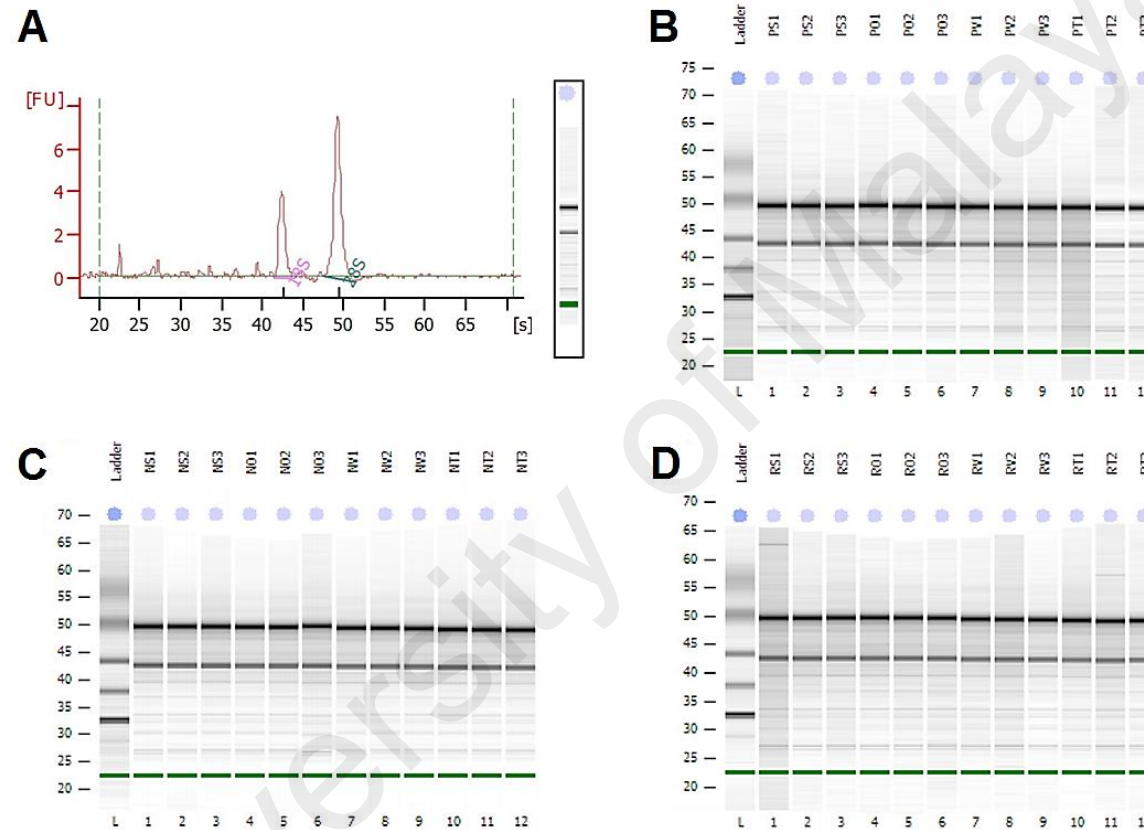


**Figure 9.1 RNA quality assessment report with Agilent Bioanalyzer.**

(A) Representative electropherogram of RNA generated from Agilent 2100 bioanalyzer. A good quality of RNA sample should produce two well-defined peaks corresponding to the 18S and 28S ribosomal RNA with the 28s/18s ratio of 2:1. Bioanalyzer gel-like images of RNA extracted from (B) paraventricular nucleus (PVN), (C) nucleus of the solitary tract (NTS) and (D) rostral ventrolateral medulla (RVLM) obtained. Visualization of two distant bands representing the 18S and 28S ribosomal RNA in all samples indicated good quality of RNA extracted. Abbreviations: P; PVN, R; RVLM, N; NTS, S; sham-operated intact male, O; orchidectomized male, V; ovariectomized female; T; testosterone-treated ovariectomized female.

### **9.2.2 cDNA library quality assessment and quantification**

In Figure 9.2, representative bioanalyzer electropherogram and gel-like images showed the distribution of all cDNA libraries between 150 to 1000 base pair (bp) with a peak maximum of approximately 260bp. In Table 9.2, the average fragment length of cDNA in all libraries ranged from 340 to 455 bp while the concentration of cDNA libraries ranged from 14 to 56ng/μl. Due to the low cDNA concentration of 5.2ng/μl, sample RV1 was subjected to further purification by using Agencourt AMPure XP (Beckman Coulter, Inc., California, United States) prior to qPCR run. Mean quantity of cDNA in all libraries, quantified by Eco real-time PCR system, ranged from 0.5 to 1.8pM.

### **9.2.3 MiSeq library quality control of pooled library**

In Table 9.3, the percentage of cluster passing filter (%PF) of each cDNA libraries ranged from 2.1 to 3.9%, with a total of 19,818,961.79 reads obtained for 36 samples in which an ideal reads number of 550,526.72 per sample was estimated (refer **Chapter 3; Section 3.9.1.6** for calculation equation).

### **9.2.4 HiSeq sequencing of pooled library**

In Table 9.4, a minimum of 30 million reads of each cDNA libraries was generated, indicating a success HiSeq sequencing run. The number of reads of each cDNA libraries ranged from 32 to 46 million reads, with a total number of 1,543 million reads in one HiSeq run.

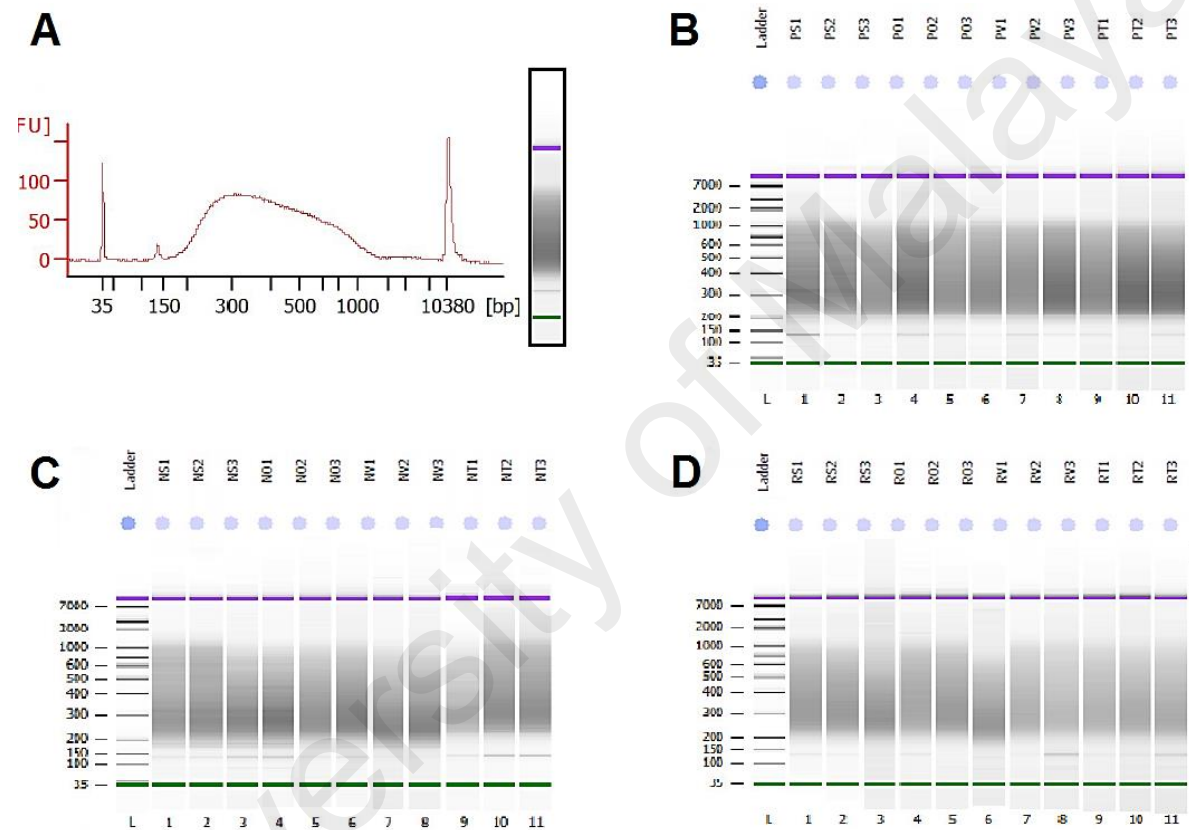


**Figure 9.2 Library quality assessment report with Agilent Bioanalyzer.**

(A) Representative electropherogram of cDNA library generated from Agilent 2100 bioanalyzer showing the library size ranging from 150-100bp with a maximal peak at approximately 260bp. Bioanalyzer gel-like images of cDNA library prepared from RNA of (B) paraventricular nucleus (PVN), (C) nucleus of the solitary tract (NTS) and (D) rostral ventrolateral medulla (RVLM). Abbreviations: P; PVN, R; RVLM, N; NTS, S; sham-operated intact male, O; orchidectomized male, V; ovariectomized female; T; testosterone-treated ovariectomized female.

**Table 9.2 Quality control assessment of cDNA library.**

Sample ID	Fragment length (bp)	Qubit (ng/ $\mu$ l)	Concentration (nM)	Eco value (pM)
PS1	392	24.0	91.84	0.5393
PS2	344	38.5	167.88	0.6923
PS3	385	30.5	118.83	0.9395
PO1	392	27.5	105.23	0.7831
PO2	386	31.8	123.58	0.5831
PO3	388	37.0	143.04	0.7045
PV1	413	38.4	139.47	0.8548
PV2	392	36.8	140.82	0.5590
PV3	404	38.1	141.46	0.6688
PT1	452	14.4	47.79	0.6692
PT2	376	37.4	149.20	0.6619
PT3	390	24.6	94.62	0.7040
NS1	423	18.1	64.18	1.1700
NS2	432	16.3	56.60	1.6275
NS3	402	14.2	52.99	1.0837
NO1	434	18.9	65.32	1.1975
NO2	440	16.8	57.27	1.4401
NO3	369	30.3	123.17	1.1652
NV1	433	23.1	80.02	1.2406
NV2	437	22.5	77.23	1.8362
NV3	428	15.4	53.97	1.3359
NT1	419	22.2	79.47	1.5495
NT2	407	22.4	82.56	1.6068
NT3	435	20.1	69.31	1.3969
RS1	411	49.3	179.93	0.9564
RS2	386	56.0	217.62	0.9844
RS3	439	44.7	152.73	0.8722
RO1	421	54.0	192.40	0.8879
RO2	344	46.3	201.89	0.5243
RO3	421	49.0	174.58	0.8624
RV1	453	5.20	17.22	1.3396
RV2	421	49.7	177.08	0.6191
RV3	403	49.0	182.38	0.5565
RT1	401	45.8	171.32	0.5870
RT2	404	48.2	178.96	0.6064
RT3	405	42.9	158.89	0.6061

A number of quality control tests were performed on the cDNA library prepared from RNA of PVN, NTS and RVLM. Using the average fragment length obtained Agilent 2100 bioanalyzer and concentrations in ng/ $\mu$ l quantified via Qubit DNA assay, the concentrations of the libraries in nM were calculated (refer **Chapter 3; Section 3.9.1.5** for all calculation equations). Eco value is the mean quantity of cDNA given by Eco real-time PCR system in pM. Abbreviations: P; PVN, R; RVLM, N; NTS, S; sham-operated intact male, O; orchidectomized male, V; ovariectomized female; T; testosterone-treated ovariectomized female.

**Table 9.3 MiSeq quality control assessment of pooled library.**

Sample ID	%PF	Reads	Reads/ $\mu$ l	Volume ( $\mu$ l)
PS1	3.01	606,460.36	202,153.45	2.72
PS2	2.40	484,648.14	161,549.38	3.41
PS3	2.68	539,687.43	179,895.81	3.06
PO1	2.89	582,267.27	194,089.09	2.84
PO2	3.42	688,656.40	229,552.13	2.40
PO3	3.04	613,113.46	204,371.15	2.69
PV1	2.18	439,991.72	146,663.91	3.75
PV2	3.87	779,723.23	259,907.74	2.12
PV3	2.85	574,424.68	191,474.89	2.88
PT1	3.41	686,559.66	228,853.22	2.41
PT2	2.67	538,941.47	179,647.16	3.06
PT3	3.00	604,484.59	201,494.86	2.73
NS1	2.70	544,344.60	181,448.20	3.03
NS2	2.70	544,183.31	181,394.44	3.03
NS3	2.66	537,227.80	179,075.93	3.07
NO1	2.81	566,824.01	188,941.34	2.91
NO2	2.25	454,487.42	151,495.81	3.63
NO3	2.45	494,567.31	164,855.77	3.34
NV1	2.63	530,373.09	176,791.03	3.11
NV2	2.79	562,932.96	187,644.32	2.93
NV3	2.41	486,039.24	162,013.08	3.40
NT1	2.63	529,647.29	176,549.10	3.12
NT2	2.19	441,423.15	147,141.05	3.74
NT3	2.41	485,111.84	161,703.95	3.40
RS1	2.59	522,207.92	174,069.31	3.16
RS2	2.37	478,599.87	159,533.29	3.45
RS3	2.60	523,941.76	174,647.25	3.15
RO1	2.63	531,078.72	177,026.24	3.11
RO2	2.55	514,022.59	171,340.86	3.21
RO3	2.22	448,459.30	149,486.43	3.68
RV1	2.27	457,068.01	152,356.00	3.61
RV2	2.90	584,484.97	194,828.32	2.83
RV3	3.02	608,053.08	202,684.36	2.72
RT1	2.90	584,545.45	194,848.48	2.83
RT2	3.30	664,664.91	221,554.97	2.48
RT3	2.91	585,714.79	195,238.26	2.82
<b>TOTAL READS</b>		<b>19,818,961.79</b>		

The efficiency of pooled libraries of PVN, NTS and RVLM was assessed via MiSeq quality run. The numbers of reads per sample per  $\mu$ l were calculated using %PF values obtained from the MiSeq reporter software. Volumes of each cDNA libraries required to be repooled were calculated (refer **Chapter 3; Section 3.9.1.6** for all calculation equations). Abbreviations: %PF: percentage of clusters passing filter; P; PVN, R; RVLM, N; NTS, S; sham-operated intact male, O; orchidectomized male, V; ovariectomized female; T; testosterone-treated ovariectomized female.

**Table 9.4 Summary report of HiSeq run.**

Sample ID	Paired-end (PE) Reads	Reads
PS1	84,438,178	42,219,089
PS2	79,526,500	39,763,250
PS3	85,353,774	42,676,887
PO1	80,994,104	40,497,052
PO2	86,426,346	43,213,173
PO3	87,124,232	43,562,116
PV1	82,350,662	41,175,331
PV2	85,145,142	42,572,571
PV3	84,938,064	42,469,032
PT1	84,689,682	42,344,841
PT2	87,752,726	43,876,363
PT3	82,728,564	41,364,282
NS1	86,561,332	43,280,666
NS2	85,278,792	42,639,396
NS3	91,961,142	45,980,571
NO1	86,728,138	43,364,069
NO2	83,359,626	41,679,813
NO3	79,244,716	39,622,358
NV1	87,370,478	43,685,239
NV2	79,910,024	39,955,012
NV3	86,903,008	43,451,504
NT1	83,518,204	41,759,102
NT2	91,757,248	45,878,624
NT3	77,709,950	38,854,975
RS1	77,607,334	38,803,667
RS2	81,088,646	40,544,323
RS3	79,908,350	39,954,175
RO1	84,038,952	42,019,476
RO2	82,431,854	41,215,927
RO3	74,940,206	37,470,103
RV1	85,232,986	42,616,493
RV2	86,332,882	43,166,441
RV3	86,905,320	43,452,660
RT1	82,855,610	41,427,805
RT2	85,140,012	42,570,006
RT3	82,728,288	41,364,144
<b>TOTAL READS</b>	<b>3,085,379,068</b>	<b>1,542,689,534</b>

The pooled library of PVN, NTS and RVLM was sequenced on HiSeq2500 sequencing platform (refer **Chapter 3; Section 3.10.1.7** for detail protocols). The table shows the summary of total numbers of paired-end and single reads per sample (refer **Appendix D** for full report). Abbreviations: P; PVN, R; RVLM, N; NTS, S; sham-operated intact male, O; orchidectomized male, V; ovariectomized female; T; testosterone-treated ovariectomized female.

## 9.2.5 Transcriptome data analysis

### 9.2.5.1 Paraventricular nucleus (PVN)

Expressions of 6,728 genes were found to be significantly changed (edgeR;  $P < 0.05$ ) in PVN of orchidectomized male when compared to sham-operated intact male SHR rats. Meanwhile, ovariectomized female SHR rats receiving chronic testosterone treatment showed marked changes (edgeR;  $P < 0.05$ ) in the expression levels of 2,741 genes in PVN as compared to those non-treated. In Figure 9.3, a total number of 2,099 genes were observed in the intersect, indicating expression changes of identical genes in PVN by orchidectomy in male rats (SMO compare to SMS) and chronic testosterone treatment in ovariectomized female rats (SFT compare to SFO). Based on the edgeR statistical method, a wide variety of genes with diverse functions that are significantly and strongly increased or decreased in expression level in PVN following orchidectomy in male and chronic testosterone treated ovariectomized female rats were selected for the subsequent determination via qPCR (Table 9.4). The majority of genes selected lied within the top 20 genes of highly up-regulated or down-regulated in their expression levels in orchidectomized males and testosterone-treated ovariectomized females as compared to sham-operated intact males (SMO compare to SMS) and non-treated ovariectomized female SHR rats (SFT compare to SFO), respectively.

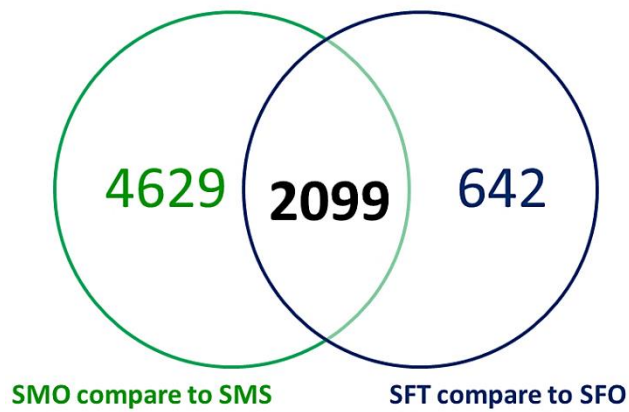


**Figure 9.3 Venn diagram showing intersection of number of genes changes in PVN in SMO compared to SMS and in SFT compared to SFO.**

Significantly changes (edgeR;  $P < 0.05$ ) of 2,099 genes were found in PVN under both cases. Abbreviations: SMS: SHR sham-operated intact male; SMO: SHR orchidectomized male; SFO: SHR ovariectomized female; SFT: SHR testosterone-treated ovariectomized female rats.

University of Manitoba

**Table 9.5 Expression changes of selected genes in PVN based on edgeR analysis of SMO compared to SMS and SFT compared to SFO.**

No.	Gene ID	Gene name	SMO compare to SMS						SFT compare to SFO					
			Average count		DESeq		edgeR		Average count		DESeq		edgeR	
			SMS	SMO	FC	PValue	FC	PValue	SFO	SFT	FC	PValue	FC	PValue
1	ENSRNOG00000019578	<b>Rps16</b>	350.31	29.64	0.08	7.42E-95	<b>0.08</b>	4.65E-97	61.42	200.98	3.27	4.65E-19	<b>3.31</b>	2.46E-10
2	ENSRNOG00000005130	<b>Ogdh</b>	4009.97	434.44	0.11	0.00E+00	<b>0.11</b>	0.00E+00	716.53	1726.91	2.41	1.18E-41	<b>2.44</b>	1.84E-12
3	ENSRNOG000000021691	<b>Ccdc92</b>	960.60	110.29	0.11	3.49E-175	<b>0.11</b>	2.44E-191	216.39	484.86	2.24	9.80E-19	<b>2.27</b>	7.13E-14
4	ENSRNOG000000020460	<b>Banf1</b>	246.18	58.26	0.24	9.66E-35	<b>0.24</b>	4.12E-54	70.62	143.38	2.03	1.33E-05	<b>2.04</b>	4.24E-09
5	ENSRNOG00000015318	<b>Heyl</b>	174.21	30.18	0.17	3.87E-34	<b>0.17</b>	1.97E-57	35.33	71.38	2.02	5.05E-03	<b>2.03</b>	4.36E-05
6	ENSRNOG00000002579	<b>Parm1</b>	381.26	27.39	0.07	2.93E-108	<b>0.07</b>	3.46E-144	67.72	132.11	1.95	1.60E-04	<b>1.96</b>	7.02E-04
7	ENSRNOG00000018680	<b>Rpl17</b>	422.47	183.72	0.43	5.20E-23	<b>0.43</b>	1.48E-27	161.05	307.59	1.91	4.15E-09	<b>1.93</b>	2.30E-11
8	ENSRNOG000000047111	<b>NOL6</b>	329.45	63.47	0.19	1.76E-54	<b>0.19</b>	4.95E-75	71.23	135.58	1.90	1.97E-04	<b>1.92</b>	3.07E-04
9	ENSRNOG00000014613	<b>Ddah1</b>	745.23	129.09	0.17	1.61E-109	<b>0.17</b>	1.85E-72	245.72	442.33	1.80	6.53E-10	<b>1.82</b>	4.64E-11
10	ENSRNOG00000018116	<b>Kcna3</b>	163.36	54.99	0.34	2.66E-16	<b>0.33</b>	1.22E-26	56.39	102.14	1.81	4.79E-03	<b>1.81</b>	9.55E-07
11	ENSRNOG00000011227	<b>Atp1b2</b>	1312.28	290.16	0.22	3.08E-125	<b>0.22</b>	2.64E-132	414.20	697.79	1.68	8.41E-10	<b>1.70</b>	1.21E-12
12	ENSRNOG00000017286	<b>Ephx2</b>	354.40	73.27	0.21	3.08E-54	<b>0.20</b>	5.60E-85	131.32	211.47	1.61	6.69E-04	<b>1.63</b>	1.31E-05
13	ENSRNOG000000025745	<b>Gpr17</b>	147.93	76.32	0.52	5.57E-07	<b>0.51</b>	9.88E-09	73.24	118.13	1.61	2.60E-02	<b>1.61</b>	1.78E-05
14	ENSRNOG00000015733	<b>Myl12b</b>	392.26	100.94	0.26	2.45E-47	<b>0.26</b>	8.55E-71	112.02	177.40	1.58	2.03E-03	<b>1.61</b>	4.50E-04
15	ENSRNOG00000013397	<b>Foxo1</b>	195.97	49.37	0.25	6.44E-27	<b>0.25</b>	1.85E-33	77.38	121.16	1.57	2.55E-02	<b>1.58</b>	8.08E-05
16	ENSRNOG00000006542	<b>Atp6v0c</b>	2290.59	627.34	0.27	1.71E-127	<b>0.27</b>	1.23E-104	784.30	1180.92	1.51	4.03E-08	<b>1.53</b>	6.84E-06
17	ENSRNOG000000021225	<b>Oxt</b>	39030.00	27806.40	0.71	7.88E-15	<b>0.70</b>	6.28E-09	31498.90	46852.00	1.49	1.56E-10	<b>1.51</b>	1.37E-03
18	ENSRNOG000000020263	<b>Atp1a3</b>	7461.31	2075.48	0.28	1.14E-172	<b>0.27</b>	2.58E-179	3000.64	4363.70	1.45	8.81E-10	<b>1.48</b>	3.35E-07
19	ENSRNOG00000003999	<b>Adcy3</b>	1516.73	521.36	0.34	3.45E-77	<b>0.34</b>	1.10E-114	661.97	961.54	1.45	2.52E-06	<b>1.47</b>	3.22E-08
20	ENSRNOG000000020533	<b>Htra1</b>	588.32	235.36	0.40	1.07E-33	<b>0.40</b>	2.35E-31	275.59	396.55	1.44	9.32E-04	<b>1.46</b>	1.39E-04

Abbreviations: FC: fold change; PValue: probability value; SMS: SHR sham-operated intact male; SMO: SHR orchidectomized male; SFO: SHR ovariectomized female; SFT: SHR testosterone-treated ovariectomized female rats.

Table 9.5 continued.

No.	Gene ID	Gene name	SMO compare to SMS						SFT compare to SFO					
			Average count		DESeq		edgeR		Average count		DESeq		edgeR	
			SMS	SMO	FC	PValue	FC	PValue	SFO	SFT	FC	PValue	FC	PValue
21	ENSRNOG00000036798	<b>Dusp3</b>	2206.52	1355.96	0.61	4.36E-21	<b>0.61</b>	4.77E-26	1455.18	1908.82	1.31	3.40E-04	<b>1.33</b>	3.52E-05
22	ENSRNOG00000022523	<b>Fkbp5</b>	318.56	226.68	0.71	4.60E-04	<b>0.71</b>	1.52E-06	261.71	342.85	1.31	5.67E-02	<b>1.32</b>	5.70E-04
23	ENSRNOG00000016684	<b>Wnk2</b>	507.00	166.22	0.33	1.45E-42	<b>0.32</b>	1.25E-65	227.14	292.98	1.29	6.62E-02	<b>1.31</b>	1.35E-02
24	ENSRNOG00000042022	<b>H1f0</b>	783.31	460.53	0.59	6.60E-16	<b>0.58</b>	2.70E-23	545.21	631.16	1.16	3.67E-01	<b>1.17</b>	4.01E-02
25	ENSRNOG00000034303	<b>Spon1</b>	1700.47	1187.05	0.70	2.41E-11	<b>0.69</b>	2.29E-14	1365.48	1541.15	1.13	2.39E-01	<b>1.15</b>	2.77E-02
26	ENSRNOG00000018454	<b>Apoe</b>	42935.60	54920.90	1.28	1.93E-08	<b>1.26</b>	4.35E-08	56439.50	47846.40	0.85	3.11E-02	<b>0.86</b>	6.38E-03
27	ENSRNOG00000017333	<b>Syt4</b>	6696.05	12460.20	1.86	1.06E-47	<b>1.84</b>	8.66E-43	11186.10	9326.04	0.83	1.01E-02	<b>0.85</b>	1.09E-03
28	ENSRNOG00000018294	<b>Hspa5</b>	21707.90	26870.80	1.24	1.92E-06	<b>1.22</b>	2.21E-05	31071.00	25851.20	0.83	5.57E-03	<b>0.84</b>	1.14E-02
29	ENSRNOG00000016356	<b>Got1</b>	2430.22	3819.33	1.57	3.01E-22	<b>1.55</b>	1.09E-21	3518.25	2861.88	0.81	5.59E-03	<b>0.83</b>	7.73E-05
30	ENSRNOG00000026455	<b>Gpd1l</b>	296.64	585.88	1.98	2.48E-20	<b>1.95</b>	1.75E-26	423.05	336.04	0.79	9.25E-02	<b>0.81</b>	1.66E-03
31	ENSRNOG00000019741	<b>Isyna1</b>	175.56	358.78	2.04	9.74E-16	<b>2.02</b>	4.04E-24	289.13	220.14	0.76	5.97E-02	<b>0.77</b>	8.89E-04
32	ENSRNOG00000003747	<b>Asna1</b>	487.77	861.22	1.77	9.99E-19	<b>1.74</b>	2.18E-28	746.85	557.88	0.75	1.30E-03	<b>0.76</b>	1.37E-06
33	ENSRNOG00000001959	<b>Mx1</b>	69.88	119.46	1.71	2.37E-04	<b>1.69</b>	5.85E-05	90.45	65.04	0.72	2.95E-01	<b>0.73</b>	1.99E-02
34	ENSRNOG00000027156	<b>Morn4</b>	441.17	1060.27	2.40	4.26E-45	<b>2.37</b>	1.09E-37	649.53	460.21	0.71	1.94E-04	<b>0.72</b>	3.13E-07
35	ENSRNOG00000016164	<b>Fcrl2</b>	110.24	218.79	1.98	4.39E-10	<b>1.96</b>	2.08E-11	174.56	122.92	0.70	5.87E-02	<b>0.72</b>	7.68E-03
36	ENSRNOG00000020435	<b>Terf2</b>	139.25	243.50	1.75	2.10E-07	<b>1.72</b>	1.15E-06	224.20	151.44	0.68	7.37E-03	<b>0.69</b>	2.20E-05
37	ENSRNOG00000032404	<b>Top2a</b>	46.38	71.45	1.54	3.46E-02	<b>1.52</b>	1.16E-03	59.53	40.11	0.67	2.38E-01	<b>0.68</b>	1.92E-02
38	ENSRNOG00000004247	<b>Nhp2</b>	160.93	199.88	1.24	1.09E-01	<b>1.22</b>	2.18E-02	215.00	144.13	0.67	4.37E-03	<b>0.68</b>	2.37E-06
39	ENSRNOG00000049075	<b>Fabp5</b>	504.58	1421.81	2.82	6.77E-70	<b>2.79</b>	7.07E-27	1166.16	679.25	0.58	3.97E-15	<b>0.59</b>	1.68E-10

Fold changes in average read counts of each gene were analyzed using DESeq and edgeR (n = 3 per group where 5 samples were pooled to obtain n = 1). 39 selected genes with significantly and strong expression changes (edgeR:  $PValue < 0.05$ ) following orchidectomy in male rats (SMO) and chronic testosterone treatment in ovariectomized female rats (SFT) for subsequent qPCR determinations (**Chapter 10**). Abbreviations: FC: fold change; PValue: probability value; SMS: SHR sham-operated intact male; SMO: SHR orchidectomized male; SFO: SHR ovariectomized female; SFT: SHR testosterone-treated ovariectomized female rats.

### 9.2.5.2 Nucleus of the solitary tract (NTS)

A total number of 644 genes showed significant changes (edgeR;  $P < 0.05$ ) in their expression levels in NTS of orchidectomized male as compared to sham-operated intact male SHR rats. When compared to non-treated ovariectomized female rats, expression levels of 673 genes were markedly change (edgeR;  $P < 0.05$ ) in NTS of testosterone-treated ovariectomized female SHR rats. Figure 9.4 showed an intersect of 76 genes, indicating the changes in expression levels of identical genes in NTS following orchidectomy in male rats (SMO compare to SMS) and testosterone treatment in ovariectomized female rats (SFT compare to SFO). Based on the edgeR statistical analysis, genes of variety functions that were significantly and strongly increased or decreased in NTS were selected for subsequent qPCR determinations (Table 9.5). The majority of genes selected lied within the top 20 in the gene list with highest fold changes, either up-regulation or down-regulation, following orchidectomy in male rats (SMO compare to SMS) and testosterone treatment in ovariectomized female SHR rats (SFT compare to SFO).

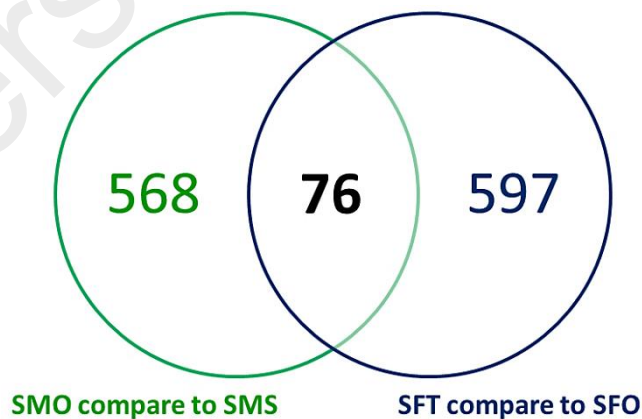


**Figure 9.4 Venn diagram showing intersection of number of genes changes in NTS in SMO compared to SMS and in SFT compared to SFO.**

Significantly changes (edgeR;  $P < 0.05$ ) of 76 genes were found in NTS under both cases. Abbreviations: SMS: SHR sham-operated intact male; SMO: SHR orchidectomized male; SFO: SHR ovariectomized female; SFT: SHR testosterone-treated ovariectomized female rats.

**Table 9.6 Expression changes of selected genes in NTS based on edgeR analysis of SMO compared to SMS and SFT compared to SFO.**

No.	Gene ID	Gene name	SMO compare to SMS						SFT compare to SFO					
			Average count		DESeq		edgeR		Average count		DESeq		edgeR	
			SMS	SMO	FC	PValue	FC	PValue	SFO	SFT	FC	PValue	FC	PValue
1	ENSRNOG00000011815	<b>Sgk1</b>	827.30	698.71	0.84	1.00E+00	<b>0.84</b>	1.32E-02	717.20	1166.10	1.63	2.98E-06	<b>1.63</b>	6.13E-04
2	ENSRNOG00000019871	<b>Prlh</b>	82.16	45.23	0.55	7.06E-01	<b>0.57</b>	5.40E-05	62.58	96.91	1.55	7.41E-01	<b>1.55</b>	1.31E-02
3	ENSRNOG00000018736	<b>Pnpla2</b>	61.36	45.04	0.73	1.00E+00	<b>0.72</b>	2.77E-02	47.98	73.28	1.53	1.00E+00	<b>1.53</b>	2.36E-03
4	ENSRNOG00000016085	<b>Mpzl2</b>	278.00	164.43	0.59	1.36E-03	<b>0.59</b>	7.17E-09	208.16	313.78	1.51	4.49E-02	<b>1.51</b>	8.29E-06
5	ENSRNOG00000019213	<b>Gpd1</b>	2336.13	1452.88	0.62	2.69E-07	<b>0.62</b>	8.81E-12	1703.66	2520.87	1.48	1.86E-04	<b>1.48</b>	2.63E-08
6	ENSRNOG00000002391	<b>Gira4</b>	161.04	70.93	0.44	8.10E-07	<b>0.43</b>	1.78E-07	90.77	133.20	1.47	7.58E-01	<b>1.47</b>	1.81E-03
7	ENSRNOG00000023162	<b>Car14</b>	722.75	624.57	0.86	1.00E+00	<b>0.86</b>	3.31E-02	589.14	829.78	1.41	3.30E-02	<b>1.41</b>	5.82E-05
8	ENSRNOG00000020030	<b>Crif1</b>	171.02	136.86	0.80	1.00E+00	<b>0.80</b>	1.62E-02	144.87	199.84	1.38	7.58E-01	<b>1.38</b>	3.09E-03
9	ENSRNOG00000017206	<b>Igfbp5</b>	10870.50	6671.71	0.61	4.87E-12	<b>0.61</b>	1.06E-05	7930.38	10868.70	1.37	8.78E-03	<b>1.37</b>	4.36E-03
10	ENSRNOG00000019211	<b>Olfml3</b>	338.54	239.11	0.71	3.18E-01	<b>0.70</b>	5.30E-05	223.09	305.72	1.37	5.20E-01	<b>1.37</b>	2.24E-03
11	ENSRNOG00000015904	<b>Wfdc1</b>	155.41	122.71	0.79	1.00E+00	<b>0.80</b>	3.64E-02	135.18	180.32	1.33	1.00E+00	<b>1.33</b>	7.93E-03
12	ENSRNOG00000014231	<b>Pnoc</b>	95.47	73.96	0.77	1.00E+00	<b>0.76</b>	2.29E-02	76.18	100.25	1.32	1.00E+00	<b>1.32</b>	3.55E-02
13	ENSRNOG00000019342	<b>Sult1a1</b>	339.19	237.59	0.70	4.76E-02	<b>0.69</b>	4.04E-03	250.42	328.35	1.31	8.13E-01	<b>1.31</b>	9.93E-03
14	ENSRNOG00000004280	<b>Tcn2</b>	702.11	548.54	0.78	9.79E-01	<b>0.78</b>	1.68E-03	516.77	670.42	1.30	5.22E-01	<b>1.30</b>	1.83E-03
15	ENSRNOG00000026953	<b>Gpr88</b>	199.00	158.54	0.80	1.00E+00	<b>0.78</b>	1.61E-02	151.01	188.73	1.25	1.00E+00	<b>1.25</b>	2.42E-02
16	ENSRNOG00000006010	<b>Slc6a20</b>	630.95	504.73	0.80	1.00E+00	<b>0.80</b>	9.14E-03	497.12	617.01	1.24	9.88E-01	<b>1.24</b>	2.81E-02
17	ENSRNOG00000012294	<b>Heph</b>	447.31	288.87	0.65	1.23E-02	<b>0.65</b>	5.50E-06	341.06	422.29	1.24	1.00E+00	<b>1.24</b>	4.07E-02
18	ENSRNOG00000042022	<b>H1f0</b>	864.94	736.57	0.85	1.00E+00	<b>0.84</b>	1.48E-02	919.78	1121.63	1.22	9.66E-01	<b>1.22</b>	2.03E-02
19	ENSRNOG00000032472	<b>Gpr64</b>	278.91	216.66	0.78	1.00E+00	<b>0.76</b>	7.17E-03	255.84	306.35	1.20	1.00E+00	<b>1.20</b>	3.83E-02

Abbreviations: FC: fold change; PValue: probability value; SMS: SHR sham-operated intact male; SMO: SHR orchidectomized male; SFO: SHR ovariectomized female; SFT: SHR testosterone-treated ovariectomized female rats.

Table 9.6 continued.

No.	Gene ID	Gene name	SMO compare to SMS						SFT compare to SFO					
			Average count		DESeq		edgeR		Average count		DESeq		edgeR	
			SMS	SMO	FC	PValue	FC	PValue	SFO	SFT	FC	PValue	FC	PValue
20	ENSRNOG00000011955	<b>RPLP1</b>	2836.09	3672.29	1.29	6.03E-02	<b>1.29</b>	2.14E-04	3384.96	2844.84	0.84	1.00E+00	<b>0.84</b>	3.13E-02
21	ENSRNOG00000008154	<b>Ramp3</b>	609.44	749.22	1.23	1.00E+00	<b>1.23</b>	7.94E-03	700.17	572.73	0.82	1.00E+00	<b>0.82</b>	1.26E-02
22	ENSRNOG00000018294	<b>Hspa5</b>	18201.00	21364.30	1.17	1.00E+00	<b>1.17</b>	1.15E-02	23021.20	18384.00	0.80	3.89E-01	<b>0.80</b>	1.77E-03
23	ENSRNOG00000000842	<b>Ddah2</b>	680.19	831.56	1.22	1.00E+00	<b>1.22</b>	1.41E-02	967.78	762.88	0.79	6.54E-01	<b>0.79</b>	7.28E-03
24	ENSRNOG00000048769	<b>Nek5</b>	160.97	204.50	1.27	1.00E+00	<b>1.26</b>	2.01E-02	215.09	168.88	0.79	1.00E+00	<b>0.79</b>	2.24E-02
25	ENSRNOG00000008521	<b>Myl6l</b>	412.49	500.03	1.21	1.00E+00	<b>1.22</b>	4.99E-02	546.25	427.23	0.78	7.58E-01	<b>0.78</b>	2.88E-03
26	ENSRNOG00000015763	<b>Cml3</b>	267.21	349.97	1.31	1.00E+00	<b>1.30</b>	1.19E-03	440.25	342.61	0.78	8.27E-01	<b>0.78</b>	1.07E-02
27	ENSRNOG00000016294	<b>Cd4</b>	126.11	164.78	1.31	1.00E+00	<b>1.28</b>	1.35E-02	196.16	152.28	0.78	1.00E+00	<b>0.78</b>	1.60E-02
28	ENSRNOG00000022286	<b>Dmrtc1b</b>	94.18	135.74	1.44	1.00E+00	<b>1.41</b>	4.28E-03	132.46	102.85	0.78	1.00E+00	<b>0.78</b>	3.71E-02
29	ENSRNOG00000018454	<b>Apoe</b>	44232.80	53101.90	1.20	9.69E-01	<b>1.20</b>	8.90E-03	57842.60	44595.20	0.77	1.38E-01	<b>0.77</b>	1.12E-04
30	ENSRNOG00000002919	<b>Gfap</b>	9196.56	12314.00	1.34	3.73E-02	<b>1.33</b>	5.14E-05	12984.50	10007.50	0.77	1.44E-01	<b>0.77</b>	3.11E-04
31	ENSRNOG00000016243	<b>Casq2</b>	45.71	62.94	1.38	1.00E+00	<b>1.39</b>	2.97E-02	66.10	49.05	0.74	1.00E+00	<b>0.74</b>	3.80E-02
32	ENSRNOG00000014171	<b>Tnfsf13</b>	299.84	361.84	1.21	1.00E+00	<b>1.21</b>	3.96E-02	416.48	307.55	0.74	3.99E-01	<b>0.74</b>	2.76E-03
33	ENSRNOG00000016983	<b>Myh7</b>	59.68	87.42	1.46	1.00E+00	<b>1.45</b>	2.77E-03	95.65	69.92	0.73	1.00E+00	<b>0.73</b>	1.81E-02
34	ENSRNOG00000021084	<b>Mpeg1</b>	298.93	362.81	1.21	1.00E+00	<b>1.20</b>	2.89E-02	388.20	271.68	0.70	1.38E-01	<b>0.70</b>	3.07E-04
35	ENSRNOG00000010079	<b>Car3</b>	106.96	138.71	1.30	1.00E+00	<b>1.28</b>	2.48E-02	136.21	87.07	0.64	3.83E-01	<b>0.64</b>	8.32E-04
36	ENSRNOG00000020151	<b>Cdh1</b>	64.19	89.90	1.40	1.00E+00	<b>1.37</b>	1.14E-02	106.40	66.00	0.62	4.16E-01	<b>0.62</b>	9.03E-05
37	ENSRNOG00000045654	<b>Hspa1b</b>	49.16	75.87	1.54	1.00E+00	<b>1.52</b>	5.25E-03	85.78	49.81	0.58	3.40E-01	<b>0.58</b>	2.04E-03
38	ENSRNOG00000016164	<b>Ferl2</b>	114.50	175.71	1.53	2.79E-01	<b>1.53</b>	2.36E-04	162.29	93.14	0.57	1.41E-02	<b>0.57</b>	4.89E-07

Fold changes in average read counts of each gene were analyzed using DESeq and edgeR (n = 3 per group where 5 samples were pooled to obtain n = 1). 38 selected genes with significantly expression changes (edgeR: *PValue*<0.05) following orchidectomy in male rats (SMO) and chronic testosterone treatment in ovariectomized female rats (SFT) for subsequent qPCR determinations (**Chapter 10**). Abbreviations: FC: fold change; PValue: probability value; SMS: SHR sham-operated intact male; SMO: SHR orchidectomized male; SFO: SHR ovariectomized female; SFT: SHR testosterone-treated ovariectomized female rats.

### 9.2.5.3 Rostral ventrolateral medulla (RVLM)

Expression levels of 1,706 genes in RVLM were found to be significantly changed (edgeR;  $P < 0.05$ ) by orchidectomy in male SHR rats. Meanwhile, a total number of 708 genes showed marked changes (edgeR;  $P < 0.05$ ) in their expression levels in RVLM following chronic testosterone treatment in ovariectomized female rats. In Figure 9.5, a total number of 130 genes lied within the intersect, indicating the identical genes that showed changes in their expression levels in RVLM of orchidectomized male and testosterone-treated ovariectomized female when compared to sham-operated intact male (SMO compare to SMS) and non-treated ovariectomized female SHR rats (SFT compare to SFO), respectively. Based on the edgeR statistical method, a number of genes of variety functions that significantly and strongly increased or decreased in their expression levels in RVLM as a result of orchidectomy in male rats and chronic testosterone exposure in ovariectomized female SHR rats were selected and subjected to qPCR determinations (Table 9.6). The majority of genes selected were found within the list of top 20 genes with highest changes in their expression levels, either up or down-regulation, in RVLM of orchidectomized male when compared to sham-operated intact male SHR rats (SMO compare to SMS) and testosterone-treated compared to non-treated ovariectomized female SHR rats (SFT compare to SFO).

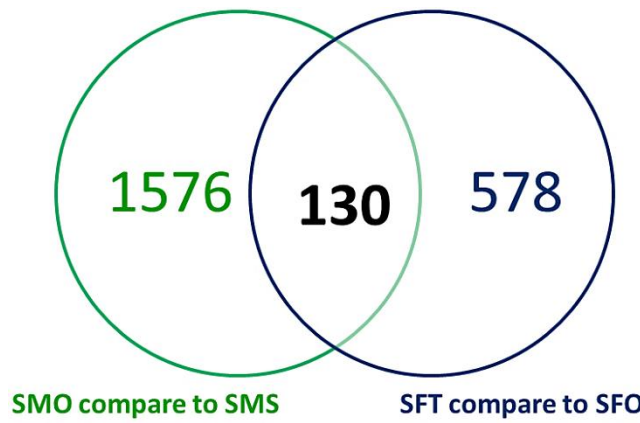


**Figure 9.5 Venn diagram showing intersection of number of genes changes in RVLM in SMO compared to SMS and in SFT compared to SFO.**

Significantly changes (edgeR;  $P < 0.05$ ) of 130 genes were found in RVLM under both cases. Abbreviations: SMS: SHR sham-operated intact male; SMO: SHR orchidectomized male; SFO: SHR ovariectomized female; SFT: SHR testosterone-treated ovariectomized female rats.

University of Manitoba

**Table 9.7 Expression changes of selected genes in RVLM based on edgeR analysis of SMO compared to SMS and SFT compared to SFO.**

No.	Gene ID	Gene name	SMO compare to SMS						SFT compare to SFO					
			Average count		DESeq		edgeR		Average count		DESeq		edgeR	
			SMS	SMO	FC	PValue	FC	PValue	SFO	SFT	FC	PValue	FC	PValue
1	ENSRNOG00000016275	<b>Ttr</b>	3733.92	744.76	0.20	1.11E-161	<b>0.20</b>	7.77E-05	938.86	2671.63	2.85	3.10E-57	<b>2.85</b>	4.74E-03
2	ENSRNOG00000039107	<b>Mfrp</b>	73.70	19.95	0.27	5.51E-09	<b>0.27</b>	2.34E-04	25.97	67.65	2.61	6.28E-04	<b>2.60</b>	4.10E-03
3	ENSRNOG00000012190	<b>Cldn2</b>	77.54	25.69	0.33	5.58E-07	<b>0.33</b>	2.79E-03	32.21	74.36	2.31	3.36E-03	<b>2.30</b>	1.16E-02
4	ENSRNOG00000001092	<b>Kl</b>	204.15	81.16	0.40	4.36E-13	<b>0.40</b>	2.65E-05	86.88	194.42	2.24	2.33E-08	<b>2.24</b>	5.84E-03
5	ENSRNOG00000010378	<b>Slc4a5</b>	150.33	97.14	0.65	2.15E-02	<b>0.64</b>	1.47E-02	87.51	164.50	1.88	3.78E-04	<b>1.88</b>	5.73E-03
6	ENSRNOG00000026870	<b>Clic6</b>	156.36	69.14	0.44	5.71E-08	<b>0.44</b>	1.71E-04	65.29	118.28	1.81	1.26E-02	<b>1.81</b>	3.54E-02
7	ENSRNOG00000015156	<b>Gal</b>	697.45	477.43	0.68	1.35E-04	<b>0.69</b>	6.33E-04	438.50	701.82	1.60	3.00E-06	<b>1.60</b>	8.01E-04
8	ENSRNOG00000047459	<b>Hist1h1d</b>	507.56	400.96	0.79	1.07E-01	<b>0.79</b>	1.97E-02	471.39	681.72	1.45	8.62E-04	<b>1.45</b>	1.21E-03
9	ENSRNOG00000015733	<b>Myl12b</b>	528.76	377.38	0.71	1.74E-03	<b>0.71</b>	8.78E-04	358.79	494.59	1.38	3.42E-02	<b>1.38</b>	1.06E-03
10	ENSRNOG00000019342	<b>Sult1a1</b>	539.87	438.05	0.81	2.21E-01	<b>0.81</b>	3.43E-02	466.35	630.45	1.35	4.47E-02	<b>1.35</b>	1.13E-02
11	ENSRNOG00000029792	<b>Ogn</b>	1000.49	784.84	0.78	3.19E-02	<b>0.78</b>	1.61E-02	839.53	1126.09	1.34	1.22E-02	<b>1.34</b>	4.86E-02
12	ENSRNOG00000012294	<b>Heph</b>	487.71	393.18	0.81	2.26E-01	<b>0.81</b>	5.71E-03	436.39	579.11	1.33	1.10E-01	<b>1.33</b>	1.11E-04
13	ENSRNOG00000025406	<b>Iqgap2</b>	248.99	167.33	0.67	1.05E-02	<b>0.67</b>	6.37E-05	172.59	226.95	1.31	8.16E-01	<b>1.32</b>	5.99E-03
14	ENSRNOG00000022523	<b>Fkbp5</b>	378.34	287.99	0.76	7.54E-02	<b>0.76</b>	7.42E-04	279.71	349.86	1.25	1.00E+00	<b>1.25</b>	6.18E-03
15	ENSRNOG00000021691	<b>Ccdc92</b>	1552.13	1312.12	0.85	1.90E-01	<b>0.84</b>	2.61E-02	1250.22	1545.95	1.24	2.70E-01	<b>1.24</b>	4.13E-04
16	ENSRNOG00000020533	<b>Htra1</b>	1901.80	1544.81	0.81	3.90E-02	<b>0.81</b>	7.87E-04	1666.90	2032.36	1.22	3.95E-01	<b>1.22</b>	3.76E-03
17	ENSRNOG00000023162	<b>Car14</b>	1056.90	915.24	0.87	4.91E-01	<b>0.87</b>	4.45E-02	1011.37	1194.38	1.18	1.00E+00	<b>1.18</b>	9.47E-03
18	ENSRNOG00000034303	<b>Spon1</b>	1079.56	964.01	0.89	7.58E-01	<b>0.89</b>	4.02E-02	1023.97	1177.45	1.15	1.00E+00	<b>1.15</b>	3.63E-02
19	ENSRNOG00000038686	<b>Ap1s2</b>	2215.45	1970.30	0.89	6.33E-01	<b>0.89</b>	4.41E-02	2069.29	2362.27	1.14	1.00E+00	<b>1.14</b>	3.20E-02
20	ENSRNOG00000036798	<b>Dusp3</b>	4330.32	3799.59	0.88	3.87E-01	<b>0.88</b>	1.80E-02	3894.67	4374.03	1.12	1.00E+00	<b>1.12</b>	1.86E-02
21	ENSRNOG00000003999	<b>Adecy3</b>	1037.61	851.91	0.82	1.08E-01	<b>0.82</b>	4.60E-03	997.19	1115.37	1.12	1.00E+00	<b>1.12</b>	4.74E-02

Abbreviations: FC: fold change; PValue: probability value; SMS: SHR sham-operated intact male; SMO: SHR orchidectomized male; SFO: SHR ovariectomized female; SFT: SHR testosterone-treated ovariectomized female rats.

Table 9.7 continued.

No.	Gene ID	Gene name	SMO compare to SMS						SFT compare to SFO					
			Average count		DESeq		edgeR		Average count		DESeq		edgeR	
			SMS	SMO	FC	PValue	FC	PValue	SFO	SFT	FC	PValue	FC	PValue
22	ENSRNOG00000006472	<b>Hspa2</b>	577.19	695.22	1.20	2.95E-01	<b>1.20</b>	1.09E-02	691.15	578.59	0.84	1.00E+00	<b>0.84</b>	3.97E-02
23	ENSRNOG00000010959	<b>Klhl25</b>	88.09	110.66	1.26	8.08E-01	<b>1.25</b>	4.88E-02	125.87	101.44	0.81	1.00E+00	<b>0.81</b>	4.22E-02
24	ENSRNOG00000016356	<b>Got1</b>	3504.67	3937.53	1.12	5.30E-01	<b>1.12</b>	3.15E-02	3686.01	2924.02	0.79	5.16E-02	<b>0.79</b>	1.48E-03
25	ENSRNOG00000003747	<b>Asna1</b>	438.83	575.27	1.31	3.19E-02	<b>1.31</b>	3.11E-03	528.63	413.79	0.78	4.17E-01	<b>0.78</b>	5.71E-03
26	ENSRNOG00000012409	<b>Exosc3</b>	142.99	180.17	1.26	5.67E-01	<b>1.26</b>	1.05E-02	176.90	138.16	0.78	1.00E+00	<b>0.78</b>	9.57E-03
27	ENSRNOG00000050464	<b>GSTA1</b>	846.33	971.14	1.15	5.52E-01	<b>1.15</b>	2.27E-02	1074.05	827.91	0.77	5.91E-02	<b>0.77</b>	1.01E-04
28	ENSRNOG00000016164	<b>Fcrl2</b>	91.86	151.40	1.65	8.30E-03	<b>1.64</b>	2.58E-07	137.42	102.42	0.75	1.00E+00	<b>0.75</b>	3.52E-02
29	ENSRNOG00000021084	<b>Mpeg1</b>	250.77	324.36	1.29	1.79E-01	<b>1.29</b>	9.53E-04	323.84	240.76	0.74	3.61E-01	<b>0.75</b>	2.00E-03
30	ENSRNOG00000046834	<b>C3</b>	551.09	725.74	1.32	1.32E-02	<b>1.32</b>	1.12E-03	767.64	562.97	0.73	2.43E-02	<b>0.73</b>	1.22E-03
31	ENSRNOG00000028368	<b>Etnk2</b>	39.91	61.62	1.54	4.38E-01	<b>1.53</b>	4.06E-03	63.79	46.25	0.72	1.00E+00	<b>0.73</b>	2.24E-02
32	ENSRNOG00000019035	<b>Trpm8</b>	94.95	140.33	1.48	1.07E-01	<b>1.48</b>	5.91E-04	126.83	89.64	0.71	9.27E-01	<b>0.71</b>	2.15E-03
33	ENSRNOG00000049075	<b>Fabp5</b>	389.82	474.36	1.22	3.12E-01	<b>1.22</b>	3.11E-03	496.69	343.59	0.69	4.69E-03	<b>0.69</b>	7.01E-04
34	ENSRNOG00000015763	<b>Cml3</b>	415.26	557.35	1.34	1.55E-02	<b>1.34</b>	2.74E-05	633.44	420.75	0.66	2.17E-04	<b>0.67</b>	4.34E-09

Fold changes in average read counts of each gene were analyzed using DESeq and edgeR (n = 3 per group where 5 samples were pooled to obtain n = 1). 34 selected genes with significantly expression changes (edgeR: *PValue*<0.05) following orchidectomy in male rats (SMO) and chronic testosterone treatment in ovariectomized female rats (SFT) for subsequent qPCR determinations (**Chapter 10**). Abbreviations: FC: fold change; PValue: probability value; SMS: SHR sham-operated intact male; SMO: SHR orchidectomized male; SFO: SHR ovariectomized female; SFT: SHR testosterone-treated ovariectomized female rats.

### 9.3 Discussion

An increase in the number of biological replicates, pooled into one sample which in this study, five biological samples were pooled as  $n = 1$ , helps to overcome the low RNA concentration as well as to minimize bias during transcriptome analysis (Robledo et al., 2014; Xu et al., 2012). RNA is a sensitive polymeric molecule and extremely susceptible to degradation. Thus, in order to ensure the success of subsequent downstream transcriptome sequencing, several methods of RNA quality assessment were carried out. The RNA quantity and purity were determined by measuring the UV absorption of the sample by using a spectrophotometer (NanoDrop). The absorbance of 230nm was taken to determine the background absorption and the presence of other organic contaminants such as guanidine salt and phenol. The A260/A280 ratio was used as an indicator of protein contamination and A260/A230 ratio as an indicator of other organic compounds. The acceptable ratios for purity vary according to the downstream application and typical requirement for A260/A280 and A260/A230 are 1.8-2.2 and above 1.7 (Glasel, 1995; Green & Sambrook, 2014). RNA extracted RVLM displayed A260/A230 value below 1.7 may be due to the low concentration of nucleic acid obtained. The A230 value is usually constant across sample extracted using the identical kit, yet the content of nucleic acid depended on the source of the sample, thus A260/A230 have been known to exhibit wider fluctuation.

The Agilent bioanalyzer is an efficient RNA quality assessment method as it only required a small amount of RNA sample (1-2 $\mu$ l) to be electrophoretically separated on a micro-fabricated chip and subsequently detected via laser induced fluorescence detection. Good quality of RNA should clearly display two distinct peaks, corresponding to the 18S and 28S of rRNA. The ribosomal ratios of 28S/18S were also estimated by bioanalyzer software where the decreased in this ratio is an indication of degradation of

the sample (Mueller et al., 2004). Imbeaud *et al.* (2005) have suggested the lack of reliability of the 28S/18S ratio to be used to assess the RNA integrity as the ratio evaluation were based on the area under the peak and therefore it heavily dependent on the start and end points of each run. Although samples with 28S/18S ratio around 2.0 were often of high quality, however it is shown that RNAs with ratio of above 1.0 could also be considered of good quality especially if no degradation can be observed in the electrophoretic trace (Imbeaud et al., 2005). Due to lack of reliability of the 28S/18S ratio, RIN number has thus become the powerful analysis tool used to assess the quality of the sample. The RIN numbers were determined by the software algorithm based on the shape of the entire electropherogram, thus it is a more reliable standard to determine the integrity of the RNA. Using the RIN number, the RNAs could be classified based on a numbering system from 1 to 10, where 1 being the most degraded and 10 being the most intact. Generally, RIN numbers higher than 8 indicated good quality of RNA in which worked well with most of the downstream experiments (Imbeaud et al., 2005). Based on the value of A260/A280, 28S/18S ratio and RIN number, all RNAs extracted were qualified for the downstream library preparation.

A high quality, non-biased, representative cDNA input library is required to generate a highly reliable HiSeq data and therefore a number of prescreening quality control tests was performed. In order to ensure that the cDNA are of proper distribution and fragment size and free from post-tagmentation and post-PCR contaminants i.e. tagging oligos and primers, prepared cDNA libraries were first assessed using Agilent Bioanalyzer. Based on the electropherograms of cDNA libraries, the absence of 18S and 28S peaks indicated the success in rRNA depletion while the absence of peaks from 100 to 150bp indicated that the respective libraries were free from any adaptor-dimer products. The concentrations of cDNAs in the libraries were quantified using qPCR in

which P5 and P7 primers were used in order to ensure specific amplification and quantification of fragments with proper adaptors at both ends as well as to mimic the amplification on the flow cell. MiSeq quality control run allowed the estimation of cluster density and efficiency of the pooled library in which adjustments could be done to maximize the yield of downstream HiSeq run.

To date, RNA-Seq, a direct sequencing of transcripts by high-throughput sequencing technologies, has become the most powerful tool for obtaining quantitative information in regards of the abundance of RNAs that are present in a specific tissue or cells (Korf, 2013). This study revealed the changes in expression levels of global genes in PVN, NTS and RVLM in response to orchidectomy and chronic testosterone treatment. The number of RNA-seq reads, mapped to a transcript, is directly proportional to that transcript's relative abundance in the sample (Trapnell et al., 2012). DESeq and edgeR statistical analyses were performed in this study however the selection of genes was based on fold changes and probability value generated by edgeR. Although both DESeq and edgeR statistical tools used raw read counts as input data, nonetheless edgeR introduces possible bias source in the model to perform an integrated normalization as well as a differential expression analysis using the negative binomial as the reference distribution (Robinson et al., 2010). In addition, edgeR provides more accurate detection of differential expressed gene with high specificity and sensitivity (Rajkumar et al., 2015).

Understanding the molecular mechanisms underlying gender-associated differences in central control on blood pressure requires examination of differential gene expression by using different approaches. The present study used the state-of-art RNA-Seq approaches to identify potential candidate genes that are differentially regulated by

testosterone in three pivotal areas of the brain. The transcriptome analysis of PVN, NTS and RVLM have resulted in a number of genes significantly changes in response to chronic testosterone treatment. Those genes that showed expression changes following chronic testosterone treatment in ovariectomized female rat were further supported by the changes observed in orchidectomized male rats, which represented the loss of testosterone effects. The outcomes of this study have greatly enriched our understanding of how testosterone leads to the changes in blood pressure in which a number of genes in PVN, NTS and RVLM were suggested to contribute to testosterone-induced differences in blood pressure regulation. Nonetheless, the expression levels of these genes are required to be assessed and further verified using qPCR (**Chapter 10**), the most reliable tool for gene expression studies(Regier & Frey, 2010).

## **CHAPTER 10: EFFECTS OF CHRONIC TESTOSTERONE TREATMENT ON SELECTED GENES EXPRESSION IN PVN, NTS AND RVLM**

### **10.1 Introduction**

The paraventricular nucleus (PVN) in the hypothalamus and the nucleus of the solitary tract (NTS) and rostral ventrolateral medulla (RVLM) in the brainstem have been known to play important roles in the central neural control of blood pressure (Martins-Pinge, 2011; Shell et al., 2016). The hypothalamic supraoptic nucleus (SON) and PVN magnocellular neurons (MCNs) mediate the neuroendocrine reflexes through their axons that terminate at the blood capillaries of the posterior pituitary (Bargmann, 1966), at which the biologically active arginine vasopressin (AVP) is stored until mobilized for secretion (Fitzsimmons et al., 1994). Intrinsic MCN osmoreceptor (Bourque et al., 2002; Zhang & Bourque, 2003) and specialized osmoreceptive neurons in the circumventricular organs (CVOs) that project to the MCNs detect a rise in plasma osmolality and provide direct excitatory inputs for AVP hormone secretion (Hu & Bourque, 1992; Nissen et al., 1994), that in turn causing water retention in kidneys. In addition, parvocellular neurons of PVN also regulate the sympathetic nervous activity, arterial pressure and blood volume via its descending projections to the brainstem, notably the RVLM, and the intermediolateral cell column of the spinal cord (Pyner, 2009; Shafton et al., 1998; Swanson et al., 1980). Meanwhile, baroreceptor activation, triggered by an increase in blood pressure, enhances NTS activity, which activates GABAergic caudal ventrolateral medulla (CVLM) neurons that inhibit RVLM activity (Calaresu & Yardley, 1988; Sun, 1995; Sun & Guyenet, 1985) and therefore mediate the reduction in the cardiovascular activity.

To date, high-throughput next generation sequencing technologies are widely applied in many biological researches. The advantage of RNA-Seq to quantify the whole transcriptomes in one run have led to the rapid growth of this application as the method of choice for gene expression studies. However, due to the high sequence production volume in parallel in a single run of these technologies (Metzker, 2010), higher chances of enormous information might be generated depending on the application used. Nonetheless, this problem can be overcome by performing a validation experiment using different biological replicated from the same population via real-time polymerase chain reaction (qPCR) (Fang & Cui, 2011). In the present study, based on the fold changes and significance values (*PValue*) generated through the RNA-Seq analysis (refer **Chapter 9**), a number of candidate genes of variety functions in PVN, NTS and RVLM were selected for further qPCR verification. The expression levels of these genes in their respective brain regions were accessed following orchidectomy in males and chronic testosterone treatment in ovariectomized female rats under both normotensive and hypertensive conditions. In addition, the protein expressions and distributions of two potential target genes in PVN were also assessed using double immunofluorescence staining.

## 10.2 Results

### 10.2.1 Verification of RNA-Seq analysis by qPCR

#### 10.2.1.1 Paraventricular nucleus (PVN)

In Figure 10.1, no significant differences in the levels of steady-state mRNA of three housekeeping genes *i.e.* *Rpl19*, *Gapdh* and *Actb* in PVN between different treatment groups indicated independent constant expression of these genes under different experimental conditions. Figure 10.2 showed the fold changes in mRNA expression levels of 25 genes that were suggested to be significantly and greatly increased by chronic testosterone treatment in ovariectomized female SHR rats, based on the previous transcriptome analysis of PVN. Of these 25 candidate genes, 18 genes (*Ogdh*, *Banf1*, *Heyl*, *Parm1*, *NOL6*, *Ddah1*, *Kcna3*, *Ephx2*, *Gpr17*, *Foxo1*, *Oxt* and *hnOxt*, *Adcy3*, *Htra1*, *Dusp3*, *Fkbp5*, *Wnk2*, *Hlf0* and *Spon1*) were shown by qPCR analysis to be significantly decreased by orchidectomy in male and increased by chronic testosterone treatment in ovariectomized female SHR rats. In addition, similar effects of testosterone treatment were observed in the expression levels of 13 genes (*Banf1*, *Heyl*, *Parm1*, *NOL6*, *Ddah1*, *Ephx2*, *Gpr17*, *Oxt* and *hnOxt*, *Adcy3*, *Htra1*, *Fkbp5*, *Wnk2* and *Spon1*) in PVN of normotensive WKY rat. In addition, a significant higher abundance of *Banf2* mRNA was observed in PVN of all normotensive WKY groups as compared to their corresponding hypertensive SHR groups ( $P < 0.001$ ). Meanwhile, *Ephx2* ( $P < 0.001$ ) and *Oxt* ( $P < 0.001$ ) as well as its pre-mature transcript, *hnOxt* ( $P < 0.001$ ) were highly expressed in PVN of hypertensive SHR when compared to normotensive WKY strain regardless of the treatments received. The gene expression fold changes obtained from the RNA-Seq (edgeR) and qPCR analysis were summarized in Table 10.1.

Figure 10.2 showed the changes in mRNA expression levels of 14 genes in PVN, identified via RNA-Seq analysis in which their expression levels were significantly and strongly decreased following chronic testosterone treatment in ovariectomized female SHR rats. Of these 14 candidate genes, significant changes in expression levels of 4 genes (*Fcrl2*, *Top2a*, *Mx1* and *ApoE*) in PVN of hypertensive SHR rats were identified via qPCR analysis, in which orchidectomy in male rats caused elevation while chronic testosterone treatment in ovariectomized female rats resulted in a reduction. In normotensive WKY rats, 2 genes (*Fcrl1* and *Mx1*) were found to be significantly changes in their expression levels in PVN following orchidectomy and chronic testosterone treatment. In overall, higher expression level of *Fcrl2* was observed in PVN of all normotensive WKY groups as compared to their corresponding hypertensive group ( $P < 0.01$  for sham-operated male;  $P < 0.05$  for orchidectomized male, non-treated ovariectomized female and testosterone-treated ovariectomized female rats). Table 10.1 shows the summary comparison of gene expression fold changes generated by RNA-Seq (edgeR) and qPCR analysis.

Based on the transcriptome analysis of PVN, *Avp* was not significantly affected by orchidectomy in male rat (SMO compare to SMS) and chronic testosterone treatment in ovariectomized female SHR rats (SFT compare to SFO). However, in Figure 10.4, orchidectomy in male rats significantly decreased ( $P < 0.01$ ) while chronic testosterone treatment in ovariectomized female rats significantly increased ( $P < 0.05$ ) the expression levels of mature AVP transcript in PVN of hypertensive SHR rats. In addition, a reduced in the expression levels of pre-mature AVP transcripts following orchidectomy in male normotensive WKY ( $P < 0.05$ ) and hypertensive SHR ( $P < 0.01$ ) were observed. Meanwhile, chronic treatment of ovariectomized female normotensive WKY and hypertensive SHR rats with testosterone increased the expression levels of pre-mature

AVP transcripts in PVN ( $P < 0.01$ ). Of sham-operated male and testosterone-treated ovariectomized female rats, higher abundance of mature and pre-mature AVP transcripts were noted in hypertensive SHR strain as compared to the corresponding normotensive WKY group.

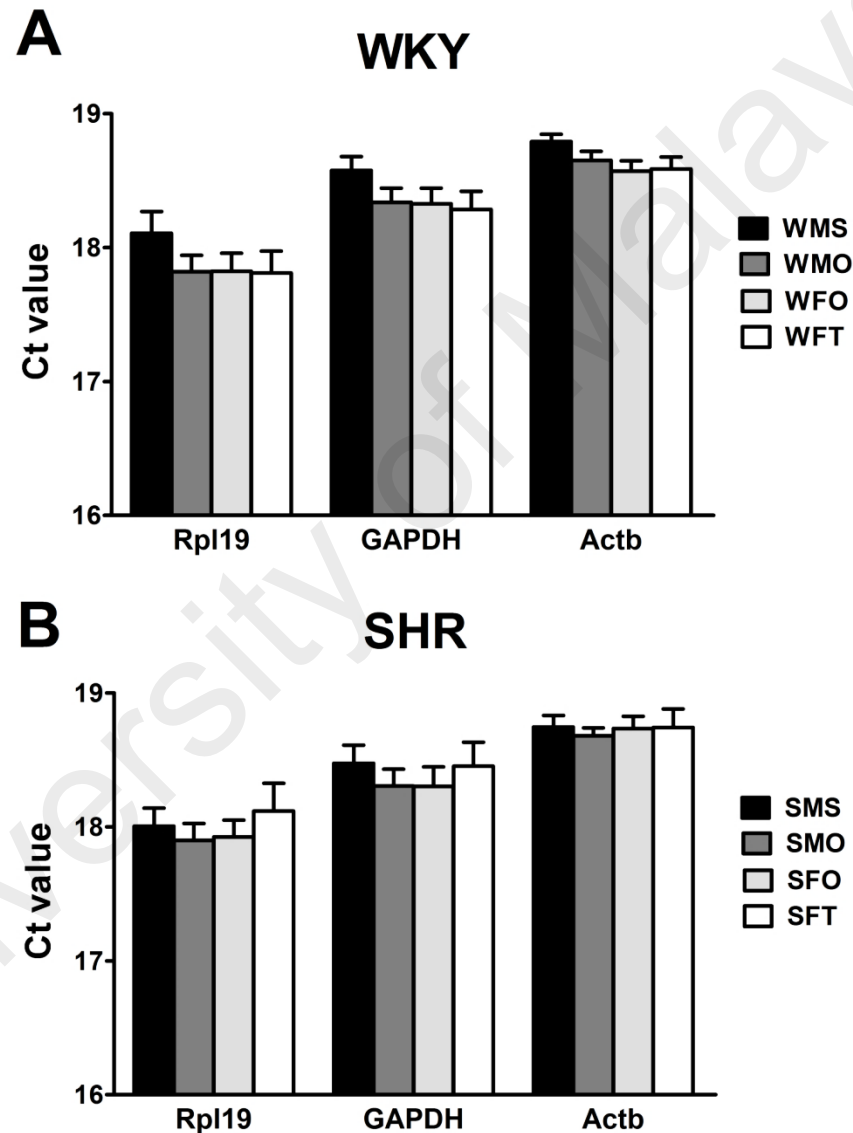


**Figure 10.1 Selection of reference gene with constant expression in PVN.**

Steady state mRNA levels of three housekeeping genes *i.e.* *Rpl19*, *Gapdh* and *Actb* in PVN of (A) WKY and (B) SHR rats were quantified using qPCR. Data are presented in mean  $\pm$  SEM ( $n = 6$ /group, unpaired student's *t*-test). Abbreviations: WMS: WKY sham-operated intact male; WMO: WKY orchidectomized male; WFO: WKY ovariectomized female; WFT: WKY testosterone-treated ovariectomized female; SHR sham-operated intact male; SMO: SHR orchidectomized male; SFO: SHR ovariectomized female; SFT: SHR testosterone-treated ovariectomized female rats.

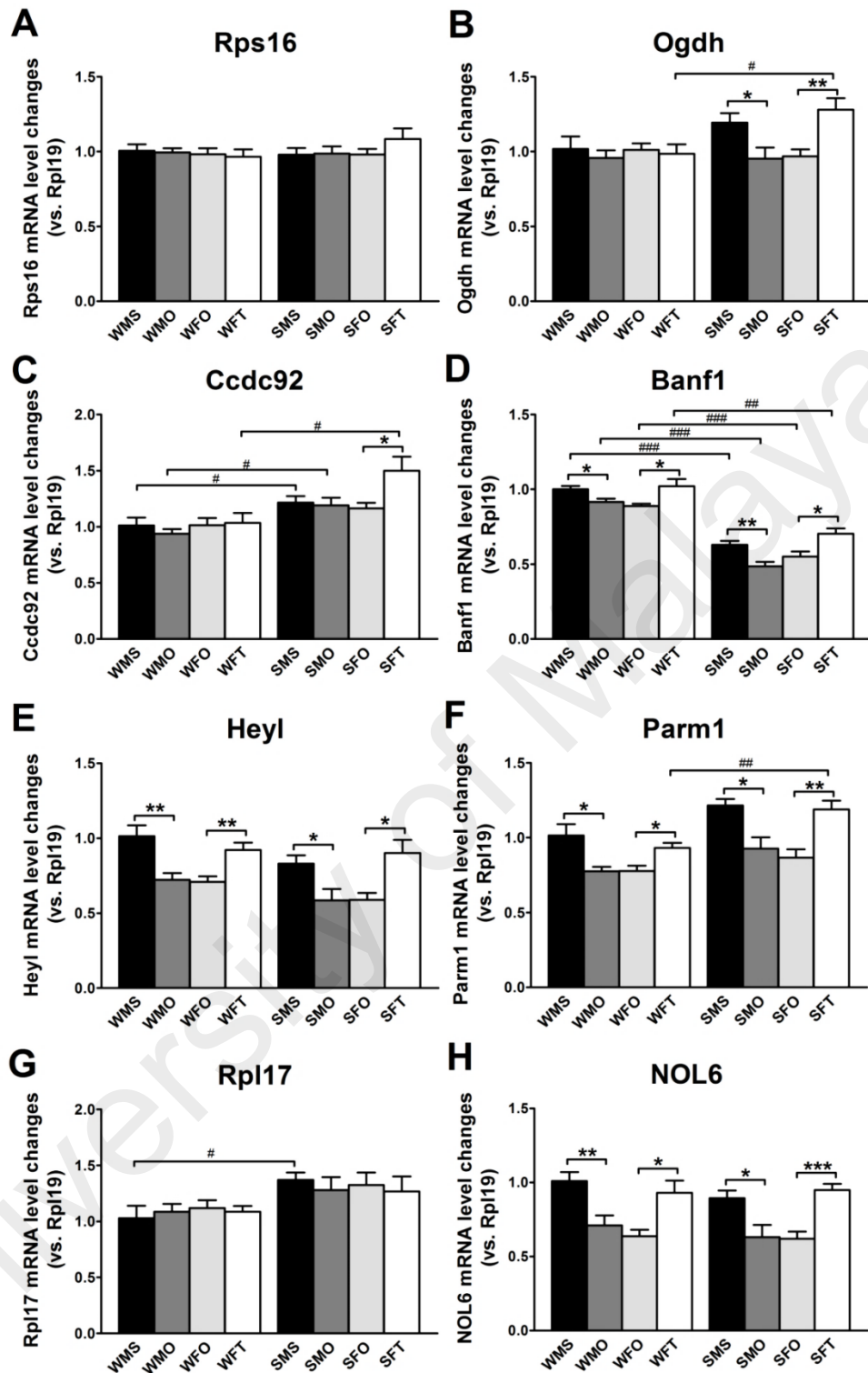


**Figure 10.2** qPCR determinations of up-regulated genes by chronic testosterone treatment based on the transcriptome analysis of PVN.

Fold changes in mRNA expression levels of (A) *Rps16*, (B) *Ogdh*, (C) *Ccdc92*, (D) *Banf1*, (E) *Heyl*, (F) *Parm1*, (G) *Rpl17* and (H) *NOL6* in PVN were quantified using qPCR. Data are presented in mean  $\pm$  SEM (n = 6/group, unpaired student's *t*-test); \* $P$ <0.05, \*\* $P$ <0.01, \*\*\* $P$ <0.001 compared to control group *i.e.* WMS, WFO, SMS and SFO; # $P$ <0.05, ## $P$ <0.01, ### $P$ <0.001 compared to normotensive WKY group. Abbreviations: WMS: WKY sham-operated intact male; WMO: WKY orchidectomized male; WFO: WKY ovariectomized female; WFT: WKY testosterone-treated ovariectomized female; SHR sham-operated intact male; SMO: SHR orchidectomized male; SFO: SHR ovariectomized female; SFT: SHR testosterone-treated ovariectomized female rats.

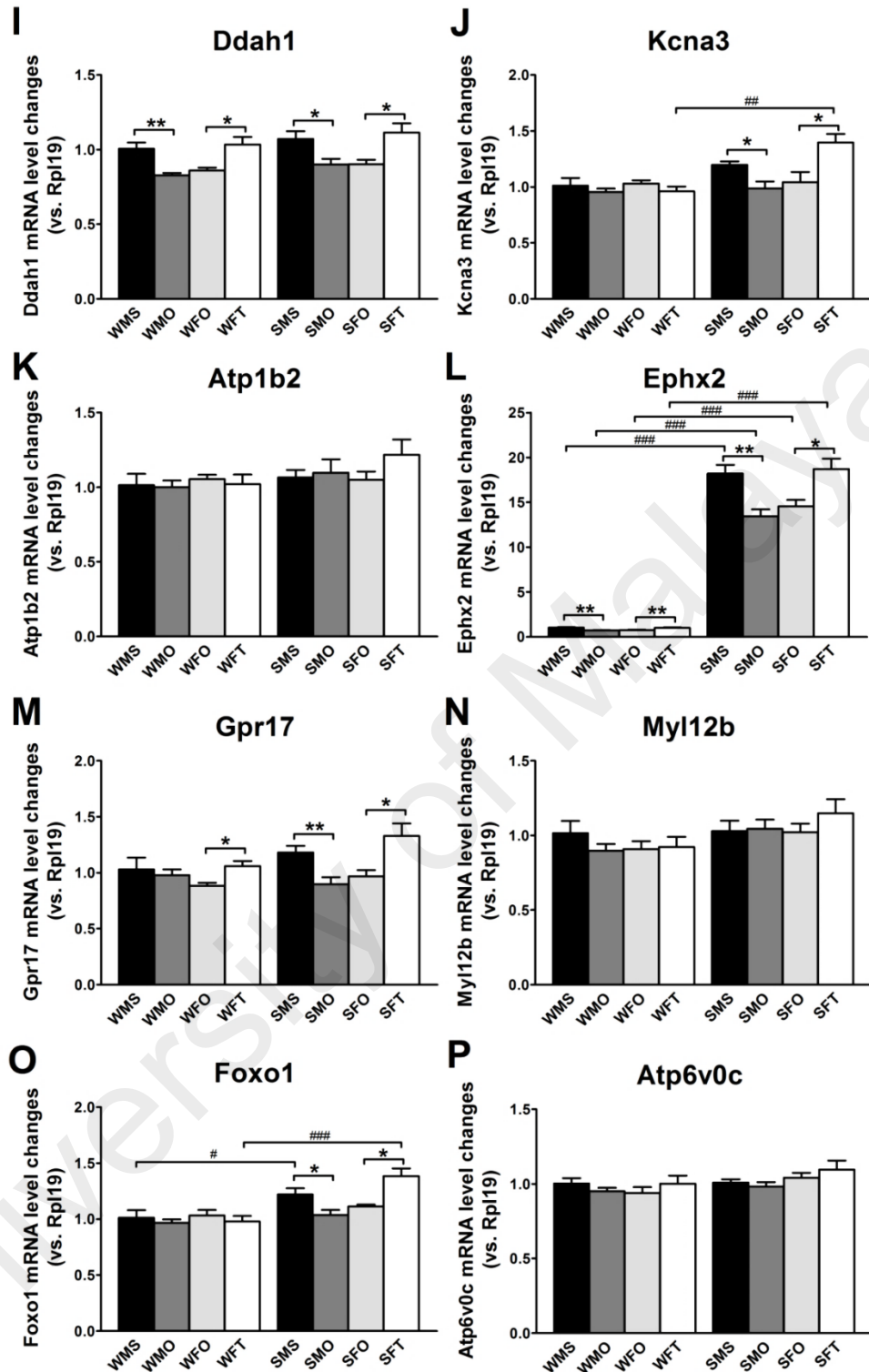


**Figure 10.2 continued.**

Fold changes in mRNA expression levels of **(I) *Ddah1***, **(J) *Kcna3***, **(K) *Atp1b2***, **(L) *Ephx2***, **(M) *Gpr17***, **(N) *Myl12b***, **(O) *Foxo1*** and **(P) *Atp6v0c*** in PVN were quantified using qPCR. Data are presented in mean  $\pm$  SEM ( $n = 6/\text{group}$ , unpaired student's  $t$ -test); \* $P < 0.05$ , \*\* $P < 0.01$ , \*\*\* $P < 0.001$  compared to control group *i.e.* WMS, WFO, SMS and SFO; # $P < 0.05$ , ## $P < 0.01$ , ### $P < 0.001$  compared to normotensive WKY group. Abbreviations: WMS: WKY sham-operated intact male; WMO: WKY orchidectomized male; WFO: WKY ovariectomized female; WFT: WKY testosterone-treated ovariectomized female; SHR sham-operated intact male; SMO: SHR orchidectomized male; SFO: SHR ovariectomized female; SFT: SHR testosterone-treated ovariectomized female rats.

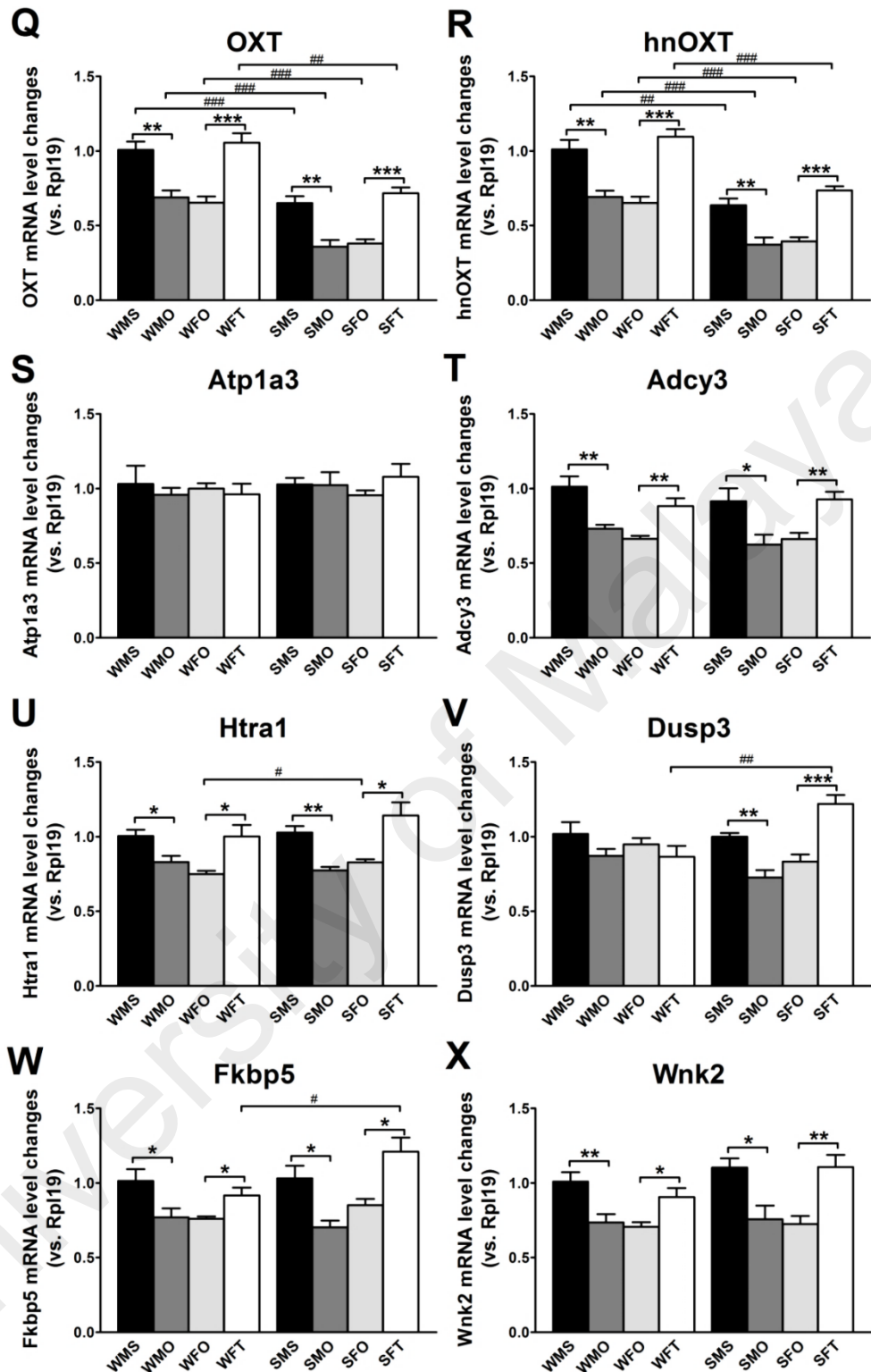


**Figure 10.2 continued.**

Fold changes in mRNA expression levels of (Q) *Oxt*, (R) *hnOxt*, (S) *Atp1a3*, (T) *Adcy3*, (U) *Htra1*, (V) *Dusp3*, (W) *Fkbp5*, (X) *Wnk2* in PVN were quantified using qPCR. Data are presented in mean  $\pm$  SEM (n = 6/group, unpaired student's *t*-test); \* $P$ <0.05, \*\* $P$ <0.01, \*\*\* $P$ <0.001 compared to control group *i.e.* WMS, WFO, SMS and SFO; # $P$ <0.05, ### $P$ <0.01, ### $P$ <0.001 compared to normotensive WKY group. Abbreviations: WMS: WKY sham-operated intact male; WMO: WKY orchidectomized male; WFO: WKY ovariectomized female; WFT: WKY testosterone-treated ovariectomized female; SHR sham-operated intact male; SMO: SHR orchidectomized male; SFO: SHR ovariectomized female; SFT: SHR testosterone-treated ovariectomized female rats.

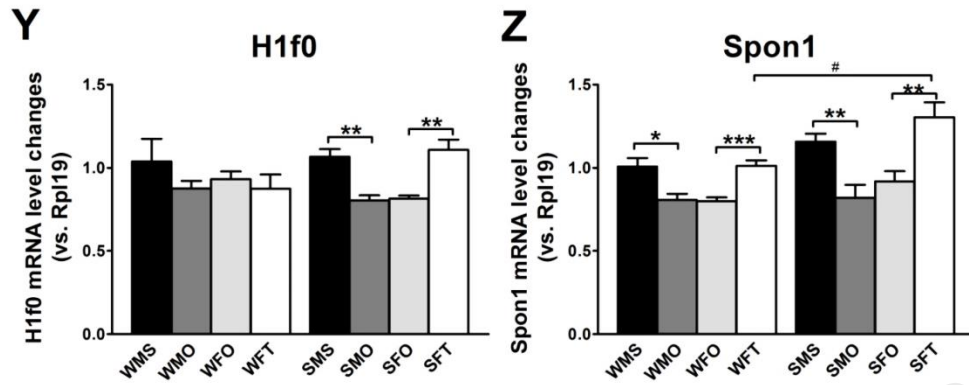


**Figure 10.2 continued.**

Fold changes in mRNA expression levels of (Y) *H1f0* and (Z) *Spon1* in PVN were quantified using qPCR. Data are presented in mean  $\pm$  SEM ( $n = 6/\text{group}$ , unpaired student's *t*-test); \* $P < 0.05$ , \*\* $P < 0.01$ , \*\*\* $P < 0.001$  compared to control group i.e. WMS, WFO, SMS and SFO; # $P < 0.05$ , ## $P < 0.01$ , ### $P < 0.001$  compared to normotensive WKY strain. Abbreviations: WMS: WKY sham-operated intact male; WMO: WKY orchidectomized male; WFO: WKY ovariectomized female; WFT: WKY testosterone-treated ovariectomized female; SHR sham-operated intact male; SMO: SHR orchidectomized male; SFO: SHR ovariectomized female; SFT: SHR testosterone-treated ovariectomized female rats.

**Table 10.1 Summary of fold changes, both from edgeR analysis of RNA-Seq data and qPCR analysis, of genes up-regulated by chronic testosterone treatment based on the transcriptome analysis of PVN.**

No.	Gene name	qPCR						Transcriptome		qPCR					
		WMO compare to WMS			WFT compare to WFO			SMO compare to SMS	SFT compare to SFO	SMO compare to SMS			SFT compare to SFO		
		WMS	WMO	<i>P</i>	WFO	WFT	<i>P</i>			SMS	SMO	<i>P</i>	SFO	SFT	<i>P</i>
1	<b>Rps16</b>	1.00	0.99		0.98	0.97		<b>0.08</b>	<b>3.31</b>	0.98	0.99		0.98	1.08	
2	<b>Ogdh</b>	1.02	0.96		1.01	0.99		<b>0.11</b>	<b>2.44</b>	1.19	<b>0.95</b>	*	0.97	<b>1.28</b>	**
3	<b>Ccdc92</b>	1.01	0.94		1.01	1.03		<b>0.11</b>	<b>2.27</b>	1.22	1.19		1.16	<b>1.50</b>	*
4	<b>Banf1</b>	1.00	<b>0.91</b>	*	0.89	<b>1.02</b>	*	<b>0.24</b>	<b>2.04</b>	0.63	<b>0.49</b>	**	0.55	<b>0.70</b>	*
5	<b>Heyl</b>	1.01	<b>0.72</b>	**	0.71	<b>0.92</b>	**	<b>0.17</b>	<b>2.03</b>	0.83	<b>0.59</b>	*	0.59	<b>0.90</b>	*
6	<b>Parm1</b>	1.01	<b>0.78</b>	*	0.78	<b>0.93</b>	*	<b>0.07</b>	<b>1.96</b>	1.22	<b>0.93</b>	*	0.87	<b>1.19</b>	**
7	<b>Rpl17</b>	1.03	1.09		1.12	1.08		<b>0.43</b>	<b>1.93</b>	1.37	1.28		1.32	1.27	
8	<b>NOL6</b>	1.01	<b>0.71</b>	**	0.64	<b>0.93</b>	*	<b>0.19</b>	<b>1.92</b>	0.89	<b>0.63</b>	*	0.62	<b>0.95</b>	***
9	<b>Ddah1</b>	1.00	<b>0.83</b>	**	0.86	<b>1.03</b>	*	<b>0.17</b>	<b>1.82</b>	1.07	<b>0.90</b>	*	0.90	<b>1.11</b>	*
10	<b>Kcna3</b>	1.01	0.95		1.03	0.96		<b>0.33</b>	<b>1.81</b>	1.20	<b>0.99</b>	*	1.04	<b>1.40</b>	*
11	<b>Atp1b2</b>	1.01	1.00		1.05	1.02		<b>0.22</b>	<b>1.70</b>	1.06	1.10		1.05	1.22	
12	<b>Ephx2</b>	1.01	<b>0.72</b>	**	0.73	<b>1.00</b>	**	<b>0.20</b>	<b>1.63</b>	18.20	<b>13.42</b>	**	14.56	<b>18.73</b>	*
13	<b>Gpr17</b>	1.03	0.96		0.87	<b>1.04</b>	*	<b>0.51</b>	<b>1.61</b>	1.18	<b>0.90</b>	**	0.97	<b>1.33</b>	*

Mean fold changes estimated from edgeR analysis of RNA-Seq data (Transcriptome) and qPCR analysis (n = 6/group, unpaired student's *t*-test where \**P*<0.05, \*\**P*<0.01, \*\*\**P*<0.001 compared to control group *i.e.* WMS, WFO, SMS and SFO) are presented in the table. Genes are listed based on the levels of expression changes (estimated by edgeR), from highest (top) to lowest (bottom) increase, following chronic testosterone treatment in ovariectomized female SHR rats (SFT compare to SFO). Green values represent significant up-regulation while red values represent significant down-regulation of mRNA levels. Abbreviations: *P*: probability value; WMS: WKY sham-operated intact male; WMO: WKY orchidectomized male; WFO: WKY ovariectomized female; WFT: WKY testosterone-treated ovariectomized female; SHR sham-operated intact male; SMO: SHR orchidectomized male; SFO: SHR ovariectomized female; SFT: SHR testosterone-treated ovariectomized female rats

Table 10.1 continued.

No.	Gene name	qPCR						Transcriptome		qPCR					
		WMO compare to WMS			WFT compare to WFO			SMO compare to SMS	SFT compare to SFO	SMO compare to SMS			SFT compare to SFO		
		WMS	WMO	P	WFO	WFT	P			SMS	SMO	P	SFO	SFT	P
14	<b>Myl12b</b>	1.01	0.90		0.91	0.92		<b>0.26</b>	<b>1.61</b>	1.03	1.04		1.02	1.15	
15	<b>Foxo1</b>	1.01	0.97		1.03	0.98		<b>0.25</b>	<b>1.58</b>	1.22	<b>1.04</b>	*	1.11	<b>1.38</b>	*
16	<b>Atp6v0c</b>	1.00	0.95		0.94	1.00		<b>0.27</b>	<b>1.53</b>	1.01	0.98		1.04	1.10	
17	<b>Oxt</b>	1.01	<b>0.69</b>	**	0.65	<b>1.05</b>	***	<b>0.70</b>	<b>1.51</b>	0.65	<b>0.36</b>	**	0.38	<b>0.72</b>	***
	<b>hnOXT</b>	1.01	<b>0.69</b>	**	0.65	<b>1.09</b>	***			0.64	<b>0.37</b>	**	0.39	<b>0.73</b>	***
18	<b>Atp1a3</b>	1.03	0.96		1.00	0.96		<b>0.27</b>	<b>1.48</b>	1.03	1.02		0.95	1.08	
19	<b>Adcy3</b>	1.01	<b>0.73</b>	**	0.66	<b>0.88</b>	**	<b>0.34</b>	<b>1.47</b>	0.92	<b>0.62</b>	*	0.66	<b>0.93</b>	**
20	<b>Htra1</b>	1.00	<b>0.83</b>	*	0.75	<b>1.00</b>	*	<b>0.40</b>	<b>1.46</b>	1.03	<b>0.77</b>	**	0.83	<b>1.14</b>	*
21	<b>Dusp3</b>	1.02	0.87		0.95	0.87		<b>0.61</b>	<b>1.33</b>	1.00	<b>0.73</b>	**	0.83	<b>1.22</b>	***
22	<b>Fkbp5</b>	1.01	<b>0.77</b>	*	0.76	<b>0.92</b>	*	<b>0.71</b>	<b>1.32</b>	1.03	<b>0.70</b>	*	0.85	<b>1.21</b>	*
23	<b>Wnk2</b>	1.01	<b>0.74</b>	**	0.71	<b>0.90</b>	*	<b>0.32</b>	<b>1.31</b>	1.10	<b>0.76</b>	*	0.72	<b>1.11</b>	**
24	<b>H1f0</b>	1.04	0.88		0.93	0.87		<b>0.58</b>	<b>1.17</b>	1.06	<b>0.80</b>	**	0.81	<b>1.11</b>	**
25	<b>Spon1</b>	1.01	<b>0.81</b>	*	0.80	<b>1.01</b>	***	<b>0.69</b>	<b>1.15</b>	1.16	<b>0.82</b>	**	0.92	<b>1.30</b>	**

Mean fold changes estimated from edgeR analysis of RNA-Seq data (Transcriptome) and qPCR analysis (n = 6/group, unpaired student's *t*-test where \**P*<0.05, \*\**P*<0.01, \*\*\**P*<0.001 compared to control group *i.e.* WMS, WFO, SMS and SFO) are presented in the table. Genes are listed based on the levels of expression changes (estimated by edgeR), from highest (top) to lowest (bottom) increase, following chronic testosterone treatment in ovariectomized female SHR rats (SFT compare to SFO). Green values represent significant up-regulation while red values represent significant down-regulation of mRNA levels. Abbreviations: *P*: probability value; WMS: WKY sham-operated intact male; WMO: WKY orchidectomized male; WFO: WKY ovariectomized female; WFT: WKY testosterone-treated ovariectomized female; SHR sham-operated intact male; SMO: SHR orchidectomized male; SFO: SHR ovariectomized female; SFT: SHR testosterone-treated ovariectomized female rats.

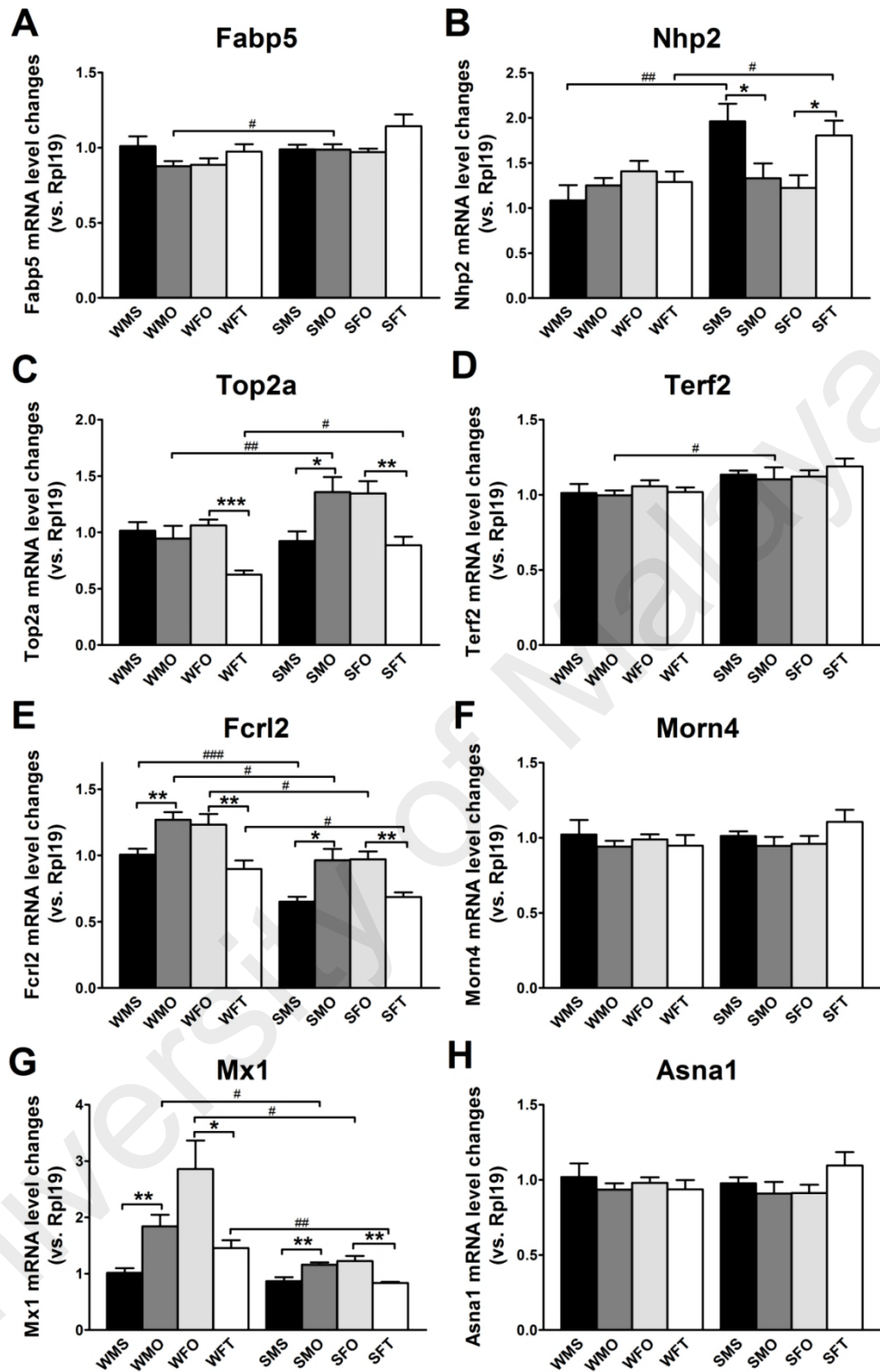


**Figure 10.3** qPCR determinations of genes down-regulated by chronic testosterone treatment based on transcriptome analysis of PVN.

Fold changes in mRNA expression levels of (A) *Fabp5*, (B) *Nhp2*, (C) *Top2a*, (D) *Terf2*, (E) *Fcrl2*, (F) *Morn4*, (G) *Mx1* and (H) *Asna1* in PVN were quantified using qPCR. Data are presented in mean  $\pm$  SEM (n = 6/group, unpaired student's *t*-test); \* $P$ <0.05, \*\* $P$ <0.01, \*\*\* $P$ <0.001 compared to control group *i.e.* WMS, WFO, SMS and SFO; # $P$ <0.05, ### $P$ <0.01, ### $P$ <0.001 compared to normotensive WKY group. Abbreviations: WMS: WKY sham-operated intact male; WMO: WKY orchidectomized male; WFO: WKY ovariectomized female; WFT: WKY testosterone-treated ovariectomized female; SHR sham-operated intact male; SMO: SHR orchidectomized male; SFO: SHR ovariectomized female; SFT: SHR testosterone-treated ovariectomized female rats.

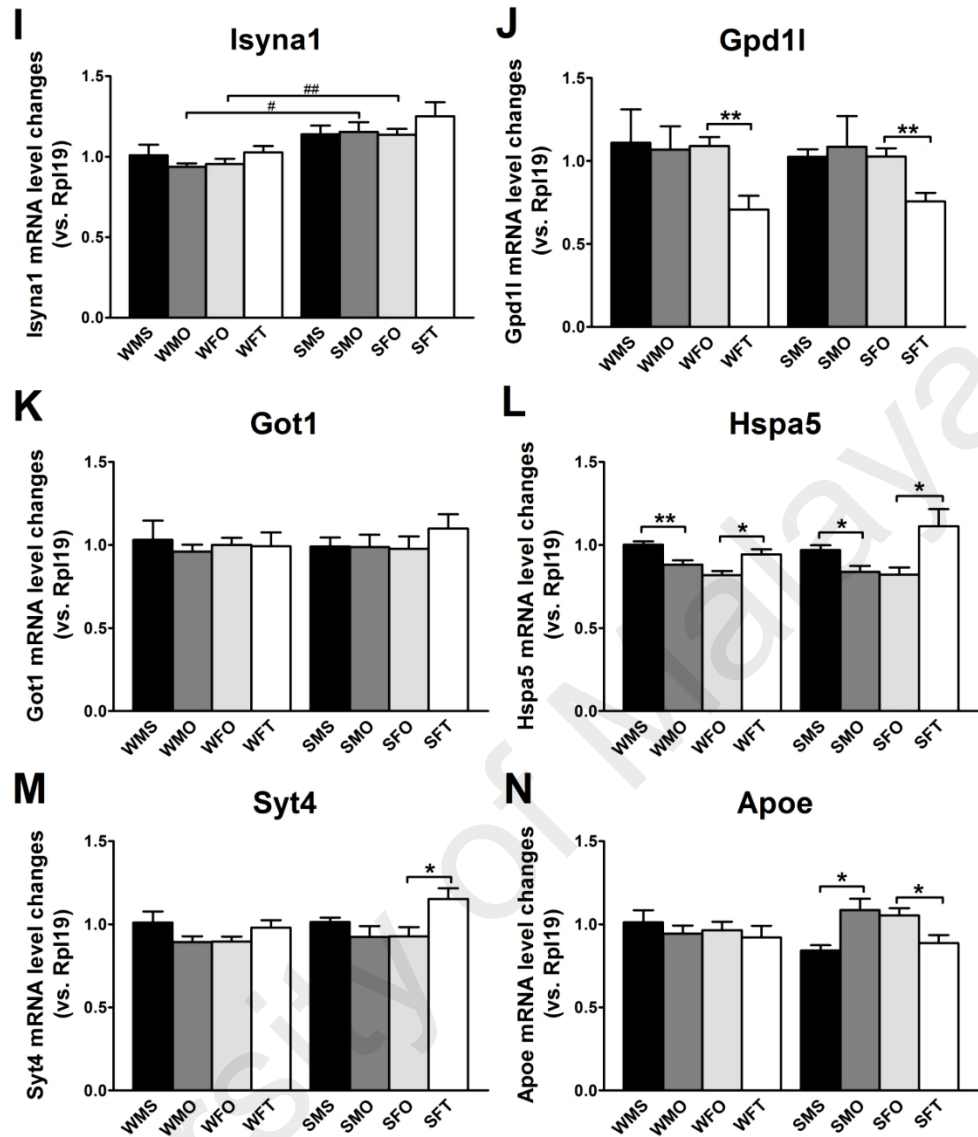


**Figure 10.3 continued.**

Fold changes in mRNA expression levels of (I) *Isyna1*, (J) *Gpd1l*, (K) *Got1*, (L) *Hspa5*, (M) *Syt4* and (N) *Apoe* in PVN were quantified using qPCR. Data are presented in mean  $\pm$  SEM (n = 6/group, unpaired student's *t*-test); \* $P$ <0.05, \*\* $P$ <0.01, \*\*\* $P$ <0.001 compared to control group i.e. WMS, WFO, SMS and SFO; # $P$ <0.05, ## $P$ <0.01, ### $P$ <0.001 compared to normotensive WKY group. Abbreviations: WMS: WKY sham-operated intact male; WMO: WKY orchidectomized male; WFO: WKY ovariectomized female; WFT: WKY testosterone-treated ovariectomized female; SHR sham-operated intact male; SMO: SHR orchidectomized male; SFO: SHR ovariectomized female; SFT: SHR testosterone-treated ovariectomized female rats.

**Table 10.2 Summary of fold changes, both from edgeR analysis of RNA-Seq data and qPCR analysis, of genes down-regulated by chronic testosterone treatment based on the transcriptome analysis of PVN.**

No.	Gene name	qPCR						Transcriptome		qPCR					
		WMO compare to WMS			WFT compare to WFO			SMO compare to SMS	SFT compare to SFO	SMO compare to SMS			SFT compare to SFO		
		WMS	WMO	<i>P</i>	WFO	WFT	<i>P</i>			SMS	SMO	<i>P</i>	SFO	SFT	<i>P</i>
1	<b>Fabp5</b>	1.01	0.88		0.89	0.97		<b>2.79</b>	<b>0.59</b>	0.99	0.99		0.97	1.14	
2	<b>Nhp2</b>	1.08	1.25		1.41	1.29		<b>1.22</b>	<b>0.68</b>	1.96	<b>1.33</b>	*	1.22	<b>1.80</b>	*
3	<b>Top2a</b>	1.01	0.94		1.06	<b>0.62</b>	**	<b>1.52</b>	<b>0.68</b>	0.92	<b>1.36</b>	*	1.34	<b>0.89</b>	**
4	<b>Terf2</b>	1.01	1.00		1.06	1.02		<b>1.72</b>	<b>0.69</b>	1.13	1.10		1.12	1.19	
5	<b>Fcrl2</b>	1.00	<b>1.27</b>	**	1.23	<b>0.90</b>	**	<b>1.96</b>	<b>0.72</b>	0.65	<b>0.96</b>	*	0.97	<b>0.69</b>	**
6	<b>Morn4</b>	1.02	0.94		0.99	0.95		<b>2.37</b>	<b>0.72</b>	1.01	0.95		0.96	1.11	
7	<b>Mx1</b>	1.02	<b>1.84</b>	**	2.86	<b>1.45</b>	*	<b>1.69</b>	<b>0.73</b>	0.87	<b>1.16</b>	*	1.22	<b>0.83</b>	**
8	<b>Asna1</b>	1.02	0.93		0.98	0.94		<b>1.74</b>	<b>0.76</b>	0.98	0.91		0.91	1.09	
9	<b>Isyna1</b>	1.01	0.94		0.96	1.03		<b>2.02</b>	<b>0.77</b>	1.14	1.15		1.14	1.25	
10	<b>Gpd1l</b>	1.11	1.07		1.09	<b>0.71</b>	**	<b>1.95</b>	<b>0.81</b>	1.02	1.09		1.03	<b>0.76</b>	**
11	<b>Got1</b>	1.03	0.96		1.00	0.99		<b>1.55</b>	<b>0.83</b>	0.99	0.99		0.98	1.10	
12	<b>Hspa5</b>	1.00	<b>0.88</b>	**	0.82	<b>0.94</b>	*	<b>1.22</b>	<b>0.84</b>	0.97	<b>0.84</b>	*	0.82	<b>1.11</b>	*
13	<b>Syt4</b>	1.01	0.89		0.89	0.98		<b>1.84</b>	<b>0.85</b>	1.01	0.92		0.93	<b>1.15</b>	*
14	<b>Apoe</b>	1.01	0.94		0.96	0.92		<b>1.26</b>	<b>0.86</b>	0.84	<b>1.09</b>	*	1.05	<b>0.89</b>	*

Mean fold changes estimated from edgeR analysis of RNA-Seq data (Transcriptome) and qPCR analysis (n = 6/group, unpaired student's *t*-test where \**P*<0.05, \*\**P*<0.01, \*\*\**P*<0.001 compared to control group *i.e.* WMS, WFO, SMS and SFO) are presented in the table. Genes are listed based on the levels of expression changes (estimated by edgeR), from highest (top) to lowest (bottom) decrease, following chronic testosterone treatment in ovariectomized female SHR rats (SFT compare to SFO). Green values represent significant up-regulation while red values represent significant down-regulation of mRNA levels. Abbreviations: *P*: probability value; WMS: WKY sham-operated intact male; WMO: WKY orchidectomized male; WFO: WKY ovariectomized female; WFT: WKY testosterone-treated ovariectomized female; SHR sham-operated intact male; SMO: SHR orchidectomized male; SFO: SHR ovariectomized female; SFT: SHR testosterone-treated ovariectomized female rats.

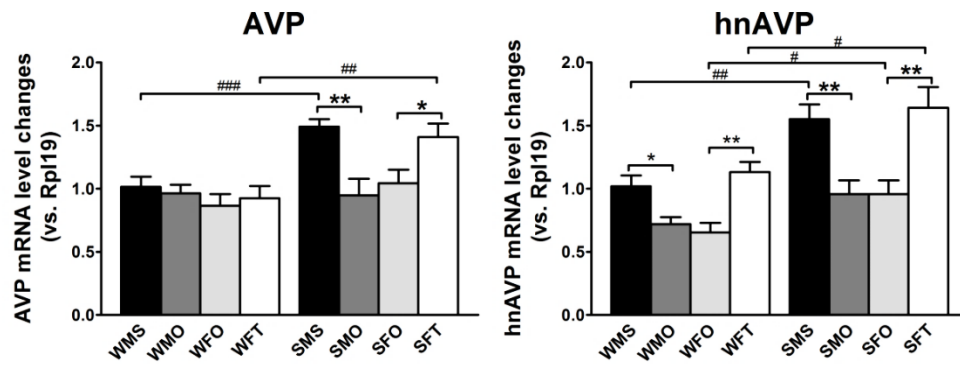


**Figure 10.4 Effects of chronic testosterone treatment on mRNA expression levels of arginine vasopressin (AVP) in PVN.**

Fold changes in expression levels of mature *AVP* and pre-mature *hnAVP* transcripts in PVN were quantified using qPCR. Data are presented in mean  $\pm$  SEM ( $n = 6/\text{group}$ , unpaired student's *t*-test); \* $P < 0.05$ , \*\* $P < 0.01$  compared to control groups *i.e.* WMS, WFO, SMS and SFO; # $P < 0.05$ , ## $P < 0.01$ , ### $P < 0.001$  compared to normotensive WKY group. Abbreviations: WMS: WKY sham-operated intact male; WMO: WKY orchidectomized male; WFO: WKY ovariectomized female; WFT: WKY testosterone-treated ovariectomized female; SHR sham-operated intact male; SMO: SHR orchidectomized male; SFO: SHR ovariectomized female; SFT: SHR testosterone-treated ovariectomized female rats.

University of Medicine and Health Sciences

### 10.2.1.2 Nucleus of Solitary tract (NTS)

In both normotensive WKY and hypertensive SHR rats, constant expressions of three housekeeping genes *i.e.* *Rpl19*, *Gapdh* and *Actb* were observed in NTS across different treatment groups (Figure 10.5), indicating independent expression of these genes in NTS regardless of the experimental conditions. Based on the NTS transcriptome analysis, 19 candidate genes that were significantly and strongly up-regulated by chronic testosterone treatment in ovariectomized female SHR rats were selected for verification via qPCR (Figure 10.6). Except for *Slc6a20*, qPCR analysis identified significant changes in expression levels of all others 18 genes (*Sgk1*, *Prlh*, *Pnpla2*, *Mpzl2*, *Gpd1*, *Glra4*, *Car14*, *Crlf1*, *Igfbp5*, *Olfml3*, *Wfdc1*, *Pnoc*, *Sult1a1*, *Tcn2*, *Gpr88*, *Heph*, *Hlf0* and *Gpr64*) in NTS of hypertensive SHR rats. As compared to sham-operated intact male SHR rat, a significantly lower expression level of these genes in orchidectomized male SHR rat was observed. In ovariectomized SHR female rats, chronic testosterone treatment significantly increased the expression levels of these genes in NTS. Of these 18 genes, the expression levels of 15 genes (*Sgk1*, *Prlh*, *Mpzl2*, *Gpd1*, *Glra4*, *Car14*, *Crlf1*, *Igfbp5*, *Olfml3*, *Wfdc1*, *Sult1a1*, *Tcn2*, *Gpr88*, *Heph* and *Hlf0*) changed in a similar pattern in NTS of normotensive WKY rats in which higher abundance of *Prlh* ( $P < 0.01$  for sham-operated male;  $P < 0.05$  for orchidectomized male, ovariectomized female and testosterone-treated ovariectomized female rats) and *Car14* ( $P < 0.01$  for sham-operated male, orchidectomized male and testosterone-treated ovariectomized female;  $P < 0.001$  for ovariectomized female rats). were observed as compared to the corresponding hypertensive group. A significant higher expression level of *Sgk1* in NTS of hypertensive SHR rats than normotensive WKY rats was also noted ( $P < 0.05$ ). Table 10.3, showing the expression fold changes of 19 candidate genes in NTS, summarized and compared the data from RNA-Seq and qPCR.

In Figure 10.7, the expression levels of steady-state mRNA of another 19 candidate genes were assessed by qPCR. These genes were suggested to be down-regulated by testosterone was selected based on RNA-Seq analysis that showed their expression levels in NTS to be markedly decreased by chronic testosterone treatment in ovariectomized female SHR rats. Based on the qPCR data, of these 19 genes, 11 genes (*Fcrl2*, *Hspa1b*, *Cdh1*, *Car3*, *Mpeg1*, *Myh7*, *Tnfsf13*, *Gfap*, *Apoe*, *Cd4* and *Cml3*) showed significant changes in their expression levels in NTS of hypertensive SHR rats. Orchidectomy caused an increased in the expression levels of these genes in NTS of male SHR rats while chronic testosterone treatment resulted in reductions in these gene expressions. In normotensive WKY rats, this similar pattern of expression changes was observed in 3 genes (*Fcrl2*, *Cdh1* and *Car3*) following orchidectomy in males and chronic testosterone treatment in ovariectomized females. Opposite effects were shown in the expression level of *Hspa5* in NTS of normotensive WKY rats in which orchidectomy in male rats caused a marked reduction ( $P<0.05$ ) while in ovariectomized females, chronic testosterone treatment induced the expression of this gene to a significant level ( $P<0.01$ ). As compared to the corresponding hypertensive group, *Fcrl2* ( $P<0.01$  for sham-operated male;  $P<0.05$  for orchidectomized male, ovariectomized female and testosterone-treated ovariectomized female rats) and *Mpeg1* ( $P<0.01$  for sham-operated male, orchidectomized male and testosterone-treated ovariectomized female;  $P<0.05$  for ovariectomized female rat) were more highly expressed in NTS of normotensive WKY. Nonetheless, higher abundance of *Cd4* ( $P<0.001$ ) and *Ramp3* ( $P<0.05$  for sham-operated male, ovariectomized female and testosterone-treated ovariectomized female;  $P<0.001$  for orchidectomized male rats) was observed in hypertensive SHR when compared to their corresponding normotensive group. Table 10.4 summarized the changes in gene expression levels, obtained from the transcriptome analysis as well as qPCR verification.

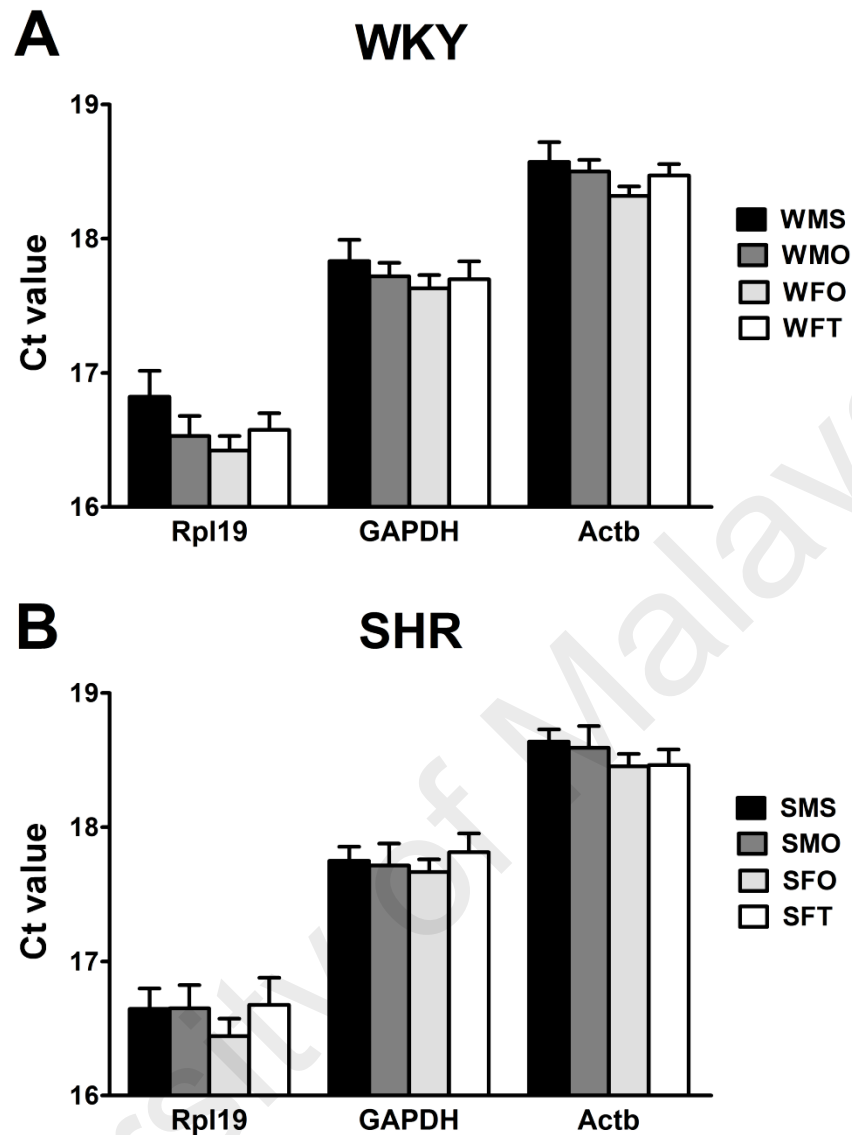


**Figure 10.5 Selection of reference gene with constant expression in NTS.**

Steady state mRNA levels of three housekeeping genes *i.e.* *Rpl19*, *Gapdh* and *Actb* in NTS of (A) WKY and (B) SHR rats were quantified using qPCR. Data are presented in mean  $\pm$  SEM ( $n = 6/\text{group}$ , unpaired student's *t*-test). Abbreviations: WMS: WKY sham-operated intact male; WMO: WKY orchidectomized male; WFO: WKY ovariectomized female; WFT: WKY testosterone-treated ovariectomized female; SHR sham-operated intact male; SMO: SHR orchidectomized male; SFO: SHR ovariectomized female; SFT: SHR testosterone-treated ovariectomized female rats.

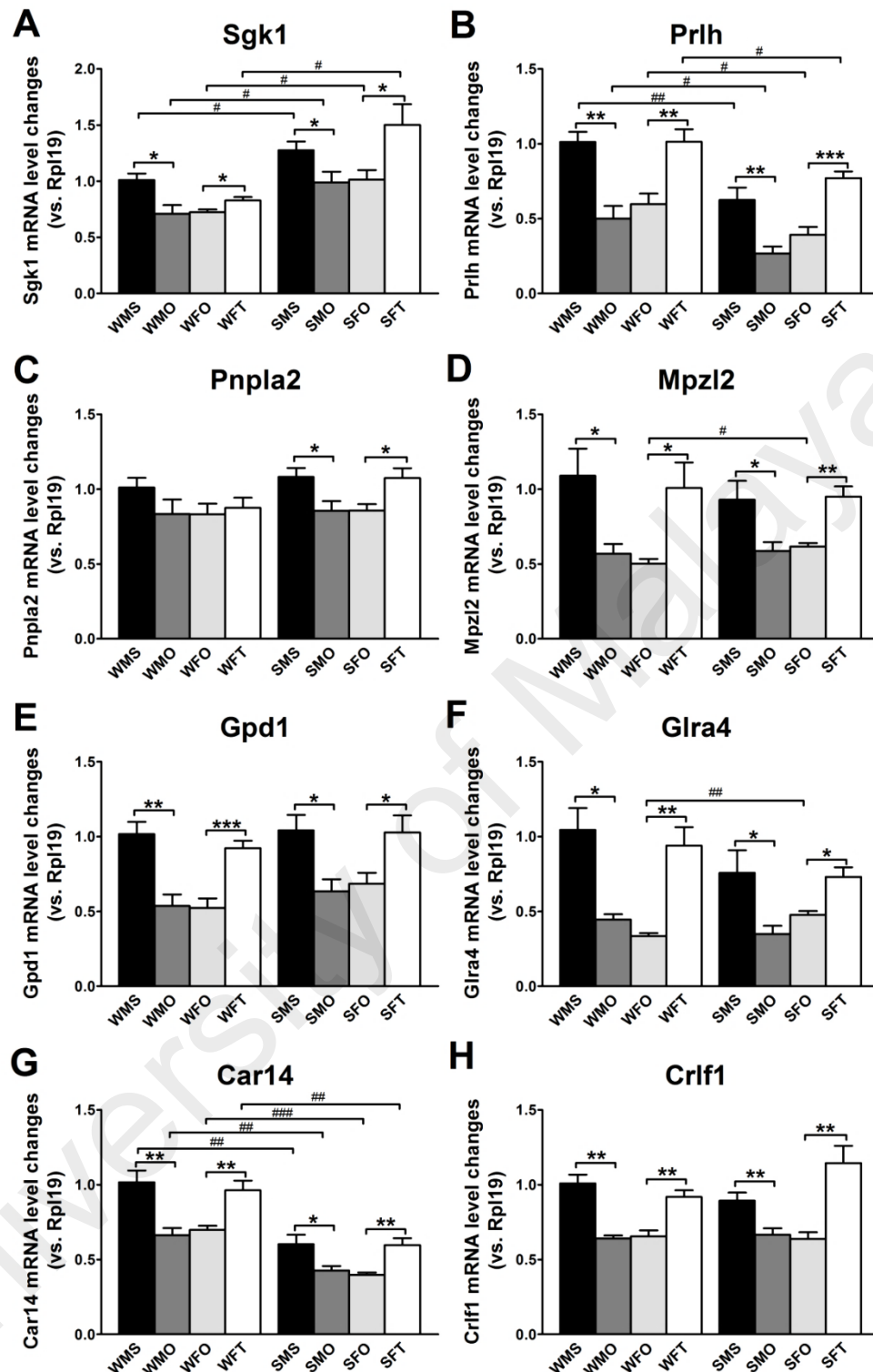


**Figure 10.6** qPCR determinations of genes up-regulated by testosterone treatment based on the transcriptome analysis of NTS.

Fold changes in mRNA expression levels of (A) *Sgk1*, (B) *Prlh*, (C) *Pnpla2*, (D) *Mpzl2*, (E) *Gpd1*, (F) *Glra4*, (G) *Car14* and (H) *Crif1* in NTS were quantified using qPCR. Data are presented in mean  $\pm$  SEM (n = 6/group, unpaired student's *t*-test); \* $P$ <0.05, \*\* $P$ <0.01, \*\*\* $P$ <0.001 compared to control group *i.e.* WMS, WFO, SMS and SFO; # $P$ <0.05, ## $P$ <0.01, ### $P$ <0.001 compared to normotensive WKY group. Abbreviations: WMS: WKY sham-operated intact male; WMO: WKY orchidectomized male; WFO: WKY ovariectomized female; WFT: WKY testosterone-treated ovariectomized female; SMS: SHR sham-operated intact male; SMO: SHR orchidectomized male; SFO: SHR ovariectomized female; SFT: SHR testosterone-treated ovariectomized female rats.

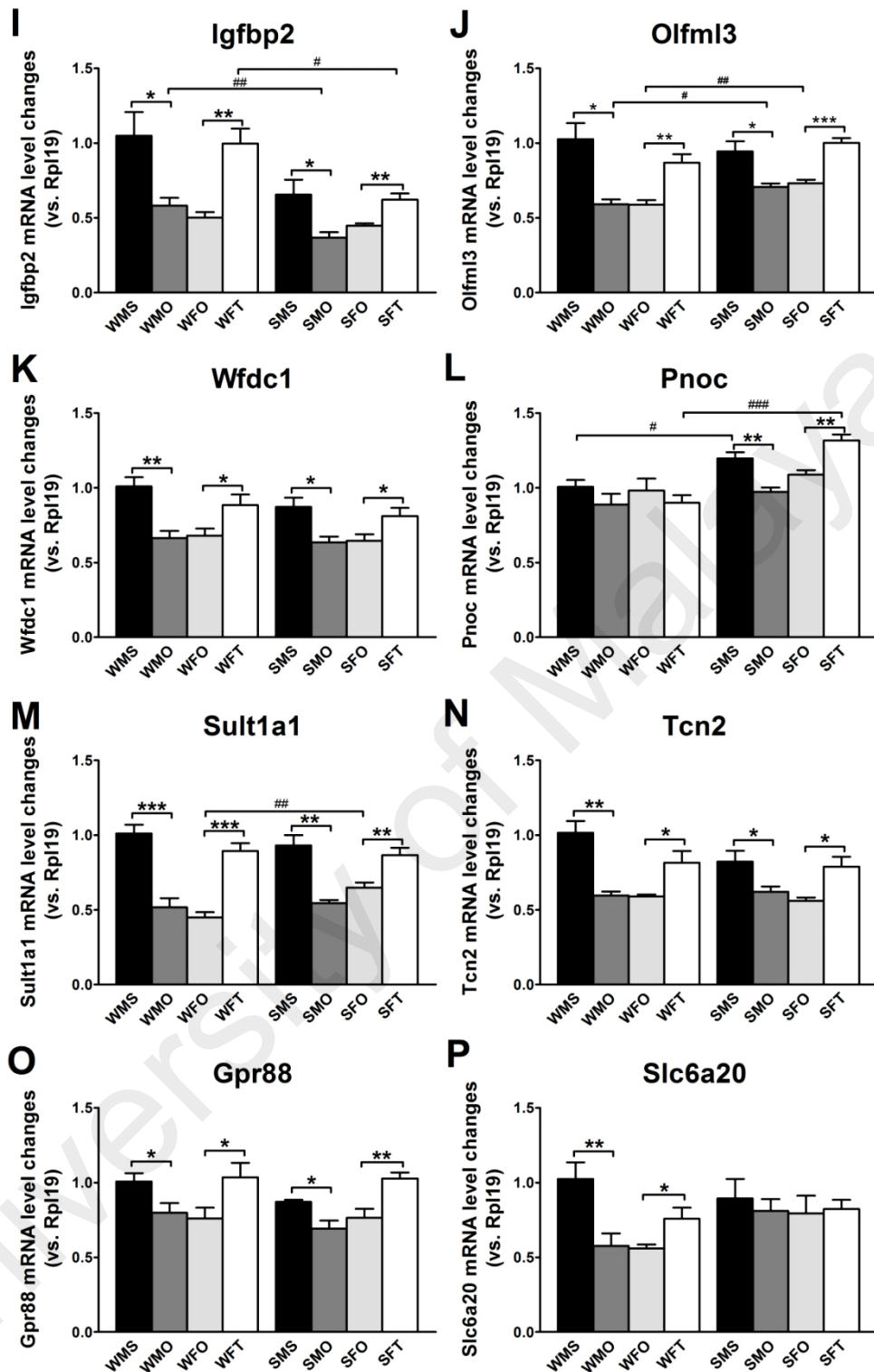


**Figure 10.8 continued.**

Fold changes in mRNA expression levels of **(I)** *Igfbp5*, **(J)** *Olfml3*, **(K)** *Wfdc1*, **(L)** *Pnoc*, **(M)** *Sult1a1*, **(N)** *Tcn2*, **(O)** *Gpr88* and **(P)** *Slc6a20* in NTS were quantified using qPCR. Data are presented in mean  $\pm$  SEM ( $n = 6$ /group, unpaired student's *t*-test); \* $P < 0.05$ , \*\* $P < 0.01$ , \*\*\* $P < 0.001$  compared to control group *i.e.* WMS, WFO, SMS and SFO; # $P < 0.05$ , ## $P < 0.01$ , ### $P < 0.001$  compared to normotensive WKY group. Abbreviations: WMS: WKY sham-operated intact male; WMO: WKY orchidectomized male; WFO: WKY ovariectomized female; WFT: WKY testosterone-treated ovariectomized female; SHR sham-operated intact male; SMO: SHR orchidectomized male; SFO: SHR ovariectomized female; SFT: SHR testosterone-treated ovariectomized female rats.

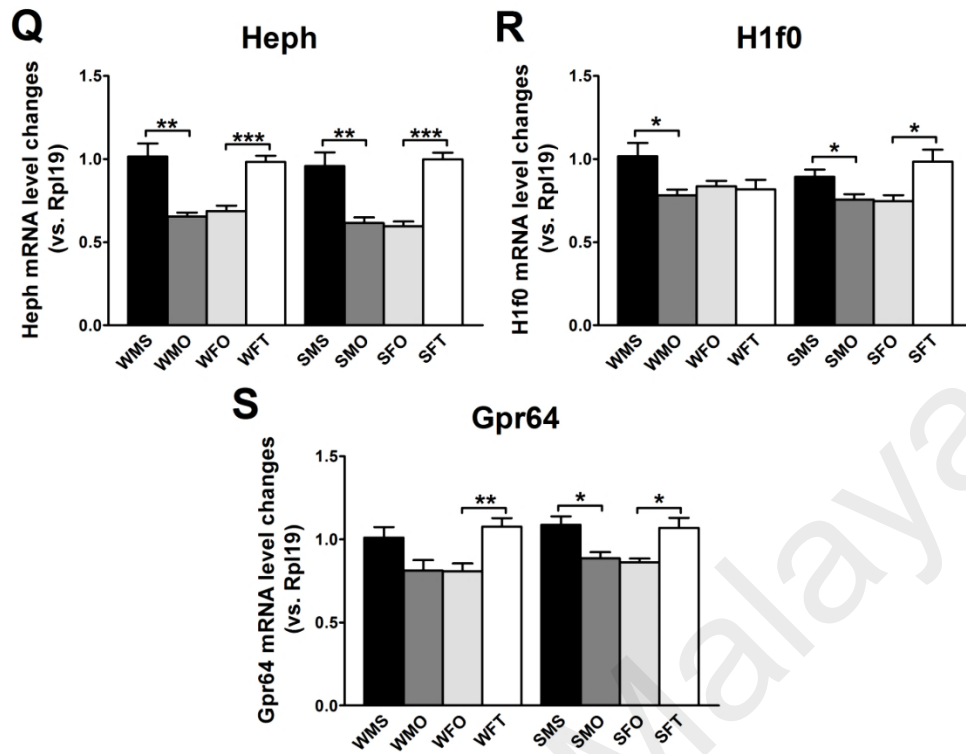


**Figure 10.8 continued.**

Fold changes in mRNA expression levels of (Q) *Heph*, (R) *H1f0* and (S) *Gpr64* in NTS were quantified using qPCR. Data are presented in mean  $\pm$  SEM ( $n = 6$ /group, unpaired student's *t*-test); \* $P < 0.05$ , \*\* $P < 0.01$ , \*\*\* $P < 0.001$  compared to control group *i.e.* WMS, WFO, SMS and SFO; # $P < 0.05$ , ## $P < 0.01$ , ### $P < 0.001$  compared to normotensive WKY group. Abbreviations: WMS: WKY sham-operated intact male; WMO: WKY orchidectomized male; WFO: WKY ovariectomized female; WFT: WKY testosterone-treated ovariectomized female; SHR sham-operated intact male; SMO: SHR orchidectomized male; SFO: SHR ovariectomized female; SFT: SHR testosterone-treated ovariectomized female rats.

**Table 10.3 Summary of fold changes, both from edgeR analysis of RNA-Seq data and qPCR analysis, of genes up-regulated by chronic testosterone treatment based on the transcriptome analysis of NTS.**

No.	Gene name	qPCR						Transcriptome		qPCR					
		WMO compare to WMS			WFT compare to WFO			SMO compare to SMS	SFT compare to SFO	SMO compare to SMS			SFT compare to SFO		
		WMS	WMO	P	WFO	WFT	P			SMS	SMO	P	SFO	SFT	P
1	<b>Sgk1</b>	1.01	<b>0.71</b>	*	0.72	<b>0.83</b>	*	<b>0.84</b>	<b>1.63</b>	1.28	<b>0.99</b>	*	1.01	<b>1.50</b>	*
2	<b>Prlh</b>	1.01	<b>0.50</b>	**	0.60	<b>1.01</b>	**	<b>0.57</b>	<b>1.55</b>	0.62	<b>0.27</b>	**	0.39	<b>0.77</b>	***
3	<b>Pnpla2</b>	1.01	0.83		0.83	0.87		<b>0.72</b>	<b>1.53</b>	1.08	<b>0.85</b>	*	0.86	<b>1.07</b>	*
4	<b>Mpzl2</b>	1.09	<b>0.57</b>	*	0.50	<b>1.01</b>	*	<b>0.59</b>	<b>1.51</b>	0.93	<b>0.59</b>	*	0.62	<b>0.95</b>	**
5	<b>Gpd1</b>	1.02	<b>0.54</b>	**	0.52	<b>0.92</b>	***	<b>0.62</b>	<b>1.48</b>	1.04	<b>0.64</b>	*	0.69	<b>1.03</b>	*
6	<b>Gira4</b>	1.04	<b>0.45</b>	*	0.33	<b>0.94</b>	**	<b>0.43</b>	<b>1.47</b>	0.76	<b>0.35</b>	*	0.48	<b>0.73</b>	*
7	<b>Car14</b>	1.02	<b>0.66</b>	**	0.70	<b>0.96</b>	**	<b>0.86</b>	<b>1.41</b>	0.60	<b>0.43</b>	*	0.40	<b>0.60</b>	**
8	<b>Crlf1</b>	1.01	<b>0.64</b>	**	0.65	<b>0.92</b>	**	<b>0.80</b>	<b>1.38</b>	0.89	<b>0.66</b>	**	0.64	<b>1.14</b>	**
9	<b>Igfbp5</b>	1.05	<b>0.58</b>	*	0.50	<b>1.00</b>	**	<b>0.61</b>	<b>1.37</b>	0.65	<b>0.37</b>	*	0.45	<b>0.62</b>	**
10	<b>Olfml3</b>	1.03	<b>0.59</b>	*	0.59	<b>0.87</b>	**	<b>0.70</b>	<b>1.37</b>	0.94	<b>0.71</b>	*	0.73	<b>1.00</b>	***
11	<b>Wfdc1</b>	1.01	<b>0.66</b>	**	0.68	<b>0.88</b>	*	<b>0.80</b>	<b>1.33</b>	0.87	<b>0.63</b>	*	0.65	<b>0.81</b>	*
12	<b>Pnoc</b>	1.01	0.89		0.98	0.90		<b>0.76</b>	<b>1.32</b>	1.20	<b>0.97</b>	**	1.09	<b>1.32</b>	**
13	<b>Sult1a1</b>	1.01	<b>0.52</b>	***	0.45	<b>0.89</b>	***	<b>0.69</b>	<b>1.31</b>	0.93	<b>0.54</b>	**	0.65	<b>0.87</b>	**

Mean fold changes estimated from edgeR analysis of RNA-Seq data (Transcriptome) and qPCR analysis (n = 6/group, unpaired student's *t*-test where \**P*<0.05, \*\**P*<0.01, \*\*\**P*<0.001 compared to control group i.e. WMS, WFO, SMS and SFO) are presented in the table. Genes are listed based on the levels of expression changes (estimated by edgeR), from highest (top) to lowest (bottom) increase, following chronic testosterone treatment in ovariectomized female SHR rats (SFT compare to SFO). Green values represent significant up-regulation while red values represent significant down-regulation of mRNA levels. Abbreviations: *P*: probability value; WMS: WKY sham-operated intact male; WMO: WKY orchidectomized male; WFO: WKY ovariectomized female; WFT: WKY testosterone-treated ovariectomized female; SHR sham-operated intact male; SMO: SHR orchidectomized male; SFO: SHR ovariectomized female; SFT: SHR testosterone-treated ovariectomized female rats.

Table 10.3 continued.

No.	Gene name	qPCR						Transcriptome		qPCR					
		WMO compare to WMS			WFT compare to WFO			SMO compare to SMS	SFT compare to SFO	SMO compare to SMS			SFT compare to SFO		
		WMS	WMO	<i>P</i>	WFO	WFT	<i>P</i>			SMS	SMO	<i>P</i>	SFO	SFT	<i>P</i>
14	<b>Tcn2</b>	1.02	<b>0.60</b>	**	0.59	<b>0.81</b>	*	<b>0.76</b>	<b>1.20</b>	0.82	<b>0.62</b>	*	0.56	<b>0.79</b>	*
15	<b>Gpr88</b>	1.01	<b>0.80</b>	*	0.76	<b>1.03</b>	*	<b>0.78</b>	<b>1.25</b>	0.87	<b>0.69</b>	*	0.76	<b>1.03</b>	**
16	<b>Slc6a20</b>	1.03	<b>0.58</b>	**	0.56	<b>0.76</b>	*	<b>0.80</b>	<b>1.24</b>	0.89	0.81		0.79	0.82	
17	<b>Heph</b>	1.01	<b>0.65</b>	**	0.69	<b>0.98</b>	***	<b>0.65</b>	<b>1.24</b>	0.96	<b>0.61</b>	**	0.59	<b>1.00</b>	***
18	<b>H1f0</b>	1.02	<b>0.78</b>	*	0.84	0.82		<b>0.84</b>	<b>1.22</b>	0.89	<b>0.76</b>	*	0.75	<b>0.98</b>	*
19	<b>Gpr64</b>	1.01	<b>0.81</b>		0.81	<b>1.08</b>	**	<b>0.78</b>	<b>1.30</b>	1.09	<b>0.88</b>	*	0.86	<b>1.07</b>	*

Mean fold changes estimated from edgeR analysis of RNA-Seq data (Transcriptome) and qPCR analysis (n = 6/group, unpaired student's *t*-test where \**P*<0.05, \*\**P*<0.01, \*\*\**P*<0.001 compared to control group *i.e.* WMS, WFO, SMS and SFO) are presented in the table. Genes are listed based on the levels of expression changes (estimated by edgeR), from highest (top) to lowest (bottom) increase, following chronic testosterone treatment in ovariectomized female SHR rats (SFT compare to SFO). Green values represent significant up-regulation while red values represent significant down-regulation of mRNA levels. Abbreviations: *P*: probability value; WMS: WKY sham-operated intact male; WMO: WKY orchidectomized male; WFO: WKY ovariectomized female; WFT: WKY testosterone-treated ovariectomized female; SHR sham-operated intact male; SMO: SHR orchidectomized male; SFO: SHR ovariectomized female; SFT: SHR testosterone-treated ovariectomized female rats.

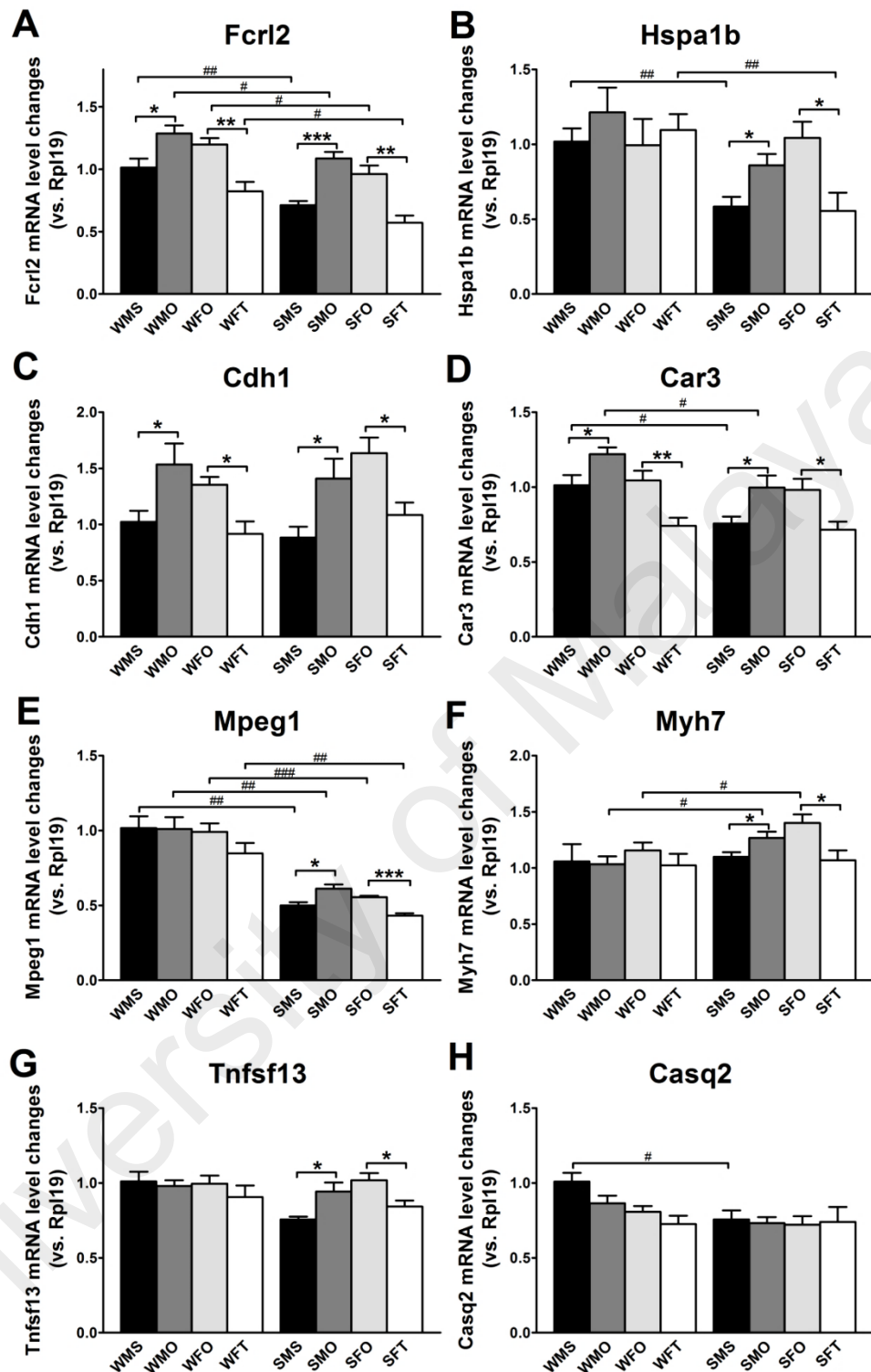


**Figure 10.7** qPCR determinations of genes down-regulated by testosterone treatment based on NTS transcriptome analysis.

Fold changes in mRNA expression levels of (A) *Fcrl2*, (B) *Hspa1b*, (C) *Cdh1*, (D) *Car3*, (E) *Mpeg1*, (F) *Myh7*, (G) *Tnfsf13* and (H) *Casq2* in NTS were quantified using qPCR. Data are presented in mean  $\pm$  SEM ( $n = 6$ /group, unpaired student's *t*-test); \* $P < 0.05$ , \*\* $P < 0.01$ , \*\*\* $P < 0.001$  compared to control group *i.e.* WMS, WFO, SMS and SFO; # $P < 0.05$ , ## $P < 0.01$ , ### $P < 0.001$  compared to normotensive WKY group. Abbreviations: WMS: WKY sham-operated intact male; WMO: WKY orchidectomized male; WFO: WKY ovariectomized female; WFT: WKY testosterone-treated ovariectomized female; SHR sham-operated intact male; SMO: SHR orchidectomized male; SFO: SHR ovariectomized female; SFT: SHR testosterone-treated ovariectomized female rats.

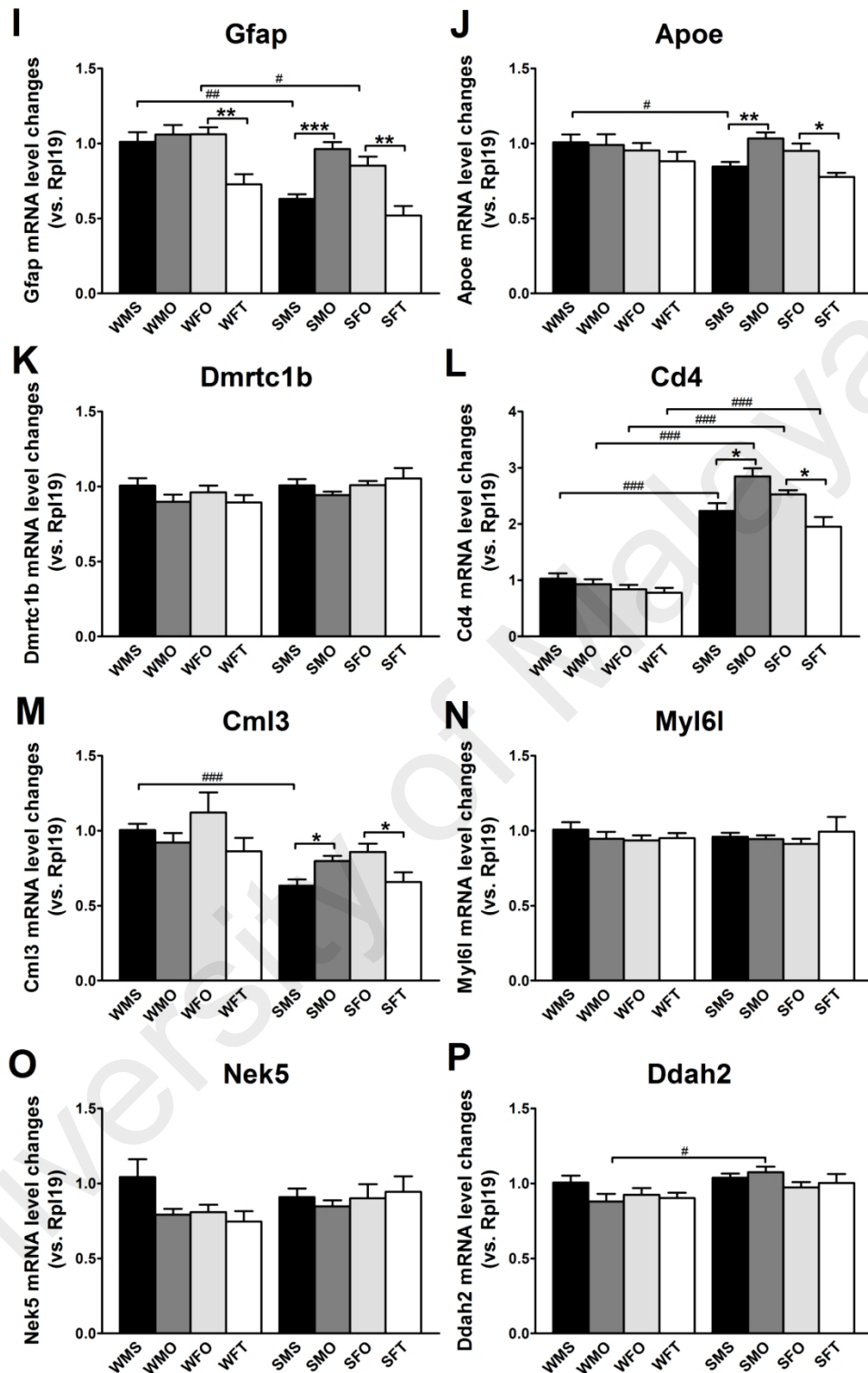


**Figure 10.7 continued.**

Fold changes in mRNA expression levels of (I) *Gfap*, (J) *Apoe*, (K) *Dmrtc1b*, (L) *Cd4*, (M) *Cml3*, (N) *Myl6l*, (O) *Nek5* and (P) *Ddah2* in NTS were quantified using qPCR. Data are presented in mean  $\pm$  SEM (n = 6/group, unpaired student's *t*-test); \* $P$ <0.05, \*\* $P$ <0.01, \*\*\* $P$ <0.001 compared to control group *i.e.* WMS, WFO, SMS and SFO; # $P$ <0.05, ## $P$ <0.01, ### $P$ <0.001 compared to normotensive WKY group. Abbreviations: WMS: WKY sham-operated intact male; WMO: WKY orchidectomized male; WFO: WKY ovariectomized female; WFT: WKY testosterone-treated ovariectomized female; SHR sham-operated intact male; SMO: SHR orchidectomized male; SFO: SHR ovariectomized female; SFT: SHR testosterone-treated ovariectomized female rats.

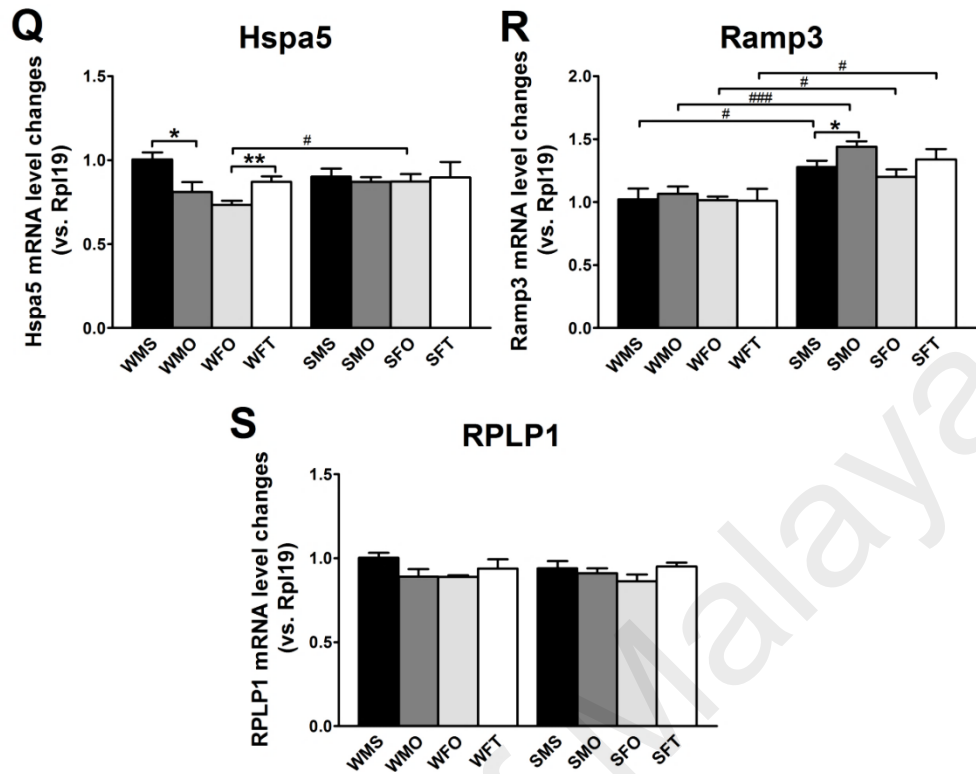


**Figure 10.7 continued.**

Fold changes in mRNA expression levels of **(Q)** *Hspa5*, **(R)** *Ramp3* and **(S)** *RPLP1* in NTS were quantified using qPCR. Data are presented in mean  $\pm$  SEM ( $n = 6$ /group, unpaired student's *t*-test); \* $P < 0.05$ , \*\* $P < 0.01$ , \*\*\* $P < 0.001$  compared to control group *i.e.* WMS, WFO, SMS and SFO; # $P < 0.05$ , ## $P < 0.01$ , ### $P < 0.001$  compared to normotensive WKY group. Abbreviations: WMS: WKY sham-operated intact male; WMO: WKY orchidectomized male; WFO: WKY ovariectomized female; WFT: WKY testosterone-treated ovariectomized female; SHR sham-operated intact male; SMO: SHR orchidectomized male; SFO: SHR ovariectomized female; SFT: SHR testosterone-treated ovariectomized female rats.

**Table 10.4 Summary of fold changes, both from edgeR analysis of RNA-Seq data and qPCR analysis, of genes down-regulated by chronic testosterone treatment based on the transcriptome analysis of NTS.**

No.	Gene name	qPCR						Transcriptome		qPCR					
		WMO compare to WMS			WFT compare to WFO			SMO compare to SMS	SFT compare to SFO	SMO compare to SMS			SFT compare to SFO		
		WMS	WMO	P	WFO	WFT	P			SMS	SMO	P	SFO	SFT	P
1	<b>Fcrl2</b>	1.01	<b>1.29</b>	*	1.20	<b>0.82</b>	**	<b>1.53</b>	<b>0.57</b>	0.71	<b>1.09</b>	***	0.96	<b>0.57</b>	**
2	<b>Hspa1b</b>	1.02	1.21		0.99	1.09		<b>1.52</b>	<b>0.58</b>	0.58	<b>0.86</b>	*	1.04	<b>0.55</b>	*
3	<b>Cdh1</b>	1.02	<b>1.53</b>	*	1.35	<b>0.92</b>	*	<b>1.37</b>	<b>0.62</b>	0.88	<b>1.41</b>	*	1.63	<b>1.08</b>	*
4	<b>Car3</b>	1.01	<b>1.22</b>	*	1.04	<b>0.74</b>	**	<b>1.28</b>	<b>0.64</b>	0.76	<b>1.00</b>	*	0.98	<b>0.72</b>	*
5	<b>Mpeg1</b>	1.02	1.01		0.99	0.85		<b>1.20</b>	<b>0.70</b>	0.50	<b>0.61</b>	*	0.55	<b>0.43</b>	***
6	<b>Myh7</b>	1.06	1.03		1.16	1.02		<b>1.45</b>	<b>0.73</b>	1.17	<b>1.27</b>	*	1.40	<b>1.07</b>	*
7	<b>Tnfsf13</b>	1.01	0.98		0.99	0.91		<b>1.21</b>	<b>0.74</b>	0.76	<b>0.94</b>	*	1.02	0.84	*
8	<b>Casq2</b>	1.01	0.86		0.81	0.73		<b>1.39</b>	<b>0.74</b>	0.76	0.73		0.72	0.74	
9	<b>Gfap</b>	1.01	1.06		1.06	<b>0.73</b>	**	<b>1.33</b>	<b>0.77</b>	0.63	<b>0.96</b>	***	0.85	<b>0.52</b>	**
10	<b>Apoe</b>	1.01	0.99		0.95	0.88		<b>1.20</b>	<b>0.77</b>	0.84	<b>1.03</b>	**	0.95	<b>0.78</b>	*
11	<b>Dmrtd1b</b>	1.01	0.90		0.96	0.89		<b>1.41</b>	<b>0.78</b>	1.01	0.94		1.01	1.05	
12	<b>Cd4</b>	1.03	0.93		0.84	0.78		<b>1.28</b>	<b>0.78</b>	2.23	<b>2.85</b>	*	2.53	<b>1.95</b>	*
13	<b>Cml3</b>	1.00	0.92		1.12	0.86		<b>1.30</b>	<b>0.78</b>	0.63	<b>0.80</b>	*	0.86	<b>0.66</b>	*

Mean fold changes estimated from edgeR analysis of RNA-Seq data (Transcriptome) and qPCR analysis (n = 6/group, unpaired student's *t*-test where \**P*<0.05, \*\**P*<0.01, \*\*\**P*<0.001 compared to control treatment group *i.e.* WMS, WFO, SMS and SFO) are presented in the table. Genes are listed based on the levels of expression changes (estimated by edgeR), from highest (top) to lowest (bottom) decrease, following chronic testosterone treatment in ovariectomized female SHR rats (SFT compare to SFO). Green values represent significant up-regulation while red values represent significant down-regulation of mRNA levels. Abbreviations: *P*: probability value; WMS: WKY sham-operated intact male; WMO: WKY orchidectomized male; WFO: WKY ovariectomized female; WFT: WKY testosterone-treated ovariectomized female; SHR sham-operated intact male; SMO: SHR orchidectomized male; SFO: SHR ovariectomized female; SFT: SHR testosterone-treated ovariectomized female rats

Table 10.4 continued.

No.	Gene name	qPCR						Transcriptome		qPCR					
		WMO compare to WMS			WFT compare to WFO			SMO compare to SMS	SFT compare to SFO	SMO compare to SMS			SFT compare to SFO		
		WMS	WMO	<i>P</i>	WFO	WFT	<i>P</i>			SMS	SMO	<i>P</i>	SFO	SFT	<i>P</i>
14	<b>Myl6l</b>	1.01	0.95		0.94	0.95		<b>1.22</b>	<b>0.78</b>	0.96	0.94		0.91	0.99	
15	<b>Nek5</b>	1.04	0.79		0.81	0.75		<b>1.26</b>	<b>0.79</b>	0.91	0.85		0.90	0.94	
16	<b>Ddah2</b>	1.01	0.88		0.92	0.90		<b>1.22</b>	<b>0.79</b>	1.04	1.08		0.97	1.00	
17	<b>Hspa5</b>	1.00	<b>0.81</b>	*	0.73	<b>0.87</b>	**	<b>1.17</b>	<b>0.80</b>	0.90	0.87		0.87	0.90	
18	<b>Ramp3</b>	1.02	1.07		1.01	1.01		<b>1.23</b>	<b>0.82</b>	1.28	<b>1.44</b>	*	1.20	1.34	
19	<b>RPLP1</b>	1.00	0.89		0.89	0.94		<b>1.29</b>	<b>0.84</b>	0.94	0.91		0.86	0.95	

Mean fold changes estimated from edgeR analysis of RNA-Seq data (Transcriptome) and qPCR analysis (n = 6/group, unpaired student's *t*-test where \**P*<0.05, \*\**P*<0.01, \*\*\**P*<0.001 compared to control treatment group *i.e.* WMS, WFO, SMS and SFO) are presented in the table. Genes are listed based on the levels of expression changes (estimated by edgeR), from highest (top) to lowest (bottom) decrease, following chronic testosterone treatment in ovariectomized female SHR rats (SFT compare to SFO). Green values represent significant up-regulation while red values represent significant down-regulation of mRNA levels. Abbreviations: *P*: probability value; WMS: WKY sham-operated intact male; WMO: WKY orchidectomized male; WFO: WKY ovariectomized female; WFT: WKY testosterone-treated ovariectomized female; SHR sham-operated intact male; SMO: SHR orchidectomized male; SFO: SHR ovariectomized female; SFT: SHR testosterone-treated ovariectomized female rats.

### 10.2.1.3 Rostral ventrolateral medulla (RVLM)

Figure 10.8 showed constant expressions of housekeeping genes, *Rpl19*, *Gapdh* and *Actb* in RVLM of both normotensive WKY and hypertensive SHR rats, with no significant differences identified. Figure 10.9 showed the quantification of steady-state mRNA of 21 genes which were shown in the transcriptome analysis of RVLM, to be significantly increased in ovariectomized female hypertensive SHR rats following chronic testosterone treatment. Based on the qPCR analysis, 11 (*Mfrp*, *Clic6*, *Gal*, *Sult1a1*, *Heph*, *Iqgap2*, *Fkbp5*, *Htra1*, *Car14*, *Spon1* and *Dusp3*) out of 21 candidate genes showed significant changes in their expression levels in RVLM of hypertensive SHR rats in which 6 (*Heph*, *Iqgap2*, *Fkbp5*, *Htra1*, *Car14* and *Spon1*) of them were also significantly altered in normotensive WKY rats. In male rats, orchidectomy caused the expression levels of these genes to decrease while in ovariectomized female rats, chronic testosterone exposure elevated the expression of these genes in RVLM. Opposite effects were observed in the expression levels of *Slc4a5* in RVLM of normotensive WKY rats in which orchidectomy resulted in a significant increase in male rats ( $P < 0.05$ ) while chronic testosterone treatment markedly reduced the expression ( $P < 0.05$ ). The comparison between the fold changes in expression levels obtained from RNA-Seq and qPCR analysis were shown in Table 10.5.

In RVLM, the changes in the expression levels of 13 genes, selected based on their significant reduction in testosterone-treated ovariectomized female SHR rats reported in RNA-Seq analysis, were determined using qPCR (Figure 10.10). Of that 13 candidate genes, the expression levels of 5 genes (*Trpm8*, *C3*, *Mpeg1*, *Fcrl2* and *GSTA1*) significantly increased by orchidectomy in male and decreased by chronic testosterone treatment in ovariectomized female SHR rats. In normotensive WKY rats, 5 genes

(*Trpm8*, *C3*, *Fcrl2*, *GSTA1* and *Klhl25*) were also shown to be significantly changed in RVLM, in which higher expression levels in orchidectomized male as compared to sham-operated intact male and lower expression levels in testosterone-treated ovariectomized female as compared to those non-treated were observed. In both normotensive WKY and hypertensive SHR rats, no significant changes in expression level of *Hspa2* were observed following orchidectomy in male rats, however the chronic administration of testosterone significantly reduced the expression levels in RVLM ( $P < 0.01$  for WKY;  $P < 0.05$  for SHR rats). When comparing to the corresponding hypertensive groups, normotensive WKY rats showed significant higher expression of *Cml3* ( $P < 0.01$  for sham-operated male, ovariectomized female and testosterone-treated ovariectomized female;  $P < 0.001$  for orchidectomized male rats), *Trpm8* ( $P < 0.01$  for sham-operated male and testosterone-treated female;  $P < 0.001$  for orchidectomized male and ovariectomized female rats) and *Mpeg1* ( $P < 0.001$  for sham-operated male and ovariectomized female;  $P < 0.01$  for orchidectomized male and testosterone-treated ovariectomized female rats) in RVLM. Meanwhile, higher expression of *Etnk2* in RVLM of hypertensive SHR rat as compared to the corresponding normotensive group was also noted ( $P < 0.01$  for sham-operated male, ovariectomized female and testosterone-treated ovariectomized female;  $P < 0.05$  for orchidectomized male). The fold changes, obtained from both RNA-Seq analysis and qPCR determinations, in the expression levels of 13 candidate genes in RVLM were shown in Table 10.6.

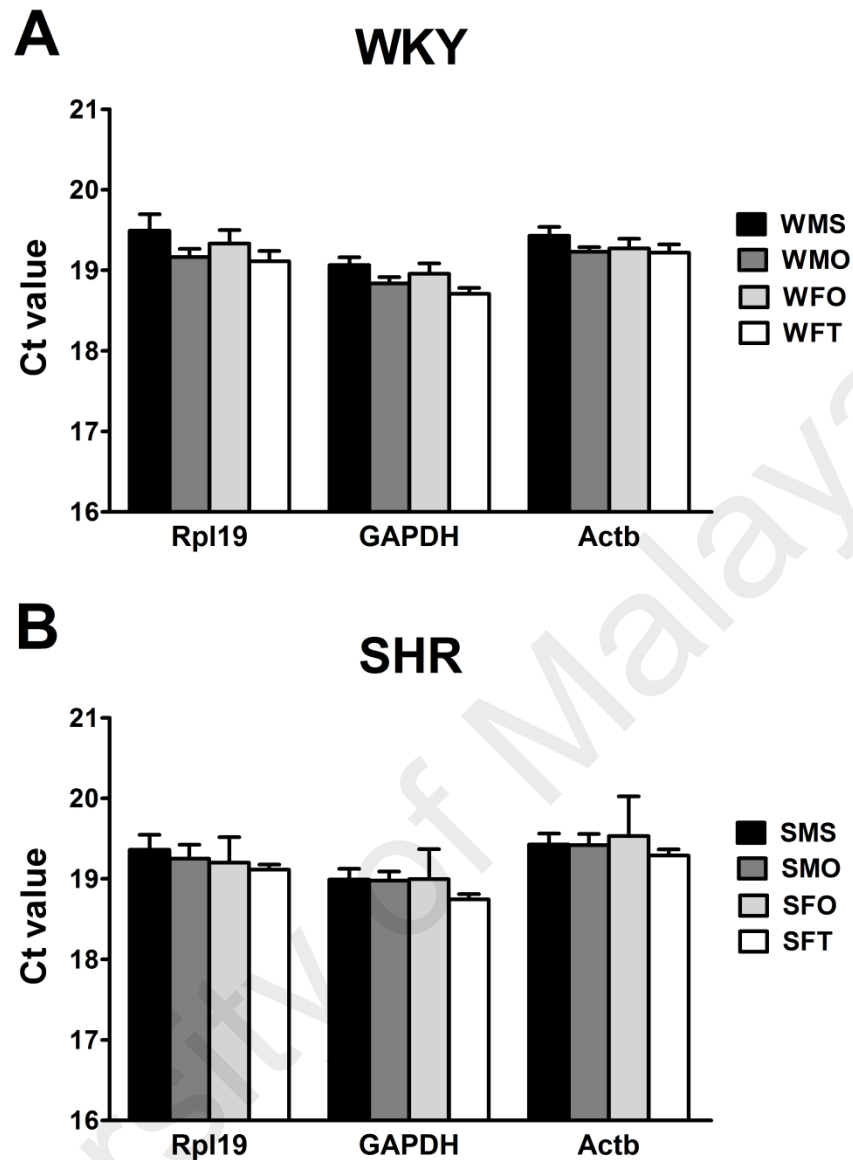


**Figure 10.8 Selection of reference gene with constant expression in RVLM.**

Steady state mRNA levels of three housekeeping genes *i.e.* *Rpl19*, *Gapdh* and *Actb* in RVLM of (A) WKY and (B) SHR rats were quantified using qPCR. Data are presented in mean  $\pm$  SEM ( $n = 6/\text{group}$ , unpaired student's *t*-test). Abbreviations: WMS: WKY sham-operated intact male; WMO: WKY orchidectomized male; WFO: WKY ovariectomized female; WFT: WKY testosterone-treated ovariectomized female; SHR sham-operated intact male; SMO: SHR orchidectomized male; SFO: SHR ovariectomized female; SFT: SHR testosterone-treated ovariectomized female rats.

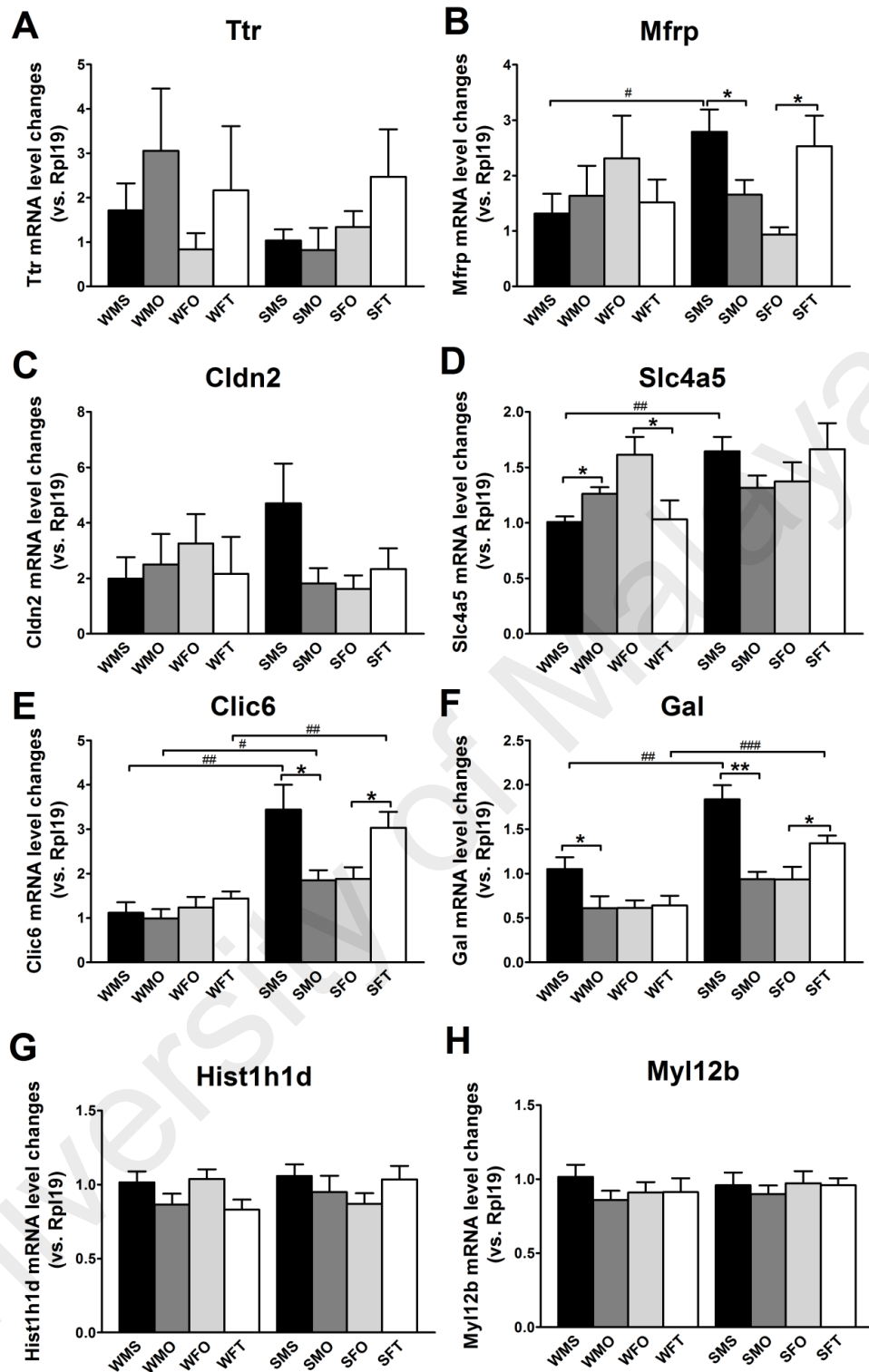


**Figure 10.9** qPCR determinations of genes up-regulated by testosterone treatment based on the transcriptome analysis of RVLM.

Fold changes in mRNA expression levels of (A) *Ttr*, (B) *Mfrp*, (C) *Cldn2*, (D) *Kl*, (E) *Slc4a5*, (F) *Clic6*, (G) *Gal* and (H) *Hist1h1d* in RVLM were quantified using qPCR. Data are presented in mean  $\pm$  SEM (n = 6/group, unpaired student's *t*-test); \* $P$ <0.05, \*\* $P$ <0.01, \*\*\* $P$ <0.001 compared to control group *i.e.* WMS, WFO, SMS and SFO; # $P$ <0.05, ## $P$ <0.01, ### $P$ <0.001 compared to normotensive WKY group. Abbreviations: WMS: WKY sham-operated intact male; WMO: WKY orchidectomized male; WFO: WKY ovariectomized female; WFT: WKY testosterone-treated ovariectomized female; SHR sham-operated intact male; SMO: SHR orchidectomized male; SFO: SHR ovariectomized female; SFT: SHR testosterone-treated ovariectomized female rats.

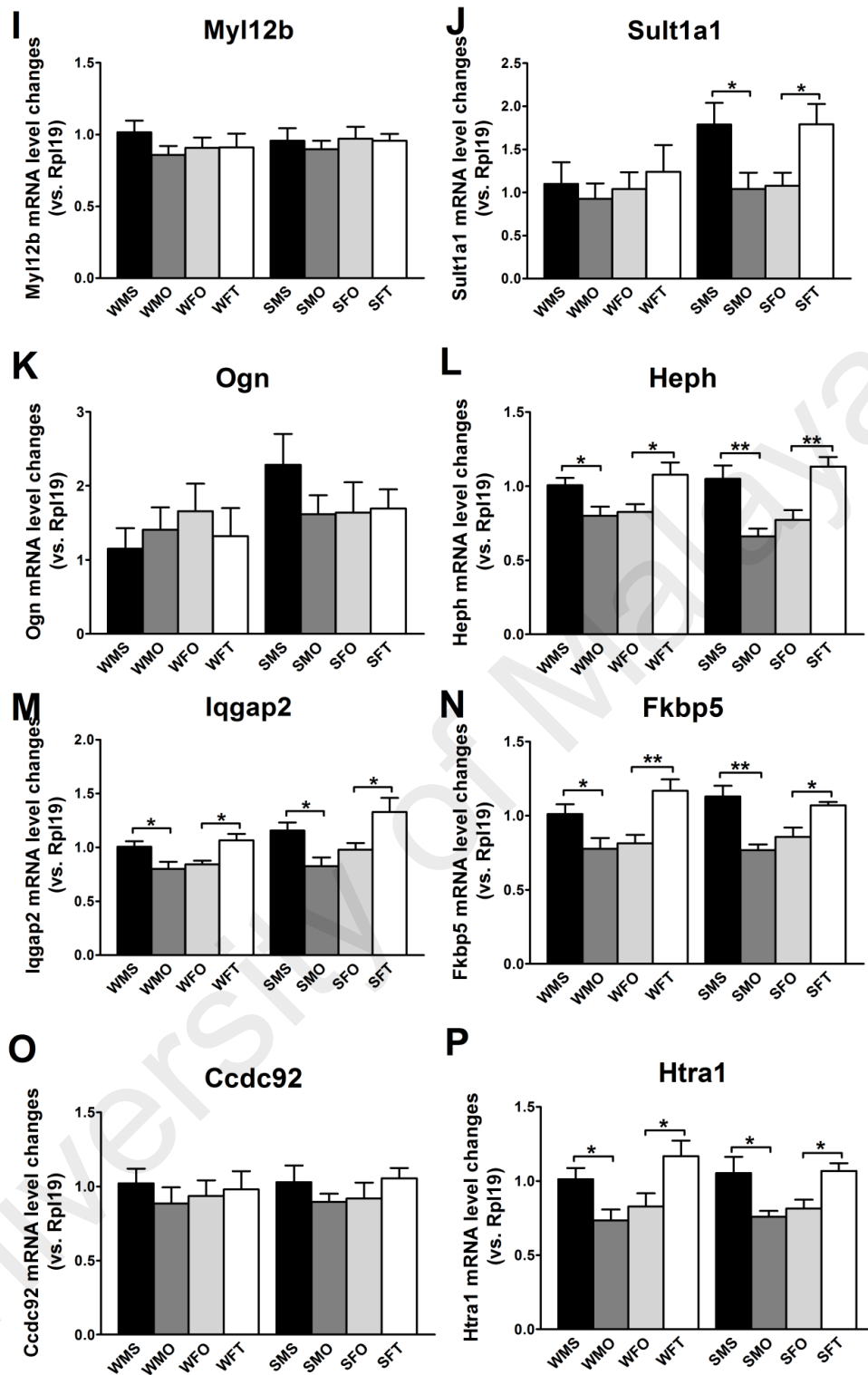


**Figure 10.9 continued.**

Fold changes in mRNA expression levels of (I) *Myl12b*, (J) *Sult1a1*, (K) *Ogn*, (L) *Heph*, (M) *Iqgap2*, (N) *Fkbp5*, (O) *Ccdc92* and (P) *Htra1* in RVLN were quantified using qPCR. Data are presented in mean  $\pm$  SEM (n = 6/group, unpaired student's *t*-test); \**P*<0.05, \*\**P*<0.01, \*\*\**P*<0.001 compared to control group *i.e.* WMS, WFO, SMS and SFO; #*P*<0.05, ##*P*<0.01, ###*P*<0.001 compared to normotensive WKY group. Abbreviations: WMS: WKY sham-operated intact male; WMO: WKY orchidectomized male; WFO: WKY ovariectomized female; WFT: WKY testosterone-treated ovariectomized female; SHR sham-operated intact male; SMO: SHR orchidectomized male; SFO: SHR ovariectomized female; SFT: SHR testosterone-treated ovariectomized female rats.

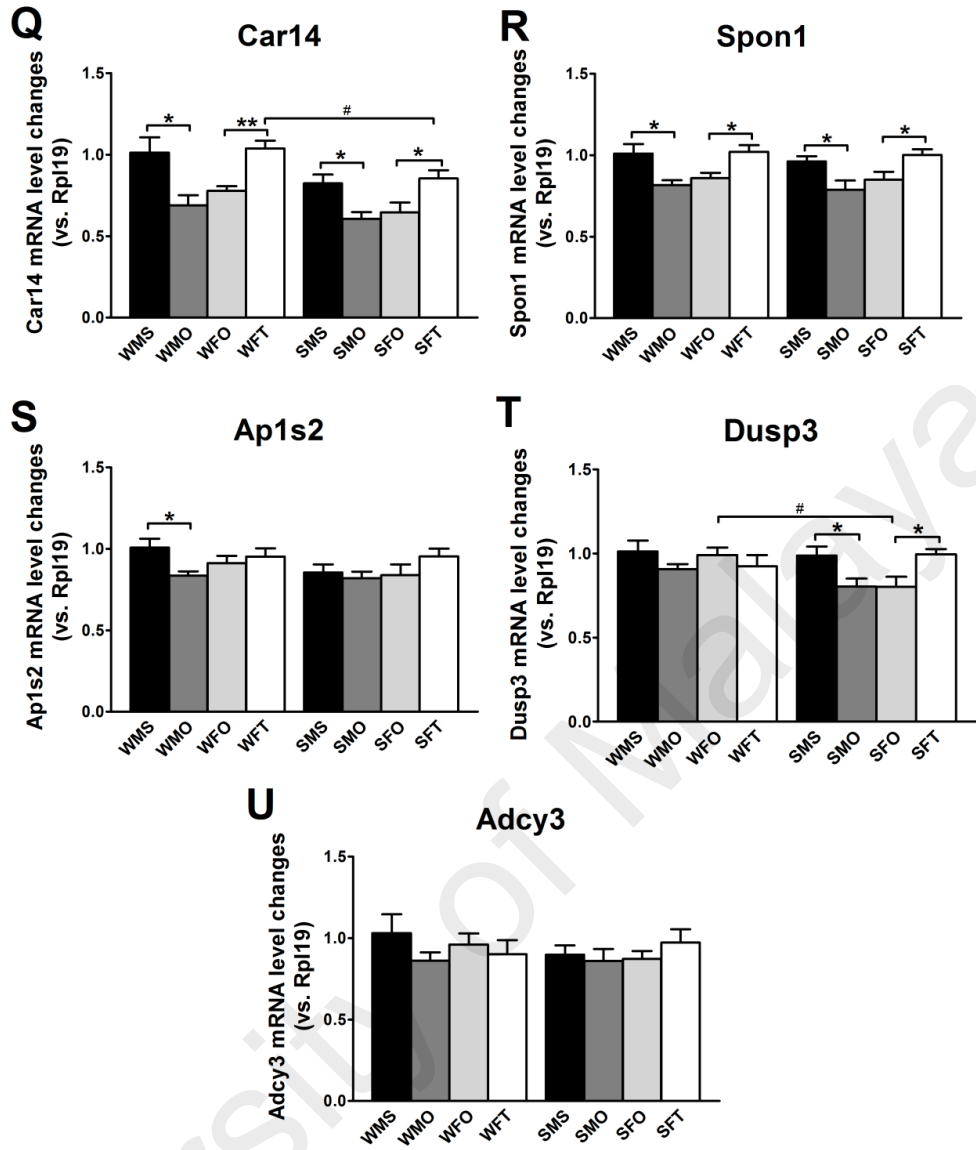


**Figure 10.9 continued.**

Fold changes in mRNA expression levels of (Q) *Car14*, (R) *Spon1*, (S) *Ap1s2*, (T) *Dusp3* and (U) *Adcy3* in RVLM were quantified using qPCR. Data are presented in mean  $\pm$  SEM (n = 6/group, unpaired student's *t*-test); \* $P$ <0.05, \*\* $P$ <0.01, \*\*\* $P$ <0.001 compared to control group *i.e.* WMS, WFO, SMS and SFO; # $P$ <0.05, ## $P$ <0.01, ### $P$ <0.001 compared to normotensive WKY group. Abbreviations: WMS: WKY sham-operated intact male; WMO: WKY orchidectomized male; WFO: WKY ovariectomized female; WFT: WKY testosterone-treated ovariectomized female; SHR sham-operated intact male; SMO: SHR orchidectomized male; SFO: SHR ovariectomized female; SFT: SHR testosterone-treated ovariectomized female rats.

**Table 10.5 Summary of fold changes, both from edgeR analysis of RNA-Seq data and qPCR analysis, of genes up-regulated by chronic testosterone treatment based on the transcriptome analysis of RVLM.**

No.	Gene name	qPCR						Transcriptome		qPCR					
		WMO compare to WMS			WFT compare to WFO			SMO compare to SMS	SFT compare to SFO	SMO compare to SMS			SFT compare to SFO		
		WMS	WMO	<i>P</i>	WFO	WFT	<i>P</i>			SMS	SMO	<i>P</i>	SFO	SFT	<i>P</i>
1	<b>Ttr</b>	1.71	3.06		0.83	2.16		<b>0.20</b>	<b>2.85</b>	1.03	0.82		1.34	2.47	
2	<b>Mfrp</b>	1.31	1.63		2.31	1.51		<b>0.27</b>	<b>2.60</b>	2.79	<b>1.65</b>	*	0.93	<b>2.53</b>	*
3	<b>Cldn2</b>	1.99	2.50		3.26	2.16		<b>0.33</b>	<b>2.30</b>	4.70	1.82		1.62	2.33	
4	<b>Kl</b>	1.05	0.85		0.99	0.87		<b>0.40</b>	<b>2.24</b>	1.20	1.04		0.93	1.09	
5	<b>Slc4a5</b>	1.01	<b>1.26</b>	*	1.61	<b>1.03</b>	*	<b>0.64</b>	<b>1.88</b>	1.64	1.31		1.37	1.66	
6	<b>Clic6</b>	1.11	0.99		1.23	1.44		<b>0.44</b>	<b>1.81</b>	3.44	<b>1.85</b>	*	1.88	<b>3.03</b>	*
7	<b>Gal</b>	1.05	<b>0.61</b>	*	0.61	0.64		<b>0.69</b>	<b>1.60</b>	1.84	<b>0.94</b>	**	0.93	<b>1.34</b>	*
8	<b>Hist1h1d</b>	1.01	0.86		1.04	0.83		<b>0.79</b>	<b>1.45</b>	1.06	0.95		0.87	1.03	
9	<b>Myl12b</b>	1.01	0.86		0.91	0.91		<b>0.71</b>	<b>1.38</b>	0.96	0.90		0.97	0.96	
10	<b>Sult1a1</b>	1.10	0.93		1.04	1.24		<b>0.81</b>	<b>1.35</b>	1.79	<b>1.04</b>	*	1.08	<b>1.79</b>	*
11	<b>Ogn</b>	1.15	1.41		1.66	1.32		<b>0.78</b>	<b>1.34</b>	2.29	1.61		1.64	1.69	
12	<b>Heph</b>	1.01	<b>0.80</b>	*	0.83	<b>1.08</b>	*	<b>0.81</b>	<b>1.33</b>	1.05	<b>0.66</b>	**	0.77	<b>1.13</b>	**
13	<b>Iqgap2</b>	1.01	<b>0.80</b>	*	0.84	<b>1.07</b>	*	<b>0.67</b>	<b>1.32</b>	1.16	<b>0.83</b>	*	0.98	<b>1.33</b>	*

Mean fold changes estimated from edgeR analysis of RNA-Seq data (Transcriptome) and qPCR analysis (n = 6/group, unpaired student's *t*-test where \**P*<0.05, \*\**P*<0.01, \*\*\**P*<0.001 compared to control group *i.e.* WMS, WFO, SMS and SFO) are presented in the table. Genes are listed based on the levels of expression changes (estimated by edgeR), from highest (top) to lowest (bottom) increase, following chronic testosterone treatment in ovariectomized female SHR rats (SFT compare to SFO). Green values represent significant up-regulation while red values represent significant down-regulation of mRNA levels. Abbreviations: *P*: probability value; WMS: WKY sham-operated intact male; WMO: WKY orchidectomized male; WFO: WKY ovariectomized female; WFT: WKY testosterone-treated ovariectomized female; SHR sham-operated intact male; SMO: SHR orchidectomized male; SFO: SHR ovariectomized female; SFT: SHR testosterone-treated ovariectomized female rats.

Table 10.5 continued.

No.	Gene name	qPCR						Transcriptome		qPCR					
		WMO compare to WMS			WFT compare to WFO			SMO compare to SMS	SFT compare to SFO	SMO compare to SMS			SFT compare to SFO		
		WMS	WMO	<i>P</i>	WFO	WFT	<i>P</i>			SMS	SMO	<i>P</i>	SFO	SFT	<i>P</i>
14	<b>Fkbp5</b>	1.01	<b>0.78</b>	*	0.81	<b>1.17</b>	**	<b>0.76</b>	<b>1.25</b>	1.13	<b>0.77</b>	**	0.86	<b>1.07</b>	*
15	<b>Ccdc92</b>	1.02	0.88		0.93	0.98		<b>0.84</b>	<b>1.24</b>	1.03	0.89		0.92	1.05	
16	<b>Htra1</b>	1.01	<b>0.73</b>	*	0.83	<b>1.17</b>	*	<b>0.81</b>	<b>1.22</b>	1.05	<b>0.76</b>	*	0.81	<b>1.07</b>	*
17	<b>Car14</b>	1.01	<b>0.69</b>	*	0.78	<b>1.04</b>	**	<b>0.87</b>	<b>1.18</b>	0.82	<b>0.61</b>	*	0.64	<b>0.85</b>	*
18	<b>Spon1</b>	1.01	<b>0.82</b>	*	0.86	<b>1.02</b>	*	<b>0.89</b>	<b>1.15</b>	0.96	<b>0.79</b>	*	0.85	<b>1.00</b>	*
19	<b>Ap1s2</b>	1.01	<b>0.83</b>	*	0.91	0.95		<b>0.89</b>	<b>1.14</b>	0.86	0.82		0.84	0.95	
20	<b>Dusp3</b>	1.01	0.91		0.99	0.92		<b>0.88</b>	<b>1.12</b>	0.99	<b>0.80</b>	*	0.80	<b>0.99</b>	*
21	<b>Adcy3</b>	1.03	0.86		0.96	0.90		<b>0.82</b>	<b>1.12</b>	0.90	0.86		0.87	0.97	

Mean fold changes estimated from edgeR analysis of RNA-Seq data (Transcriptome) and qPCR analysis (n = 6/group, unpaired student's *t*-test where \**P*<0.05, \*\**P*<0.01, \*\*\**P*<0.001 compared to control group *i.e.* WMS, WFO, SMS and SFO) are presented in the table. Genes are listed based on the levels of expression changes (estimated by edgeR), from highest (top) to lowest (bottom) increase, following chronic testosterone treatment in ovariectomized female SHR rats (SFT compare to SFO). Green values represent significant up-regulation while red values represent significant down-regulation of mRNA levels. Abbreviations: *P*: probability value; WMS: WKY sham-operated intact male; WMO: WKY orchidectomized male; WFO: WKY ovariectomized female; WFT: WKY testosterone-treated ovariectomized female; SHR sham-operated intact male; SMO: SHR orchidectomized male; SFO: SHR ovariectomized female; SFT: SHR testosterone-treated ovariectomized female rats.

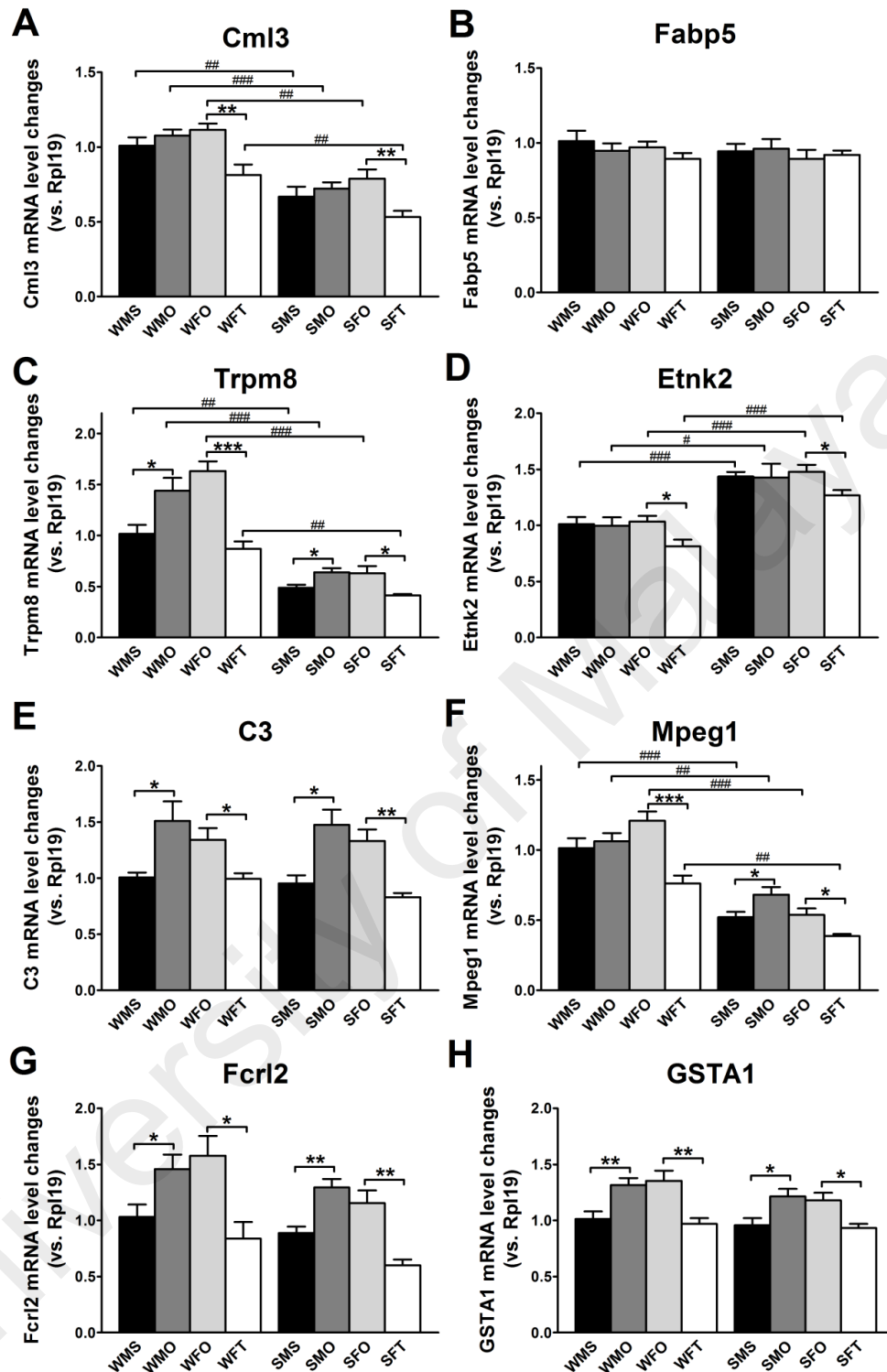


**Figure 10.10 qPCR determinations of genes down-regulated by testosterone treatment based on the transcriptome analysis of RVLM.**

Fold changes in mRNA expression levels of (A) *Cml3*, (B) *Fabp5*, (C) *Trpm8*, (D) *Etnk2*, (E) *C3*, (F) *Mpeg1*, (G) *Fcrl2* and (H) *GSTA1* in RVLM were quantified using qPCR. Data are presented in mean  $\pm$  SEM ( $n = 6/\text{group}$ , unpaired student's  $t$ -test); \* $P < 0.05$ , \*\* $P < 0.01$ , \*\*\* $P < 0.001$  compared to control group *i.e.* WMS, WFO, SMS and SFO; # $P < 0.05$ , ## $P < 0.01$ , ### $P < 0.001$  compared to normotensive WKY group. Abbreviations: WMS: WKY sham-operated intact male; WMO: WKY orchidectomized male; WFO: WKY ovariectomized female; WFT: WKY testosterone-treated ovariectomized female; SHR sham-operated intact male; SMO: SHR orchidectomized male; SFO: SHR ovariectomized female; SFT: SHR testosterone-treated ovariectomized female rats.

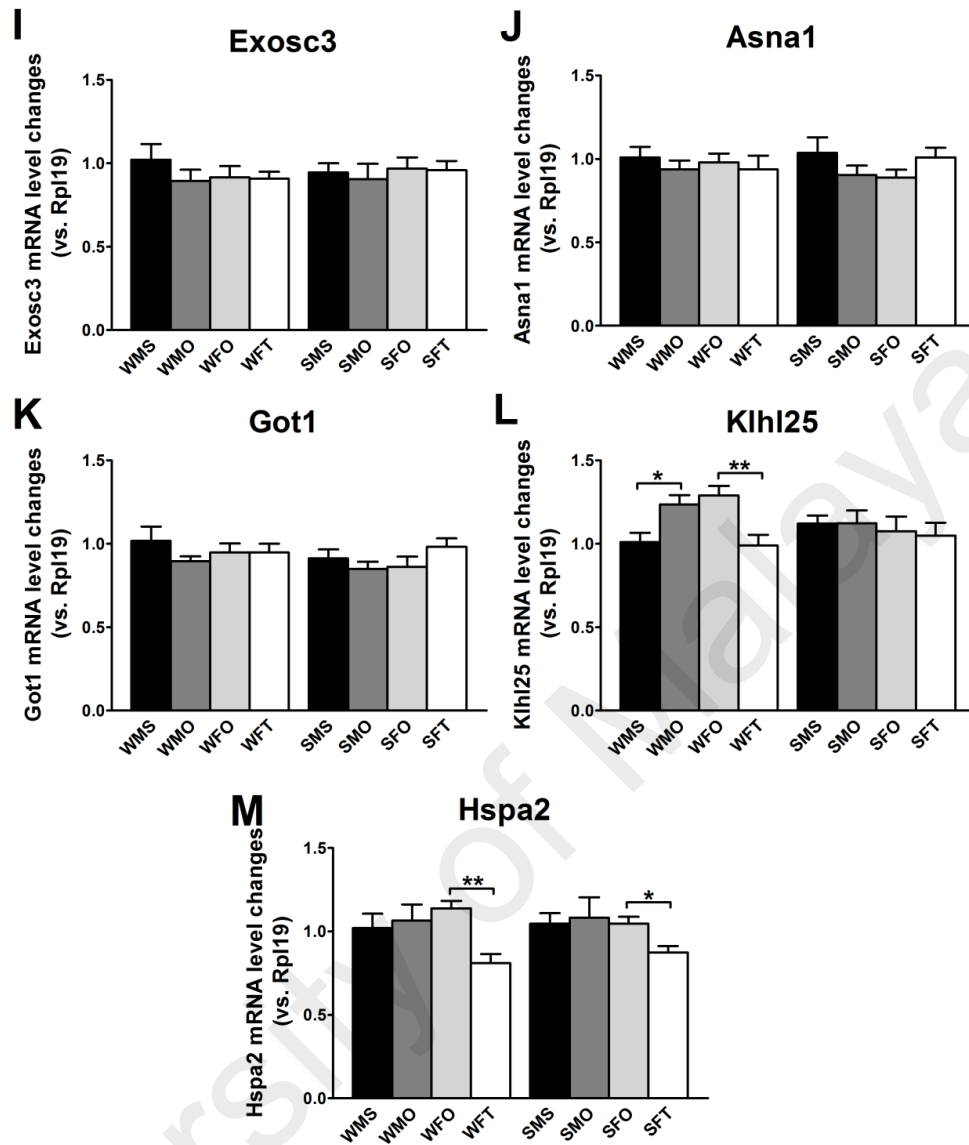


**Figure 10.10 continued.**

Fold changes in mRNA expression levels of (I) *Exosc3*, (J) *Asna1*, (K) *Got1*, (L) *Klh25* and (M) *Hspa2* in RVLM were quantified using qPCR. Data are presented in mean  $\pm$  SEM (n = 6/group, unpaired student's *t*-test); \* $P$ <0.05, \*\* $P$ <0.01, \*\*\* $P$ <0.001 compared to control group *i.e.* WMS, WFO, SMS and SFO; # $P$ <0.05, ## $P$ <0.01, ### $P$ <0.001 compared to normotensive WKY group. Abbreviations: WMS: WKY sham-operated intact male; WMO: WKY orchidectomized male; WFO: WKY ovariectomized female; WFT: WKY testosterone-treated ovariectomized female; SHR sham-operated intact male; SMO: SHR orchidectomized male; SFO: SHR ovariectomized female; SFT: SHR testosterone-treated ovariectomized female rats.

**Table 10.6 Summary of fold changes, both from edgeR analysis of RNA-Seq data and qPCR analysis, of genes down-regulated by chronic testosterone treatment based on the transcriptome analysis of RVLM.**

No.	Gene name	qPCR						Transcriptome		qPCR					
		WMO compare to WMS			WFT compare to WFO			SMO compare to SMS	SFT compare to SFO	SMO compare to SMS			SFT compare to SFO		
		WMS	WMO	P	WFO	WFT	P			SMS	SMO	P	SFO	SFT	P
1	<b>Cml3</b>	1.01	1.08		1.11	<b>0.81</b>	**	<b>1.34</b>	<b>0.67</b>	0.67	0.72		0.79	<b>0.53</b>	**
2	<b>Fabp5</b>	1.01	0.95		0.97	0.89		<b>1.22</b>	<b>0.69</b>	0.94	0.96		0.89	0.92	
3	<b>Trpm8</b>	1.02	<b>1.44</b>	*	1.63	<b>0.87</b>	***	<b>1.48</b>	<b>0.71</b>	0.49	<b>0.64</b>	*	0.63	<b>0.41</b>	*
4	<b>Etnk2</b>	1.01	1.00		1.03	<b>0.81</b>	*	<b>1.53</b>	<b>0.73</b>	1.43	1.43		1.48	<b>1.27</b>	*
5	<b>C3</b>	1.01	<b>1.51</b>	*	1.34	<b>0.99</b>	*	<b>1.32</b>	<b>0.73</b>	0.95	<b>1.47</b>	*	1.33	<b>0.83</b>	**
6	<b>Mpeg1</b>	1.01	1.06		1.21	<b>0.76</b>	***	<b>1.29</b>	<b>0.75</b>	0.52	<b>0.68</b>	*	0.54	<b>0.39</b>	*
7	<b>Fcrl2</b>	1.03	<b>1.46</b>	*	1.58	<b>0.84</b>	*	<b>1.64</b>	<b>0.75</b>	0.89	<b>1.29</b>	**	1.16	<b>0.60</b>	**
8	<b>GSTA1</b>	1.01	<b>1.32</b>	**	1.35	<b>0.97</b>	**	<b>1.15</b>	<b>0.77</b>	0.96	<b>1.21</b>	*	1.18	<b>0.93</b>	*
9	<b>Exosc3</b>	1.02	0.89		0.91	0.91		<b>1.26</b>	<b>0.78</b>	0.94	0.90		0.97	0.96	
10	<b>Asna1</b>	1.01	0.94		0.98	0.94		<b>1.31</b>	<b>0.78</b>	1.04	0.90		0.89	1.01	
11	<b>Got1</b>	1.02	0.89		0.95	0.95		<b>1.12</b>	<b>0.79</b>	0.91	0.85		0.86	0.98	
12	<b>Klhl25</b>	1.01	<b>1.23</b>	*	1.29	<b>0.99</b>	**	<b>1.25</b>	<b>0.81</b>	1.12	1.12		1.07	1.05	
13	<b>Hspa2</b>	1.02	1.06		1.14	<b>0.81</b>	**	<b>1.20</b>	<b>0.84</b>	1.05	1.08		1.05	<b>0.87</b>	*

Mean fold changes estimated from edgeR analysis of RNA-Seq data (Transcriptome) and qPCR analysis (n = 6/group, unpaired student's *t*-test where \**P*<0.05, \*\**P*<0.01, \*\*\**P*<0.001 compared to control group *i.e.* WMS, WFO, SMS and SFO) are presented in the table. Genes are listed based on the levels of expression changes (estimated by edgeR), from highest (top) to lowest (bottom) decrease, following chronic testosterone treatment in ovariectomized female SHR rats (SFT compare to SFO). Green values represent significant up-regulation while red values represent significant down-regulation of mRNA levels. Abbreviations: *P*: probability value; WMS: WKY sham-operated intact male; WMO: WKY orchidectomized male; WFO: WKY ovariectomized female; WFT: WKY testosterone-treated ovariectomized female; SHR sham-operated intact male; SMO: SHR orchidectomized male; SFO: SHR ovariectomized female; SFT: SHR testosterone-treated ovariectomized female rats.

### 10.2.2 Distribution of Ephx2 and Fcrl2 proteins in PVN

Distribution and co-localization of epoxide hydrolase 2 (Ephx2) and Fc receptor-like 2 (Fcrl2) proteins in PVN were assessed via double immunofluorescence staining. In Figure 10.11, immunofluorescence images revealed that Ephx2 (red fluorescent signals) and Fcrl2 (green fluorescent signals) were expressed abundantly in the MCNs of PVN, which located further from the third ventricle. A relatively lower distribution of Ephx2 proteins in PVN was observed following orchidectomy in male normotensive WKY rat. Meanwhile, in ovariectomized female rats, chronic exposure of testosterone resulted in relatively higher expression level of Ephx2 proteins when compared to those non-treated. In contrast, the expression of Fcrl2 proteins in PVN was relatively lower in orchidectomized male as compared to sham-operated intact normotensive WKY male rats. Nonetheless, a comparably higher distribution of this protein was found in PVN of testosterone-treated ovariectomized female as compared to those non-treated rats.

The immunofluorescence images showed the distribution and co-localization of Ephx2 (red fluorescent signals) and Fcrl2 (green fluorescent signals) in PVN of hypertensive SHR rats (Figure 10.12). A comparably highest red fluorescent signals were noted in PVN of testosterone-treated ovariectomized female rats, indicating a high expression level. In male SHR rats, the expression level of this protein was relatively decreased by orchidectomy. On the other hand, a relatively highest expression of Fcrl2 proteins was found in orchidectomized male hypertensive SHR rats. However, in ovariectomized female rats, the chronic administration of testosterone caused the expression of this protein to reduce as compared to those non-treated.

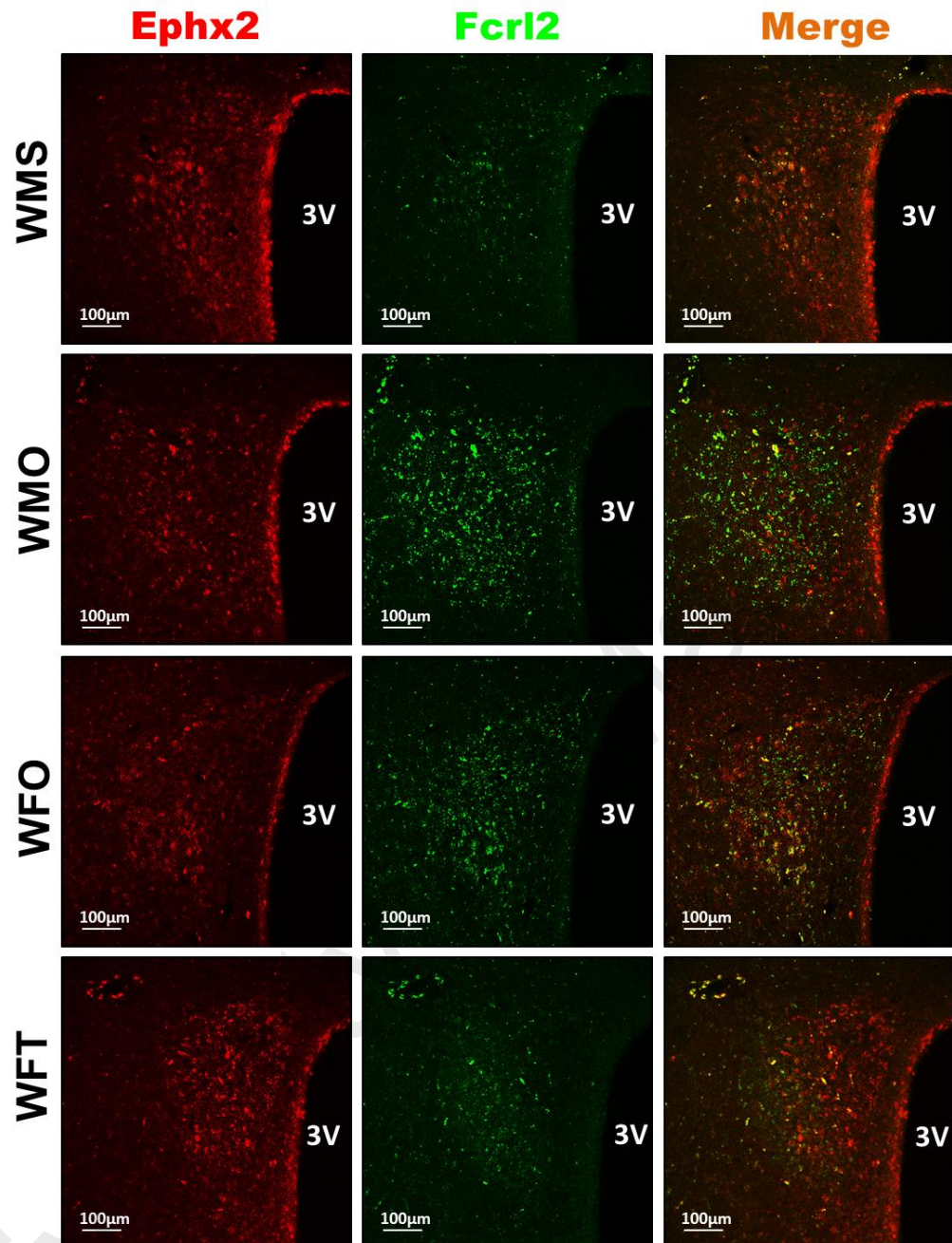


**Figure 10.11 Effects of chronic testosterone treatment on the distribution of Ephx2 (red) and Fcrl2 (green) in PVN of normotensive WKY rats.**

Representative double immunofluorescence images (n = 4/group) showing the distribution and localization of epoxide hydrolase 2 (Ephx2) and Fc receptor-like 2 (Fcrl2) proteins in PVN of normotensive WKY rats. Ephx2 proteins, represented by red fluorescent signals and Fcrl2 proteins, represented by green fluorescent signals were abundantly expressed in the PVN. In merged images, yellow signals indicated the co-localization of both proteins in PVN. Abbreviations: 3V: third ventricle; WMS: WKY sham-operated intact male; WMO: WKY orchidectomized male; WFO: WKY ovariectomized female; WFT: WKY testosterone-treated ovariectomized female rats. Scale bar = 100µm.

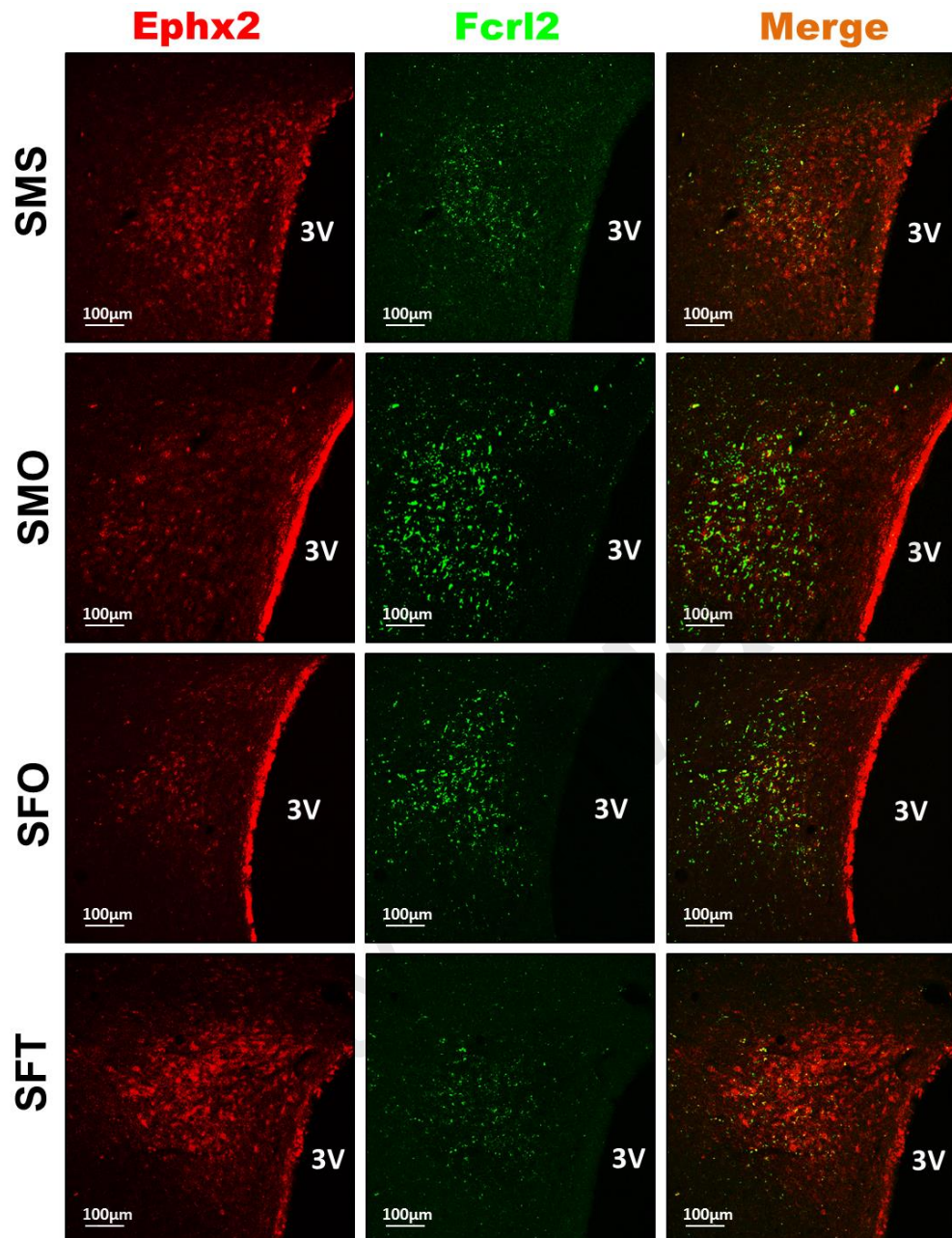


**Figure 10.12 Effects of chronic testosterone treatment on the distribution of Ephx2 (red) and Fcrl2 (green) in PVN of hypertensive SHR rats.**

Representative double immunofluorescence images (n = 4/group) showing the distribution and localization of epoxide hydrolase 2 (Ephx2) and Fc receptor-like 2 (Fcrl2) protein in PVN of hypertensive SHR rats. Ephx2 proteins, represented by red fluorescent signals and Fcrl2 proteins, represented by green fluorescent signals were abundantly expressed in the PVN. In merged images, yellow signals indicated the co-localization of both proteins in PVN. Abbreviations: 3V: third ventricle; SMS: SHR sham-operated intact male; SMO: SHR orchidectomized male; SFO: SHR ovariectomized female; SFT: SHR testosterone-treated ovariectomized female rats. Scale bar = 100µm.

### 10.3 Discussion

Although qPCR has been known as the method of choice to produce a reliable gene expression analysis with high accuracy, however many different factors could eventually affect the outcomes of the study, including the selection of appropriate housekeeping gene to be used as the reference genes (Aithal & Rajeswari, 2015). Prior to any qPCR determinations, the steady-state of mRNA levels of three housekeeping gene *i.e.* ribosomal protein L19 (RPL19), glyceraldehyde 3-phosphate dehydrogenase (GAPDH) and beta-actin (ACTB) were quantified in PVN, NTS and RVLM. Constant expression levels in these genes were observed across the treatment groups, indicating that the expression levels of these genes were not affected by the treatments performed in the current experiment. Therefore, these genes can be selected as the reference genes to normalize the absolute quantification of a specific gene expression in PVN, NTS and RVLM, in which the relative abundance value of a specific target gene could be estimated and compared against different treatment groups.

The roles of PVN oxytocin (OXT) and vasopressin (AVP)-synthesizing neurons in central control of blood pressures have been well documented in which gender-related differences in the expression levels of OXT and AVP in PVN were shown (Ishunina & Swaab, 1999; Thomas et al., 1996; Viau et al., 1999). In this study, the levels of pre-mature transcripts of OXT (hnOXT) and AVP (hnAVP) in PVN were quantified in addition to the mature transcripts detection. The heterogeneous nuclear RNA (hnRNA), also known as precursor mRNA, is an immature single strand mRNA, that subsequently modified and processed into mature transcripts. Due to its very short half-life, the changes in hnRNA levels could thus provide a more sensitive and effective detection of

gene transcription changes in compare with the detection of more stable mRNAs (Ma et al., 1997b).

In PVN, 13 genes i.e. *Banf1*, *Heyl*, *Parm1*, *NOL6*, *Ddah1*, *Ephx2*, *Gpr17*, *Oxt* and *hnOxt*, *Adcy3*, *Htra1*, *Fkbp5*, *Wnk2* and *Spon1* were found to be up-regulated while 2 genes i.e. *Fcrl2* and *Mx1* were down-regulated by testosterone in both normotensive and hypertensive rats. Recently, an association between *Banf1* (barrier-to-autointegration factor 1) mutation and pulmonary hypertension were shown in patients with progeroid syndrome (Puente et al., 2011). Meanwhile, *Parm1* (prostate androgen-regulated mucin-like protein 1) was previously reported to be highly up-regulated in prostate following orchidectomy in male rats (Bruyninx et al., 1999). However, in the present study, orchidectomy was found to significantly decrease while chronic testosterone exposure increased the expression of this gene in PVN, thus suggesting the possible tissue-dependent effects of testosterone. Despite the limited information available, *Parm1* that expressed predominantly in the endoplasmic reticulum (ER) of heart and skeletal muscle, have been reported to be involved in the development of hypertensive heart disease by inducing the ER stress and apoptotic cell death events (Isodono et al., 2010). Recently, there is an increase in the numbers of researches on *Ephx2* (epoxide hydrolase 2) gene. Genetic polymorphisms of EPHX2 gene have been reported to be associated with essential hypertension in human (Zhu et al., 2015). In addition, previous studies have reported the elevated expression of this gene in the kidneys of hypertensive inherited stress-induced arterial hypertension (ISIAH) rats where its role in controlling and modulating the vascular tone in the kidneys were suggested (Abramova et al., 2013). Meanwhile, the present study have demonstrated the up-regulation of *Ephx2* gene expression, with significantly higher abundances found in hypertensive rats than

normotensive rats, in PVN by testosterone. This finding has indicated the important roles of *Ephx2* gene in maintaining the hypertensive state and suggested a potential underlying mechanism by which testosterone increases the blood pressure (refer **Chapter 4**).

Higher accuracy of RNA-Seq analysis was observed in NTS in which the expression levels of as much as 15 genes *i.e.* *Sgk1*, *Prlh*, *Mpzl2*, *Gpd1*, *Glra4*, *Car14*, *Crlf1*, *Igfbp5*, *Olfml3*, *Wfdc1*, *Sult1a1*, *Tcn2*, *Gpr88*, *Heph* and *Hlf0* were increased while *Fcrl2*, *Cdh1* and *Car3* were decreased by testosterone. The higher accuracy of RNA-Seq could be in part due to the high amount of RNA from NTS, as compared to PVN and RVLM, that could reduce the chances of biasness during the sequencing run. In contrast, lesser numbers of genes were found to be regulated by testosterone in RVLM. The expression levels of *Heph*, *Iqgap2*, *Fkbp5*, *Htra1*, *Car14* and *Spon1* were increased while *Trpm8*, *C3*, *Fcrl2* and *GSTA1* were decreased by testosterone in RVLM of both normotensive and hypertensive rats. It is noted that *Fcrl2* (Fc receptor-like 2) was consistently regulated in a parallel pattern by testosterone in all three targeted areas, PVN, NTS and RVLM, thus indicating the potential roles of this gene in the central control of blood pressure. The expression levels of this gene were significantly increased by orchidectomy, which represented the loss of testosterone, and decreased when testosterone was administrated. These findings have suggested the possible protective effects of *Fcrl2* in which higher expression of this gene was found in PVN, NTS and RVLM of orchidectomized male and ovariectomized female with lower blood pressure. In addition, it is also postulated that testosterone reduces the expression level of this gene, causing the loss of protection and thus more likely to develop high blood pressure.

Meanwhile, as PVN has been known to play an important role in blood pressure regulation with strong literature backgrounds (Carmichael & Wainford, 2015; Holbein et al., 2014) and thus the protein distribution and localization of two highly potential genes, *Ephx2* and *Fcrl2* in PVN were assessed using double immunofluorescence staining method. PVN is a bilateral structure, located beside the top of the third ventricle in the anterior hypothalamus. Using the visual aid of third ventricle, PVN can thus be identified easily. The protein levels of *Ephx2* were increased while *Fcrl2* was decreased in PVN by testosterone. These results have thus further supported the hypothesis that testosterone-induced increases in blood pressure could involve the regulation of these genes in PVN. Together, the outcomes of this study have provided a better understanding of the expression changes in central cardiovascular control of the brain by which testosterone could exert its effects on blood pressure. In addition, this study has also discovered two highly potential target genes *i.e.* *Ephx2* and *Fcrl2* in the PVN, which could be involved in mediating the testosterone-induced increases in blood pressure (refer **Chapter 4**) and might in part responsible for the high blood pressure in men than age-matched premenopausal women.

## CHAPTER 11: CONCLUSION AND FUTURE STUDIES

### 11.1 Conclusion

The present study demonstrated that testosterone causes the increases in mean arterial pressure (MAP) in animal models in which these effects were further supported by the observed decreased in MAP following orchidectomy *i.e.* loss of endogenous testosterone. In the meantime, the effects of testosterone on the expression of epithelial sodium channels (ENaC) in kidneys were found to be dependent on the route and time frame of testosterone administration. Sub-chronic testosterone treatment (seven days) increased while chronic testosterone treatment (six weeks) decreased the expression levels of these proteins. Nevertheless, the study have however documented the roles of testosterone in regulating the expression of ENaC in kidney, which was accompanied by the alteration of some biochemical parameters *i.e.* plasma levels of sodium and osmolality. In addition, there were also changes in the expression levels of aquaporin subunits in the kidneys. Testosterone generally increased the expressions of the majority of aquaporin subunits in the kidney. The up-regulation of aquaporin subunits in the kidney could result in the enhanced water reabsorption activity, which eventually causes the increases in blood volume and blood pressure. Therefore, it is suggested that testosterone could influence the blood pressure by regulating the expression of water channel, aquaporin in the kidneys.

Meanwhile, the roles of central neural control of the cardiovascular system in mediating the testosterone-induced increase in blood pressure were also investigated. Following the study on the changes in the transcriptome profiles of three important cardiovascular control regions *i.e.* PVN, NTS and RVLM in the brain using RNASeq, a large number of genes of variety functions were shown to be significantly regulated by

testosterone in these areas, in which a number of candidate genes were then selected, based on their fold changes and significant values, for subsequent qPCR determination. Based on the qPCR data, 13 genes *i.e.* *Banfl*, *Heyl*, *Parm1*, *NOL6*, *Ddah1*, *Ephx2*, *Gpr17*, *Oxt* and *hnOxt*, *Adcy3*, *Htra1*, *Fkbp5*, *Wnk2* and *Spon1* were found to be up-regulated while 2 genes *i.e.* *Fcrl2* and *Mx1* down-regulated by testosterone in PVN under both normotensive and hypertensive conditions. Nonetheless, in NTS, testosterone increased the expression levels of as much as 15 genes *i.e.* *Sgk1*, *Prlh*, *Mpzl2*, *Gpd1*, *Glra4*, *Car14*, *Crlf1*, *Igfbp5*, *Olfml3*, *Wfdc1*, *Sult1a1*, *Tcn2*, *Gpr88*, *Heph* and *Hlf0* while the expressions of 3 genes *i.e.* *Fcrl2*, *Cdh1* and *Car3* were decreased. Meanwhile, the least number of genes regulated by testosterone was found in RVLM. Following testosterone treatment, the gene expression levels of 6 genes *i.e.* *Heph*, *Iqgap2*, *Fkbp5*, *Htra1*, *Car14* and *Spon1* were increased while 4 genes *i.e.* *Trpm8*, *C3*, *Fcrl2* and *GSTA1* were decreased in RVLM. Taken together, these data have revealed the down-regulation of *Fcrl2* by testosterone in all three regions, suggesting potential roles of this gene in the testosterone-induced increase in blood pressure. In addition, testosterone was also found to cause an increase in the distribution of EPHX2 proteins while a decrease in FCRL2 proteins in PVN. These findings have not only further supported the protective roles of FCRL2, yet also highlighted the roles of EPHX2 in accelerating the development of high blood pressure in men. In fact, the qPCR data have also reported that the *Ephx2* mRNA expression levels were 13-18 folds higher in the PVN of hypertensive rats than normotensive rats.

The present study has revealed a number of potential underlying mechanisms by which testosterone could cause increased blood pressure. The current finding has at least, in part, explain the high blood pressure in men than women before menopause and the increased blood pressure following menopause in women, which could be due to the

higher testosterone levels or changes in the ratio of testosterone to estradiol (T/E). In addition, the transcriptome data of PVN, NTS and RVLM could also serve as a reference source for better understanding of gender-associated differences in central neural control of blood pressure.

University of Malaya

## 11.2 Limitation of the present study

This study has several limitations. Rat models were used to reflect the natural course and causative background of human essential hypertension and thus one of the limitations of the current study are lack of confirmation of the results by using human samples. In the present study, the blood pressure measurements were carried out in anesthetized rats, which might not reflect the exact changes in blood pressure as in the conscious animals. Meanwhile, due to the limited amount of samples (PVN, NTS and RVLM) from small sized animals studied, the transcriptome study was conducted using pooled samples in which biases might be introduced during sample pooling, thus resulting in an increase the chances of false discovery.

## 11.3 Future studies

The findings of the current study pave interesting avenues for future studies in discovering more genes that contributed to the gender-differences in blood pressure. Functional studies could be carried out to investigate the roles of genes identified *i.e.* EPHX2 and FCRL2. In view of the advance in bioinformatics tools today, in addition to the differential expression studies, more analysis can be performed on the transcriptome datasets in order to identify the potential transcriptional factors (*i.e.* small RNA or non-coding RNA) and alternative splicing events that may be regulated by testosterone and thus improving the understanding of gender-related difference in blood pressure regulation. Further, translation studies could be performed by comparing these transcriptome datasets (rat) with the available comprehensive human genetic data, thus allowing the identification of potential concordant genes that are also found in human.

## REFERENCES

- Abhishekh, H. A., Nisarga, P., Kisan, R., Meghana, A., Chandran, S., Trichur, Raju, & Sathyaprabha, T. N. (2013). Influence of age and gender on autonomic regulation of heart. *Journal of Clinical Monitoring and Computing*, 27(3): 259-264. doi: 10.1007/s10877-012-9424-3
- Abramova, T. O., Redina, O. E., Smolenskaya, S. E., & Markel, A. L. (2013). Elevated expression of the Ephx2 mRNA in the kidney of hypertensive ISIAH rats. *Molecular Biology*, 47(6): 821-826. doi: 10.1134/S0026893313060022
- Accorsi-Mendonça, D., & Machado, B. H. (2013). Synaptic transmission of baro- and chemoreceptors afferents in the NTS second order neurons. *Autonomic Neuroscience*, 175(1-2): 3-8. doi: 10.1016/j.autneu.2012.12.002
- Adams, M. D., Kelley, J. M., Gocayne, J. D., Dubnick, M., Polymeropoulos, M. H., Xiao, H., . . . Venter, J. C. (1991). Complementary-DNA sequencing - Expressed sequence tags and human genom project. *Science*, 252(5013): 1651-1656. doi: 10.1126/science.2047873
- Affleck, V. S., Coote, J. H., & Pyner, S. (2012). The projection and synaptic organisation of NTS afferent connections with presympathetic neurons, GABA and nNOS neurons in the paraventricular nucleus of the hypothalamus. *Neuroscience*, 219: 48-61. doi: 10.1016/j.neuroscience.2012.05.070
- Agarwal, S. K., Gelsema, A. J., & Calaresu, F. R. (1990). Inhibition of rostral VLM by baroreceptor activation is relayed through caudal VLM. *American Journal of Physiology*, 258(5 Pt 2): R1271-1278.
- Agarwal, S. K., & Gupta, A. (2008). Aquaporins: The renal water channels. *Indian Journal of Nephrology*, 18(3): 95-100. doi: 10.4103/0971-4065.43687
- Aithal, M. G. S., & Rajeswari, N. (2015). Validation of Housekeeping Genes for Gene Expression Analysis in Glioblastoma Using Quantitative Real-Time Polymerase Chain Reaction. *Brain Tumor Research and Treatment*, 3(1): 24-29. doi: 10.14791/btrt.2015.3.1.24
- Akaishi, T., Negoro, H., & Kobayasi, S. (1980). Responses of paraventricular and supraoptic units to angiotensin II, sar1-ile8-angiotensin II and hypertonic NaCl administered into the cerebral ventricle. *Brain Research*, 188(2): 499-511.
- Alexandru, I. (2011). Experimental use of animals in research spa. *Balneo-Research Journal* 2(1): 65-69.
- Ammar, E. M., Said, S. A., & Hassan, M. S. (2004). Enhanced vasoconstriction and reduced vasorelaxation induced by testosterone and nandrolone in hypercholesterolemic rabbits. *Pharmacological Research*, 50(3): 253-259. doi: 10.1016/j.phrs.2004.03.010
- Amory, J. K., & Bremner, W. (2001). Endocrine regulation of testicular function in men: implications for contraceptive development. *Molecular and Cellular Endocrinology*, 182(2): 175-179.

- Anders, S., & Huber, W. (2010). Differential expression analysis for sequence count data. *Genome Biology*, 11(10): R106. doi: 10.1186/gb-2010-11-10-r106
- Anders, S., McCarthy, D. J., Chen, Y. F., Okoniewski, M., Smyth, G. K., Huber, W., & Robinson, M. D. (2013). Count-based differential expression analysis of RNA sequencing data using R and Bioconductor. *Nature Protocols*, 8(9): 1765-1786. doi: 10.1038/nprot.2013.099
- Anders, S., Pyl, P. T., & Huber, W. (2015). HTSeq--a Python framework to work with high-throughput sequencing data. *Bioinformatics*, 31(2): 166-169. doi: 10.1093/bioinformatics/btu638
- Anderson, J. W., Washburn, D. L., & Ferguson, A. V. (2000). Intrinsic osmosensitivity of subfornical organ neurons. *Neuroscience*, 100(3): 539-547.
- Andresen, M. C., Doyle, M. W., Bailey, T. W., & Jin, Y. H. (2004). Differentiation of autonomic reflex control begins with cellular mechanisms at the first synapse within the nucleus tractus solitarius. *Brazilian Journal of Medical and Biological Research*, 37: 549-558.
- Ashton, N., & Balment, R. J. (1991). Sexual dimorphism in renal function and hormonal status of New Zealand genetically hypertensive rats. *Acta Endocrinologica (Copenhagen)*, 124(1): 91-97.
- Auger, C. J., Coss, D., Auger, A. P., & Forbes-Lorman, R. M. (2011). Epigenetic control of vasopressin expression is maintained by steroid hormones in the adult male rat brain. *Proceedings of the National Academy of Sciences U S A*, 108(10): 4242-4247. doi: 10.1073/pnas.1100314108
- Badaut, J., Lasbennes, F., Magistretti, P. J., & Regli, L. (2002). Aquaporins in brain: distribution, physiology, and pathophysiology. *Journal of Cerebral Blood Flow and Metabolism*, 22(4): 367-378. doi: 10.1097/00004647-200204000-00001
- Badoer, E. (2001). Hypothalamic paraventricular nucleus and cardiovascular regulation. *Clinical and Experimental Pharmacology and Physiology*, 28(1-2): 95-99.
- Bainbridge, M. N., Warren, R. L., Hirst, M., Romanuik, T., Zeng, T., Go, A., . . . Jones, S. J. M. (2006). Analysis of the prostate cancer cell line LNCaP transcriptome using a sequencing-by-synthesis approach. *BMC Genomics*, 7(1): 1-11. doi: 10.1186/1471-2164-7-246
- Bargmann, W. (1966). Neurosecretion. *International Review of Cytology*, 19: 183-201.
- Barnett, S. R., Morin, R. J., Kiely, D. K., Gagnon, M., Azhar, G., Knight, E. L., . . . Lipsitz, L. A. (1999). Effects of age and gender on autonomic control of blood pressure dynamics. *Hypertension*, 33(5): 1195-1200.
- Barrett, K. E., Brooks, H. L., Boitano, S., & Barman, S. M. (2010). Renal Physiology *Ganong's review of medical physiology* (Vol. 23, pp. 639-686): The McGraw-Hill Companies.

- Barsha, G., Denton, K. M., Mirabito, C., & Katrina, M. (2016). Sex- and age-related differences in arterial pressure and albuminuria in mice. *Biology of Sex Differences*, 7(57): 1-15. doi: 10.1186/s13293-016-0110-x
- Benga, G. (2004). The first water channel protein (later called aquaporin 1) was first discovered in Cluj-Napoca, Romania. *Romanian journal of physiology*, 41(1-2): 3-20.
- Benga, G. (2009). Water channel proteins (later called aquaporins) and relatives: Past, present, and future. *IUBMB Life*, 61(2): 112-133. doi: 10.1002/iub.156
- Benga, G. (2012). The first discovered water channel protein, later called aquaporin 1: molecular characteristics, functions and medical implications. *Molecular Aspects of Medicine*, 33(5-6): 518-534. doi: 10.1016/j.mam.2012.06.001
- Berecek, K. H., & Swords, B. H. (1990). Central role for vasopressin in cardiovascular regulation and the pathogenesis of hypertension. *Hypertension*, 16(3): 213-224.
- Bhalla, V., & Hallows, K. R. (2008). Mechanisms of ENaC regulation and clinical implications. *Journal of the American Society of Nephrology*, 19(10): 1845-1854. doi: 10.1681/asn.2008020225
- Bingham, B., Williamson, M., & Viau, V. (2006). Androgen and estrogen receptor-beta distribution within spinal-projecting and neurosecretory neurons in the paraventricular nucleus of the male rat. *Journal of Comparative Neurology*, 499(6): 911-923. doi: 10.1002/cne.21151
- Blair, M. L., Piekut, D., Want, A., & Olschowka, J. A. (1996). Role of the hypothalamic paraventricular nucleus in cardiovascular regulation. *Clinical and Experimental Pharmacology and Physiology*, 23(2): 161-165.
- Blanks, A. M., & Thornton, S. (2003). The role of oxytocin in parturition. *BJOG*, 110 Suppl 20: 46-51.
- Bourassa, E. A., Sved, A. F., & Speth, R. C. (2009). Angiotensin modulation of rostral ventrolateral medulla (RVLM) in cardiovascular regulation. *Molecular and Cellular Endocrinology*, 302(2): 167-175. doi: 10.1016/j.mce.2008.10.039
- Bourque, C. W., Oliet, S. H., & Richard, D. (1994). Osmoreceptors, osmoreception, and osmoregulation. *Frontiers in Neuroendocrinology*, 15(3): 231-274. doi: 10.1006/frne.1994.1010
- Bourque, C. W., Voisin, D. L., & Chakfe, Y. (2002). Stretch-inactivated cation channels: cellular targets for modulation of osmosensitivity in supraoptic neurons. *Progress in Brain Research*, 139: 85-94.
- Boynton, R. E., & Todd, R. L. (1947). Blood pressure readings of 75,258 university students. *Archives of internal medicine (Chicago)*, 80(4): 454-462.
- Braga, V. A. (2011). Differential brain angiotensin-II type I receptor expression in hypertensive rats. *Journal of Veterinary Science*, 12(3): 291-293. doi: 10.4142/jvs.2011.12.3.291

- Broulik, P. D., Kochakian, C. D., & Dubovsky, J. (1973). Influence of Castration and Testosterone Propionate on Cardiac Output, Renal Blood Flow, and Blood Volume in Mice. *Experimental Biology and Medicine*, *144*(2): 671-673. doi: 10.3181/00379727-144-37659
- Brownlow, M. A., & Hutchins, D. R. (1982). The concept of osmolality: its use in the evaluation of "dehydration" in the horse. *Equine Veterinary Journal*, *14*(2): 106-110.
- Bruyninx, M., Hennuy, B., Cornet, A., Houssa, P., Daukandt, M., Reiter, E., . . . Hennen, G. (1999). A novel gene overexpressed in the prostate of castrated rats: hormonal regulation, relationship to apoptosis and to acquired prostatic cell androgen independence. *Endocrinology*, *140*(10): 4789-4799. doi: 10.1210/endo.140.10.7097
- Bubien, J. K. (2010). Epithelial Na<sup>(+)</sup> channel (ENaC), hormones, and hypertension. *The Journal of Biological Chemistry*, *285*(31): 23527-23531.
- Buemi, M., Nostro, L., Di Pasquale, G., Cavallaro, E., Sturiale, A., Floccari, F., . . . Frisina, N. (2004). Aquaporin-2 water channels in spontaneously hypertensive rats. *American Journal of Hypertension*, *17*(12 Pt 1): 1170-1178. doi: 10.1016/j.amjhyper.2004.07.003
- Burbach, J. P.H., Luckman, S. M., Murphy, D., & Gainer, H. (2001). Gene regulation in the magnocellular hypothalamo-neurohypophysial system. *Physiological Reviews*, *81*(3): 1197-1267.
- Burns, J., Sivananthan, M. U., Ball, S. G., Mackintosh, A. F., Mary, D. A., & Greenwood, J. P. (2007). Relationship between central sympathetic drive and magnetic resonance imaging-determined left ventricular mass in essential hypertension. *Circulation*, *115*(15): 1999-2005. doi: 10.1161/circulationaha.106.668863
- Burt, V. L., Whelton, P., Roccella, E. J., Brown, C., Cutler, J. A., Higgins, M., . . . Labarthe, D. (1995). Prevalence of hypertension in the US adult population. Results from the Third National Health and Nutrition Examination Survey, 1988-1991. *Hypertension*, *25*(3): 305-313.
- Butterworth, M. B. (2010). Regulation of the epithelial sodium channel (ENaC) by membrane trafficking. *Biochimica et Biophysica Acta (BBA) - Molecular Basis of Disease*, *1802*(12): 1166-1177. doi: 10.1016/j.bbadis.2010.03.010
- Byers, S. L., Wiles, M. V., Dunn, S. L., & Taft, R. A. (2012). Mouse estrous cycle identification tool and images. *PLoS One*, *7*(4): e35538. doi: 10.1371/journal.pone.0035538
- Calaresu, F. R., & Yardley, C. P. (1988). Medullary basal sympathetic tone. *Annual Review of Physiology*, *50*: 511-524. doi: 10.1146/annurev.ph.50.030188.002455
- Campelo, A. E., Cutini, P. H., & Massheimer, V. L. (2012). Testosterone modulates platelet aggregation and endothelial cell growth through nitric oxide pathway. *Journal of Endocrinology*, *213*(1): 77-87. doi: 10.1530/joe-11-0441

- Capone, C., Anrather, J., Milner, T. A., & Iadecola, C. (2009). Estrous cycle dependent neurovascular dysfunction induced by angiotensin II in the mouse neocortex. *Hypertension*, *54*(2): 302-307. doi: 10.1161/hypertensionaha.109.133249
- Carbajosa, N. A. L., Corradi, G., Verrilli, M. A. L., Guil, M. J., Vatta, M. S., & Gironacci, M. M. (2015). Tyrosine hydroxylase is short-term regulated by the ubiquitin-proteasome system in PC12 cells and hypothalamic and brainstem neurons from Spontaneously Hypertensive Rats: possible implications in hypertension. *PLoS One*, *10*(2): e0116597. doi: 10.1371/journal.pone.0116597
- Carmichael, C. Y., & Wainford, R. D. (2015). Hypothalamic Signaling Mechanisms in Hypertension. *Current Hypertension Reports*, *17*(39): 1-9. doi: 10.1007/s11906-015-0550-4
- Catudioc-Vallero, J., Sands, J. M., Klein, J. D., Sidorowicz, H. E., & Sladek, C. D. (2000). Effect of age and testosterone on the vasopressin and aquaporin responses to dehydration in Fischer 344/Brown-Norway F1 rats. *Journals of Gerontology Series A - Biological Sciences and Medical Sciences*, *55*(1): B26-34.
- Ceballos, G., Figueroa, L., Rubio, I., Gallo, G., Garcia, A., Martinez, A., . . . Chamorro, G. (1999). Acute and nongenomic effects of testosterone on isolated and perfused rat heart. *Journal of Cardiovascular Pharmacology*, *33*(5): 691-697.
- Chakrabarti, N., Tajkhorshid, E., Roux, B., & Pomès, R. (2004). Molecular Basis of Proton Blockage in Aquaporins. *Structure*, *12*(1): 65-74. doi: 10.1016/j.str.2003.11.017
- Charkoudian, N., & Rabbitts, J. A. (2009). Sympathetic neural mechanisms in human cardiovascular health and disease. *Mayo Clinic Proceedings*, *84*(9): 822-830.
- Cheema, M. U., Irsik, D. L., Wang, Y., Miller-Little, W., Hyndman, K. A., Marks, E. S., . . . Norregaard, R. (2015). Estradiol regulates AQP2 expression in the collecting duct: a novel inhibitory role for estrogen receptor  $\alpha$ . *American Journal of Physiology-Renal Physiology*, *309*(4): F305-F317.
- Chen, M., Cai, H., Klein, J. D., Laur, O., & Chen, G. (2015). Dexamethasone increases aquaporin-2 protein expression in ex vivo inner medullary collecting duct suspensions. *Frontiers in Physiology*, *6*: 310. doi: 10.3389/fphys.2015.00310
- Chen, M. J., Yang, W. S., Yang, J. H., Chen, C. L., Ho, H. N., & Yang, Y. S. (2007). Relationship between androgen levels and blood pressure in young women with polycystic ovary syndrome. *Hypertension*, *49*(6): 1442-1447. doi: 10.1161/hypertensionaha.106.083972
- Chen, Y. F., & Meng, Q. C. (1991). Sexual dimorphism of blood pressure in spontaneously hypertensive rats is androgen dependent. *Life Sciences*, *48*(1): 85-96. doi: 10.1016/0024-3205(91)90428-e
- Chen, Y. F., Naftilan, A. J., & Oparil, S. (1992). Androgen-dependent angiotensinogen and renin messenger RNA expression in hypertensive rats. *Hypertension*, *19*(5): 456-463.

- Chignalia, A. Z., Schuldt, E. Z., Camargo, L. L., Montezano, A. C., Callera, G. E., Laurindo, F. R., . . . Tostes, R. C. (2012). Testosterone induces vascular smooth muscle cell migration by NADPH oxidase and c-Src-dependent pathways. *Hypertension*, 59(6): 1263-1271. doi: 10.1161/hypertensionaha.111.180620
- Chinnathambi, V., Balakrishnan, M., Yallampalli, C., & Sathishkumar, K. (2012). Prenatal testosterone exposure leads to hypertension that is gonadal hormone-dependent in adult rat male and female offspring. *Biology of reproduction*, 86(5): 1-7.
- Chinnathambi, V., Yallampalli, C., & Sathishkumar, K. (2013). Prenatal testosterone induces sex-specific dysfunction in endothelium-dependent relaxation pathways in adult male and female rats. *Biology of Reproduction*, 89(4): 97. doi: 10.1095/biolreprod.113.111542
- Choe, K. Y., & Bourque, C. W. (2014). The osmotic control of vasopressin-releasing neurons. In W. E. Armstrong & J. G. Tasker (Eds.), *Neurophysiology of Neuroendocrine Neurons*. United Kingdom: John Wiley & Sons. Copyright. .
- Chou, C. L., Ma, T., Yang, B., Knepper, M. A., & Verkman, A. S. (1998). Fourfold reduction of water permeability in inner medullary collecting duct of aquaporin-4 knockout mice. *American Journal of Physiology - Cell Physiology*, 274(2): C549-C554.
- Chow, P. K. H., Ng, R. T. H., & Ogden, B. E. (2007). *Using animal models in biomedical research: A primer for the investigator*. United Kingdom: World Scientific Publishing Co. Pte. Ltd.
- Chu, Y., & Corey, D. R. (2012). RNA Sequencing: Platform selection, experimental design, and data interpretation. *Nucleic Acid Therapeutics*, 22(4): 271-274. doi: 10.1089/nat.2012.0367
- Ciura, S., & Bourque, C. W. (2006). Transient receptor potential vanilloid 1 is required for intrinsic osmoreception in organum vasculosum lamina terminalis neurons and for normal thirst responses to systemic hyperosmolality. *Journal of Neuroscience*, 26(35): 9069-9075. doi: 10.1523/jneurosci.0877-06.2006
- Coffman, T. M., & Crowley, S. D. (2008). Kidney in hypertension: Guyton redux. *Hypertension*, 51(4): 811-816. doi: 10.1161/hypertensionaha.105.063636
- Cohen, P. E., & Milligan, S. R. (1993). Silastic implants for delivery of oestradiol to mice. *Journal of reproduction and fertility*, 99(1): 219-223.
- Colombari, E., Sato, M. A., Cravo, S. L., Bergamaschi, C. T., Campos, R. R., & Lopes, O. U. (2001). Role of the medulla oblongata in hypertension. *Hypertension*, 38(3): 549-554. doi: 10.1161/01.hyp.38.3.549
- Cooke, B. A., Choi, M. C. K., Dirami, G., Lopez-Ruiz, M. P., & West, A. P. (1992). Control of steroidogenesis in Leydig cells. *The Journal of Steroid Biochemistry and Molecular Biology*, 43(5): 445-449. doi: 10.1016/0960-0760(92)90083-U

- Coote, J. H., Gardner, J., Gladwell, S., Sermasi, E., Ranson, R., Motawei, K., & Pyner, S. (1997). The hypothalamic paraventricular nucleus and blood pressure control. *Fundamental and Clinical Pharmacology*, *11*(S1): 26s-30s. doi: 10.1111/j.1472-8206.1997.tb00870.x
- Cora, M. C., Kooistra, L., & Travlos, G. (2015). Vaginal cytology of the laboratory rat and mouse: Review and criteria for the staging of the estrous cycle using stained vaginal smears. *Toxicologic Pathology*, *43*(6): 776-793. doi: 10.1177/0192623315570339
- Coutinho, T., Borlaug, B. A., Pellikka, P. A., Turner, S. T., & Kullo, I. J. (2013). Sex Differences in Arterial Stiffness and Ventricular-Arterial Interactions. *Journal of the American College of Cardiology*, *61*(1): 96-103. doi: 10.1016/j.jacc.2012.08.997
- Cowley, A. W., & Roman, R. J. (1989). Control of blood and extracellular volume. *Baillière's Clinical Endocrinology and Metabolism*, *3*(2): 331-369.
- Crofton, J. T., & Share, L. (1997). Gonadal hormones modulate deoxycorticosterone-salt hypertension in male and female rats. *Hypertension*, *29*(1): 494-499.
- Crofton, J. T., Ota, M., & Share, L. (1993). Role of vasopressin, the renin-angiotensin system and sex in Dahl salt-sensitive hypertension. *Journal of Hypertension*, *11*(10): 1031-1038. doi: 10.1097/00004872-199310000-00005
- Crowley, S. D., Gurley, S. B., Herrera, M. J., Ruiz, P., Griffiths, R., Kumar, A. P., . . . Coffman, T. M. (2006). Angiotensin II causes hypertension and cardiac hypertrophy through its receptors in the kidney. *Proceedings of the National Academy of Sciences USA*, *103*(47): 17985-17990. doi: 10.1073/pnas.0605545103
- Csaki, A., Kocsis, K., Halasz, B., & Kiss, J. (2000). Localization of glutamatergic/aspartatergic neurons projecting to the hypothalamic paraventricular nucleus studied by retrograde transport of [<sup>3</sup>H]D-aspartate autoradiography. *Neuroscience*, *101*(3): 637-655.
- Cui, L. N., Coderre, E., & Renaud, L. P. (2001). Glutamate and GABA mediate suprachiasmatic nucleus inputs to spinal-projecting paraventricular neurons. *American Journal of Physiology - Regulatory, Integrative and Comparative Physiology*, *281*(4): R1283-1289.
- Curtis, K. S. (2009). Estrogen and the central control of body fluid balance. *Physiology and Behavior*, *97*(2): 180-192. doi: 10.1016/j.physbeh.2009.02.027
- Cutler, J. A., Sorlie, P. D., Wolz, M., Thom, T., Fields, L. E., & Roccella, E. J. (2008). Trends in hypertension prevalence, awareness, treatment, and control rates in United States adults between 1988-1994 and 1999-2004. *Hypertension*, *52*(5): 818-827. doi: 10.1161/hypertensionaha.108.113357
- Dalmasso, C., Maranon, R. O., Patil, C. N., Moulana, M., Romero, D. G., & Reckelhoff, J. F. (2016). 20-HETE and CYP4A2  $\omega$ -hydroxylase contribute to the elevated

blood pressure in hyperandrogenemic female rats. *American Journal of Physiology - Renal Physiology*, 311(1): F71-F77.

- Dalpia, P. L. M., Lamas, A. Z., Caliman, I. F., Ribeiro, R. F., Abreu, G. R., Moyses, M. R., . . . Bissoli, N. S. (2015). Sex hormones promote opposite effects on ACE and ACE2 activity, hypertrophy and cardiac contractility in spontaneously hypertensive rats. *PLoS One*, 10(5): e0127515. doi: 10.1371/journal.pone.0127515
- Dampney, R. A. (1994). Functional organization of central pathways regulating the cardiovascular system. *Physiological Reviews*, 74(2): 323-364.
- Dampney, R. A., Goodchild, A. K., & McAllen, R. M. (1987). Vasomotor control by subretrofacial neurones in the rostral ventrolateral medulla. *Canadian Journal of Physiology and Pharmacology*, 65(8): 1572-1579.
- Dampney, R. A., & Horiuchi, J. (2003). Functional organisation of central cardiovascular pathways: studies using c-fos gene expression. *Progress Neurobiology*, 71(5): 359-384.
- Danziger, J., & Zeidel, M. L. (2015). Osmotic homeostasis. *Clinical Journal of the American Society of Nephrology*, 10(5): 852-862. doi: 10.2215/cjn.10741013
- Dart, A. M., Du, X. J., & Kingwell, B. A. (2002). Gender, sex hormones and autonomic nervous control of the cardiovascular system. *Cardiovascular Research*, 53(3): 678-687.
- Davern, P. J., & Head, G. A. (2007). Fos-related antigen immunoreactivity after acute and chronic angiotensin II-induced hypertension in the rabbit brain. *Hypertension*, 49(5): 1170-1177. doi: 10.1161/hypertensionaha.106.086322
- Davidson, S. M., & Duchon, M. R. (2007). Endothelial mitochondria: contributing to vascular function and disease. *Circulation Research*, 100(8): 1128-1141. doi: 10.1161/01.RES.0000261970.18328.1d
- Davis, D. D., Ruiz, A. L., Yanes, L. L., Iliescu, R., Yuan, K., Moulana, M., . . . Reckelhoff, J. F. (2012). Testosterone supplementation in male obese Zucker rats reduces body weight and improves insulin sensitivity, but increases blood pressure. *Hypertension*, 59(3): 726-731. doi: 10.1161/hypertensionaha.111.180943
- De Melo, V. U., Saldanha, R. R. M., Dos Santos, C. R., De Campos Cruz, J., Lira, V. A., Santana-Filho, V. J., & Michelini, Li. C. (2016). Ovarian hormone deprivation reduces oxytocin expression in paraventricular nucleus preautonomic neurons and correlates with baroreflex impairment in rats. *Frontiers in Physiology*, 7: Article 461. doi: 10.3389/fphys.2016.00461
- de Seigneux, S., Nielsen, J., Olesen, E. T. B., Dimke, H., Kwon, T. H., Frøkiær, J., & Nielsen, S. (2007). Long-term aldosterone treatment induces decreased apical but increased basolateral expression of AQP2 in CCD of rat kidney. *American Journal of Physiology-Renal Physiology*, 293(1): F87-F99.

- de Simone, G., Devereux, R. B., Roman, M. J., Ganau, A., Chien, S., Alderman, M. H., . . . Laragh, J. H. (1991). Gender differences in left ventricular anatomy, blood viscosity and volume regulatory hormones in normal adults. *The American Journal of Cardiology*, *68*(17): 1704-1708.
- Deen, P. M., Verdijk, M. A., Knoers, N. V., Wieringa, B., Monnens, L. A., van Os, C. H., & van Oost, B. A. (1994). Requirement of human renal water channel aquaporin-2 for vasopressin-dependent concentration of urine. *Science*, *264*(5155): 92-95. doi: 10.1126/science.8140421
- Denayer, T., Stöhr, T., & Van Roy, M. (2014). Animal models in translational medicine: Validation and prediction. *New Horizons in Translational Medicine*, *2*(1): 5-11. doi: 10.1016/j.nhtm.2014.08.001
- Denker, B. M., Smith, B. L., Kuhajda, F. P., & Agre, P. (1988). Identification, purification, and partial characterization of a novel Mr 28,000 integral membrane protein from erythrocytes and renal tubules. *Journal of Biological Chemistry*, *263*(30): 15634-15642.
- Dias, D.P.M., Oliveira, M., Salgado, H.C., & Fazan Jr., R. (2010). Ovariectomy does not affect the cardiac sympathovagal balance of female SHR but estradiol does. *Brazilian Journal of Medical and Biological Research*, *43*: 969-975.
- Dimkpa, U., Ugwu, A. C., & Oshi, D. C. . (2008). Assessment of sex differences in systolic blood pressure responses to exercise in healthy non-athletic young adults. *Journal of Exercise Physiology Online*, *11*(2): 18–25.
- Doggrell, S. A., & Brown, L. (1998). Rat models of hypertension, cardiac hypertrophy and failure. *Cardiovascular Research*, *39*(1): 89-105. doi: 10.1016/s0008-6363(98)00076-5
- Drago, F., Lo Presti, L., Nardo, F., Panella, I., Matera, M., & Scapagnini, U. (1982). Aromatization of testosterone by adipose tissue and sexual behavior of castrated male rats. *Biology of Reproduction*, *27*(4): 765-770.
- Dubey, R. K., & Jackson, E. K. (2001). Estrogen-induced cardiorenal protection: potential cellular, biochemical, and molecular mechanisms. *American Journal of Physiology - Renal Physiology*, *280*(3): F365-388.
- Dubey, R. K., Oparil, S., Imthurn, B., & Jackson, E. K. (2002). Sex hormones and hypertension. *Cardiovasc Res*, *53*: 688-708. doi: 10.1016/s0008-6363(01)00527-2
- Duskova, M., & Pospisilova, H. (2011). The role of non-aromatizable testosterone metabolite in metabolic pathways. *Physiological Research*, *60*(2): 253-261.
- Eaton, D. C., Becchetti, A., Ma, H., & Ling, B. N. (1995). Renal sodium channels: Regulation and single channel properties. *Kidney International*, *48*(4): 941-949. doi: 10.1038/ki.1995.375
- Ebine, T., Toriumi, H., Shimizu, T., Unekawa, M., Takizawa, T., Kayama, Y., . . . Suzuki, N. (2016). Alterations in the threshold of the potassium concentration to

evoke cortical spreading depression during the natural estrous cycle in mice. *Neuroscience Research*, 112: 57-62. doi: 10.1016/j.neures.2016.06.001

- Ecelbarger, C. A., Terris, J., Frindt, G., Echevarria, M., Marples, D., Nielsen, S., & Knepper, M. A. (1995). Aquaporin-3 water channel localization and regulation in rat kidney. *American Journal of Physiology - Renal Physiology*, 269(5): F663-F672.
- Echiburú, B., Crisosto, N., Maliqueo, M., Pérez-Bravo, F., de Guevara, A. L., Hernández, P., . . . Sir-Petermann, T. (2016). Metabolic profile in women with polycystic ovary syndrome across adult life. *Metabolism*, 65(5): 776-782. doi: 10.1016/j.metabol.2016.01.006
- Edinger, R. S., Bertrand, C. A., Rondandino, C., Apodaca, G. A., Johnson, J. P., & Butterworth, M. I. B. (2012). The epithelial sodium channel (ENaC) establishes a trafficking vesicle pool responsible for its regulation. *PLoS One*, 7(9): e46593.
- Ellis, J. A., Stebbing, M., & Harrap, S. B. (2000). Association of the human Y chromosome with high blood pressure in the general population. *Hypertension*, 36(5): 731-733.
- Ellison, K. E., Ingelfinger, J. R., Pivor, M., & Dzau, V. J. (1989). Androgen regulation of rat renal angiotensinogen messenger RNA expression. *Journal of Clinical Investigation*, 83(6): 1941-1945. doi: 10.1172/jci114102
- Ely, D., Falvo, J., Dunphy, G., Caplea, A., Salisbury, R., & Turner, M. (1994). The spontaneously hypertensive rat Y chromosome produces an early testosterone rise in normotensive rats. *Journal of Hypertension*, 12(7): 769-774.
- Ely, D. L., Salisbury, R., Hadi, D., Turner, M., & Johnson, M. L. (1991). Androgen receptor and the testes influence hypertension in a hybrid rat model. *Hypertension*, 17(6 Pt 2): 1104-1110.
- Ely, D., Underwood, A., Dunphy, G., Boehme, S., Turner, M., & Milsted, A. (2010). Review of the y chromosome, Sry and hypertension. *Steroids*, 75(11): 747-753. doi: 10.1016/j.steroids.2009.10.015
- Ermisch, A., Landgraf, R., & Ruhle, H. J. (1992). Circumventricular organs and brain fluid environment: Molecular and brain fluid environment *Progress in brain research* (Vol. 91). Netherlands: Elsevier Science Publishers.
- Eroschenko, V. P. (2005). Urinary System. In M. S. H. d. Fiore (Ed.), *Di Fiore's atlas of histology with functional correlations* (10th ed. / ed., pp. 355-382). Philadelphia: Lippincott Williams & Wilkins.
- Estrada, M., Varshney, A., & Ehrlich, B. E. (2006). Elevated testosterone induces apoptosis in neuronal cells. *Journal of Biological Chemistry*, 281(35): 25492-25501. doi: 10.1074/jbc.M603193200
- Eyster, K. M., Mark, C. J., Gayle, R., & Martin, D. S. (2007). The effects of estrogen and testosterone on gene expression in the rat mesenteric arteries. *Vascular Pharmacology*, 47(4): 238-247. doi: 10.1016/j.vph.2007.06.007

- Falvo, R. E., Buhl, A., & Nalbandov, A. V. (1974). Testosterone concentrations in the peripheral plasma of androgenized female rats and in the estrous cycle of normal female rats. *Endocrinology*, *95*(1): 26-29. doi: doi:10.1210/endo-95-1-26
- Fan, L., Curtis, K., Toal, S., Kudo, L., & Rouch, A. (2015). Differential effects of sex steroids on mRNA expression of renal sodium transporters in mice. *The FASEB Journal*, *29*(1).
- Fang, Z., & Cui, X. (2011). Design and validation issues in RNA-seq experiments. *Briefings in Bioinformatics*, *12*(3): 280-287. doi: 10.1093/bib/bbr004
- Ferguson, A. V., Latchford, K. J., & Samson, W. K. (2008). The paraventricular nucleus of the hypothalamus a potential target for integrative treatment of autonomic dysfunction. *Expert Opinion on Therapeutic Targets* *12*(6): 717-727.
- Filgueira, F. P., Lobato, N. S., DosSantos, R. A., Oliveira, M. A., Akamine, E. H., Tostes, R. C., . . . Carvalho, M. H. (2012). Endogenous testosterone increases leukocyte-endothelial cell interaction in spontaneously hypertensive rats. *Life Sciences*, *90*(17-18): 689-694. doi: 10.1016/j.lfs.2012.03.009
- Fink, G. D., Haywood, J. R., Bryan, W. J., Packwood, W., & Brody, M. J. (1980). Central site for pressor action of blood-borne angiotensin in rat. *American Journal of Physiology - Regulatory, Integrative and Comparative Physiology*, *239*(3): R358-R361.
- Finkle, W. D., Greenland, S., Ridgeway, G. K., Adams, J. L., Frasco, M. A., Cook, M. B., . . . Hoover, R. N. (2014). Increased risk of non-fatal myocardial infarction following testosterone therapy prescription in men. *PLoS One*, *9*(1): e85805. doi: 10.1371/journal.pone.0085805
- Fitzsimmons, M. D., Roberts, M. M., & Robinson, A. G. (1994). Control of posterior pituitary vasopressin content: implications for the regulation of the vasopressin gene. *Endocrinology*, *134*(4): 1874-1878. doi: 10.1210/endo.134.4.8137755
- Fogari, R., Preti, P., Zoppi, A., Fogari, E., Rinaldi, A., Corradi, L., & Mugellini, A. (2005). Serum testosterone levels and arterial blood pressure in the elderly. *Hypertension Research*, *28*(8): 625-630. doi: 10.1291/hypres.28.625
- Folkow, B. (1982). Physiological aspects of primary hypertension. *Physiological Reviews*, *62*(2): 347-504.
- Foradori, C. D., Weiser, M. J., & Handa, R. J. (2008). Non-genomic actions of androgens. *Front Neuroendocrinol*, *29*(2): 169-181. doi: 10.1016/j.yfrne.2007.10.005
- Freeman, E. R., Bloom, D. A., & McGuire, E. J. (2001). A brief history of testosterone. *Journal of Urology*, *165*(2): 371-373. doi: 10.1097/00005392-200102000-00004
- Frindt, G., Ergonul, Z., & Palmer, L. G. (2008). Surface Expression of Epithelial Na Channel Protein in Rat Kidney. *The Journal of General Physiology*, *131*(6): 617-627. doi: 10.1085/jgp.200809989

- Gage, G. J., Kipke, D. R., & Shain, W. (2012). Whole Animal Perfusion Fixation for Rodents. (65): e3564. doi: doi:10.3791/3564
- Gambling, L., Dunford, S., Wilson, C. A., McArdle, H. J., & Baines, D. L. (2004). Estrogen and progesterone regulate alpha, beta, and gamma ENaC subunit mRNA levels in female rat kidney. *Kidney International*, 65(5): 1774-1781. doi: 10.1111/j.1523-1755.2004.00593.x
- Ganten, U., Schroder, G., Witt, M., Zimmermann, F., Ganten, D., & Stock, G. (1989). Sexual dimorphism of blood pressure in spontaneously hypertensive rats: effects of anti-androgen treatment. *Journal of Hypertension*, 7(9): 721-726.
- Garcia-Lopez, P., Perez-Urizar, J., Ibarra, A., Grijalva, I., Madrazo, I., Flores-Murrieta, F., . . . Guizar-Sahagun, G. (1996). Comparison between Sprague-Dawley and Wistar rats as an experimental model of pharmacokinetic alterations induced by spinal cord injury. *Archives of Medical Research*, 27(4): 453-457.
- Garty, H. (2000). Regulation of the epithelial Na<sup>+</sup> channel by aldosterone: Open questions and emerging answers. *Kidney International*, 57(4): 1270-1276.
- Gill, J. R. (1979). Neural control of renal tubular sodium reabsorption. *Nephron*, 23(2-3): 116-118.
- Giltay, E. J., Hoogeveen, E. K., Elbers, J. M., Gooren, L. J., Asscheman, H., & Stehouwer, C. D. (1998). Effects of sex steroids on plasma total homocysteine levels: a study in transsexual males and females. *The Journal of Clinical Endocrinology and Metabolism*, 83(2): 550-553. doi: 10.1210/jcem.83.2.4574
- Giménez, J., García, M. P., Serna, M., Bonacasa, B., Carbonell, L. F., Quesada, T., & Hernández, I. (2006). 17 $\beta$ -Oestradiol enhances the acute hypotensive effect of captopril in female ovariectomized spontaneously hypertensive rats. *Experimental Physiology*, 91(4): 715-722. doi: 10.1113/expphysiol.2006.033449
- Ginzinger, D. G. (2002). Gene quantification using real-time quantitative PCR: An emerging technology hits the mainstream. *Experimental Hematology*, 30(6): 503-512. doi: 10.1016/S0301-472X(02)00806-8
- Glasel, J. A. (1995). Validity of nucleic acid purities monitored by 260nm/280nm absorbance ratios. *Biotechniques*, 18(1): 62-63.
- Golden, K. L., Marsh, J. D., & Jiang, Y. (2004). Testosterone regulates mRNA levels of calcium regulatory proteins in cardiac myocytes. *Hormone and Metabolic Research*, 36(4): 197-202. doi: 10.1055/s-2004-814445
- Goldman, R. K., Azar, A. S., Mulvaney, J. M., Hinojosa-Laborde, C., Haywood, J. R., & Brooks, V. L. (2009). Baroreflex sensitivity varies during the rat estrous cycle: role of gonadal steroids. *American Journal of Physiology - Regulatory, Integrative and Comparative Physiology*, 296(5): R1419-R1426. doi: 10.1152/ajpregu.91030.2008
- Gomes, D., Agasse, A., Thiébaud, P., Delrot, S., Gerós, H., & Chaumont, F. (2009). Aquaporins are multifunctional water and solute transporters highly divergent in

living organisms. *Biochimica et Biophysica Acta (BBA) - Biomembranes*, 1788(6): 1213-1228. doi: 10.1016/j.bbamem.2009.03.009

- Gonzales, R. J., Ghaffari, A. A., Duckles, S. P., & Krause, D. N. (2005). Testosterone treatment increases thromboxane function in rat cerebral arteries. *American Journal of Physiology - Heart and Circulatory Physiology*, 289(2): H578-585. doi: 10.1152/ajpheart.00958.2004
- Graceli, J. B., Cicilini, M. A., Bissoli, N. S., Abreu, G. R., & Moysés, M. R. (2013). Roles of estrogen and progesterone in modulating renal nerve function in the rat kidney. *Brazilian Journal of Medical and Biological Research*, 46: 521-527.
- Graffe, C. C., Bech, J. N., Lauridsen, T. G., Vase, H., & Pedersen, E. B. (2012). Abnormal increase in urinary aquaporin-2 excretion in response to hypertonic saline in essential hypertension. *BMC Nephrology*, 13(1): 1-15. doi: 10.1186/1471-2369-13-15
- Grassi, D., Bellini, M. J., Acaz-Fonseca, E., Panzica, G., & Garcia-Segura, L. M. (2013). Estradiol and testosterone regulate arginine-vasopressin expression in SH-SY5Y human female neuroblastoma cells through estrogen receptors-alpha and -beta. *Endocrinology*, 154(6): 2092-2100. doi: 10.1210/en.2012-2137
- Green, M. R., & Sambrook, J. (2014). *Molecular Cloning: A Laboratory Manual (Fourth Edition)*: Cold Spring Harbor Laboratory, NY.
- Grossman, R. C. (2010). Experimental models of renal disease and the cardiovascular system. *The Open Cardiovascular Medicine Journal*, 4: 257-264. doi: 10.2174/1874192401004010257
- Gu, F., Hata, R., Toku, K., Yang, L., Ma, Y. J., Maeda, N., . . . Tanaka, J. (2003). Testosterone up-regulates aquaporin-4 expression in cultured astrocytes. *Journal of Neuroscience Research*, 72(6): 709-715. doi: 10.1002/jnr.10603
- Guyton, A. C., Coleman, T. G., Cowley, A. V., Jr., Scheel, K. W., Manning, R. D., Jr., & Norman, R. A., Jr. (1972). Arterial pressure regulation. Overriding dominance of the kidneys in long-term regulation and in hypertension. *American Journal of Medicine*, 52(5): 584-594.
- Haanwinckel, M. A., Elias, L. K., Favaretto, A. L., Gutkowska, J., McCann, S. M., & Antunes-Rodrigues, J. (1995). Oxytocin mediates atrial natriuretic peptide release and natriuresis after volume expansion in the rat. *Proceedings of the National Academy of Sciences U S A*, 92(17): 7902-7906.
- Hall, J. E. (2003). The kidney, hypertension, and obesity. *Hypertension*, 41(3): 625-633. doi: 10.1161/01.hyp.0000052314.95497.78
- Hall, J. E. (2016). The body fluids and kidneys *Guyton and Hall textbook of medical physiology* (Vol. 13, pp. 285-302): Saunders Elsevier.
- Hall, J. E., Mizelle, H. L., Hildebrandt, D. A., & Brands, M. W. (1990). Abnormal pressure natriuresis. A cause or a consequence of hypertension? *Hypertension*, 15(6 Pt 1): 547-559.

- Hamm, L. L., Feng, Z., & Hering-Smith, K. S. (2010). Regulation of sodium transport by ENaC in the kidney. *Current Opinion in Nephrology and Hypertension*, 19(1): 98-105. doi: 10.1097/MNH.0b013e328332bda4
- Hamson, D. K., Jones, B. A., & Watson, N. V. (2004). Distribution of androgen receptor immunoreactivity in the brainstem of male rats. *Neuroscience*, 127(4): 797-803. doi: 10.1016/j.neuroscience.2004.06.006
- Han, Y., Gao, S., Muegge, K., Zhang, W., & Zhou, B. (2015). Advanced applications of RNA sequencing and challenges. *Bioinformatics and Biology Insights*, 9(Suppl 1): 29-46. doi: 10.4137/bbi.s28991
- Hanukoglu, I., & Hanukoglu, A. (2016). Epithelial sodium channel (ENaC) family: Phylogeny, structure-function, tissue distribution, and associated inherited diseases. *Gene*, 579(2): 95-132. doi: 10.1016/j.gene.2015.12.061
- Hara-Chikuma, M., & Verkman, A. S. (2006). Physiological roles of glycerol-transporting aquaporins: the aquaglyceroporins. *Cellular and Molecular Life Sciences*, 63(12): 1386-1392. doi: 10.1007/s00018-006-6028-4
- Harrison-Bernard, L. M. (2009). The renal renin-angiotensin system. *Advances in Physiology Education*, 33(4): 270-274. doi: 10.1152/advan.00049.2009
- Hart, E. C., & Joyner, M. J. (2010). The curse of the sympathetic nervous system: are men or women more unfortunate? *The Journal of Physiology*, 588(Pt 22): 4345-4346. doi: 10.1113/jphysiol.2010.199935
- Hay, M. (2016). Sex, the brain and hypertension: brain oestrogen receptors and high blood pressure risk factors. *Clinical science (London)*, 130(1): 9-18. doi: 10.1042/cs20150654
- Haywood, S. A., Simonian, S. X., van der Beek, E. M., Bicknell, R. J., & Herbison, A. E. (1999). Fluctuating estrogen and progesterone receptor expression in brainstem norepinephrine neurons through the rat estrous cycle. *Endocrinology*, 140(7): 3255-3263. doi: 10.1210/endo.140.7.6869
- Hazell, G. G. J., Hindmarch, C. C., Pope, G. R., Roper, J. A., Lightman, S. L., Murphy, D., . . . Lolait, S. J. (2012). G protein-coupled receptors in the hypothalamic paraventricular and supraoptic nuclei – serpentine gateways to neuroendocrine homeostasis. *Frontiers in Neuroendocrinology*, 33(1): 45-66.
- Heo, N. J., Son, M. J., Lee, J. W., Jung, J. Y., Kim, S., Oh, Y. K., . . . Han, J. S. (2013). Effect of estradiol on the expression of renal sodium transporters in rats. *Climacteric*, 16(2): 265-273. doi: 10.3109/13697137.2012.672494
- Herak-Kramberger, C. M., Breljak, D., Ljubojevic, M., Matokanovic, M., Lovric, M., Rogic, D., . . . Sabolic, I. (2015). Sex-dependent expression of water channel AQP1 along the rat nephron. *American Journal of Physiology - Renal Physiology*, 308(8): F809-821. doi: 10.1152/ajprenal.00368.2014
- Heritage, A. S., Stumpf, W. E., Sar, M., & Grant, L. D. (1981). (3-H)-dihydrotestosterone in catecholamine neurons of rat brain stem: combined

localization by autoradiography and formaldehyde-induced fluorescence. *Journal of Comparative Neurology*, 200(2): 289-307. doi: 10.1002/cne.902000208

Hermo, L., Krzeczunowicz, D., & Ruz, R. (2004). Cell specificity of aquaporins 0, 3, and 10 expressed in the testis, efferent ducts, and epididymis of adult rats. *Journal of Andrology*, 25(4): 494-505.

Herrera, M., & Garvin, J. L. (2011). Aquaporins as gas channels. *Pflügers Archiv: European Journal of Physiology*, 462(4): 623-630. doi: 10.1007/s00424-011-1002-x

Herzberg, N. H., Goudsmit, E., Kruisbrink, J., & Boer, G. J. (1989). Testosterone treatment restores reduced vasopressin-binding sites in the kidney of the ageing rat. *Journal of Endocrinology*, 123(1): 59-63. doi: 10.1677/joe.0.1230059

Hinojosa-Laborde, C., Chapa, I., Lange, D., & Haywood, J. R. (1999). Gender differences in sympathetic nervous system regulation. *Clinical and Experimental Pharmacology and Physiology*, 26(2): 122-126.

Hinojosa-Laborde, C., Craig, T., Zheng, W., Ji, H., Haywood, J. R., & Sandberg, K. (2004). Ovariectomy augments hypertension in aging female Dahl salt-sensitive rats. *Hypertension*, 44(4): 405-409.

Hinojosa-Laborde, C., Lange, D. L., & Haywood, J. R. (2000). Role of female sex hormones in the development and reversal of dahl hypertension. *Hypertension*, 35(1 Pt 2): 484-489.

Hofmann, P. J., Michaelis, M., Götz, F., Bartel, C., Kienitz, T., & Quinkler, M. (2012). Flutamide increases aldosterone levels in gonadectomized male but not female wistar rats. *American Journal of Hypertension*, 25(6): 697-703. doi: 10.1038/ajh.2012.21

Holbein, W. W., Bardgett, M. E., & Toney, G. M. (2014). Blood pressure is maintained during dehydration by hypothalamic paraventricular nucleus-driven tonic sympathetic nerve activity. *Journal of Physiology*, 592(Pt 17): 3783-3799. doi: 10.1113/jphysiol.2014.276261

Hosoya, Y., Sugiura, Y., Okado, N., Loewy, A. D., & Kohno, K. (1991). Descending input from the hypothalamic paraventricular nucleus to sympathetic preganglionic neurons in the rat. *Experimental Brain Research*, 85(1): 10-20.

Hu, B., & Bourque, C. W. (1992). NMDA receptor-mediated rhythmic bursting activity in rat supraoptic nucleus neurones in vitro. *The Journal of Physiology*, 458: 667-687.

Hu, J., Tan, S., & Zhong, Y. (2011). Effects of testosterone on renal function in salt-loaded rats. *The American Journal of the Medical Sciences*, 342(1): 38-43. doi: 10.1097/MAJ.0b013e31820f835b

- Hu, J., Zhang, Z., Shen, W. J., & Azhar, S. (2010). Cellular cholesterol delivery, intracellular processing and utilization for biosynthesis of steroid hormones. *Nutrition and Metabolism (London)*, 7(47): 1-25. doi: 10.1186/1743-7075-7-47
- Huang, C. K., Lee, S. O., Chang, E., Pang, H., & Chang, C. (2016). Androgen receptor (AR) in cardiovascular diseases. *J Endocrinol*, 229(1): R1-R16. doi: 10.1530/joe-15-0518
- Huang, H. F., He, R. H., Sun, C. C., Zhang, Y., Meng, Q. X., & Ma, Y. Y. (2006). Function of aquaporins in female and male reproductive systems. *Human Reproduction Update*, 12(6): 785-795. doi: 10.1093/humupd/dml035
- Hughes, G. S., Mathur, R. S., & Margolius, H. S. (1989). Sex steroid hormones are altered in essential hypertension. *Journal of Hypertension*, 7(3): 181-187.
- Idris, A. I. (2012). Ovariectomy/orchidectomy in rodents. *Methods in Molecular Biology*, 816: 545-551. doi: 10.1007/978-1-61779-415-5\_34
- Illiescu, R., Hancianu, M., & Reckelhoff, J. F. (2014). Testosterone supplements accelerate progression of kidney injury in a rat model of reduced renal mass. *Farmacologia*, 62(1): 119-128.
- Imbeaud, S., Graudens, E., Boulanger, V., Barlet, X., Zaborski, P., Eveno, E., . . . Auffray, C. (2005). Towards standardization of RNA quality assessment using user-independent classifiers of microcapillary electrophoresis traces. *Nucleic Acids Research*, 33(6): e56. doi: 10.1093/nar/gni054
- Ishibashi, K. (2006). Aquaporin superfamily with unusual npa boxes: S-aquaporins (superfamily, sip-like and subcellular-aquaporins). *Cellular and Molecular Biology (Noisy-le-grand, France)*, 52(7): 20-27.
- Ishibashi, K., Hara, S., & Kondo, S. (2009). Aquaporin water channels in mammals. *Clinical and Experimental Nephrology*, 13(2): 107-117. doi: 10.1007/s10157-008-0118-6
- Ishikawa, Y., & Ishida, H. (2000). Aquaporin water channel in salivary glands. *The Japan Journal of Pharmacology*, 83(2): 95-101.
- Ishunina, T. A., & Swaab, D. F. (1999). Vasopressin and oxytocin neurons of the human supraoptic and paraventricular nucleus: size changes in relation to age and sex. *The Journal of Clinical Endocrinology and Metabolism*, 84(12): 4637-4644. doi: 10.1210/jcem.84.12.6187
- Isodono, K., Takahashi, T., Imoto, H., Nakanishi, N., Ogata, T., Asada, S., . . . Matsubara, H. (2010). PARM-1 is an endoplasmic reticulum molecule involved in endoplasmic reticulum stress-induced apoptosis in rat cardiac myocytes. *PLoS One*, 5(3): e9746. doi: 10.1371/journal.pone.0009746
- Isselhard, W. H., & Kusche, J. (1998). Animal experimentation. In H. Troidl, M. F. McKneally, D. S. Mulder, A. S. Wechsler, B. McPeck & W. O. Spitzer (Eds.), *Surgical Research: Basic Principles and Clinical Practice* (pp. 419-433). New York, NY: Springer New York.

- Ito, K., Hirooka, Y., Kimura, Y., Sagara, Y., & Sunagawa, K. (2006). Ovariectomy augments hypertension through rho-kinase activation in the brain stem in female spontaneously hypertensive rats. *Hypertension*, 48(4): 651-657. doi: 10.1161/01.HYP.0000238125.21656.9e
- Ivy, J. R., & Bailey, M. A. (2014). Pressure natriuresis and the renal control of arterial blood pressure. *The Journal of Physiology*, 592(Pt 18): 3955-3967. doi: 10.1113/jphysiol.2014.271676
- Jazbutyte, V., Hu, K., Kruchten, P., Bey, E., Maier, S. K.G., Fritzscheier, K. H., . . . Pelzer, T. (2006). Aging Reduces the Efficacy of Estrogen Substitution to Attenuate Cardiac Hypertrophy in Female Spontaneously Hypertensive Rats. *Hypertension*, 48(4): 579-586. doi: 10.1161/01.HYP.0000240053.48517.c7
- Jean, A. (1991). The nucleus tractus solitarius: neuroanatomic, neurochemical and functional aspects. *Archives Internationales de Physiologie, de Biochimie et de Biophysique (Liege)*, 99(5): A3-52.
- Jenkins, C., Salisbury, R., & Ely, D. (1994). Castration lowers and testosterone restores blood pressure in several rat strains on high sodium diets. *Clinical and Experimental Hypertension*, 16(5): 611-625.
- Ji, H., Zheng, W., Wu, X., Liu, J., Ecelbarger, C. M., Watkins, R., . . . Sandberg, K. (2010). Sex chromosome effects unmasked in angiotensin II-induced hypertension. *Hypertension*, 55(5): 1275-1282. doi: 10.1161/hypertensionaha.109.144949
- Jin-Gon, J., Maeda, S., Kuwahara-Otani, S., Tanaka, K., Hayakawa, T., & Makoto, S. (2014). Expression of adrenergic and cholinergic receptors in murine renal intercalated cells. *Journal of Veterinary Medical Science*, 76(11): 1493-1500.
- Johnson, A. L., & Rendano, V. T. (1984). Effects of castration, with and without testosterone replacement, on leg bone integrity in the domestic fowl. *American Journal of Veterinary Research*, 45(2): 319-325.
- Jones, J. E., Natarajan, A. R., & Jose, P. A. (2004). Cardiovascular and autonomic influences on blood pressure. In R. J. Portman, J. M. Sorof & J. R. Ingelfinger (Eds.), *Pediatric Hypertension* (pp. 23-43). Totowa, NJ: Humana Press.
- Jones, T. J., Dunphy, G., Milsted, A., & Ely, D. (1998). Testosterone effects on renal norepinephrine content and release in rats with different Y chromosomes. *Hypertension*, 32(5): 880-885. doi: 10.1161/01.hyp.32.5.880
- Joseph, A., Shur, B. D., & Hess, R. A. (2011). Estrogen, Efferent Ductules, and the Epididymis. *Biology of Reproduction*, 84(2): 207-217. doi: 10.1095/biolreprod.110.087353
- Joyner, M. J., Charkoudian, N., & Wallin, B. G. (2010). Sympathetic nervous system and blood pressure in humans: Individualized patterns of regulation and their implications. *Hypertension*, 56(1): 10-16. doi: 10.1161/hypertensionaha.109.140186

- Kamat, S. S. (2013). Normal water balance *Practical applications of intravenous fluids in surgical patients* (pp. 1-37). India: JayPee Brothers Medical Publisher (P) Ltd.
- Kamynina, E., & Staub, O. (2002). Concerted action of ENaC, Nedd4–2, and Sgk1 in transepithelial Na<sup>+</sup> transport. *American Journal of Physiology - Renal Physiology*, 283(3): F377-F387. doi: 10.1152/ajprenal.00143.2002
- Kanagy, N. L. (2005).  $\alpha$ 2-Adrenergic receptor signalling in hypertension. *Clinical Science*, 109(5): 431-437. doi: 10.1042/cs20050101
- Kang, N. N., Fu, L., Xu, J., Han, Y., Cao, J. X., Sun, J. F., & Zheng, M. (2012). Testosterone improves cardiac function and alters angiotensin II receptors in isoproterenol-induced heart failure. *Archives of Cardiovascular Diseases*, 105(2): 68-76. doi: 10.1016/j.acvd.2011.12.002
- Kau, M. M., Lo, M. J., Wang, S. W., Tsai, S. C., Chen, J. J., Chiao, Y. C., . . . Wang, P. S. (1999). Inhibition of aldosterone production by testosterone in male rats. *Metabolism*, 48(9): 1108-1114.
- Kelly, D. M., & Jones, T. H. (2013a). Testosterone: a metabolic hormone in health and disease. *Journal of Endocrinology*, 217(3): R25-45. doi: 10.1530/joe-12-0455
- Kelly, D. M., & Jones, T. H. (2013b). Testosterone: a vascular hormone in health and disease. *Journal of Endocrinology*, 217(3): R47-R71. doi: 10.1530/joe-12-0582
- Khalid, M., Ilhami, N., Giudicelli, Y., & Dausse, J. P. (2002). Testosterone dependence of salt-induced hypertension in Sabra rats and role of renal alpha(2)-adrenoceptor subtypes. *Journal of Pharmacology and Experimental Therapeutics*, 300(1): 43-49.
- Khaw, K. T., & Barrett-Connor, E. (1988). Blood pressure and endogenous testosterone in men: an inverse relationship. *Journal of Hypertension*, 6(4): 328-332.
- Khurana, I. (2014). *Medical Physiology for Undergraduate Students* (Vol. 2). India: Elsevier Health Sciences APAC.
- Kienitz, T., Allolio, B., Strasburger, C. J., & Quinkler, M. (2006a). Renal expression of alpha-ENaC is increased in testosterone treated rats. *Endocrine Abstracts*, 11: P302.
- Kienitz, T., Allolio, B., Strasburger, C. J., & Quinkler, M. (2006b). Testosterone treatment in rats increases expression of the alpha-subunit of the epithelial sodium channel (alpha-ENaC) in the kidney. *Experimental and Clinical Endocrinology & Diabetes*, 114(S 1): P14\_176. doi: 10.1055/s-2006-933061
- Kienitz, T., Allolio, B., Strasburger, C. J., & Quinkler, M. (2009). Sex-specific regulation of ENaC and androgen receptor in female rat kidney. *Hormone and metabolic research*, 41(5): 356-362.
- Kienitz, T., Allolio, B., Strasburger, C., & Quinkler, M. (2006c). Testosterone treatment in rats increases expression of the alpha-subunit of the epithelial sodium channel

(alpha-ENaC) in the kidney. *Exp Clin Endocrinol Diabetes*, 114(S 1): P14\_176.  
doi: 10.1055/s-2006-933061

King, L. S., Kozono, D., & Agre, P. (2004). From structure to disease: the evolving tale of aquaporin biology. *Nature Reviews Molecular Cell Biology*, 5(9): 687-698.  
doi: 10.1038/nrm1469

Klabunde, R. E. (2011). Cardiovascular Integration, Adaptation and Pathophysiology *Cardiovascular Pharmacology Concepts* (Vol. 2): Lippincott Williams & Wilkins.

Koizumi, K., & Yamashita, H. (1978). Influence of atrial stretch receptors on hypothalamic neurosecretory neurones. *The Journal of Physiology*, 285: 341-358.

Komukai, K., Mochizuki, S., & Yoshimura, M. (2010). Gender and the renin-angiotensin-aldosterone system. *Fundamental and Clinical Pharmacology*, 24(6): 687-698. doi: 10.1111/j.1472-8206.2010.00854.x

Korf, I. (2013). Genomics: the state of the art in RNA-seq analysis. *Nature Methods*, 10(12): 1165-1166. doi: 10.1038/nmeth.2735

Koshiya, N., & Guyenet, P. G. (1996). *NTS neurons with carotid chemoreceptor inputs arborize in the rostral ventrolateral medulla* (Vol. 270).

Kraus, A. L. (1979). Research Methodology. In H. J. Baker, J. R. Lindsey & S. H. Wesibroth (Eds.), *The Laboratory Rat: Biology and Diseases* (Vol. 1). New York: Academic Press Inc. (London) Ltd.

Kruse, E., Uehlein, N., & Kaldenhoff, R. (2006). The aquaporins. *Genome Biology*, 7(2): 206. doi: 10.1186/gb-2006-7-2-206

Kumagai, H., Oshima, N., Matsuura, T., Iigaya, K., Imai, M., Onimaru, H., . . . Saruta, T. (2012). Importance of rostral ventrolateral medulla neurons in determining efferent sympathetic nerve activity and blood pressure. *Hypertension Research*, 35(2): 132-141.

Kumai, T., Tanaka, M., Watanabe, M., Nakura, H., & Kobayashi, S. (1995). Influence of androgen on tyrosine hydroxylase mRNA in adrenal medulla of spontaneously hypertensive rats. *Hypertension*, 26(1): 208-212.

Kurtz, T. W., & Morris, R. C. (1987). Biological variability in Wistar-Kyoto rats. Implications for research with the spontaneously hypertensive rat. *Hypertension*, 10(1): 127-131.

Kwon, T. H., Frøkiær, J., & Nielsen, S. (2013). Regulation of aquaporin-2 in the kidney: A molecular mechanism of body-water homeostasis. *Kidney Research and Clinical Practice*, 32(3): 96-102. doi: 10.1016/j.krcp.2013.07.005

Laemmli, U. K. (1970). Cleavage of Structural Proteins during the Assembly of the Head of Bacteriophage T4. *Nature*, 227(5259): 680-685.

- Lambert, E. A., Teede, H., Sari, C. I., Jona, E., Shorakae, S., Woodington, K., . . . Lambert, G. W. (2015). Sympathetic activation and endothelial dysfunction in polycystic ovary syndrome are not explained by either obesity or insulin resistance. *Clinical Endocrinology*, 83(6): 812-819. doi: 10.1111/cen.12803
- Lane, P. H. (2008). Estrogen receptors in the kidney: lessons from genetically altered mice. *Gender Medicine*, 5 Suppl A: S11-18. doi: 10.1016/j.genm.2008.03.003
- Lara, H., Galleguillos, X., Arrau, J., & Belmar, J. (1985). Effect of castration and testosterone on norepinephrine storage and on the release of [(3)H]norepinephrine from rat vas deferens. *Neurochemistry International*, 7(4): 667-674.
- Laragh, J. H. (1986). The endocrine control of blood volume, blood pressure and sodium balance: atrial hormone and renin system interactions. *Journal of hypertension. Supplement: official journal of the International Society of Hypertension*, 4(2): S143-156.
- Latendresse, J. R., Newbold, R. R., Weis, C. C., & Delclos, K. B. (2001). Polycystic kidney disease induced in F1 Sprague-Dawley rats fed para-nonylphenol in a soy-free, casein-containing diet. *Toxicological Sciences*, 62(1): 140-147. doi: 10.1093/toxsci/62.1.140
- Laudański, K., & Cudnoch-Jędrzejewska, A. (2001). Effects of ovariectomy on the regulation of cardiovascular functions in female Wistar rats. *Medical Science Monitor*, 7(6): BR1188-BR1192.
- Lee, B. H., & Kwon, T. H. (2007). Regulation of AQP2 in collecting duct: An emphasis on the effects of angiotensin II or aldosterone. *Electrolyte and Blood Pressure*, 5(1): 15-22.
- Lee, C. H., Kuo, S. W., Hung, Y. J., Hsieh, C. H., He, C. T., Yang, T. C., . . . Pei, D. (2005). The effect of testosterone supplement on insulin sensitivity, glucose effectiveness, and acute insulin response after glucose load in male type 2 diabetics. *Endocrine Research*, 31(2): 139-148.
- Lee, J., Kang, D. G., & Kim, Y. (2000). Increased expression and shuttling of aquaporin-2 water channels in the kidney in DOCA-salt hypertensive rats. *Clinical and Experimental Hypertension*, 22(5): 531-541.
- Lee, J., Kim, S., Kim, J., Jeong, M. H., Oh, Y., & Choi, K. C. (2006). Increased expression of renal aquaporin water channels in spontaneously hypertensive rats. *Kidney and Blood Pressure Research*, 29(1): 18-23. doi: 10.1159/000092483
- Lehmann, G. L., Larocca, M. C., Soria, L. R., & Marinelli Rú, A. (2008). Aquaporins: Their role in cholestatic liver disease. *World Journal of Gastroenterology*, 14(46): 7059-7067. doi: 10.3748/wjg.14.7059
- Leng, G., Caquineau, C., & Sabatier, N. (2005). Regulation of oxytocin secretion. *Vitamins and Hormones*, 71: 27-58. doi: 10.1016/s0083-6729(05)71002-5

- Leong, X. F., Ng, C. Y., & Jaarin, K. (2015). Animal models in cardiovascular research: Hypertension and atherosclerosis. *BioMed Research International*, 2015(528757): 1-11. doi: 10.1155/2015/528757
- Li, C., & Wang, W. (2014). Urea transport mediated by aquaporin water channel proteins. *Subcellular Biochemistry*, 73: 227-265. doi: 10.1007/978-94-017-9343-8\_14
- Li, C., Wang, W., Rivard, C. J., Lanaspá, M. A., Summer, S., & Schrier, R. W. (2011). Molecular mechanisms of angiotensin II stimulation on aquaporin-2 expression and trafficking. *American Journal of Physiology-Renal Physiology*, 300(5): F1255-F1261.
- Li, D. P., & Pan, H. L. (2007). Glutamatergic inputs in the hypothalamic paraventricular nucleus maintain sympathetic vasomotor tone in hypertension. *Hypertension*, 49(4): 916-925. doi: 10.1161/01.hyp.0000259666.99449.74
- Liang, P., & Pardee, A. B. (1992). Differential display of eukaryotic messenger RNA by means of the polymerase chain reaction. *Science*, 257(5072): 967-971.
- Linton, L., Taylor, M., Dunn, S., Martin, L., Chavez, S., Stanitz, G., . . . Boyd, N. (2016). Associations of Serum Levels of Sex Hormones in Follicular and Luteal Phases of the Menstrual Cycle with Breast Tissue Characteristics in Young Women. *PLoS One*, 11(10): e0163865. doi: 10.1371/journal.pone.0163865
- Litman, T., Sogaard, R., & Zeuthen, T. (2009). Ammonia and urea permeability of mammalian aquaporins. *Handbook of Experimental Pharmacology*(190): 327-358. doi: 10.1007/978-3-540-79885-9\_17
- Liu, B., & Ely, D. (2011). Testosterone increases: Sodium reabsorption, blood pressure, and renal pathology in female Spontaneously Hypertensive Rats on a high sodium diet. *Advances in Pharmacological Sciences*, 2011.
- Liu, P. Y., Death, A. K., & Handelsman, D. J. (2003). Androgens and cardiovascular disease. *Endocrine Reviews*, 24(3): 313-340. doi: 10.1210/er.2003-0005
- Liu, Y., Zhou, J. Y., Zhou, Y. H., Wu, D., He, J. L., Han, L. M., . . . Li, B. Y. (2016). Unique Expression of Angiotensin Type-2 Receptor in Sex-Specific Distribution of Myelinated A<sub>h</sub>-Type Baroreceptor Neuron Contributing to Sex-Dimorphic Neurocontrol of Circulation. *Hypertension*, 67(4): 783-791. doi: 10.1161/hypertensionaha.115.06815
- Livak, K. J., & Schmittgen, T. D. (2001). Analysis of relative gene expression data using real-time quantitative PCR and the 2<sup>-</sup>( $\Delta\Delta C_T$ ) Method. *Methods*, 25(4): 402-408. doi: 10.1006/meth.2001.1262
- Loffing, J., & Schild, L. (2005). Functional domains of the epithelial sodium channel. *Journal of the American Society of Nephrology*, 16(11): 3175-3181. doi: 10.1681/asn.2005050456
- Lohmeier, T. E. (2001). The sympathetic nervous system and long-term blood pressure regulation. *American Journal of Hypertension*, 14(6 Pt 2): 147s-154s.

- Lopes, R. A. M., Neves, K. B., Pestana, C. R., Queiroz, A. L., Zanotto, C. Z., Chignalia, A. Z., . . . Tostes, R. C. (2014). Testosterone induces apoptosis in vascular smooth muscle cells via extrinsic apoptotic pathway with mitochondria-generated reactive oxygen species involvement. *American Journal of Physiology - Heart and Circulatory Physiology*, 306(11): H1485-1495. doi: 10.1152/ajpheart.00809.2013
- Lopez-Ruiz, A. F., Iliescu, R., & Reckelhoff, J. F. (2010). Refractory blood pressure in female SHR to increased oxidative stress is not mediated by NO or by upregulation of renal antioxidant enzymes. *American Journal of Physiology - Regulatory, Integrative and Comparative Physiology*, 298(2): R266-R271.
- Luo, L., Chen, H., Stocco, D. M., & Zirkin, B. R. (1998). Leydig cell protein synthesis and steroidogenesis in response to acute stimulation by luteinizing hormone in rats. *Biology of Reproduction*, 59(2): 263-270.
- Ma, T., Yang, B., Gillespie, A., Carlson, E. J., Epstein, C. J., & Verkman, A. S. (1997a). Generation and phenotype of a transgenic knockout mouse lacking the mercurial-insensitive water channel aquaporin-4. *Journal of Clinical Investigation*, 100(5): 957-962.
- Ma, X. M., Levy, A., & Lightman, S. L. (1997b). Emergence of an isolated arginine vasopressin (AVP) response to stress after repeated restraint: a study of both AVP and corticotropin-releasing hormone messenger ribonucleic acid (RNA) and heteronuclear RNA. *Endocrinology*, 138(10): 4351-4357. doi: 10.1210/endo.138.10.5446
- Maas, A., & Appelman, Y. (2010). Gender differences in coronary heart disease. *Netherlands Heart Journal*, 18(12): 598-602.
- Mahmood, T., & Yang, P. C. (2012). Western Blot: Technique, theory, and trouble shooting. *North American Journal of Medical Sciences*, 4(9): 429-434. doi: 10.4103/1947-2714.100998
- Mancia, G., & Grassi, G. (2014). The autonomic nervous system and hypertension. *Circulation Research*, 114(11): 1804-1814. doi: 10.1161/circresaha.114.302524
- Manna, P. R., Jo, Y., & Stocco, D. M. (2007). Regulation of Leydig cell steroidogenesis by extracellular signal-regulated kinase 1/2: role of protein kinase A and protein kinase C signaling. *Journal of Endocrinology*, 193(1): 53-63. doi: 10.1677/joe-06-0201
- Manrique, C., Lastra, G., Gardner, M., & Sowers, J. R. (2009). The renin angiotensin aldosterone system in hypertension: Roles of insulin resistance and oxidative stress. *Medical Clinics of North America*, 93(3): 569-582. doi: 10.1016/j.mcna.2009.02.014
- Mantione, K. J., Kream, R. M., Kuzelova, H., Ptacek, R., Raboch, J., Samuel, J. M., & Stefano, G. B. (2014). Comparing bioinformatic gene expression profiling methods: Microarray and RNA-Seq. *Medical Science Monitor Basic Research*, 20: 138-141. doi: 10.12659/msmbr.892101

- Maranon, R., Lima, R., Spradley, F. T., do Carmo, J. M., Zhang, H., Smith, A. D., . . . Hall, J. E. (2015). Roles for the sympathetic nervous system, renal nerves, and CNS melanocortin-4 receptor in the elevated blood pressure in hyperandrogenemic female rats. *American Journal of Physiology - Regulatory, Integrative and Comparative Physiology*, 308(8): R708-R713.
- Maranon, R., & Reckelhoff, J. F. (2013). Sex and gender differences in control of blood pressure. *Clinical Science (London)*, 125(7): 311-318.
- Marcondes, F. K., Bianchi, F. J., & Tanno, A. P. (2002). Determination of the estrous cycle phases of rats: some helpful considerations. *Brazilian Journal of Biology*, 62: 609-614.
- Maria, S., Kamath, V. V., Krishnanand, P. S., & Komali, R. (2015). Sprague-Dawley rats are a sustainable and reproducible animal model for induction and study of oral submucous fibrosis. *Journal of Orofacial Sciences*, 7(1): 11-18.
- Maric-Bilkan, C., & Manigrasso, M. B. (2012). Sex differences in hypertension: contribution of the renin–angiotensin system. *Gender medicine*, 9(4): 287-291.
- Maris, M. E., Melchert, R. B., Joseph, J., & Kennedy, R. H. (2005). Gender differences in blood pressure and heart rate in spontaneously hypertensive and Wistar-Kyoto rats. *Clinical and Experimental Pharmacology and Physiology*, 32(1-2): 35-39. doi: 10.1111/j.1440-1681.2005.04156.x
- Marlar, S., Arnspang, E. C., Koffman, J. S., Løcke, E. M., Christensen, B. M., & Nejsum, L. N. (2014). Elevated cAMP increases aquaporin-3 plasma membrane diffusion. *American Journal of Physiology-Cell Physiology*, 306(6): C598-C606.
- Marples, D., Knepper, M. A., Christensen, E. I., & Nielsen, S. (1995). Redistribution of aquaporin-2 water channels induced by vasopressin in rat kidney inner medullary collecting duct. *American Journal of Physiology*, 269(3 Pt 1): C655-664.
- Martin, D. S., Biloft, S., Redetzke, R., & Vogel, E. (2005). Castration reduces blood pressure and autonomic venous tone in male spontaneously hypertensive rats. *Journal of Hypertension*, 23(12): 2229-2236.
- Martin, D. S., Klinkova, O., & Eyster, K. M. (2012). Regional differences in sexually dimorphic protein expression in the spontaneously hypertensive rat (SHR). *Molecular and Cellular Biochemistry*, 362(1): 103-114. doi: 10.1007/s11010-011-1132-7
- Martins-Pinge, M.C. (2011). Cardiovascular and autonomic modulation by the central nervous system after aerobic exercise training. *Brazilian Journal of Medical and Biological Research*, 44: 848-854.
- Marunaka, Y., Marunaka, R., Sun, H., Yamamoto, T., Kanamura, N., & Taruno, A. (2016). Na(+) homeostasis by epithelial Na(+) channel (ENaC) and Na(x) channel (Na(x)): cooperation of ENaC and Na(x). *Annals of Translational Medicine*, 4(Suppl 1): S11. doi: 10.21037/atm.2016.10.42

- Marvar, P. J., Lob, H., Vinh, A., Zarreen, F., & Harrison, D. G. (2011). The Central Nervous System and Inflammation in Hypertension. *Current Opinion in Pharmacology*, *11*(2): 156-161. doi: 10.1016/j.coph.2010.12.001
- Masilamani, S., Kim, G. H., Mitchell, C., Wade, J. B., & Knepper, M. A. (1999). Aldosterone-mediated regulation of ENaC  $\alpha$ ,  $\beta$ , and  $\gamma$  subunit proteins in rat kidney. *Journal of Clinical Investigation*, *104*(7): R19–R23.
- Masubuchi, Y., Kumai, T., Uematsu, A., Komoriyama, K., & Hirai, M. (1982). Gonadectomy-induced reduction of blood pressure in adult spontaneously hypertensive rats. *Acta Endocrinologica (Copenhagen)*, *101*(1): 154-160.
- Matsubara, M. (2004). Renal sodium handling for body fluid maintenance and blood pressure regulation. *Yakugaku Zasshi*, *124*(6): 301-309.
- McGettigan, P. A. (2013). Transcriptomics in the RNA-seq era. *Current Opinion in Chemical Biology*, *17*(1): 4-11. doi: 10.1016/j.cbpa.2012.12.008
- McKinley, M. J., Mathai, M. L., McAllen, R. M., McClear, R. C., Miselis, R. R., Pennington, G. L., . . . Oldfield, B. J. (2004). Vasopressin secretion: osmotic and hormonal regulation by the lamina terminalis. *Journal of Neuroendocrinology*, *16*(4): 340-347. doi: 10.1111/j.0953-8194.2004.01184.x
- McLeod-Sordjan, R. (2015). Prostatic hyperplasia and male genital. In J. K. Singleton, R. V. DiGregorio, C. Green-Hernandez, S. P. Holzemer, E. S. Faber, L. R. Ferrara & J. T. Slyer (Eds.), *Primary Care, Second Edition: An Interprofessional Perspective* (Vol. 2, pp. 932-959). New York: Springer Publishing Company.
- Meneton, P., Jeunemaitre, X., de Wardener, H. E., & Macgregor, G. A. (2005). Links between dietary salt intake, renal salt handling, blood pressure, and cardiovascular diseases. *Physiological Reviews*, *85*(2): 679-715. doi: 10.1152/physrev.00056.2003
- Metzker, M. L. (2010). Sequencing technologies - the next generation. *Nature Reviews Genetics*, *11*(1): 31-46. doi: 10.1038/nrg2626
- Michels, G., & Hoppe, U. C. (2008). Rapid actions of androgens. *Frontiers in Neuroendocrinology*, *29*(2): 182-198. doi: 10.1016/j.yfrne.2007.08.004
- Milner, T. A., Hernandez, F. J., Herrick, S. P., Pierce, J. P., Iadecola, C., & Drake, C. T. (2007). Cellular and subcellular localization of androgen receptor immunoreactivity relative to C1 adrenergic neurons in the rostral ventrolateral medulla of male and female rats. *Synapse*, *61*(5): 268-278. doi: 10.1002/syn.20370
- Mironova, E., Bugaj, V., Roos, K. P., Kohan, D. E., & Stockand, J. D. (2012). Aldosterone-independent regulation of the epithelial Na<sup>+</sup> channel (ENaC) by vasopressin in adrenalectomized mice. *Proceedings of the National Academy of Sciences*, *109*(25): 10095-10100. doi: 10.1073/pnas.1201978109

- Mishra, J. S., Hankins, G. D., & Kumar, S. (2016). Testosterone downregulates angiotensin II type-2 receptor via androgen receptor-mediated ERK1/2 MAP kinase pathway in rat aorta. *Journal of the Renin-Angiotensin-Aldosterone System*, 17(4): 1-16. doi: 10.1177/1470320316674875
- Miura, M., & Reis, D. J. (1972). The role of the solitary and paramedian reticular nuclei in mediating cardiovascular reflex responses from carotid baro- and chemoreceptors. *The Journal of Physiology*, 223(2): 525-548.
- Moehren, U., Denayer, S., Podvinec, M., Verrijdt, G., & Claessens, F. (2008). Identification of androgen-selective androgen-response elements in the human aquaporin-5 and Rad9 genes. *Biochemical Journal*, 411(3): 679-686. doi: 10.1042/bj20071352
- Mohd Mokhtar, H., Giribabu, N., Kassim, N. M., Muniandy, S., & Salleh, N. (2014). Testosterone decreases fluid and chloride secretions in the uterus of adult female rats via down-regulating cystic fibrosis transmembrane regulator (CFTR) expression and functional activity. *The Journal of steroid biochemistry and molecular biology*, 144(Pt B): 361-372.
- Molina, E., Clarence, E. M., Ahmady, F., Chew, G. S., & Charchar, F. J. (2016). Coronary Artery Disease: Why We should Consider the Y Chromosome. *Heart Lung Circ*, 25(8): 791-801. doi: 10.1016/j.hlc.2015.12.100
- Momoi, H., Ikomi, F., & Ohhashi, T. (2003). Estrogen-induced augmentation of endothelium-dependent nitric oxide-mediated vasodilation in isolated rat cerebral small arteries. *The Japan Journal of Physiology*, 53(3): 193-203.
- Montano, L. M., Calixto, E., Figueroa, A., Flores-Soto, E., Carbajal, V., & Perusquia, M. (2008). Relaxation of androgens on rat thoracic aorta: testosterone concentration dependent agonist/antagonist L-type Ca<sup>2+</sup> channel activity, and 5 $\beta$ -dihydrotestosterone restricted to L-type Ca<sup>2+</sup> channel blockade. *Endocrinology*, 149(5): 2517-2526.
- Moreno, C., Maier, K. G., Hoagland, K. M., Yu, M., & Roman, R. J. (2001). Abnormal pressure-natriuresis in hypertension: role of cytochrome P450 metabolites of arachidonic acid. *American Journal of Hypertension*, 14(6 Pt 2): 90s-97s.
- Morin, R., Bainbridge, M., Fejes, A., Hirst, M., Krzywinski, M., Pugh, T., . . . Marra, M. (2008). Profiling the HeLa S3 transcriptome using randomly primed cDNA and massively parallel short-read sequencing. *Biotechniques*, 45(1): 81-94. doi: 10.2144/000112900
- Mortazavi, A., Williams, B. A., McCue, K., Schaeffer, L., & Wold, B. (2008). Mapping and quantifying mammalian transcriptomes by RNA-Seq. *Nature Methods*, 5(7): 621-628. doi: 10.1038/nmeth.1226
- Mueller, O., Lightfoot, S., & Schroeder, A. (2004). RNA integrity number (RIN) - standardization of RNA quality control. *Agilent Application Note, Publication 5989-1165EN*: 1-8.

- Muraoka, K. (2001). Effects of testosterone replacement on renal function and apoptosis on mesangial and renal tubule cells in rats. *Yonago Acta Medica*, 44(1): 37-44.
- Nadar, S., & Lip, G. (2009). *Hypertension*: OUP Oxford.
- Navar, L. G. (1997). The kidney in blood pressure regulation and development of hypertension. *Medical Clinics of North America*, 81(5): 1165-1198.
- Nesterov, V., Dahlmann, A., Krueger, B., Bertog, M., Loffing, J., & Korbmacher, C. (2012). Aldosterone-dependent and -independent regulation of the epithelial sodium channel (ENaC) in mouse distal nephron. *American Journal of Physiology - Renal Physiology*, 303(9): F1289-F1299. doi: 10.1152/ajprenal.00247.2012
- Nettleship, J. E., Jones, R. D., Channer, K. S., & Jones, T. H. (2009). Testosterone and coronary artery disease. *Frontiers of Hormone Research*, 37: 91-107. doi: 10.1159/000176047
- Ng, A. V., Callister, R., Johnson, D. G., & Seals, D. R. (1993). Age and gender influence muscle sympathetic nerve activity at rest in healthy humans. *Hypertension*, 21(4): 498-503.
- Nheu, L., Nazareth, L., Xu, G., Xiao, F., Luo, R., Komesaroff, P., & Ling, S. (2011). Physiological effects of androgens on human vascular endothelial and smooth muscle cells in culture. *Steroids*, 76(14): 1590-1596. doi: 10.1016/j.steroids.2011.09.015
- Nielsen, S., Frøkiær, J., Marples, D., Kwon, T. H., Agre, P., & Knepper, M. A. (2002). Aquaporins in the kidney: From molecules to medicine. *Physiological Reviews*, 82(1): 205-244. doi: 10.1152/physrev.00024.2001
- Nielsen, S., Kwon, T., Christensen, B. M., Promeneur, D., Frøkiær, J., & Marples, D. (1999). Physiology and Pathophysiology of Renal Aquaporins. *Journal of the American Society of Nephrology*, 10(3): 647-663.
- Nissen, R., Hu, B., & Renaud, L. P. (1994). N-methyl-D-aspartate receptor antagonist ketamine selectively attenuates spontaneous phasic activity of supraoptic vasopressin neurons in vivo. *Neuroscience*, 59(1): 115-120.
- O'Keefe, J. A., Crowley, R. S., Hrivnak, P., Kim, N. B., & Amico, J. A. (1995). Effect of testosterone and its metabolites upon the level of vasopressin messenger ribonucleic acid in the hypothalamus of the hyperosmotically stimulated male rat. *Neuroendocrinology*, 61(4): 405-411.
- O'Donoghue, T. L., Resta, T. C., & Walker, B. R. (2002). Laboratory demonstration of baroreflex control of heart rate in conscious rats. *Advances in Physiology Education*, 26(4): 309-316. doi: 10.1152/advan.00040.2001
- O'Hagan, T. S., Wharton, W., & Kehoe, P. G. (2012). Interactions between oestrogen and the renin angiotensin system - potential mechanisms for gender differences in Alzheimer's disease. *American Journal of Neurodegenerative Disease*, 1(3): 266-279.

- Ofner, P. (1955). A preliminary investigation of the products of the metabolism of testosterone by rat liver in vitro. *Biochemical Journal*, 61(2): 287-297.
- Ojeda, N. B., Royals, T. P., Black, J. T., Dasinger, J. H., Johnson, J. M., & Alexander, B. T. (2010). Enhanced sensitivity to acute angiotensin II is testosterone dependent in adult male growth-restricted offspring. *American Journal of Physiology - Regulatory, Integrative and Comparative Physiology*, 298(5): R1421-1427. doi: 10.1152/ajpregu.00096.2010
- Okamoto, K., & Aoki, K. (1963). Development of a strain of spontaneously hypertensive rats. *Japanese Circulation Journal*, 27: 282-293.
- Oparil, S., Zaman, M. A., & Calhoun, D. A. (2003). Pathogenesis of hypertension. *Annals of Internal Medicine*, 139(9): 761-776.
- Osborn, J. L. (1991). Relation between sodium intake, renal function, and the regulation of arterial pressure. *Hypertension*, 17(1 Suppl): I91-96.
- Osterberg, E. C., Bernie, A. M., & Ramasamy, R. (2014). Risks of testosterone replacement therapy in men. *Indian Journal of Urology*, 30(1): 2-7. doi: 10.4103/0970-1591.124197
- Ouchi, Y., Share, L., Crofton, J. T., Iitake, K., & Brooks, D. P. (1987). Sex difference in the development of deoxycorticosterone-salt hypertension in the rat. *Hypertension*, 9(2): 172-177.
- Pao, Alan C. (2012). Landscape of ENaC regulation in the kidney. *American Journal of Physiology - Renal Physiology*, 303(9): F1287-F1288. doi: 10.1152/ajprenal.00518.2012
- Papadopoulos, V. (2010). How is the synthesis of testosterone regulated? In B. Robaire & P. Chan (Eds.), *Handbook of Andrology* (Vol. 2). Canada: The American Society of Andrology.
- Parasuraman, S., & Raveendran, R. (2012). Measurement of invasive blood pressure in rats. *Journal of Pharmacology and Pharmacotherapeutics*, 3(2): 172-177. doi: 10.4103/0976-500x.95521
- Parhizkar, S., Ibrahim, R., & Latiff, L. A. (2008). Incision choice in laparotomy: A comparison of two incision techniques in ovariectomy of rats. *World Applied Sciences Journal*, 4(4): 537-540.
- Park, E. J., & Kwon, T. H. (2015). A minireview on vasopressin-regulated aquaporin-2 in kidney collecting duct cells. *Electrolyte and Blood Pressure*, 13(1): 1-6. doi: 10.5049/EBP.2015.13.1.1
- Parker, K. L., & Schimmer, B. P. (1995). Transcriptional regulation of the genes encoding the cytochrome P-450 steroid hydroxylases. *Vitamins and Hormones*, 51: 339-370.

- Patel, K. P., & Schmid, P. G. (1988). Role of paraventricular nucleus (PVH) in baroreflex-mediated changes in lumbar sympathetic nerve activity and heart rate. *Journal of the Autonomic Nervous System*, 22(3): 211-219.
- Paxinos, G., & Watson, C. (2007). *The Rat Brain in Stereotaxic Coordinates* (Vol. 6): Academic Press.
- Payne, A. H., & Hales, D. B. (2004). Overview of steroidogenic enzymes in the pathway from cholesterol to active steroid hormones. *Endocrine Reviews*, 25(6): 947-970. doi: 10.1210/er.2003-0030
- Pearce, D., Soundararajan, R., Trimpert, C., Kashlan, O. B., Deen, P. M. T., & Kohan, D. E. (2014). Collecting duct principal cell transport processes and their regulation. *Clinical Journal of the American Society of Nephrology: CJN*. 05760513.
- Pearson, L. J., Yandle, T. G., Nicholls, M. G., & Evans, J. J. (2008). Regulation of endothelin-1 release from human endothelial cells by sex steroids and angiotensin-II. *Peptides*, 29(6): 1057-1061. doi: 10.1016/j.peptides.2008.02.003
- Pease, J., & Sooknanan, R. (2012). A rapid, directional RNA-seq library preparation workflow for Illumina® sequencing. *Nature Methods*, 9(3): 1-2.
- Phillip, M., Palese, T., Hernandez, E. R., Roberts, C. T., Jr., LeRoith, D., & Kowarski, A. A. (1992). Effect of testosterone on insulin-like growth factor-I (IGF-I) and IGF-I receptor gene expression in the hypophysectomized rat. *Endocrinology*, 130(5): 2865-2870. doi: 10.1210/endo.130.5.1315260
- Phillips, J. K. (2005). Pathogenesis of hypertension in renal failure: role of the sympathetic nervous system and renal afferents. *Clinical and Experimental Pharmacology and Physiology*, 32(5-6): 415-418. doi: 10.1111/j.1440-1681.2005.04204.x
- Piantadosi, C. A. (2003). Water and Salt *The biology of human survival: Life and death in extreme environments* (pp. 41-53). New York: Oxford University.
- Pijacka, W., Clifford, B., Walas, D., Tilburgs, C., Joles, J.A., McMullen, S., & Langley-Evans, S.C. (2016). Impact of gonadectomy on blood pressure regulation in ageing male and female rats. *Biol Sex Differ*: ISSN 2042-6410 (In Press).
- Pinto, Y. M., Paul, M., & Ganten, D. (1998). Lessons from rat models of hypertension: from Goldblatt to genetic engineering. *Cardiovasc Res*, 39(1): 77-88. doi: 10.1016/s0008-6363(98)00077-7
- Pitteloud, N., Mootha, V. K., Dwyer, A. A., Hardin, M., Lee, H., Eriksson, K. F., . . . Hayes, F. J. (2005). Relationship between testosterone levels, insulin sensitivity, and mitochondrial function in men. *Diabetes Care*, 28(7): 1636-1642. doi: 10.2337/diacare.28.7.1636
- Plut, C., Ribiere, C., Giudicelli, Y., & Dausse, J. P. (2002). Gender differences in hypothalamic tyrosine hydroxylase and  $\alpha$ 2-adrenoceptor subtype gene expression in cafeteria diet-induced hypertension and consequences of neonatal

androgenization. *Journal of Pharmacology and Experimental Therapeutics*, 302(2): 525-531. doi: 10.1124/jpet.302.2.525

Pol, H. E. H., Cohen-Kettenis, P. T., Van Haren, N. E. M., Peper, J. S., Brans, R. G. H., Cahn, W., . . . Kahn, R. S. (2006). Changing your sex changes your brain: influences of testosterone and estrogen on adult human brain structure. *European Journal of Endocrinology*, 155(suppl 1): S107-S114. doi: 10.1530/eje.1.02248

Probst, R. J., Lim, J. M., Bird, D. N., Pole, G. L., Sato, A. K., & Claybaugh, J. R. (2006). Gender Differences in the Blood Volume of Conscious Sprague-Dawley Rats. *Journal of the American Association for Laboratory Animal Science*, 45(2): 49-52.

Puente, X. S., Quesada, V., Osorio, F. G., Cabanillas, R., Cadiñanos, J., Fraile, J. M., . . . López-Otín, C. (2011). Exome Sequencing and Functional Analysis Identifies BANF1 Mutation as the Cause of a Hereditary Progeroid Syndrome. *American Journal of Human Genetics*, 88(5): 650-656. doi: 10.1016/j.ajhg.2011.04.010

Pyner, S. (2009). Neurochemistry of the paraventricular nucleus of the hypothalamus: implications for cardiovascular regulation. *Journal of Chemical Neuroanatomy*, 38(3): 197-208. doi: 10.1016/j.jchemneu.2009.03.005

Pyner, S., & Coote, J. H. (2000). Identification of branching paraventricular neurons of the hypothalamus that project to the rostroventrolateral medulla and spinal cord. *Neuroscience*, 100(3): 549-556.

Quan, A., Chakravarty, S., Chen, J. K., Chen, J. C., Loleh, S., Saini, N., . . . Quigley, R. (2004). Androgens augment proximal tubule transport. *American Journal of Physiology - Renal Physiology*, 287(3): F452-F459. doi: 10.1152/ajprenal.00188.2003

Quinkler, M., Bujalska, I. J., Kaur, K., Onyimba, C. U., Buhner, S., Allolio, B., . . . Stewart, P. M. (2005). Androgen receptor-mediated regulation of the alpha-subunit of the epithelial sodium channel in human kidney. *Hypertension*, 46(4): 787-798. doi: 10.1161/01.HYP.0000184362.61744.c1

Quinn, S., Harvey, B. J., & Thomas, W. (2014). Rapid aldosterone actions on epithelial sodium channel trafficking and cell proliferation. *Steroids*, 81: 43-48.

Quispe, R., Trappschuh, M., Gahr, M., & Goymann, W. (2015). Towards more physiological manipulations of hormones in field studies: comparing the release dynamics of three kinds of testosterone implants, silastic tubing, time-release pellets and beeswax. *General and comparative endocrinology*, 212: 100-105.

Rajkumar, A. P., Qvist, P., Lazarus, R., Lescai, F., Ju, J., Nyegaard, M., . . . Christensen, J. H. (2015). Experimental validation of methods for differential gene expression analysis and sample pooling in RNA-seq. *BMC Genomics*, 16: 1-8. doi: 10.1186/s12864-015-1767-y

- Rao, P. M., Kelly, D. M., & Jones, T. H. (2013). Testosterone and insulin resistance in the metabolic syndrome and T2DM in men. *Nature Reviews Endocrinology*, 9(8): 479-493. doi: 10.1038/nrendo.2013.122
- Rastogi, S. C., Rastogi, P., & Mendiratta, N. (2008). Ion channels and aquaporins as potential drug targets *Bioinformatics Methods And Applications: Genomics Proteomics And Drug Discovery* (Vol. 3). New Dehli: PHI Learning Private Limited.
- Reckelhoff, J. F. (2001). Gender differences in the regulation of blood pressure. *Hypertension*, 37(5): 1199-1208. doi: 10.1161/01.hyp.37.5.1199
- Reckelhoff, J. F. (2004). Basic research into the mechanisms responsible for postmenopausal hypertension. *International journal of clinical practice. Supplement*(139): 13-19.
- Reckelhoff, J. F., & Granger, J. P. (1999). Role of androgens in mediating hypertension and renal injury. *Clinical and Experimental Pharmacology and Physiology*, 26(2): 127-131.
- Reckelhoff, J. F., Yanes, L. L., Ilescu, R., Fortepiani, L. A., & Granger, J. P. (2005). Testosterone supplementation in aging men and women: possible impact on cardiovascular-renal disease. *American Journal of Physiology - Renal Physiology*, 289(5): F941-F948. doi: 10.1152/ajprenal.00034.2005
- Reckelhoff, J. F., Zhang, H., & Granger, J. P. (1998). Testosterone exacerbates hypertension and reduces pressure-natriuresis in male spontaneously hypertensive rats. *Hypertension*, 31(1 Pt 2): 435-439.
- Reckelhoff, J. F., Zhang, H., & Srivastava, K. (2000). Gender differences in development of hypertension in spontaneously hypertensive rats: role of the renin-angiotensin system. *Hypertension*, 35(1 Pt 2): 480-483.
- Reckelhoff, J. F., Zhang, H., Srivastava, K., & Granger, J. P. (1999). Gender differences in hypertension in Spontaneously Hypertensive Rats role of androgens and androgen receptor. *Hypertension*, 34(4): 920-923.
- Regier, N., & Frey, B. (2010). Experimental comparison of relative RT-qPCR quantification approaches for gene expression studies in poplar. *BMC Mol Biol*, 11: 57. doi: 10.1186/1471-2199-11-57
- Regitz-Zagrosek, V. (2012). Sex and gender differences in health: Science and society series on sex and science. *EMBO Reports*, 13(7): 596-603. doi: 10.1038/embor.2012.87
- Regitz-Zagrosek, V., & Seeland, U. (2012). Sex and gender differences in clinical medicine. *Handbook of Experimental Pharmacology*(214): 3-22. doi: 10.1007/978-3-642-30726-3\_1
- Renaud, L. P. (1994). Hypothalamic magnocellular neurosecretory neurons: intrinsic membrane properties and synaptic connection. In B. F. E. (Ed.), *Neuroscience:*

*From the Molecular to the Cognitive* (Vol. 100, pp. 133-137). Netherland: Elsevier Science Publishers.

- Robinson, M. D., McCarthy, D. J., & Smyth, G. K. (2010). edgeR: A bioconductor package for differential expression analysis of digital gene expression data. *Bioinformatics*, 26(1): 139-140. doi: 10.1093/bioinformatics/btp616
- Robledo, D., Ronza, P., Harrison, P. W., Losada, A. P., Bermudez, R., Pardo, B. G., . . . Martinez, P. (2014). RNA-seq analysis reveals significant transcriptome changes in turbot (*Scophthalmus maximus*) suffering severe enteromyxosis. *BMC Genomics*, 15: 1149. doi: 10.1186/1471-2164-15-1149
- Roland, B. L., & Sawchenko, P. E. (1993). Local origins of some GABAergic projections to the paraventricular and supraoptic nuclei of the hypothalamus in the rat. *Journal of Comparative Neurology*, 332(1): 123-143. doi: 10.1002/cne.903320109
- Rossi, N. F., & Chen, H. (2001). PVN lesions prevent the endothelin 1-induced increase in arterial pressure and vasopressin. *American Journal of Physiology - Endocrinology and Metabolism*, 280(2): E349-E356.
- Rossier, B. C. (2014). Epithelial sodium channel (ENaC) and the control of blood pressure. *Current Opinion in Pharmacology*, 15: 33-46. doi: 10.1016/j.coph.2013.11.010
- Rothman, M. S., Carlson, N. E., Xu, M., Wang, C., Swerdloff, R., Lee, P., . . . Wierman, M. E. (2011). Reexamination of testosterone, dihydrotestosterone, estradiol and estrone levels across the menstrual cycle and in postmenopausal women measured by liquid chromatography–tandem mass spectrometry. *Steroids*, 76(1–2): 177-182. doi: 10.1016/j.steroids.2010.10.010
- Rotin, D., & Schild, L. (2008). ENaC and its regulatory proteins as drug targets for blood pressure control. *Current Drug Targets*, 9(8): 709-716.
- Rouch, A., Curtis, K., Fan, L., Kudo, L., Toal, S., & Naukam, R. (2012). Estrogen supplementation in female mice yields higher sodium (Na) retention than that of testosterone in male mice. *The FASEB Journal*, 26(1): 1096-1098.
- Ruiz-Cortés, Z. T. (2012). Gonadal sex steroids: Production, action and interactions in mammals. In S. M. Ostojic (Ed.), *Steroids - From Physiology to Clinical Medicine* (pp. 3-44): InTech.
- Rush, M. E., & Blake, C. A. (1982). Serum testosterone concentrations during the 4-day estrous cycle in normal and adrenalectomized rats. *Experimental Biology and Medicine*, 169(2): 216-221. doi: 10.3181/00379727-169-41334
- Saad, F. (2009). The role of testosterone in type 2 diabetes and metabolic syndrome in men. *Archives of Endocrinology and Metabolism*, 53(8): 901-907.
- Sabolic, I., Asif, A. R., Budach, W. E., Wanke, C., Bahn, A., & Burckhardt, G. (2007). Gender differences in kidney function. *Pflügers Archiv: European Journal of Physiology*, 455(3): 397-429. doi: 10.1007/s00424-007-0308-1

- Safari, T., Nematbakhsh, M., Evans, R. G., & Denton, K. M. (2015). High-dose estradiol-replacement therapy enhances the renal vascular response to angiotensin II via an AT<sub>2</sub>-receptor dependent mechanism. *Advances in Pharmacological Sciences*, 2015: Article ID 682745. doi: 10.1155/2015/682745
- Saigusa, T., Granger, N. S., Godwin, S. J., & Head, G. A. (2003). The rostral ventrolateral medulla mediates sympathetic baroreflex responses to intraventricular angiotensin II in rabbits. *Autonomic Neuroscience*, 107(1): 20-31. doi: 10.1016/s1566-0702(03)00104-8
- Salleh, N., Mohd Mokhtar, H., Kassim, N. M., & Giribabu, N. (2015). Testosterone induces increase in aquaporin (AQP)-1, 5, and 7 expressions in the uteri of ovariectomized rats. *Journal of Membrane Biology*, 248(6): 1097-1105. doi: 10.1007/s00232-015-9823-8
- Sandberg, K., & Ji, H. (2012). Sex differences in primary hypertension. *Biology of Sex Differences*, 3: 1-21. doi: 10.1186/2042-6410-3-7
- Sandhu, S., Silbiger, S. R., Lei, J., & Neugarten, J. (1997). Effects of sex hormones on fluid and solute transport in Madin-Darby canine kidney cells. *Kidney International*, 51(5): 1535-1539.
- Sanger, F., Nicklen, S., & Coulson, A. R. (1977). DNA sequencing with chain-terminating inhibitors. *Proceedings of the National Academy of Sciences U S A*, 74(12): 5463-5467.
- Sangiao-Alvarellos, S., Polakof, S., Arjona, F. J., Garcia-Lopez, A., Martin del Rio, M. P., Martinez-Rodriguez, G., . . . Soengas, J. L. (2006). Influence of testosterone administration on osmoregulation and energy metabolism of gilthead sea bream *Sparus auratus*. *General and Comparative Endocrinology*, 149(1): 30-41. doi: 10.1016/j.ygcen.2006.05.003
- Sar, M., & Stumpf, W. E. (1980). Simultaneous localization of [3H]estradiol and neurophysin I or arginine vasopressin in hypothalamic neurons demonstrated by a combined technique of dry-mount autoradiography and immunohistochemistry. *Neuroscience Letters*, 17(1-2): 179-184.
- Sato, M. A., Menani, J. V., Lopes, O. U., & Colombari, E. (1999). Commissural NTS lesions and cardiovascular responses in aortic baroreceptor-denervated rats. *Hypertension*, 34(4): 739-743. doi: 10.1161/01.hyp.34.4.739
- Schena, M., Shalon, D., Davis, R. W., & Brown, P. O. (1995). Quantitative monitoring of gene expression patterns with a complementary DNA microarray. *Science*, 270(5235): 467-470.
- Schild, L. (2010). The epithelial sodium channel and the control of sodium balance. *Biochimica et Biophysica Acta (BBA) - Molecular Basis of Disease*, 1802(12): 1159-1165. doi: 10.1016/j.bbadis.2010.06.014
- Schild, L., Lu, Y., Gautschi, I., Schneeberger, E., Lifton, R. P., & Rossier, B. C. (1996). Identification of a PY motif in the epithelial Na channel subunits as a target

sequence for mutations causing channel activation found in Liddle syndrome. *EMBO Journal*, 15(10): 2381-2387.

- Schnermann, J., Huang, Y., & Mizel, D. (2013). Fluid reabsorption in proximal convoluted tubules of mice with gene deletions of claudin-2 and/or aquaporin1. *American Journal of Physiology - Renal Physiology*, 305(9): F1352-F1364.
- Schorr, K., Morinelli, T. A., Masuda, A., Matsuda, K., Mathur, R. S., & Halushka, P. V. (1994). Testosterone treatment enhances thromboxane A2 mimetic induced coronary artery vasoconstriction in guinea pigs. *European Journal of Clinical Investigation*, 24 Suppl 1: 50-52.
- Schulster, M., Bernie, A. M., & Ramasamy, R. (2016). The role of estradiol in male reproductive function. *Asian Journal of Andrology*, 18(3): 435-440.
- Schuoler, C., Haider, T., Leuenberger, C., Gassmann, M., Kohler, M., Huber, L., & Brock, M. (2015). Expression and function of aquaporin 1 in hypoxia-induced pulmonary hypertension. *European Respiratory Journal*, 46(suppl 59): PA4906. doi: 10.1183/13993003.congress-2015.PA4906
- Secreto, G., Sieri, S., Agnoli, C., Grioni, S., Muti, P., Zumoff, B., . . . Krogh, V. (2016). A novel approach to breast cancer prevention: reducing excessive ovarian androgen production in elderly women. *Breast Cancer Res Treat*, 158(3): 553-561. doi: 10.1007/s10549-016-3901-1
- Seftel, A. D. (2015). Re: Testosterone products: Drug safety communication - FDA Cautions about using testosterone products for low testosterone due to aging; Requires labeling change to inform of possible increased risk of heart attack and stroke. *Journal of Urology*, 194(3): 759-760. doi: 10.1016/j.juro.2015.06.058
- Sevre, K., Lefrandt, J. D., Nordby, G., Os, I., Mulder, M., Gans, R. O., . . . Smit, A. J. (2001). Autonomic function in hypertensive and normotensive subjects: the importance of gender. *Hypertension*, 37(6): 1351-1356.
- Shafton, A. D., Ryan, A., & Badoer, E. (1998). Neurons in the hypothalamic paraventricular nucleus send collaterals to the spinal cord and to the rostral ventrolateral medulla in the rat. *Brain Research*, 801(1-2): 239-243.
- Shankar, R. R., Eckert, G. J., Saha, C., Tu, W., & Pratt, J. H. (2005). The change in blood pressure during pubertal growth. *The Journal of Clinical Endocrinology & Metabolism*, 90(1): 163-167. doi: doi:10.1210/jc.2004-0926
- Shell, B., Faulk, K., & Cunningham, J. T. (2016). Neural Control of Blood Pressure in Chronic Intermittent Hypoxia. *Current Hypertension Reports*, 18(3): 1-9. doi: 10.1007/s11906-016-0627-8
- Sherbet, D. P., & Auchus, R. J. (2007). Peripheral testosterone metabolism. In A. Payne & M. Hardy (Eds.), *The Leydig Cell in Health and Disease* (pp. 181-188): Humana Press.
- Shores, M. M., Biggs, M. L., Arnold, A. M., Smith, N. L., Longstreth, W. T., Kizer, J. R., . . . Matsumoto, A. M. (2014). Testosterone, dihydrotestosterone, and

incident cardiovascular disease and mortality in the cardiovascular health study. *The Journal of Clinical Endocrinology & Metabolism*, 99(6): 2061-2068. doi: 10.1210/jc.2013-3576

- Simerly, R. B., Swanson, L. W., Chang, C., & Muramatsu, M. (1990). Distribution of androgen and estrogen receptor mRNA-containing cells in the rat brain: An in situ hybridization study. *Journal of Comparative Neurology*, 294(1): 76-95. doi: 10.1002/cne.902940107
- Sjahfirdi, L. , Azis, S. N. , Maheshwari, H., Astuti, P., Suyatna, F. D., & Nasikin, M. (2011). Estrus period determination of female rats (*Rattus norvegicus*) by fourier transform infrared (ftir) through identification of reproductive hormones metabolites in urine samples. *International Journal of Basic and Applied Sciences*, 11(3): 128-133.
- Smith, P. K., Krohn, R. I., Hermanson, G. T., Mallia, A. K., Gartner, F. H., Provenzano, M. D., . . . Klenk, D. C. (1985). Measurement of protein using bicinchoninic acid. *Analytical Biochemistry*, 150(1): 76-85.
- Snyder, E. M., Small, C. L., Li, Y., & Griswold, M. D. (2009). Regulation of gene expression by estrogen and testosterone in the proximal mouse reproductive tract. *Biology of Reproduction*, 81(4): 707-716. doi: 10.1095/biolreprod.109.079053
- Soares, T. J., Coimbra, T. M., Martins, A. R., Pereira, A. G. F., Carnio, E. C., Branco, L. G. S., . . . Antunes-Rodrigues, J. (1999). Atrial natriuretic peptide and oxytocin induce natriuresis by release of cGMP. *Proceedings of the National Academy of Sciences U S A*, 96(1): 278-283. doi: 10.1073/pnas.96.1.278
- Sohara, E., Rai, T., Sasaki, S., & Uchida, S. (2006). Physiological roles of AQP7 in the kidney: lessons from AQP7 knockout mice. *Biochimica et Biophysica Acta (BBA)-Biomembranes*, 1758(8): 1106-1110.
- Sohara, E., Uchida, S., & Sasaki, S. (2009). Function of aquaporin-7 in the kidney and the male reproductive system *Aquaporins* (pp. 219-231): Springer.
- Solomon, E. P. (2016). *The Central Nervous System Introduction to human anatomy and physiology* (Vol. 4). USA: Saunders Elsevier.
- Somponpun, S., & Sladek, C. D. (2002). Role of Estrogen Receptor- $\beta$  in Regulation of Vasopressin and Oxytocin Release in Vitro. *Endocrinology*, 143(8): 2899-2904. doi: doi:10.1210/endo.143.8.8946
- Song, J., Eyster, K. M., Kost, C. K., Jr., Kjellsen, B., & Martin, D. S. (2010). Involvement of protein kinase C-CPI-17 in androgen modulation of angiotensin II-renal vasoconstriction. *Cardiovasc Res*, 85(3): 614-621. doi: 10.1093/cvr/cvp326
- Song, J., Hu, X., Riazi, S., Tiwari, S., Wade, J. B., & Ecelbarger, C. A. (2006). Regulation of blood pressure, the epithelial sodium channel (ENaC), and other key renal sodium transporters by chronic insulin infusion in rats. *American*

*Journal of Physiology - Renal Physiology*, 290(5): F1055-1064. doi: 10.1152/ajprenal.00108.2005

- Soundararajan, R., Pearce, D., & Ziera, T. (2012). The role of the ENaC-regulatory complex in aldosterone-mediated sodium transport. *Molecular and Cellular Endocrinology*, 350(2): 242-247. doi: 10.1016/j.mce.2011.11.003
- Stachenfeld, N. S. (2008). Sex hormone effects on body fluid regulation. *Exercise and Sport Sciences Reviews*, 36(3): 152-159. doi: 10.1097/JES.0b013e31817be928
- Stachenfeld, N. S., Splenser, A. E., Calzone, W. L., Taylor, M. P., & Keefe, D. L. (2001). Sex differences in osmotic regulation of AVP and renal sodium handling. *Journal of Applied Physiology*, 91(4): 1893-1901.
- Stachowiak, A., Nussdorfer, G. G., & Malendowicz, L. K. (1991). Ovariectomy-induced changes in the adrenal cortex of spontaneously hypertensive rats. *Histology and Histopathology*, 6(2): 257-259.
- Stamler, J., Stamler, R., Riedlinger, W. F., Algera, G., & Roberts, R. H. (1976). Hypertension screening of 1 million Americans. Community Hypertension Evaluation Clinic (CHEC) program, 1973 through 1975. *Journal of the American Medical Association (JAMA)*, 235(21): 2299-2306.
- Stockand, J. D. (2010). Vasopressin regulation of renal sodium excretion. *Kidney International*, 78(9): 849-856. doi: 10.1038/ki.2010.276
- Stockand, J. D., Edinger, R. S., Eaton, D. C., & Johnson, J. P. (2000). Toward understanding the role of methylation in aldosterone-sensitive Na<sup>+</sup> transport. *Physiology*, 15(4): 161-165.
- Stocker, S. D., Monahan, K. D., & Browning, K. N. (2013). Neurogenic and sympathoexcitatory actions of NaCl in hypertension. *Current Hypertension Reports*, 15(6): 538-546. doi: 10.1007/s11906-013-0385-9
- Stocker, S. D., Osborn, J. L., & Carmichael, S. P. (2008). Forebrain osmotic regulation of the sympathetic nervous system. *Clinical and Experimental Hypertension*, 35(5-6): 695-700. doi: 10.1111/j.1440-1681.2007.04835.x
- Ström, J. O., Theodorsson, E., & Theodorsson, A. (2008). Order of magnitude differences between methods for maintaining physiological 17 $\beta$  - oestradiol concentrations in ovariectomized rats. *Scandinavian journal of clinical and laboratory investigation*, 68(8): 814-822.
- Subramanian, M., Balasubramanian, P., Garver, H., Northcott, C., Zhao, H., Haywood, J. R., . . . MohanKumar, P. S. (2011). Chronic estradiol-17 $\beta$  exposure increases superoxide production in the rostral ventrolateral medulla and causes hypertension: reversal by resveratrol. *American Journal of Physiology - Regulatory, Integrative and Comparative Physiology*, 300(6): R1560-1568. doi: 10.1152/ajpregu.00020.2011

- Sun, M. K. (1995). Central neural organization and control of sympathetic nervous system in mammals. *Progress in Neurobiology*, 47(3): 157-233.
- Sun, M. K., & Guyenet, P. G. (1985). GABA-mediated baroreceptor inhibition of reticulospinal neurons. *American Journal of Physiology*, 249(6 Pt 2): R672-680.
- Suzuki, H., & Saruta, T. (2004). An overview of blood pressure regulation associated with the kidney. In H. Suzuki & T. Saruta (Eds.), *Kidney and Blood Pressure Regulation* (Vol. 143, pp. 1-15): Karger.
- Suzuki, S., Takeshita, A., Imaizumi, T., Hirooka, Y., Yoshida, M., Ando, S., & Nakamura, M. (1989). Central nervous system mechanisms involved in inhibition of renal sympathetic nerve activity induced by arginine vasopressin. *Circulation Research*, 65(5): 1390-1399.
- Svartberg, J., von Muhlen, D., Schirmer, H., Barrett-Connor, E., Sundfjord, J., & Jorde, R. (2004). Association of endogenous testosterone with blood pressure and left ventricular mass in men. The Tromso Study. *European Journal of Endocrinology*, 150(1): 65-71. doi: 10.1530/eje.0.1500065
- Sved, A. F., Ito, S., Madden, C. J., Stocker, S. D., & Yajima, Y. (2001). Excitatory inputs to the RVLM in the context of the baroreceptor reflex. *Annals of the New York Academy of Sciences*, 940: 247-258.
- Swanson, L. W., Sawchenko, P. E., Wiegand, S. J., & Price, J. L. (1980). Separate neurons in the paraventricular nucleus project to the median eminence and to the medulla or spinal cord. *Brain Research*, 198(1): 190-195.
- Tagawa, T., & Dampney, R. A. (1999). AT(1) receptors mediate excitatory inputs to rostral ventrolateral medulla pressor neurons from hypothalamus. *Hypertension*, 34(6): 1301-1307.
- Takata, K., Matsuzaki, T., & Tajika, Y. (2004). Aquaporins: water channel proteins of the cell membrane. *Progress in Histochemistry and Cytochemistry*, 39(1): 1-83.
- Takata, K., Matsuzaki, T., Tajika, Y., Ablimit, A., & Hasegawa, T. (2008). Localization and trafficking of aquaporin 2 in the kidney. *Histochemistry Cell Biology*, 130(2): 197-209. doi: 10.1007/s00418-008-0457-0
- Takezawa, H., Hayashi, H., Sano, H., & Ebihara, S. (1994). Estrous-related variations of blood pressure and heart rate in female rats. *Frontiers of Medical and Biological Engineering*, 6(2): 131-137.
- Tambo, A., Roshan, M. H. K., & Pace, N. P. (2016). Testosterone and cardiovascular disease. *The Open Cardiovascular Medicine Journal*, 10: 1-10. doi: 10.2174/1874192401610010001
- Tasker, J. G., Boudaba, C., & Schrader, L. A. (1998). Local glutamatergic and GABAergic synaptic circuits and metabotropic glutamate receptors in the hypothalamic paraventricular and supraoptic nuclei. In H. Zingg, C. Bourque & D. Bichet (Eds.), *Vasopressin and Oxytocin* (Vol. 449, pp. 117-121): Springer US.

- Tatchum-Talom, R., Eyster, K. M., Kost, C. K., & Martin, D. S. (2011). Blood pressure and mesenteric vascular reactivity in SHR seven months after gonadectomy. *Journal of Cardiovascular Pharmacology*, 57(3): 357-364.
- Thangjam, P., & Wangkheimayum, K. (2015). Comparison of sympathetic nervous activity among male and female patients of bronchial asthma. *National Journal of Physiology, Pharmacy and Pharmacology*, 5(2): 116-118.
- Thomas, A., Kim, N. B., & Amico, J. A. (1996). Differential regulation of oxytocin and vasopressin messenger ribonucleic acid levels by gonadal steroids in postpartum rats. *Brain Res*, 738(1): 48-52.
- Tivesten, Å., Pinthus, J. H., Clarke, N., Duivenvoorden, W., & Nilsson, J. (2015). Cardiovascular risk with androgen deprivation therapy for prostate cancer: Potential mechanisms. *Urologic Oncology: Seminars and Original Investigations*, 33(11): 464-475. doi: 10.1016/j.urolonc.2015.05.030
- Toney, G. M., & Stocker, S. D. (2010). Hyperosmotic activation of CNS sympathetic drive: implications for cardiovascular disease. *The Journal of Physiology*, 588(18): 3375-3384. doi: 10.1113/jphysiol.2010.191940
- Toot, J. D., Reho, J. J., Novak, J., Dunphy, G., Ely, D. L., & Ramirez, R. J. (2011). Colony social stress differentially alters blood pressure and resistance-sized mesenteric artery reactivity in SHR/y and WKY male rats. *Stress*, 14(1): 33-41. doi: 10.3109/10253890.2010.491876
- Toot, J. D., Reho, J. J., Ramirez, R. J., Novak, J., & Ely, D. L. (2012). Alterations in vasomotor systems and mechanics of resistance-sized mesenteric arteries from SHR and WKY male rats following in vivo testosterone manipulation. *Biology of Sex Differences*, 3(1): 1. doi: 10.1186/2042-6410-3-1
- Toot, J., Jenkins, C., Dunphy, G., Boehme, S., Hart, M., Milsted, A., . . . Ely, D. (2008). Testosterone influences renal electrolyte excretion in SHR/y and WKY males. *BMC Physiology*, 8(1): 1-10. doi: 10.1186/1472-6793-8-5
- Towbin, H., Staehelin, T., & Gordon, J. (1979). Electrophoretic transfer of proteins from polyacrylamide gels to nitrocellulose sheets: procedure and some applications. *Proceedings of the National Academy of Sciences U S A*, 76(9): 4350-4354.
- Trapnell, C., Roberts, A., Goff, L., Pertea, G., Kim, D., Kelley, D. R., . . . Pachter, L. (2012). Differential gene and transcript expression analysis of RNA-seq experiments with TopHat and Cufflinks. *Nature Protocols*, 7(3): 562-578. doi: 10.1038/nprot.2012.016
- Trapnell, C., Williams, B. A., Pertea, G., Mortazavi, A., Kwan, G., van Baren, M. J., . . . Pachter, L. (2010). Transcript assembly and quantification by RNA-Seq reveals unannotated transcripts and isoform switching during cell differentiation. *Nature Biotechnology*, 28(5): 511-515. doi: 10.1038/nbt.1621

- Trippodo, N. C., & Frohlich, E. D. (1981). Similarities of genetic (spontaneous) hypertension. Man and rat. *Circulation Research*, 48(3): 309-319. doi: 10.1161/01.res.48.3.309
- Vallon, V., Verkman, A. S., & Schnermann, J. (2000). Luminal hypotonicity in proximal tubules of aquaporin-1-knockout mice. *American Journal of Physiology - Renal Physiology*, 278(6): F1030-F1033.
- van den Pol, A. N. (1982). The magnocellular and parvocellular paraventricular nucleus of rat: intrinsic organization. *Journal of Comparative Neurology*, 206(4): 317-345. doi: 10.1002/cne.902060402
- Van Kesteren, P. J., Kooistra, T., Lansink, M., van Kamp, G. J., Asscheman, H., Gooren, L. J., . . . Stehouwer, C. D. (1998). The effects of sex steroids on plasma levels of marker proteins of endothelial cell functioning. *Thrombosis and Haemostasis*, 79(5): 1029-1033.
- Vasudevan, H., Yuen, V. G., & McNeill, J. H. (2012). Testosterone-dependent increase in blood pressure is mediated by elevated Cyp4A expression in fructose-fed rats. *Molecular and Cellular Biochemistry*, 359(1): 409-418. doi: 10.1007/s11010-011-1035-7
- Verkman, A. (2012). Aquaporins in Clinical Medicine. *Annu Rev Med*, 63: 303-316. doi: 10.1146/annurev-med-043010-193843
- Verkman, A. S. (2011). Aquaporins at a glance. *Journal of Cell Science*, 124(13): 2107-2112. doi: 10.1242/jcs.079467
- Verkman, A. S., Anderson, M. O., & Papadopoulos, M. C. (2014). Aquaporins: important but elusive drug targets. *Nature Reviews Drug Discovery*, 13(4): 259-277. doi: 10.1038/nrd4226
- Verkman, A. S., Matthay, M. A., & Song, Y. (2000). Aquaporin water channels and lung physiology. *American Journal of Physiology - Lung Cellular and Molecular Physiology*, 278(5): L867-879.
- Verkman, A. S., & Mitra, A. K. (2000). Structure and function of aquaporin water channels. *American Journal of Physiology - Renal Physiology*, 278(1): F13-28.
- Verrey, F., Hummler, E., Schild, L., & Rossier, B. C. (2008). Mineralocorticoid action in the aldosterone-sensitive distal nephron. *The Kidney Physiology and Pathophysiology*: 889-924.
- Viau, V., Chu, A., Soriano, L., & Dallman, M. F. (1999). Independent and overlapping effects of corticosterone and testosterone on corticotropin-releasing hormone and arginine vasopressin mRNA expression in the paraventricular nucleus of the hypothalamus and stress-induced adrenocorticotrophic hormone release. *Journal of Neuroscience*, 19(15): 6684-6693.
- Vlachopoulos, C., Pietri, P., Ioakeimidis, N., Aggelis, A., Terentes-Printzios, D., Abdelrasoul, M., . . . Tousoulis, D. (2016). Inverse association of total testosterone with central haemodynamics and left ventricular mass in

hypertensive men. *Atherosclerosis*, 250: 57-62. doi: 10.1016/j.atherosclerosis.2016.04.018

- Vodo, S., Bechi, N., Petroni, A., Muscoli, C., & Aloisi, A. M. (2013). Testosterone-induced effects on lipids and inflammation. *Mediators of Inflammation*, 2013: 8. doi: 10.1155/2013/183041
- Vukićević, T., Schulz, M., Faust, D., & Klussmann, E. (2016). The trafficking of the water channel aquaporin-2 in renal principal cells—A potential target for pharmacological intervention in cardiovascular diseases. *Frontiers in Pharmacology*, 7.
- Wadei, H. M., & Textor, S. C. (2012). The role of the kidney in regulating arterial blood pressure. *Nature Reviews Nephrology*, 8(10): 602-609.
- Wang, Y. B., Leroy, V., Maunsbach, A. B., Doucet, Al., Hasler, U., Dizin, E., . . . Féraille, E. (2014). Sodium transport is modulated by p38 kinase-dependent cross-talk between ENaC and Na, K-ATPase in collecting duct principal cells. *Journal of the American Society of Nephrology*, 25(2): 250-259.
- Wang, Y., & Tajkhorshid, E. (2010). Nitric Oxide Conduction by the Brain Aquaporin AQP4. *Proteins*, 78(3): 661-670. doi: 10.1002/prot.22595
- Wang, Y. X., Edwards, R. M., Nambi, P., Stack, E. J., Pullen, M., Share, L., . . . Brooks, D. P. (1993). Sex difference in the antidiuretic activity of vasopressin in the rat. *American Journal of Physiology - Regulatory, Integrative and Comparative Physiology*, 265(6): R1284-R1290.
- Wang, Y., Xie, B. Q., Gao, W. H., Yan, D. Y., Zheng, W. L., Lv, Y. B., . . . Mu, J. J. (2015). Effects of renin-angiotensin system inhibitors on renal expression of renalase in Sprague-Dawley rats fed with high salt diet. *Kidney and Blood Pressure Research*, 40(6): 605-613.
- Wang, Z., Gerstein, M., & Snyder, M. (2009). RNA-Seq: A revolutionary tool for transcriptomics. *Nature Reviews Genetics*, 10(1): 57-63. doi: 10.1038/nrg2484
- Warnock, D. G., & Rossier, B. C. (2005). Renal sodium handling: The role of the epithelial sodium channel. *Journal of the American Society of Nephrology*, 16(11): 3151-3153. doi: 10.1681/asn.2005080886
- Wei, H., Wang, G., Xu, J., Yuan, W., & Wei, J. (2014-05). Effects of reduced estrogen and progesterone on renal aquaporin expression in rats. *Journal of Zhengzhou University (Medical Sciences)*(R692).
- Weinberger, M. H., Aoi, W., & Henry, D. P. (1975). Direct effect of beta-adrenergic stimulation on renin release by the rat kidney slice in vitro. *Circulation Research*, 37(3): 318-324.
- Wenner, M. M., & Stachenfeld, N. S. (2012). Blood pressure and water regulation: understanding sex hormone effects within and between men and women. *The Journal of Physiology*, 590(23): 5949-5961. doi: 10.1113/jphysiol.2012.236752

- Wiinberg, N., Hoegholm, A., Christensen, H. R., Bang, L. E., Mikkelsen, K. L., Nielsen, P. E., . . . Bentzon, M. W. (1995). 24-h ambulatory blood pressure in 352 normal Danish subjects, related to age and gender. *American Journal of Hypertension*, *8*(10 Pt 1): 978-986. doi: 10.1016/0895-7061(95)00216-2
- Williamson, M., & Viau, V. (2008). Selective contributions of the medial preoptic nucleus to testosterone-dependant regulation of the paraventricular nucleus of the hypothalamus and the HPA axis. *American Journal of Physiology - Regulatory, Integrative and Comparative Physiology*, *295*(4): R1020-R1030. doi: 10.1152/ajpregu.90389.2008
- Wilson, C., Maass, R., & Estrada, M. (2011). Cardiovascular Effects of Androgens. In F. Akin (Ed.), *Basic and Clinical Endocrinology Up-to-Date* (October, 2011 ed., pp. 63-78): InTech.
- Wilson, J. L. L., Miranda, C. A., & Knepper, M. A. (2013). Vasopressin and the regulation of aquaporin-2. *Clinical and Experimental Nephrology*, *17*(6): 751-764. doi: 10.1007/s10157-013-0789-5
- Wolf, J. B. W. (2013). Principles of transcriptome analysis and gene expression quantification: an RNA-seq tutorial. *Molecular Ecology Resources*, *13*(4): 559-572. doi: 10.1111/1755-0998.12109
- Wu, D., Lin, G., & Gore, A. C. (2009). Age-related changes in hypothalamic androgen receptor and estrogen receptor alpha in male rats. *Journal of Comparative Neurology*, *512*(5): 688-701. doi: 10.1002/cne.21925
- Wyss, J. M. (1993). The role of the sympathetic nervous system in hypertension. *Current Opinion in Nephrology and Hypertension*, *2*(2): 265-273.
- Xia, Y., & Krukoff, T. L. (2003). Differential neuronal activation in the hypothalamic paraventricular nucleus and autonomic/neuroendocrine responses to I.C.V. endotoxin. *Neuroscience*, *121*(1): 219-231.
- Xu, J., Sun, J., Chen, J., Wang, L., Li, A., Helm, M., . . . Chen, X. (2012). RNA-Seq analysis implicates dysregulation of the immune system in schizophrenia. *BMC Genomics*, *13*(8): 1-10. doi: 10.1186/1471-2164-13-s8-s2
- Xu, Q., Prabhu, A., Xu, S., Manigrasso, M. B., & Maric, C. (2009). Dose-dependent effects of dihydrotestosterone in the streptozotocin-induced diabetic rat kidney. *American Journal of Physiology - Renal Physiology*, *297*(2): F307-F315. doi: 10.1152/ajprenal.00135.2009
- Xue, B., Badaue-Passos, D., Guo, F., Gomez-Sanchez, C. E., Hay, M., & Johnson, A. K. (2009). Sex differences and central protective effect of 17 $\beta$ -estradiol in the development of aldosterone/NaCl-induced hypertension. *American Journal of Physiology-Heart and Circulatory Physiology*, *296*(5): H1577-H1585.
- Xue, B., Johnson, A. K., & Hay, M. (2007). Sex differences in angiotensin II- induced hypertension. *Brazilian Journal of Medical and Biological Research*, *40*: 727-734.

- Xue, B., Zhang, Z., Beltz, T. G., Johnson, R. F., Guo, F., Hay, M., & Johnson, A. K. (2013). Estrogen receptor- $\beta$  in the paraventricular nucleus and rostroventrolateral medulla plays an essential protective role in aldosterone/salt-induced hypertension in female rats. *Hypertension*, *61*(6): 1255.
- Yanes, L. L., Sartori-Valinotti, J. C., Iliescu, R., Romero, D. G., Racusen, L. C., Zhang, H., & Reckelhoff, J. F. (2009). Testosterone-dependent hypertension and upregulation of intrarenal angiotensinogen in Dahl salt-sensitive rats. *American Journal of Physiology - Renal Physiology*, *296*(4): F771-F779. doi: 10.1152/ajprenal.90389.2008
- Yanes, L. L., Sartori-Valinotti, J. C., & Reckelhoff, J. F. (2008). Sex steroids and renal disease: lessons from animal studies. *Hypertension*, *51*(4): 976-981. doi: 10.1161/hypertensionaha.107.105767
- Yang, S. H., Shi, J., Day, A. L., & Simpkins, J. W. (2000). Estradiol exerts neuroprotective effects when administered after ischemic insult. *Stroke*, *31*(3): 745-749; discussion 749-750.
- Yasui, M., Kwon, T. H., Knepper, M. A., Nielsen, S., & Agre, P. (1999). Aquaporin-6: an intracellular vesicle water channel protein in renal epithelia. *Proceedings of the National Academy of Sciences*, *96*(10): 5808-5813.
- Yasui, T., Matsui, S., Tani, A., Kunimi, K., Yamamoto, S., & Irahara, M. (2012). Androgen in postmenopausal women. *The Journal of Medical Investigation*, *59*(1-2): 12-27.
- Ye, L., Su, Z. J., & Ge, R. S. (2011). Inhibitors of testosterone biosynthetic and metabolic activation enzymes. *Molecules*, *16*(12): 9983-10001. doi: 10.3390/molecules16129983
- Yeum, C. H., Kim, S. W., Kim, N. H., Choi, K. C., & Lee, J. (2002). Increased expression of aquaporin water channels in hypothyroid rat kidney. *Pharmacological Research*, *46*(1): 85-88.
- Yong, L. C., Kuller, L. H., Rutan, G., & Bunker, C. (1993). Longitudinal study of blood pressure: changes and determinants from adolescence to middle age. The Dormont High School follow-up study, 1957-1963 to 1989-1990. *American Journal of Epidemiology*, *138*(11): 973-983.
- Yusef, Y. R., Thomas, W., & Harvey, B. J. (2014). Estrogen increases ENaC activity via PKC $\delta$  signaling in renal cortical collecting duct cells. *Physiological Reports*, *2*(5): e12020. doi: 10.14814/phy2.12020
- Zeisberger, E., Roth, J., & Simon, E. (1988). Changes in water balance and in release of arginine vasopressin during thermal adaptation in guinea-pigs. *Pflügers Archiv: European Journal of Physiology*, *412*(3): 285-291.
- Zhang, Z., & Bourque, C. W. (2003). Osmometry in osmosensory neurons. *Nature Neuroscience*, *6*(10): 1021-1022. doi: 10.1038/nn1124

Zhu, X. L., Wang, L., Wang, Z., Chen, S. Z., Zhang, W. Q., & Ma, M. M. (2015). Relationship between EPHX2 gene polymorphisms and essential hypertension in Uygur, Kazakh, and Han. *Genet Mol Res*, *14*(2): 3474-3480. doi: 10.4238/2015.April.15.11

Ziemens, B., Wallaschofski, H., Völzke, H., Rettig, R., Dörr, M., Nauck, M., . . . Haring, R. (2013). Positive association between testosterone, blood pressure, and hypertension in women: longitudinal findings from the Study of Health in Pomerania. *Journal of Hypertension*, *31*(6): 1106-1113. doi: 10.1097/HJH.0b013e3283603eb1

University of Malaya

## LIST OF PUBLICATIONS AND PAPERS PRESENTED

### Publication:

1. Loh, S. Y., Giribabu, N. & Salleh, N. (2016). Sub-chronic testosterone treatment increases the levels of epithelial sodium channel (ENaC)- $\alpha$ ,  $\beta$  and  $\gamma$  in the kidney of orchidectomized adult male Sprague Dawley rats. *PeerJ*, 4:e2145; doi: 10.7717/peerj.2145
2. Loh, S.Y. & Salleh, N. (2016) Influence of testosterone on mean arterial pressure: A physiological study in male and female normotensive WKY and hypertensive SHR rats. *Physiology International (Acta Physiologica Hungarica)*. 104(1): 25-34. doi: 10.1556/2060.104.2017.1.3
3. Loh, S.Y., Giribabu, N., Gholami, K. & Salleh, N. (2016) Effects of testosterone on mean arterial pressure and aquaporin (AQP)-1, 2, 3, 4, 6 and 7 expressions in the kidney of orchidectomized, adult male Sprague-Dawley rats. *Archives of Biochemistry and Biophysics*. 614: 41-49. doi: 10.1016/j.abb.2016.12.008
4. Loh, S.Y., Giribabu, N. & Salleh, N. (2017). Effects of gonadectomy and testosterone treatment on aquaporin expression in the kidney of normotensive and hypertensive rats. *Experimental Biology and Medicine (Maywood)*. doi: 10.1177/1535370217703360
5. Gholami, K., Loh, S.Y., Salleh, N., Lam, S.K. & Hoe, S.Z. (2017) Selection of suitable endogenous reference genes for qPCR in kidney and hypothalamus of rats under testosterone influence. *PLoS One*. 12(6): e0176368. doi: 10.1371/journal.pone.0176368
6. Konopacka, A., Greenwood, M., Loh, S.Y., Paton, J. & Murphy, D. (2015) RNA binding protein Caprin-2 is a pivotal regulator of the central osmotic defense response. *eLife*. 4. doi: 10.7554/eLife.09656.001

### Manuscripts under review:

1. Changes in plasma aldosterone and electrolytes levels, kidney epithelial sodium channel (ENaC) and blood pressure in normotensive WKY and hypertensive SHR rats following gonadectomy and chronic testosterone treatment. *Steroids*.

**Papers presented:**

1. Poster: Castration reduces mean arterial pressure (MAP) in male spontaneous hypertensive rats (SHR). *Faculty of Medicine Research Week 2015*, 11-15 May 2015 (Faculty of Medicine, University Malaya - University).
2. Poster: Selection of suitable endogenous reference genes in rat kidney and hypothalamus under the influence of testosterone for qPCR. *29th Scientific Meeting of Malaysian Society of Pharmacology and Physiology (MSPP)*, 24-25 Aug 2015 (Setia Alam, Selangor, Malaysia – National).
3. Poster: Enhanced expression of epithelial sodium channel (ENaC) -  $\alpha$ ,  $\beta$  and  $\gamma$  in kidneys of orchidectomized rats by testosterone. *8th Federation of the Asian and Oceanian Physiological Societies Congress*, 22-25 November 2015 (Bangkok, Thailand – International).
4. Oral: Effects of testosterone treatment on blood pressure, plasma aldosterone and kidney ENaC expression in normotensive WKY and hypertensive SHR rat. *21<sup>st</sup> Biological Science Graduate Congress (BSGC) 2016*, 15-16 December 2016 (Kuala Lumpur, Malaysia – International).